AD-A956 216

DTIC
ELECTE
APR 22 1996
S
C

Scientific and Engineering Studies

Spectral Estimation

NAVAL UNDERWATER SYSTEMS CENTER

DISTRIBUTION STATEMENT A
Approved for public release;
Distribution unlimited

Accesion For
NTIS CRA&I ☑
DTIC TAB ☐
Unannounced ☐
Justification
By
Distribution /
Availability Codes
Dist | Avail and / or Special
A-1

UNANNOUNCED

Scientific and Engineering Studies

Spectral Estimation

Albert H. Nuttall, et al.

93-08379



PUBLISHED BY

NAVAL UNDERWATER SYSTEMS CENTER

NEWPORT LABORATORY, NEWPORT, RHODE ISLAND

NEW LONDON LABORATORY, NEW LONDON, CONNECTICUT

Foreword

This collection of technical reports deals with estimation of spectra of stationary processes, both by the now-standard direct approach and by the more recent autoregressive approach. The topics range over numerical procedures involving Fast Fourier Transforms, cross-spectral estimation, minimum bias windows, vernier FFTs, coherence, univariate and multivariate maximum entropy spectral estimation, and probability distributions of spectral estimates. These results, which were new when published, are still of great relevance to anyone doing spectral analysis who is interested in obtaining good resolution and stability from limited record lengths.

Dr. William A. Von Winkle
Associate Technical Director
for Technology
NAVAL UNDERWATER SYSTEMS CENTER

$$\mathrm{Im}\left\{ f(0) \right\} = 0 \tag{8}$$

and

$$\lim_{\xi \to 0} \frac{\sin(\xi X)}{\xi} = X. \tag{9}$$

Equation (7) is the general equation allowing numerical evaluation of the MDF $P(X)$ directly from the CF $f(\xi)$. For a discontinuous CDF, in order to minimize inaccuracies in a numerical evaluation of Eq. (7), values of the MDF $P(X)$ at points removed from the discontinuity locations (if known) should be computed. In particular, for a discrete random variable, values of the MDF at points midway between discontinuities should be computed when using Eq. (7).

The integral in Eq. (7) is confined to the real axis. Since

$$|f(\xi)| \leq \int dx\, p(x) = 1 \qquad \text{for } \xi \text{ real}, \tag{10}$$

there are no singular points along the ξ axis. Also some CF's are defined only for ξ real; for example, for

$$p(x) = \frac{1}{\pi} \frac{1}{1+x^2}, \tag{11}$$

$$f(\xi) = \exp(-|\xi|), \qquad \text{real } \xi, \tag{12}$$

but $f(\xi)$ is not defined for complex ξ. Thus, the CF $f(\xi)$ does not have to be analytic at the origin to apply Eq. (7). Nor do any moments of the random variable have to exist.

DISCRETE DISTRIBUTIONS

The expression (7) applies to all MDF's (and CDF's through Eq. (5)); however, it requires an infinite integral for each value of X. Here we shall alleviate this requirement for a special class of random variables. Namely, we consider discrete random variables that can only take on values which are multiples of some fundamental increment Δ. That is, the PDF of interest takes the form

$$p(x) = \sum_k c_k\, \delta(x - k\Delta). \tag{13}$$

Table of Contents

TR 1032 Numerical Evaluation of Cumulative Probability Distribution Functions Directly from Characteristic Functions

A. H. Nuttall

TR 3012 Alternate Forms and Computational Considerations for Numerical Evaluation of Cumulative Probability Distributions Directly from Characteristic Functions

A. H. Nuttall

TR 4113 Comparison of Four Fast Fourier Transform Algorithms

J. F. Ferrie and A. H. Nuttall

TR 4169 Spectral Estimation by Means of Overlapped Fast Fourier Transform Processing of Windowed Data

A. H. Nuttall

TR 4169-S Estimation of Cross-Spectra Via Overlapped Fast Fourier Transform Processing

A. H. Nuttall

TR 4513 Minimum-Bias Windows for Spectral Estimation by Means of Overlapped Fast Fourier Transform Processing

A. H. Nuttall

TR 4767 An Approximate Fast Fourier Transform Technique for Vernier Spectral Analysis

A. H. Nuttall

TR 5291 Approximations for Statistics of Coherence Estimators

A. H. Nuttall and G. C. Carter

TR 5303 Spectral Analysis of a Univariate Process With Bad Data Points, Via Maximum Entropy and Linear Predictive Techniques

A. H. Nuttall

TR 5419 FORTRAN Program for Multivariate Linear Predictive Spectral Analysis, Employing Forward and Backward Averaging

A. H. Nuttall

TR 5501 Multivariate Linear Predictive Spectral Analysis Employing Weighted Forward and Backward Averaging: A Generalization of Burg's Algorithm

A. H. Nuttall

TR 5505 FORTRAN Program for Linear Predictive Spectral Analysis of a Complex Univariate Process

A. H. Nuttall

TR 5529 Probability Distribution of Spectral Estimates Obtained Via Overlapped FFT Processing of Windowed Data

A. H. Nuttall

SUBJECT MATTER INDEX

Copies of the studies included in this volume may be purchased from the National Technical Information Service, U. S. Department of Commerce, Springfield, Va. 22161.

NUSL Report No 1032
11 August 1969

Numerical Evaluation of Cumulative Probability Distribution Functions Directly from Characteristic Functions

Albert H. Nuttall

ABSTRACT

A method for direct numerical evaluation of the cumulative probability distribution function from the characteristic function in terms of a single integral is presented. No moment evaluations or series expansions are required. Intermediate evaluation of the probability density function is circumvented. The method takes on a special form when the random variables are discrete.

Approved for public release; distribution unlimited

TABLE OF CONTENTS

Page

INTRODUCTION 1

ANALYSIS 1
General Distributions 2
Discrete Distributions 4
Nonnegative Discrete Random Variables 5
General Discrete Random Variables 6

EXAMPLES 8

CONCLUSIONS 10

LIST OF REFERENCES 13

INITIAL DISTRIBUTION LIST . . . . . Inside Back Cover

LIST OF TABLES

Table

1 Numerical Computation of Exponential Distribution 9

2 Numerical Computation of Poisson Distribution 10

REVERSE BLANK

NUMERICAL EVALUATION OF CUMULATIVE PROBABILITY DISTRIBUTION FUNCTIONS DIRECTLY FROM CHARACTERISTIC FUNCTIONS

INTRODUCTION

When several independent random variables are added, the characteristic function of the sum is the product of the characteristic functions of the individual random variables. This rule holds regardless of the distributions of the individual random variables, and whether they are identically distributed or not. Evaluation of the cumulative probability distribution of the sum variable in closed form is often very tedious or impossible to achieve. This is especially so when the number of random variables added is large, but not large enough to employ the Central Limit Theorem with accuracy.

In many signal-detection problems, the characteristic function of the decision variable can be derived in closed form (or evaluated numerically fairly easily). Often, however, neither the probability density function of the decision variable, nor its integral, the cumulative probability distribution function, can be obtained in closed form. Even if they can, they are frequently tedious and time-consuming to evaluate (see, for example, Marcum[1]). In this report, we present a technique for numerically evaluating cumulative probability distribution functions directly from specified characteristic functions in terms of a single integral. Intermediate evaluations of the probability density functions are not necessary, and no moment evaluations or series expansions are required. The technique takes on a special form when the decision variable is discrete.

When the characteristic function of the decision variable (which is compared with a threshold) can be evaluated for both the signal-present and signal-absent cases, the technique can be applied to the problem of obtaining receiver operating characteristics (probability of detection versus probability of false alarm).

ANALYSIS

This section is composed of two subsections. In the first, a general formula for direct evaluation of the cumulative probability distribution function from the characteristic function is derived; in the second, an alternate and more useful form for discrete random variables is presented.

GENERAL DISTRIBUTIONS

Let random variable x have probability density function (PDF) p(x) and characteristic function (CF) f(ξ):

$$f(\xi) = \int dx \exp(i\xi x)\, p(x), \tag{1}$$

and

$$p(x) = \frac{1}{2\pi} \int d\xi \exp(-i\xi x)\, f(\xi). \tag{2}$$

(An integral without limits is over the real axis from $-\infty$ to $+\infty$.)

The cumulative distribution function (CDF) $\Pr(X)$ is defined as the probability that random variable x is less than or equal to X:

$$\Pr(X) = \int_{-\infty}^{X+} dx\, p(x). \tag{3}$$

The upper limit means that an impulse in PDF p(x) at $x = X$ is to be included in full. It will be convenient to define the modified distribution function (MDF):

$$P(X) = \int_{-\infty}^{X} dx\, p(x), \tag{4}$$

where an impulse in p(x) at $x = X$ is only half included. At points of continuity of the CDF, $\Pr(X)$ and $P(X)$ are equal. At a point of discontinuity of the CDF, the MDF $P(X)$ takes on a value halfway between the limit values on either side of the discontinuity.[2] The CDF $\Pr(X)$ can be obtained from the MDF $P(X)$ via

$$\Pr(X) = \lim_{\epsilon \to 0+} P(X + \epsilon). \tag{5}$$

Therefore, we can direct our effort to evaluating either the CDF $\Pr(X)$ or the MDF $P(X)$, depending on which is more convenient.

When Eq. (2) is substituted into Eq. (4), we note that the MDF becomes[3]

$$P(X) = \int_{-\infty}^{X} dx \frac{1}{2\pi} \int d\xi \exp(-i\xi x) f(\xi)$$

$$= \frac{1}{2\pi} \int d\xi f(\xi) \int_{-\infty}^{X} dx \exp(-i\xi x)$$

$$= \frac{1}{2\pi} \int d\xi f(\xi) \left[\pi\delta(\xi) - \frac{1}{i\xi} \exp(-i\xi X) \right]$$

$$= \frac{1}{2} - \frac{1}{i2\pi} \int \frac{d\xi}{\xi} f(\xi) \exp(-i\xi X), \tag{6}$$

where the last integral is a principal value integral. Since the PDF $p(x)$ is real, the real part of the CF $f(\xi)$ is even, and the imaginary part of the CF $f(\xi)$ is odd; i.e., $f(-\xi) = f^*(\xi)$. This allows Eq. (6) to be manipulated into the forms

$$P(X) = \frac{1}{2} - \frac{1}{\pi} \int_0^\infty \frac{d\xi}{\xi} \operatorname{Im}\left\{ f(\xi) \exp(-i\xi X) \right\}$$

$$= \frac{1}{2} - \frac{1}{\pi} \int_0^\infty \frac{d\xi}{\xi} \left[\operatorname{Im}\left\{ f(\xi) \right\} \cos(\xi X) - \operatorname{Re}\left\{ f(\xi) \right\} \sin(\xi X) \right]. \tag{7}$$

Convergence of the integrals† at the origin is guaranteed by the fact that

† ξ^ν is integrable at the origin if $\nu > -1$. No moments of the distribution are required to exist.

(A sum without limits is over the integers from $-\infty$ to $+\infty$.) Then the CF is

$$f(\xi) = \sum_k c_k \exp(ik\Delta\xi), \tag{14}$$

which is periodic with period $2\pi/\Delta$. Therefore, the coefficients $\{c_k\}$ can be determined from the CF $f(\xi)$ by

$$c_k = \frac{\Delta}{2\pi} \int_{2\pi/\Delta} d\xi \exp(-ik\Delta\xi) f(\xi), \tag{15}$$

where the integral is over any interval of length $2\pi/\Delta$.

Equation (15) gives the area of any impulse in the PDF $p(x)$ in terms of a finite integral of the CF $f(\xi)$. Since we are interested in the CDF $\Pr(X)$, a sum over $\{c_k\}$ is required. At this point, it is convenient to distinguish two cases: (1) nonnegative discrete random variables and (2) general discrete random variables.

NONNEGATIVE DISCRETE RANDOM VARIABLES

If x is a nonnegative discrete random variable, the CDF is, at integer value M,

$$\Pr(M) = \sum_{k=0}^{M} c_k = \frac{\Delta}{2\pi} \int_{2\pi/\Delta} d\xi\, f(\xi) \sum_{k=0}^{M} \exp(-ik\Delta\xi), \quad M \geq 0, \tag{16}$$

where we have substituted Eq. (15). Now

$$\sum_{k=0}^{M} \exp(-ik\Delta\xi) = \frac{1 - \exp[-i(M+1)\Delta\xi]}{1 - \exp[-i\Delta\xi]}, \tag{17}$$

which must be interpreted as $M + 1$ at $\xi = 0, \pm 2\pi/\Delta, \pm 4\pi/\Delta, \ldots$. Using Eq. (17) and the fact that $f(-\xi) = f^*(\xi)$, we note that Eq. (16) becomes

$$\Pr(M) = \frac{\Delta}{2\pi} \int_{2\pi/\Delta} d\xi \, f(\xi) \exp(-iM\Delta\xi/2) \frac{\sin[(M+1)\Delta\xi/2]}{\sin[\Delta\xi/2]}$$

$$= \frac{\Delta}{\pi} \int_0^{\pi/\Delta} d\xi \frac{\sin[(M+1)\Delta\xi/2]}{\sin[\Delta\xi/2]} \operatorname{Re}\left\{f(\xi)\exp(-iM\Delta\xi/2)\right\}, \quad M \geq 0, \tag{18}$$

where the interval $(-\pi/\Delta, \pi/\Delta)$ has been selected for integration. The ratio of sines is interpreted as $M + 1$ at the origin $\xi = 0$. Equation (18) is a single finite integral from which the CDF $\Pr(M)$ can be evaluated at any M directly from the CF $f(\xi)$.

A special case of Eq. (18) is

$$\Pr(0) = c_0 = \frac{\Delta}{\pi} \int_0^{\pi/\Delta} d\xi \operatorname{Re}\left\{f(\xi)\right\}. \tag{19}$$

(Actually, c_0 is always given by this formula, even for general discrete random variables, as may be seen from the general formula (Eq. (15)).)

The case of a discrete random variable taking on values in a semi-infinite range (i.e., $(-\infty, N)$ or (N, ∞), where N is finite but can be positive or negative) can be handled in a similar fashion. The key is that a finite sum of exponentials (like Eq. (17)) can be evaluated without requiring a summation.

GENERAL DISCRETE RANDOM VARIABLES

Here we shall consider discrete random variables which can take on values in the range $(-\infty, \infty)$. From Eqs. (7), (4), and (13),

$$P(0) = \frac{1}{2} - \frac{1}{\pi} \int_0^{\infty} \frac{d\xi}{\xi} \operatorname{Im}\left\{f(\xi)\right\} \tag{20}$$

$$= \sum_{k=-\infty}^{-1} c_k + \frac{1}{2} c_0 \tag{21}$$

That is, the value of the MDF $P(\mathbb{X})$ at the origin can be evaluated by a single infinite integral. There does not seem to be any simpler way of obtaining this number, which will be necessary in the development to follow. In some cases, it may be possible to evaluate the particular value $P(0)$ from the integral Eq. (20) in closed form, or expand it in a rapidly convergent series, while $P(\mathbb{X})$ could not be so evaluated generally for $\mathbb{X} \neq 0$. In any event, Eq. (20) will be the only infinite integral necessary to evaluate in order to get the complete CDF for this general discrete case.

The area of the impulse at the origin is given by Eq. (15) as

$$c_o = \frac{\Delta}{\pi} \int_0^{\pi/\Delta} d\xi \, \mathrm{Re}\left\{f(\xi)\right\} . \tag{22}$$

Now let us define auxiliary functions

$$S_+(M) = \sum_{k=0}^{M} c_k , \quad M \geq 0 , \tag{23}$$

$$S_-(M) = \sum_{k=-M}^{0} c_k , \quad M \geq 0 . \tag{24}$$

By a development similar to Eqs. (16) through (18), we find that these auxiliary functions can be expressed directly in terms of the CF $f(\xi)$ as

$$S_{\pm}(M) = \frac{\Delta}{\pi} \int_0^{\pi/\Delta} d\xi \, \frac{\sin\left[(M+1)\Delta\xi/2\right]}{\sin\left[\Delta\xi/2\right]} \, \mathrm{Re}\left\{f(\xi) \exp(\mp i M \Delta \xi/2)\right\} , \; M \geq 0, \tag{25}$$

where the ratio of sines is interpreted as $M + 1$ at the origin $\xi = 0$.

The CDF $Pr(M)$ then can be evaluated at any M according to

$$Pr(M) = \begin{cases} P(0) - \frac{1}{2} c_o + S_+(M), & M \geq 0 \\ P(0) + \frac{1}{2} c_o - S_-(|M+1|), & M < 0 \end{cases} . \tag{26}$$

Here $P(0)$ is given by Eq. (20), c_o by Eq. (22), and $S_+(M)$ by Eq. (25). The constants $P(0)$ and c_o need be evaluated once, but Eq. (25) must be evaluated for each M of interest. However, Eq. (25) is a finite integral.

EXAMPLES

We shall consider two examples recently examined by Helstrom[4] for purposes of comparison.

Example 1 - Exponential Distribution

$$p(x) = \left\{ \begin{array}{ll} \exp(-x), & x \geq 0 \\ 0, & x < 0 \end{array} \right\}, \tag{27}$$

$$\Pr(\mathbb{X}) = P(\mathbb{X}) = \left\{ \begin{array}{ll} 1 - \exp(-\mathbb{X}), & \mathbb{X} \geq 0 \\ 0, & \mathbb{X} < 0 \end{array} \right\}, \tag{28}$$

$$f(\xi) = (1 - i\xi)^{-1} . \tag{29}$$

The exact CDF is given in Eq. (28). Approximate values for the CDF are obtained by substituting Eq. (29) into Eq. (7) and approximating the infinite integral by a finite sum. Results are indicated in Table 1.

The integral of Eq. (7) was sampled in ξ at values indicated by column four of Table 1 and approximated by the trapezoidal rule for integration. The limit of integration in Eq. (7) was taken to be the value above 60 where the finite sum deviated most from the exact answer. Thus, the finite sum in column three of Table 1 is the worst approximation to the exact answer in column two.

For this example, the largest error occurred at the origin. This happened because the integrand of Eq. (7) oscillates for $\mathbb{X} \neq 0$, thereby converging fairly rapidly, whereas the integrand decreases monotonically only as $(1 + \xi^2)^{-1}$ for $\mathbb{X} = 0$.

Table 1

NUMERICAL COMPUTATION OF EXPONENTIAL DISTRIBUTION

X	Pr(X)	Finite Sum via Eq. (7)	Increment in ξ	Approximate Limit of Integration
-10	0	.00001	.1	60
-2	0	-.00007	.5	60
-1	0	.00008	.5	60
0	0	.00532	.5	60
.2	.18127	.18096	.5	60
1	.63212	.63220	.5	60
2	.86466	.86470	.5	60
10	.9999546	.9999637	.1	60

Example 2 - Poisson Distribution

$$p(x) = \exp(-\lambda) \sum_{k=0}^{\infty} \frac{\lambda^k}{k!} \delta(x-k), \tag{30}$$

$$\Pr(M) = \left\{ \begin{array}{ll} \exp(-\lambda) \displaystyle\sum_{k=0}^{M} \frac{\lambda^k}{k!}, & M \geq 0 \\ 0, & M < 0 \end{array} \right\}, \tag{31}$$

$$f(\xi) = \exp\left[\lambda\left\{\exp(i\xi)-1\right\}\right] . \tag{32}$$

The exact CDF is given in Eq. (31). Approximate values for the CDF are obtained by substituting Eq. (32) into Eq. (18), with $\Delta = 1$, and approximating the finite integral by a finite sum. Results are indicated in Table 2.

Table 2

NUMERICAL COMPUTATION OF POISSON DISTRIBUTION

M	Pr(M)	Finite Sum via Eq. (18)	Number of Intervals
0	.00000 03059	.00000 03059	25
1	.00000 48944	.00000 48945	25
6	.00763 18996	.00763 18998	25
14	.46565 37089	.46565 37089	25
16	.66412 32005	.66412 32004	25
20	.91702 90899	.91702 90895	25
29	.99958 15502	.99958 15500	25
30	.99980 26867	.99980 26865	25
40	.99999 99765	.99999 99764	25

The integral of Eq. (18) was divided into 25 equal intervals and approximated by the trapezoidal rule for integration. Columns two and three of Table 2 show that the error in the approximation occurs in the tenth place (and may be due to computer inaccuracies rather than sampling errors). Also, the accuracy holds on the tails of the CDF as well as near the mean.

CONCLUSIONS

The numerical technique suggested for obtaining CDF's directly from CF's has considerable merit. It requires no moment evaluations or series expansions (like Edgeworth or Laguerre) for the distributions. It does not depend upon evaluation of derivatives of CF's, but depends only upon the values of the CF itself. (Evaluation of high-order derivatives can be extremely tedious and time-consuming even if an analytic form for the CF is available.) The accuracy of the suggested technique can be estimated and controlled by decreasing the increment in the integral evaluations or lengthening the interval of

integration or both; the change in the approximation is a measure of the error at that point. The method does not require an inordinate number of samples of the CF, at least for the examples considered, and the additional functions requiring evaluation are sines and cosines. Intermediate evaluation of the PDF is entirely circumvented. (Of course, estimates of the PDF are available as differences of the CDF, if desired.)

REVERSE BLANK

LIST OF REFERENCES

1. J. I. Marcum, A Statistical Theory of Target Detection by Pulsed Radar: Mathematical Appendix, Rand Corporation Report No. RM-753, 1 July 1948.

2. A. Papoulis, The Fourier Integral and Its Applications, McGraw-Hill Book Co., Inc., New York, 1962, sect. 2.1.

3. Ibid, Eqs. (3-12), (3-6), (3-9), and (2-36) and sect. 2.1.

4. C. W. Helstrom, "Approximate Calculation of Cumulative Probability from a Moment-Generating Function," Proceedings of the IEEE, vol. 57, no. 3, March 1969, pp. 368-369.

REVERSE BLANK

NUSC Report No. NL-3012
12 August 1970

Alternate Forms and Computational Considerations for Numerical Evaluation of Cumulative Probability Distributions Directly from Characteristic Functions

Albert H. Nuttall

ABSTRACT

Alternate integral forms for the cumulative probability distribution in terms of the characteristic function are given. In particular, forms that can utilize a fast Fourier transform (FFT) algorithm and special forms for one-sided probability density functions are derived. For a special class of discrete random variables, all integral evaluations are over a finite range. Some computational aspects of utilizing the FFT are discussed.

Approved for public release; distribution unlimited.

TABLE OF CONTENTS

Page

Section

1. INTRODUCTION 1

2. ANALYSIS 1

2.1 General Distributions 1

2.2 Nonnegative Distributions 4

2.3 Discrete Distributions 8

2.4 Nonnegative Discrete Distributions 10

2.5 Use of FFT for Fourier Transforms 12

3. CONCLUSIONS 16

LIST OF REFERENCES 17

APPENDIX A — BEHAVIOR OF INTEGRAND OF EQ. (3) AT ORIGIN . . 19

APPENDIX B — EVALUATION OF $\sum_{n=1}^{\infty} \exp(inx)$ 21

APPENDIX C — ALIASED SPECTRUM 25

REVERSE BLANK

ALTERNATE FORMS AND COMPUTATIONAL CONSIDERATIONS FOR NUMERICAL EVALUATION OF CUMULATIVE PROBABILITY DISTRIBUTIONS DIRECTLY FROM CHARACTERISTIC FUNCTIONS

1. INTRODUCTION

A recent report [1] on numerical evaluation of cumulative probability distribution functions directly from characteristic functions (CF) gave the cumulative distribution functions (CDF) in terms of a single integral on the CF for both continuous and discrete random variables (RV). In this report some alternate forms for the CDF in terms of the CF will be presented, with an aim toward more accurate, efficient, and expeditious calculations. For the motivation of this study and utility of the results, as well as numerical examples, see Reference 1.

2. ANALYSIS

This section is composed of five subsections. In the first, general distributions are considered; in the second, specialization to a nonnegative random variable is made. In both subsections, forms that utilize a fast Fourier transform (FFT) are derived and their applicability is discussed. In the third and fourth subsections, discrete random variables are considered. The former subsection shows that the distribution function can be evaluated entirely in terms of finite integrals; the latter subsection specializes to nonnegative discrete random variables. The fifth subsection treats some computational aspects of the FFT.

2.1 GENERAL DISTRIBUTIONS

Let RV x have probability density function (PDF) p(x) and CF f(ξ):

$$f(\xi) = \int dx \, \exp(i\xi x) \, p(x) \quad , \tag{1}$$

$$p(x) = \frac{1}{2\pi} \int d\xi \, \exp(-i\xi x) \, f(\xi) \quad . \tag{2}$$

(Integrals without limits are over the real axis from $-\infty$ to ∞.) The CDF $\Pr(X)$ is defined as the probability that RV x is less than or equal to X. The modified distribution function (MDF) $P(X)$ is defined equal to $\Pr(X)$ at points of continuity, but it takes a value midway between limit values on either side of a discontinuity.

The MDF $P(X)$ can be obtained from the CF by [1, Eq. (7), or 2, Eq. (4.14)]

$$P(X) = \frac{1}{2} - \frac{1}{\pi}\int_0^\infty \frac{d\xi}{\xi} \operatorname{Im}\left\{f(\xi)\, \exp(-i\xi X)\right\}, \quad \text{all } X\,. \tag{3}$$

If we attempt to remove the Imaginary operation from under the integral sign, we obtain an infinite integral since $f(0) = 1$. However, if we express

$$f(\xi) = \left[f(\xi) - a(\xi)\right] + a(\xi)\,, \tag{4}$$

where $a(0) = 1$, and split (3) into two integrals, we can move the Imaginary operation out of the first integral in (3). One particularly useful choice for $a(\xi)$, which results in a closed form expression for the second integral in (3), is

$$a_1(\xi) = \exp\left[i\mu\xi - \frac{1}{2}\sigma^2\xi^2\right], \quad \xi > 0\,, \tag{5}$$

where* μ and σ^2 are the mean and variance of RV x. The mean and variance are available from $f'(0)$ and $f''(0)$, if these quantities can be evaluated; if not, the method to be described is still applicable with arbitrary constants used for μ and σ^2. When (4) and (5) are substituted into (3), there results [3, Eq. 3.896 4; integrate both sides with respect to b]

$$P(X) = \Phi\left(\frac{X-\mu}{\sigma}\right) - \frac{1}{\pi}\operatorname{Im}\left\{\int_0^\infty d\xi\, \frac{f(\xi) - a_1(\xi)}{\xi}\, \exp(-i\xi X)\right\}, \quad \text{all } X\,, \tag{6}$$

---

*Actually, μ and σ^2 could be assigned arbitrary values in the form (5); this particular choice gives a second-order fit to $f(\xi)$ at the origin.

where

$$\Phi(y) \equiv \int_{-\infty}^{y} dt(2\pi)^{-1/2} \exp(-t^2/2) \tag{7}$$

is the Gaussian CDF.

Equation (6) is now in a form where an FFT can be utilized in the integration on ξ (See Subsection 2.5). This equation is exact; we are not making a Gaussian approximation in (6). There is no problem in the integration at $\xi = 0$ because, for the choice of μ and σ^2 as the mean and variance of RV x,

$$\frac{f(\xi) - a_1(\xi)}{\xi} = O(\xi^2) \quad \text{as} \quad \xi \to 0+ . \tag{8}$$

Also, since $|a_1(\xi)|$ decays as $\exp(-\sigma^2\xi^2/2)$, the decay of the left side of (8) for large ξ will often depend on the decay of $f(\xi)/\xi$; this decay will dictate how far the integral in (6) must be carried out for specified accuracy in $P(X)$.

Other choices for $a(\xi)$ are possible and sometimes recommended. For example, if the mean and variance of RV x do not exist (e.g., $p(x) = \pi^{-1} \cdot (1 + x^2)^{-1}$, all x), we might choose

$$a_2(\xi) = \exp(-b\xi), \quad \xi > 0 . \tag{9}$$

To best match $f(\xi)$ near the origin, we could choose

$$b = -f'(0+) = |f'(0+)| \text{ (assuming } f'(0+) \text{ real)} . \tag{10}$$

Then by substituting (4) and (9) into (3) [3, Eq. 3.941 1], we get

$$P(X) = \frac{1}{2} + \frac{1}{\pi} \arctan(X/b) - \frac{1}{\pi} \operatorname{Im} \left\{ \int_0^\infty d\xi \frac{f(\xi) - a_2(\xi)}{\xi} \exp(-i\xi X) \right\}, \quad \text{all } X . \tag{11}$$

For the choice of b in (10),

$$\frac{f(\xi) - a_2(\xi)}{\xi} = O(\xi) \quad \text{as} \quad \xi \to 0+ , \tag{12}$$

so no problem in integration arises at the origin. We must be able to evaluate $f'(0+)$ in this case so that b is known, and it must be real. In cases where $f'(0+)$ is not known or is infinite (See Appendix A, for example), the above methods are inapplicable, and special techniques such as subtracting out the singularity are required.

2.2 NONNEGATIVE DISTRIBUTIONS

When RV x is limited to nonnegative values, some simplifications in the general form (3) occur. (The case of nonpositive RV x can be treated in a similar fashion.) First, if $X < 0$ in (3), then $P(X) = 0$. Letting $X = -a$ yields

$$\frac{1}{2} = \frac{1}{\pi} \int_0^\infty \frac{d\xi}{\xi} \left[f_r(\xi) \sin(a\xi) + f_i(\xi) \cos(a\xi) \right], \quad a > 0 , \tag{13}$$

where subscripts r and i denote real and imaginary parts, respectively. Employing (13) in (3) for $X > 0$, we get

$$P(X) = \frac{2}{\pi} \int_0^\infty \frac{d\xi}{\xi} f_r(\xi) \sin(\xi X), \quad X > 0 , \tag{14}$$

or

$$P(X) = 1 - \frac{2}{\pi} \int_0^\infty \frac{d\xi}{\xi} f_i(\xi) \cos(\xi X), \quad X > 0 . \tag{15}$$

Thus, the MDF $P(X)$ can be evaluated from knowledge of either the real part or the imaginary part of the CF $f(\xi)$. For $X = 0$, neither (14) nor (15) is necessarily valid, and we must resort to (3).

There are computational reasons for choosing (14) over (15), or vice versa. The first has to do with ease of calculating $f_r(\xi)$ versus $f_i(\xi)$. For example, in Appendix A, for $p(x) = 2/\pi\ (1 + x^2)^{-1}$ for $x > 0$, we find that $f_r(\xi)$ is a simple exponential, whereas $f_i(\xi)$ is a sum of exponential integrals. Converse examples, where $f_i(\xi)$ is simpler to compute, can also be found.

The second reason has to do with the rate of decay of $f_r(\xi)$ versus $f_i(\xi)$. We have

$$f_r(\xi) = \int_0^\infty dx\ p(x)\ \cos(\xi x) = \int dx\ p_e(x)\ \cos(\xi x) = \int dx\ p_e(x)\ \exp(i\xi x)\ , \quad (16)$$

$$f_i(\xi) = \int_0^\infty dx\ p(x)\ \sin(\xi x) = \int dx\ p_o(x)\ \sin(\xi x) = i^{-1} \int dx\ p_o(x)\ \exp(i\xi x)\ , \quad (17)$$

where subscripts e and o denote even and odd parts, respectively. Now, if $p(0+) > 0$, then $p_o(x)$ is discontinuous at the origin, and $f_i(\xi)$ decays only as ξ^{-1} for large ξ. An example is

$$p(x) = e^{-x},\ x > 0;\quad f(\xi) = (1 - i\xi)^{-1}\ ,$$

$$f_r(\xi) = \left(1 + \xi^2\right)^{-1},\quad f_i(\xi) = \xi\left(1 + \xi^2\right)^{-1}\ . \quad (18)$$

In (18), $f_r(\xi)$ decays as ξ^{-2} for large ξ, giving rise to an integral in (14) that can be terminated earlier than the one in (15). On the other hand, consider that $p(0+) = 0$ and that $p(x)$ and its derivative are continuous except at the origin, but $p'(0+) > 0$. Then $p_o(x)$ and its derivative are continuous, whereas $p'_e(x)$ is discontinuous. In this case, $f_r(\xi)$ decays only as ξ^{-2} for large ξ. An example is

$$p(x) = xe^{-x},\ x > 0;\quad f(\xi) = (1 - i\xi)^{-2}\ ,$$

$$f_r(\xi) = \left(1 - \xi^2\right)\left(1 + \xi^2\right)^{-2},\quad f_i(\xi) = 2\xi\left(1 + \xi^2\right)^{-2}\ . \quad (19)$$

Here (15) could be terminated earlier than (14).

The third reason has to do with the region of X of interest. For large X, where P(X) is near unity, Eq. (15), in the form

$$1 - P(X) = \frac{2}{\pi}\int_0^\infty \frac{d\xi}{\xi} f_i(\xi) \cos(\xi X), \quad X > 0 , \tag{20}$$

is to be recommended, since it is an alternating sum of small quantities and retains significance. Equation (14), for large X, is an alternating sum of large quantities and loses significance. But for small X, Eq. (14) would be recommended.

Equation (15) can be immediately manipulated into a form where an FFT can be utilized. Namely,

$$P(X) = 1 - \frac{2}{\pi} \mathrm{Re}\left\{\int_0^\infty d\xi \, \frac{f_i(\xi)}{\xi} \exp(-i\xi X)\right\}, \quad X > 0 . \tag{21}$$

From Appendix A, we have $f_i(\xi)/\xi \sim \mu_x$ as $\xi \to 0$, if μ_x exists and is finite.

If we attempt to express (14) in the form

$$\mathrm{Im}\left\{\frac{2}{\pi}\int_0^\infty \frac{d\xi}{\xi} f_r(\xi) \exp(i\xi X)\right\} ,$$

we obtain an integral that does not converge at the origin. However, if we express

$$f_r(\xi) = [f_r(\xi) - b(\xi)] + b(\xi) , \tag{22}$$

where $b(0) = 1$ and $b(\xi)$ is real, then (14) becomes

$$P(X) = \frac{2}{\pi}\,\mathrm{Im}\left\{\int_0^\infty d\xi\,\frac{f_r(\xi) - b(\xi)}{\xi}\exp(i\xi X)\right\} + \frac{2}{\pi}\int_0^\infty d\xi\; b(\xi)\,\frac{\sin(\xi X)}{\xi}, \quad X > 0\,, \tag{23}$$

and an FFT can be used on the first integral. Preferably, the second integral should be integrable in closed form. A particularly useful choice is

$$b(\xi) = \exp\left(-\frac{1}{2}\,\mu_2\xi^2\right), \quad \xi > 0\,, \tag{24}$$

where* μ_2 is the mean-square value of RV x. This quantity is available from $f_r''(0)$ if it can be evaluated. When (24) is substituted into (23), we get (See (3) through (7))

$$P(X) = 2\Phi\left(\frac{X}{\mu_2^{1/2}}\right) - 1 + \frac{2}{\pi}\,\mathrm{Im}\left\{\int_0^\infty d\xi\,\frac{f_r(\xi) - \exp\left(-\frac{1}{2}\,\mu_2\xi^2\right)}{\xi}\exp(i\xi X)\right\}, \quad X > 0\,. \tag{25}$$

The function

$$\frac{f_r(\xi) - \exp\left(-\frac{1}{2}\,\mu_2\xi^2\right)}{\xi} \to 0 \text{ as } \xi \to 0+$$

in (25) if the mean-square value μ_2 exists. In many cases, it decays as $f_r(\xi)/\xi$ for large ξ.

The fact that MDF P(X) can be obtained from either the real or imaginary parts of the CF for a nonnegative distribution are manifestations of the fact that $f_r(\xi)$ and $f_i(\xi)$ can be found from each other; in fact, they are related by Hilbert transforms. For $p(x) = 0$ for $x < 0$, and no impulses at the origin, we see that [4, p. 38]

*As in the footnote to Eq. (5), μ_2 could be assigned any convenient value.

$$f(\xi) = \int dx\ p(x)\ \exp(i\xi x) = \int dx\ p(x)\ U(x)\ \exp(i\xi x) = \mathfrak{F}\{p(x)\ U(x)\}$$

$$= \mathfrak{F}\{p(x)\} \circledast \mathfrak{F}\{U(x)\} = f(\xi) \circledast \left[\frac{1}{2}\ \delta(\xi) + \frac{i}{2\pi\xi}\right] = \frac{1}{2}\left[f(\xi) + i\mathcal{H}\{f(\xi)\}\right] , \tag{26}$$

where $U(x)$ is the unit step function, $\mathfrak{F}$ denotes a Fourier transform, $\circledast$ denotes convolution, and $\mathcal{H}$ denotes a Hilbert transform. Therefore,

$$f(\xi) = i\mathcal{H}\{f(\xi)\} , \tag{27}$$

or

$$f_i(\xi) = \mathcal{H}\{f_r(\xi)\}, \quad f_r(\xi) = -\mathcal{H}\{f_i(\xi)\} . \tag{28}$$

For the cases when $p(x)$ contains an impulse at the origin of area c_o, the first part of (28) is still correct, but the second part is incorrect by the additive constant c_o. However, we can still find $f_r(\xi)$ from $f_i(\xi)$ by utilizing the fact that $f_r(0) = 1$. Thus, either the real or the imaginary part of the CF constitutes complete knowledge about the MDF in the case of a nonnegative distribution.

2.3 DISCRETE DISTRIBUTIONS

In this subsection, the RV x is restricted to take on values that are multiples of some fundamental increment Δ, and can be either positive or negative. Although the equations in Subsection 2.2 are applicable here, it is advantageous to have forms for the distribution function that require finite integrals rather than infinite ones. We have for the PDF

$$p(x) = \sum_k c_k\ \delta(x - k\Delta) , \tag{29}$$

where the sum ranges from $-\infty$ to ∞. The CDF Pr(M) for integer M is given in Reference 1, Eqs. (20) through (26). All the integrals are finite integrals except for the one in (20) for MDF value P(0):

$$P(0) = \frac{1}{2} - \frac{1}{\pi} \int_0^\infty d\xi \, \frac{f_i(\xi)}{\xi} \, .$$

We now rectify this situation and obtain a finite integral for P(0) also. From Reference 1, Eq. (15),

$$c_k = \frac{\Delta}{2\pi} \int_{-\pi/\Delta}^{\pi/\Delta} d\xi \; f(\xi) \; \exp(-ik\Delta\xi) \, . \tag{30}$$

Therefore, by using Appendix B and $f(-\xi) = f^*(\xi)$, we get

$$\sum_{k=-\infty}^{-1} c_k = \frac{\Delta}{2\pi} \int_{-\pi/\Delta}^{\pi/\Delta} d\xi \; f(\xi) \sum_{k=-\infty}^{-1} \exp(ik\Delta\xi)$$

$$= \frac{\Delta}{2\pi} \int_{-\pi/\Delta}^{\pi/\Delta} d\xi \; f(\xi) \left[-\frac{1}{2} + \pi \sum_k \delta(\Delta\xi - k2\pi) + i \, \frac{1}{2} \cot\left(\frac{\Delta\xi}{2}\right) \right]$$

$$= -\frac{1}{2} c_o + \frac{1}{2} + i \, \frac{1}{2} \, \frac{\Delta}{2\pi} \int_{-\pi/\Delta}^{\pi/\Delta} d\xi \; f(\xi) \cot\left(\frac{\Delta\xi}{2}\right)$$

$$= -\frac{1}{2} c_o + \frac{1}{2} - \frac{\Delta}{2\pi} \int_0^{\pi/\Delta} d\xi \, \frac{f_i(\xi)}{\tan(\Delta\xi/2)} \, . \tag{31}$$

Then, we obtain the desired result

$$P(0) = \sum_{k=-\infty}^{-1} c_k + \frac{1}{2} c_o = \frac{1}{2} - \frac{\Delta}{2\pi} \int_0^{\pi/\Delta} d\xi \, \frac{f_i(\xi)}{\tan(\Delta\xi/2)} \, . \tag{32}$$

As $\xi \to 0+$, the integrand of (32) approaches $2\mu_x/\Delta$ if μ_x exists and is finite. (There is no integral expression for $P(0)$ in terms of $f_r(\xi)$. Since $f_r(\xi)$ is the Fourier transform of $p_e(x)$ (See Eq. (16)), and since

$$\int_{-\infty}^{o} dx \; p_e(x) = \frac{1}{2} ,$$

irrespective of the form of $p(x)$, $f_r(\xi)$ contains no inform ion about $P(0)$. This is analogous to the general distribution case where $P(0)$ follows from (3) as

$$P(0) = \frac{1}{2} - \frac{1}{\pi} \int_0^{\infty} d\xi \; f_i(\xi)/\xi \; . \;)$$

2.4 NONNEGATIVE DISCRETE DISTRIBUTIONS

When RV x is limited to nonnegative values, the CDF $Pr(M)$ takes on forms requiring either the real or imaginary parts of the CF for its evaluation, just as in Subsection 2.2. To see this, we note that c_k in (29) is zero for $k < 0$. By letting $k = -m$ in (30), we get

$$\int_0^{\pi/\Delta} d\xi \; \sin(m\Delta\xi) \; f_i(\xi) = \int_0^{\pi/\Delta} d\xi \; \cos(m\Delta\xi) \; f_r(\xi) \text{ for } m > 0 \; . \tag{33}$$

When we employ (33) into (30) for $k > 0$, we get

$$c_k = \frac{2\Delta}{\pi} \int_0^{\pi/\Delta} d\xi \; \cos(k\Delta\xi) \; f_r(\xi), \quad k > 0 \; , \tag{34}$$

or

$$c_k = \frac{2\Delta}{\pi} \int_0^{\pi/\Delta} d\xi \ \sin(k\Delta\xi) \ f_i(\xi), \quad k > 0 \ . \tag{35}$$

Therefore, the CDF Pr(M) for integer M is given by

$$\Pr(M) = \sum_{k=0}^{M} c_k = \frac{2\Delta}{\pi} \int_0^{\pi/\Delta} d\xi \ f_r(\xi) \left[\frac{1}{2} + \sum_{k=1}^{M} \cos(k\Delta\xi) \right]$$

$$= \frac{\Delta}{\pi} \int_0^{\pi/\Delta} d\xi \ f_r(\xi) \frac{\sin\left[\left(M + \frac{1}{2}\right)\Delta\xi\right]}{\sin\left[\frac{1}{2} \ \Delta\xi\right]}, \quad M \geq 0 \ , \tag{36}$$

where we have used (34), (30), the fact that $f(-\xi) = f^*(\xi)$, and Eq. 1.342 2 in Reference 3. Equation (36) enables evaluating the CDF in terms of the real part of the CF alone.

To represent Pr(M) in terms of $f_i(\xi)$, we first note that for nonnegative RV, the general formula for P(0) in (32) becomes

$$P(0) = \frac{1}{2} \ c_o = \frac{1}{2} - \frac{\Delta}{2\pi} \int_0^{\pi/\Delta} d\xi \ \frac{f_i(\xi)}{\tan(\Delta\xi/2)} \ . \tag{37}$$

Now,

$$\Pr(M) = \sum_{k=0}^{M} c_k = c_o + \frac{2\Delta}{\pi} \int_0^{\pi/\Delta} d\xi \ f_i(\xi) \sum_{k=1}^{M} \sin(k\Delta\xi)$$

$$= 1 - \frac{\Delta}{\pi} \int_0^{\pi/\Delta} d\xi \; f_i(\xi) \frac{\cos\left[\left(M + \frac{1}{2}\right)\Delta\xi\right]}{\sin\left[\frac{1}{2}\Delta\xi\right]}, \quad M \geq 0 , \tag{38}$$

where we have employed (35), (37), and Eq. 1.342 1 in Reference 3. Equation (38) is complementary to (36) in the sense that only the imaginary part of the CF is necessary for evaluating the CDF. The reasons given in Subsection 2.2 for selecting (36) or (38) in a particular application are again relevant.

2.5 USE OF FFT FOR FOURIER TRANSFORMS

Many of the integrals in this report take the form

$$\int_0^\infty dt \; g(t) \; \exp(-i2\pi ft) \; .$$

Suppose a limit T on the integration can be found such that

$$\left| \int_T^\infty dt \; g(t) \; \exp(-i2\pi ft) \right| < \epsilon \text{ for all } f \; , \tag{39}$$

where ϵ is some specified tolerance or error. Then, attention can be focused on evaluating

$$G_T(f) \equiv \int_0^T dt \; g(t) \; \exp(-i2\pi ft) \; . \tag{40}$$

Since the integration in (40) is over an interval of length T, it is seen that $G_T(f)$ will undergo a significant change in value in an interval no smaller than $1/T$ in f. Thus, one might initially anticipate that (40) should be evaluated at values of $f = n/T$, $n = 1, 2, \ldots$. However, in many cases, this resolution, $1/T$, may be much too fine, and be the result of satisfying (39) with a very small ϵ. In such cases, values of $G_T(f)$ at some multiple of the fundamental

resolution may be satisfactory, say m/T, where m is an integer. Thus, we might be interested only in evaluating $G_T\left(n\frac{m}{T}\right)$, $n = 1, 2, \ldots$. But from (40)

$$G_T\left(n\frac{m}{T}\right) = \int_0^T dt\ g(t)\ \exp(-i2\pi nmt/T)$$

$$= \sum_{k=0}^{m-1} \int_{kT/m}^{(k+1)T/m} dt\ g(t)\ \exp(-i2\pi nmt/T)\,. \tag{41}$$

In making the substitution $u = t - kT/m$ in (41) and defining the collapsed function

$$g_c(u) = \left\{ \begin{array}{ll} \displaystyle\sum_{k=0}^{m-1} g\left(u + k\,\frac{T}{m}\right), & 0 \le u \le T/m \\ 0 \qquad\qquad , & \text{otherwise} \end{array} \right\}, \tag{42}$$

we note that (41) becomes

$$G_T\left(n\,\frac{m}{T}\right) = \int_0^{T/m} du\ g_c(u)\ \exp\left(-i2\pi\frac{n}{T/m}\,u\right)\,. \tag{43}$$

The collapsed function g_c is obtained from g by "pre-aliasing" g into the interval T/m. If we define the Fourier transform of g_c as

$$G_c(f) = \int_0^{T/m} du\ g_c(u)\ \exp(-i2\pi fu)\ , \tag{44}$$

then (43) yields

$$G_T\left(n\,\frac{m}{T}\right) = G_c\left(n\,\frac{m}{T}\right). \tag{45}$$

That is, $G_T(f)$ can be evaluated at $f = m/T,\ 2m/T, \ldots,$ in terms of the Fourier transform of the collapsed function.

Now suppose $g_c(u)$ is sampled at increments of h in (44), where $h = \frac{T/m}{M}$, and weighting $\{w_k\}$ applied to the samples in an effort to approximate* (44). That is,

$$G_c(f) \cong h \sum_{k=0}^{M} w_k\, g_c(kh)\, \exp(-i2\pi fkh) \equiv \hat{G}_c(f)\ . \tag{46}$$

The approximation in (46) will be good if g_c and the exponential are sampled frequently enough. Thus, if the exponential is not to vary by more than a radian between samples, we require

$$|f| < \frac{1}{2\pi h}\ . \tag{47}$$

When (45) through (47) are combined, the desired values are given by

$$G_T\left(n\,\frac{m}{T}\right) = G_c\left(n\,\frac{m}{T}\right) \cong \hat{G}_c\left(n\,\frac{m}{T}\right) = h \sum_{k=0}^{M} w_k\, g_c(kh)\, \exp(-i2\pi kn/M) \tag{48}$$

if

$$|n|\,\frac{m}{T} < \frac{1}{2\pi h}, \quad \text{or} \quad |n| < \frac{1}{\pi}\,\frac{M}{2}\ . \tag{49}$$

By defining

---

*For example, Simpson's rule has $w_0 = 1/3$, $w_{2n+1} = 4/3$, $w_{2n+2} = 2/3$, $w_M = 1/3$.

$$d_k = \left\{ \begin{array}{l} hw_k\ g_c(kh), \quad 1 \le k \le M-1 \\ \\ hw_o\ g_c(0) + hw_M\ g_c(T/m), \quad k = 0 \end{array} \right\}, \tag{50}$$

we can express (48) as

$$G_T\left(n\,\frac{m}{T}\right) = G_c\left(n\,\frac{m}{T}\right) \cong \hat{G}_c\left(n\,\frac{m}{T}\right) = \sum_{k=0}^{M-1} d_k\ \exp(-i2\pi kn/M)\ , \tag{51}$$

which is an M-point discrete Fourier transform (DFT) of the sequence $\{d_k\}$. The factor $1/\pi$ in the upper bound on $|n|$ in (49) is due to the aliasing in the frequency domain that takes place at $|n| = M/2$. In fact, letting $\{w_k\}$ be the samples of waveform $w(t)$ at $t = kh$ and $W(f)$ its Fourier transform, it can be shown that (Appendix C)

$$\hat{G}_c(f) = W(f) \circledast \sum_k G_c\left(f - kM\,\frac{m}{T}\right). \tag{52}$$

Thus, the value $\hat{G}_c\left(\frac{M}{2}\,\frac{m}{T}\right)$ is composed of at least two overlapping tails of $G_c(f)$. In order to avoid this aliasing, we must observe (49).

To summarize, the values of $G_T(f)$ at $f = n\frac{m}{T}$ are given approximately as an M-point DFT in (51) of the sequence $\{d_k\}$ in (50). When (42) is substituted into (50), this sequence can be expressed as

$$d_k = \left\{ \begin{array}{l} hw_k \displaystyle\sum_{j=0}^{m-1} g\left(kh + j\frac{T}{m}\right), \quad 1 \le k \le M-1 \\ \\ hw_o \displaystyle\sum_{j=0}^{m-1} g\left(j\frac{T}{m}\right) + hw_M \sum_{j=1}^{m} g\left(j\frac{T}{m}\right), \quad k = 0 \end{array} \right\}. \tag{53}$$

As is obvious from (53), $g(t)$ must still be evaluated from 0 to T in increments of h, that is, at $mM + 1$ values. However, collapsing reduces the

size of the FFT from mM to M, with an attendant reduction in computation time and round-off error. This method is related to one given in Reference 5, p. 81.

In applying this technique to numerical integration of CF's, since the exponentials take the form $\exp(\pm i\xi X)$, we note that the increment in X at which values are obtained by employing an FFT are $2\pi/T$, or $2\pi m/T$ for coarser resolution as above.

3. CONCLUSIONS

Several alternate forms for direct numerical evaluation of the CDF or MDF from the CF have been presented that have utility in different situations, including ease of calculation, rate of decay of the integrands, and the probability region of interest. Also, the speed of the FFT and the large number of values of the distribution functions that are quickly available make the formulas presented attractive in a large number of practical applications.

In the case of discrete distributions with RV that can take on positive as well as negative values, all integrals for the CDF are finite and over a half-period of the CF. Reevaluation of the sines or cosines, as in (36) or (38) for different values of M, can be avoided if one notes that

$$\sin\left[\left(M+\frac{1}{2}\right)a\right] = \sin\left[\left(M-\frac{1}{2}\right)a + a\right] = \sin\left[\left(M-\frac{1}{2}\right)a\right]\cos[a] + \cos\left[\left(M-\frac{1}{2}\right)a\right]\sin[a],$$

with a similar result for cosine. Thus, if a table of sin(a) and cos(a) for the values of a $(\Delta\xi)$ is constructed, this recurrence relation can be used to obtain the higher order M-dependence required in (36) and (38) without reevaluating sines and cosines.

LIST OF REFERENCES

1. A. H. Nuttall, Numerical Evaluation of Cumulative Probability Distribution Functions Directly fr\ m Characteristic Functions, NUSL* Report No. 1032, 11 August 1969. For an abbreviated version of this report, see IEEE Proceedings (Letters), vol. 57, no. 11, November 1969, pp. 2071-2072.

2. M. G. Kendall and A. Stuart, The Advanced Theory of Statistics, vol. 1, Hafner Publishing Company, New York, 1958.

3. I. S. Gradshteyn and I. M. Ryzhik, Tables of Integrals, Series, and Products, Academic Press, New York, 1965.

4. A. Papoulis, The Fourier Integral and Its Applications, McGraw-Hill Book Co., New York, 1962.

5. J. W. Cooley, P. A. W. Lewis, and P. D. Welch, "Application of the Fast Fourier Transform to Computation of Fourier Integrals, Fourier Series, and Convolution Integrals," IEEE Transactions on Audio and Electroacoustics, vol. AU-15, no. 2, June 1967, pp. 79-84.

*Reports prepared by the New London Laboratory prior to 1 July 1970 bear the Laboratory's earlier acronym NUSL.

REVERSE BLANK

Appendix A

BEHAVIOR OF INTEGRAND OF EQ. (3) AT ORIGIN

The integrand of (3) is given by

$$\frac{1}{\xi} \operatorname{Im} \left\{ f(\xi) \exp(-i\xi X) \right\} = \frac{f_i(\xi) \cos(\xi X)}{\xi} - \frac{f_r(\xi) \sin(\xi X)}{\xi} ,$$

where subscripts r and i denote real and imaginary parts, respectively. Now,

$$\frac{f_r(\xi) \sin(\xi X)}{\xi} \to X \quad \text{as} \quad \xi \to 0+ .$$

And

$$\frac{f_i(\xi) \cos(\xi X)}{\xi} = \int dx \, \frac{\sin(\xi x)}{\xi} \, p(x) \cos(\xi X) .$$

$$\sim \int dx \; x \; p(x) \equiv \mu_x \quad \text{as} \quad \xi \to 0+ \quad \text{if} \quad \mu_x \quad \text{exists and is finite.}$$

Here μ_x is the mean of RV x. Therefore, the integrand of (3) approaches

$$\mu_x - X \quad \text{as} \quad \xi \to 0+ \quad \text{if} \quad \mu_x \quad \text{exists and is finite.}$$

An example where μ_x is infinite is given by

$$p(x) = \left\{ \begin{array}{l} 0, \; x < 0 \\ \dfrac{2/\pi}{1 + x^2}, \; x > 0 \end{array} \right\} .$$

Then,[A1]

$$f_r(\xi) = \exp(-|\xi|) ,$$

$$f_i(\xi) = \operatorname{sgn}(\xi) \frac{1}{\pi} \left\{ \exp(-|\xi|) \operatorname{Ei}(|\xi|) - \exp(|\xi|) \operatorname{Ei}(-|\xi|) \right\} .$$

Since[A2]

$$\operatorname{Ei}(-|\xi|) = \ln |\xi| + C - |\xi| + \frac{1}{4} |\xi|^2 + O(|\xi|^3) \quad \text{as } |\xi| \to 0 ,$$

$$\operatorname{Ei}(|\xi|) = \ln |\xi| + C + |\xi| + \frac{1}{4} |\xi|^2 + O(|\xi|^3) \quad \text{as } |\xi| \to 0 ,$$

there follows

$$f_i(\xi) = \operatorname{sgn}(\xi) \left\{ \frac{2}{\pi} |\xi| (-\ln |\xi| + 1 - C + \frac{1}{4} |\xi|^2) + O\left(|\xi|^3\right) \right\}$$

$$\sim \frac{2}{\pi} \xi \ln\left(\frac{1}{|\xi|}\right) \quad \text{as } |\xi| \to 0 .$$

Therefore,

$$\frac{f_i(\xi) \cos(\xi X)}{\xi} \sim \frac{2}{\pi} \ln\left(\frac{1}{|\xi|}\right) \quad \text{as} \quad |\xi| \to 0 ,$$

which is unbounded, but integrable. So, in those cases where μ_X is infinite, the behavior of $f_i(\xi)/\xi$ at the origin must be handled carefully in order to accurately evaluate the integral. One possibility is to subtract out the singularity and integrate it analytically.

[A1] I. S. Gradshteyn and I. M. Ryzhik, Table of Integrals, Series and Products, Academic Press, New York, 1965, Eq. (3.723 1).

[A2] Ibid., Eqs. (8.214 1) and (8.214 2).

Appendix B

EVALUATION OF $\sum_{n=1}^{\infty} \exp(inx)$

Consider the ordinary function

$$f(x) = \ln\left|\sin\frac{x}{2}\right|, \quad x \neq 0, \pm 2\pi, \pm 4\pi, \ldots .$$

Since $(1 + x^2)^{-1} f(x)$ is absolutely integrable from $-\infty$ to ∞, the generalized function $f(x)$ corresponding to ordinary function $f(x)$ can be defined.[B1] In fact, the generalized function $f(x)$ equals the ordinary function $f(x)$ (See definition 8 by Lighthill[B2]). Furthermore, the generalized function $f(x)$ is periodic, with period 2π,[B3] and, therefore, can be expressed as[B4]

$$f(x) = \sum_{n=-\infty}^{\infty} c_n e^{inx} .$$

The generalized function $f(x)$ is absolutely integrable over a period, since the ordinary function $f(x)$ is absolutely integrable over a period.[B5] Therefore, the coefficients $\{c_n\}$ in the expansion of the generalized function $f(x)$ are given by[B6]

$$c_n = \frac{1}{2\pi}\int_{-\pi}^{\pi} dx\, f(x)\, e^{-inx} = \frac{1}{2\pi}\int_{-\pi}^{\pi} dx \ln\left|\sin\frac{x}{2}\right| e^{-inx}$$

$$= \frac{1}{\pi}\int_{0}^{\pi} dx \ln\left(\sin\frac{x}{2}\right)\cos(nx) = 2\int_{0}^{1/2} dt \ln(\sin\pi t)\cos(2n\pi t)$$

[B1] M. J. Lighthill, An Introduction to Fourier Analysis and Generalized Functions, Cambridge University Press, New York, 1959, p. 21, definition 7.

[B2] Ibid, p. 25.

[B3] Ibid, p. 60, definition 22.

[B4] Ibid, p. 66, Theorem 26.

[B5] Ibid, p. 48, definition 19.

[B6] Ibid, p. 66, Theorem 26, Note.

$$= \begin{Bmatrix} -\ln 2, & n = 0 \\ \\ -\dfrac{1}{2|n|}, & n \neq 0 \end{Bmatrix},$$

where we have used Eq. (4.384 3) by Gradshteyn and Ryzhik.[B7] Therefore, the generalized function $\ln|\sin(x/2)|$ can be expressed as

$$\ln\left|\sin\frac{x}{2}\right| = -\ln 2 - \frac{1}{2}\sum_{\substack{n=-\infty \\ n\neq 0}}^{\infty} \frac{\mathrm{sgn}(n)}{n}\, e^{inx}.$$

If we define the derivative of the generalized function $\ln|\sin(x/2)|$ as the generalized function $\cot(x/2)/2$, differentiation of the last equation yields the expression of the generalized function $\cot(x/2)/2$ as[B8]

$$\frac{1}{2}\cot\left(\frac{x}{2}\right) = -i\,\frac{1}{2}\sum_{n=-\infty}^{\infty} \mathrm{sgn}(n)\, e^{inx}.$$

(This equation says that the spectrum of the generalized function $\cot(x/2)$ is the odd impulse train.[B9]) And since[B10]

$$\pi\sum_{n=-\infty}^{\infty} \delta(x - n2\pi) = \frac{1}{2}\sum_{n=-\infty}^{\infty} e^{inx},$$

we obtain

$$\pi\sum_{n=-\infty}^{\infty} \delta(x - n2\pi) + i\,\frac{1}{2}\cot\left(\frac{x}{2}\right) = \frac{1}{2} + \sum_{n=1}^{\infty} e^{inx},$$

[B7] I. S. Gradshteyn and I. M. Ryzhik, Table of Integrals, Series and Products, Academic Press, New York, 1965.

[B8] Op. cit., M. J. Lighthill, p. 28, Theorem 15.

[B9] Ibid., p. 66, Theorem 26, Eq. (36).

[B10] Ibid., p. 67, Example 38.

or

$$\sum_{n=1}^{\infty} e^{inx} = -\frac{1}{2} + \pi \sum_{n=-\infty}^{\infty} \delta(x - n2\pi) + i\,\frac{1}{2}\cot\left(\frac{x}{2}\right)$$

in the sense of generalized functions.

REVERSE BLANK

Appendix C

ALIASED SPECTRUM

If we define the infinite impulse train

$$\delta_h(t) = \sum_n \delta(t - nh)$$

and use the time-limited character of g_c, as given in (42), it is possible to manipulate (46) as follows:

$$\hat{G}_c(f) = h \sum_{k=0}^{M} w_k \, g_c(kh) \, \exp(-i2\pi fkh)$$

$$= \int_0^T dt \; w(t) \; g_c(t) \; h \; \delta_h(t) \; \exp(-i2\pi ft)$$

$$= \int dt \; w(t) \; g_c(t) \; h \; \delta_h(t) \; \exp(-i2\pi ft)$$

$$= \mathfrak{F} \left\{ w(t) \; g_c(t) \; h \; \delta_h(t) \right\} = W(f) \circledast G_c(f) \circledast \delta_{1/h}(f)$$

$$= W(f) \circledast \sum_k G_c\left(f - k \frac{1}{h}\right) .$$

Using $h = \frac{T/m}{M}$, we see that (52) results.

REVERSE BLANK

NUSC Report No. 4113
3 June 1971

Comparison of Four Fast Fourier Transform Algorithms

James F. Ferrie
Albert H. Nuttall

ABSTRACT

Comparisons of four FFT (Fast Fourier Transform) algorithms (Brenner's, Cooley's, Fisher's, and Singleton's) have been made on the basis of program execution time, storage, and accuracy. Major modifications have been made in the generation of the trigonometric values in the Cooley and Fisher algorithms, with significant improvements in accuracy. Entry of constants in all algorithms has been changed: the constants are approximated by the best binary representation for the UNIVAC 1108 computer. Three waveform examples are used in the comparisons, namely, linear FM, random numbers, and a unit ramp. Also, the sizes of the FFT's considered are limited to powers of 2, from 16 through 8192.

The results indicate that Singleton's and Brenner's algorithms have the shortest execution times and occupy the least amount of computer storage, whereas Cooley's and Fisher's algorithms are the most accurate. For example, for an FFT of size 1024 on the linear FM waveform, the maximum relative errors for the four algorithms are 0.17×10^{-6}, 0.63×10^{-7}, 0.64×10^{-7}, 0.41×10^{-5}, respectively. Thus, there is no single best algorithm for all three criteria considered; rather, each algorithm has its own area of most effective applicability.

Approved for public release; distribution unlimited.

TABLE OF CONTENTS

	Page
LIST OF ILLUSTRATIONS	iii
1.0 INTRODUCTION	1
2.0 RESULTS	1
2.1 Execution Time	2
2.2 Storage Requirements	2
2.3 Accuracy	5
3.0 CONCLUSIONS	16
REFERENCES	17
APPENDIX — TABULATION OF ERRORS	19

REVERSE BLANK

LIST OF ILLUSTRATIONS

Figure		Page
1	Forward FFT Execution Times	3
2	Storage Requirements	4
3	One-Way FFT Error Calculation for Linear FM	7
4	RMS Error for Linear FM (Forward FFT)	8
5	Average Magnitude Error for Linear FM (Forward FFT)	9
6	Maximum Error for Linear FM (Forward FFT)	10
7	Two-Way FFT Error Calculation for Random Numbers and Unit Ramp	12
8	RMS Error for Linear FM (Inverse FFT)	13
9	RMS Error for Random Numbers (Inverse FFT)	14
10	RMS Error for Unit Ramp (Inverse FFT)	15

LIST OF TABLES

Table		Page
1	Relative Error for One-Way FFT of Linear FM Waveform	20
2	Relative Error for Two-Way FFT of Linear FM Waveform	21
3	Relative Error for Two-Way FFT of Random Numbers	22
4	Relative Error for Two-Way FFT of Unit Ramp	24

REVERSE BLANK

COMPARISON OF FOUR FAST FOURIER TRANSFORM ALGORITHMS

1.0 INTRODUCTION

Since the advent of the Fast Fourier Transform (FFT), several algorithms, each with its own claim to optimality, have been advanced to effect the Discrete Fourier Transformation. In an effort to determine quantitatively the relative advantages and disadvantages of the various procedures, four algorithms (Brenner's,[1] Cooley's,[2] Fisher's,[3] and Singleton's[4]) have been selected for operational comparison on the basis of program execution time, storage, and accuracy. The comparison is restricted to FFT sizes which are powers of 2, from 16 through 8192. (Cooley's and Fisher's algorithms are able to handle powers of 2 only, while Brenner's and Singleton's can handle other radices.)

In order to allow general conclusions (conclusions not restricted to results which are waveform-dependent), three different waveform examples are used for the comparison: linear frequency modulation (FM), random numbers, and a unit ramp. Both one-way and two-way error calculations are carried out for the linear FM waveform, whereas only the two-way errors are calculated for the random numbers and unit ramp waveforms.

Three measures of error are employed: rms, average magnitude, and maximum. Theoretical results on floating-point accuracy are available only for the rms measure of error.[5] It was deemed important, therefore, to evaluate the accuracy of the algorithms for all three error measures to see if any significantly different conclusions are obtained.

2.0 RESULTS

The comparison of the four FFT algorithms in terms of execution time, storage, and accuracy is carried out on the UNIVAC 1108. The forward FFT for a complex sequence $x_0, x_1, \ldots, x_{N-1}$ is defined as

$$X_n = \sum_{m=0}^{N-1} x_m \exp(-i\,2\pi\,mn/N), \quad 0 \le n \le N-1 \ .$$

The inverse FFT is defined as

$$x_m = \frac{1}{N} \sum_{n=0}^{N-1} X_n \exp(i 2\pi nm/N), \quad 0 \leq m \leq N-1 .$$

Some modifications to the algorithms have been made; however, since these modifications affect mainly the accuracy, and not execution time or storage, they are discussed in detail in Section 2.3, Accuracy.

2.1 EXECUTION TIME

Execution time is independent of the particular waveform example employed in the FFT. Figure 1 depicts the execution time of the four algorithms versus the size of the transform. The results indicate that Fisher's and Cooley's algorithms take the most time; for example, for an FFT size of 8192, Fisher's algorithm takes 3.75 seconds, while Singleton's algorithm takes 2.33 seconds. This significant difference in time is somewhat obscured in Fig. 1 by the logarithmic ordinate; however, it is worth noting. The other two algorithms, for size 8192, require 3.13 seconds for Cooley and 2.62 seconds for Brenner.

Since the curves are virtually straight lines in Fig. 1, they can be extrapolated to powers of 2 beyond 8192. However, one can not interpolate between powers of 2 to evaluate execution times for intermediate FFT sizes.

2.2 STORAGE REQUIREMENTS

Figure 2 depicts the number of storage locations required for the four algorithms as a function of the size of the FFT. The amount required represents both the number of data storage locations and the number of instructions that the algorithms need. Singleton's and Brenner's algorithms need approximately the same amount of storage, but Cooley's and Fisher's algorithms need an increasing amount of storage as the size of the FFT increases because their algorithms store the trigonometric values and scratch storage in arrays, rather than calculate values as needed.

Again, extrapolation to other powers of 2 is possible, but interpolation between powers of 2 is not.

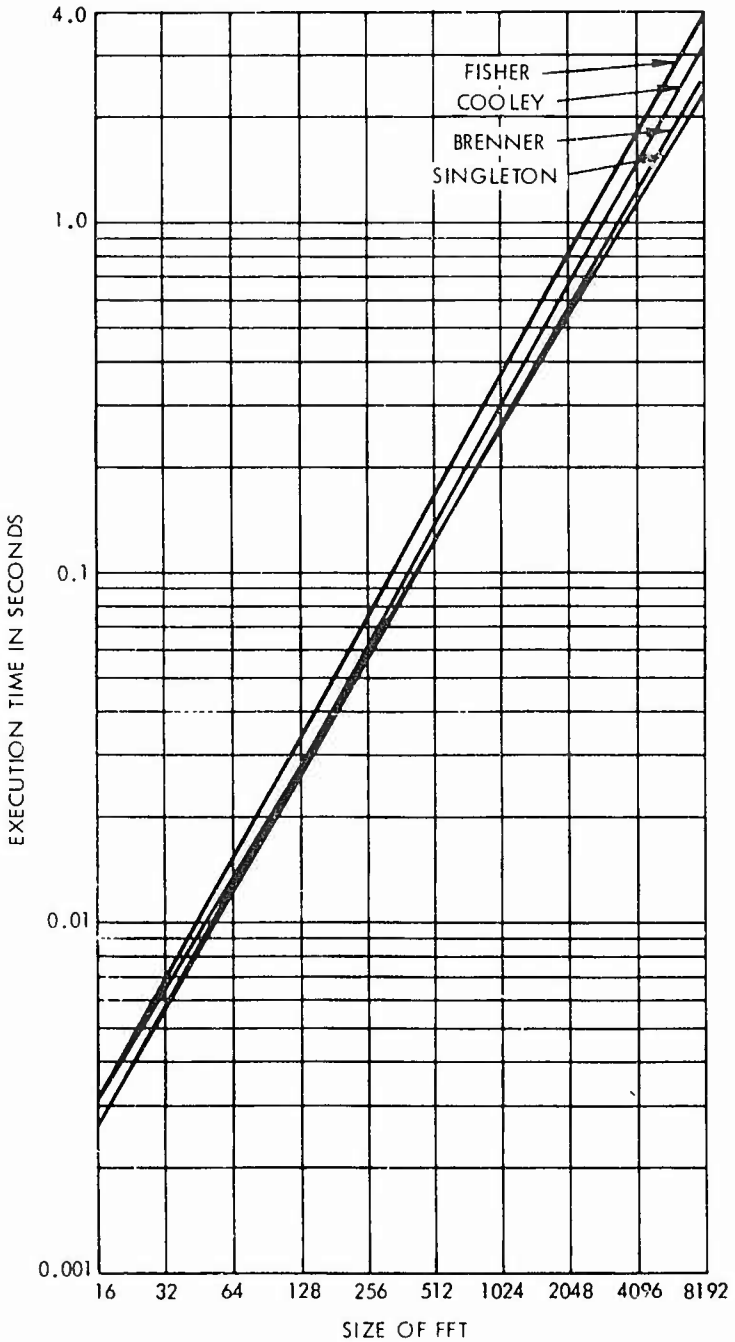


Fig. 1. Forward FFT Execution Times

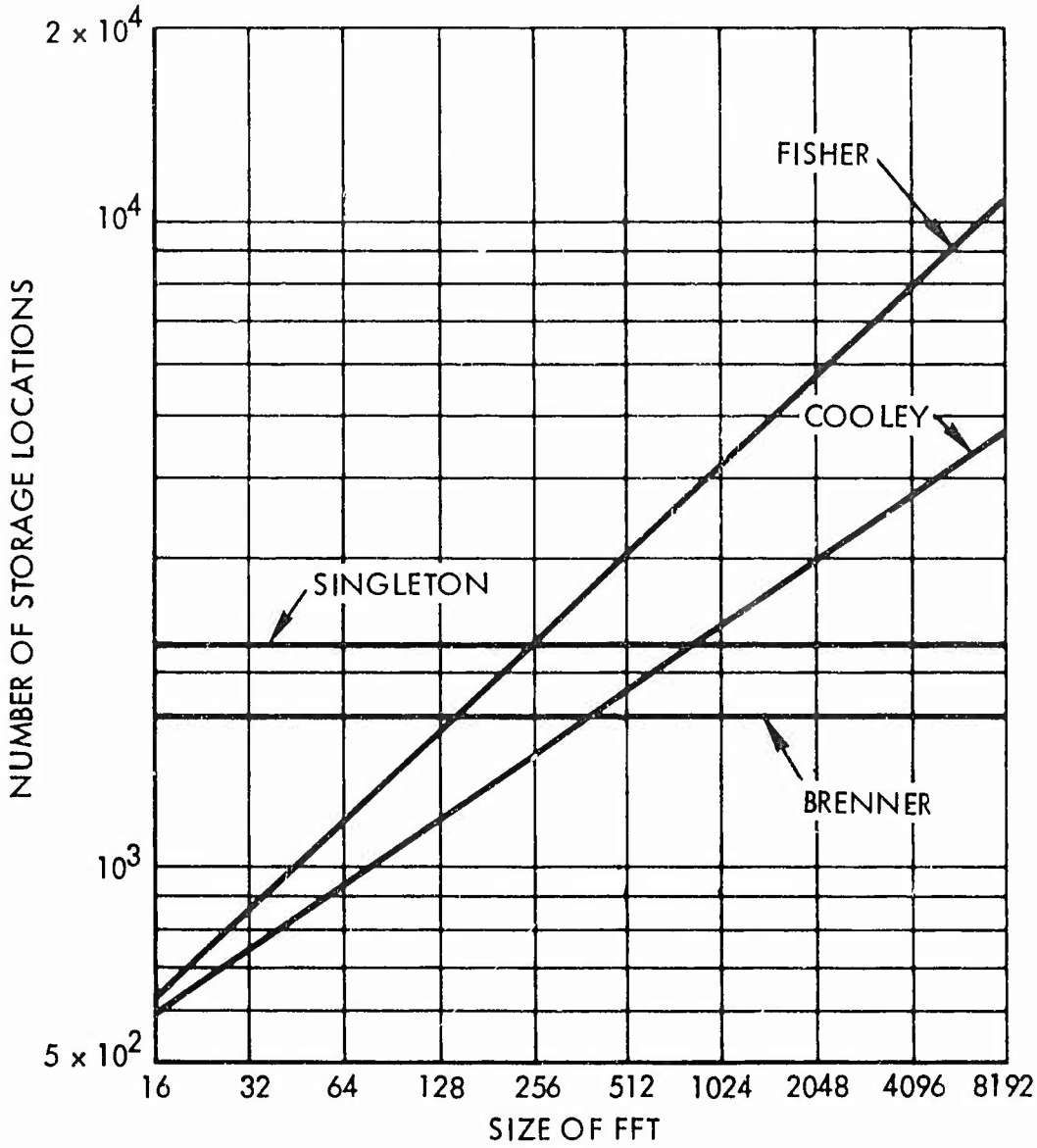


Fig. 2. Storage Requirements

2.3 ACCURACY

Three measures of error are used in the accuracy comparison: rms error, average magnitude error, and maximum error. If the result of a calculation yields the sequence of complex numbers $\hat{z}_0, \hat{z}_1, \ldots, \hat{z}_{N-1}$, whereas the desired result is the sequence $z_0, z_1, \ldots, z_{N-1}$, the three errors are defined as

$$\text{rms error} = \left(\frac{1}{N} \sum_{n=0}^{N-1} \left| z_n - \hat{z}_n \right|^2 \right)^{1/2},$$

$$\text{average magnitude error} = \frac{1}{N} \sum_{n=0}^{N-1} \left| z_n - \hat{z}_n \right|,$$

$$\text{maximum error} = \max_n \left\{ \left| z_n - \hat{z}_n \right| \right\}.$$

The three errors obey the rule that the average magnitude error is never larger than the rms error, which, in turn, is never larger than the maximum error. (The proof of the first inequality follows from Schwartz's inequality.) Thus, the rms error is an intermediate measure insofar as severity of error is concerned. The only way any of the error measures can be equal is if all the terms $|z_n - \hat{z}_n|$ are equal, i.e., independent of n.

Modifications have been made in all four FFT algorithms to improve their accuracy. These modifications include the changing of constant values to the best binary representation for the computer, and the generation of the trigonometric values in the Cooley and Fisher algorithms by calculating one pair of sine and cosine values in double precision, followed by double precision recursion, and rounding to single precision. This procedure keeps execution time to a minimum and improves the accuracy of the generated trigonometric values, which often are the major source of error in FFT algorithms.

Three different waveforms are considered in the error comparison in order to eliminate any waveform-dependent conclusions. The first waveform is linear FM, characterized by the sequence

$$x_m = \exp(i \pi m^2/N), \quad 0 \leq m \leq N-1 \quad (N \text{ even})$$

The FFT of this sequence[6] is

$$X_n = \sum_{m=0}^{N-1} \exp(i\pi m^2/N) \exp(-i 2\pi mn/N)$$

$$= N^{1/2} \exp(i\pi/4) \exp(-i\pi n^2/N), \quad 0 \leq n \leq N-1 .$$

We have here a simple closed-form theoretical expression for the one-way FFT that can be used for comparison with the numerical FFT calculations, according to the error measures above. Figure 3 is a flow chart for the error calculation.

The results of the rms-error comparison on the one-way (forward) FFT are given in Fig. 4, for N ranging from 16 through 2048, in powers of 2.* The corresponding results for average magnitude error and maximum error are given in Figs. 5 and 6, respectively. Actually, all these errors are relative errors, obtained by dividing the errors above by the average magnitude of the correct answer.

There is considerable similarity between the results of Figs. 4, 5, and 6 for the three error measures. Accordingly, in the remainder of this section attention is confined to the rms-error measure. (Tabulations of all three errors for all three waveforms are provided in the appendix to this report.)

The increased error of Singleton's algorithm is strikingly evident in Figs. 4, 5, and 6. It is almost two orders of magnitude less accurate than the Cooley and Fisher algorithms for an FFT size at 2048 and is degrading rapidly. The Brenner algorithm is approximately three times less accurate at size 2048 and has the same rate of error growth as the Cooley and Fisher algorithms.

It is worthwhile, at this point, to compare the numerical investigation with some theoretical calculations of error conducted by Weinstein.[5] From Eqs. (28) and (24) of Weinstein, we obtain the error (for a one-way FFT) as

$$\frac{\sigma_E}{\sigma_x} = 2^{1/2} \sigma_\epsilon \left(\nu - \frac{3}{2} + 2^{1-\nu} \right)^{1/2}$$

where

$$\sigma_\epsilon = 0.46 \cdot 2^{-t}$$

*Storage limitations in the auxiliary error computation program for the Cooley and Fisher algorithms prevented us from investigating the 4096 and 8192 cases for the linear FM waveform.

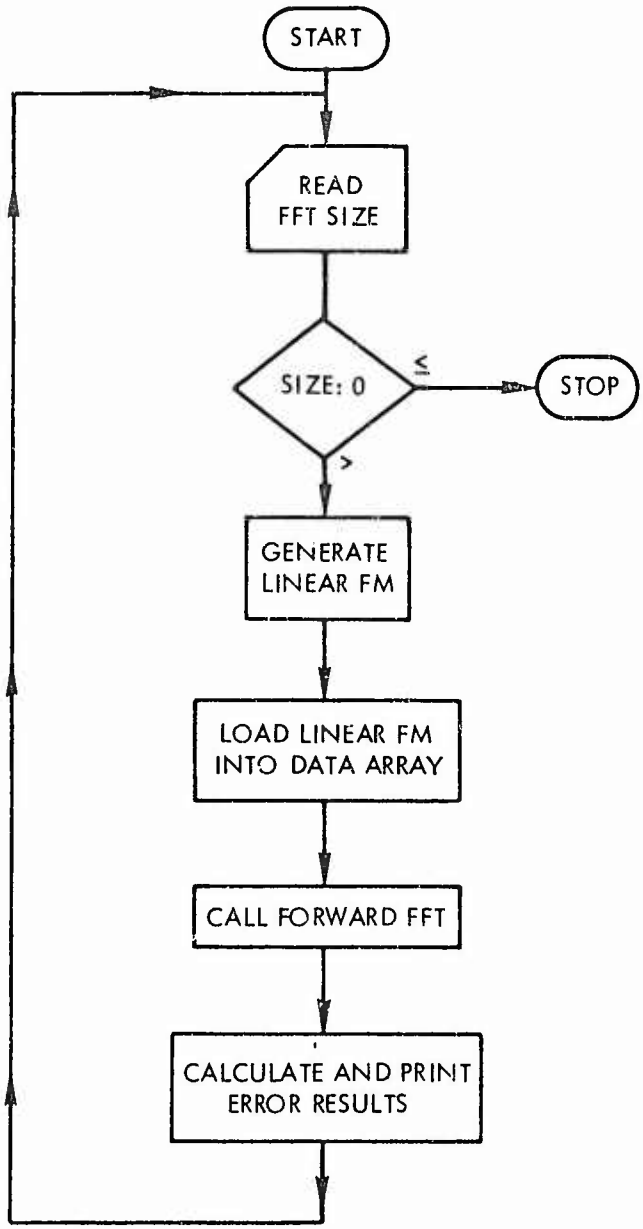


Fig. 3. One-Way FFT Error Calculation for Linear FM

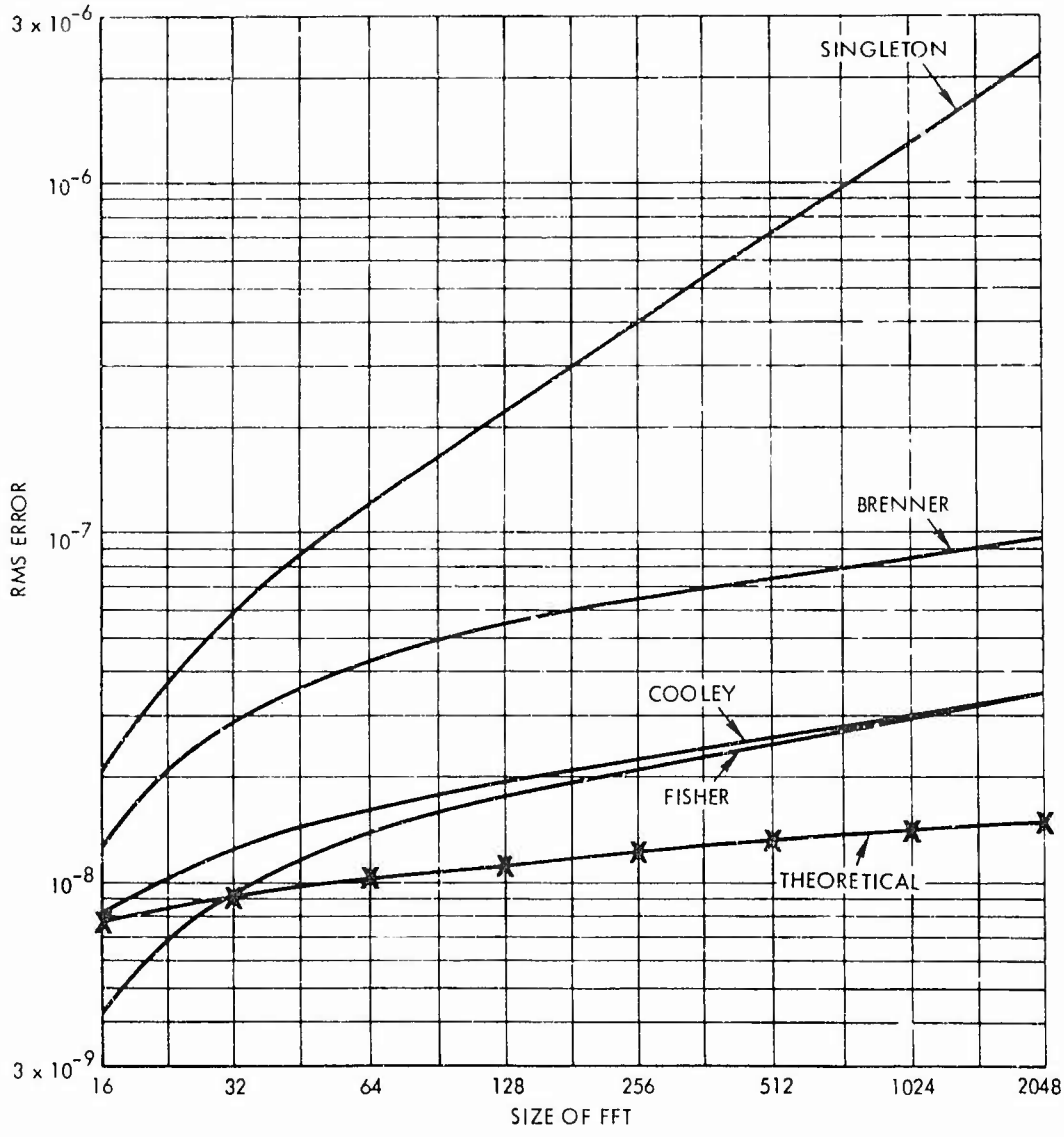


Fig. 4. RMS Error for Linear FM (Forward FFT)

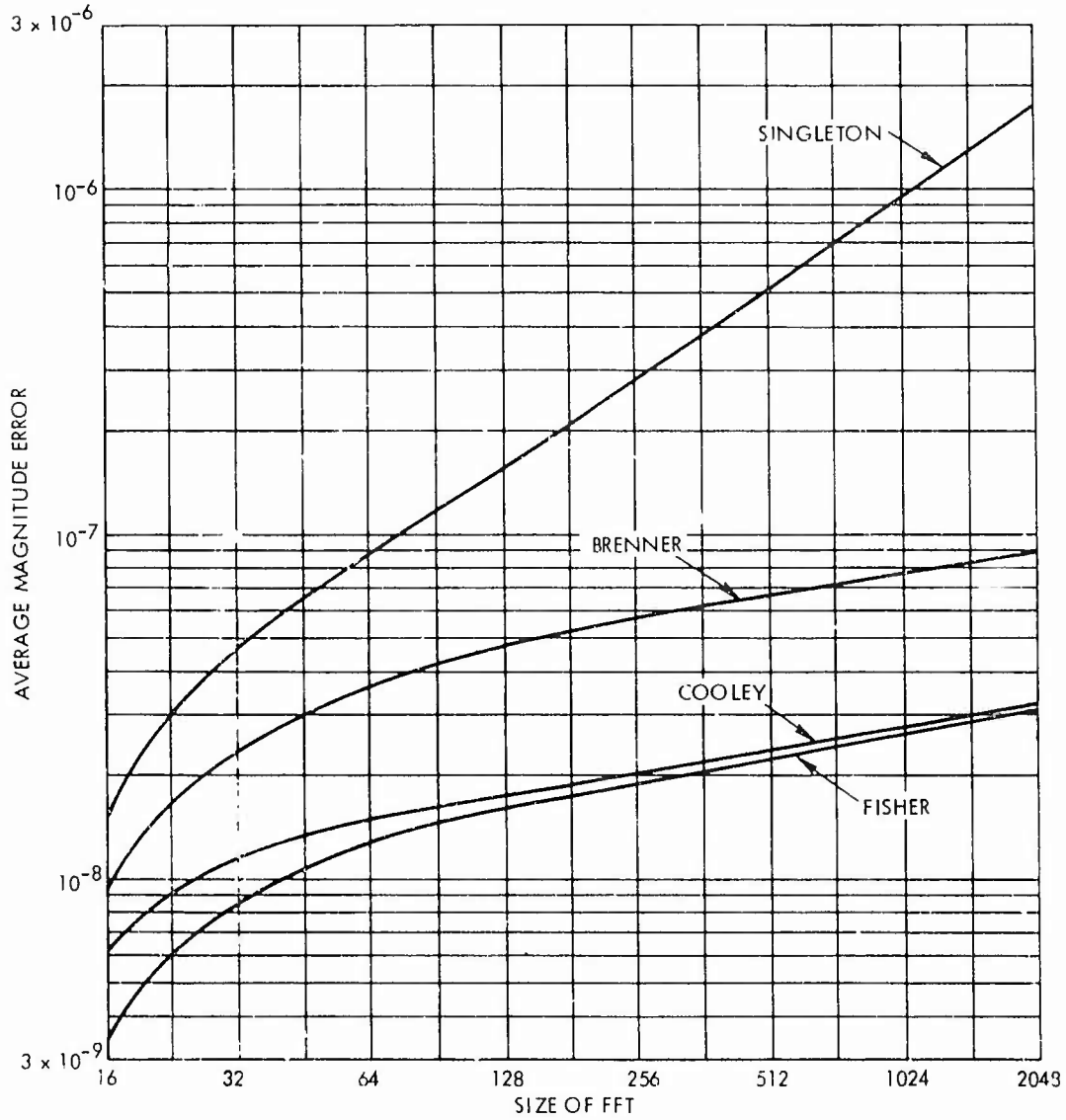


Fig. 5. Average Magnitude Error for Linear FM (Forward FFT)

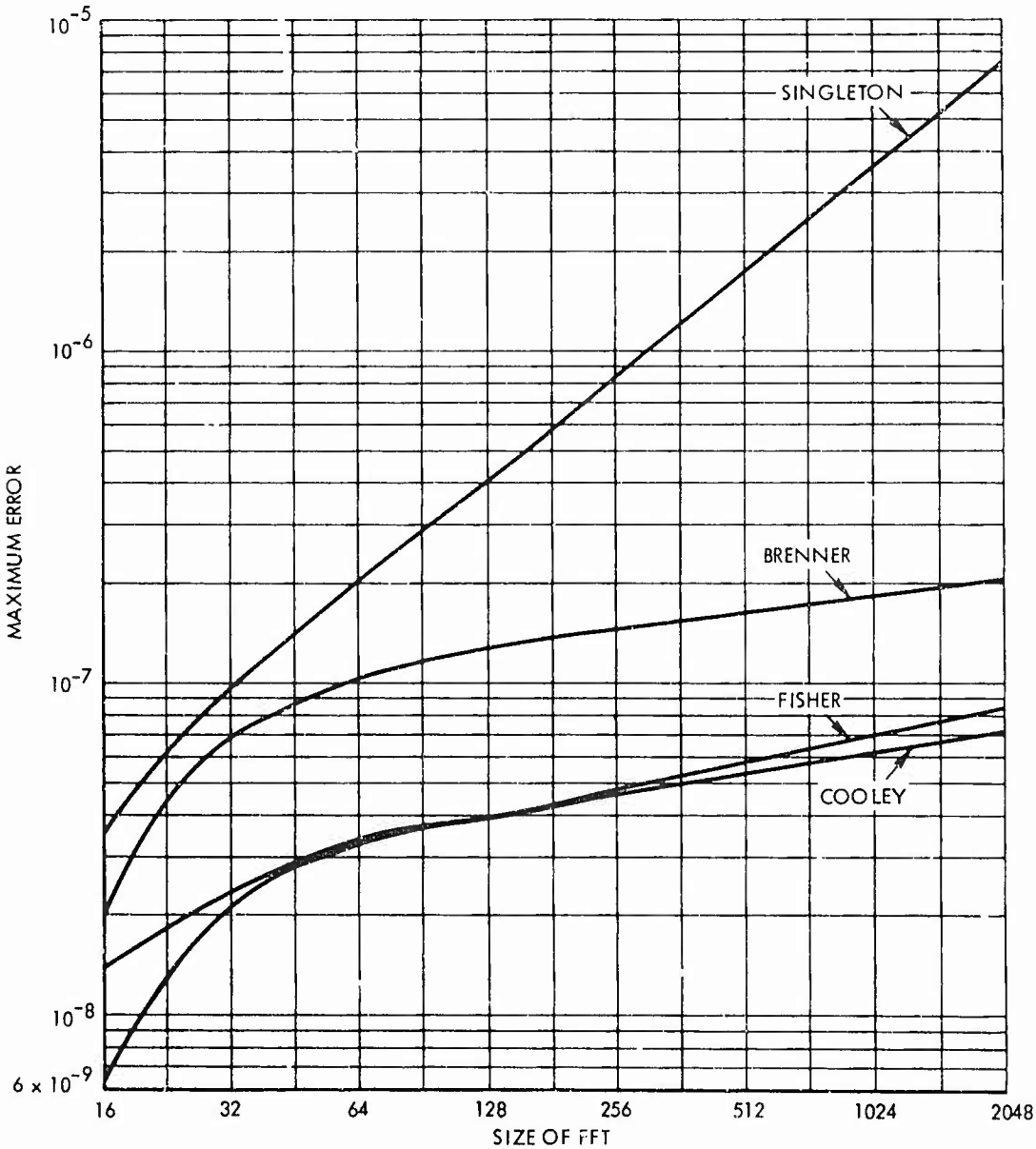


Fig. 6. Maximum Error for Linear FM (Forward FFT)

Here, ν is the logarithm (to the base 2) of the size of the transform ($N = 2^{\nu}$), and t is the number of bits used to represent the mantissa of a number. *

As shown in Fig. 4 (where the theoretical equation is plotted as x's, with $\sigma_x^2 = 1$), Weinstein's calculations underestimate the rms error by a fair amount over most of the range of FFT sizes. Also, his calculations indicate a slower rate of error growth with FFT size than was actually obtained. As Weinstein himself notes, this is probably due to the truncated arithmetic employed in the UNIVAC 1108. In fact, if truncated arithmetic is employed instead of rounding, the rms error is greater by a factor of $\sqrt{32}$ at N = 2048 (see Ref. 5). This increased error would move the theoretical curve in Fig. 4 to a very close approximation to the Brenner curve. Fisher's and Cooley's error curves are somewhat better because their trigonometric values are obtained by rounding while the remaining arithmetic is truncation; thus, they constitute a mixed procedure.

For the other two waveforms considered, the error is computed after a two-way FFT is performed; i.e., the FFT is retransformed back into the original (time) domain to obtain the error estimate (see Fig. 7). The primary reason for doing this is that, since all the array entries in the time domain are approximately unity in magnitude, it is easy to form a meaningful relative error in the time domain. A relative error formed in the frequency domain, where the range of values is several orders of magnitude for the random numbers and unit ramp waveforms, would be less meaningful. The linear FM waveform, on the other hand, possesses constant magnitude for all array entries in <u>both</u> domains, a characteristic which makes it particularly appealing.

The results for the rms error for the three waveforms are given in Figs. 8, 9, and 10. (The average magnitude error and maximum error are tabulated in the appendix.) The two-way error results are similar in form to the one-way error results, with the exception of Singleton's curve. A comparison of Figs. 4 and 8 reveals that the two-way error for Singleton's algorithm is less than the one-way error, a discrepancy which must be due to fortuitous error-cancellation in the two-way results. Since one would never use a two-way FFT without performing some transformations on the one-way results, the two-way Singleton results must be used with reservation. Where Singleton's algorithm is concerned, it would be more reasonable to double the one-way error of Fig. 4 than to use the two-way error of Fig. 8.

---

* For the UNIVAC 1108, t equals 27 in single precision.

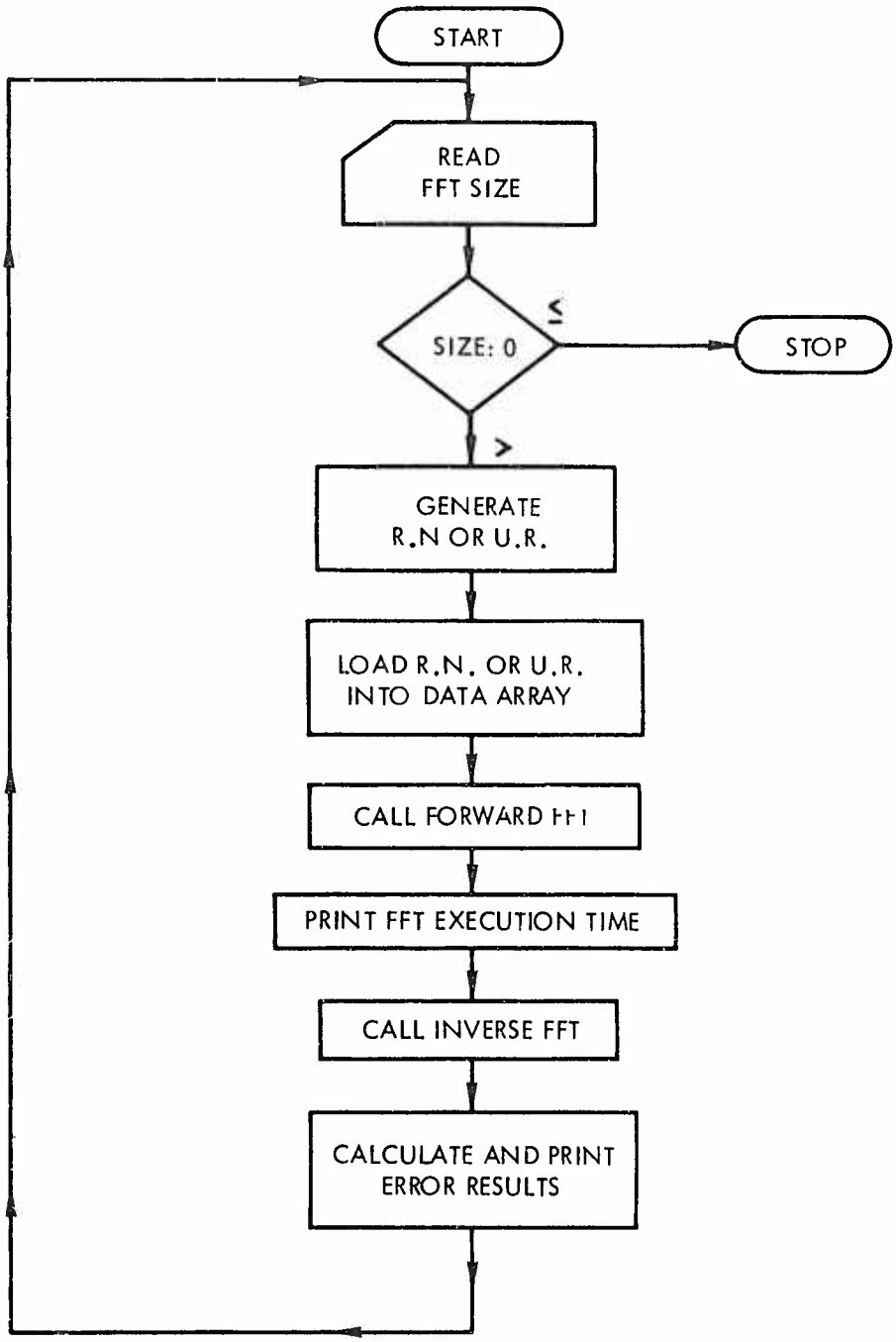


Fig. 7. Two-Way FFT Error Calculation for Random Numbers and Unit Ramp

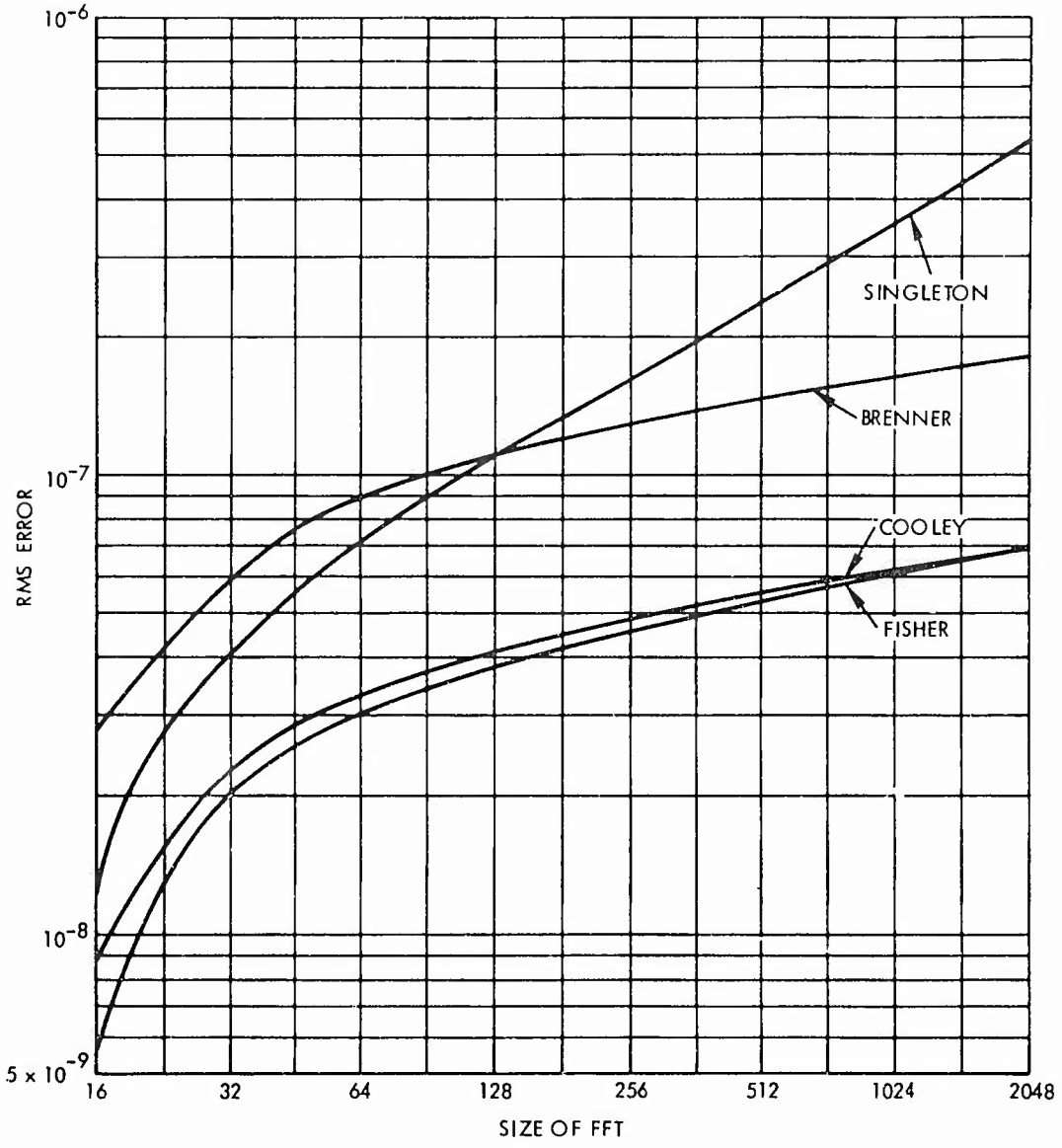


Fig. 8. RMS Error for Linear FM (Inverse FFT)

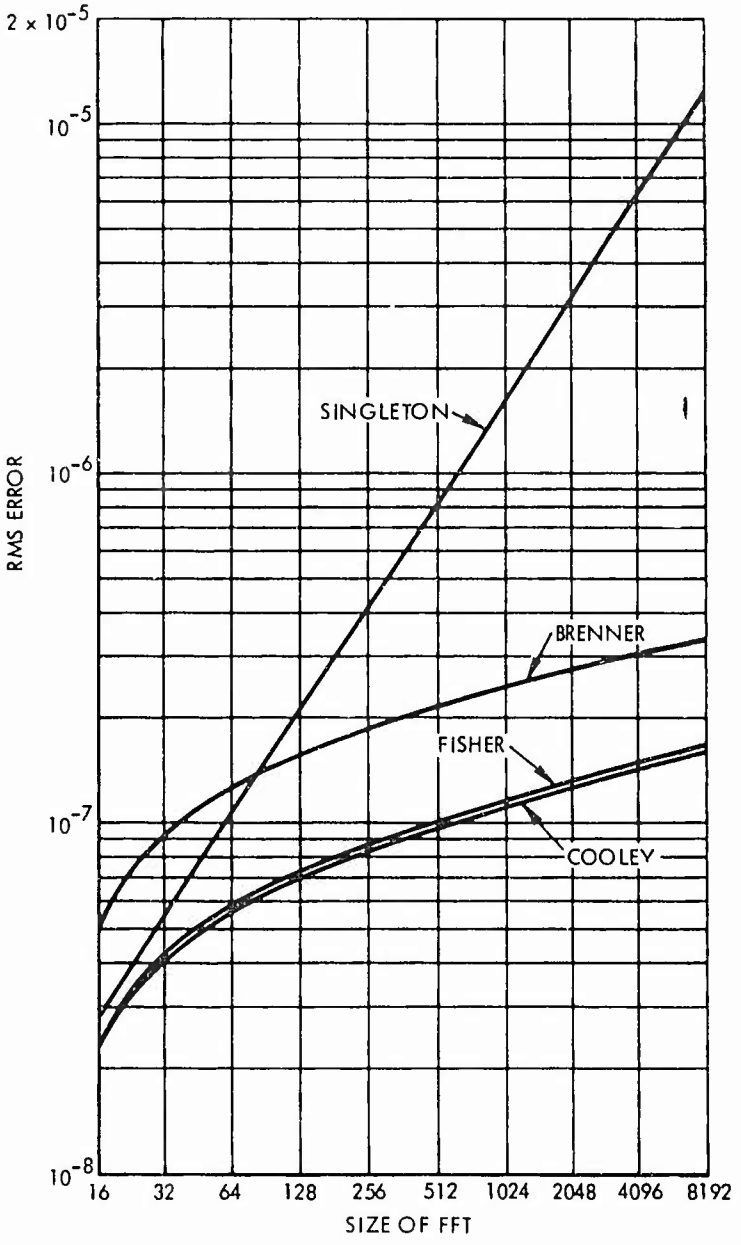


Fig. 9. RMS Error for Random Numbers (Inverse FFT)

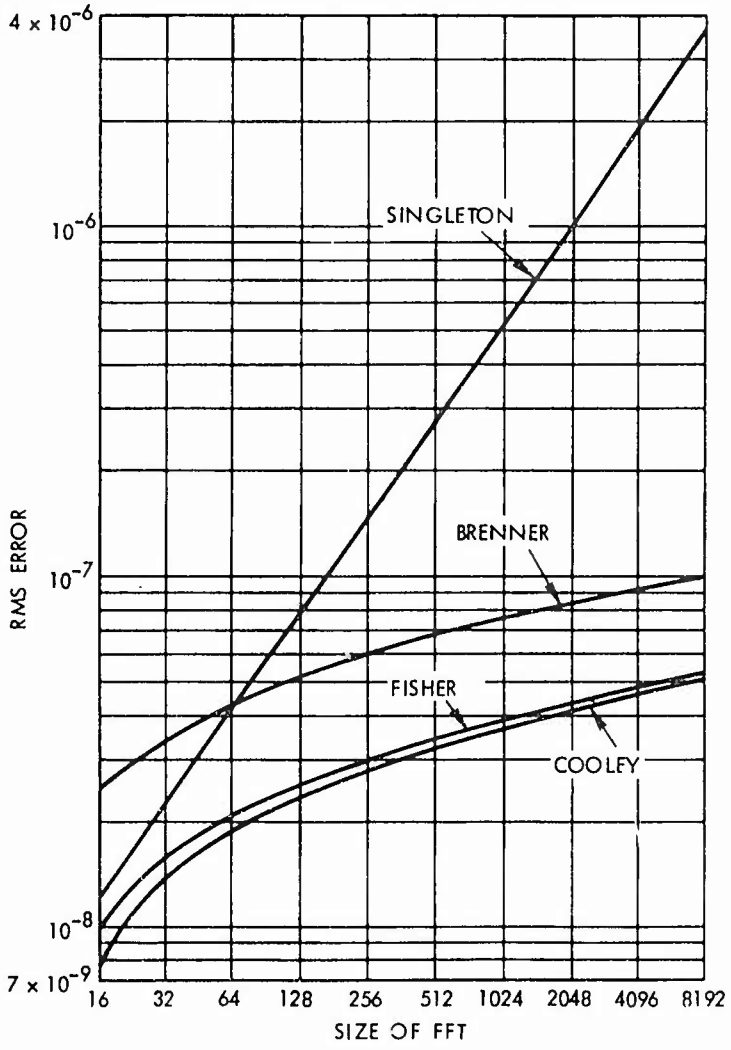


Fig. 10. RMS Error for Unit Ramp (Inverse FFT)

Direct comparison between errors for different waveforms is not possible because the average values of the array entries are not identical; e.g., the rms value for the linear FM waveform is 1, for the random numbers $\sqrt{2}$, and for the unit ramp $\sqrt{2/3}$. Such scale factors would have to be included in order to obtain a valid comparison between waveforms.

3.0 CONCLUSIONS

The trade-off between the four algorithms considered is readily apparent: the best accuracy is achieved only at the expense of increased execution time and storage. If we are severely limited by execution time and storage, we may have to select a less accurate FFT algorithm; how important the errors are will depend upon the particular application.

In summary, no single FFT algorithm represents a best choice; it must be left to the user to determine the best algorithm, based on the criteria of most importance to him.

REFERENCES

1. N. M. Brenner, Three Fortran Programs that Perform the Cooley-Tukey Fourier Transform, MIT Lincoln Lab Publication AD 657019, 28 July 1967.

2. J. W. Cooley, Harmonic Analysis-Complex Fourier Series, Share Program Library No. SDA3425, 7 February 1966.

3. J. R. Fisher, Fortran Program for Fast Fourier Transform, NRL Report 7041, 16 April 1970.

4. R. C. Singleton, "An Algorithm for Computing the Mixed Radix Fast Fourier Transform," IEEE Transactions on Audio and Electroacoustics, vol. AU-17, June 1969, pp. 99-103.

5. C. Weinstein, "Roundoff Noise in Floating Point Fast Fourier Transform Computation," IEEE Transactions on Audio and Electroacoustics, vol. AU-17, no. 3, September 1969.

6. E. S. Eby and A. H. Nuttall, "Some Sums of the Form $\sum_{k=0}^{M} \exp(i\pi k^2/N)$," NUSC Technical Memorandum No. 2020-181-70, 23 September 1970.

REVERSE BLANK

APPENDIX

TABULATION OF ERRORS

(NOTE: In the following tables, notations such as .124-07 mean $.124 \times 10^{-7}$.)

Table 1

RELATIVE ERROR FOR ONE-WAY FFT OF LINEAR FM WAVEFORM

Algorithm	FFT Size	RMS	Average Magnitude	Maximum
Brenner	16	.124-07	.951-08	.199-07
Cooley	16	.800-08	.611-08	.142-07
Fisher	16	.416-08	.349-08	.631-08
Singleton	16	.208-07	.152-07	.354-07
Brenner	32	.421-07	.326-07	.826-07
Cooley	32	.150-07	.119-07	.226-07
Fisher	32	.103-07	.792-08	.220-07
Singleton	32	.728-07	.570-07	.133-06
Brenner	64	.448-07	.351-07	.942-07
Cooley	64	.155-07	.121-07	.345-07
Fisher	64	.130-07	.893-08	.331-07
Singleton	64	.136-06	.101-06	.311-06
Brenner	128	.612-07	.518-07	.132-06
Cooley	128	.197-07	.171-07	.386-07
Fisher	128	.198-07	.160-07	.384-07
Singleton	128	.175-06	.128-06	.444-06
Brenner	256	.586-07	.494-07	.118-06
Cooley	256	.213-07	.181-07	.431-07
Fisher	256	.205-07	.160-07	.459-07
Singleton	256	.334-06	.250-06	.869-06
Brenner	512	.765-07	.682-07	.178 06
Cooley	512	.264-07	.239-07	.549-07
Fisher	512	.279-07	.242-07	.593-07
Singleton	512	665-06	.520-06	.189-05
Brenner	1024	.806-07	.718-07	.173-06
Cooley	1024	.283-07	.249-07	.626-07
Fisher	1024	.271-07	.228-07	.642-07
Singleton	1024	.126-05	.968-06	.355-05
Brenner	2048	.969-07	.890-07	.203-06
Cooley	2048	.349-07	.321-07	.654-07
Fisher	2048	.344-07	.311-07	.828-07
Singleton	2048	.235-05	.176-05	.755-05

Table 2

RELATIVE ERROR FOR TWO-WAY FFT OF LINEAR FM WAVEFORM

Algorithm	FFT Size	RMS	Average Magnitude	Maximum
Brenner	16	.279-07	.197-07	.395-07
Cooley	16	.884-08	.590-08	.159-07
Fisher	16	.543-08	.373-08	.931-08
Singleton	16	.124-07	.843-08	.218-07
Brenner	32	.800-07	.628-07	.159-06
Cooley	32	.230-07	.177-07	.401-07
Fisher	32	.204-07	.169-07	.333-07
Singleton	32	.425-07	.280-07	.897-07
Brenner	64	.828-07	.659-07	.157-06
Cooley	64	.237-07	.180-07	.525-07
Fisher	64	.222-07	.165-07	.449-07
Singleton	64	.376-07	.289-07	.802-07
Brenner	128	.108-06	.931-07	.211-06
Cooley	128	.344-07	.291-07	.619-07
Fisher	128	.381-07	.326-07	.673-07
Singleton	128	.678-07	.562-07	.157-06
Brenner	256	.115-06	.980-07	.214-06
Cooley	256	.380-07	.324-07	.760-07
Fisher	256	.383-07	.315-07	.792-07
Singleton	256	.898-07	.685-07	.242-06
Brenner	512	.142-06	.127-06	.306-06
Cooley	512	.510-07	.452-07	.954-07
Fisher	512	.539-07	.484-07	.989-07
Singleton	512	.227-06	.178-06	.696-06
Brenner	1024	.150-06	.135-06	.308-06
Cooley	1024	.544-07	.487-07	.934-06
Fisher	1024	.520-07	.461-07	.105-06
Singleton	1024	.294-06	.211-06	.126-05
Brenner	2048	.181-06	.166-06	.344-06
Cooley	2048	.683-07	.623-07	.127-06
Fisher	2048	.688-07	.638-07	.119-06
Singleton	2048	.557-06	.397-06	.289-05

Table 3

RELATIVE ERROR FOR TWO-WAY FFT OF RANDOM NUMBERS

Algorithm	FFT Size	RMS	Average Magnitude	Maximum
Brenner	16	.499-07	.359-07	.141-06
Cooley	16	.221-07	.165-07	.632-07
Fisher	16	.220-07	.153-07	.632-07
Singleton	16	.276-07	.209-07	.802-07
Brenner	32	.787-07	.612-07	.224-06
Cooley	32	.369-07	.308-07	.954-07
Fisher	32	.332-07	.267-07	.666-07
Singleton	32	.543-07	.458-07	.114-06
Brenner	64	.105-06	.838-07	.256-06
Cooley	64	.464-07	.366-07	.128-06
Fisher	64	.516-07	.403-07	.128-06
Singleton	64	.966-07	.820-07	.187-06
Brenner	128	.166-06	.132-06	.592-06
Cooley	128	.733-07	.571-07	.253-06
Fisher	128	.719-07	.603-07	.211-06
Singleton	128	.223-06	.178-06	.716-06
Brenner	256	.184-06	.148-06	.530-06
Cooley	256	.881-07	.711-07	.298-06
Fisher	256	.862-07	.709-07	.233-06
Singleton	256	.326-06	.261-06	.943-06
Brenner	512	.215-06	.172-06	.718-06
Cooley	512	.102-06	.813-07	.382-06
Fisher	512	.101-06	.825-07	.340-06
Singleton	512	.737-06	.602-06	.259-05
Brenner	1024	.255-06	.204-06	.894-06
Cooley	1024	.123-06	.992-07	.443-[illegible]
Fisher	1024	.124-06	.102-06	.424-06
Singleton	1024	.152-05	.124-05	.524-05
Brenner	2048	.288-06	.230-06	.110-05
Cooley	2048	.136-06	.109-06	.506-06
Fisher	2048	.137-06	.111-06	.554-06
Singleton	2048	.317-05	.257-05	.128-04

Table 3 (Cont'd)

RELATIVE ERROR FOR TWO-WAY FFT OF RANDOM NUMBERS

Algorithm	FFT Size	RMS	Average Magnitude	Maximum
Brenner	4096	.306-06	.245-06	.117-05
Cooley	4096	.149-06	.119-06	.569-06
Fisher	4096	.150-06	.122-06	.654-06
Singleton	4096	.619-05	.502-05	.275-04
Brenner	8192	.339-06	.272-06	.154-05
Cooley	8192	.163-06	.131-06	.654-06
Fisher	8192	.165-06	.133-06	.674-06
Singleton	8192	.122-04	.991-05	.563-04

Table 4

RELATIVE ERROR FOR TWO-WAY FFT OF UNIT RAMP

Algorithm	FFT Size	RMS	Average Magnitude	Maximum
Brenner	16	.250-07	.188-07	.537-07
Cooley	16	.774-08	.492-08	.211-07
Fisher	16	.101-07	.889-08	.211-07
Singleton	16	.121-07	.833-08	.239-07
Brenner	32	.361-07	.305-07	1.000-07
Cooley	32	.129-07	.102-07	.421-07
Fisher	32	.172-07	.142-07	.421-07
Singleton	32	.213-07	.183-07	.421-07
Brenner	64	.411-07	.337-07	.120-06
Cooley	64	.180-07	.141-07	.632-07
Fisher	64	.206-07	.171-07	.477-07
Singleton	64	.367-07	.296-07	.107-06
Brenner	128	.529-07	.449-07	.180-06
Cooley	128	.238-07	.181-07	.954-07
Fisher	128	.246-07	.195-07	.745-07
Singleton	128	.702-07	.564-07	.249-06
Brenner	256	.575-07	.483-07	.208-06
Cooley	256	.284-07	.222-07	.116-06
Fisher	256	.298-07	.241-07	.105-06
Singleton	256	.107-06	.820-07	.463-06
Brenner	512	.696-07	.593-07	.283-06
Cooley	512	.331-07	.255-07	.149-06
Fisher	512	.342-07	.273-07	.126-06
Singleton	512	.236-06	.178-06	.119-05
Brenner	1024	.743-07	.628-07	.316-06
Cooley	1024	.366-07	.279-07	.191-06
Fisher	1024	.396-07	.319-07	.158-06
Singleton	1024	.440-06	.328-06	.270-05

Table 4 (Cont'd)

RELATIVE ERROR FOR TWO-WAY FFT OF UNIT RAMP

Algorithm	FFT Size	RMS	Average Magnitude	Maximum
Brenner	2048	.872-07	.750-07	.401-06
Cooley	2048	.412-07	.315-07	.233-06
Fisher	2048	.438-07	.350-07	.191-06
Singleton	2048	.936-06	.694-06	.642-05
Brenner	4096	.899-07	.760-07	.434-06
Cooley	4096	.464-07	.359-07	.277-06
Fisher	4096	.491-07	.395-07	.244-06
Singleton	4096	.185-05	.137-05	.144-04
Brenner	8192	.101-06	.870-07	.517-06
Cooley	8192	.502-07	.384-07	.310-06
Fisher	8192	.530-07	.422-07	.265-06
Singleton	8192	.370-05	.273-05	.328-04

REVERSE BLANK

NUSC Report No. 4169
13 October 1971

Spectral Estimation by Means of Overlapped Fast Fourier Transform Processing of Windowed Data

Albert H. Nuttall

ABSTRACT

An investigation of power-density autospectrum estimation by means of overlapped Fast Fourier Transform (FFT) processing of windowed data is conducted for four candidate spectral windows with good side-lobe behavior. A comparison of the four spectral windows is made on the basis of equal half-power resolution bandwidths. The criteria for comparison are: (1) statistical stability of the spectral estimates, (2) leakage (side lobes) of the spectral windows, (3) number of FFTs (number of overlapped pieces) required, and (4) size of each FFT required. The dependence of these criteria on the amount of overlap is investigated quantitatively.

Some striking invariances are discovered. Specifically, it is shown that the ultimate variance-reduction capabilities of the four windows, as measured by the equivalent number of degrees of freedom (EDF), are virtually identical under the constraint of equal half-power bandwidths. Furthermore, when the proper overlap is used for each window, the stability of this method of spectral estimation is identical to that of the "indirect" correlation approach. Also, the number of FFTs required to realize 99 percent (or less) of the maximum EDF is virtually independent of the particular window employed. The required fractional overlap of the four data windows for 99 percent (or less) of the maximum EDF is virtually independent of the product of the available time and the resolution bandwidth, although it does depend on the particular window. Tables of required overlap are presented. The only tradeoff among the four windows is that those with better side lobes require larger-size FFTs. All of these results are derived for a Gaussian random process, under the assumption that the resolution bandwidth of the spectral window is smaller than the finest detail in the true spectrum.

Rules of thumb for the maximum EDF and the number of FFTs required to realize 99 percent of the maximum EDF are given. The possibility of weighting individual spectral estimates unequally in order to optimize the EDF is investigated; the gain is found to be negligible for cases of practical interest.

Approved for public release; distribution unlimited.

TABLE OF CONTENTS

	Page
LIST OF FIGURES	iii
LIST OF TABLES	v
GLOSSARY	vi
INTRODUCTION	1
PROBLEM DEFINITION	2
LIMITING VALUE OF EQUIVALENT NUMBER OF DEGREES OF FREEDOM	7
DATA WINDOWS AND CHARACTERISTICS	10
RESULTS	18
OPTIMUM WEIGHTING OF INDIVIDUAL SPECTRAL ESTIMATES	26
DISCUSSION	27
APPENDIX A — DERIVATION OF MEAN AND VARIANCE	29
APPENDIX B — CORRELATIONS OF DATA WINDOWS	33
APPENDIX C — OPTIMUM WEIGHTS FOR EDF	35
APPENDIX D — COVARIANCE OF SPECTRAL ESTIMATES	37
REFERENCES	39

REVERSE BLANK

LIST OF FIGURES

Figure		Page
1	Overlapped Data Windows	3
2	Data Window	3
3	Spectral Window for Triangular Data Window	14
4	Spectral Window for Cosine Data Window	15
5	Spectral Window for Quadratic Data Window	16
6	Spectral Window for Cubic Data Window	17

REVERSE BLANK

LIST OF TABLES

Table		Page
1	Bandwidth Constants	13
2	First Three Side Lobes of Spectral Windows	18
3	Equivalent Degrees of Freedom Versus Number of Pieces; BT = 8, Cosine Data Window	19
4	Number of Pieces Required (P) and Corresponding Fractional Overlap (FO) for a Specified Fraction of the Maximum EDF .	22-23
5	Required Fractional Overlap for .99 max EDF.	24
6	Attainable Fraction of max EDF at .50 Fractional Overlap .	24
7	Attainable Fraction of max EDF at .625 Fractional Overlap .	25
8	Optimum EDF Values	26

GLOSSARY

T	available record length
B	desired frequency resolution, half-power bandwidth
x	random process
t	time
f, f_1	frequency
G	power-density spectrum of process x
w	data window
L	segment length
S	shift of data windows
P	number of pieces; number of FFTs
p	integer in range (1, P)
Y_p	Fourier transform of weighted p-th piece
$\hat{G}$, $\tilde{G}$	estimate of power density
Δt	sampling increment of x
W	Fourier transform of w
$\|W\|^2$, Q_i	spectral window
$E\{A\}$	statistical average of A
$Var\{A\}$	variance of A
ϕ_w, ϕ_u	correlations of data windows w, u

K, K_ω	equivalent degrees of freedom
u	normalized data window
B_{st}	statistical bandwidth
C_{st}	statistical-bandwidth constant
U	Fourier transform of u
$\mathrm{sinc}(x)$	$\sin(\pi x)/(\pi x)$
C	half-power-bandwidth constant
N_s	number of samples in segment length
w_p	weighting applied to $\lvert Y_p \rvert^2$
R	correlation of process x
γ_k	correlation of weights $\{w_p\}$
M_k	normalized correlation(Eq. (C-6))
χ	ambiguity function of data window w

Abbreviations

FFT	Fast Fourier Transform
EDF	Equivalent Degrees of Freedom
max	Maximum
FO	Fractional Overlap

REVERSE BLANK

SPECTRAL ESTIMATION BY MEANS OF OVERLAPPED FAST FOURIER TRANSFORM PROCESSING OF WINDOWED DATA

INTRODUCTION

Estimation of the power-density spectra of stationary random processes is an important problem and occurs frequently in many fields. The resolution of closely spaced frequency components, with limited amounts of data, presents inherent limitations on the statistical stability of the estimates. Also, the prevention of leakage of undesired frequency components into the frequency being analyzed dictates a careful choice of data weighting. Lastly, the extent and complexity of the data processing required to realize the desired resolution, stability, and leakage control are important considerations.

The fundamental, conflicting desires involved in spectral estimation become painfully obvious when the amount of data available for analysis is limited and can not be augmented by additional measurements. For example, the available record length may be limited by

a. nonstationary conditions (changing environment),

b. storage limitations,

c. equipment failure, and

d. time-sharing requirements.

Although factors b, c, and d can often be remedied or corrected, factor a often can not be controlled. Thus, only a small segment of the time record may be usable for each spectral analysis. If fine frequency resolution is desired, the limited number of independent observations available makes stable estimation impossible in some cases. One must then be willing to accept coarser, but more stable, spectral estimates.

The two fundamental parameters that control the performance of spectral estimation are the available record length, T, in which the sample of the random process is assumed stationary, and the desired frequency resolution, B, of the spectral analysis. Large values of the fundamental BT product yield good performance of the analysis technique, but small values are often forced upon us by too small a record length T or too fine a desired resolution B. The problem here is to make maximum use of the available data.

Spectral analysis has received much attention in the past [1-6], especially since the advent of the Fast Fourier Transform (FFT) [7, 8]. In particular, the method of averaging short modified periodograms [9] is a prime candidate for spectral analysis — for several reasons. First of all, nonstationary trends in the data are more readily observable through the time-local spectral estimates of each segment. Second, the size of each FFT can be kept reasonably small, thereby reducing storage, execution time, and round-off error. Third, the frequency resolution is easily controlled by the choice of segment length, and leakage (side lobes) can be controlled by the proper choice of window in the time domain. Lastly, overlapped segments of windowed data utilize more fully the variance-reduction capability of a given record length.

The problem to be addressed here has to do with the choice of window and amount of overlap to employ for a particular application. Specifically, if we employ a window with very small spectral side lobes, how much should the segments be overlapped, and does the overlap vary greatly with the particular window selected? (Fifty-percent overlap has been suggested as a reasonable procedure for the triangular data window [9, p. 72].) How many FFTs of what size have to be performed for the different windows? Is the variance-reduction capability dependent on the particular window?

Four windows will be investigated. They are called data windows in the time domain, where they are multiplied by the available data record; they will be called spectral windows in the frequency domain, where their main effect enters via convolution. The four data windows are called triangular, cosine,* quadratic, and cubic and will be documented in a later section. Hamming weighting [2, p. 14], although it possesses good adjacent side lobes, is not considered here because the spectral window decays very slowly with frequency, thereby responding to frequencies far removed from the analysis band of interest.

PROBLEM DEFINITION

Consider that stationary random process x has been observed for a time interval T seconds; that is, $x(t)$ for $0 < t < T$ is available. Let the power-density autospectrum of this process at frequency f be denoted by $G(f)$, where double-sided spectral notation will be employed. We wish to estimate spectrum G with a resolution of B hertz, where B is the half-power (-3 dB) bandwidth of the desired resolution.

*Also called Hanning weighting.

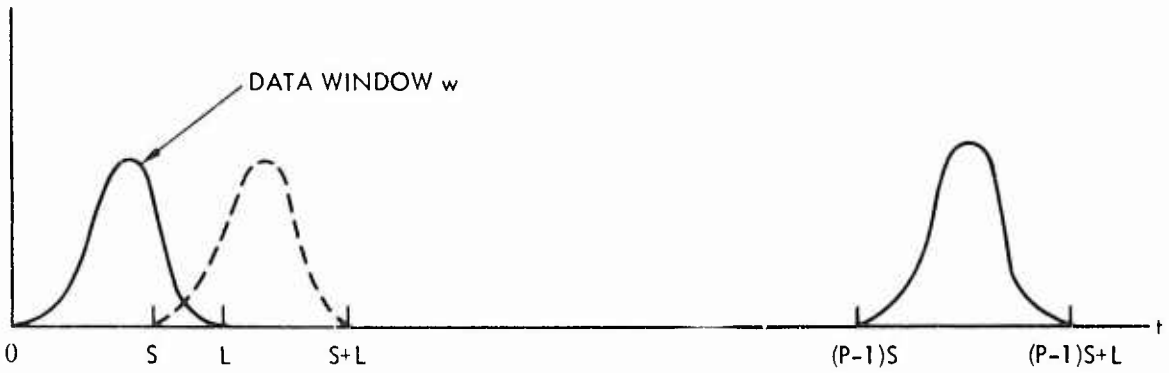


Fig. 1. Overlapped Data Windows

The method of obtaining the spectral estimates is depicted in Fig. 1. A data window w of duration L seconds is applied successively to the available data x in the overlapping intervals (0, L), (S, S+L), ... , ((P-1)S, (P-1)S+L). S is the amount of shift each adjacent data window undergoes, and P is the total number of pieces or segments employed. Since only T seconds of data are available, we must have

$$(P-1)S+L \leq T . \tag{1}$$

The segment length L should be large enough that the correlation function of process x is effectively zero for delays larger than L/2. (The relation between frequency resolution B and segment length L is discussed quantitatively later.) The form of the data window, depicted in Fig. 2, is even about the origin and real. Also, w(t) is zero for $|t| > L/2$.

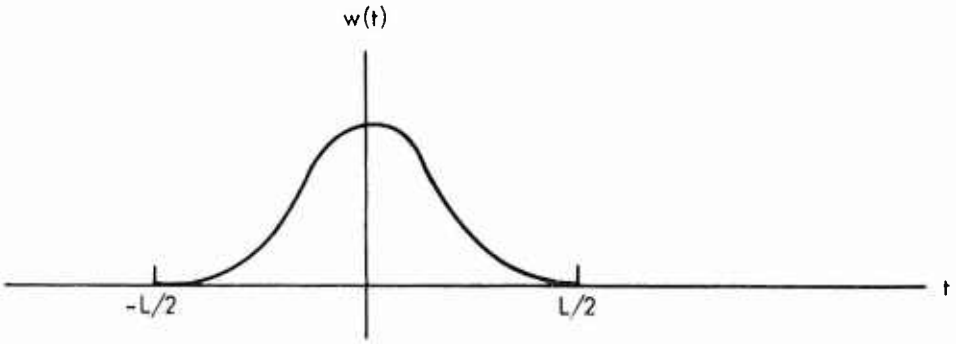


Fig. 2. Data Window

When the overlap in Fig. 1 is a significant fraction of the segment length, the effective use of the available data x is fairly uniform over the entire interval T except for the edges of the data, where a gradual taper over an interval of length $L/2$ takes place. This is consistent with earlier suggestions [10, p. 58] for maximum use of the available data. Notice that the percentage of taper depends on the desired frequency resolution and available record length, and is not a constant, such as 10 percent, as has occasionally been suggested.

The estimate of the power-density spectrum G is obtained as follows. First, a Fourier transform on the p-th windowed section is performed*:

$$Y_p(f) = \int dt\, \exp(-i2\pi ft)\, x(t)\, w\left[t - \frac{L}{2} - (p-1)S\right], \qquad 1 \le p \le P. \tag{2}$$

The spectral estimate at frequency f is then available as the average of the P pieces:

$$\hat{G}(f) = \frac{1}{P} \sum_{p=1}^{P} \left|Y_p(f)\right|^2 . \tag{3}$$

Equation (2) assumes a continuous, rather than discrete, form of signal processing [2, Secs. 4-11 versus 12-21]. However, if the discrete version of Eq. (2), where samples of x are taken Δt seconds apart, is such that aliasing is negligible, there is little difference between the two methods of spectral analysis [2, pp. 37-39 and 123-125]. We shall assume that Δt is so chosen and confine attention here to the continuous processing technique of Eq. (2). Of course, in practice, Eq. (2) is approximated by a discrete Fourier transform [9, p. 70], in which case dc and linear-trend removal should be considered for the sampled data [2, pp. 47-49].

The spectral estimate $\hat{G}(f)$ in Eq. (3) is a random variable. Its mean and variance are evaluated in Appendix A under the assumptions that x is a Gaussian random process and that the frequency resolution of the spectral window $|W|^2$, where

$$W(f) = \int dt\, \exp(-i2\pi ft)\, w(t), \tag{4}$$

is narrower than the finest detail in the true spectrum G. (This latter assumption is equivalent to that given under Eq. (1) for segment length L.) The results are

*Integrals without limits are over the range of non-zero integrand.

$$E\{\hat{G}(f)\} = \int d\nu\ G(f-\nu)\ |W(\nu)|^2 \cong G(f) \int d\nu\ |W(\nu)|^2 , \tag{5}$$

$$\mathrm{Var}\{\hat{G}(f)\} \cong \frac{1}{P} \sum_{k=-(P-1)}^{P-1} \left(1 - \frac{|k|}{P}\right) \left| \int d\mu\ \exp(i2\pi\mu kS)\ G(\mu)\ |W(f-\mu)|^2 \right|^2$$

$$\cong G^2(f)\ \frac{1}{P} \sum_{k=-(P-1)}^{P-1} \left(1 - \frac{|k|}{P}\right) \left|\phi_w(kS)\right|^2 , \tag{6}$$

where

$$\phi_w(\tau) = \int dt\ w(t)\ w^*(t - \tau) . \tag{7}$$

Relation (5) shows that the mean of the spectral estimate is equal to the convolution of the true spectrum G with the spectral window $|W|^2$. Relation (6) expresses the variance of the spectral estimate in terms of the number of pieces P, the shift S, and the autocorrelation ϕ_w of the data window. The result, Eq. (6), holds if f is greater than the bandwidth of the spectral window; the right side of Eq. (6) must be doubled if $f = 0$ [see also 9, p. 71].

The equivalent number of degrees of freedom (EDF) in spectral estimate $\hat{G}$ is defined as [2, p. 22]

$$K = 2\ \frac{E^2\ \{\hat{G}(f)\}}{\mathrm{Var}\ \{\hat{G}(f)\}}$$

$$= \frac{2P}{\displaystyle\sum_{k=-(P-1)}^{P-1} \left(1 - \frac{|k|}{P}\right) \left|\frac{\phi_w(kS)}{\phi_w(0)}\right|^2} , \tag{8}$$

employing Eqs. (4) through (6). Notice that under the assumptions given above, K is independent of the value of frequency f and true spectrum G; for $f = 0$, K is given by one half of Eq. (8).

For computational purposes, it is convenient to define a normalized data window u according to

$$u(x) = w(Lx) . \tag{9}$$

Then u contains the shape information of data window w but extends only over the interval (-1/2, 1/2). It follows that

$$\phi_w(\tau) = L\ \phi_u(\tau/L)\ , \tag{10}$$

where

$$\phi_u(\tau) = \int dt\ u(t)\ u^*(t-\tau)\ . \tag{11}$$

The EDF in Eq. (8) then becomes

$$K = \frac{2P}{\sum_{k=-(P-1)}^{P-1} \left(1 - \frac{|k|}{P}\right) \left| \frac{\phi_u(kS/L)}{\phi_u(0)} \right|^2}\ . \tag{12}$$

In order to minimize the fluctuations in the spectral estimate $\hat{G}$, we should maximize K in Eq. (12). To accomplish this for a given number of pieces P and segment length L, the shift S in Eq. (12) should be chosen as large as possible so that ϕ_u is as small as possible at S/L, 2S/L, etc. However, since Eq. (1) dictates a constraint among these variables, the best choice of shift S — for given record length T, number of pieces P, and segment length L — is given by equality in Eq. (1):

$$S = \frac{T-L}{P-1} \quad (\text{for } P \geq 2)\ . \tag{13}$$

Substituting Eq. (13) in Eq. (12), we have

$$K = \frac{2P}{\sum_{k=-(P-1)}^{P-1} \left(1 - \frac{|k|}{P}\right) \left| \frac{\phi_u\left(k \frac{\frac{T}{L} - 1}{P - 1}\right)}{\phi_u(0)} \right|^2}\ . \tag{14}$$

Equation (14) expresses the EDF as a function of

P, number of pieces in the average,

T/L, ratio of record length to segment length, and

ϕ_u, autocorrelation of shape of data window.

The problem now is to maximize the EDF in Eq. (14) by choosing, subject to specified record length T and desired half-power frequency resolution B, the number of pieces, P, for several data windows, w. It will turn out that the optimum value for P is <u>not</u> infinite.

One special case of Eq. (14) is worth comment: if $P \leq T/L$, the values of ϕ_u in Eq. (14) are zero since u extends only over (-1/2, 1/2). Then K equals 2P; that is, regardless of the window, the EDF increases linearly with the number of pieces P until overlap occurs (see Eq. (13)). As P increases somewhat beyond T/L, K continues to increase, although at a slower rate, because the overlapped pieces are progressively more statistically dependent. Of importance in the behavior of K are the rate of increase of K with P, and the maximum value of K attainable through the choice of P.

LIMITING VALUE OF EQUIVALENT NUMBER OF DEGREES OF FREEDOM

As the number of pieces P tends to infinity, the overlap approaches 100 percent, and the denominator of Eq. (14) approaches an integral, yielding

$$K_\infty \equiv \frac{2}{\int_{-1}^{1} dx\,(1-|x|)\left|\frac{\phi_u\left(\left(\frac{T}{L}-1\right)x\right)}{\phi_u(0)}\right|^2}$$

$$= \frac{2\left(\frac{T}{L}-1\right)}{\int_{-\frac{T}{L}+1}^{\frac{T}{L}-1} d\tau\left(1-\left|\frac{\tau}{\frac{T}{L}-1}\right|\right)\left|\frac{\phi_u(\tau)}{\phi_u(0)}\right|^2}. \qquad (15)$$

This limiting value depends only on T/L and the correlation ϕ_u of the shape u of the window. It is finite because the overlapped pieces are statistically dependent.

For large values of T/L (ratio of record length to segment length), an alternate form of Eq. (15) is very illuminating. If Eq. (10) is utilized, the denominator approaches

$$\int d\tau \left| \frac{\phi_u(\tau)}{\phi_u(0)} \right|^2 = \int d\tau \left| \frac{\phi_w(L\tau)}{\phi_w(0)} \right|^2 = \frac{1}{L} \int dt \left| \frac{\phi_w(t)}{\phi_w(0)} \right|^2 ; \tag{16}$$

but from Eqs. (7) and (4),

$$\phi_w(0) = \int dt \, |w(t)|^2 = \int df \, |W(f)|^2 , \tag{17}$$

and

$$\phi_w(t) = \int df \exp(i2\pi ft) \, |W(f)|^2 , \tag{18}$$

giving

$$\int dt \, |\phi_w(t)|^2 = \int df \, |W(f)|^4 \tag{19}$$

by Parseval's Theorem. Combining Eqs. (15) through (19), we obtain

$$K_{(\omega)} \cong 2 \, (T - L) \frac{\left[\int df \, |W(f)|^2 \right]^2}{\int df \, |W(f)|^4} , \quad \text{for } \frac{T}{L} \gg 1 . \tag{20}$$

If we define the statistical bandwidth [5, p. 265] of spectral window $|W|^2$ as

$$B_{st} = \frac{\left[\int df \, |W(f)|^2 \right]^2}{\int df \, |W(f)|^4} \equiv \frac{C_{st}}{L} , \tag{21}$$

then

$$K_{\omega} \cong 2 \, (T - L) \, B_{st} = 2 \left(\frac{T}{L} - 1 \right) C_{st} , \quad \text{for } \frac{T}{L} \gg 1 . \tag{22}$$

The constant C_{st} is dimensionless and of the order of unity; it depends only on the shape of the window:

$$C_{st} = \frac{\left[\int df\, |U(f)|^2\right]^2}{\int df\, |U(f)|^4}, \tag{23}$$

where U is the Fourier transform of u (see also Eq. (9)).

The first form in Eq. (22) for K_{∞} indicates that if windows are compared on the basis of equal statistical bandwidths (by appropriate choice of segment length L for each data window), then all windows have the same value of K_{∞} for large T/L; that is, all windows have the same variance-reduction capability, when compared on the basis of equal statistical bandwidths, if the available record length is much larger than the segment length. For other measures of bandwidth, such as the half-power bandwidth B, we are led to anticipate this same result. In a later section, we will demonstrate this quantitatively not only for $T/L \gg 1$ but for small values of this ratio as well, and for finite values of P, the number of pieces.

It is of interest to compare Eq. (20) with the results of Blackman and Tukey [2, Secs. B6-B8] for spectral estimation via the "indirect" correlation function approach. Their EDF at frequency f_1 is given approximately by

$$2T\, \frac{\left[\int_0^{\infty} df\, \left[Q_i(f+f_1) + Q_i(f-f_1)\right]\, G(f)\right]^2}{\int_0^{\infty} df\, \left[Q_i(f+f_1) + Q_i(f-f_1)\right]^2\, G^2(f)} \tag{24}$$

for long records, where Q_i is their spectral window. For frequencies f_1 greater than the width of spectral window Q_i, and assuming that Q_i is narrow compared with the finest detail in true spectrum G, Eq. (24) becomes approximately

$$2T\, \frac{\left[\int_0^{\infty} df\, Q_i(f-f_1)\right]^2}{\int_0^{\infty} df\, Q_i^2(f-f_1)}. \tag{25}$$

In order to relate the EDF in Eq. (25) to the one used here, we note that the mean value of Blackman and Tukey's spectral estimate is given by the convolution of Q_i with G. We then identify Q_i with $|W|^2$, obtaining for the EDF in Eq. (25):

$$2T \frac{\left[\int_{-\infty}^{\infty} df\, |W(f)|^2\right]^2}{\int_{-\infty}^{\infty} df\, |W(f)|^4}, \tag{26}$$

which is in agreement with Eq. (20) for long records. Thus, under the assumptions given above, the same limiting value of EDF is realized by both the "indirect" correlation approach and the present "direct" FFT approach; that is, both methods are capable of the same statistical stability if the proper overlap is used in the FFT approach.

DATA WINDOWS AND CHARACTERISTICS

Four data windows will be considered here. They are all continuous; however, they have differing degrees of continuity in their derivatives, leading to different rates of decay of their spectral windows for large frequencies. The triangular data window, made up of two straight-line segments, has a discontinuous first derivative. The cosine data window (Hanning) has a discontinuous second derivative. The quadratic data window is made up of segments of quadratic curves so chosen that the first derivative is everywhere continuous, but the second derivative is discontinuous; thus, the quadratic data window has behavior similar to that of the cosine data window. The cubic data window is made up of segments of cubic curves so chosen that the second derivative is everywhere continuous, but the third derivative is discontinuous. This sequence of windows will have progressively better high-frequency decay and, as will be seen shortly, better side lobes at low frequencies. (Hamming weighting is not considered because its discontinuous data window yields a slowly decaying spectral window for large frequencies.) Computation of the quadratic and cubic data windows is easier and faster than computation of the cosine data window in the time domain.* Their computational advantage and better sidelobe behavior, make them attractive candidates for spectral analysis.

---

*In the frequency domain, the cosine data window is equivalent to convolution with the sequence -1/4, 1/2, -1/4, which is easily implemented.

The four windows are detailed below in Eqs. (27) through (30). They have been normalized in such a way that $U(0) = 1$. From Eq. (9) and Fig. 1, notice that $u(t) = 0$ for $|t| \geq 1/2$. (The expressions for the correlations ϕ_u of the windows are collected in Appendix B; these correlations are necessary for the evaluation of Eq. (14).) In the following, $\mathrm{sinc}(x) \equiv \sin(\pi x)/(\pi x)$.

Triangular Data Window

$$u(t) = 2\,(1 - 2|t|), \qquad |t| \leq \frac{1}{2}$$

$$U(f) = \mathrm{sinc}^2(f/2) \quad . \tag{27}$$

Cosine Data Window

$$u(t) = 1 + \cos(2\pi t), \qquad |t| \leq \frac{1}{2}$$

$$U(f) = \frac{\mathrm{sinc}(f)}{1 - f^2} \quad . \tag{28}$$

Quadratic Data Window

$$u(t) = \begin{cases} \dfrac{9}{4}\left(1 - 12t^2\right), & |t| \leq \dfrac{1}{6} \\ \dfrac{27}{8}\left(1 - 2|t|\right)^2, & \dfrac{1}{6} \leq |t| \leq \dfrac{1}{2} \end{cases}$$

$$U(f) = \mathrm{sinc}^3(f/3) \quad . \tag{29}$$

Cubic Data Window

$$u(t) = \begin{cases} \frac{8}{3}\left(1 - 24t^2 + 48|t|^3\right), & |t| \le \frac{1}{4} \\ \frac{16}{3}\left(1 - 2|t|\right)^3, & \frac{1}{4} \le |t| \le \frac{1}{2} \end{cases}$$

$$U(f) = \text{sinc}^4(f/4) \ . \tag{30}$$

The function $W(f)$ is available from the normalized function $U(f)$ according to

$$W(f) = L\, U(Lf) \ , \tag{31}$$

upon Fourier transformation of Eq. (9). We define the half-power bandwidth of spectral window $|W|^2$ as the frequency range over which $|W|^2$ is greater than half of its peak value:

$$\left|W\left(\pm \frac{1}{2}B\right)\right|^2 = \frac{1}{2}\left|W(0)\right|^2 . \tag{32}$$

In addition to the statistical-bandwidth constant C_{st} defined in Eq. (21), we define a half-power-bandwidth constant C according to

$$B = \frac{C}{L} \ . \tag{33}$$

Numerical values for both of these dimensionless constants for the four windows are given in Table 1.

The bandwidth constants are larger for the "smoother" data windows; thus, their bandwidths are larger for a given segment length L (Fig. 1). Alternatively, if the bandwidths are to be kept equal for the four windows, the segment lengths must be larger for the smoother data windows.

In the bottom row of Table 1, the ratio of the statistical-bandwidth constant to the half-power-bandwidth constant is found to be relatively constant for the four windows considered. Thus, the statistical stability of the spectral esti-

Table 1

BANDWIDTH CONSTANTS

	Data Window			
	Triangular	Cosine	Quadratic	Cubic
C_{st}	1.854	2.079	2.304	2.686
C	1.276	1.441	1.572	1.820
C_{st}/C	1.454	1.443	1.466	1.476

mates can be discussed in terms of either bandwidth without fear of changing significantly the quantitative aspects. For example, Eq. (22) becomes

$$K_{\infty} \approx 2.9(T-L)B, \quad \text{for } \frac{T}{L} \gg 1, \tag{34}$$

in terms of half-power bandwidth B, where Eqs. (21) and (33) and Table 1 have been employed. A more precise relation than Eq. (34) will be given for K in the next section, where the number of pieces P will be finite.

Half of each symmetric spectral window is plotted in dB versus f/B in Figs. 3 through 6. Here

$$dB \equiv 10 \log_{10} |U|^2, \tag{35}$$

since the power-density spectrum G is seen through a window proportional to $|U|^2$. All the plots go through -3.01 dB at f/B = 1/2, since B is the half-power bandwidth. The slow spectral decay of the triangular data window and the fast spectral decay of the cubic data window are evident. The cosine and quadratic data windows exhibit intermediate behavior. The first three side lobes of the spectral windows are given in Table 2, where it is seen that the quadratic window offers an 8.3-dB improvement relative to the cosine window in the size of the first side lobe, and the cubic window yields an additional 13.3-dB improvement.

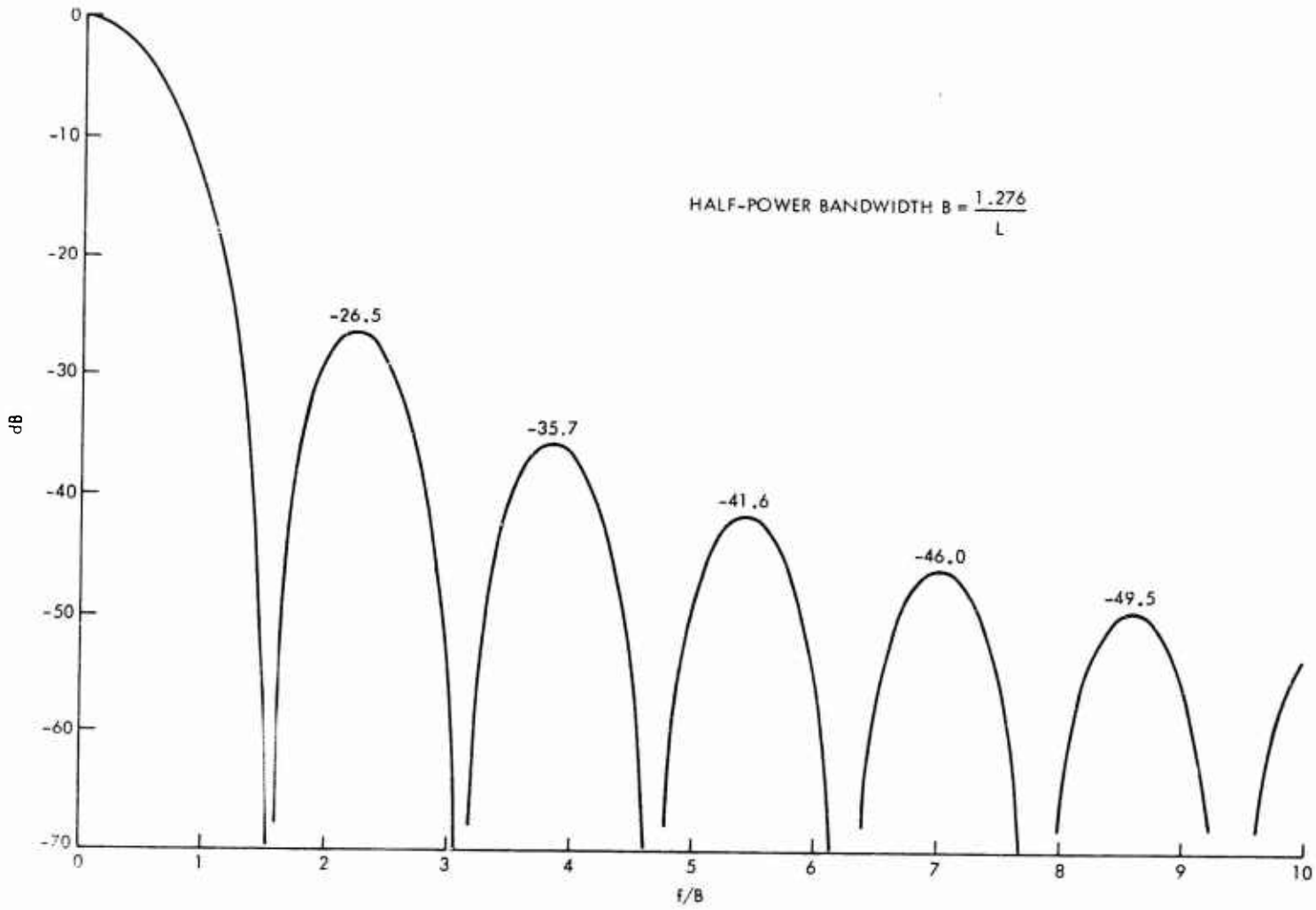


Fig. 3. Spectral Window for Triangular Data Window

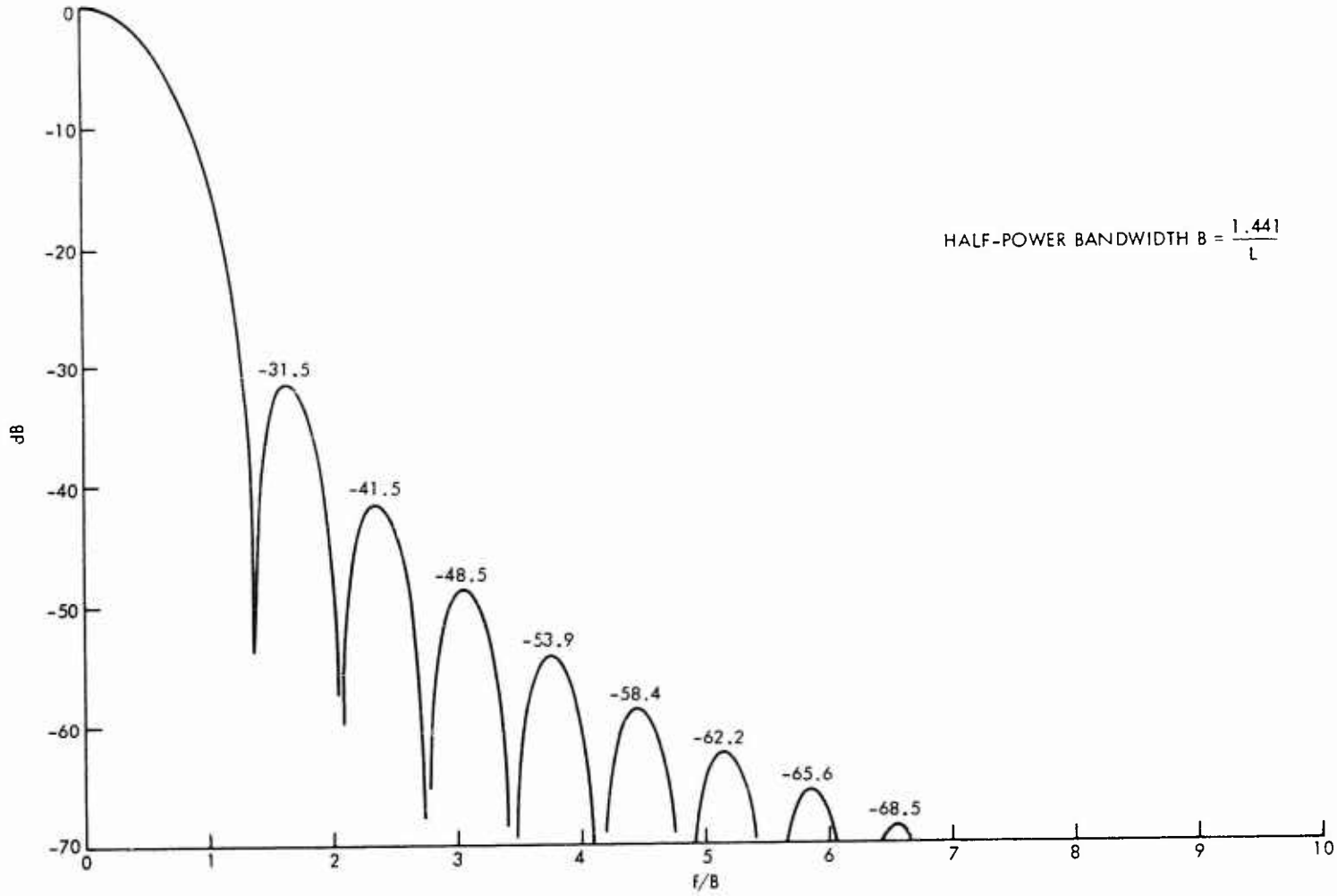


Fig. 4. Spectral Window for Cosine Data Window

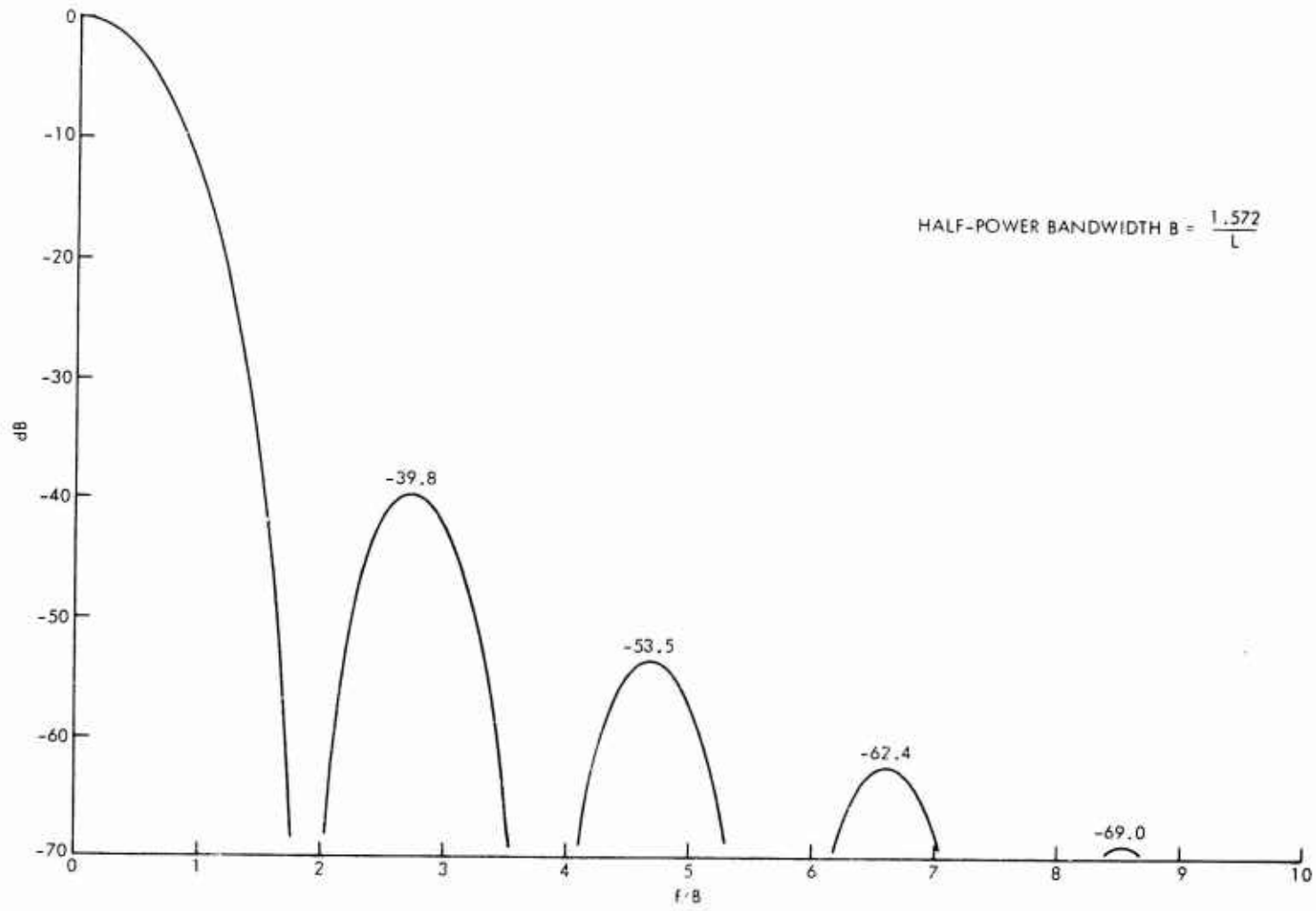


Fig. 5. Spectral Window for Quadratic Data Window

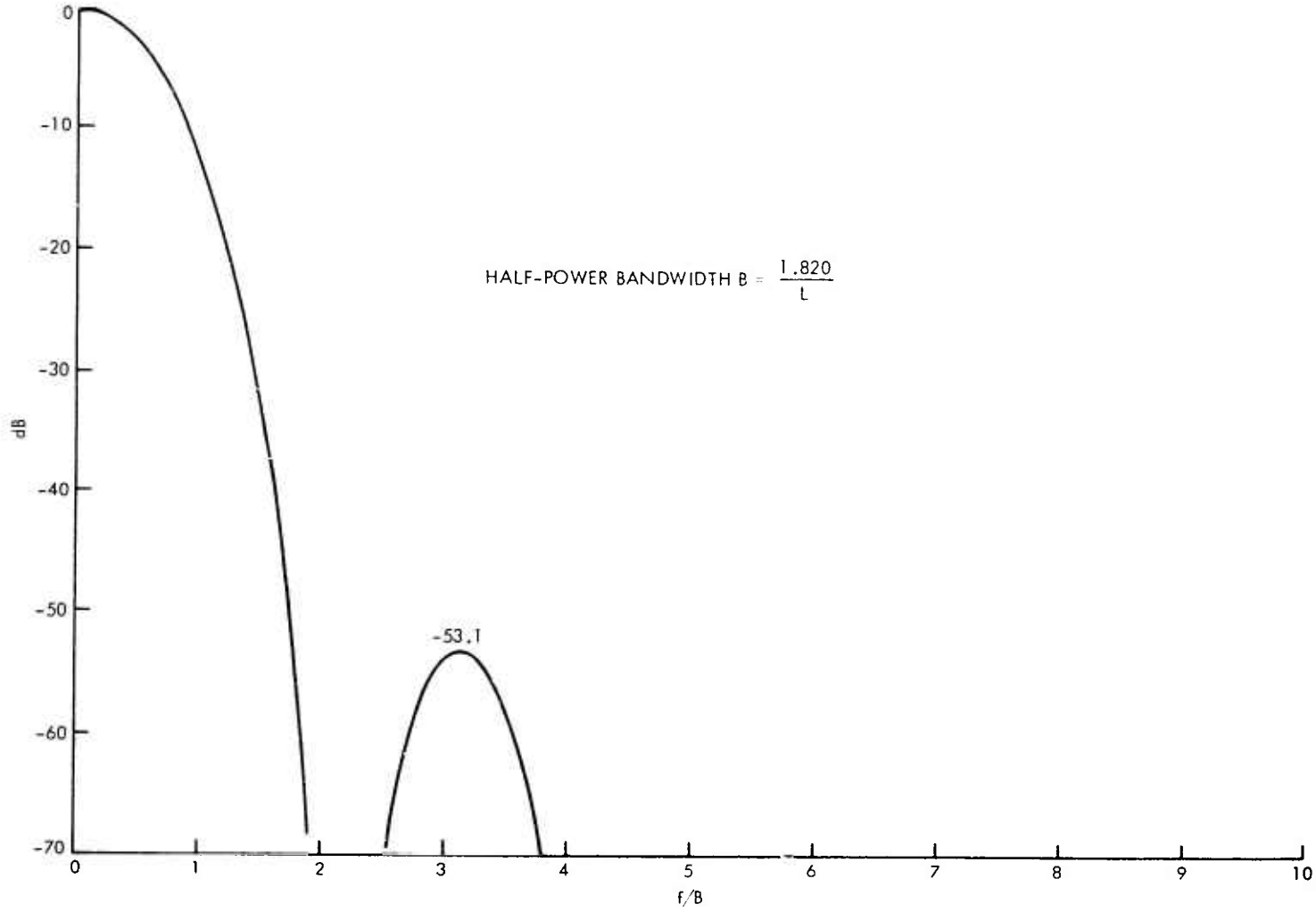


Fig. 6. Spectral Window for Cubic Data Window

Table 2

FIRST THREE SIDE LOBES OF
SPECTRAL WINDOWS

Data Window	Side Lobes (dB)		
Triangular	-26.5	-35.7	-41.6
Cosine	-31.5	-41.5	-48.5
Quadratic	-39.8	-53.5	-62.4
Cubic	-53.1	-71.3	-83.2

RESULTS

The general expression for EDF is given in Eq. (14). We eliminate the segment length L in this expression in favor of the half-power bandwidth B by using Eq. (33) to obtain the dependence on the fundamental parameter BT (see Introduction). It follows that

$$K = \frac{2P}{\sum_{k=-(P-1)}^{P-1} \left(1 - \frac{|k|}{P}\right) \left| \frac{\phi_u\left(k\frac{BT/C-1}{P-1}\right)}{\phi_u(0)} \right|^2} . \qquad (36)$$

For a particular window u and value of BT, K is computed versus P. A sample tabulation for the cosine data window and BT = 8 is given in Table 3. The column headed "Fractional Overlap" is a measure of how much the individual data windows overlap in the spectral processing technique depicted in Fig. 1 and is given by

Table 3

EQUIVALENT DEGREES OF FREEDOM
VERSUS NUMBER OF PIECES,
BT = 8, COSINE DATA WINDOW

P	K	Fractional Overlap
2	4.00	.00
3	6.00	.00
4	8.00	.00
5	10.00	.00
6	12.00	.09
7	14.00	.24
8	15.96	.35
9	17.74	.43
10	19.13	.49
11	20.03	.54
12	20.50	.59
13	20.69	.62
14	20.73	.65
15	20.71	.67
16	20.66	.70
17	20.61	.72
18	20.56	.73
19	20.52	.75
20	20.48	.76
30	20.19	.84
40	20.04	.88
50	19.95	.91
100	19.77	.95
200	19.67	.98

$$FO = \frac{L-S}{L} = \frac{P-T/L}{P-1} = \frac{P-BT/C}{P-1} \quad , \tag{37}$$

when non-negative. Equations (13) and (33) were employed in Eq. (37).

Several points in Table 3 are worth noting. For no overlap, the EDF increases linearly with P, and even as overlap begins to occur, the rate of increase of EDF remains the same. Thus, 24% overlap still yields the maximum possible EDF for P = 7. However, as P and the overlap increase further, the EDF increases more slowly, eventually reaching a maximum,* after which it decreases slightly for further increases in P. A point of diminishing returns is reached somewhere near P = 12, where 98% of the maximum (max) EDF is realized. The extra computational effort in spectral analysis for P > 12 is not worth the return in stability. The fractional overlap for 98% of max EDF is .59; the EDF is then 20.5, whereas it was only 10.0 for the last non-overlapped example. The case for overlapped processing is well demonstrated by Table 3.

Similar results for all four windows and BT = 2, 4, 8, 16, 32, and 64 are condensed in Table 4, which gives the required number of pieces and the corresponding fractional overlap for a specified fraction of the max EDF. For example, in Table 4B for the cosine data window, in order to realize a specified fraction of 98% of the max EDF at BT = 8, the number of pieces required is 12, and the corresponding fractional overlap is .59. The bottom row of each data-window table gives the max EDF for the corresponding value of BT. Also provided is an equation for max EDF, which was empirically determined to fit through the numerical values obtained.

Several striking invariances are apparent upon inspection of Table 4. First, for a given record length T and desired frequency resolution B, the max

---

* The existence of a finite value of P for maximum EDF is similar to the situation cited in Reference 11.

EDF is virtually independent* of the window employed; that is, all the windows considered have the same variance-reduction capability in spectral estimation when compared under the same frequency-resolution constraint. A simple, approximate rule of thumb for all four windows is given by

$$\max \text{EDF} \approx 3\,(\text{BT} - 1). \tag{38}$$

Recall that B is the half-power bandwidth of the spectral window.

For a given window and specified fraction of the max EDF, it will be observed from Table 4 that for $\text{BT} > 4$, the required fractional overlap is approximately constant (independent of BT). Therefore, in the last column of Table 4 is entered a representative or "average" fractional overlap required for the specified fraction of max EDF entered in the first column. (This simple rule does not hold well when 100% of the max EDF is required; accordingly, no value is entered for this case.)

For a given value of BT, the number of pieces required to realize .99 (or less) of max EDF is virtually independent of the particular window employed in spectral analysis. This independence is very important; it says that all four windows require the same number of FFTs in order to realize the same EDF and that selection among the windows, therefore, can not be based upon the number of FFTs required, but must be based upon some other consideration such as side-lobe level or size of FFT (to be discussed). An approximate rule of thumb for the number of pieces required is given by

$$\text{Number of pieces required} \sim 1.75\ \text{BT} \quad \text{for .99 of max EDF.} \tag{39}$$

For large BT products, the number of pieces required to realize max EDF is significantly larger than the number required to realize 99% of max EDF; thus, this large amount of additional processing yields insignificant improvement and is to be avoided.

---

*Very small values of BT are an exception; these are of little practical interest however.

Table 4

NUMBER OF PIECES REQUIRED (P) AND CORRESPONDING FRACTIONAL OVERLAP (FO) FOR A SPECIFIED FRACTION OF THE MAXIMUM EDF

Table 4A. Triangular Data Window

Specified Fraction of max EDF	BT												"Average" Fractional Overlap
	2		4		8		16		32		64		
	P	FO	P	FO	P	FO	P	FO	P	FO	P	FO	
.90	2	.43	5	.47	10	.41	21	.42	43	.43	87	.43	.43
.95	2	.43	5	.47	11	.47	23	.48	48	.49	96	.48	.48
.96	2	.43	5	.47	11	.47	24	.50	49	.50	99	.50	.50
.97	2	.43	6	.57	11	.47	25	.52	50	.51	102	.51	.52
.98	2	.43	6	.57	12	.52	25	.52	52	.53	107	.54	.54
.99	2	.43	6	.57	13	.56	27	.56	56	.56	115	.57	.56
1.00	2	.43	6	.57	14	.59	31	.62	100	.76	211	.77	—
max EDF	3.90		9.74		21.25		44.31		90.68		183.62		
max EDF ≈ 2.91 BT - 2.27													

Table 4B. Cosine Data Window

Specified Fraction of max EDF	BT												"Average" Fractional Overlap
	2		4		8		16		32		64		
	P	FO	P	FO	P	FO	P	FO	P	FO	P	FO	
.90	2	.36	5	.56	10	.49	21	.49	43	.51	86	.49	.50
.95	2	.36	5	.56	11	.54	23	.54	47	.54	95	.54	.54
.96	2	.36	5	.56	11	.54	24	.56	48	.55	98	.55	.55
.97	2	.36	5	.56	12	.59	24	.56	50	.57	101	.57	.57
.98	2	.36	5	.56	12	.59	25	.58	52	.58	105	.58	.58
.99	2	.36	6	.64	13	.62	27	.61	55	.61	112	.61	.61
1.00	2	.36	6	.64	14	.65	31	.66	68	.68	146	.70	—
max EDF	3.55		9.24		20.73		43.76		89.87		182.15		
max EDF ≈ 2.88 BT - 2.43													

Table 4C. Quadratic Data Window

Specified Fraction of max EDF	BT												"Average" Fractional Overlap
	2		4		8		16		32		64		
	P	FO	P	FO	P	FO	P	FO	P	FO	P	FO	
.90	2	.73	5	.61	10	.55	21	.54	43	.54	88	.54	.54
.95	2	.73	5	.61	11	.59	23	.58	48	.59	98	.59	.59
.96	2	.73	5	.61	11	.59	24	.60	49	.60	100	.60	.60
.97	2	.73	5	.61	12	.63	25	.62	51	.61	104	.61	.62
.98	2	.73	5	.61	12	.63	26	.63	53	.63	108	.63	.63
.99	2	.73	5	.61	13	.66	27	.65	56	.65	115	.65	.65
1.00	2	.73	6	.69	14	.69	32	.70	69	.72	146	.73	—
max EDF	3.10		8.96		20.64		44.05		90.91		184.67		

max EDF $\approx$ 2.93 BT - 2.87

Table 4D. Cubic Data Window

Specified Fraction of max EDF	BT												"Average" Fractional Overlap
	2		4		8		16		32		64		
	P	FO	P	FO	P	FO	P	FO	P	FO	P	FO	
.90	2	.90	4	.60	10	.62	21	.61	43	.61	88	.61	.61
.95	2	.90	5	.70	11	.66	23	.65	48	.65	98	.65	.65
.96	2	.90	5	.70	11	.66	24	.66	50	.66	101	.66	.66
.97	2	.90	5	.70	11	.66	25	.68	51	.67	105	.67	.67
.98	2	.90	5	.70	12	.69	26	.69	53	.68	109	.68	.69
.99	2	.90	5	.70	12	.69	27	.70	57	.70	116	.70	.70
1.00	2	.90	5	.70	14	.74	32	.75	70	.76	150	.77	—
max EDF	2.22		8.28		20.03		43.59		90.78		185.18		

max EDF $\approx$ 2.95 BT - 3.65

Table 5

REQUIRED FRACTIONAL OVERLAP FOR .99 max EDF

	Data Window			
	Triangular	Cosine	Quadratic	Cubic
Fractional Overlap	.56	.61	.65	.70

The required fractional overlap is greater for the better-side-lobe windows. Thus, for example, to realize .99 of max EDF, we have (virtually independent of the BT product) the values listed in Table 5. Notice that rather large overlaps are required for some windows.

The difficulty of realizing general fractional overlaps, such as .56, raises the question as to what fraction of max EDF is attainable if one restricts overlaps to a few easily realized overlaps such as .50 and .625. This question is answered in Tables 6 and 7.* Table 6 indicates that the cosine data window at 50% overlap (a popular case) yields 92% of the max EDF. However, the cubic data window realizes only 75% of its potential at 50% overlap. Table 7 shows that when the fractional overlap is increased to 5/8, the cosine and quadratic data windows realize virtually their ultimate capability. If the overlap is increased to 75%, the cubic data window then realizes its max EDF.

Table 6

ATTAINABLE FRACTION OF max EDF
AT .50 FRACTIONAL OVERLAP

	Data Window			
	Triangular	Cosine	Quadratic	Cubic
Fraction of max EDF	.96	.92	.85	.75

*These values are not attainable from Table 4 but come from the complete tabular results, of which Table 3 is one example.

Table 7

ATTAINABLE FRACTION OF MAX EDF
AT .625 FRACTIONAL OVERLAP

	Data Window		
	Cosine	Quadratic	Cubic
Fraction of max EDF	1.00	.98	.93

Thus far, no trade-off has been necessary to realize the better side lobes of the smoother data windows; that is, by proper choice of overlap, equal statistical stability is attainable, and an equal number of FFTs is required, for all four windows. However, there is one trade-off that enters as follows: if the original record length T is composed of samples of a process at increments* Δt, more samples are contained in the segment length L for the better-side-lobe windows; that is, the number of samples in interval L is

$$N_s = \frac{L}{\Delta t} = \frac{C}{B\,\Delta t} \quad , \tag{40}$$

employing Eq. (33). N_s is directly proportional to half-power-bandwidth constant C for a specified sampling increment Δt and resolution B. Thus, using Table 1, the cosine data window requires 1.13 times as many samples as the triangular data window requires. The corresponding ratios for the quadratic and cubic data windows are 1.23 and 1.43, respectively. Thus, better side lobes in spectral analysis can be realized at the expense of larger-size FFTs, rather than at the expense of statistical stability or number of FFTs. These comments hold for equal half-power bandwidths of the windows.

For a specified sampling increment Δt, desired resolution B, and particular window, Eq. (40) will generally not be a power of 2. Since FFTs run

*The sampling increment Δt must be chosen small enough to avoid aliasing; this is the only area where the bandwidth of the process comes into consideration.

faster when conducted at powers of 2, it is recommended that the desired resolution B be changed somewhat (increased or decreased) so as to make N_s a power of 2. This is generally a tolerable situation since B is often a "guesstimate" in the first place.

OPTIMUM WEIGHTING OF INDIVIDUAL SPECTRAL ESTIMATES

In Eq. (3), the p-th estimate $|Y_p(f)|^2$ of the power-density spectrum was weighted equally with all other estimates. In this section, we consider whether unequal weighting will yield additional worthwhile variance reduction. Inasmuch as the edge pieces in Fig. 1 are weighted only once by a data window, whereas the interior pieces are weighted more than once, perhaps heavier weighting of the edge pieces will yield additional stability. The power-density estimate is formed as

$$\tilde{G}(f) = \sum_{p=1}^{P} w_p \left| Y_p(f) \right|^2. \tag{41}$$

The derivation of the EDF of this estimate is given in Appendix C, which also presents the optimization of the EDF by choice of weights for a given P, record length, and window. A summary of the numerical results is given in Table 8, where P is varied up to 64. The largest value of EDF attained over that range of P is quoted in Table 8, except for BT = 16 where, with the exception of the triangular data window, P = 64 was not yet great enough to reach the max EDF by weighting.

Table 8

OPTIMUM EDF VALUES

Data Window	BT			
	2	4	8	16
Triangular	4.37	10.12	21.65	44.72
Cosine	4.50	10.15	21.44	>43.87
Quadratic	4.07	9.80	21.29	>44.18
Cubic	3.82	9.52	20.94	>43.72

A comparison of Table 8 with the max EDF values of Fig. 4 reveals that very little is to be gained by optimum weighting, except for small values of BT. However, small values of BT are not of great practical interest because the estimates are very unstable statistically. Also, the number of pieces P required to realize the optimum EDF is rather large; for example, in order to gain an improvement in EDF of 0.5 over the max EDF in Table 4, 19 pieces are required for the cosine data window, 20 pieces for the quadratic data window, and 15 pieces for the cubic data window. Moreover, the optimum weights are found to alternate in sign for some cases, causing a loss in significance.

DISCUSSION

This investigation of four good data windows indicates that there is no best window for spectral estimation. Rather, there is a trade-off to be made when choosing a window: the better-side-lobe windows require larger-size FFTs. When the proper overlap is used for each data window, the selection of windows can not be made on the basis of statistical stability or the number of FFTs required.

The quadratic and cubic data windows are simpler and quicker to compute than the cosine data window in the time domain (but not in the frequency domain as regards their effects). In addition, the quadratic and cubic windows have better side-lobe behavior and, therefore, merit serious consideration for spectral analysis. However, they require larger-size (but not more) FFTs than does the cosine data window.

The reason that the better-side-lobe windows do not require more FFTs than do the other windows is as follows. For a fixed half-power bandwidth B, the better-side-lobe windows require larger segment lengths L; however, the corresponding data windows tend to be more peaked near the center of the segment length. In order to utilize a given record length for maximum statistical stability, these data windows must, therefore, overlap for a greater percentage of the segment length. It turns out that the increased segment length and increased overlap almost exactly compensate each other, so that a constant number of FFTs is required regardless of the window selection.

This report has concentrated on the variance of the spectral estimates. In Appendix D, it is shown that the covariance of spectral estimates at two different frequencies is always positive but is essentially zero when the frequencies differ by more than the width of the spectral window. Thus, spectral estimates at frequencies farther apart than B are statistically linearly independent of each other.

REVERSE BLANK

Appendix A

DERIVATION OF MEAN AND VARIANCE

From Eqs. (2) and (3), the spectral estimate at frequency f is

$$\hat{G}(f) = \frac{1}{P}\sum_{p=1}^{P}\iint du\, dv\, \exp\left(-i2\pi f(u-v)\right)\, x(u)x^*(v) \cdot$$

$$w\left[u - \frac{L}{2} - (p-1)S\right]\, w^*\left[v - \frac{L}{2} - (p-1)S\right] . \qquad (A-1)$$

(For completeness, process x and window w are allowed to be complex.) The mean value of $\hat{G}(f)$ is obtained by ensemble-averaging Eq. (A-1) over the possible realizations of process x. Expressing the correlation of x as a Fourier transform of spectrum G, we find the average value

$$E\left\{\hat{G}(f)\right\} = \frac{1}{P}\sum_{p=1}^{P}\iint du\, dv\, \exp\left(-i2\pi f(u-v)\right)\int d\nu\, \exp\left(i2\pi(u-v)\nu\right)\, G(\nu) \cdot$$

$$w\left[u - \frac{L}{2} - (p-1)S\right]\, w\left[v - \frac{L}{2} - (p-1)S\right]$$

$$= \int d\nu\, G(\nu)\left|W(f-\nu)\right|^2 = \int d\nu\, G(f-\nu)\left|W(\nu)\right|^2 , \qquad (A-2)$$

where we have utilized Eq. (4). If spectral window $|W|^2$ is narrower than the finest detail in the true spectrum G, Eq. (A-2) becomes

$$E\left\{\hat{G}(f)\right\} \cong G(f)\int d\nu\, \left|W(\nu)\right|^2 . \qquad (A-3)$$

Equation (A-2) is not limited to Gaussian processes but is, in fact, true for any stationary process.

In order to evaluate the variance of the spectral estimate, we start with

$$E\{\hat{G}^2(f)\} = \frac{1}{P^2}\sum_{p=1}^{P}\sum_{q=1}^{P}\iiiint du\,dv\,dr\,ds\,\exp\left(-i2\pi f(u-v+r-s)\right)\,E\{x(u)x^*(v)x(r)x^*(s)\}\cdot$$

$$w\left[u-\frac{L}{2}-(p-1)S\right]\,w^*\left[v-\frac{L}{2}-(p-1)S\right]\,w\left[r-\frac{L}{2}-(q-1)S\right]\,w^*\left[s-\frac{L}{2}-(q-1)S\right]\,. \tag{A-4}$$

In order to simplify this expression, we must be able to evaluate the fourth-order average. If x is a real Gaussian random process, the average in Eq. (A-4) becomes

$$R(u-v)\,R(r-s) + R(u-r)\,R(v-s) + R(u-s)\,R(r-v)\,, \tag{A-5}$$

where R is the correlation of process x. (If x is a complex envelope of a Gaussian process, the middle term in Eq. (A-5) is absent [12].) When we express correlation R as a Fourier transform of spectrum G and substitute Eq. (A-5) in Eq. (A-4), we obtain

$$E\{\hat{G}^2(f)\} = \frac{1}{P^2}\sum_{p=1}^{P}\sum_{q=1}^{P}\iiiint du\,dv\,dr\,ds\,\exp\left(-i2\pi f(u-v+r-s)\right)\cdot$$

$$w\left[u-\frac{L}{2}-(p-1)S\right]\,w^*\left[v-\frac{L}{2}-(p-1)S\right]\,w\left[r-\frac{L}{2}-(q-1)S\right]\,w^*\left[s-\frac{L}{2}-(q-1)S\right]\cdot$$

$$\iint d\mu\,d\nu\,G(\mu)\,G(\nu)\,\left[\exp\left(i2\pi\mu(u-v)+i2\pi\nu(r-s)\right) + \exp\left(i2\pi\mu(u-r)+i2\pi\nu(v-s)\right)\right.$$

$$\left. + \exp\left(i2\pi\mu(u-s)+i2\pi\nu(r-v)\right)\right]$$

$$= \frac{1}{P^2}\sum_{p=1}^{P}\sum_{q=1}^{P}\iint d\mu\,d\nu\,G(\mu)\,G(\nu)\,\left[|W(f-\mu)|^2\,|W(f-\nu)|^2 + \exp(i2\pi(\mu+\nu)(p-q)S)\cdot\right.$$

$$\left. W(f-\mu)\,W^*(f+\nu)\,W(f+\mu)\,W^*(f-\nu) + \exp(i2\pi(\mu-\nu)(p-q)S)\,|W(f-\mu)|^2\,|W(f-\nu)|^2\right]\,, \tag{A-6}$$

using Eq. (4). The first term in Eq. (A-6) is recognized from Eq. (A-2) as the square of the mean of $\hat{G}$. Therefore,

$$\mathrm{Var}\{\hat{G}(f)\} = \frac{1}{P^2}\sum_{p=1}^{P}\sum_{q=1}^{P}\left|\int d\mu\, G(\mu)\, \exp(i2\pi\mu(p-q)S)\, W(f-\mu)\, W(f+\mu)\right|^2$$

$$+\frac{1}{P^2}\sum_{p=1}^{P}\sum_{q=1}^{P}\left|\int d\mu\, G(\mu)\, \exp(i2\pi\mu(p-q)S)\, |W(f-\mu)|^2\right|^2 . \quad (A-7)$$

Now if f, the frequency of interest, is greater than the bandwidth of the spectral window $|W|^2$ (i.e., a couple of resolution cells away from the origin), then $W(f-\mu)$ and $W(f+\mu)$ do not overlap significantly. Letting B be the half-power bandwidth of the spectral window $|W|^2$, we therefore have the excellent approximation* for $f > B$,

$$\mathrm{Var}\{\hat{G}(f)\} \cong \frac{1}{P^2}\sum_{p=1}^{P}\sum_{q=1}^{P}\left|\int d\mu\, G(\mu)\, \exp(i2\pi\mu(p-q)S)\, |W(f-\mu)|^2\right|^2 . \quad (A-8)$$

(For $f = 0$, the two terms in Eq. (A-7) are equal if data window w is real, in which case $\mathrm{Var}\{\hat{G}(0)\}$ is double that given by Eq. (A-8) at $f = 0$.) Making the change of variable $k = p-q$ in Eq. (A-8), we obtain

$$\mathrm{Var}\{\hat{G}(f)\} \cong \frac{1}{P}\sum_{k=-(P-1)}^{P-1}\left(1 - \frac{|k|}{P}\right)\left|\int d\mu\, \exp(i2\pi\mu kS)\, G(\mu)\, |W(f-\mu)|^2\right|^2 . \quad (A-9)$$

But if the bandwidth B of spectral window $|W|^2$ is narrower than the finest detail in spectrum G, the integral on μ in Eq. (A-9) can be approximated by

$$G(f)\int d\mu\, \exp(i2\pi\mu kS)\, |W(f-\mu)|^2$$

$$= G(f)\, \exp(i2\pi fkS)\, \phi_W^*(kS) , \quad (A-10)$$

where we have utilized Eqs. (4) and (7). Then Eq. (A-9) becomes

---

*When x is a complex envelope, Eq. (A-8) is exact; see comment under Eq. (A-5).

$$\mathrm{Var}\{\hat{G}(f)\} \cong G^2(f)\frac{1}{P}\sum_{k=-(P-1)}^{P-1}\left(1-\frac{|k|}{P}\right)\left|\phi_w(kS)\right|^2 \quad . \qquad \text{(A-11)}$$

This equation is similar to that given in [9, p. 71].

Equations (A-3) and (A-11) are the main products of this appendix.

Appendix B

CORRELATIONS OF DATA WINDOWS

The correlation of the normalized data window u is given by Eq. (11) as

$$\phi_u(\tau) = \int dt\, u(t)\, u^*(t-\tau) \,. \tag{B-1}$$

This quantity is required for the calculation of EDF, K, in Eq. (14). Since $u(t) = 0$ for $|t| \geq 1/2$, then $\phi_u(\tau) = 0$ for $|\tau| \geq 1$. Thus, for the:

Triangular Data Window

$$\frac{\phi_u(\tau)}{\phi_u(0)} = \left\{ \begin{array}{ll} 1 - 6\tau^2 + 6|\tau|^3, & |\tau| \leq \frac{1}{2} \\ 2\,(1 - |\tau|)^3, & \frac{1}{2} \leq |\tau| \leq 1 \end{array} \right\} . \tag{B-2}$$

Cosine Data Window

$$\frac{\phi_u(\tau)}{\phi_u(0)} = \frac{2}{3}(1 - |\tau|)\left[1 + \frac{1}{2}\cos(2\pi\tau)\right] + \frac{1}{2\pi}\sin(2\pi|\tau|), \quad |\tau| \leq 1 \,. \tag{B-3}$$

Quadratic Data Window

$$\frac{\phi_u(\tau)}{\phi_u(0)} = \left\{ \begin{array}{ll} \frac{81}{22}(1 - |\tau|)^5 \equiv Q_1(\tau), & \frac{2}{3} \leq |\tau| \leq 1 \\ Q_1(\tau) - \frac{243}{11}\left(\frac{2}{3} - |\tau|\right)^5 \equiv Q_2(\tau), & \frac{1}{3} \leq |\tau| \leq \frac{2}{3} \\ Q_2(\tau) + \frac{1215}{22}\left(\frac{1}{3} - |\tau|\right)^5, & |\tau| \leq \frac{1}{3} \end{array} \right\} . \tag{B-4}$$

Cubic Data Window

$$\frac{\phi_u(\tau)}{\phi_u(0)} = \begin{cases} \frac{1024}{151}(1 - |\tau|)^7 \equiv C_1(\tau), & \frac{3}{4} \le |\tau| \le 1 \\ C_1(\tau) - \frac{8192}{151}\left(\frac{3}{4} - |\tau|\right)^7 \equiv C_2(\tau), & \frac{1}{2} \le |\tau| \le \frac{3}{4} \\ C_2(\tau) + \frac{28672}{151}\left(\frac{1}{2} - |\tau|\right)^7 \equiv C_3(\tau), & \frac{1}{4} \le |\tau| \le \frac{1}{2} \\ C_3(\tau) - \frac{57344}{151}\left(\frac{1}{4} - |\tau|\right)^7, & |\tau| \le \frac{1}{4} \end{cases} . \qquad \text{(B-5)}$$

The forms for the correlation of the quadratic and cubic data windows are compact and very useful for computer programming.

Appendix C

OPTIMUM WEIGHTS FOR EDF

The estimate of the power-density spectrum is given by Eq. (41). By generalizing the results in Appendix A, we have

$$\mathrm{Var}\left\{\tilde{G}(f)\right\} \cong \sum_{k=-(P-1)}^{P-1} \gamma_k \left| \int d\mu \, \exp(i2\pi\mu kS) \, G(\mu) \, |W(f-\mu)|^2 \right|^2 , \qquad \text{(C-1)}$$

where

$$\gamma_k = \sum_q w_{q+k} \, w_q^* . \qquad \text{(C-2)}$$

The sum is over all non-zero terms. Utilizing the same assumptions used in Appendix A, we have

$$\mathrm{Var}\left\{\tilde{G}(f)\right\} \cong G^2(f) \sum_{k=-(P-1)}^{P-1} \gamma_k \left| \phi_w(kS) \right|^2 , \qquad \text{(C-3)}$$

$$E\left\{\tilde{G}(f)\right\} \cong G(f) \sum_p w_p \, \phi_w(0) , \qquad \text{(C-4)}$$

yielding

$$\tilde{K} = 2 \frac{\left| \sum_p w_p \right|^2}{\sum_{k=-(P-1)}^{P-1} \gamma_k \, M_k} , \qquad \text{(C-5)}$$

where

$$M_k \equiv \left| \frac{\phi_w(kS)}{\phi_w(0)} \right|^2 = M_{-k} \, . \tag{C-6}$$

Partially differentiating $\tilde{K}$ with respect to w_j^* [13, Appendix] and noting that the absolute scale of weights $\{w_p\}$ does not enter in $\tilde{K}$, we see that the optimum weights must satisfy the equation

$$\sum_k M_k \, w_{j+k} = 1, \quad 1 \le j \le P \, . \tag{C-7}$$

If we define the matrices

$$M = \left[M_{m-n} \right], \quad 1 \le m, \, n \le P \, ,$$

$$1^T = [1 \;\; 1 \ldots \;\; 1], \; w^T = [w_1 \;\; w_2 \ldots \;\; w_P] \, , \tag{C-8}$$

then the optimum weights are

$$w = M^{-1} 1 \, , \tag{C-9}$$

and the optimum EDF is

$$\tilde{K} = 2 \;\; 1^T M^{-1} 1 \, . \tag{C-10}$$

Appendix D

COVARIANCE OF SPECTRAL ESTIMATES

A generalization of the technique in Appendix A leads to the following expression for the covariance between spectral estimates at frequencies f_1 and f_2:

$$\mathrm{Cov}\{\hat{G}(f_1), \hat{G}(f_2)\} = \frac{1}{P^2}\sum_{p=1}^{P}\sum_{q=1}^{P}\left|\int d\mu\, G(\mu)\, W(f_1-\mu)\, W(f_2+\mu)\, \exp(i2\pi\mu(p-q)S)\right|^2$$

$$+\frac{1}{P^2}\sum_{p=1}^{P}\sum_{q=1}^{P}\left|\int d\mu\, G(\mu)\, W(f_1-\mu)\, W^*(f_2-\mu)\exp(i2\pi\mu(p-q)S\right|^2 . \tag{D-1}$$

Now if f_1+f_2 is greater than the bandwidth of the spectral window, $W(f_1-\mu)$ and $W(f_2+\mu)$ are essentially non-overlapping. Then,

$$\mathrm{Cov} \cong \frac{1}{P}\sum_{k=-(P-1)}^{P-1}\left(1-\frac{|k|}{P}\right)\left|\int d\mu\, G(\mu)\, W(f_1-\mu)\, W^*(f_2-\mu)\exp(i2\pi\mu kS)\right|^2 . \tag{D-2}$$

This quantity is always positive. However, it is very small when $|f_2-f_1|>B$ because $W(f_1-\mu)$ and $W(f_2-\mu)$ do not overlap then.

When true spectrum G varies but slightly over a frequency range B,

$$\mathrm{Cov} \cong G(f_1)\, G(f_2)\sum_{k=-(P-1)}^{P-1}\left(1-\frac{|k|}{P}\right)\left|\chi(kS,\, f_2-f_1)\right|^2 , \tag{D-3}$$

where

$$\chi(\tau, f) \equiv \int d\mu \exp(i2\pi\mu\tau)\, W(\mu+f)W^*(\mu)$$

$$= \int dt \exp(-i2\pi ft)\, w(t)\, w^*(t-\tau) \qquad \text{(D-4)}$$

is the ambiguity function of window w. Again, if $|f_1-f_2| > B$, Eq. (D-3) is essentially zero, as shown by the first form in Eq. (D-4).

As an example, for the cosine window and 0% overlap, the covariance coefficient (ratio of Cov to the square-root of the product of variances) is $1, \frac{4}{9}, \frac{1}{36}, 0, 0, \ldots$, for $|f_2-f_1| = 0, \frac{1}{L}, \frac{2}{L}, \frac{3}{L}, \frac{4}{L}, \ldots$, respectively. Thus spectral estimates $\frac{2}{L}$ Hz apart are essentially uncorrelated. For 50% overlap (and large P), the corresponding covariance coefficients are slightly larger, being 1, .495, .068, .005, 0, ...

REFERENCES

1. M. S. Bartlett, An Introduction to Stochastic Processes, with Special Reference to Methods and Applications, Cambridge University Press, Cambridge, 1953.

2. R. B. Blackman and J. W. Tukey, The Measurement of Power Spectra from the Point of View of Communications Engineering, Dover Publications, Inc., New York, 1959.

3. E. Parzen, "Mathematical Considerations in the Estimation of Spectra," Technometrics, vol. 3, 1961, p. 167.

4. R. B. Blackman, Data Smoothing and Prediction, Addison-Wesley Publishing Company, Inc., Reading, Mass., 1965.

5. J. S. Bendat and A. G. Piersol, Measurement and Analysis of Random Data, J. Wiley & Sons, Inc., New York, 1966.

6. G. M. Jenkins and D. G. Watts, Spectral Analysis and Its Applications, Holden-Day Company, San Francisco, 1968.

7. IEEE Transactions on Audio and Electroacoustics, Special Issue on Fast Fourier Transform, vol. AU-15, no. 2, June 1967.

8. IEEE Transactions on Audio and Electroacoustics, Special Issue on Fast Fourier Transform, vol. AU-17, no. 2, June 1969.

9. P. D. Welch, "The Use of FFT for the Estimation of Power Spectra: a Method Based on Time Averaging over Short Modified Periodograms," IEEE Transactions on Audio and Electroacoustics, vol. AU-15, no. 2, June 1967, pp. 70-73.

10. C. Bingham, M. D. Godfrey, and J. W. Tukey, "Modern Techniques of Power Spectrum Estimation," IEEE Transactions on Audio and Electroacoustics, vol. AU-15, no. 2, June 1967.

11. H. T. Balch et al., "Estimation of the Mean of a Stationary Random Process by Periodic Sampling," Bell System Technical Journal, May-June 1966, pp. 733-741.

12. A. H. Nuttall, "High-Order Covariance Functions for Complex Gaussian Processes," IEEE Transactions on Information Theory, vol. IT-8, no. 3, April 1962, pp. 255-256.

13. A. H. Nuttall, "Trigonometric Smoothing and Interpolation of Sampled Complex Functions, via the FFT," NUSC Technical Memorandum No. TC-94-71, 19 April 1971.

NUSC Technical Report 4169-S
11 July 1975

Estimation of Cross-Spectra Via Overlapped Fast Fourier Transform Processing

Albert H. Nuttall

ABSTRACT

The optimum overlap to be used for estimation of cross-spectra via FFT processing of windowed data is shown to be identical to that for estimation of auto-spectra. In addition, a useful geometric interpretation of the random errors in cross-spectral estimation, and their covariances, is furnished.

Approved for public release; distribution unlimited.

TABLE OF CONTENTS

	Page
LIST OF ILLUSTRATIONS	ii
INTRODUCTION	1
PROBLEM DEFINITION	1
PROBLEM SOLUTION	2
VARIANCES OF QUADRATURE COMPONENTS OF CROSS-SPECTRUM ESTIMATE	4
VARIANCES OF AMPLITUDE AND PHASE ESTIMATES	7
EFFECT OF CLOSELY SPACED TONES	8
APPENDIX — DERIVATION OF MOMENTS	9
REFERENCES	15

LIST OF ILLUSTRATIONS

Figure		Page
1	Complex Random Variables in Cross-Spectrum Estimation	4
2	Projections of Random Error $\hat{g}(f)$	4
3	Scatter of Cross-Spectral Estimates	6

ESTIMATION OF CROSS-SPECTRA VIA OVERLAPPED FAST FOURIER TRANSFORM PROCESSING

INTRODUCTION

In a recent report (Ref. 1), the use of overlapped fast Fourier transform (FFT) processing of windowed data for estimation of auto-spectra was thoroughly investigated. It is now desired to extend these results to estimation of cross-spectra. The method of overlapped FFT processing is often used for cross-spectral and coherence estimation with good results (see, for example, Ref. 2); here we wish to give analytical back-up to its optimality.

PROBLEM DEFINITION

Consider that stationary random processes $x(t)$ and $y(t)$ have been observed for a time interval of T seconds, $0<t<T$. Let the auto-spectra of the processes at frequency f be $G_{xx}(f)$ and $G_{yy}(f)$, respectively, and let the (complex) cross-spectrum be $G_{xy}(f)$. The method of estimating the cross-spectrum is discussed thoroughly on pages 2-4 of Ref. 1, and will not be repeated here; the reader is referred to that reference for notation, related past work, and qualifications. We let $w(t)$ denote the fundamental data window, and S the shift of each successive overlapped window, and define

$$W_k(t) = w\left(t - \frac{L}{2} - (k-1)S\right), \quad 1 \le k \le P, \tag{1}$$

where P is the total number of overlapped segments fitting into the $(0,T)$ interval. The estimate of the cross-spectrum is*

$$\hat{G}_{xy}(f) = \frac{1}{P}\sum_{k=1}^{P} X_k(f)\, Y_k^*(f), \tag{2}$$

where

$$X_k(f) = \int dt\, \exp(-i2\pi ft)\, W_k(t)\, x(t),$$

$$Y_k(f) = \int dt\, \exp(-i2\pi ft)\, W_k(t)\, y(t). \tag{3}$$

(The continuous versus discrete versions of (3) are discussed on page 4 of Ref. 1.)

The estimate in (2) is a complex random variable (RV) which it is hoped will approximate the true cross-spectrum $G_{xy}(f)$ for sufficiently large P and proper choice of shift S. The problem is to evaluate the stability of the RV $\hat{G}_{xy}(f)$, and optimize the stability by choice of overlap. At the

*Carets denote random variables, and integrals without limits are over the range of non-zero integrand.

same time, we wish to investigate the dependence of the stability on the fundamental parameters such as observation time T, desired frequency resolution B, spectra $G_{xx}(f)$, $G_{yy}(f)$, $G_{xy}(f)$, etc.

PROBLEM SOLUTION

In Appendix A, the mean of RV $\hat{G}_{xy}(f)$ is determined to be

$$E\{\hat{G}_{xy}(f)\} = \int d\mu\, G_{xy}(\mu)\,|W(f-\mu)|^2 \tag{4A}$$

$$\cong G_{xy}(f)\int d\mu\,|W(\mu)|^2 = G_{xy}(f), \tag{4B}$$

where

$$W(f) \equiv \int dt\, \exp(-i2\pi ft)\, w(t), \tag{5}$$

and we have assumed, with no loss of generality, that $\int df\,|W(f)|^2 = 1$. The exact relation (4A) indicates that the mean is equal to the convolution of the true spectrum $G_{xy}(f)$ with a spectral window $|W(f)|^2$. (Desirable aspects of windows are discussed on pages 10-18 of Ref. 1.) The approximation (4B) is valid when the frequency width B of spectral window $|W(f)|^2$ is narrower than the finest detail in the true spectrum $G_{xy}(f)$. These results are not restricted to Gaussian processes, but hold for any stationary processes $x(t)$ and $y(t)$.

We now define the zero-mean complex RV

$$\hat{g}(f) = \hat{G}_{xy}(f) - E\{\hat{G}_{xy}(f)\} = \hat{G}_{xy}(f) - G_{xy}(f). \tag{6}$$

This RV measures the deviation of the estimate of cross-spectrum from its true value. In Appendix A, the following two relations are demonstrated:

$$E\{|\hat{g}^2(f)|\} \cong G_{xx}(f)G_{yy}(f)\frac{1}{P}\sum_{k=-P+1}^{P-1}\left(1-\frac{|k|}{P}\right)\left|\phi_w(kS)\right|^2, \tag{7A}$$

$$E\{\hat{g}^2(f)\} \cong G_{xy}^2(f)\frac{1}{P}\sum_{k=-P+1}^{P-1}\left(1-\frac{|k|}{P}\right)\left|\phi_w(kS)\right|^2, \tag{7B}$$

where

$$\phi_w(\tau) \equiv \int dt\, w(t)\, w^*(t-\tau). \tag{8}$$

Three assumptions are required for the validity of (7): the processes $x(t)$ and $y(t)$ are jointly Gaussian; the frequency f of interest must be greater than bandwidth B of window $|W(f)|^2$; and bandwidth B must be less

than the narrowest detail in $G_{xx}(f)$, $G_{yy}(f)$, and $G_{xy}(f)$. (A case where B is greater than the narrowest detail is discussed later.)

A measure of the stability of a RV is afforded by its equivalent number of degrees of freedom (EDF); see Ref. 3, p. 22. For a complex RV $\hat{z}$, we extend the definition to

$$EDF = 2 \frac{\left|E\{\hat{z}\}\right|^2}{E\left\{\left|\hat{z} - E\{\hat{z}\}\right|^2\right\}} . \tag{9}$$

The denominator of (9) could be interpreted as the variance of complex RV $\hat{z}$. Interpreting $\hat{z}$ as $\hat{G}_{xy}(f)$, and using (4B), (6), (7A), (8), and Parseval's Theorem, there follows for the EDF at frequency f,

$$EDF = \left|\gamma_{xy}(f)\right|^2 K, \tag{10}$$

where

$$\gamma_{xy}(f) \equiv \frac{G_{xy}(f)}{\left[G_{xx}(f)\, G_{yy}(f)\right]^{1/2}} , \tag{11}$$

and

$$K \equiv \frac{2P}{\sum_{k=-P+1}^{P-1} \left(1 - \frac{|k|}{P}\right) \left|\frac{\phi_w(kS)}{\phi_w(0)}\right|^2} . \tag{12}$$

The quantity $\gamma_{xy}(f)$ is the complex coherence at frequency f of processes x(t) and y(t). Equation (10) indicates that the EDF at frequency f of RV $\hat{G}_{xy}(f)$ is given by the product of two factors, one frequency-dependent solely on the processes' spectra (over which we have no control*), and the other depending solely on the method of processing, but being frequency-independent. Specifically, K depends on the number of pieces P in the average (2), the shift S of each window in (1), and the autocorrelation $\phi_w(\tau)$ of the window w(t). Furthermore, this factor K is precisely the same quantity encountered in Ref. 1 as the EDF for auto-spectral estimation. Therefore all the results of Ref. 1 on maximization of K by choice of shift S are immediately brought to bear on the present problem of cross-spectral estimation. Thus, the optimum choice of overlap for cross-spectral estimation is identical to that for auto-spectral estimation.**

*Linear filtering of x(t) and/or y(t), such as pre-whitening, would not affect $|\gamma_{xy}(f)|^2$, and therefore not affect EDF. A related observation on this aspect is made in Ref. 4, p. 379.

**More generally, since all the variances of the estimates in the following sections depend inversely on K, maximization of K is appropriate, regardless of the particular definition of stability.

VARIANCES OF QUADRATURE COMPONENTS OF CROSS-SPECTRUM ESTIMATE

The zero-mean complex RV $\hat{g}(f)$ in (6) is the random error in estimation of the cross-spectrum. The diagram in Fig. 1 depicts the

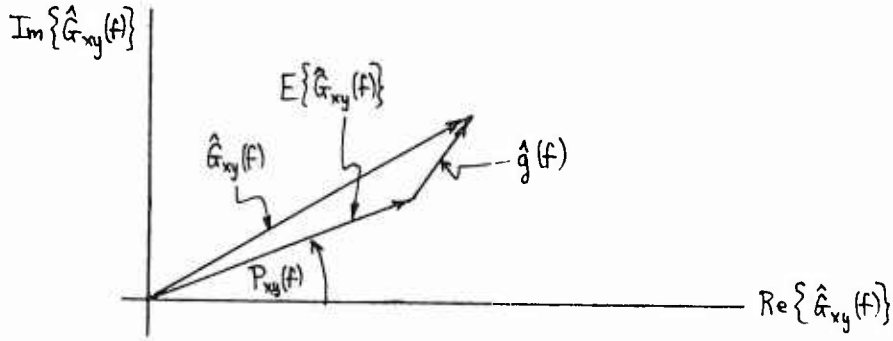


Fig. 1. Complex Random Variables in Cross-Spectrum Estimation

relationships between the various complex RVs. Here

$$P_{xy}(f) = \arg\{G_{xy}(f)\} \tag{13}$$

is the true phase of the cross-spectrum.

It is convenient to represent complex RV $\hat{g}(f)$ in terms of its real and imaginary components,

$$\hat{g}(f) = \hat{\ell}(f) + i\,\hat{q}(f), \tag{14}$$

as shown in Fig. 2. Also depicted are the projections of $\hat{g}(f)$ on a

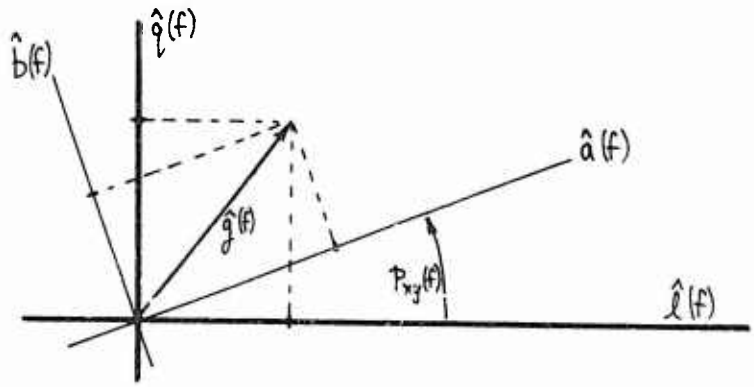


Fig. 2. Projections of Random Error $\hat{g}(f)$

different rectangular coordinate system $(\hat{a}(f), \hat{b}(f))$ aligned with the direction of the true phase $P_{xy}(f)$ of the cross-spectrum. That is, we also represent

$$\hat{g}(f) \exp\left[-i P_{xy}(f)\right] = \hat{a}(f) + i\,\hat{b}(f), \tag{15}$$

where $\hat{a}(f)$ and $\hat{b}(f)$ are real. We note immediately that all the RVs in (14) and (15) have zero mean; this follows from the definition (6).

In order to evaluate the covariances of these various quadrature components, we first note from (7), (12), and the fact that $\phi_w(o)$ has been assumed unity, that

$$E\left\{|\hat{g}(f)|^2\right\} = 2\,G_{xx}(f)\,G_{yy}(f)/K, \tag{16A}$$

$$E\left\{\hat{g}^2(f)\right\} = 2\,G_{xy}^2(f)/K. \tag{16B}$$

Equation (16A) (or (7A)) affords the interesting interpretation that the average squared-length of the random error $\hat{g}(f)$ in the estimate of the cross-spectrum is, in fact, independent of the true cross-spectrum, but depends on the auto-spectra of the two processes involved. (See also (A15) more generally.)

Substituting (14) in (16), there immediately follows

$$\begin{aligned} E\left\{\begin{matrix}\hat{\ell}^2(f) \\ \hat{q}^2(f)\end{matrix}\right\} &= \left[G_{xx}(f)\,G_{yy}(f) \pm \mathrm{Re}\left\{G_{xy}^2(f)\right\}\right]/K \\ &= \left[G_{xx}(f)\,G_{yy}(f) \pm \mathrm{Re}^2\left\{G_{xy}(f)\right\} \mp \mathrm{Im}^2\left\{G_{xy}(f)\right\}\right]/K \\ &= G_{xx}(f)\,G_{yy}(f)\left[1 \pm \mathrm{Re}\left\{\gamma_{xy}^2(f)\right\}\right]/K, \end{aligned} \tag{17A}$$

$$\begin{aligned} E\left\{\hat{\ell}(f)\,\hat{q}(f)\right\} &= \mathrm{Im}\left\{G_{xy}^2(f)\right\}/K = 2\,\mathrm{Re}\left\{G_{xy}(f)\right\}\mathrm{Im}\left\{G_{xy}(f)\right\}/K \\ &= G_{xx}(f)\,G_{yy}(f)\,\mathrm{Im}\left\{\gamma_{xy}^2(f)\right\}/K. \end{aligned} \tag{17B}$$

The quantities in (17) are the covariances of the real and imaginary parts of the cross-spectrum estimate; that is, using (6) and (14),

$$\begin{aligned} \mathrm{Var}\left[\mathrm{Re}\left\{\hat{G}_{xy}(f)\right\}\right] &= E\left\{\hat{\ell}^2(f)\right\}, \\ \mathrm{Var}\left[\mathrm{Im}\left\{\hat{G}_{xy}(f)\right\}\right] &= E\left\{\hat{q}^2(f)\right\}, \\ \mathrm{Cov}\left[\mathrm{Re}\left\{\hat{G}_{xy}(f)\right\}, \mathrm{Im}\left\{\hat{G}_{xy}(f)\right\}\right] &= E\left\{\hat{\ell}(f)\,\hat{q}(f)\right\}. \end{aligned} \tag{18}$$

Equations (17) and (18) are basically identical to Ref. 4, p. 378; however, the scale factor K is different.

The projections $\hat{a}(f)$ and $\hat{b}(f)$ have simpler properties than $\hat{\ell}(f)$ and $\hat{q}(f)$. From (15), (16), and (13), there follows

$$E\left\{\begin{matrix}\hat{a}^2(f)\\ \hat{b}^2(f)\end{matrix}\right\} = \left[G_{xx}(f)\,G_{yy}(f) \pm |G_{xy}(f)|^2\right]/K$$

$$= G_{xx}(f)\,G_{yy}(f)\left[1 \pm |\gamma_{xy}(f)|^2\right]/K,$$

$$E\{\hat{a}(f)\hat{b}(f)\} = 0. \qquad (19)$$

Thus the projections of the random error along and perpendicular to the direction of the true phase of the cross-spectrum are uncorrelated. Furthermore, the variance of the projection $\hat{a}(f)$ along the direction of the true phase is <u>always</u> greater than or equal to the variance of the projection $\hat{b}(f)$ perpendicular to the true phase. In fact, if the magnitude-squared coherence is unity at some frequency f_1, then the variance of $\hat{b}(f_1)$ is zero; in this case, all random fluctuations of $\hat{G}_{xy}(f_1)$ lie along the line with phase $\theta_{xy}(f_1)$ in Fig. 1.

On the other hand, if the magnitude-squared coherence is zero at some frequency f_2, then the variances of $\hat{a}(f_2)$ and $\hat{b}(f_2)$ are equal; in this case, the "scatter" of random perturbations $\hat{g}(f_2)$ in Fig. 1 is a circle centered at the origin.

Generally, the scatter of random perturbations is like an ellipse, as depicted in Fig. 3, where the major axis of the ellipse lies on the line

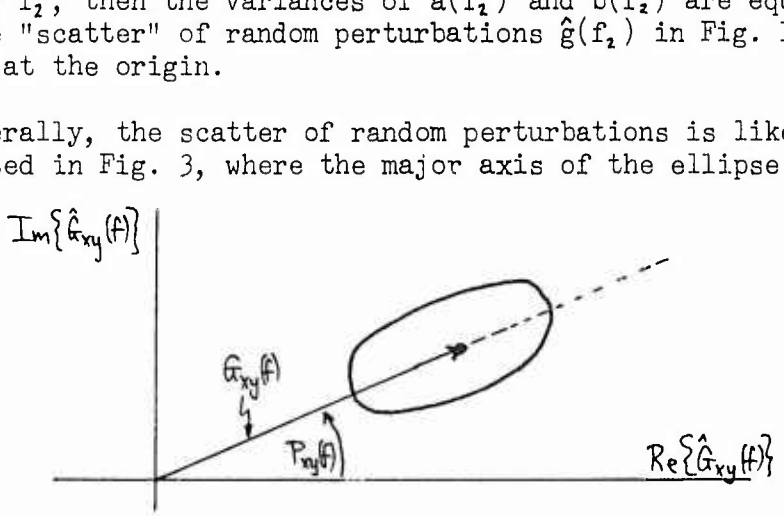


Fig. 3. Scatter of Cross-Spectral Estimates

with phase $\theta_{xy}(f)$. If RVs $\hat{a}(f)$ and $\hat{b}(f)$ are Gaussian, as they would be (approximately) if K is large, then the elliptical diagram can be made quantitative and interpreted as contours of iso-probability.

VARIANCES OF AMPLITUDE AND PHASE ESTIMATES

Estimates of the amplitude and phase of the cross-spectrum are available according to

$$\hat{G}_{xy}(f) = \hat{A}_{xy}(f) \exp\left[i \hat{P}_{xy}(f)\right]. \tag{20}$$

In order to estimate the means and variances of $\hat{A}_{xy}(f)$ and $\hat{P}_{xy}(f)$, we will assume that the scatter of points in Fig. 3 is small in comparison with the distance out to the center of the ellipse. That is, using (9) and (10), we will assume that

$$|\gamma_{xy}(f)|^2 K \gg 1. \tag{21}$$

This requires that the product of observation time and desired frequency resolution be much larger than unity (Ref. 1), but it also requires that the magnitude-squared coherence not be too small at the frequency of interest.

We first utilize (20), (6), and (15) to express

$$\hat{G}_{xy}(f) = \left[|G_{xy}(f)| + \hat{a}(f) + i\,\hat{b}(f)\right] \exp\left[i\,P_{xy}(f)\right]. \tag{22}$$

Then

$$\hat{A}_{xy}(f) = \left| |G_{xy}(f)| + \hat{a}(f) + i\,\hat{b}(f) \right| \tag{23A}$$

$$\cong |G_{xy}(f)| + \hat{a}(f), \tag{23B}$$

$$\hat{P}_{xy}(f) = P_{xy}(f) + \arg\left\{|G_{xy}(f)| + \hat{a}(f) + i\,\hat{b}(f)\right\} \tag{24A}$$

$$\cong P_{xy}(f) + \frac{\hat{b}(f)}{|G_{xy}(f)|}. \tag{24B}$$

Equations (23A) and (24A) are actually exact, whereas (23B) and (24B) require the assumption of (21). Combining (23B), (24B), and (19), there follows immediately

$$\mathrm{Var}\left\{\hat{A}_{xy}(f)\right\} = \left[G_{xx}(f)G_{yy}(f) + |G_{xy}(f)|^2\right]/K$$

$$= G_{xx}(f)G_{yy}(f)\left[1 + |\gamma_{xy}(f)|^2\right]/K, \tag{25A}$$

$$\mathrm{Var}\left\{\hat{P}_{xy}(f)\right\} = \frac{1 - |\gamma_{xy}(f)|^2}{|\gamma_{xy}(f)|^2 K}, \tag{25B}$$

$$\mathrm{Cov}\left\{\hat{A}_{xy}(f), \hat{P}_{xy}(f)\right\} = 0. \tag{25C}$$

Thus the amplitude and phase estimates are uncorrelated. The variance of the phase estimate in (25B) is much smaller than unity, when we recall that assumption (21) is necessary for (25) to be true; that is, the denominator of (25B) must always be large. It should also be noticed that none of the covariances in eqs. (19) or (25) depend on the actual phase of the cross-spectrum, but only on its magnitude. Some additional relations on the covariances of estimates of coherence are given in Ref. 4, pp. 378-9; of course, the phase estimates of complex coherence and cross-spectrum are identical.

EFFECT OF CLOSELY SPACED TONES

All the earlier results have presumed that the bandwidth B of the spectral window $|W(f)|^2$ is narrower than the finest detail in the spectra $G_{xx}(f)$, $G_{yy}(f)$, and $G_{xy}(f)$. We now consider a case where this is not so, and investigate the variance of the cross-spectrum estimate.

Suppose the spectra are approximately pure tones:

$$G_{xx}(f) \cong \tfrac{1}{2} P_x \left[\delta(f-f_x) + \delta(f+f_x)\right],$$

$$G_{yy}(f) \cong \tfrac{1}{2} P_y \left[\delta(f-f_y) + \delta(f+f_y)\right]. \tag{26}$$

Then from (A27) in the appendix,

$$E\left\{|\hat{g}^2(f)|\right\} \cong \tfrac{1}{4} P_x P_y \left|W(f-f_x)\right|^2 \left|W(f-f_y)\right|^2 \left[\frac{\sin(P\pi(f_x-f_y)S)}{P\sin(\pi(f_x-f_y)S)}\right]^2, \tag{27}$$

which can be interpreted as the variance of the complex RV $\hat{G}_{xy}(f)$. Now if $|f_x-f_y| < B$, and if the frequency f of interest lies near or between f_x and f_y, then the window functions in (27) are near their peak value $W(0)$. Also, if $|f_x-f_y| < (2PS)^{-1} \cong (2T)^{-1}$, then the bracketed term in (27) is near unity. Then the variance in the cross-spectrum estimate is large; in fact, it has the same value as for $P=1$, no averaging. Yet the true cross-spectrum may in fact be zero. Thus estimation of the cross-spectrum will be in error, even for a large TB product, in a frequency range near f_x and f_y. It should be noted that this noisy estimation case requires the frequency separation of the tones to be less than $(2T)^{-1}$, not $(2L)^{-1}$; thus the tone separation must be much closer than the fundamental resolution of $B \approx L^{-1}$.

If the tone separation, on the other hand, satisfies $|f_x-f_y| > (PS)^{-1} = T^{-1}$, then the variance of estimation is greatly reduced, as inspection of the bracketed term in (27) indicates. In fact, (27) becomes

$$E\left\{|\hat{g}^2(f)|\right\} \lesssim \tfrac{1}{4} P_x P_y \left|W(f-f_x)\right|^2 \left|W(f-f_y)\right|^2 \left[P\pi(f_x-f_y)S\right]^{-2}, \text{ if } |f_x-f_y| < (4S)^{-1}, \tag{28}$$

which has the desirable P^{-2} dependence on the number of pieces in the average (2). Of course, when $|f_x-f_y| > B$, then the window functions in (27) decay rapidly and indicate a greatly reduced variance, even if B is greater than the finest detail in the spectra.

APPENDIX A. DERIVATION OF MOMENTS

From (2),

$$E\left\{\hat{G}_{xy}(f)\right\} = \frac{1}{P}\sum_{k=1}^{P} E\left\{X_k(f)\,Y_k^*(f)\right\}. \tag{A1}$$

But from (3),

$$E\left\{X_k(f)\,Y_k^*(f)\right\} = \iint dt_1\,dt_2\,\exp\left(-i2\pi f(t_1-t_2)\right)w_k(t_1)\,w_k^*(t_2)\,R_{xy}(t_1-t_2), \tag{A2}$$

where

$$R_{xy}(\tau) = E\left\{x(t)\,y^*(t-\tau)\right\} \tag{A3}$$

is the cross-correlation of x(t) and y(t). We are allowing all processes and windows to be complex, for generality, and have utilized joint-stationarity in (A3). The cross-spectrum of x(t) and y(t) is

$$G_{xy}(f) = \int d\tau\,\exp(-i2\pi f\tau)R_{xy}(\tau). \tag{A4}$$

Utilizing (A4) and (5) in (A2), there follows for (A1),

$$E\left\{\hat{G}_{xy}(f)\right\} = \int d\mu\,G_{xy}(\mu)\left|W(f-\mu)\right|^2; \tag{A5}$$

we have also employed the fact that

$$W_k(f) = W(f)\exp\left[-i2\pi f\left(\tfrac{1}{2}+(k-1)S\right)\right], \tag{A6}$$

which follows from (1). Equation (A5) is the fundamental relation for the mean of the cross-spectral estimate. However, when $\mathcal{B}$ is less than the finest detail in $G_{xy}(f)$,

$$E\left\{\hat{G}_{xy}(f)\right\} \cong G_{xy}(f)\int d\mu\left|W(\mu)\right|^2 = G_{xy}(f), \tag{A7}$$

upon setting $\int df\,|W(f)|^2 = 1$, without loss of generality.

To evaluate the variance of $\hat{G}_{xy}(f)$, the following steps are required: from (2),

$$E\left\{\left|\hat{G}_{xy}^2(f)\right|\right\} = \frac{1}{P^2}\sum_{k,m=1}^{P} E\left\{X_k(f)\,Y_k^*(f)\,X_m^*(f)\,Y_m(f)\right\}. \tag{A8}$$

But the statistical average in (A8) is, using (3),

$$E\left\{\cdots_{kkmm}\right\} = \iiint\!\!\int dt_1\,dt_2\,dt_3\,dt_4\,\exp\left[-i2\pi f(t_1-t_2-t_3+t_4)\right]w_k(t_1)\,w_k^*(t_2)\,w_m^*(t_3)\,w_m(t_4)$$
$$\cdot\,E\left\{x(t_1)\,y^*(t_2)\,x^*(t_3)\,y(t_4)\right\}. \tag{A9}$$

Further, the statistical average in (A9) is given by

$$E\{\dots\} = R_{xy}(t_1-t_2)R^*_{xy}(t_3-t_4) + R_{xx}(t_1-t_3)R^*_{yy}(t_2-t_4) + R_{xy}(t_1-t_4)R^*_{xy}(t_3-t_2), \tag{A10}$$

where we have assumed that $x(t)$ and $y(t)$ are joint Gaussian, and have defined

$$\begin{aligned} R_{xx}(\tau) &= E\{x(t)\,x^*(t-\tau)\}, \\ R_{yy}(\tau) &= E\{y(t)\,y^*(t-\tau)\}, \\ R_{xy}(\tau) &= E\{x(t)\,y(t-\tau)\}. \end{aligned} \tag{A11}$$

(The last function in (A11) is generally different from (A3).) Denoting the Fourier transforms of the three functions in (A11) by $G_{xx}(f)$, $G_{yy}(f)$, $\mathcal{G}_{xy}(f)$ respectively, in a manner similar to (A4), (A10) becomes

$$\begin{aligned} E\{\dots\} = \iint d\mu\, d\nu \Big\{ & \exp[i2\pi\mu(t_1-t_2)]G_{xy}(\mu)\exp[-i2\pi\nu(t_3-t_4)]\,G^*_{xy}(\nu) \\ & + \exp[i2\pi\mu(t_1-t_3)]G_{xx}(\mu)\exp[-i2\pi\nu(t_2-t_4)]\,G_{yy}(\nu) \\ & + \exp[i2\pi\mu(t_1-t_4)]\mathcal{G}_{xy}(\mu)\exp[-i2\pi\nu(t_3-t_2)]\,\mathcal{G}^*_{xy}(\nu)\Big\}. \end{aligned} \tag{A12}$$

($G_{xx}(f)$ and $G_{yy}(f)$ must always be real.) Substituting (A12) in (A9), there follows

$$\begin{aligned} E\{\dots\} = \iint d\mu\, d\nu \iiiint & dt_1\,dt_2\,dt_3\,dt_4 \exp[-i2\pi f(t_1-t_2-t_3+t_4)]W_k(t_1)W^*_k(t_2)W^*_m(t_3)W_m(t_4) \\ \cdot\Big[& G_{xy}(\mu)G^*_{xy}(\nu)\exp[i2\pi\mu(t_1-t_2)-i2\pi\nu(t_3-t_4)] \\ & + G_{xx}(\mu)G_{yy}(\nu)\exp[i2\pi\mu(t_1-t_3)-i2\pi\nu(t_2-t_4)] \\ & + \mathcal{G}_{xy}(\mu)\mathcal{G}^*_{xy}(\nu)\exp[i2\pi\mu(t_1-t_4)-i2\pi\nu(t_3-t_2)]\Big] \end{aligned}$$

$$\begin{aligned} = \iint d\mu\, d\nu \Big[& G_{xy}(\mu)G^*_{xy}(\nu)W_k(f-\mu)W^*_k(f-\mu)W^*_m(f-\nu)W_m(f-\nu) \\ & + G_{xx}(\mu)G_{yy}(\nu)W_k(f-\mu)W^*_k(f-\nu)W^*_m(f-\mu)W_m(f-\nu) \\ & + \mathcal{G}_{xy}(\mu)\mathcal{G}^*_{xy}(\nu)W_k(f-\mu)W^*_k(f+\nu)W^*_m(f-\nu)W_m(f+\mu)\Big] \end{aligned}$$

$$= \iint d\mu\, d\nu \Big[G_{xy}(\mu)\, G^*_{xy}(\nu) \big|W(f-\mu)\big|^2 \big|W(f-\nu)\big|^2$$

$$+ G_{xx}(\mu)\, G_{yy}(\nu) \big|W(f-\mu)\big|^2 \big|W(f-\nu)\big|^2 \exp\big[i2\pi S(k-m)(\mu-\nu)\big]$$

$$+ \mathcal{G}_{xy}(\mu;\nu)\, \mathcal{G}^*_{xy}(\nu) W(f-\mu) W^*(f+\nu) W(f+\mu) W^*(f-\nu) \exp\big[i2\pi S(k-m)(\mu+\nu)\big] \Big]$$

$$= \left| \int d\mu\, G_{xy}(\mu) \big|W(f-\mu)\big|^2 \right|^2$$

$$+ \int d\mu\, G_{xx}(\mu) \big|W(f-\mu)\big|^2 \exp\big[i2\pi(k-m)\mu S\big] \int d\nu\, G_{yy}(\nu) \big|W(f-\nu)\big|^2 \exp\big[-i2\pi(k-m)\nu S\big]$$

$$+ \int d\mu\, \mathcal{G}_{xy}(\mu) W(f-\mu) W(f+\mu) \exp\big[i2\pi(k-m)\mu S\big] \int d\nu\, \mathcal{G}^*_{xy}(\nu) W^*(f-\nu) W^*(f+\nu) \exp\big[i2\pi(k-m)\nu S\big]. \quad (A13)$$

Upon substitution of (A13) in (A8), we obtain

$$E\big\{ \big| \hat{G}^2_{xy}(f) \big| \big\} = \left| \int d\mu\, G_{xy}(\mu) \big|W(f-\mu)\big|^2 \right|^2$$

$$+ \frac{1}{P^2} \sum_{k,m=1}^{P} \Big\{ \int d\mu\, G_{xx}(\mu) \big|W(f-\mu)\big|^2 \exp\big[i2\pi(k-m)\mu S\big] \int d\nu\, G_{yy}(\nu) \big|W(f-\nu)\big|^2 \exp\big[-i2\pi(k-m)\nu S\big]$$

$$+ \int d\mu\, \mathcal{G}_{xy}(\mu) W(f-\mu) W(f+\mu) \exp\big[i2\pi(k-m)\mu S\big] \int d\nu\, \mathcal{G}^*_{xy}(\nu) W^*(f-\nu) W^*(f+\nu) \exp\big[i2\pi(k-m)\nu S\big] \Big\}$$

$$= \Big| E\big\{ \hat{G}_{xy}(f) \big\} \Big|^2 + E\big\{ \big| \hat{g}^2(f) \big| \big\}, \quad (A14)$$

where we have used (6). If the frequency f of interest is greater than the bandwidth B of the window $|W(f)|^2$, then $W(f-\mu)$ and $W(f+\mu)$ do not overlap on the μ-scale. Then

$$E\big\{ \big| \hat{g}^2(f) \big| \big\} \cong \frac{1}{P^2} \sum_{k,m=1}^{P} \int d\mu\, G_{xx}(\mu) \big|W(f-\mu)\big|^2 \exp\big[i2\pi(k-m)\mu S\big]$$
$$\cdot \int d\nu\, G_{yy}(\nu) \big|W(f-\nu)\big|^2 \exp\big[-i2\pi(k-m)\nu S\big]$$

$$= \frac{1}{P} \sum_{k=-P+1}^{P-1} \left(1 - \frac{|k|}{P}\right) \int d\mu\, G_{xx}(\mu) \big|W(f-\mu)\big|^2 \exp\big(i2\pi k \mu S\big)$$
$$\cdot \int d\nu\, G_{yy}(\nu) \big|W(f-\nu)\big|^2 \exp\big(-i2\pi k \nu S\big). \quad (A15)$$

This is a general relation for $E\{|\hat{g}^2(f)|\}$; it will be noticed to be independent of cross-spectrum $G_{xy}(f)$, and depend only on auto-spectra $G_{xx}(f)$ and $G_{yy}(f)$.

Also, there is no need to know $\mathcal{G}_{xy}(f)$.

If B is less than the narrowest detail in $G_{xx}(f)$ and $G_{yy}(f)$ near the frequency f of interest, the integral on μ in (A15) becomes approximately

$$G_{xx}(f)\exp(i2\pi f k S)\,\phi_w^*(kS), \tag{A16}$$

and (A15) yields

$$E\{|\hat{g}^2(f)|\} \cong G_{xx}(f)\,G_{yy}(f)\frac{1}{P}\sum_{k=-P+1}^{P-1}\left(1-\frac{|k|}{P}\right)|\phi_w(kS)|^2. \tag{A17}$$

Since $\hat{G}_{xy}(f)$ is a complex RV, it is necessary also to evaluate the quantity $E\{\hat{G}_{xy}^2(f)\}$, in addition to (A8), in order to complete the second-order moments. Due to the similarity to the derivations above, the steps will be presented in a more cursory fashion.

$$E\{\hat{G}_{xy}^2(f)\} = \frac{1}{P^2}\sum_{k,m=1}^{P} E\{X_k(f)Y_k^*(f)X_m(f)Y_m^*(f)\}. \tag{A18}$$

$$E\{\cdots\} = \iiiint dt_1\,dt_2\,dt_3\,dt_4\,\exp[-i2\pi f(t_1-t_2+t_3-t_4)]\,w_k(t_1)\,w_k^*(t_2)\,w_m(t_3)\,w_m^*(t_4)$$
$$\cdot E\{x(t_1)\,y^*(t_2)\,x(t_3)\,y^*(t_4)\}. \tag{A19}$$

$$E\{\cdots\} = R_{xy}(t_1-t_2)R_{xy}(t_3-t_4) + R_{xx}(t_1-t_3)R_{yy}^*(t_2-t_4) + R_{xy}(t_1-t_4)R_{xy}(t_3-t_2)$$

$$= \iint d\mu\,d\nu\Big\{\exp[i2\pi\mu(t_1-t_2)]\,G_{xy}(\mu)\exp[i2\pi\nu(t_3-t_4)]\,G_{xy}(\nu)$$
$$+ \exp[i2\pi\mu(t_1-t_3)]\,\mathcal{G}_{xx}(\mu)\exp[-i2\pi\nu(t_2-t_4)]\,\mathcal{G}_{yy}^*(\nu)$$
$$+ \exp[i2\pi\mu(t_1-t_4)]\,G_{xy}(\mu)\exp[i2\pi\nu(t_3-t_2)]\,G_{xy}(\nu)\Big\}. \tag{A20}$$

$$E\{\cdots\} = \iint d\mu\,d\nu\Big[G_{xy}(\mu)\,G_{xy}(\nu)W_k(f-\mu)W_k^*(f-\mu)W_m(f-\nu)W_m^*(f-\nu)$$
$$+\mathcal{G}_{xx}(\mu)\,\mathcal{G}_{yy}^*(\nu)W_k(f-\mu)\,W_k^*(f-\nu)\,W_m(f+\mu)\,W_m^*(f+\nu)$$
$$+ G_{xy}(\mu)\,G_{xy}(\nu)W_k(f-\mu)\,W_k^*(f-\nu)\,W_m(f-\nu)\,W_m^*(f-\mu)\Big]$$

$$= \iint d\mu\,d\nu\Big[G_{xy}(\mu)\,G_{xy}(\nu)|W(f-\mu)|^2\,|W(f-\nu)|^2$$
$$+\mathcal{G}_{xx}(\mu)\,\mathcal{G}_{yy}^*(\nu)W(f-\mu)W^*(f-\nu)W(f+\mu)W^*(f+\nu)\exp[i2\pi S(k-m)(\mu-\nu)]$$
$$+ G_{xy}(\mu)\,G_{xy}(\nu)W(f-\mu)W^*(f-\nu)W^*(f-\mu)W(f-\nu)\exp[i2\pi S(k-m)(\mu-\nu)]\Big]$$

$$= \left[\int d\mu\, G_{xy}(\mu)\,|W(f-\mu)|^2\right]^2$$

$$+\int d\mu\, \mathcal{G}_{xx}(\mu)W(f-\mu)W(f+\mu)\exp[i2\pi(k-m)\mu S]\int d\nu\, \mathcal{G}^*_{yy}(\nu)W^*(f-\nu)W^*(f+\nu)\exp[-i2\pi(k-m)\nu S]$$

$$+\int d\mu\, G_{xy}(\mu)|W(f-\mu)|^2\exp[i2\pi(k-m)\mu S]\int d\nu\, G_{xy}(\nu)|W(f-\nu)|^2\exp[-i2\pi(k-m)\nu S]. \qquad (A21)$$

$$E\{\hat{G}^2_{xy}(f)\} = \left[\int d\mu\, G_{xy}(\mu)\,|W(f-\mu)|^2\right]^2$$

$$+\frac{1}{P^2}\sum_{k,m=1}^{P}\Big\{\int d\mu\, \mathcal{G}_{xx}(\mu)W(f-\mu)W(f+\mu)\exp[i2\pi(k-m)\mu S]\int d\nu\, \mathcal{G}^*_{yy}(\nu)W^*(f-\nu)W^*(f+\nu)\exp[-i2\pi(k-m)\nu S]$$

$$+\int d\mu\, G_{xy}(\mu)|W(f-\mu)|^2\exp[i2\pi(k-m)\mu S]\int d\nu\, G_{xy}(\nu)|W(f-\nu)|^2\exp[-i2\pi(k-m)\nu S]\Big\}$$

$$= \left[E\{\hat{G}_{xy}(f)\}\right]^2 + E\{\hat{q}^2(f)\}. \qquad (A22)$$

If f is greater than B ,

$$E\{\hat{q}^2(f)\} \cong \frac{1}{P^2}\sum_{k,m=1}^{P}\int d\mu\, G_{xy}(\mu)\,|W(f-\mu)|^2\exp[i2\pi(k-m)\mu S]$$
$$\cdot\int d\nu\, G_{xy}(\nu)\,|W(f-\nu)|^2\exp[-i2\pi(k-m)\nu S]$$

$$= \frac{1}{P}\sum_{k=-P+1}^{P-1}\left(1-\frac{|k|}{P}\right)\int d\mu\, G_{xy}(\mu)\,|W(f-\mu)|^2\exp(i2\pi k\mu S)$$
$$\cdot\int d\nu\, G_{xy}(\nu)\,|W(f-\nu)|^2\exp(-i2\pi k\nu S). \qquad (A23)$$

This general relation for $E\{\hat{q}^2(f)\}$ depends only on the cross-spectrum $G_{xy}(f)$, and not on the auto-spectra $G_{xx}(f)$ and $G_{yy}(f)$. Also, there is no need to know $\mathcal{G}_{xx}(f)$ or $\mathcal{G}_{yy}(f)$.

If B is less the narrowest detail in $G_{xy}(f)$ near the frequency f of interest, the integral on μ in (A23) becomes approximately

$$G_{xy}(f)\exp(i2\pi fkS)\,\phi^*_w(kS), \qquad (A24)$$

and (A23) yields

$$E\{\hat{q}^2(f)\} \cong G^2_{xy}(f)\frac{1}{P}\sum_{k=-P+1}^{P-1}\left(1-\frac{|k|}{P}\right)\left|\phi_w(kS)\right|^2. \qquad (A25)$$

For the case where x(t) and y(t) contain pure tones (eq. (26) of main text), the general relation (A15) for $E\{|\hat{g}^2(f)|\}$ takes on the following form: first the integral on μ in (A15) is approximately

$$\tfrac{1}{2}P_x\left|W(f-f_x)\right|^2 \exp\left(i2\pi k f_x S\right). \tag{A26}$$

Then (A15) becomes

$$E\{|\hat{g}^2(f)|\} \cong \tfrac{1}{4}P_x P_y\left|W(f-f_x)\right|^2\left|W(f-f_y)\right|^2 \frac{1}{P}\sum_{K=-P+1}^{P-1}\left(1-\frac{|k|}{P}\right)\exp\left(i2\pi k(f_x-f_y)S\right)$$

$$= \tfrac{1}{4}P_x P_y\left|W(f-f_x)\right|^2\left|W(f-f_y)\right|^2\left[\frac{\sin\left(P\pi(f_x-f_y)S\right)}{P\sin\left(\pi(f_x-f_y)S\right)}\right]^2, \tag{A27}$$

using Ref. 5, (418) and (428); this relation is used in (27).

REFERENCES

1. A. H. Nuttall, Spectral Estimation by Means of Overlapped Fast Fourier Transform Processing of Windowed Data, NUSC Technical Report 4169, 13 October 1971.

2. G. C. Carter, Estimation of the Magnitude-Squared Coherence Function (Spectrum), NUSC Technical Report 4343, 19 May 1972.

3. R. B. Blackman and J. W. Tukey, The Measurement of Power Spectra from the Point of View of Communications Engineering, Dover Publications, Inc., New York, 1959.

4. G. M. Jenkins and D. G. Watts, Spectral Analysis and its Applications, Holden-Day, San Francisco, 1969.

5. L. B. W. Jolley, Summation of Series, Second Revised Edition, Dover Publications, Inc., New York, 1961.

REVERSE BLANK

NUSC Technical Report 4513
11 April 1973

Minimum-Bias Windows for Spectral Estimation by Means of Overlapped Fast Fourier Transform Processing

Albert H. Nuttall

ABSTRACT

The time-limited nonnegative data windows that minimize the bias in auto- and cross-spectral estimation of stationary random processes by means of overlapped Fast Fourier Transform (FFT) processing are derived for a variety of constraints. When the time duration L of the data window is constrained, the optimum data window is $(2/L)^{1/2} \cos(\pi t/L)$, $|t| < L/2$; when the equivalent-noise bandwidth is constrained, the optimum data window is $(8/3L)^{1/2} \cos^2(\pi t/L)$, which is the Hanning window; when the half-power bandwidth is constrained, the optimum data window is $L^{-1/2}$ [1.682 + 4.261 cos (4.434 t/L)- 4.337 cos (3.552 t/L)], which is very similar to the Hanning window; and when the root-mean-square bandwidth is constrained, the optimum data window is $4/(5L)^{1/2} \cos^3(\pi t/L)$. In the three bandwidth-constrained cases, the window duration L is adjusted to meet the constraint.

The Hanning window is a reasonable compromise for achieving minimum bias, because in addition to being the optimum for one bandwidth constaint, it is very close to the optima for two other bandwidth constraints. The relative merits of the spectral characteristics of the windows are also discussed.

Approved for public release; distribution unlimited.

TABLE OF CONTENTS

Page

LIST OF ILLUSTRATIONS iii

LIST OF SYMBOLS v

INTRODUCTION 1

PROBLEM DEFINITION 1

PROBLEM SOLUTION 4
Duration Constraint 4
Equivalent-Noise-Bandwidth Constraint 5
Half-Power-Bandwidth Constraint 6
Root-Mean-Square-Bandwidth Constraint 7

COMPARISON OF WINDOW CHARACTERISTICS 8

CONCLUSIONS 10

APPENDIX A — DERIVATION OF THE OPTIMUM DATA WINDOW FOR AN EQUIVALENT-NOISE-BANDWIDTH CONSTRAINT . . 15

APPENDIX B — DERIVATION OF THE OPTIMUM DATA WINDOW FOR A HALF-POWER-BANDWIDTH CONSTRAINT 19

APPENDIX C — DERIVATION OF THE OPTIMUM DATA WINDOW FOR AN RMS-BANDWIDTH CONSTRAINT 23

LIST OF REFERENCES 29

REVERSE BLANK

LIST OF ILLUSTRATIONS

Figure		Page
1	Equivalent-Noise-Bandwidth Interpretation	5
2	Three Bandwidth-Constrained Data Windows; L = 1, Unit Energy	9
3	Comparison of RMS-Bandwidth Data Window with Quadratic and Cubic Data Windows; L = 1, Unit Energy . .	9
4	Spectral Window for Duration-Limited Data Window . . .	11
5	Spectral Window for Half-Power-Bandwidth Data Window .	12
6	Spectral Window for Equivalent-Noise-Bandwidth Data Window (Hanning)	13
7	Spectral Window for RMS-Bandwidth Data Window	14
C-1	Relationship of α and β in (C-20)	26
C-2	Relationship of α and β in (C-32)	27

LIST OF SYMBOLS

L	data window duration
t	time
E	ensemble average
f	frequency
$G(f)$	true spectrum
$\hat{G}(f)$	estimate of spectrum
$w(t)$	data window
$W(f)$	spectral window
T	available record length
$B(f)$	bias
D_1, D_2	bias constants
B_{st}	statistical bandwidth
$\phi_w(\tau)$	correlation of $w(t)$
B_e	equivalent-noise bandwidth
B_h	half-power bandwidth
B_r	root-mean-square bandwidth
prime	derivative
*	conjugate

REVERSE BLANK

MINIMUM-BIAS WINDOWS FOR SPECTRAL ESTIMATION BY MEANS OF OVERLAPPED FAST FOURIER TRANSFORM PROCESSING

INTRODUCTION

The selection of good data windows in spectral estimation of stationary random processes, to minimize leakage, is an important consideration and has received much attention [1-8]. In [6], a thorough investigation of four good data windows revealed virtually the same variance-reduction capabilities of overlapped Fast Fourier Transform (FFT) processing when the proper overlap was used for each window. The ultimate variance reduction of this direct procedure was also demonstrated to be identical to that attained by the older (indirect) analysis procedure in [4].

In this report, attention is focused on the bias in the estimation of power density spectra by means of overlapped FFT processing. Specifically, the bias is minimized by the choice of data windows that are restricted to be time-limited and nonnegative and are subject to either a time-duration constraint or a bandwidth constraint. These results complement and extend those of [8] for the indirect approach to spectral estimation.

PROBLEM DEFINITION

The overlapped FFT method for spectral estimation and the reasons for its use are documented in [6]. The mean of the spectral estimate is given by [6, eq. (5)] for auto-spectral estimation, and by [7, eq. (4A)] for cross-spectral estimation. In both cases, the mean takes the form*

$$E\{\hat{G}(f)\} = \int d\nu\, G(f-\nu)\, |W(\nu)|^2 , \tag{1}$$

where $\hat{G}(f)$ is the estimate of the true (auto or cross) spectrum $G(f)$, and

$$W(f) = \int dt\, \exp(-i2\pi ft)\, w(t), \tag{2}$$

*Integrals without limits are over the range of nonzero integrand.

where w(t) is the data window multiplied in the time domain by the available data. It is assumed that the data window is time-limited and nonnegative:

$$w(t) \quad \begin{cases} = 0 \text{ for } |t| > L/2 \\ \geq 0 \text{ for } |t| \leq L/2 \end{cases}, \tag{3}$$

where L is the window duration. The restriction to nonnegative data windows guarantees that the spectral window W(f) peaks at the origin. It should be noted that (1) is true with no restriction on the available record length T and with no restriction on the statistics of the random processes involved, except that the processes must be stationary; they need not be Gaussian for (1) to apply.

The desired value of (1) is the true value G(f); therefore the bias in estimation is defined as

$$B(f) = E\left\{\hat{G}(f)\right\} - G(f). \tag{4}$$

We approximate this bias by expanding $G(f-\nu)$ in (1) according to

$$G(f-\nu) \cong G(f) - \nu G'(f) + 1/2\ G''(f)\nu^2 - 1/6\ G'''(f)\nu^3 + 1/24\ G''''(f)\nu^4, \tag{5}$$

where the prime denotes a derivative. Substitution of (5) and (1) into (4) yields

$$B(f) \cong 1/2\ G''(f)\int d\nu\ \nu^2 |W(\nu)|^2 + 1/24\ G''''(f)\int d\nu\ \nu^4 |W(\nu)|^2, \tag{6}$$

where we have assumed (without loss of generality) that

$$\int d\nu\, |W(\nu)|^2 = \int dt\ w^2(t) = 1, \tag{7}$$

and that $|W(\nu)|^2$ is even about the origin; that is, w(t) is a unit-energy real waveform.

We express (6) as

$$B(f) \cong 1/2\ G''(f)\ D_1 + 1/24\ G''''(f)\ D_2 \equiv B_1(f) + B_2(f), \tag{8}$$

where window constants

$$\begin{aligned} D_1 &= \int d\nu\ \nu^2\ |W(\nu)|^2, \\ D_2 &= \int d\nu\ \nu^4\ |W(\nu)|^2, \end{aligned} \tag{9}$$

are independent of the true spectrum G(f). To minimize the bias, we must therefore minimize D_1 and/or D_2, subject to (3) and (7). To this aim, it is useful to express (9) in terms of the time domain. There follows, by use of (2),

$$D_1 = (2\pi)^{-2} \int dt \ [w'(t)]^2 \tag{10}$$

and

$$D_2 = (2\pi)^{-4} \int dt \ [w''(t)]^2. \tag{11}$$

Strictly, the approximation (8) to the bias is due only to local variations in true spectrum G(f) about the frequency point f of interest; equation (5) is not necessarily a good approximation for larger ν. Thus, peaks in the true spectrum that are distant from the point f under investigation are not accounted for by (5). To minimize the effects of remote spectral peaks on bias, we must also require that the spectral window W(f) decay sufficiently rapidly for large $|f|$. Thus the results of the following optimizations are not final, but must be investigated to see if they also meet the requirement of sufficiently rapid decay with frequency.

In addition to constraints (3) and (7), we shall be interested in constraining the bandwidth of the window; this is in keeping with the philosophy of requesting a specified frequency resolution for spectral estimation, and letting the window duration L and overlap be whatever is necessary to meet this requirement [6].

It should also be noted that constraints on bandwidth tend to equalize the variance-reduction capabilities of the windows. This may be seen from [6, eq. (22)], where the equivalent number of degrees of freedom is given approximately by

$$2TB_{st} \quad \text{for} \quad T \gg L, \tag{12}$$

where B_{st} is the statistical bandwidth [9, p. 278] of the window. Thus, if all windows were constrained to have the same statistical bandwidth, they would all have the same variance-reduction capabilities, and we could minimize the bias subject to this constraint. However, this constraint is not mathematically tractable.* Therefore, we resort to constraints on other, more tractable, bandwidth measures, with confidence that they too will yield comparable variance in spectral estimation (see [6, table 1]).

---

*We have not been able to express the time-domain constraint (3) directly in the frequency domain, nor have we been able to express the requirement that $\phi_w(\tau)$ be a legal correlation function directly in the time domain; see [6, eqs. (7) and (17)-(21)].

PROBLEM SOLUTION

Four different constrained problems will be addressed in this section: constrained window duration L ; constrained equivalent-noise bandwidth; constrained half-power bandwidth; and constrained root-mean-square (rms) bandwidth. The window duration L is adjusted to meet the bandwidth constraint in the latter three cases.

DURATION CONSTRAINT

Here we wish to minimize D_1 in (10), subject to constraints (3) and (7) and a fixed value of window duration L. In order that (10) be finite, w(t) must be continuous; therefore $w(\pm L/2) = 0$ from (3). When we use a calculus-of-variations approach, the optimum window $w_o(t)$ must satisfy the differential equation

$$w_o''(t) + \lambda w_o(t) = 0, \quad |t| < L/2, \tag{13}$$

where λ is a constant (Lagrange multiplier). The solution of (13) that satisfies the boundary conditions and (7), and has minimum D_1, is

$$w_o(t) = \left(\frac{2}{L}\right)^{1/2} \cos(\pi t/L), \quad |t| \le L/2. \tag{14}$$

The corresponding value of (10) is

$$D_1 = \frac{1}{4L^2} \cdot \tag{15}$$

Several windows are compared in table 1. It is seen that the Hanning window has 33 percent greater bias, as measured by $B_1(f)$, than the optimum window, under a duration constraint.

Table 1. Window Bias Constants D_1

Data Window	$4L^2D_1$
Optimum, (14)	1
Parabola	$10/\pi^2 = 1.01$
Triangle	$12/\pi^2 = 1.22$
Hanning	$4/3 = 1.33$

The spectral window corresponding to the optimum data window, (14), is

$$W_o(f) = \frac{2}{\pi} (2L)^{1/2} \frac{\cos(\pi L f)}{1-4L^2 f^2} . \tag{16}$$

The decay for large frequencies is only as f^{-2}. The sidelobes of this and the following windows will be discussed later.

EQUIVALENT-NOISE-BANDWIDTH CONSTRAINT

The equivalent-noise bandwidth B_e of spectral window $W(f)$ is defined as

$$B_e = \frac{\int df\, |W(f)|^2}{|W(0)|^2} = \frac{1}{\left[\int dt\, w(t)\right]^2} , \tag{17}$$

where we have used (7) and (2). The quantity B_e can be interpreted physically as the bandwidth of an ideal rectangular filter that would pass the same amount of power as a filter $W(f)$, when subjected to white noise; see figure 1. The peak of $|W(f)|^2$ occurs at the origin, since data window $w(t)$ is nonnegative.

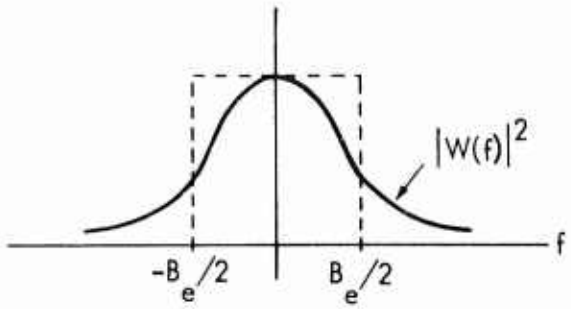


Figure 1. Equivalent-Noise-Bandwidth Interpretation

The problem here is to minimize D_1 in (10), subject to constraints (3), (7), and (17). This problem is solved in appendix A, with the result that the optimum data window is

$$w_o(t) = \left(\frac{8}{3L}\right)^{1/2} \cos^2(\pi t/L), \quad |t| \le L/2 . \tag{18}$$

This is the familiar Hanning window. The window duration L must be chosen as

$$L = \frac{3}{2}\,\frac{1}{B_e} \quad , \tag{19}$$

according to (17). The minimum value of D_1 is

$$D_1 = \frac{1}{3L^2} = \frac{4}{27}\,B_e^2 \, . \tag{20}$$

The specified equivalent-noise bandwidth dictates the window duration L and the minimum attainable bias constant D_1. The spectral window corresponding to (18) is

$$W_o(f) = \left(\frac{2L}{3}\right)^{1/2} \frac{\sin(\pi Lf)}{\pi Lf(1-L^2f^2)} \quad , \tag{21}$$

where L must be determined from (19). The decay for large frequencies varies as f^{-3}.

HALF-POWER-BANDWIDTH CONSTRAINT

The half-power bandwidth B_h of spectral window W(f) is defined as

$$\left|\frac{W(\pm B_h/2)}{W(0)}\right|^2 = \frac{1}{2} \, . \tag{22}$$

We desire to minimize D_1 in (10), subject to constraints (3), (7), and (22). Converting (22) into the time domain and restricting w(t) to be even, * constraint (22) takes a desirable integral form:

$$\int dt\; w(t)[\cos(\pi B_h t) - 2^{-1/2}] = 0 \, . \tag{23}$$

The solution to this minimization problem is presented in appendix B. The optimum data window is

$$w_o(t) = L^{-1/2}\,[1.682 + 4.261\cos(4.434t/L) - 4.337\cos(3.552t/L)], \quad |t| \le L/2 \, . \tag{24}$$

---

*An odd component in w(t) increases the rate of variation and therefore increases D_1.

The window duration L must be chosen as

$$L = \frac{1.411}{B_h} , \tag{25}$$

according to (23). The minimum value of D_1 is

$$D_1 = 0.1604\ B_h^2 . \tag{26}$$

The spectral window corresponding to (24) is obtained by employing (2); this will be discussed in the next section. It is shown in appendix B that $w_0'(\pm L/2) = 0$; therefore the decay of the spectral window is according to f^{-3}.

For comparison, if the time duration of the Hanning window is adjusted to realize the specified half-power bandwidth, namely $L = 1.441/B_h$ [6, eq. (33) and table 1], it follows that $D_1 = 0.1606\ B_h^2$. Thus the Hanning window has virtually the same bias as the optimum window under a half-power-bandwidth constraint. Further comparisons are made in the next section.

ROOT-MEAN-SQUARE-BANDWIDTH CONSTRAINT

The rms bandwidth B_r of spectral window W(f) is defined as

$$B_r^2 = \frac{\int df\ f^2 |W(f)|^2}{\int df\ |W(f)|^2} . \tag{27}$$

Inspection of (7) and (9) immediately reveals that

$$D_1 = B_r^2 . \tag{28}$$

Thus if the rms bandwidth is constrained, bias constant D_1 is fixed. In this case, it is reasonable to resort to minimization of the second bias constant D_2 in (9) or (11). Thus, we wish to minimize (11), subject to constraints (3), (7), and

$$\int dt\ [w'(t)]^2 = (2\pi B_r)^2 . \tag{29}$$

The solution to this problem is presented in appendix C. The optimum data window is

$$w_o(t) = \frac{4}{(5L)^{1/2}} \cos^3(\pi t/L), \quad |t| \le L/2 . \tag{30}$$

The window duration L must be chosen as

$$L = \frac{3}{2\sqrt{5}} \frac{1}{B_r} , \tag{31}$$

according to (29). The minimum value of D_2 is

$$D_2 = \frac{25}{9} B_r^4 . \tag{32}$$

The spectral window corresponding to (30) is

$$W_o(f) = \frac{16}{15\pi} (5L)^{1/2} \frac{\cos(\pi L f)}{(1-4L^2f^2)(1-4L^2f^2/9)} , \tag{33}$$

where L is determined from (31). The decay for large frequencies is according to f^{-4}.

For comparison, let the time duration of the Hanning window be adjusted to realize the specified rms bandwidth B_r. Then employing (18) in (29), we find $L = 1/(\sqrt{3}\, B_r)$, and (11) yields $D_2 = 3\, B_r^4$. Thus the Hanning window has 8 percent more bias than the optimum window under an rms bandwidth constraint, as measured by bias constant D_2.

COMPARISON OF WINDOW CHARACTERISTICS

In figure 2, one-half of the symmetric optimum data windows for the three bandwidth-constrained cases are drawn for a common time duration of L = 1. The equivalent-noise-bandwidth data window (Hanning) and the half-power-bandwidth data window are virtually identical and are continuous in value and derivative at 0.5. The rms-bandwidth data window is more peaked, and goes to zero in value, in derivative, and in second derivative at 0.5. Thus the last window would require greater overlap than the first two, in order to realize the same variance reduction; see [6].

In order to deduce the required overlap for the rms bandwidth data window, the quadratic and cubic data windows [6, pp. 10-18] are superposed in figure 3. Over most of the range, the quadratic and rms-bandwidth windows are very close. Near the end of the range, however, the taper of the rms-bandwidth window approaches that of the cubic; in fact, both are continuous in second derivative at 0.5. Thus, it is anticipated from earlier results [6, table 4] that slightly over 65 percent overlap would be required for the rms bandwidth data window to realize 99 percent of its maximum equivalent degrees of freedom [4, p. 22].

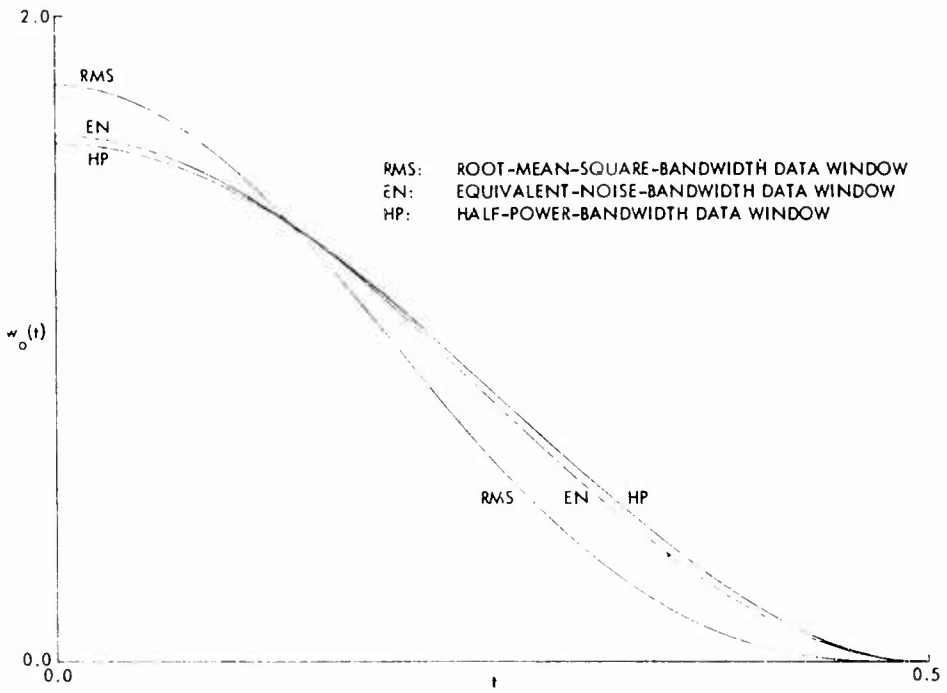


Figure 2. Three Bandwidth-Constrained Data Windows; L = 1, Unit Energy

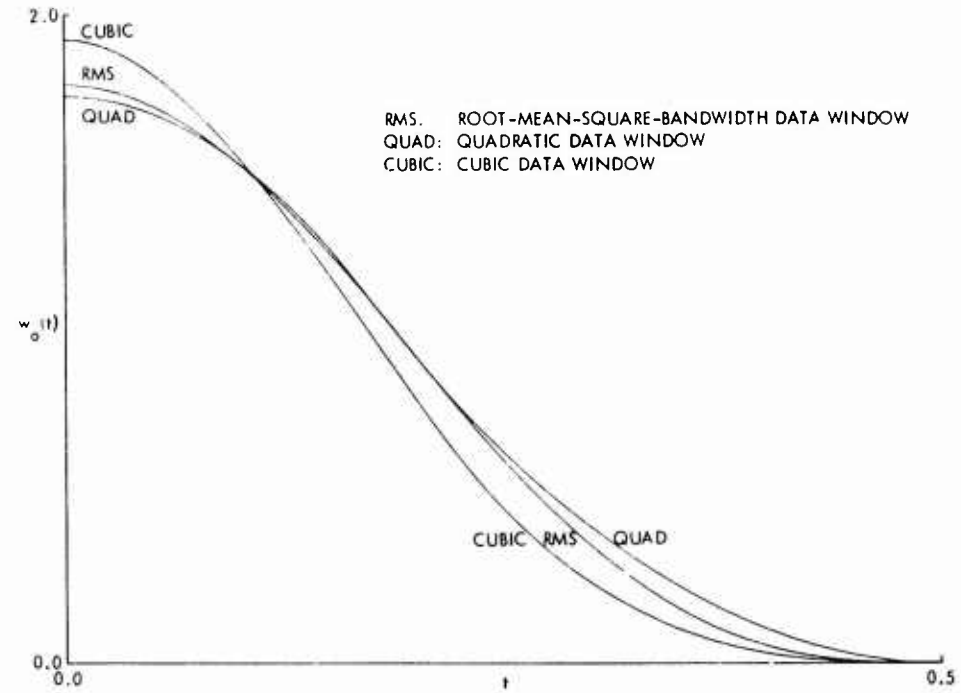


Figure 3. Comparison of RMS-Bandwidth Data Window with Quadratic and Cubic Data Windows; L = 1, Unit Energy

The spectral characteristics of the four windows derived in this report are presented in figures 4 through 7. The abscissas on every plot are in units of the half-power bandwidth; thus all the curves go through half-power (-3.01 dB) at $f/B_h = 0.5$. The duration-limited window, (14), is plotted in figure 4 and exhibits relatively slow decay with frequency, since the data window is discontinuous in derivative at its edge. The equivalent-noise-bandwidth (Hanning) and half-power-bandwidth spectral windows, plotted in figures 5 and 6, are virtually identical and have good decay with frequency, since the data windows are continuous in derivative at their edges. The spectral window for the rms-bandwidth data window is plotted in figure 7 and exhibits very rapid decay with frequency. However, as noted above, by virtue of requiring greater overlap for maximum variance reduction, this window will require somewhat greater-size FFTs than do the other windows.

CONCLUSIONS

The Hanning window is optimum under an equivalent-noise-bandwidth constraint, as far as minimization of bias constant D_1 is concerned. Furthermore, it is near the optima for two other bandwidth constraints. Its spectral decay is also sufficient for most cases that the bias is relatively unaffected by distant spectral peaks. And with 50 percent overlap, it realizes 92 percent of the maximum number of equivalent degrees of freedom [6, table 6]. Thus, the Hanning window is a reasonable compromise to utilize in spectral estimation of random stationary data.

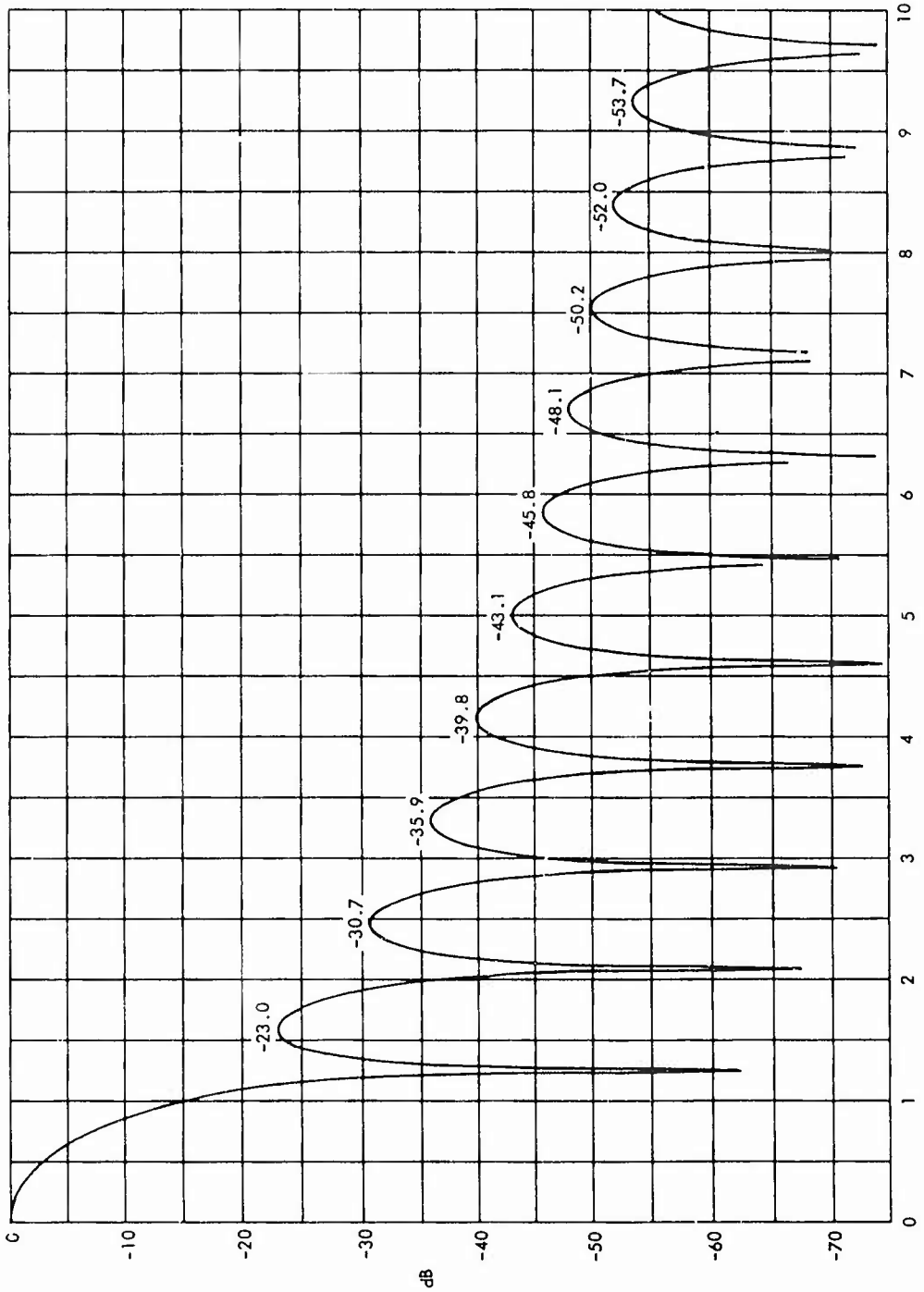


Figure 4. Spectral Window for Duration-Limited Data Window

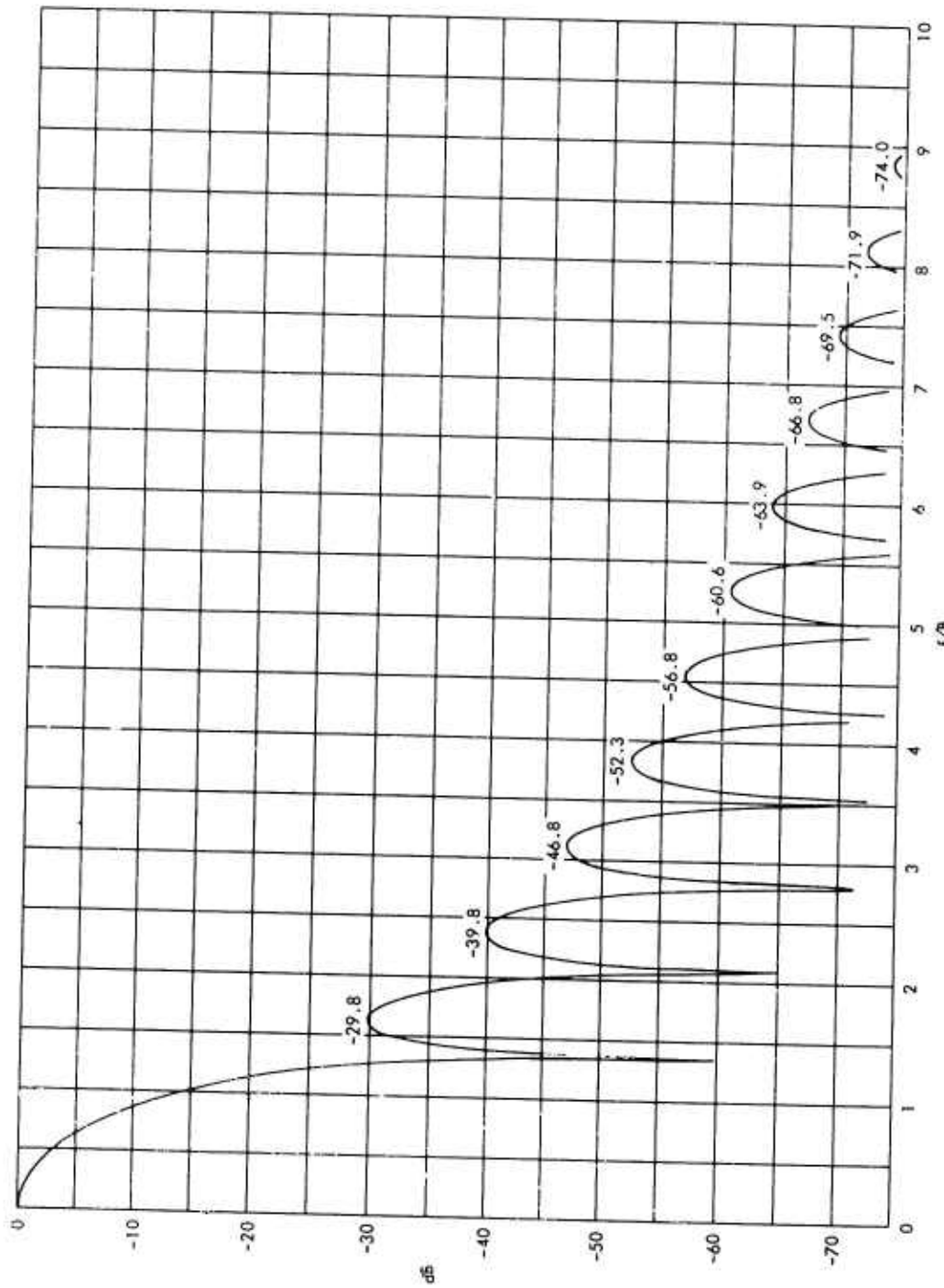


Figure 5. Spectral Window for Half-Power-Bandwidth Data Window

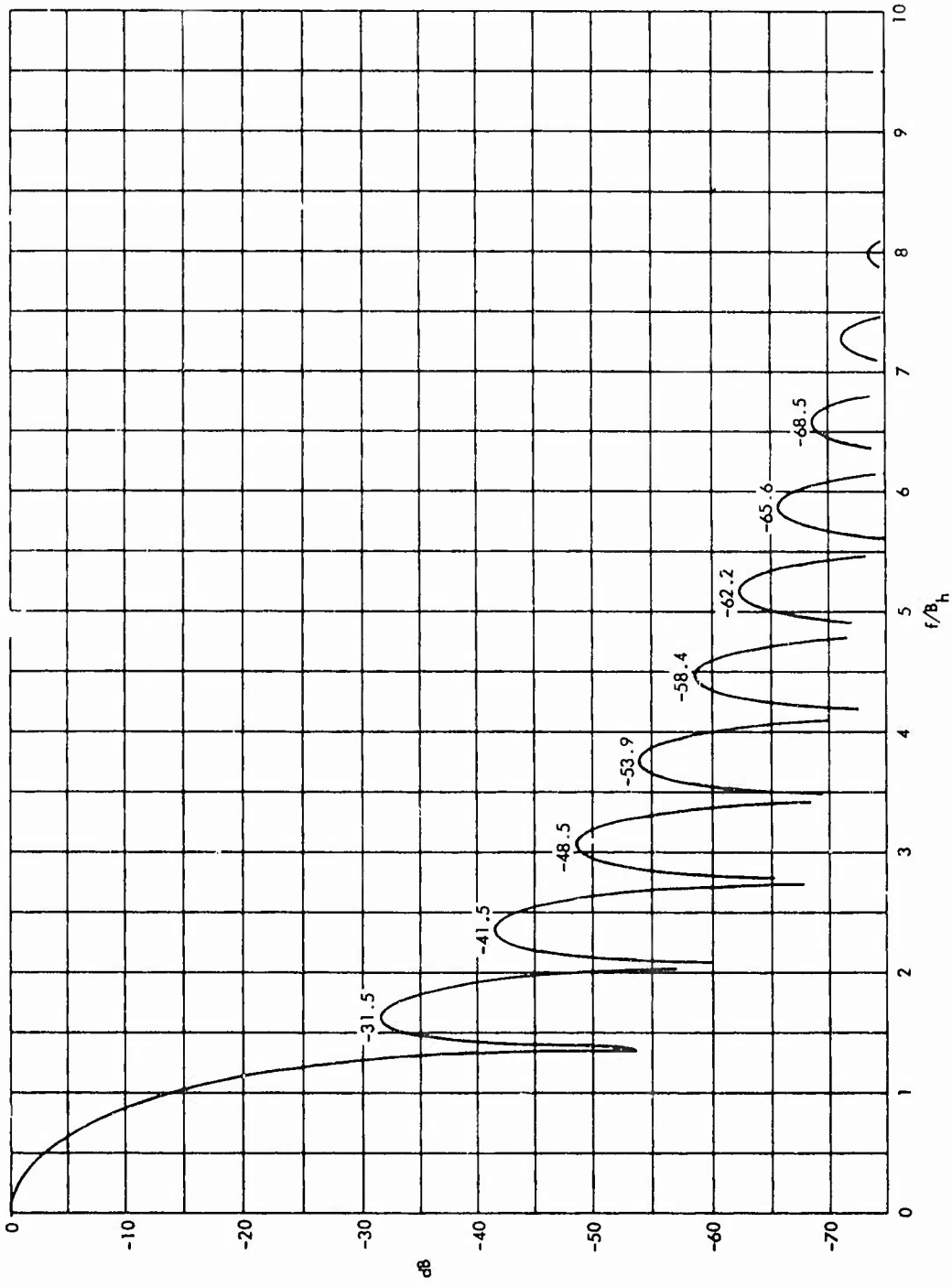


Figure 6. Spectral Window for Equivalent-Noise-Bandwidth Data Window (Hanning)

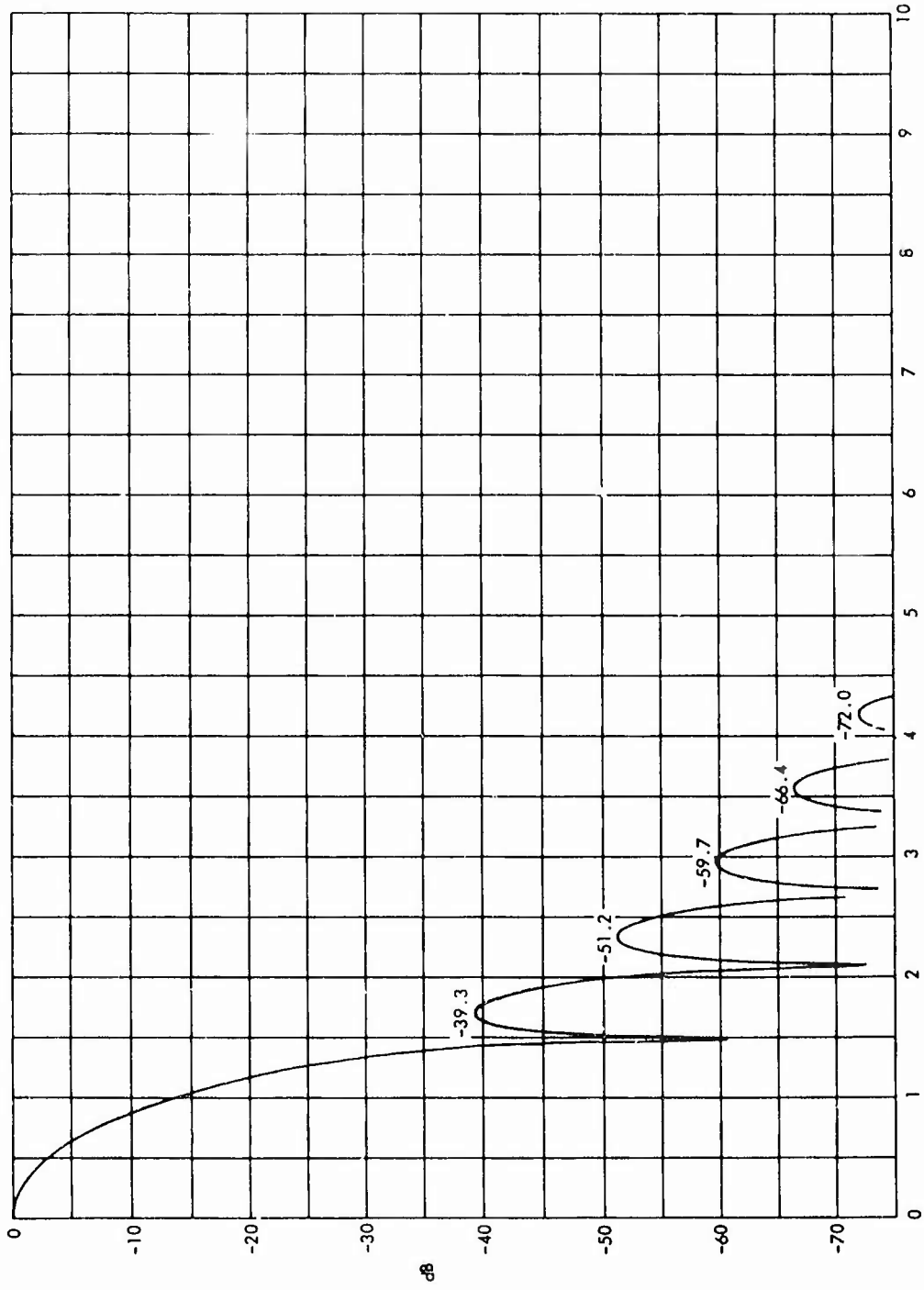


Figure 7. Spectral Window for RMS-Bandwidth Data Window

Appendix A

DERIVATION OF THE OPTIMUM DATA WINDOW FOR AN EQUIVALENT-NOISE-BANDWIDTH CONSTRAINT

We wish to minimize (10) (from the main text), subject to constraints (3), (7), and (17). Equations (7) and (17) are integral constraints and are in a convenient form for a calculus-of-variations approach. The way we handle (3) is to first ignore the nonnegative limitation; then, out of the class of allowable solutions, we restrict attention only to the nonnegative solutions and pick the best.

In order that (10) be finite, w(t) must be continuous. Using (3), we see that this means that

$$w(\pm L/2) = 0. \tag{A-1}$$

A calculus-of-variations approach tells us to minimize the quantity

$$Q = \int dt\,[w'(t)]^2 - \lambda_1 \int dt\; w^2(t) + 2\lambda_2 \int dt\; w(t), \tag{A-2}$$

where λ_1 and λ_2 are Lagrange multipliers; the resulting differential equation for the optimum window is

$$w_0''(t) + \lambda_1 w_0(t) = \lambda_2, \quad |t| < L/2. \tag{A-3}$$

We employed (A-1) on the allowed variations in deriving (A-3).

The general solution of (A-3) is

$$w_0(t) = \left\{ \begin{array}{l} A\cos(\alpha t) + B\sin(\alpha t) + C \\ \qquad \text{OR} \\ A\cosh(\alpha t) + B\sinh(\alpha t) + C \\ \qquad \text{OR} \\ A + Bt \end{array} \right\}, \quad |t| < L/2, \tag{A-4}$$

where α is real and positive. The third alternative in (A-4) yields the trivial solution when (A-1) is imposed.

The second alternative reduces to

$$w_0(t) = A\left[\cosh(at) - \cosh(aL/2)\right], \quad |t| \le L/2. \tag{A-5}$$

Since A can be chosen to satisfy the energy constraint (7), and L can be chosen to satisfy the bandwidth constraint (17), there is left only the variable a in (A-5) to vary; $w_0(t)$ is certainly nonnegative by the choice of proper polarity for A. In order to find the best value of a for this second alternative of (A-4), we compute D_1 in (10) versus a and pick the minimum.

To accomplish this goal, we define

$$y_{0}(u) \equiv w_0\left(\tfrac{L}{2}u\right) = A\,h(u), \quad |u| \le 1, \tag{A-6}$$

where

$$h(u) = \cosh(\alpha u) - \cosh(\alpha), \quad |u| \le 1 \tag{A-7}$$

and

$$\alpha = aL/2. \tag{A-8}$$

The bandwidth constraint (17) then becomes

$$A\frac{L}{2}K_0 = Be^{-1/2}, \tag{A-9}$$

where

$$K_0 \equiv \int_{-1}^{1} du\, h(u). \tag{A-10}$$

The energy constraint (7) becomes

$$A^2\frac{L}{2}K_2 = 1, \tag{A-11}$$

where

$$K_2 \equiv \int_{-1}^{1} du\, h^2(u). \tag{A-12}$$

The window constant (10) becomes

$$D_1 = \frac{1}{2\pi^2}\frac{A^2}{L}K_1, \tag{A-13}$$

where

$$K_1 \equiv \int_{-1}^{1} du \left[h'(u)\right]^2. \tag{A-14}$$

If we eliminate A and L by using (A-9) and (A-11), then (A-13) becomes

$$D_1 = \frac{1}{4\pi^2} \frac{K_0^4 K_1}{K_2^3} B_e^2. \tag{A-15}$$

The quantities necessary in (A-15) follow from (A-7), (A-10), (A-12), and (A-14):

$$\begin{aligned} K_0 &= 2\left[\cosh(\alpha) - \frac{\sinh(\alpha)}{\alpha}\right], \\ K_1 &= \alpha^2\left[\frac{\sinh(2\alpha)}{2\alpha} - 1\right], \\ K_2 &= 2\left[1 + \tfrac{1}{2}\cosh(2\alpha) - \frac{3}{2}\frac{\sinh(2\alpha)}{2\alpha}\right]. \end{aligned} \tag{A-16}$$

When (A-16) is substituted in (A-15), D_1 is found to increase monotonically with increasing α ; the limit as $\alpha \to 0+$ is

$$\frac{125}{72\pi^2} B_e^2 = .1759\, B_e^2. \tag{A-17}$$

The first alternative in (A-4), when subjected to boundary condition (A-1), breaks into two subcases. In the first, if $\sin(\alpha) = 0$, then B is arbitrary. Then $\alpha = k\pi$, $k \geq 1$. The function with smallest D_1 corresponds to $k = 1$, and yields

$$w_0(t) = A\left[\cos(2\pi t/L) + 1\right] + B\sin(2\pi t/L), \quad |t| \leq L/2. \tag{A-18}$$

However, we must have $B = 0$; otherwise $w_0(t)$ would go negative somewhere. Imposition of the energy constraint (7) and bandwidth constraint (17) yields

$$w_0(t) = \left(\frac{8}{3L}\right)^{1/2} \cos^2(\pi t/L), \quad |t| \leq L/2, \tag{A-19}$$

where

$$L = \frac{3}{2}\frac{1}{B_e}. \tag{A-20}$$

The corresponding value of D_1 is

$$D_1 = \frac{1}{3L^2} = \frac{4}{27} B_e^2 , \tag{A-21}$$

which is smaller than (A-17).

The second subcase occurs if $\sin(\alpha) \neq 0$. Then B in (A-4) must be zero, and we get

$$w_0(t) = A\left[\cos(at) - \cos(\alpha)\right], \quad |t| \leq L/2, \tag{A-22}$$

where $\alpha \neq k\pi$. The comments and method immediately below (A-5) apply equally well here. Therefore we define

$$h(u) = \cos(\alpha u) - \cos(\alpha), \quad |u| \leq 1, \quad \alpha \neq k\pi, \tag{A-23}$$

and find

$$K_0 = 2\left[\frac{\sin(\alpha)}{\alpha} - \cos(\alpha)\right],$$

$$K_1 = \alpha^2\left[1 - \frac{\sin(2\alpha)}{2\alpha}\right], \tag{A-24}$$

$$K_2 = 2\left[1 + \tfrac{1}{2}\cos(2\alpha) - \tfrac{3}{2}\frac{\sin(2\alpha)}{2\alpha}\right].$$

When (A-24) is substituted in (A-15), D_1 is found to decrease monotonically with increasing α , at least for α up to π. However, when $\alpha > \pi$, $h(u)$ becomes negative somewhere; this may be seen by noting that $h'(1) = -\alpha \sin(\alpha)$ is positive if $\alpha > \pi$. Thus the limiting member of this subclass, which is (A-19), is the optimum window.

Appendix B

DERIVATION OF THE OPTIMUM DATA WINDOW FOR A HALF-POWER-BANDWIDTH CONSTRAINT

Here we will minimize (10), subject to constraints (3), (7), and (23). In order that (10) be finite, (A-1) must again be true. A calculus-of-variations approach tells us to minimize

$$Q = \int dt \left[w'(t)\right]^2 - \lambda_1 \int dt\, w^2(t) + 2\lambda_2 \int dt\, w(t)\, c(t), \tag{B-1}$$

where

$$c(t) \equiv \cos(\omega t) - G, \quad \omega \equiv \pi B_h, \quad G = 2^{-1/2}, \tag{B-2}$$

and λ_1 and λ_2 are Lagrange multipliers; the resulting differential equation for the optimum window is

$$w_0''(t) + \lambda_1 w_0(t) = \lambda_2 c(t), \quad |t| < L/2. \tag{B-3}$$

If λ_1 is negative, the form for $w_0(t)$ includes sinh and cosh terms, which lead to a progressively larger value of D_1 as λ_1 becomes more negative, similar to the result of appendix A. If λ_1 is zero, the only solution to (B-3) and (A-1) is the trivial solution. If λ_1 is positive, the general solution to (B-3) is

$$w_0(t) = \left\{ \begin{array}{c} A\cos(\lambda t) + B\sin(\lambda t) + \frac{\lambda_2}{\lambda^2-\omega^2}\cos(\omega t) - \frac{\lambda_2}{\lambda^2} G, \ \lambda \neq \omega \\ \text{OR} \\ A\cos(\omega t) + B\sin(\omega t), \ \lambda = \omega \end{array} \right\}, \ |t| < \tfrac{L}{2}. \tag{B-4}$$

We discard the odd solutions for the reason given in the footnote to (23).

If we attempt to use the second alternative in (B-4), we can eliminate A by means of energy constraint (7). However, the bandwidth constraint (23) can not be satisfied for any value of $\omega L \neq 0$. Therefore, we must discard the second alternative.

To handle the first alternative in (B-4) conveniently, we define a function

$$y_0(u) \equiv w_0\left(\tfrac{L}{2}u\right) = A\cos\left(\frac{\alpha}{L}u\right) + \frac{q^2\lambda_2/\lambda^2}{q^2-1}\cos(\alpha u) - \frac{\lambda_2}{\lambda^2} G, \quad |u| < 1, \tag{B-5}$$

where

$$q \equiv \frac{\lambda}{\omega} \neq 1, \quad \alpha \equiv \frac{\omega L}{2} = \frac{\pi}{2} B_n L. \tag{B-6}$$

Imposition of (A-1) forces (B-5) into the form

$$y_0(u) = C\left[\frac{\cos(q\alpha u)}{\cos(q\alpha)} - \frac{q^2\cos(\alpha u) + G(1-q^2)}{q^2\cos(\alpha) + G(1-q^2)}\right] \equiv C\,A(u), \quad |u| \leq 1, \tag{B-7}$$

where C is a constant. The energy constraint (7) yields

$$C = \left(\frac{2}{L K_0}\right)^{1/2}, \tag{B-8}$$

where we have used (B-5) and (B-7), and defined

$$K_0 = \int du\, A^2(u). \tag{B-9}$$

Satisfaction of bandwidth constraint (23) demands that

$$0 = \int du \left[\cos(\alpha u) - G\right] A(u), \tag{B-10}$$

where we employed (B-6) and (B-7). Substitution of the detailed form for $A(u)$, (B-7), into (B-10) yields the relation

$$\begin{aligned} &\cos(\alpha q)\left[2G\,S(\alpha) - 2G^2 + q^2\left\{1 + 2G^2 + S(2\alpha) - 4G\,S(\alpha)\right\}\right] \\ &\quad = \left[q^2\cos(\alpha) + G(1-q^2)\right]\left[S(\alpha q + \alpha) + S(\alpha q - \alpha) - 2G\,S(\alpha q)\right], \end{aligned} \tag{B-11}$$

where

$$S(x) \equiv \frac{\sin(x)}{x}. \tag{B-12}$$

For a given value of q, (B-11) must be solved for the smallest value of α; G is a known specified constant. In order to find the best value of q, we compute D_1 versus q and pick the minimum, always being careful that $A(u)$ remain nonnegative for all $|u| \leq 1$. The quantity

$$\begin{aligned} D_1 &= \frac{1}{4\pi^2}\int dt\left[w_0'(t)\right]^2 = \frac{1}{4\pi^2}\,\frac{2}{L}\int du\left[y_0'(u)\right]^2 \\ &= \frac{1}{\pi^2 L^2}\,\frac{K_1}{K_0} = \frac{K_1}{4\alpha^2 K_0}\,B_n^2, \end{aligned} \tag{B-13}$$

using (B-5), (B-7), (B-8), (B-6), and defining

$$K_1 = \int du \left[h'(u)\right]^2 . \tag{B-14}$$

The quantities K_0 and K_1 are available upon substitution of (B-7) in (B-9) and (B-14). There follows, upon use of (23),

$$K_0 = C_1^2\left[1 + S(2\alpha q)\right] + 2C_2^2 G\left[q^2 S(\alpha) + G(1-q^2)\right]$$
$$+ C_1 C_2\left[2G(2-q^2)S(\alpha q) + q^2 S(\alpha q+\alpha) + q^2 S(\alpha q-\alpha)\right], \tag{B-15}$$

$$K_1 = \alpha^2 q^2\left[C_1^2\left\{1 - S(2\alpha q)\right\} + q^2 C_2^2\left\{1 - S(2\alpha)\right\}\right.$$
$$\left. + 2q C_1 C_2\left\{S(\alpha q-\alpha) - S(\alpha q+\alpha)\right\}\right], \tag{B-16}$$

where

$$C_1 = \left[\cos(\alpha q)\right]^{-1}, \quad C_2 = -\left[q^2\cos(\alpha) + G(1-q^2)\right]^{-1}. \tag{B-17}$$

The numerical approach may now be summarized as follows. A value of q is picked, and (B-11) is solved for α. Then (B-17) is computed and substituted in (B-15) and (B-16), thereby enabling evaluation of D_1 in (B-13) for that choice of q. (Up to this point, G could be any desired constant; we now restrict $G = 1/12$). When this approach is tried, it is found that D_1 increases monotonically with increasing q. On the other hand, when q is made too small, $h(u)$ becomes negative near $u=1$. The optimum value of q is realized when $h'(1) = 0$. From (B-7) and (B-17), this requirement is

$$C_1 \sin(\alpha q) + C_2 q \sin(\alpha) = 0. \tag{B-18}$$

The simultaneous solution of (B-11) and (B-18), with smallest α, is then given by

$$q = .8011\,1996\,, \quad \alpha = 2.217\,0595. \tag{B-19}$$

The optimum value of D_1 then follows from (B-13) as

$$D_1 = .1604\,4830\,B_h^2\,, \tag{B-20}$$

and the segment length follows from (B-6) as

$$L = \frac{2\pi}{\alpha}\cdot\frac{1}{B_h} = \frac{1.411\,4239}{B_h}\,. \tag{B-21}$$

Finally, the optimum window $w_0(t)$ follows from (B-5) as

$$w_0(t) = L^{-1/2}\left[1.681\,6731 + 1.261\,0617\cos(4.434\,1191\,t/L)\right.$$
$$\left. - 1.337\,3899\cos(3.552\,2613\,t/L)\right], \quad |t| \le L/2. \tag{B-22}$$

REVERSE BLANK

Appendix C

DERIVATION OF THE OPTIMUM DATA WINDOW FOR AN RMS-BANDWIDTH CONSTRAINT

The problem here is to minimize (11), subject to constraints (3), (7), and (29). In order that (11) be finite, $w'(t)$ must be continuous. Using (3), this means that

$$w(\pm L/2) = 0, \quad w'(\pm L/2) = 0. \tag{C-1}$$

A calculus-of-variations approach tells us to minimize the quantity

$$Q = \int dt\,[w''(t)]^2 + \lambda \int dt\,[w'(t)]^2 + \mu \int dt\, w^2(t), \tag{C-2}$$

where λ and μ are Lagrange multipliers; the resulting differential equation for the optimum window is

$$w_0''''(t) - \lambda w_0''(t) + \mu w_0(t) = 0, \quad |t| < L/2. \tag{C-3}$$

We employed (C-1) on the allowed variations in deriving (C-3).

To solve (C-3), we assume a form $\exp(st)$ for $w_0(t)$. Substitution in (C-3) requires that s be chosen to satisfy

$$s^4 - \lambda s^2 + \mu = 0 \; ; \quad s^2 = \tfrac{1}{2}\left[\lambda \pm (\lambda^2 - 4\mu)^{1/2}\right]. \tag{C-4}$$

At this point, several alternatives are possible. The first case we pursue is a negative discriminant in (C-4). Then the four values for s in (C-4) can be expressed as

$$s = z, z^*, -z, -z^*, \tag{C-5}$$

where z is a complex constant with nonzero imaginary part. For distinct roots (i.e., z not purely real), the optimum window is

$$w_0(t) = A\exp(zt) + B\exp(z^*t) + C\exp(-zt) + D\exp(-z^*t). \tag{C-6}$$

In order that (C-1) be satisfied with a nontrivial solution, it is necessary that the determinant

$$\begin{vmatrix} E & E^* & 1/E & 1/E^* \\ 1/E & 1/E^* & E & E^* \\ zE & z^*E^* & -z/E & -z^*/E^* \\ z/E & z^*/E^* & -zE & -z^*E^* \end{vmatrix} \tag{C-7}$$

equal zero, where $E = \exp(zL/2)$. This requires that

$$(z+z^*)(z-z^*)(E^4-1)(E^{*4}-1) = 0. \tag{C-8}$$

But none of the factors in (C-8) can be zero without double roots resulting for s, in which case the form (C-6) is not appropriate. Therefore, the negative-discriminant case is self-destroying.

The second case corresponds to a zero discriminant in (C-4). Then we have three subcases:

$$s = \left\{ \begin{array}{c} a,\ a,\ -a,\ -a \\ \text{OR} \\ ia,\ ia,\ -ia,\ -ia \\ \text{OR} \\ 0,\ 0,\ 0,\ 0 \end{array} \right\}, \qquad a \text{ real and positive.} \tag{C-9}$$

For subcase 1, the form for $w_0(t)$ is

$$w_0(t) = A\cosh(at) + B\sinh(at) + Ct\cosh(at) + Dt\sinh(at). \tag{C-10}$$

Imposition of (C-1) requires that

$$\sinh(aL) = \pm aL \tag{C-11}$$

for a nontrivial solution. But (C-11) has no solutions for positive real a .

For subcase 2 in (C-9), the form for $w_0(t)$ is

$$w_0(t) = A\cos(at) + B\sin(at) + Ct\cos(at) + Dt\sin(at). \tag{C-12}$$

Imposition of (C-1) requires that

$$\sin(aL) = \pm aL \tag{C-13}$$

for a nontrivial solution. Again this is disallowed.

For subcase 3 in (C-9), the form is

$$w_0(t) = A + Bt + Ct^2 + Dt^3. \tag{C-14}$$

Imposition of (C-1) yields only the trivial solution.

The third, and last, case we must now consider is a positive discriminant in (C-4). Then we have three subcases:

$$s = \left\{ \begin{array}{c} \pm a, \pm b \\ \pm a, \pm ib \\ \pm ia, \pm ib \end{array} \right\}, \qquad a \text{ and } b \text{ real.} \tag{C-15}$$

For subcase 1, we have

$$w_0(t) = A\cosh(at) + B\sinh(at) + C\cosh(bt) + D\sinh(bt). \tag{C-16}$$

Imposition of (C-1) requires that

$$\alpha \tanh(\alpha) = \beta \tanh(\beta) \quad \text{or} \quad \frac{\tanh(\alpha)}{\alpha} = \frac{\tanh(\beta)}{\beta}, \tag{C-17}$$

where

$$\alpha \equiv aL/2, \quad \beta \equiv bL/2. \tag{C-18}$$

The only solutions of (C-17) are $\alpha = \beta$; that is, $a = b$. However, these have been considered already in (C-10) and found inadequate.

For subcase 2 in (C-15), we have

$$w_0(t) = A\cosh(at) + B\sinh(at) + C\cos(bt) + D\sin(bt). \tag{C-19}$$

Satisfaction of (C-1) demands that

$$-\alpha \tanh(\alpha) = \beta \tan(\beta) \quad \text{or} \quad \frac{\tanh(\alpha)}{\alpha} = \frac{\tan(\beta)}{\beta}. \tag{C-20}$$

The second alternative in (C-20) leads to odd solutions only, in (C-19), and they must be discarded because of their higher variation rate. The first alternative in (C-20) leads to

$$w_0(t) = C\left[\frac{\cosh(at)}{\cosh(\alpha)} - \frac{\cos(bt)}{\cos(\beta)}\right], \quad |t| \le \frac{L}{2}, \tag{C-21}$$

which is a legal nontrivial solution. The values of α and β are related as shown in figure C-1. To handle this alternative conveniently, we define a function

$$y_0(u) = w_0\left(\frac{L}{2}u\right) = C\left[\frac{\cosh(\alpha u)}{\cosh(\alpha)} - \frac{\cos(\beta u)}{\cos(\beta)}\right] \equiv C\,k(u), \quad |u| \le 1. \tag{C-22}$$

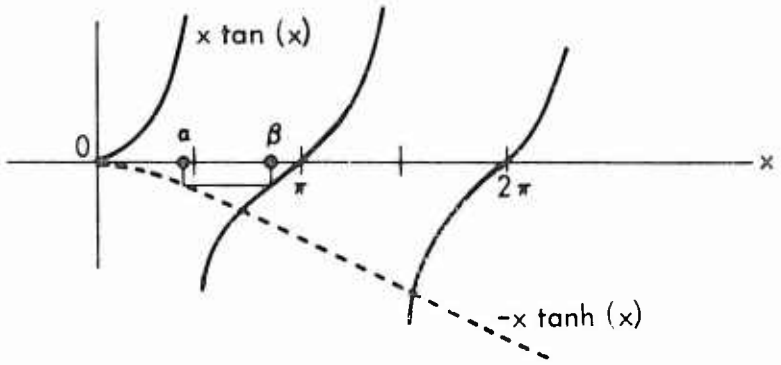


Figure C-1. Relationship of α and β in (C-20)

Then

$$y_0'(u) = \frac{L}{2} w_0'\left(\frac{L}{2}u\right), \quad y_0''(u) = \left(\frac{L}{2}\right)^2 w_0''\left(\frac{L}{2}u\right). \tag{C-23}$$

The energy constraint (7) requires that

$$C = \left(\frac{2}{LK_0}\right)^{1/2}, \tag{C-24}$$

where

$$K_j \equiv \int du \left[A^{(j)}(u)\right]^2. \tag{C-25}$$

The bandwidth constraint (29) requires that

$$L = \frac{1}{\pi}\left(\frac{K_1}{K_0}\right)^{1/2} \frac{1}{B_r}, \tag{C-26}$$

where we have employed (C-23), (C-24), and (C-25). Then we use (C-23) through (C-26) to determine the bias constant D_2 as

$$D_2 = \frac{1}{(2\pi)^4}\int dt \left[w_0''(t)\right]^2 = \frac{K_0 K_2}{K_1^2} B_r^4. \tag{C-27}$$

For the curren example in (C-22), we evaluate

$$K_0 = \frac{R(2\alpha)+1}{\cosh^2(\alpha)} + \frac{1+S(2\beta)}{\cos^2(\beta)},$$

$$K_1 = \alpha^2 \frac{R(2\alpha)-1}{\cosh^2(\alpha)} + \frac{4\alpha\beta}{\alpha^2+\beta^2}\left[\alpha\tan(\beta) - \beta\tanh(\alpha)\right] + \beta^2 \frac{1-S(2\beta)}{\cos^2(\beta)},$$

$$K_2 = \alpha^4 \frac{R(2\alpha)+1}{\sinh^2(\alpha)} + \beta^4 \frac{1+S(2\beta)}{\cos^2(\beta)}, \qquad \text{(C-28)}$$

where we have employed the first alternative in (C-20), and defined

$$R(x) = \frac{\sinh(x)}{x}, \quad S(x) = \frac{\sin(x)}{x}. \qquad \text{(C-29)}$$

For an arbitrary α, we solve the first alternative in (C-20) for β, and then compute D_2, by means of (C-27) and (C-28). It is found that D_2 increases monotonically with α. The minimum is realized when $\alpha = 0$, namely

$$D_2 = 3B_r^4. \qquad \text{(C-30)}$$

The third subcase in (C-15) yields the form

$$W_0(t) = A\cos(at) + B\sin(at) + C\cos(bt) + D\sin(bt). \qquad \text{(C-31)}$$

The boundary conditions (C-1) demand that

$$\alpha\tan(\alpha) = \beta\tan(\beta) \qquad \text{or} \qquad \frac{\tan(\alpha)}{\alpha} = \frac{\tan(\beta)}{\beta}. \qquad \text{(C-32)}$$

However, the second alternative in (C-32) yields odd solutions and is discarded. The first alternative yields

$$W_0(t) = C\left[\frac{\cos(at)}{\cos(\alpha)} - \frac{\cos(bt)}{\cos(\beta)}\right], \quad |t| \le \frac{L}{2}, \quad \alpha \ne \frac{\pi}{2}. \qquad \text{(C-33)}$$

The values of α and β are related as shown in figure C-2. As above,

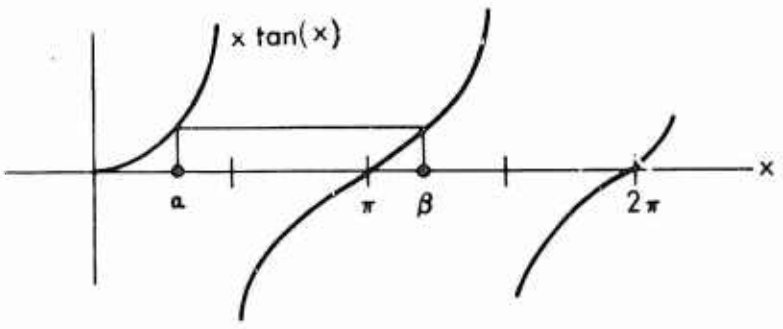


Figure C-2. Relationship of α and β in (C-32)

we define a function

$$y_0(u) = W_0\left(\tfrac{1}{2}u\right) = C\,h(u) = C\left[\frac{\cos(\alpha u)}{\cos(\alpha)} - \frac{\cos(\beta u)}{\cos(\beta)}\right]. \tag{C-34}$$

We can now employ (C-25) through (C-27) immediately. We evaluate

$$K_0 = \frac{1+S(2\alpha)}{\cos^2(\alpha)} - 2\,\frac{S(\alpha+\beta)+S(\alpha-\beta)}{\cos(\alpha)\cos(\beta)} + \frac{1+S(2\beta)}{\cos^2(\beta)},$$

$$K_1 = \alpha^2\frac{1-S(2\alpha)}{\cos^2(\alpha)} - 2\alpha\beta\,\frac{S(\alpha-\beta)-S(\alpha+\beta)}{\cos(\alpha)\cos(\beta)} + \beta^2\,\frac{1-S(2\beta)}{\cos^2(\beta)}, \tag{C-35}$$

$$K_2 = \alpha^4\frac{1+S(2\alpha)}{\cos^2(\alpha)} - 2\alpha^2\beta^2\,\frac{S(\alpha+\beta)+S(\alpha-\beta)}{\cos(\alpha)\cos(\beta)} + \beta^4\,\frac{1+S(2\beta)}{\cos^2(\beta)}.$$

For an arbitrary $\alpha\,(\neq \pi/2)$, we solve the first alternative in (C-32) for β, and then compute D_2 using (C-27) and (C-35). It is found that D_2 decreases monotonically with increasing α, at least for α up to $\pi/2$, the limit being 25/9 at $\alpha = \pi/2 -$. However, when $\alpha > \pi/2$, $h(u)$ goes negative somewhere and is unacceptable. For $\alpha = \pi/2$, (C-32) is not an adequate form; we note instead that $\beta = 3\pi/2$ from (C-31), and then

$$h(u) = A\cos\left(\tfrac{\pi}{2}u\right) - B\cos\left(\tfrac{3\pi}{2}u\right). \tag{C-36}$$

The boundary conditions (C-1) force $A = -3B$, giving

$$h(u) = \cos^3\left(\tfrac{\pi}{2}u\right). \tag{C-37}$$

We then find

$$K_0 = \frac{5}{8},\quad K_1 = \frac{9\pi^2}{32},\quad K_2 = \frac{45\pi^4}{128}, \tag{C-38}$$

yielding

$$L = \frac{3}{2\sqrt{5}}\,\frac{1}{B_r},$$

$$D_2 = \frac{25}{9}\,B_r^4, \tag{C-39}$$

which is smaller than (C-30). Thus (C-37) is the optimum window. (Notice that $h''(1) = 0$.)

LIST OF REFERENCES

1. M. S. Bartlett, An Introduction to Stochastic Processes, Cambridge University Press, New York, 1955.

2. E. Parzen, "On Consistent Estimates of the Spectrum of a Stationary Time Series," Annals of Mathematical Statistics, vol. 28, 1957, pp. 329-348.

3. U. Grenander and M. Rosenblatt, Statistical Analysis of Stationary Time Series, John Wiley and Sons, Inc., New York, 1957.

4. R. B. Blackman and J. W. Tukey, The Measurement of Power Spectra, Dover Publications, New York, 1959.

5. G. M. Jenkins and D. G. Watts, Spectral Analysis and Its Applications, Holden-Day Inc., San Francisco, 1968.

6. A. H. Nuttall, Spectral Estimation by Means of Overlapped Fast Fourier Transform Processing of Windowed Data, NUSC Report 4169, 13 October 1971.

7. A. H. Nuttall, "Estimation of Cross-Spectra via Overlapped FFT Processing," NUSC Technical Memorandum TC-83-72, 18 April 1972.

8. A. Papoulis, "Minimum-Bias Windows for High-Resolution Spectral Estimates," IEEE Transactions on Information Theory, vol. IT-9, no. 1, January 1973, pp. 9-12.

9. J. S. Bendat and A. G. Piersol, Random Data: Analysis and Measurement Procedures, John Wiley and Sons, Inc., New York, 1971.

REVERSE BLANK

NUSC Technical Report 4767
16 August 1974

An Approximate Fast Fourier Transform Technique for Vernier Spectral Analysis

Albert H. Nuttall

ABSTRACT

An approximate and quick fast Fourier transform technique for vernier spectral analysis is derived and tested for several condidate time and delay weightings, and for overlaps of the time weightings. For 50 percent overlap, the use of a simple cosine lobe for the time weighting yields spurious spectral sidelobes at least 23 dB below the main peak, whereas Dolph-Chebyshev time weighting achieves -33 dB sidelobes. For 75 percent overlap, use of a $(\text{cosine})^5$ lobe for the time weighting yields sidelobes at least 54 dB down, whereas Dolph-Chebyshev time weighting achieves -86 dB sidelobes. In both cases of overlap, use of delay weighting is also required and is taken as a Hanning weighting. Extensions to other overlaps and weightings are possible.

Approved for public release; distribution unlimited.

TABLE OF CONTENTS

Page

LIST OF TABLES iii

LIST OF ILLUSTRATIONS iii

LIST OF SYMBOLS v

INTRODUCTION 1

FUNDAMENTAL SPECTRAL RELATIONSHIPS 2

Large-Size FFT Approach 2
Approximate FFT Technique 4
Interpretation of the Vernier Spectrum 7
FFT Considerations 9

EXAMPLES 10

50 Percent Overlap 10
75 Percent Overlap 13

CONCLUSIONS 14

APPENDIX A — TWO METHODS OF COMPUTING

$$\sum_{n=n_o}^{n_o+N-1} \exp(-i2\pi pn/N)\, q_n \quad \ldots \quad A\text{-}1$$

APPENDIX B — DERIVATION OF VERNIER SPECTRUM B-1

APPENDIX C — SAMPLE PROGRAM C-1

APPENDIX D — EFFECT OF (COSINE)^n TIME WEIGHTING D-1

REFERENCES R-1

REVERSE BLANK

LIST OF TABLES

Table		Page
1	Examples of Temporal and Delay Weightings	11
2	Convolutional Sequences	12

LIST OF ILLUSTRATIONS

Figure		Page
1	Time and Frequency Relationships	3
2	Temporal and Delay Weightings	5
3	Vernier Spectrum	8
4	Vernier Spectrum for Cosine Temporal Weighting, 50 percent Overlap	16-20
5	Vernier Spectrum for $(\text{Cosine})^2$ Temporal Weighting, 50 percent Overlap	21
6	Vernier Spectrum for Dolph-Chebyshev Temporal Weighting, 50 percent Overlap	22-23
7	Vernier Spectrum for $(\text{Cosine})^2$ Temporal Weighting, 75 percent Overlap	24-25
8	Vernier Spectrum for $(\text{Cosine})^3$ Temporal Weighting, 75 percent Overlap	26-27
9	Vernier Spectrum for $(\text{Cosine})^4$ Temporal Weighting, 75 percent Overlap	28-29
10	Vernier Spectrum for $(\text{Cosine})^5$ Temporal Weighting, 75 percent Overlap	30-31
11	Vernier Spectrum for Dolph-Chebyshev Temporal Weighting, 75 percent Overlap	32-33
12	Vernier Spectrum for Flat Delay Weighting	34
13	Vernier Spectrum for $(\text{Cosine})^2$ Delay Weighting, Two Tones	35
14	Vernier Spectrum for Flat Delay Weighting, Two Tones	36

REVERSE BLANK

LIST OF SYMBOLS

t	time
$x(t)$	data waveform
Δ	sampling increment in time
f	frequency; analysis frequency
$V(f)$	voltage density spectrum
$u(t)$, $w(t)$	temporal weighting
$\delta_\Delta(t)$	impulse train, equation (2)
$X(f)$	voltage density spectrum of $x(t)$
$U(f)$, $W(f)$	temporal window
L	number of samples in duration of temporal weighting $u(t)$
τ	delay
$a(f, \tau)$	spectral-delay function
ν	vernier frequency
$d(\tau)$	delay weighting
$Y(f, \nu)$	vernier spectrum
L_w, L_d	length of temporal weighting, delay weighting
S	separation of delays
M	number of delay increments
N	number of samples in duration of temporal weighting $w(t)$
I_S	integer number of sampling increments in delay S
$D(\nu)$	delay window
f_o	excitation frequency of pure tone

REVERSE BLANK

AN APPROXIMATE FAST FOURIER TRANSFORM TECHNIQUE FOR VERNIER SPECTRAL ANALYSIS

INTRODUCTION

To detect the presence of very narrowband weak signals in noise, and to measure their center frequencies accurately, it is necessary to Fourier transform a long time segment of the available process. When the center frequencies of the signal components are unknown and the total search bandwidth of interest is large, this procedure demands storage and computation of many degrees of freedom, that is, search of a large time-bandwidth product space. It would be advantageous if a quick, coarse search for narrowband components could be conducted, followed by a finer vernier analysis over a limited band where the presence of narrowband components has been indicated. Such an adaptive procedure would be less time-consuming and require less storage. Also, if the procedure did not need to be exact, but yielded an approximation with acceptable sidelobes, the required storage and computation might be reduced further.

This report presents just such a technique, which

1. accepts the input process in smaller time segments as they are available,

2. performs a reasonable-size weighted fast Fourier transform (FFT) on each overlapped segment,

3. stores only that frequency portion (at each segment) where narrowband components are indicated to be present, and

4. performs a small-size weighted FFT over the total data record available, for each frequency bin stored.

Steps 1 and 2 permit smaller-size FFTs than would be required if the total data record were spectrally analyzed in one operation. Steps 3 and 4 constitute the adaptive feature of this technique. The last transform over time (delay) in step 4, for each frequency bin, is a vernier frequency analysis, measured from the center of each bin; the degree of approximation of this technique is the subject of this report.

Some past work on performing large-size FFTs by means of several smaller FFTs is reported in references 1 and 2. The methods reported there are exact, but they consume more time and require more storage than the method to be presented here. In particular, the two methods of reference 1 require too many small-size FFTs, and the method of reference 2 requires additional multiplications by complex exponentials and a fair amount of storage. The approximate technique of reference 3 is similar to the one outlined above, up to step 4, with the notable exception of overlapped weighting; at that point the technique of reference 3 requires transformation back to the time domain followed by another transform to the desired frequency domain. Additional transforms are required in this last technique, and it produces greater sidelobes than the new technique, especially when the temporal weighting is judiciously selected.

FUNDAMENTAL SPECTRAL RELATIONSHIPS

LARGE-SIZE FFT APPROACH

Before embarking on the approximate technique, we review the standard large-size FFT approach to spectral analysis. Suppose a data waveform $x(t)$ is sampled at time instants $n\Delta$, n integer. Then the voltage density spectrum that can be computed is*

$$\begin{aligned} V(f) &\equiv \int dt \exp(-i2\pi ft)\ x(t)\ u(t)\ \Delta\ \delta_\Delta(t) \\ &= \Delta \sum_n \exp(-i2\pi fn\Delta)\ x(n\Delta)\ u(n\Delta)\ , \end{aligned} \tag{1}$$

where $u(t)$ is a temporal weighting deliberately imposed to control spectral sidelobes, as will be discussed shortly; see figure 1A. The finite duration of $u(t)$ terminates the integral and sum in equation (1) at finite limits. The impulse-train function in (1) is defined as the infinite sum

$$\delta_\Delta(t) \equiv \sum_n \delta(t - n\Delta)\ . \tag{2}$$

The integral representation in (1) allows us to express†

$$V(f) = X(f) \circledast U(f) \circledast \delta_{1/\Delta}(f)\ , \tag{3}$$

*All integrals are over the range of nonzero integrand.

†The Fourier transform of the lower-case time function $x(t)$ is the upper-case frequency function $X(f)$; this notation is used throughout.

where $\circledast$ denotes convolution, and, in keeping with (2),

$$\delta_{1/\Delta}(f) = \sum_m \delta\left(f - \frac{m}{\Delta}\right) . \qquad (4)$$

Thus, the observed spectrum V(f) is the convolution of X(f) with the set of windows* $U(f) \circledast \delta_{1/\Delta}(f)$, which is depicted in figure 1B.

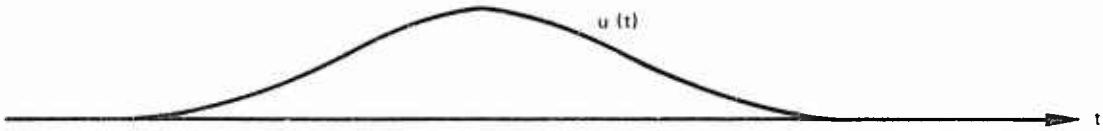


Figure 1A. Temporal Weighting

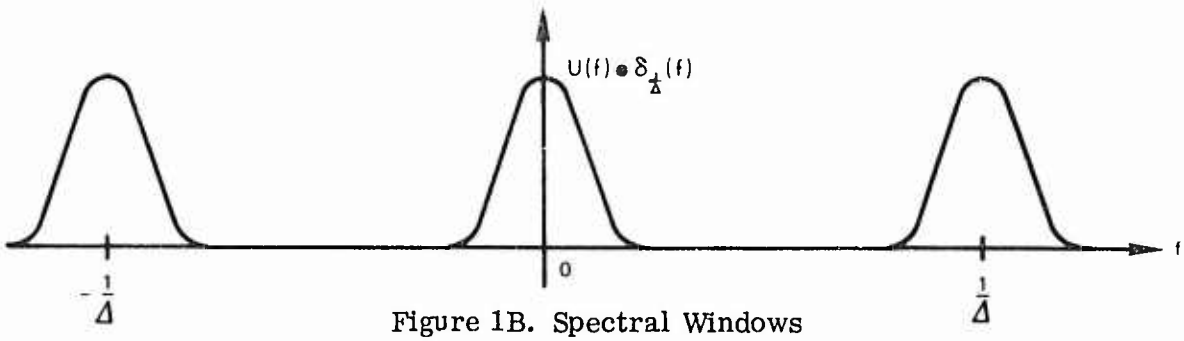


Figure 1B. Spectral Windows

Figure 1. Time and Frequency Relationships

Because the ideal spectral window is a single impulse at f = 0, the aliased mainlobes at m/Δ, $m \neq 0$, are undesired. Also, the window U(f) is desired to be narrow, with very small sidelobes. Since the weighting u(t) is of limited duration, the mainlobe width of U(f) is not zero, but is inversely proportional to the time duration.

Now, if the voltage density spectrum V(f) is computed at multiples of $(L\Delta)^{-1}$, where $L\Delta$ is the time duration of u(t), we obtain

$$V\left(\frac{p}{L\Delta}\right) = \Delta \sum_n \exp(-i2\pi np/L)\, x(n\Delta)\, u(n\Delta) , \quad p \text{ integer} . \qquad (5)$$

*In the time domain, u(t) is called a weighting; the corresponding Fourier transform in the frequency domain, U(f), is called a window. This nomenclature is used throughout.

Since V(f) is periodic of period $1/\Delta$ (see (1)), (5) need be computed at L different points; thus it can be realized as an L-point FFT of sequence $\{x(n\Delta)\ u(n\Delta)\}$. For fine frequency analysis (that is, large $L\Delta$) the size L of the FFT may be too large to compute easily, under storage and time limitations. The values in (5) are samples of the convolution of figure 1B with voltage density spectrum X(f).

APPROXIMATE FFT TECHNIQUE

Just as we started above with an integral definition of a spectrum, then showed that samples of this spectrum were attainable with an FFT, we begin with the spectral-delay function, a, defined as

$$\begin{aligned} a(f,\tau) &\equiv \int dt \exp(-i2\pi ft)\ x(t)\ w(t-\tau)\ \Delta\delta_\Delta(t) \\ &= \Delta \sum_n \exp(-i2\pi fn\Delta)\ x(n\Delta)\ w(n\Delta-\tau)\ . \end{aligned} \tag{6}$$

The temporal weighting w is now delayed by τ seconds; if the duration of w is L_W seconds, the function $w(t-\tau)$ picks out a delayed portion of data x of length L_W, and subjects it to the same transform as in (1). This operation is depicted in figure 2A, where the temporal weighting can be located at aa, bb, ..., cc. This figure is drawn for 50 percent overlap of the temporal weightings; however, other overlaps are possible and recommended in some cases.

The next step, consistent with step 4 in the Introduction, is to perform a Fourier transformation on the delay variable τ, while holding frequency variable f fixed. The general definition is the vernier spectrum

$$\begin{aligned} Y(f,\nu) &\equiv \int d\tau \exp(-i2\pi\nu\tau)\ a(f,\tau)\ d(\tau)\ S\delta_S(\tau) \\ &= S \sum_k \exp(-i2\pi\nu kS)\ a(f,kS)\ d(kS)\ , \end{aligned} \tag{7}$$

where ν is the vernier frequency, $d(\tau)$ is called the delay weighting, and S is the separation increment in delay τ at which $a(f,\tau)$ must be computed; that is, S is the shift between temporal weighting locations (see figure 2A). Since the separation S in delays can be taken to be smaller than the temporal weighting duration L_W, (7) allows for overlapped weighted transformation of the available data (see (6)).

The operation described by (7) is depicted in figure 2B. When the Fourier transform (6) on weighted time segment aa is completed, the set of frequency components denoted by the vertical line of Xs at the end of segment aa are available. Similarly, frequency component values at the ends of segments bb, . . . , cc are indicated in figure 2B; these components correspond to delayed locations of the temporal weighting w. Now, for a fixed frequency, say f_1, the array of (delayed) frequency components indicated in a horizontal box in figure 2B is subjected to a delay weighting and is Fourier transformed according to (7), thereby yielding vernier spectrum $Y(f_1, \nu)$. Similar outputs are available for other (adjacent) frequencies of interest, such as f_2 or f_3 .

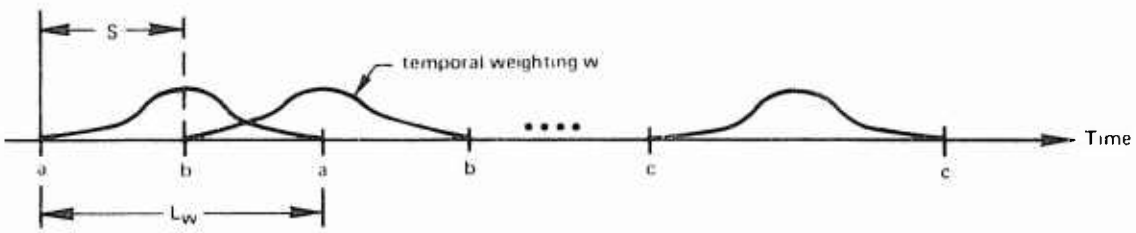


Figure 2A. Overlapped Temporal Weightings

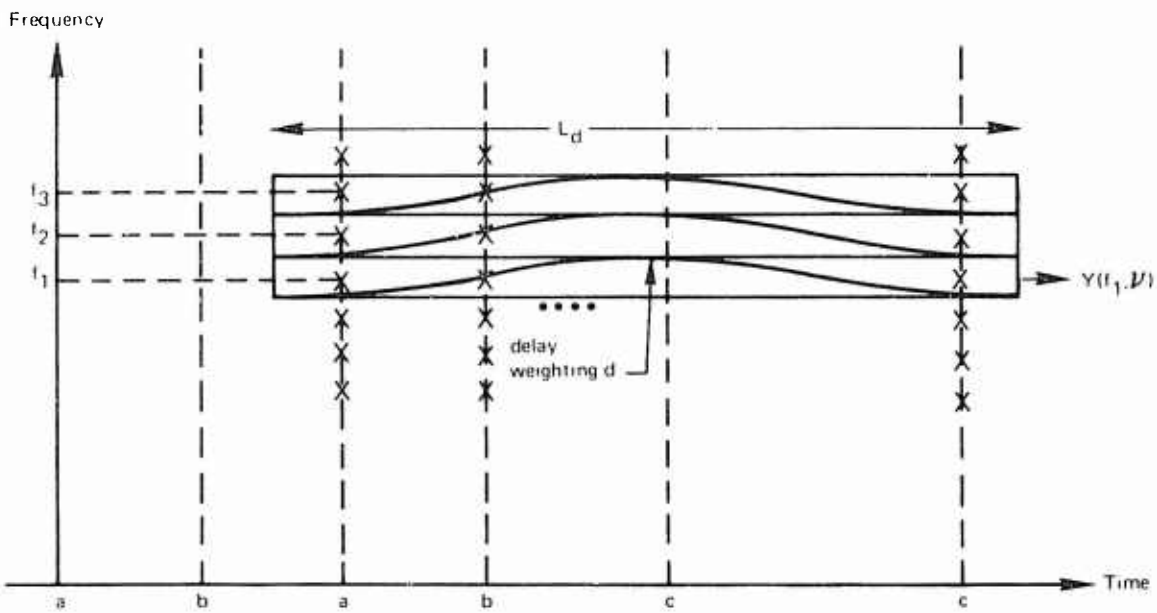


Figure 2B. Adjacent Delay Weightings

Figure 2. Temporal and Delay Weightings

Samples of the vernier spectrum in ν at multiples of $(MS)^{-1}$, where MS is the duration of delay weighting $d(\tau)$, are given by

$$Y\left(f, \frac{m}{MS}\right) = S \sum_k \exp(-i2\pi mk/M)\, a(f, kS)\, d(kS), \quad m \text{ integer}, \tag{8}$$

which can be realized as an M-point FFT of the sequence $\{a(f, kS)\, d(kS)\}$ of length M. The periodicity of $Y(f, \nu)$ in ν, of period $1/S$ (see (7)), means that (8) need be computed only at M different values of m.

Finally, samples of vernier spectrum Y in frequency f at multiples of $(N\Delta)^{-1}$ are given by (using (8))

$$Y\left(\frac{p}{N\Delta}, \frac{m}{MS}\right) = S \sum_{k=0}^{M-1} \exp(-i2\pi mk/M)\, a\left(\frac{p}{N\Delta}, kS\right) d(kS), \tag{9}$$

$$p = 0, 1, \ldots, N-1; \quad m = 0, 1, \ldots, M-1,$$

where delay weighting $d(\tau)$ has been selected so that samples $\{d(kS)\}$ are nonzero only for $k = 0, 1, \ldots, M-1$. The values of a needed in (9) are (using (6)) given by

$$a\left(\frac{p}{N\Delta}, kS\right) = \Delta \sum_n \exp(-i2\pi pn/N)\, x(n\Delta)\, w(n\Delta - kS). \tag{10}$$

In order to put (10) directly in the form of a standard FFT, we assume that the delay separation S is taken as an integer multiple of the sampling increment Δ:

$$S = I_S \Delta. \tag{11}$$

Then, if temporal weighting w has nonzero samples $\{w(n\Delta)\}$ only for $0 \le n \le N-1$, (10) becomes

$$a\left(\frac{p}{N\Delta}, kS\right) = \exp(-i2\pi pkI_S/N)\, \Delta \sum_{m=0}^{N-1} \exp(-i2\pi pm/N)\, x(m\Delta + kI_S\Delta)\, w(m\Delta), \tag{12}$$

$$0 \le p \le N-1, \quad 0 \le k \le M-1.$$

The exponential phase factor preceding the sum (FFT) in (12) takes on particularly simple forms for two special cases of delay separation S: For $I_S = N/2$, delay S is equal to half the temporal weighting duration L_W and is termed 50 percent overlap; for $I_S = N/4$, delay S is one-quarter of L_W and is termed 75 percent overlap. For these two cases,

$$\text{50 percent overlap, } I_S = N/2, \text{ phase factor} = (-1)^{pk} ; \tag{13A}$$

$$\text{75 percent overlap, } I_S = N/4, \text{ phase factor} = (-i)^{pk} . \tag{13B}$$

By proper branching in a computer program, no storage or complex multiplications are necessary to incorporate these phase factors in (12), prior to its usage in (9). (An alternative approach that completely circumvents the phase factor in (12) is described in appendix A.)

Equations (12) and (9) are the essential results of interest. We now interpret them by means of simple examples that will enable us to make good choices of temporal weighting w, delay weighting d, and separation (overlap) S.

INTERPRETATION OF THE VERNIER SPECTRUM

In appendix B, the vernier spectrum is shown to be given in terms of X by

$$Y(f, \nu) = \left[W(-\nu) \sum_m X\left(f + \nu - \frac{m}{\Delta}\right) \right] \circledast D(\nu) \circledast \delta_{1/S}(\nu) , \tag{14}$$

where all the convolutions are on ν, with f held fixed. $D(\nu)$ is the delay window corresponding to the delay weighting $d(\tau)$.

The linearity of the two Fourier transforms, (6) and (7), on the data x(t) indicates that we can investigate the behavior for data components separately and merely add the results. The fundamental component is

$$x(t) = \exp(i2\pi f_0 t), \quad X(f) = \delta(f - f_0) . \tag{15}$$

At this point, we shall make a series of reasonable assumptions and requirements, and deduce desirable properties about the weightings and separations. The first assumptions are

(a) excitation frequency $f_0 < (2\Delta)^{-1}$,

(b) coarse analysis frequency $f < (2\Delta)^{-1}$,

(c) $L_W >> \Delta$.

Assumption (a) avoids aliasing, (b) restricts analysis to the fundamental range, and (c) requires the temporal weighting to cover many samples of the process x(t). Furthermore, if

(d) temporal window W has low sidelobes,

the only term in the sum in (14), after substituting (15), that has substantial value is that for $m = 0$, and it yields

$$Y(f, \nu) \cong \left[W(f - f_o)\, D(\nu + f - f_o)\right] \circledast \delta_{1/S}(\nu) \quad . \tag{16}$$

A plot of this equation versus vernier frequency ν is given in figure 3, where L_d is the length (duration) of delay weighting $d(\tau)$. The narrow lobe at $\nu = f_o - f$ is the desired component; this component is displaced from the coarse analysis frequency f (corresponding to $\nu = 0$) by $f_o - f$ Hz, which places it at absolute frequency $f + (f_o - f) = f_o$, as desired. The shape of this lobe is governed by the delay window D; thus, if

(e) $L_d >> S$,

(f) delay window D has low sidelobes,

the large lobes separated by 1/S Hz in figure 3 will not overlap significantly, and potentially good spectral estimation is possible. The necessity of delay weighting is made obvious by these observations.

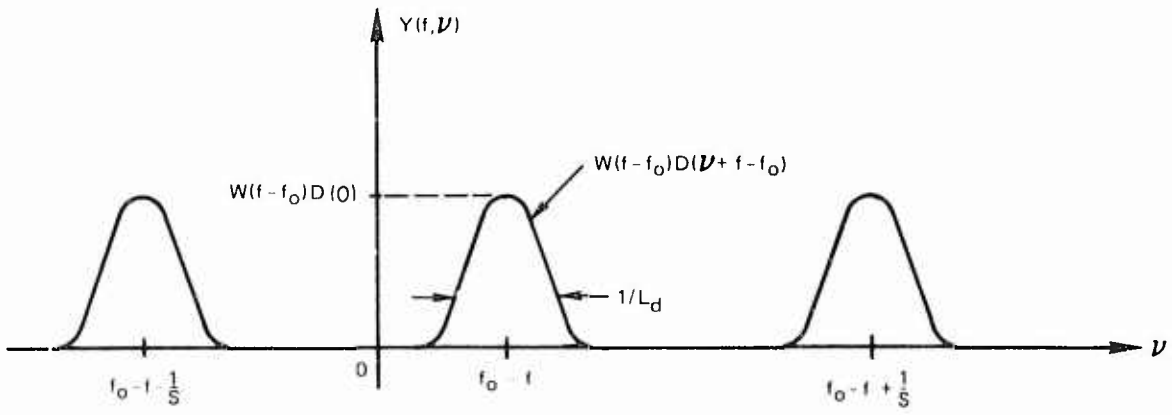


Figure 3. Vernier Spectrum

There are a few additional points worth noting about figure 3. The peak height of the lobes, $W(f - f_o)\, D(0)$, is a function of the exact location of the excitation frequency f_o and the coarse analysis frequency f. This undesirable picket-fence effect* (which was not present in figure 1) can be minimized:

(g) choose analysis frequencies $\{f_k\}$ closely spaced (see figure 2B).

Then $|f_k - f_o|$ is small for some value of k. Also, since the width of the lobes in figure 3 is $1/L_d$, where L_d is the delay weighting duration and will be taken of the order of the <u>total</u> record length available or utilized, very fine resolution in ν is possible. Hence, narrowband components closer than $1/L_w$, the resolution capability of a single time segment, can be resolved by using this technique.

FFT CONSIDERATIONS

Samples of the vernier spectrum $Y(f, \nu)$ were given in (9). The locations of the samples are†

$$\begin{aligned} f&: \ 0, \ \frac{1}{N\Delta}, \ \frac{2}{N\Delta}, \ \ldots, \ \frac{N-1}{N\Delta}; \\ \nu&: \ 0, \frac{1}{MS}, \ \frac{2}{MS}, \ \ldots, \ \frac{M-1}{MS} \ . \end{aligned} \tag{17}$$

The range covered by the vernier frequency ν is S^{-1}, and will be greater than the increment in f, which is $(N\Delta)^{-1}$, if overlapped temporal weighting is used. And since the full range, S^{-1}, would encompass a spurious lobe for values of $|f_o - f|$ near $(2S)^{-1}$ (see figure 3), overlapping is necessary.

The approach adopted here is to utilize <u>all</u> the samples in f at separations of $(N\Delta)^{-1}$, and use only samples in ν which cover a range of $(N\Delta)^{-1}$; that is, we use the <u>central</u> portion of Y centered around $\nu = 0$, including negative frequencies. In terms of figure 2B, adjacent delay weightings at f_1, f_2, f_3 will be employed. The alternative time-saving procedure of attempting to utilize all of the M samples in ν, and using only enough samples in f to fill in the frequency axis, can lead to a very bad picket-fence effect, in addition to large spurious lobes at undesired frequency locations. These conclusions follow upon piecing together several vernier spectra like figure 3 for appropriate values of f and excitation frequency f_o.

*See reference 4, page 47.

†The upper half of the array of numbers in (17) corresponds to negative frequencies. Thus the last samples in each array correspond to $f = -(N\Delta)^{-1}$ and $\nu = -(MS)^{-1}$, respectively.

EXAMPLES

The general guidelines furnished in the previous section do not yet enable us to make quantitative selection of good weightings for different degrees of overlap. To make this selection, several examples are considered and compared. The numerical examples utilize

$$\Delta = \frac{1}{1024} \text{ seconds}, \quad N = 1024, \quad \frac{1}{MS} = \frac{1}{8} \text{ Hz}, \qquad f_o = 256 \left(\frac{1}{16}\right) \quad 256\frac{1}{2} \text{ Hz} . \tag{18}$$

(A sample program utilizing (9), (10), (11), (18), and the method of appendix A is given in appendix C for 75 percent overlap.)

50 PERCENT OVERLAP

At 50 percent overlap of the temporal weighting,* several possibilities were tried. They included

$$\left.\begin{array}{r} \text{cosine lobe} : \; w(t) = \cos(\pi t/L_w) \\ \text{cosine}^2 \text{ lobe (Hanning)} ; \; w(t) = \cos^2(\pi t/L_w) \\ \text{Dolph-Chebyshev (Reference 5)}\dagger \end{array}\right\} \; |t| < L_w/2 . \tag{19}$$

A complete list of cases is presented in table 1.

In figures 4A through 4I,‡ decibel plots of the magnitude of the estimated spectrum are given for cosine temporal weighting and for (cosine)^2 delay weighting. All plots are normalized with respect to a maximum of 0 dB, which occurs for $f_o = f = 256$ Hz, $\nu = 0$ Hz. Figure 4A, for example, demonstrates the behavior predicted by figure 3, namely, the presence of spurious sidelobes every $S^{-1} = (.5 \times 1 \text{ s})^{-1} = 2$ Hz. The largest spurious lobe in figure 4A is -23.5 dB at 258 Hz. The slow rate of decay of the peaks at $256 \pm 2n$ Hz is due to the discontinuity of slope of $w(t)$ at $\pm L_w/2$ for this example. The desirable feature of a narrow mainlobe is attained, as indicated in figure 4. The succession of plots in figure 4 shows that the extent of the picket fence varies greatly

*When these weightings are employed in the FFT, they are delayed by $L_w/2$ seconds, thereby being nonzero in the interval $(0, L_w)$.

†A quick and accurate method of generating the Dolph-Chebyshev weights by means of efficient use of an FFT is presented in reference 6.

‡Figures 4 through 14 follow the text, beginning on page 16.

Table 1. Examples of Temporal and Delay Weightings

Figure	Temporal Weighting	Delay Weighting	Overlap (%)	Number of Tones
4	cosine	cosine^2	50	1
5	cosine^2	cosine^2	50	1
6	Dolph-Chebyshev	cosine^2	50	1
7	cosine^2	cosine^2	75	1
8	cosine^3	cosine^2	75	1
9	cosine^4	cosine^2	75	1
10	cosine^5	cosine^2	75	1
11	Dolph-Chebyshev	cosine^2	75	1
12	cosine^2	flat	75	1
13	cosine^2	cosine^2	75	2
14	cosine^2	flat	75	2

with excitation frequency, reaching a maximum of -3.20 dB in figure 4H for f_0 = 256 7/16 Hz. (The figures for f_0 > 256 1/2 Hz repeat the behavior shown.) The worst sidelobe of -23.0 dB occurs for f_0 = 256 1/8 Hz, as shown in figure 4C.

It should be noted that if sidelobes were to be measured with respect to the peak on that same plot, figure 4C would yield a sidelobe of -23.0 + 0.13 = -22.9 dB. Thus, the convention adopted here must be kept in mind in the following discussion.

Instead of applying the weighting directly in the time domain by means of multiplication on the data x, the effect of cosine weighting can be accomplished in the frequency domain by means of convolution of the spectrum with the sequence $(i/2)\{1, -1\}$; however, the resultant must be interpreted as the spectral value between the two quantities convolved at each frequency step.* More generally, $(\text{cosine})^n$ time weighting can be accomplished alternatively by means of convolution of the (unweighted) spectrum with the sequence

$$\left(\frac{i}{2}\right)^n \left\{1, -n, \binom{n}{2}, -\binom{n}{3}, \ldots, (-1)^n\right\} \qquad (20)$$

*This possibility and its interpretation were pointed out by Dr. N. L. Owsley.

of length $n + 1$, and then interpreted as the spectral value at the center of the region convolved, for each frequency step; see appendix D. The convolutional sequences in (20) are given in table 2 for $n = 1$ through 5.

Table 2. Convolution Sequences

n	Convolution Sequence
1	$i\ 1/2\{1, -1\}$
2	$1/4\{-1, 2, -1\}$
3	$i\ 1/8\{-1, 3, -3, 1\}$
4	$1/16\{1, -4, 6, -4, 1\}$
5	$i\ 1/32\{1, -5, 10, -10, 5, -1\}$

Since the effect of $(\text{cosine})^2$ temporal weighting is very easy to incorporate in the frequency domain by means of convolution, it must be considered as a candidate for weighting. The results in figures 5A and 5B show that although the picket fence is reduced to -2.70 dB, the peak sidelobe increases to -15.4 dB. (For brevity, we are now presenting only selected cases of worst excitation frequencies.) The reason for the increased sidelobes for this temporal weighting is that 50 percent overlap is not yet great enough to realize the deeper first sidelobe level of -31.5 dB; that is, we are still sampling, according to figure 3, on the skirts of the mainlobe for some excitation frequencies. Generally, for 50 percent overlap, the peak sidelobe will occur approximately at the excitation frequency such that the worst sidelobe (or mainlobe) of the temporal window beyond $f = 1.5/L_W$ is encountered; this may be seen by considering figure 3 and recalling that we plot only the central portion of $Y(f, \nu)$. Thus the $(\text{cosine})^n$ weightings in tables 1 and 2 for $n > 2$ are not acceptable for 50 percent overlap, since sampling of the mainlobe is encountered.

The realization of minimum sidelobe level for a specified beamwidth (to the first null) is exactly the problem addressed by Dolph, reference 5. Accordingly, this weighting is of considerable importance in spectral estimation. In figures 6A-6C, the effects of Dolph-Chebyshev time weighting are presented. The worst sidelobe of -33.2 dB occurs for $f_0 = 256\ 1/8$ Hz (figure 6C). These results are noticeably better than in figures 4 and 5.

When triangular temporal weighting was tried, it had a peak sidelobe of -20.2 dB; again, we are sampling the skirts of the mainlobe. Thus, if 50 percent overlap is all that can be utilized for some applications, due perhaps to limited computation time, the cosine-lobe temporal weighting is the best of the simply applied windows (that is, by means of frequency domain convolution), but the Dolph-Chebyshev time weighting is 10 dB better than the cosine lobe weighting.

75 PERCENT OVERLAP

At 75 percent overlap of the temporal weightings the following examples were utilized:

$$\left.\begin{array}{ll} \text{cosine}^2 \text{ lobe (Hanning)} & : w(t) = \cos^2 (\pi t/L_W) \\ \text{cosine}^3 \text{ lobe} & : w(t) = \cos^3 (\pi t/L_W) \\ \text{cosine}^4 \text{ lobe} & : w(t) = \cos^4 (\pi t/L_W) \\ \text{cosine}^5 \text{ lobe} & : w(t) = \cos^5 (\pi t/L_W) \\ \text{Dolph-Chebyshev} & \text{----} \end{array}\right\} |t| < L_W/2 \, . \qquad (21)$$

The results for the Hanning weighting are given in figure 7. The peak sidelobe is -41.8 dB at f_o = 256 1/2 Hz in figure 7C, and the picket fence is -2.60 dB at f_o = 256 7/16 Hz in figure 7B. Thus, a much improved sidelobe level is realized relative to 50 percent overlap, at the expense of increased computation effort, that is, increased overlap and number of FFTs.

In an effort to further improve performance, the (cosine)^3 weighting, which has a higher degree of continuous derivatives at $\pm L_W/2$, was tried. The results in figure 8 show a maximum sidelobe of -51.2 dB and a picket fence of -2.34 dB.

Continuation of this effort to smoother weightings such as (cosine)^4, figure 9, shows a peak sidelobe of -48.1 dB and a picket fence of -2.18 dB. The peak sidelobe has increased over that for (cosine)^3 weighting because, for 75 percent overlap, the peak sidelobe (or main lobe) of the temporal window beyond approximately $f = 3.5/L_W$ is encountered. It so happens that the worst case in this region is larger for (cosine)^4 than for (cosine)^3 temporal weighting.

For (cosine)^5 temporal weighting, the peak sidelobe is reduced further to -54.1 dB. Also, the picket fence is improved to -2.07 dB; see figure 10. This weighting is easily accomplished via frequency domain manipulations; see table 2. An alternative temporal weighting of virtually equal quality to (cosine)^5 is cubic, that is, sections of cubic curves that have continuous derivatives of as high order as possible. The temporal window is proportional to

$$\left[\frac{\sin (\pi L_W f/4)}{\pi L_W f/4}\right]^4 \qquad (22)$$

and has a worst sidelobe of -53.1 dB. (The picket fence was not computed.) However, a cubic temporal weighting is not easily accomplished in the frequency domain.

When (cosine)^6 temporal weighting is considered, it is found that 75 percent overlap forces us to sample the temporal window on the skirts of its mainlobe. This is an unacceptable weighting because the peak sidelobe in the vernier spectrum increases significantly.

The possibilities of Dolph-Chebyshev weighting are indicated in figure 11. The worst sidelobe is -86 dB in figure 11B for f_0 = 256 1/4 Hz, and the picket fence is -2.29 dB in figure 11C for f_0 = 256 7/16 Hz. This is a 32-dB improvement in sidelobe level compared with (cosine)^5 weighting. The picket fence is degraded by 0.22 dB.

To determine the effect of not using delay weighting, figure 12 was computed for (cosine)^2 temporal weighting and flat delay weighting. For certain excitation frequencies, a very narrow mainlobe is realized; see figure 12A. However, for other excitation frequencies, the lack of delay weighting creates broad "shoulders" of significant level; see figure 12B. Also, the sampling in f and ν, inherent in the FFT, produces a picket fence of -5.0 dB. Thus, although a low peak sidelobe is attained, lack of delay weighting is very detrimental to performance, as will be further demonstrated below. Notice from figure 7 that (cosine)^2 delay weighting also yields a peak sidelobe of -41.8 dB, but has no broad shoulders and has a picket fence of only -2.60 dB.

The detrimental effects of no delay weighting are best illustrated by a comparison of figures 13 and 14, which have two tones separated by 1/2 Hz, one 15 dB stronger than the other. It is seen that these two tones are resolved, even though they are closer than the resolution capability of the individual time segments, that is, closer than 1 Hz. In figure 13, (cosine)^2 delay weighting is employed; in figure 14, none is employed. A comparison of part A of these figures reveals that, for excitation frequencies 256 and 256 1/2 Hz, the flat delay weighting is better. However, for excitation frequencies 256 1/16 and 256 9/16 Hz, the presence of the weaker tone is clearly evident in figure 13B, but hardly discernible in figure 14B (no delay weighting). The presence of noise would obscure the weaker peak. Thus, although the peak sidelobe may be very small, the presence of high-level broad shoulders must also be eliminated by use of delay weighting.

CONCLUSIONS

An approximate and quick FFT technique for vernier spectral analysis is possible by employing overlapped temporal weighting and delay weighting. For 50 percent overlap and Hanning delay weighting, the best simply-applied temporal weighting discovered was a single cosine lobe, realizing a peak sidelobe

of -23 dB. However, Dolph-Chebyshev temporal weighting achieves -33 dB sidelobes. For 75 percent overlap and Hanning delay weighting, the best simply applied temporal weighting discovered was (cosine)^5, which realized a peak sidelobe of -54 dB. However, Dolph-Chebyshev temporal weighting is capable of -86 dB sidelobes. Which overlap and weighting to employ depends on the limitations on computation time and storage, and on the relative strength and location of interfering tones.

The overlap is not limited to the above choices. It could, for example, be 67 percent. The best weightings were not investigated in this case, because it was felt that the above overlaps were easier to implement in most cases of practical interest. However, Dolph-Chebyshev weighting is always a strong candidate and is quickly and accurately generated (reference 6).

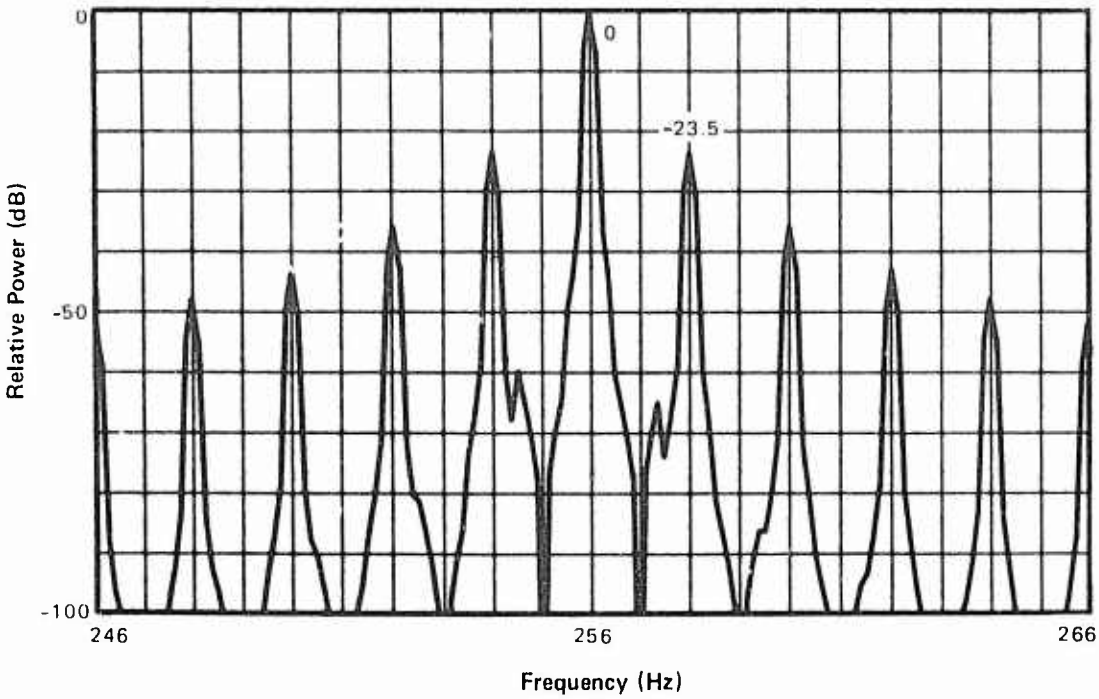


Figure 4A. f_0 = 256 Hz

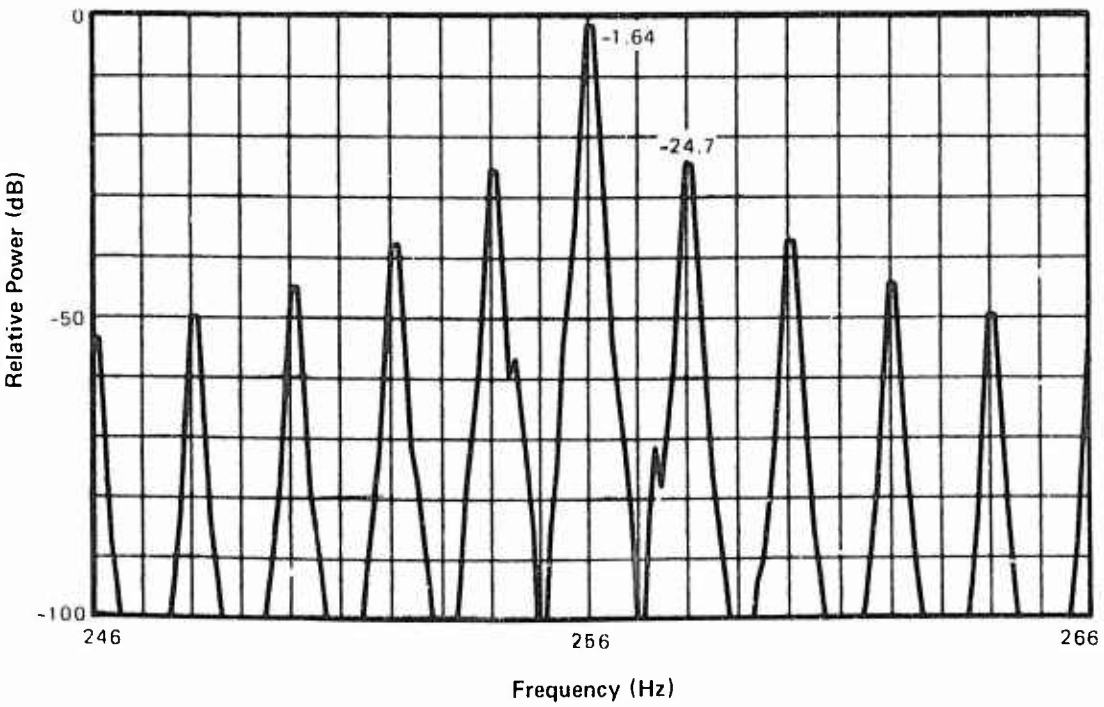


Figure 4B. f_0 = 256 1/16 Hz

Figure 4. Vernier Spectrum for Cosine Temporal Weighting, 50 percent Overlap

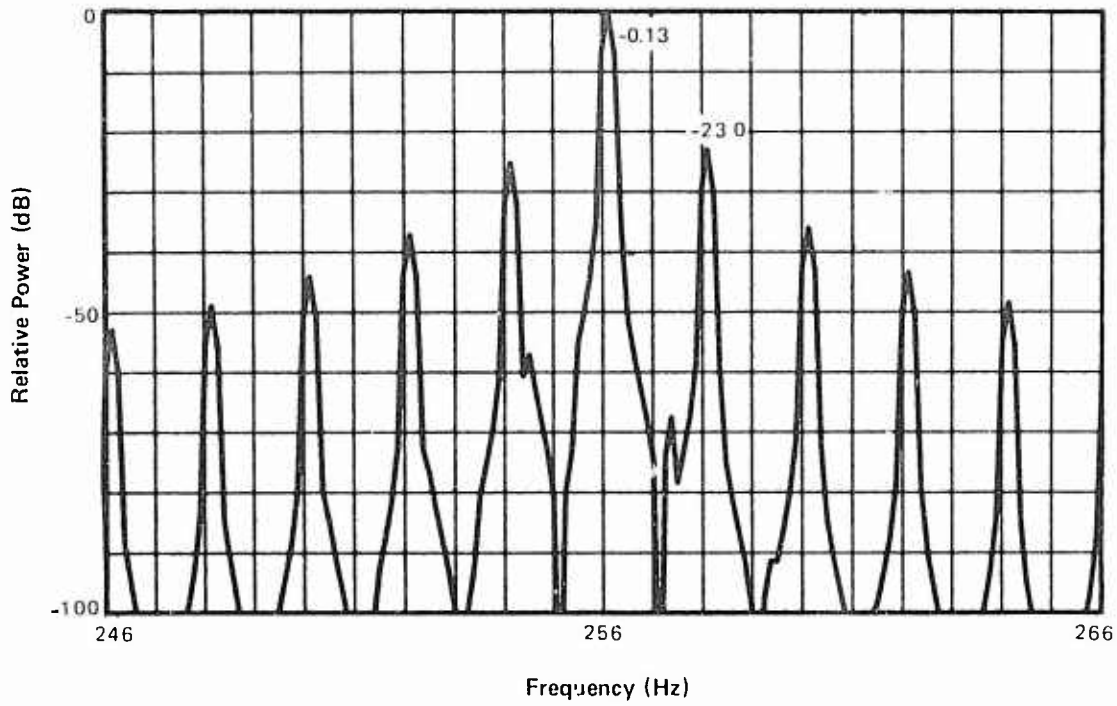


Figure 4C. f_o = 256 2/16 Hz

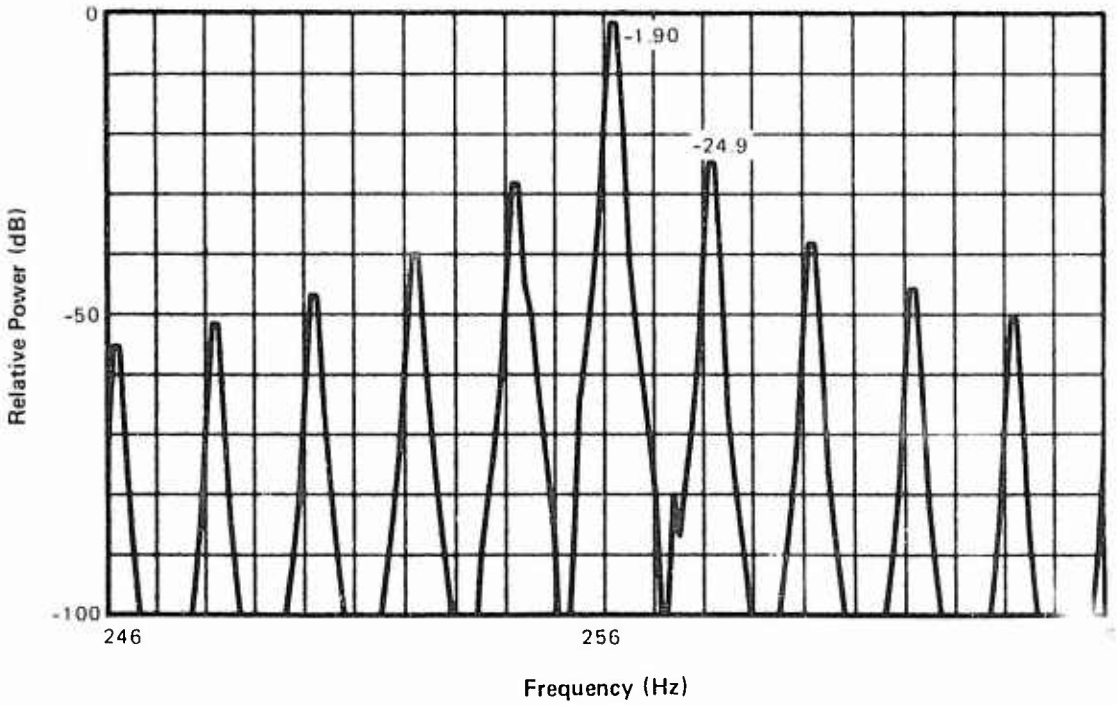


Figure 4D. f_o = 256 3/16 Hz

Figure 4 (Cont'd). Vernier Spectrum for Cosine Temporal Weighting, 50 percent Overlap

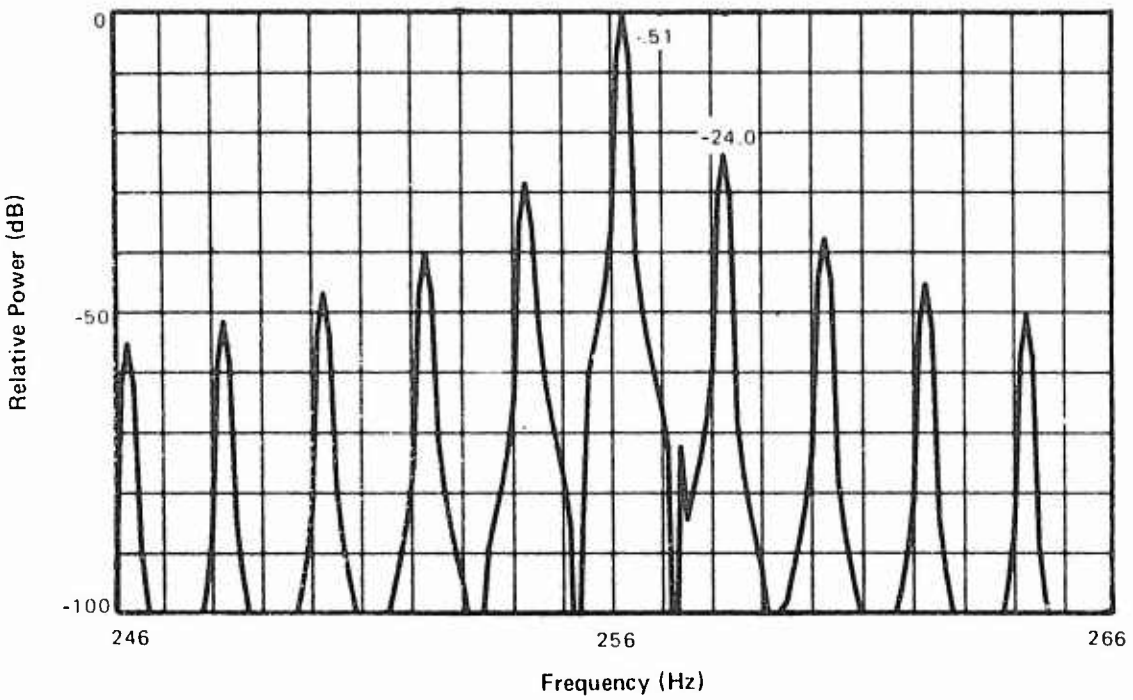


Figure 4E. f_o = 256 4/16 Hz

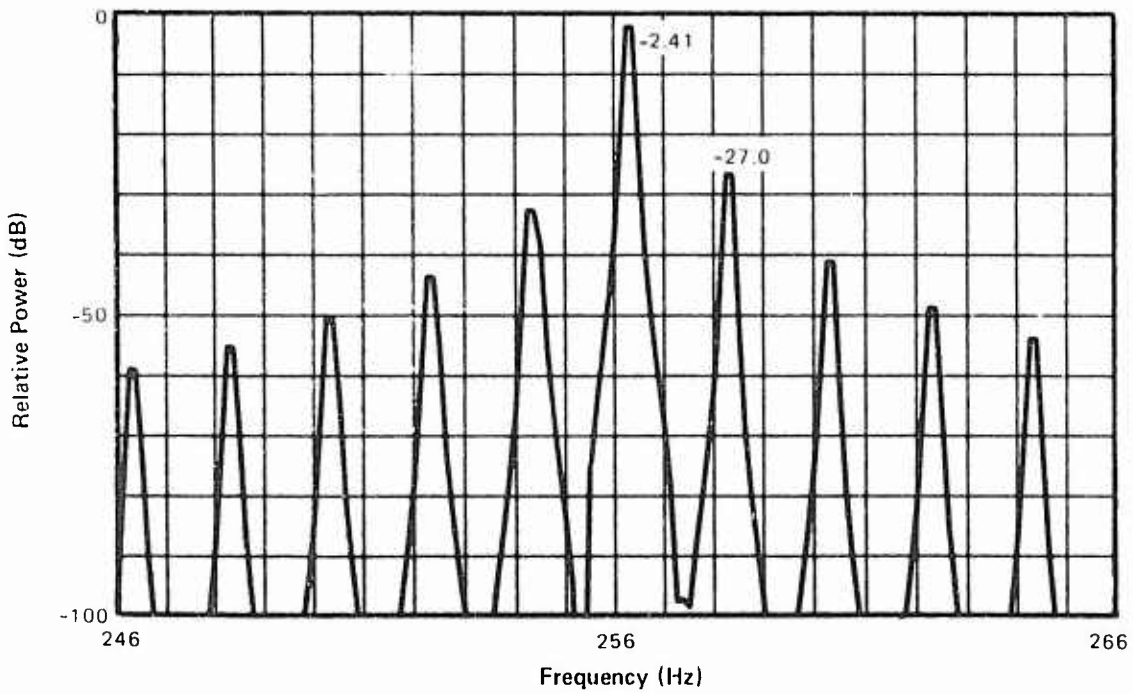


Figure 4F. f_o = 256 5/16 Hz

Figure 4 (Cont'd). Vernier Spectrum for Cosine Temporal Weighting, 50 percent Overlap

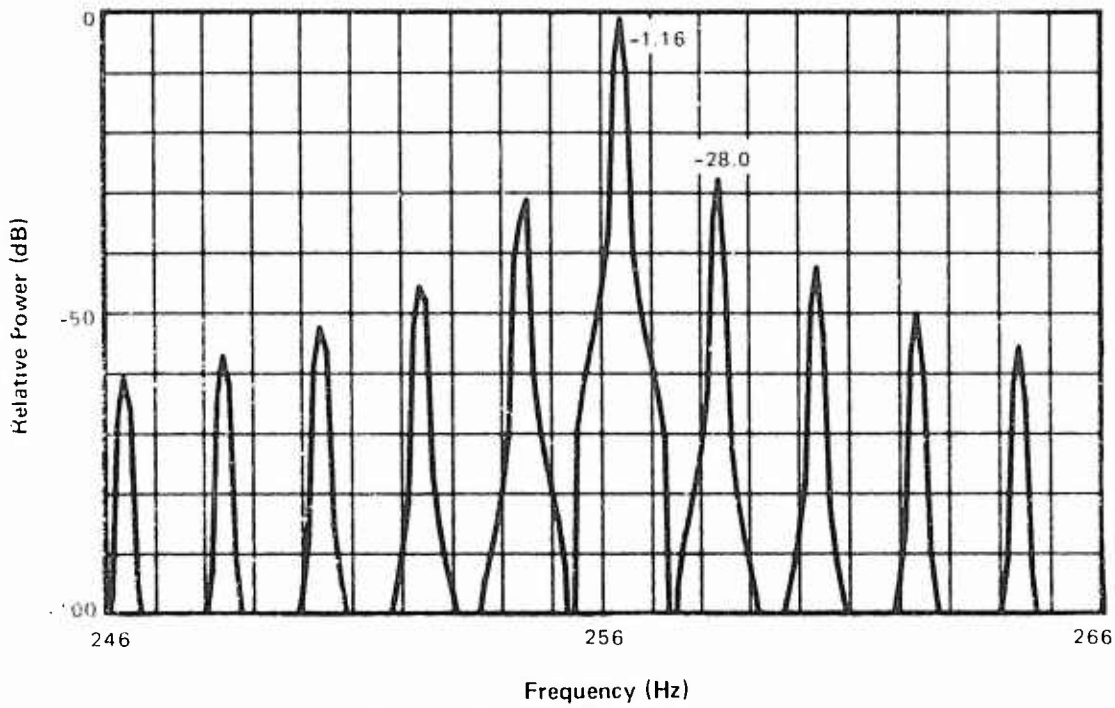


Figure 4G. f_o = 256 6/16 Hz

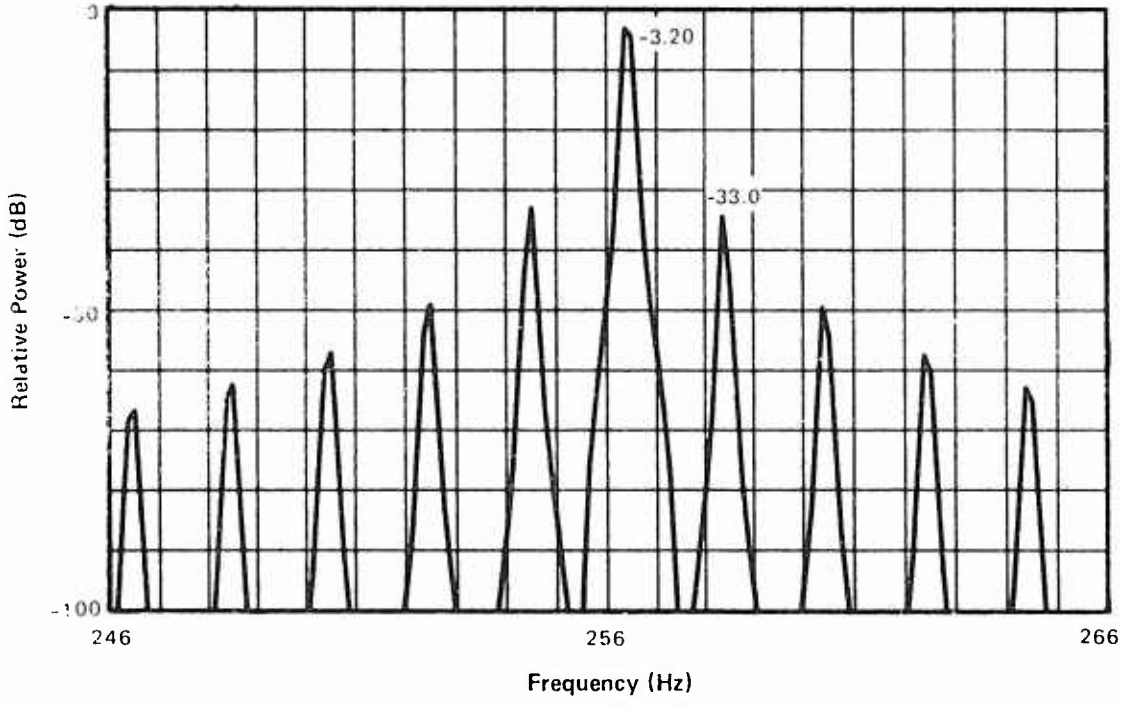


Figure 4H. f_o = 256 7/16 Hz

Figure 4 (Cont'd). Vernier Spectrum for Cosine Temporal Weighting, 50 percent Overlap

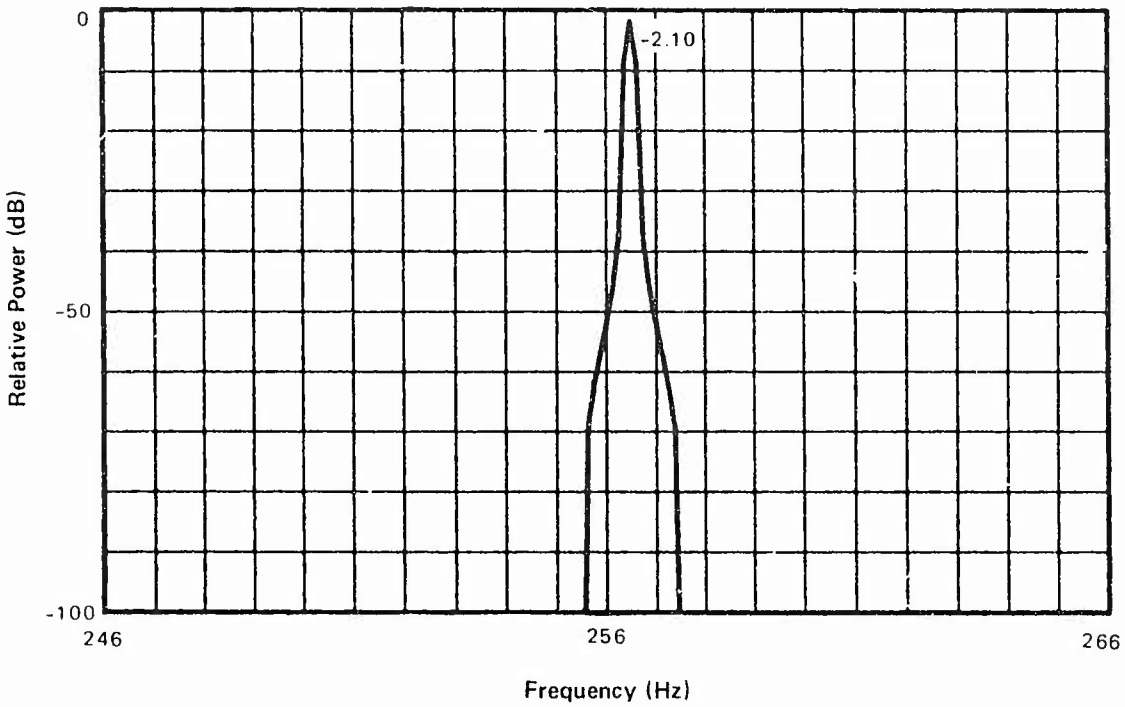


Figure 4I. f_o = 256 1/2 Hz

Figure 4 (Cont'd). Vernier Spectrum for Cosine Temporal Weighting, 50 percent Overlap

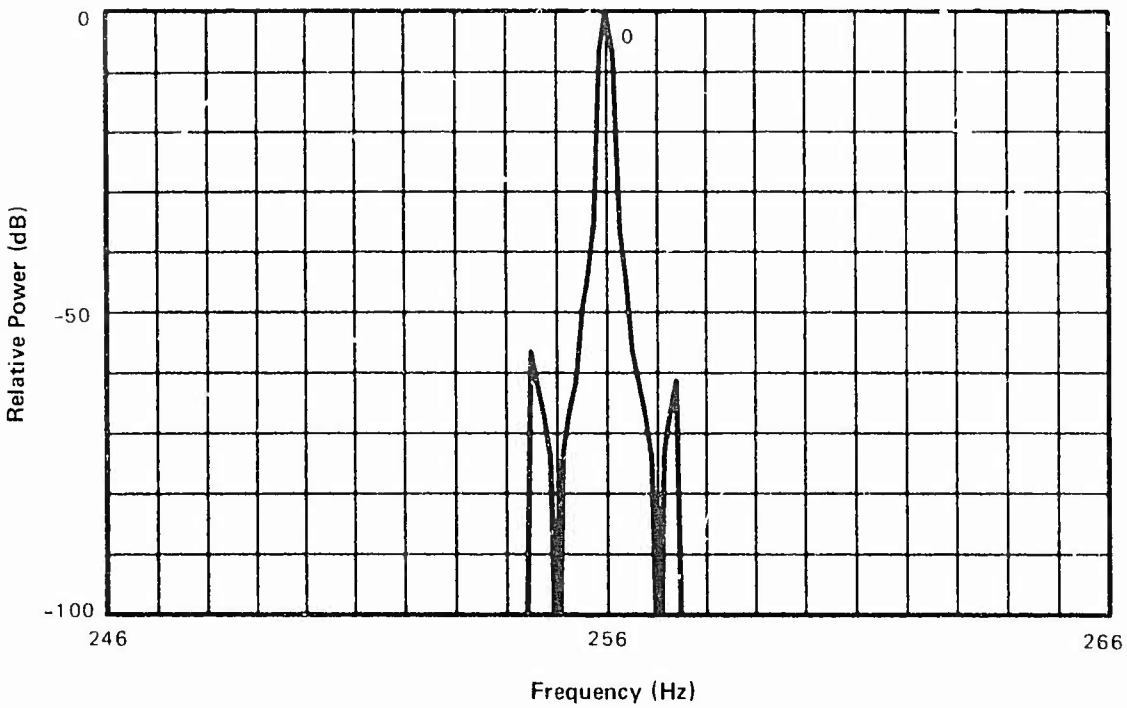


Figure 5A. f_o = 256 Hz

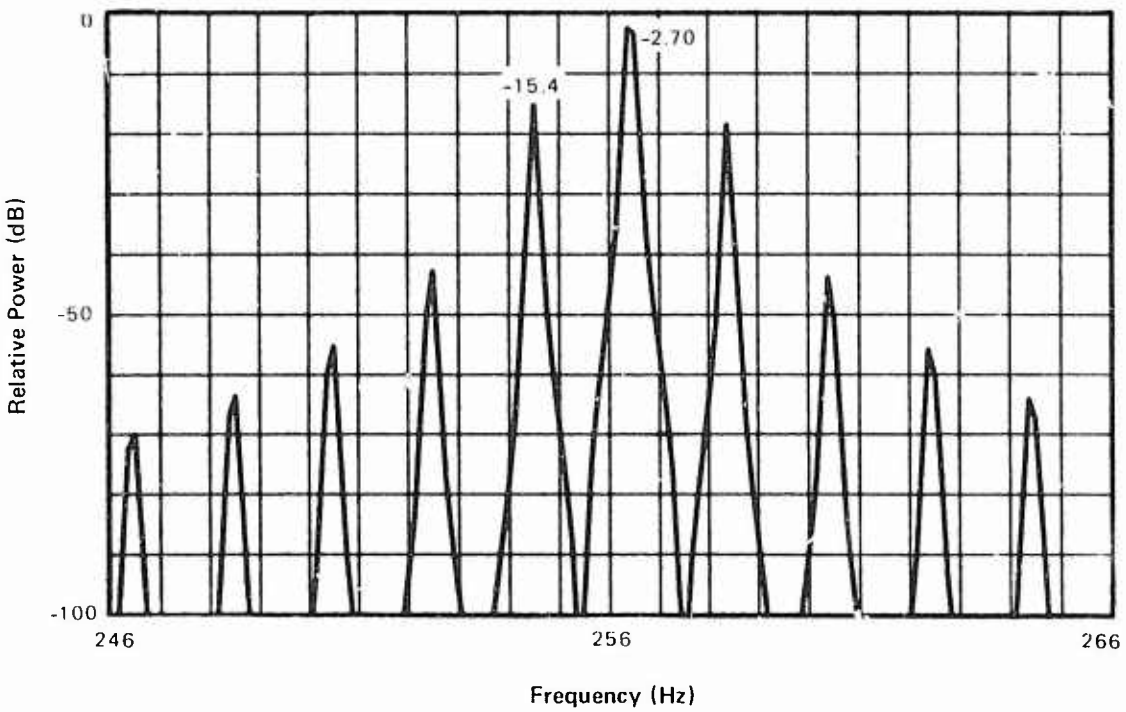


Figure 5B. f_o = 256 7/16 Hz

Figure 5. Vernier Spectrum for (Cosine)^2 Temporal Weighting, 50 percent Overlap

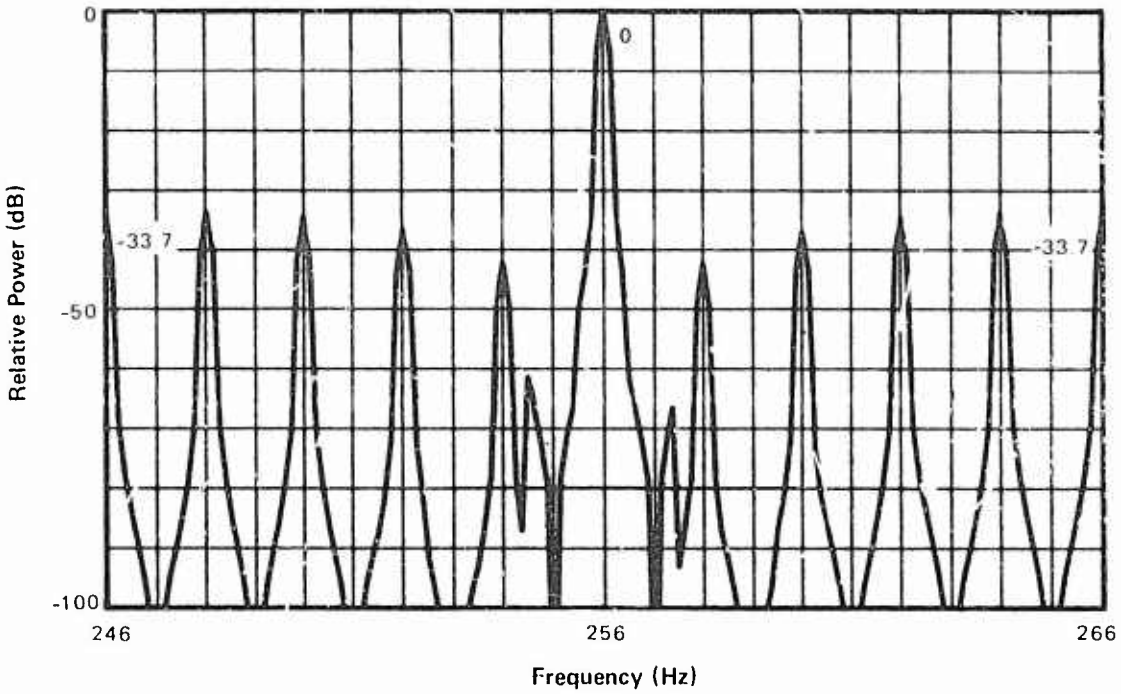


Figure 6A. f_o = 256 Hz

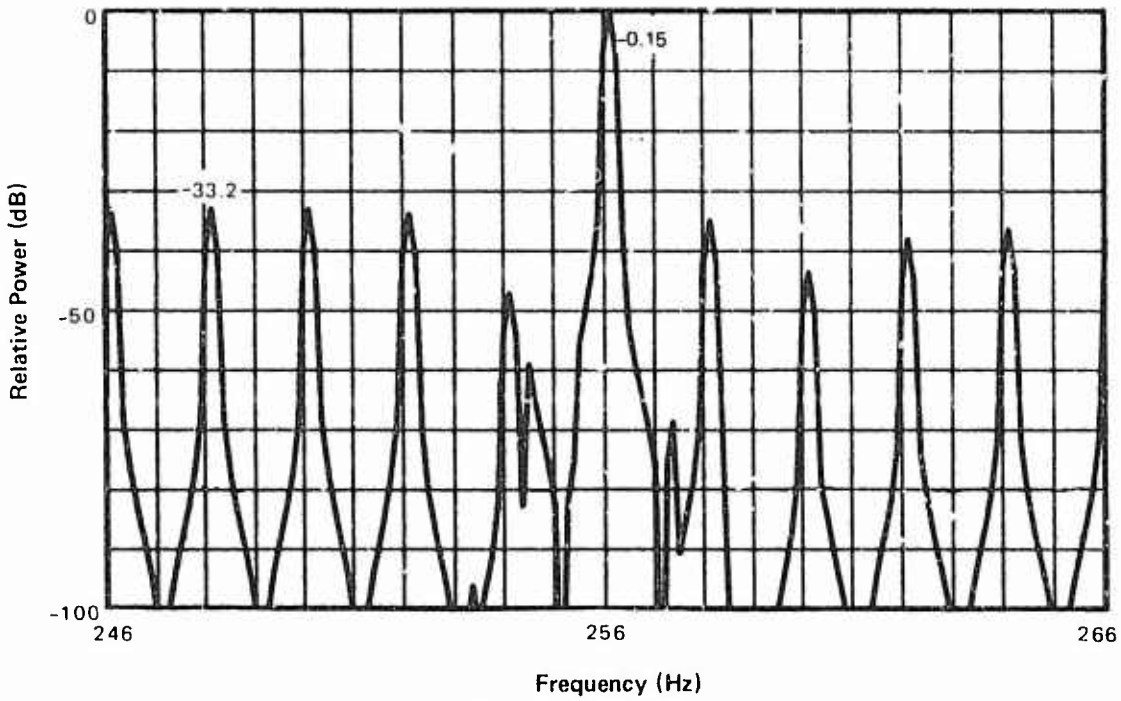


Figure 6B. f_o = 256 1/8 Hz

Figure 6. Vernier Spectrum for Dolph-Chebyshev Temporal Weighting, 50 percent Overlap

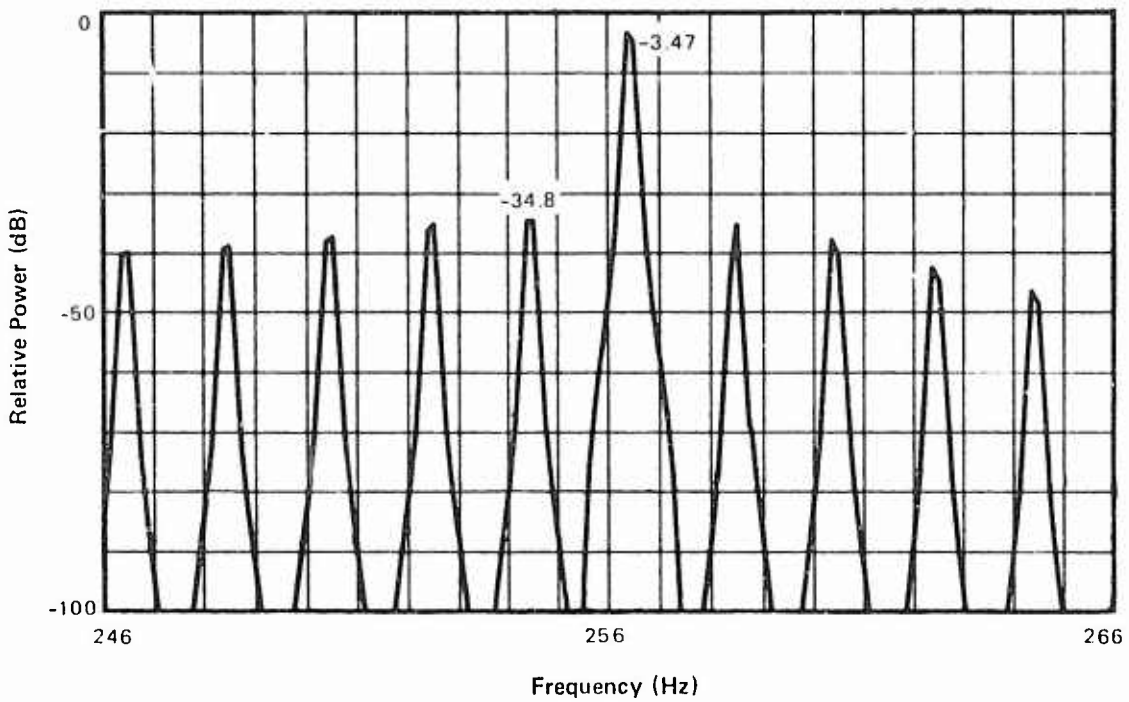


Figure 6C. f_o = 256 7/16 Hz

Figure 6 (Cont'd). Vernier Spectrum for Dolph-Chebyshev Temporal Weighting, 50 percent Overlap

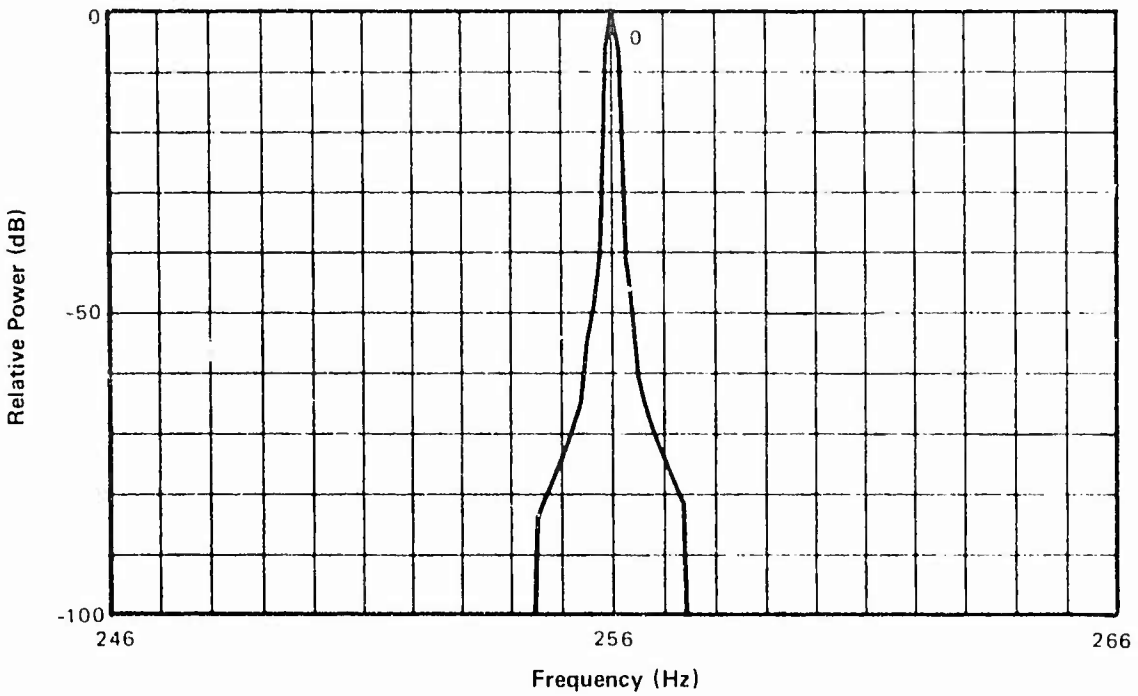


Figure 7A. f_o = 256 Hz

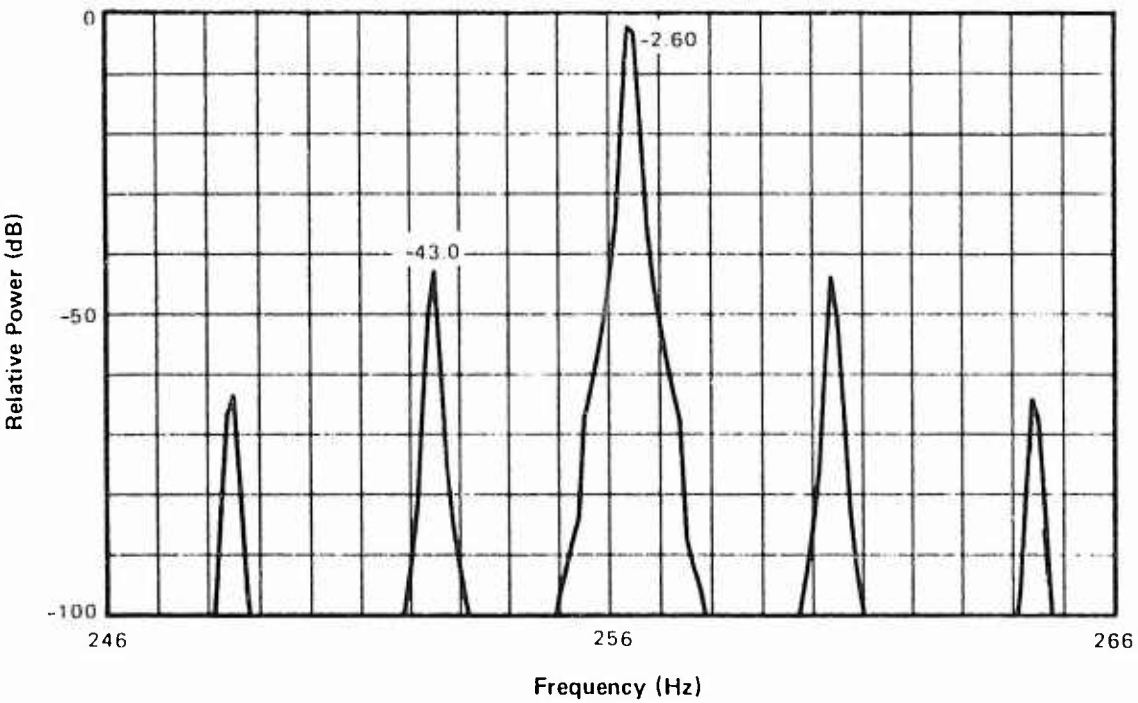


Figure 7B. f_o = 256 7/16 Hz

Figure 7. Vernier Spectrum for (Cosine)^2 Temporal Weighting, 75 percent Overlap

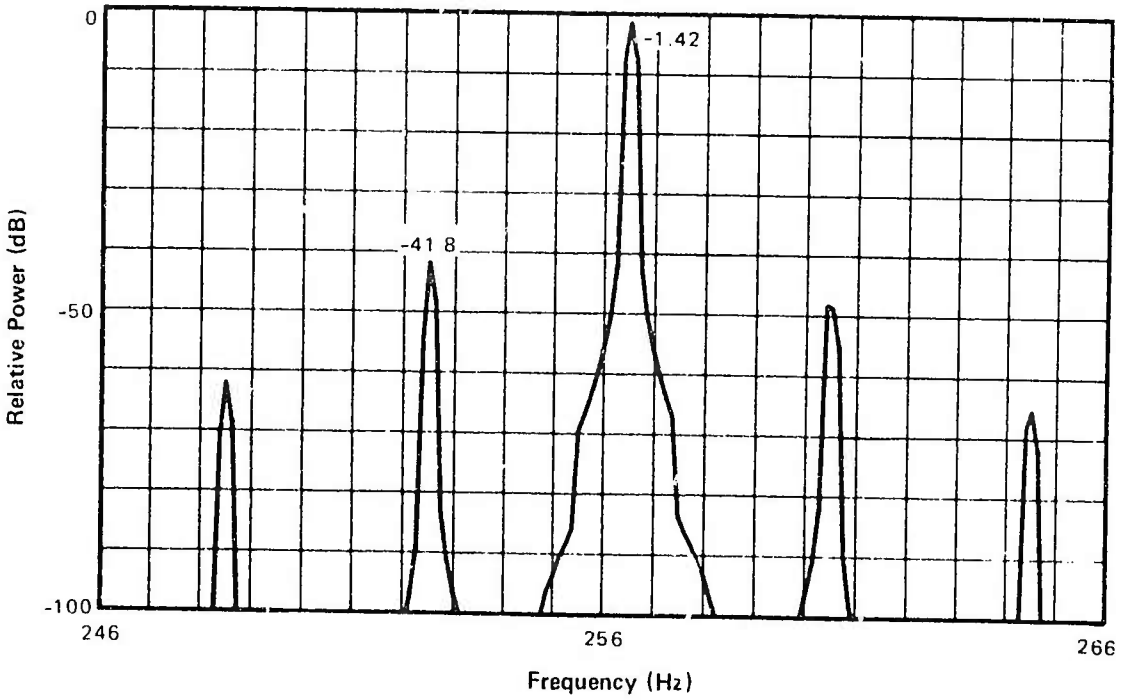


Figure 7C. f_0 = 256 1/3 Hz

Figure 7 (Cont'd). Vernier Spectrum for (Cosine)^2 Temporal Weighting, 75 percent Overlap

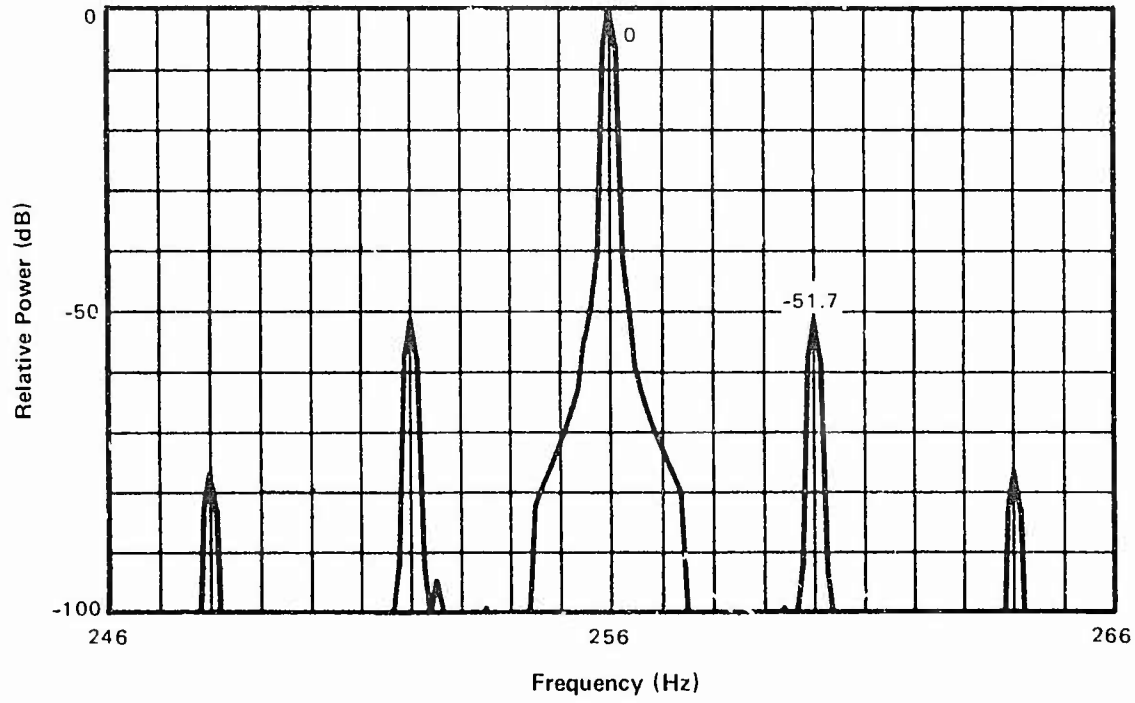


Figure 8A. f_o = 256 Hz

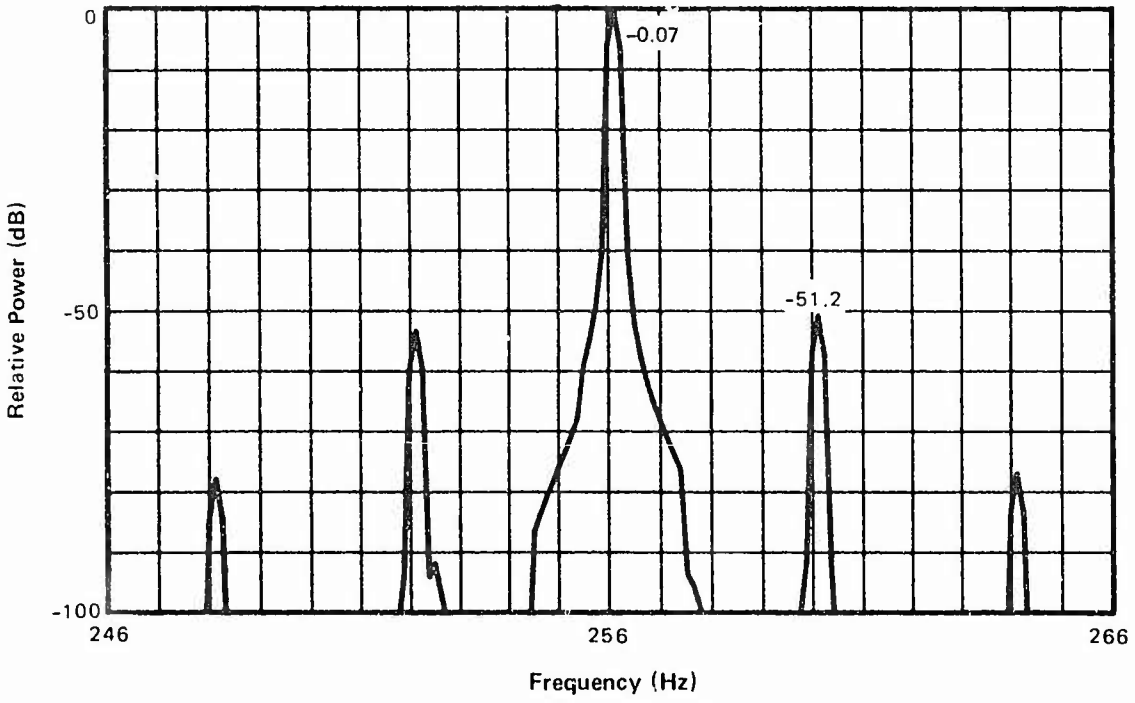


Figure 8B. f_o = 256 1/8 Hz

Figure 8. Vernier Spectrum for (Cosine)^3 Temporal Weighting, 75 percent Overlap

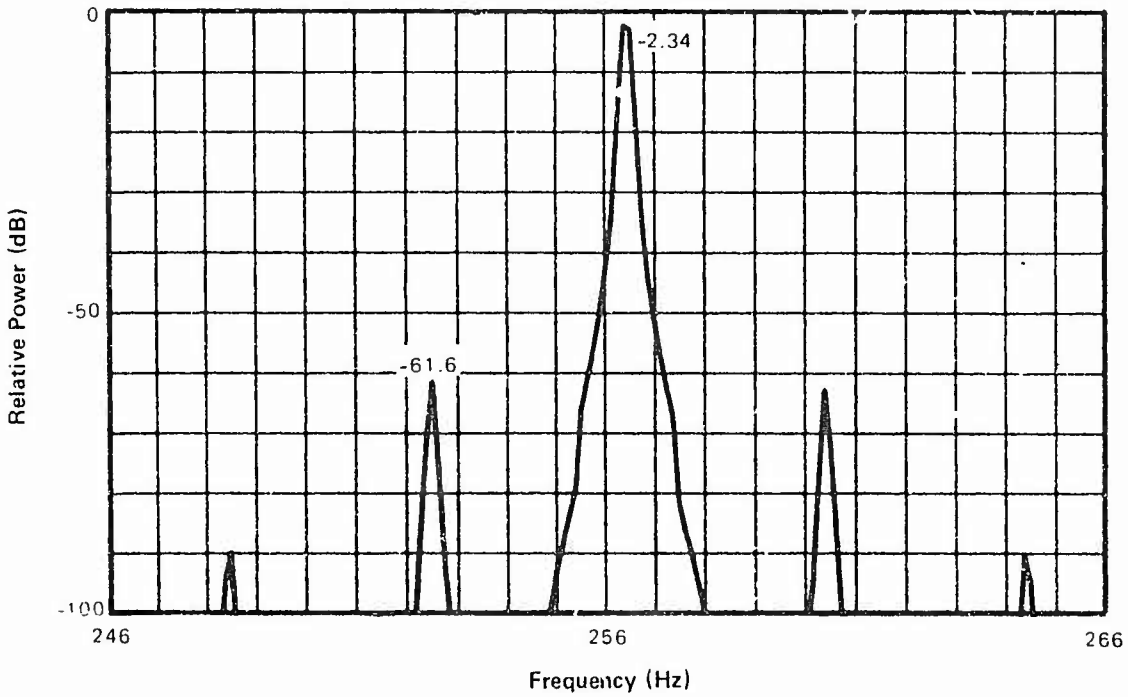


Figure 8C. f_o = 256 7/16 Hz

Figure 8 (Cont'd). Vernier Spectrum for (Cosine)^3 Temporal Weighting, 75 percent Overlap

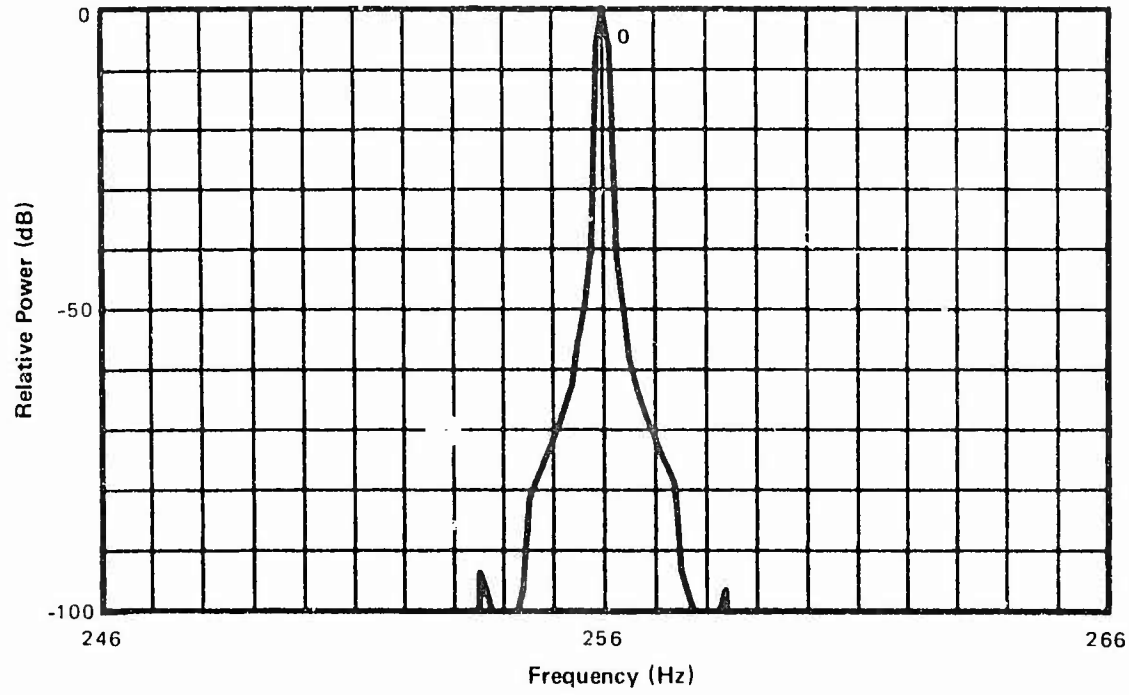


Figure 9A. f_o = 256 Hz

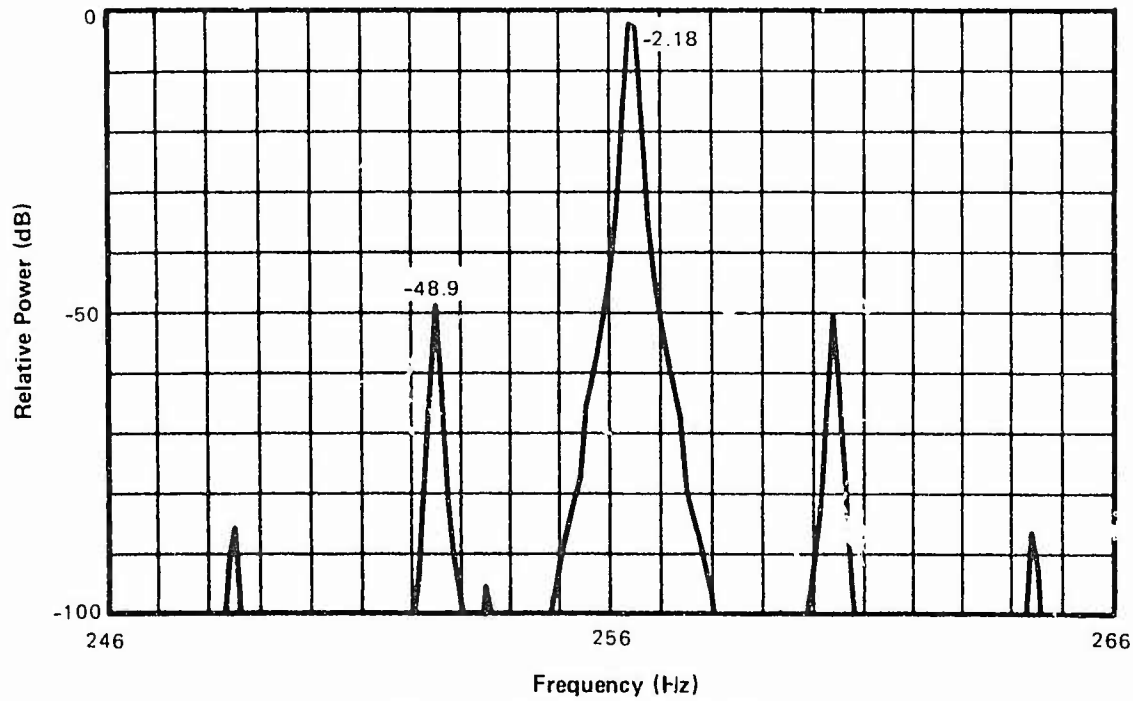


Figure 9B. f_o = 256 7/16 Hz

Figure 9. Vernier Spectrum for (Cosine)^4 Temporal Weighting, 75 percent Overlap

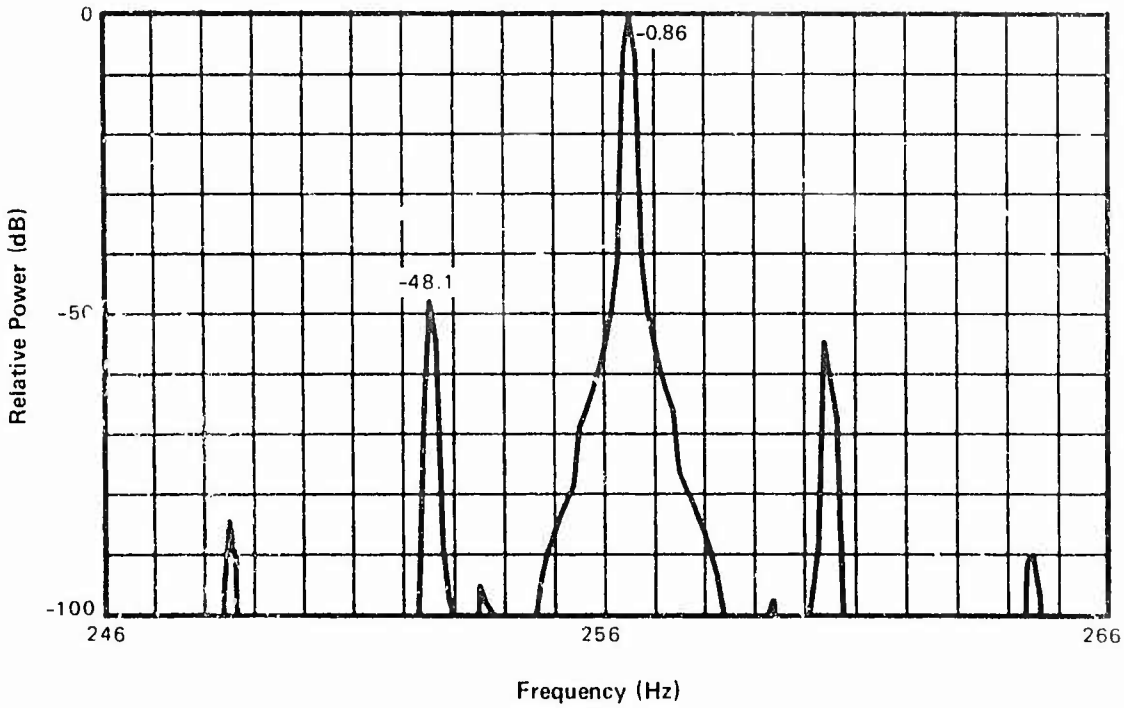


Figure 9C. f_o = 256 1/2 Hz

Figure 9 (Cont'd). Vernier Spectrum for (Cosine)^4 Temporal Weighting, 75 percent Overlap

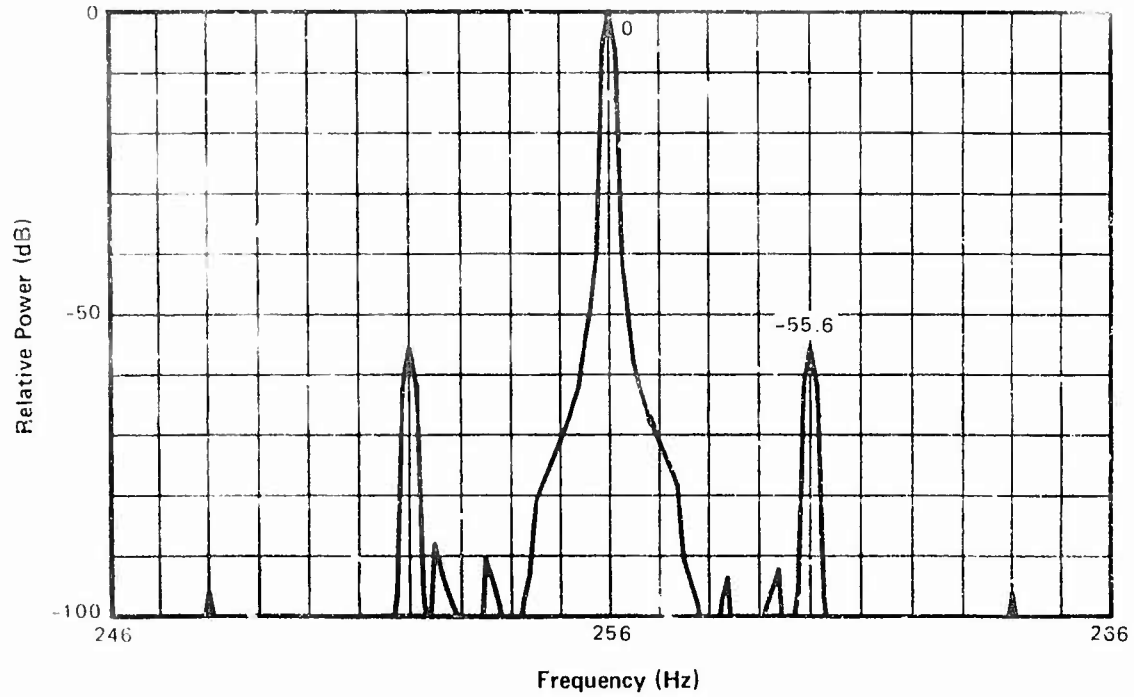


Figure 10A. f_o = 256 Hz

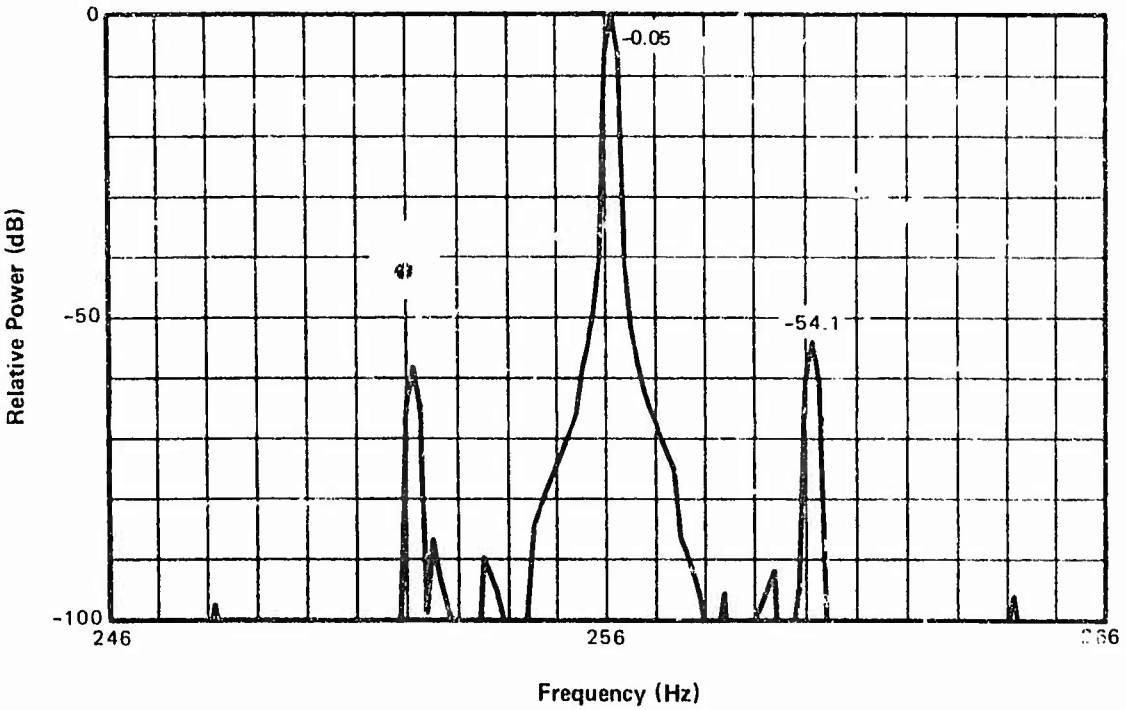


Figure 10B. f_o = 256 1/8 Hz

Figure 10. Vernier Spectrum for (Cosine)^5 Temporal Weighting, 75 percent Overlap

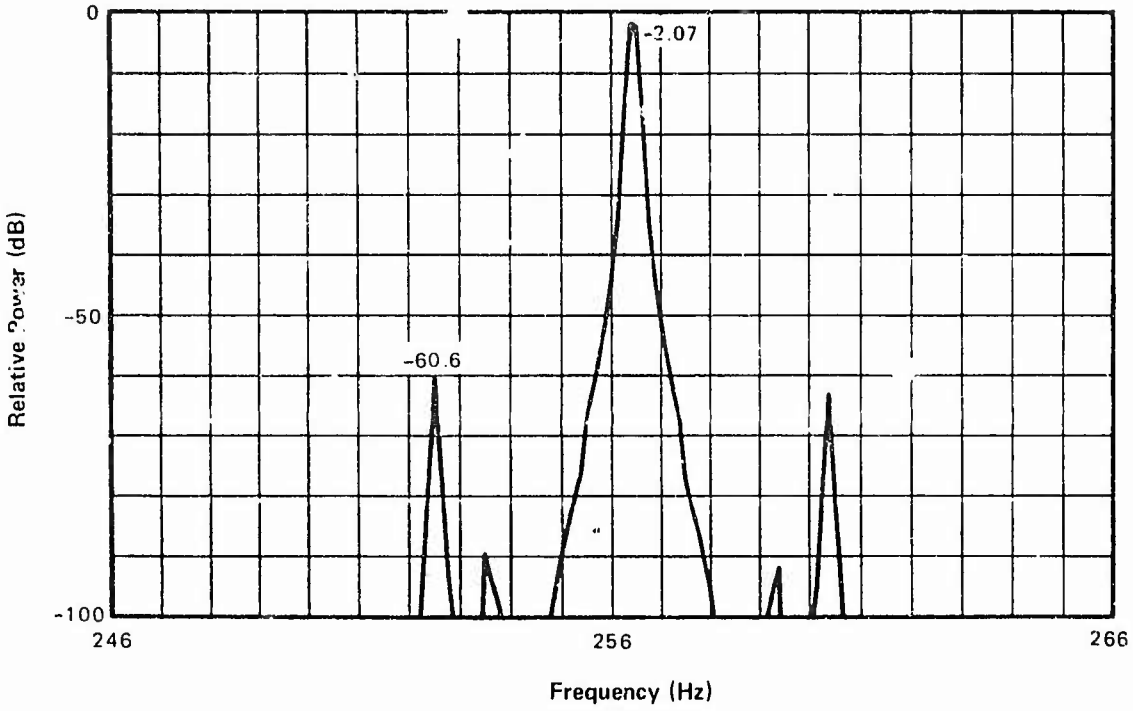


Figure 10C. f_o = 256 7/16 Hz

Figure 10 (Cont'd). Vernier Spectrum for (Cosine)^5 Temporal Weighting, 75 percent Overlap

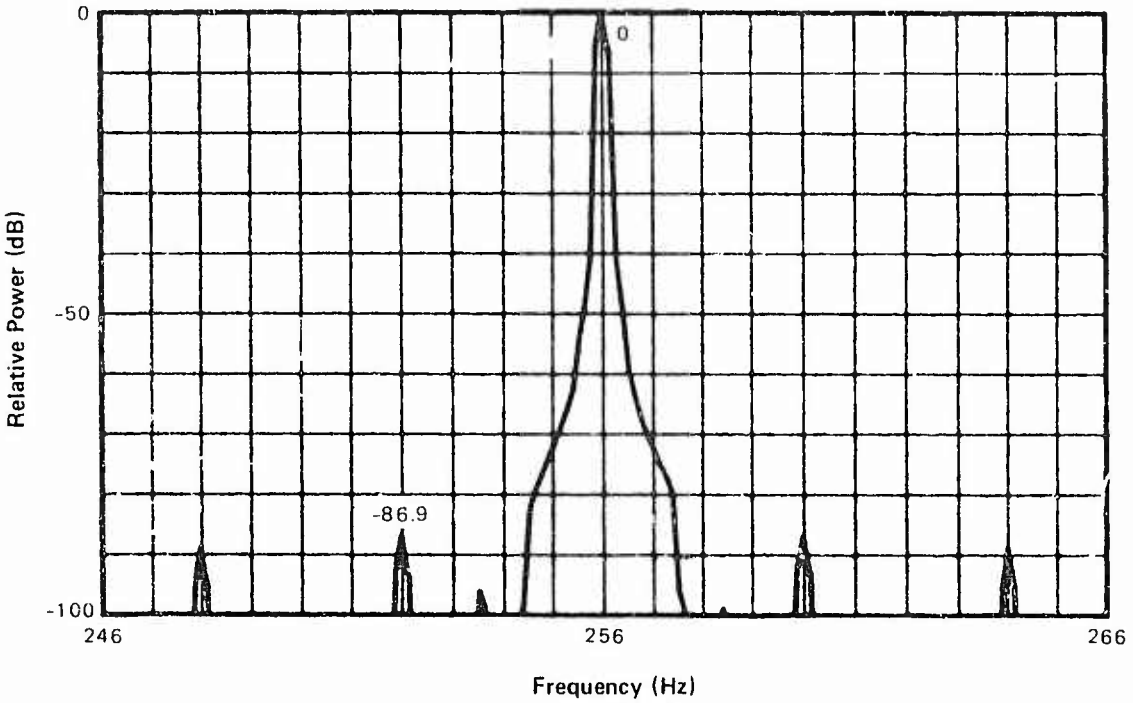


Figure 11A. f_0 = 256 Hz

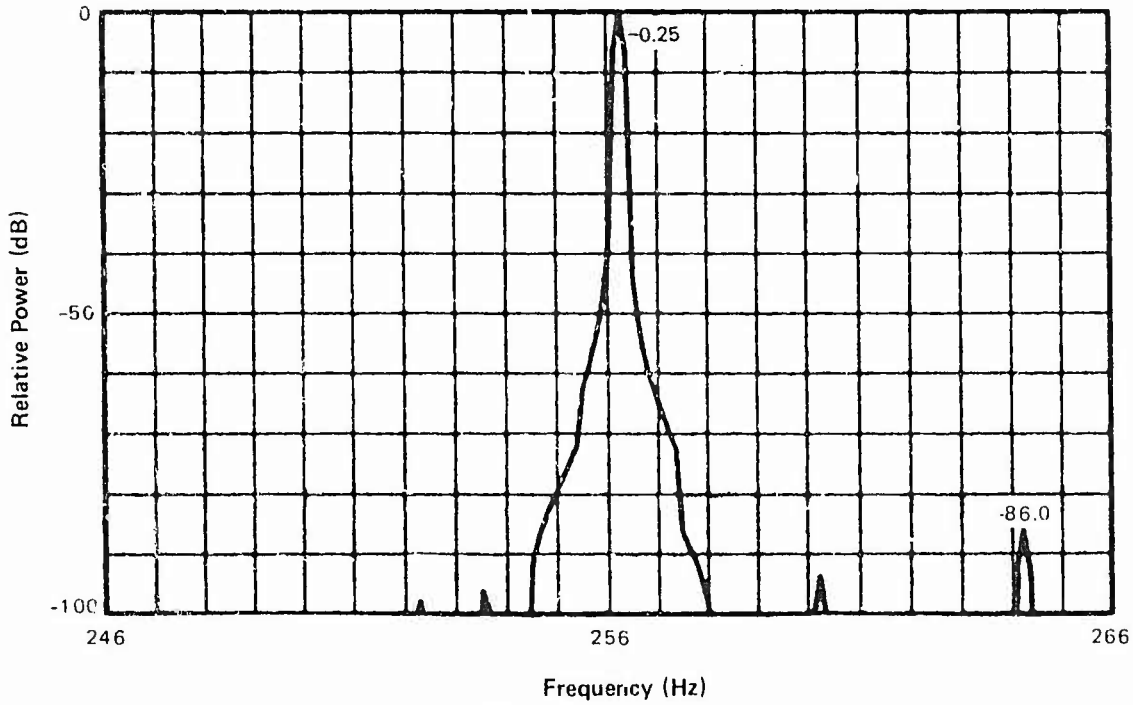


Figure 11B. f_0 = 256 1/4 Hz

Figure 11. Vernier Spectrum for Dolph-Chebyshev Temporal Weighting, 75 percent Overlap

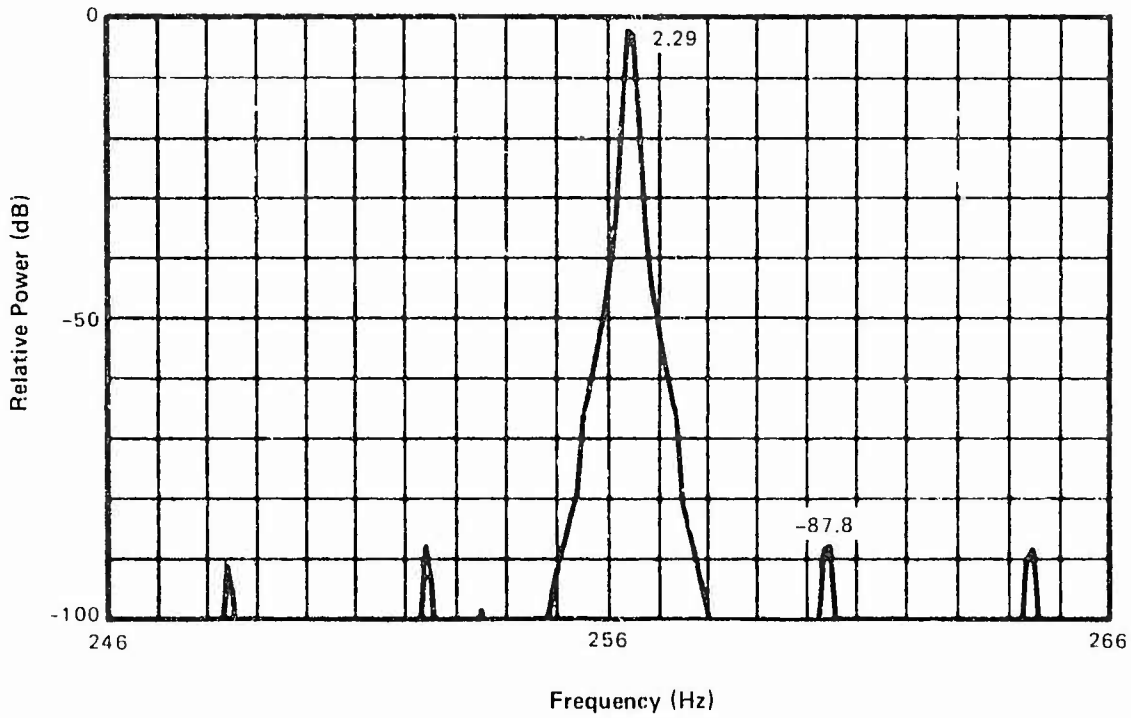


Figure 11C. f_0 = 256 7/16 Hz

Figure 11 (Cont'd). Vernier Spectrum for Dolph-Chebyshev Temporal Weighting, 75 percent Overlap

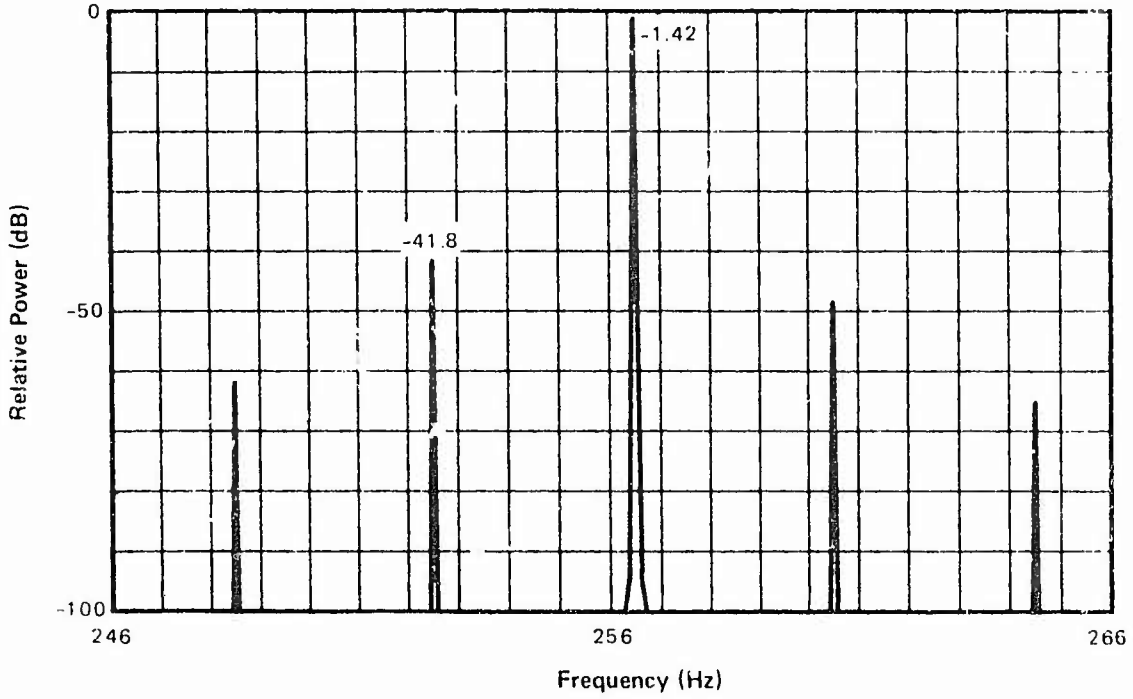


Figure 12A. f_o = 256 1/2 Hz

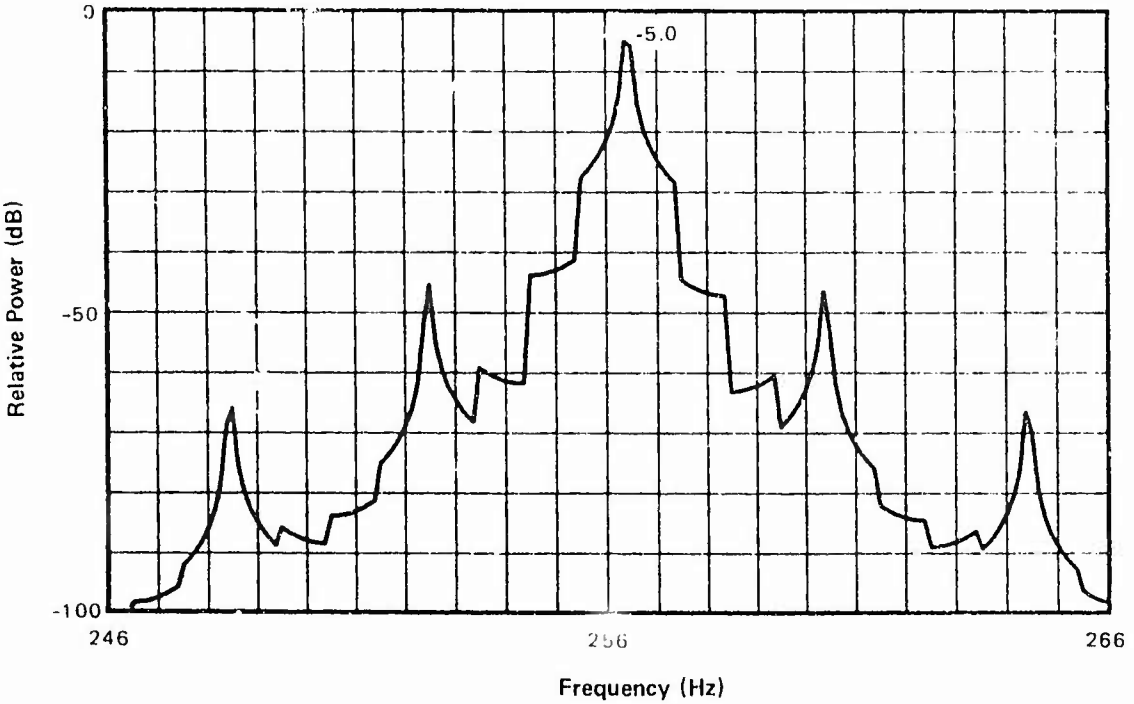


Figure 12B. f_o = 256 7/16 Hz

Figure 12. Vernier Spectrum for Flat Delay Weighting

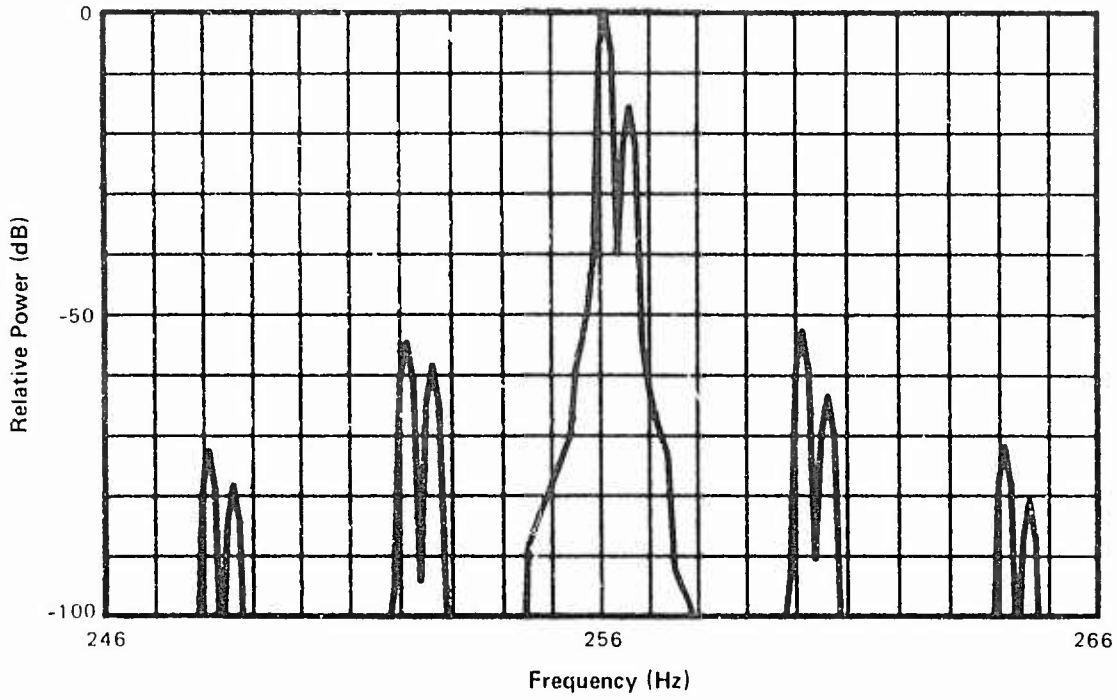


Figure 13A. f_o = 256 1/8 Hz

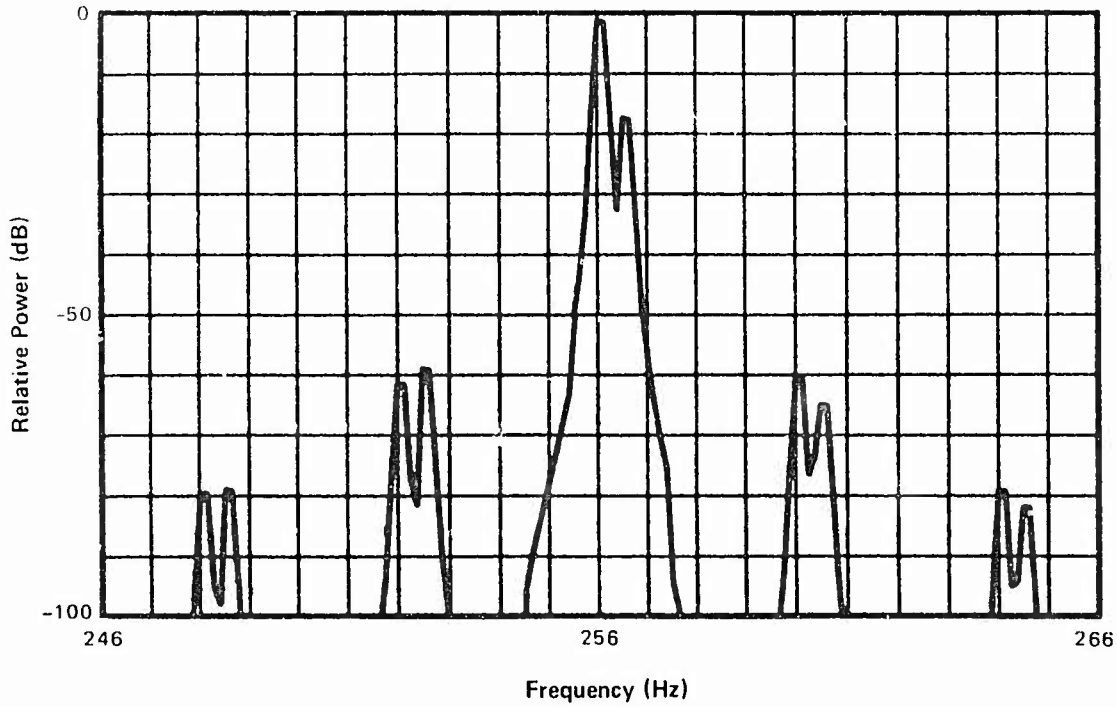


Figure 13B. f_o = 256 1/16 Hz

Figure 13. Vernier Spectrum for $(\text{Cosine})^2$ Delay Weighting, Two Tones

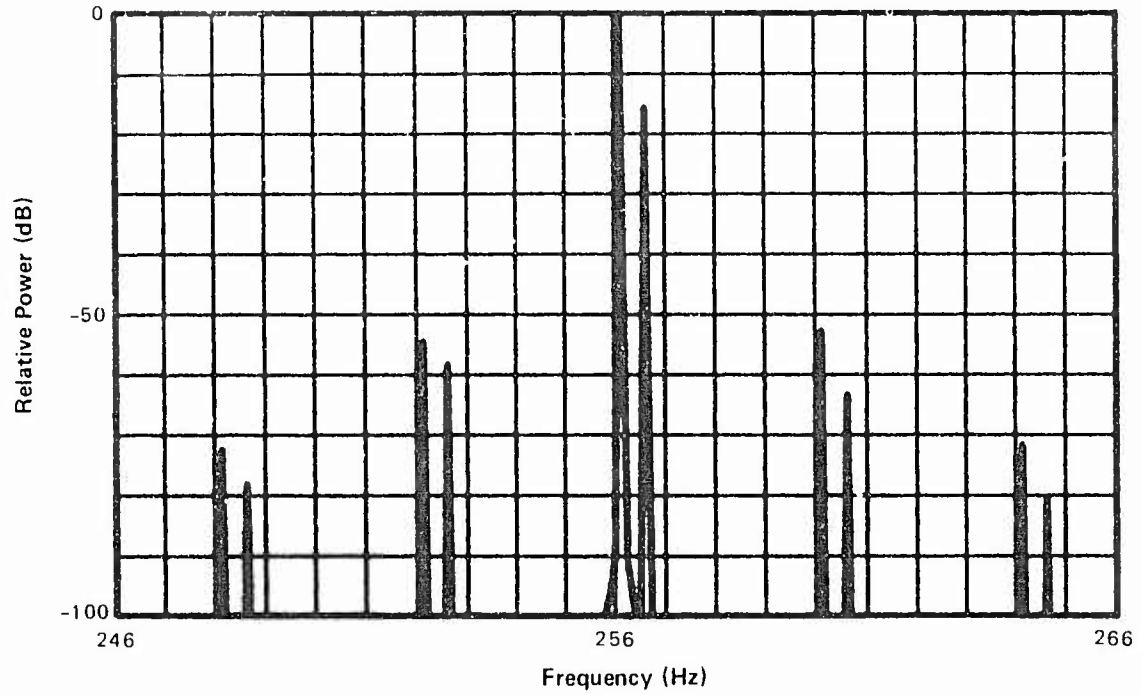


Figure 14A. f_o = 256 1/8 Hz

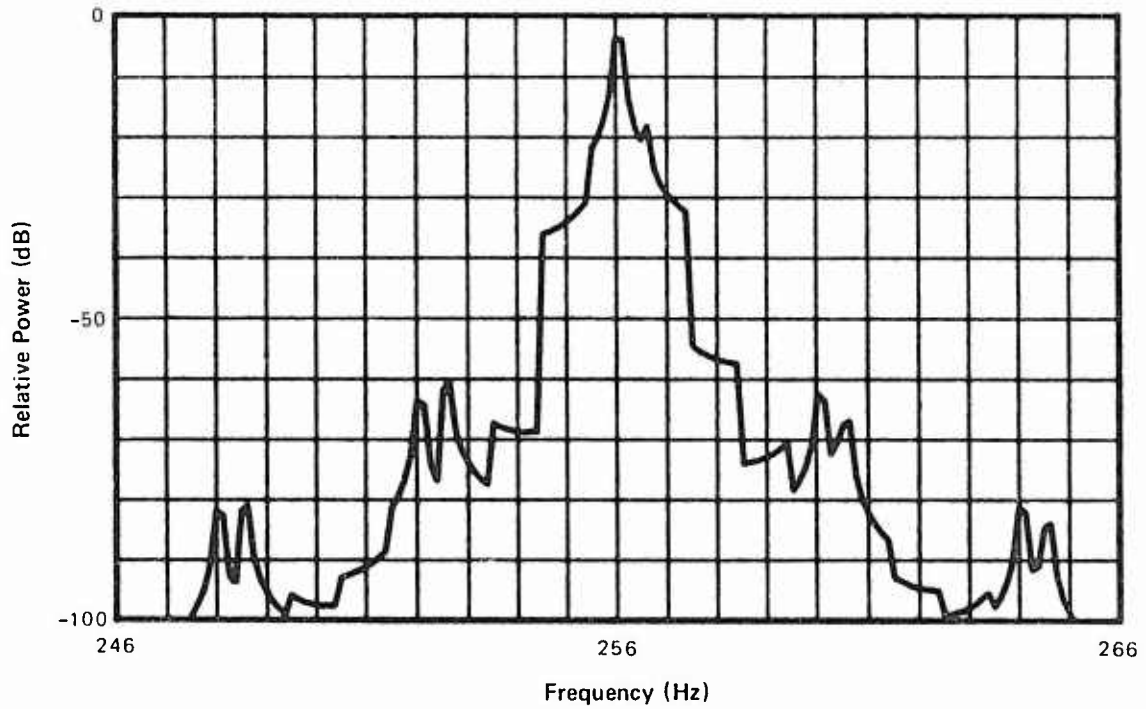


Figure 14B. f_o = 256 1/16 Hz

Figure 14. Vernier Spectrum for Flat Delay Weighting, Two Tones

Appendix A

TWO METHODS OF COMPUTING $\sum_{n=n_o}^{n_o+N-1} \exp(-i2\pi pn/N)\, q_n$

Define

$$Q_p = \sum_{n=n_o}^{n_o+N-1} \exp(-i2\pi pn/N)\, q_n, \quad 0 \le p \le N-1 , \tag{A-1}$$

where $n_o \ge 0$. If we let $m = n - n_o$, (A-1) becomes

$$Q_p = \exp(-i2\pi pn_o/N) \sum_{m=0}^{N-1} \exp(-i2\pi pm/N)\, q_{m+n_o} . \tag{A-2}$$

The sum in (A-2) is an FFT of the sequence $\{q_n\}_{n_o}^{n_o+N-1}$.

For an alternative method, consider the general term q_n in (A-1). Then, if

(a) $n = 0, N, 2N, \ldots$, q_n gets weight $\exp(-i0)$;

(b) $n = 1, N+1, 2N+1, \ldots$, q_n gets weight $\exp(-i2\pi p/N)$; (A-3)

$\vdots$

(c) $n = N-1, 2N-1, 3N-1, \ldots$, q_n gets weight $\exp(-i2\pi p(N-1)/N)$.

So, if we define $\tilde{n} = n \mod N$, then case

(a) corresponds to $\tilde{n} = 0$;

(b) corresponds to $\tilde{n} = 1$; (A-4)

$\vdots$

(c) corresponds to $\tilde{n} = N - 1$.

Therefore, let

$$V_{\tilde{n}} = q_n , \quad n_o \le n \le n_o + N - 1 , \tag{A-5}$$

in which case

$$Q_p = \sum_{\tilde{n}=0}^{N-1} \exp(-i2\pi p\tilde{n}/N)\, v_{\tilde{n}} \;,\quad 0 \le p \le N-1 \;; \tag{A-6}$$

this is simply an FFT of $\{v_{\tilde{n}}\}_0^{N-1}$, with no phase factor necessary. Equation (A-5) corresponds to filling up the $v_{\tilde{n}}$ array, from the given quantities q_n, starting from the nonzero position, $n_o \bmod N$, and cycling around to position 0.

To apply these results to (10), suppose weight w is nonzero for $t > 0$. Then if n_o is the smallest integer such that $n_o \ge k\,S/\Delta$, (10) can be expressed as

$$a\left(\frac{p}{N\Delta}, kS\right) = \Delta \sum_{n=n_o}^{n_o+N-1}{}' \exp(-i2\pi pn/N)\, x(n\Delta)\, w(n\Delta - kS) \;. \tag{A-7}$$

This is of the form of (A-1) if we identify

$$q_n = x(n\Delta)\, w(n\Delta - kS) \;. \tag{A-8}$$

Appendix B

DERIVATION OF VERNIER SPECTRUM

From the first line of (7) in the main text, there follows immediately

$$Y(f, \nu) = A(f, \nu) \circledast D(\nu) \circledast \delta_{1/s}(\nu) , \tag{B-1}$$

where all convolutions are on ν, for f fixed. Then using (6), we obtain

$$\begin{aligned} A(f, \nu) &= \int d\tau \ \exp(-i2\pi\nu\tau)\ a(f, \tau) \\ &= \int d\tau \ \exp(-i2\pi\nu\tau) \int dt \ \exp(-i2\pi ft)\ x(t)\ w(t-\tau)\ \Delta\delta_{\Delta}(t) \\ &= W(-\nu) \int dt \ \exp(-i2\pi(f+\nu)\ t)\ x(t)\ \Delta\delta_{\Delta}(t) \\ &= W(-\nu) \sum_{m} X\left(f + \nu - \frac{m}{\Delta}\right) . \end{aligned} \tag{B-2}$$

Substituting (B-2) in (B-1), we have

$$Y(f, \nu) = \left[W(-\nu) \sum_{m} X\left(f + \nu - \frac{m}{\Delta}\right)\right] \circledast D(\nu) \circledast \delta_{1/s}(\nu) . \tag{B-3}$$

Appendix C

SAMPLE PROGRAM

The program furnished below is illustrative of the vernier technique. It has been written for

$$\Delta\,(\mathrm{DEL}) = \frac{1}{1024}\ \text{seconds},\ \mathrm{N} = 1024,\ \mathrm{M} = 32,\ \mathrm{S} = \frac{1}{4}\ \text{sec}$$
$$f_o(\mathrm{F0}) = 256(1/16)\ 256\frac{1}{2}\ , \qquad \text{(C-1)}$$

but could be easily changed to other cases. The input data are furnished by internal functions XREAL and XIMAG; currently, two tones of relative strength -15 dB and separation 1/2 Hz are incorporated. Loop 1 in the main program accomplishes Hanning temporal weighting, while loop 2 accomplishes Hanning delay weighting. The subroutines MKLFFT and QTRCOS are detailed in reference 7. The method in this program employed the cycling technique described in appendix A.

```
      PARAMETER N=1024,M=32,N4=N/4+1,M4=M/4+1
      INTEGER PS
      DIMENSION ZR(N),ZI(N),W(N),D(M),AR(21,M),AI(21,M),ADR(M),ADI(M),
     $DB(M),CN(N4),CM(M4),Z(200),X(168),Y(168)
      SQ=10.**(-.75)
      TPIM=2.*3.141592654/(M+1)
      TPIN=2.*3.141592654/N
      M1=M-1
      N1=N-1
      DEL=1./N
      IS=N/4
      S=IS*DEL
      IM=INT(LOG(FLOAT(M))*1.4427+.5)
      CALL QTRCOS(CN,N)
      CALL QTRCOS(CM,M)
      CALL MODESG(Z,0)
      CALL SUBJEG(Z,5.,-100.,165.,0.)
      CALL OBJCTG(Z,800.,1400.,2425.,2350.)
      DO 1 MS=0,N1
1     W(MS+1)=1.-COS(TPIN*MS)
      DO 2 KS=0,M1
```

```
2       D(KS+1)=1.-COS(TPIM*(KS+1))
        DO 13 IC=1,168
13      X(IC)=IC
        DO 12 IF=0,8
        FO=256.+IF*.0625
        DO 3 KS=0,M1
        NO=IS*KS
        NU=NO+N1
        DO 4 NS=NO,NU
        NT=MOD(NS,N)
        ZR(NT+1)=XREAL(NS*DEL)*W(NS-NO+1)
        ZI(NT+1)=XIMAG(NS*DEL)*W(NS-NO+1)
4       CONTINUE
        CALL MKLFFT(ZR,ZI,LN,10,-1)
        DO 5 PS=246,266
        AR(PS-245,KS+1)= DEL*ZR(PS+1)
        AI(PS-245,KS+1)= DEL*ZI(PS+1)
5       CONTINUE
3       CONTINUE
        DO 6 PS=246,266
        DO 7 KS=0,M1
        ADR(KS+1)=S*AR(PS-245,KS+1)*D(KS+1)
        ADI(KS+1)=S*AI(PS-245,KS+1)*D(KS+1)
7       CONTINUE
        CALL MKLFFT(ADR,ADI,CM,IM,-1)
        IF(IF.EQ.0.AND.PS.EQ.256) PEAK=10.*LOG10(ADR(1)**2+ADI(1)**2)
        DO 8 KS=0,M1
        AR(PS-245,KS+1)=ADR(KS+1)
        AI(PS-245,KS+1)=ADI(KS+1)
8       CONTINUE
6       CONTINUE
        DO 9 PS=246,266
        IC=(PS-246)*8
        DO 10 MS=0,M1
        A=AR(PS-245,MS+1)**2+AI(PS-245,MS+1)**2
        A=MAX(A,1.E-36)
        DB(MS+1)=10.*LOG10(A)-PEAK
10      CONTINUE
        PRINT 14, PS
14      FORMAT(///I10/)
        PRINT 11, DB
11      FORMAT(/8E15.6)
        Y(IC+1)=DB(M-3)
        Y(IC+2)=DB(M-2)
        Y(IC+3)=DB(M-1)
        Y(IC+4)=DB(M)
        Y(IC+5)=DB(1)
        Y(IC+6)=DB(2)
        Y(IC+7)=DB(3)
        Y(IC+8)=DB(4)
9       CONTINUE
        SIDE=-200.
        DO 17 IC=1,168
        IF(IC.GE.69.AND.IC.LE.109) GO TO 17
        SIDE=MAX(SIDE,Y(IC))
```

```
17    CONTINUE
      PRINT 18, SIDE
18    FORMAT(/' PEAK SIDELOBE IS',E14.8)
      CALL SETSMG(Z,30,1.)
      DO 15 IP=10,90,10
      CALL LINESG(Z,0.  5.,-FLOAT(IP))
15    CALL LINESG(Z,1.165.,-FLOAT(IP))
      DO 16 IP=13,157,8
      CALL LINESG(Z,0.FLOAT(IP),0.)
16    CALL LINESG(Z,1.FLOAT(IP),-100.)
      CALL SETSMG(Z,30,2.)
      CALL LINESG(Z,0.5.,-100.)
      CALL LINESG(Z,1,5.,0.)
      CALL LINESG(Z,1.165.,0.)
      CALL LINESG(Z,1.165.,-100.)
      CALL LINESG(Z,1.5.,-100.)
      CALL LINESG(Z,168,X,Y)
      CALL PAGEG(Z,0,3,1)
12    CONTINUE
      CALL EXITG(Z)
      PRINT 11, PEAK
      FUNCTION XREAL(T)
      XREAL=COS(2.*3.141592654*F0*T)
     $     +COS(2.*3.141592654*(F0+.5)*T)*SQ
      RETURN
      FUNCTION XIMAG(T)
      XIMAG=SIN(2.*3.141592654*F0*T)
     $     +SIN(2.*3.141592654*(F0+.5)*T)*SQ
      RETURN
      END
```

Appendix D

EFFECT OF (COSINE)^n TIME WEIGHTING

Let us define the spectrum of unweighted data x as

$$Z(f) \equiv \int dt \exp(-i2\pi ft)\, x(t)\, \Delta\delta_\Delta(t) = \Delta \sum_{k=0}^{N-1} \exp(-i2\pi k\Delta f)\, x(k\Delta), \qquad (D\text{-}1)$$

and that corresponding to weighting w as

$$\begin{aligned} Z_w(f) &\equiv \int dt \exp(-i2\pi ft)\, x(t)\, w(t)\, \Delta\delta_\Delta(t) = Z(f) \circledast W(f) \\ &= \Delta \sum_{k=0}^{N-1} \exp(-i2\pi k\Delta f)\, x(k\Delta)\, w(k\Delta) \quad . \end{aligned} \qquad (D\text{-}2)$$

Now for (cosine)^n time weighting, we have*

$$w(k\Delta) = \sin^n(k\pi/N), \quad 0 \le k \le N-1 \, . \qquad (D\text{-}3)$$

Substituting (D-3) in (D-2), there follows

$$\begin{aligned} Z_w(f) &= \Delta \sum_{k=0}^{N-1} \exp(-i2\pi k\Delta f)\, x(k\Delta) \left(\frac{1}{i2}\right)^n \left[\exp(ik\pi/N) - \exp(-ik\pi/N)\right]^n \\ &= \Delta \sum_{k=0}^{N-1} \exp(-i2\pi k\Delta f)\, x(k\Delta) \left(\frac{1}{i2}\right)^n \sum_{j=0}^{n} (-1)^j \binom{n}{j} \exp\left[i\frac{k\pi}{N}(n-2j)\right] \\ &= \Delta\left(\frac{1}{i2}\right)^n \sum_{j=0}^{n} (-1)^j \binom{n}{j} \sum_{k=0}^{N-1} x(k\Delta) \exp\left[-i2\pi k\Delta\left(f - \frac{n-2j}{2N\Delta}\right)\right] \\ &= \left(\frac{1}{i2}\right)^n \sum_{j=0}^{n} (-1)^j \binom{n}{j} Z\left(f - \frac{n-2j}{2N\Delta}\right) \, , \end{aligned} \qquad (D\text{-}4)$$

the last step via use of (D-1). This result yields (20).

*See the first footnote to equation (19) of the main text for the explanation of $\sin^n$ in (D-3).

For the special case of $n = 1$, (D-4) becomes

$$Z_W(f) = i\ 1/2 \left[Z\left(f - \frac{1}{2N\Delta}\right) - Z\left(f + \frac{1}{2N\Delta}\right)\right], \qquad \text{(D-5)}$$

and in particular,

$$Z_W\left(\frac{n}{N\Delta} + \frac{1}{2N\Delta}\right) = i\ 1/2 \left[Z\left(\frac{n}{N\Delta}\right) - Z\left(\frac{n+1}{N\Delta}\right)\right]. \qquad \text{(D-6)}$$

The right-hand side of (D-6) involves two adjacent spectral values as afforded by the standard N-point FFT in (D-1). The left-hand side of (D-6) is the spectral value of Z_W at the frequency halfway between the above two spectral locations. Thus, under this interpretation of the right-hand side of (D-6), the desirable sidelobe control predicted by the convolution in (D-2) can be attained. A similar interpretation is possible for (D-4) for general n.

REFERENCES

1. A. H. Nuttall, "Two Methods of Performing a Large-Size FFT by Means of Several Smaller FFTs," NUSC Technical Memorandum TC-185-72, 6 October 1972.

2. J. F. Ferrie, C. W. Nawrocki, and G. Clifford Carter, "Implementation and Results of the Modified Chirp Z-Transform," NUSC Technical Memorandum TC-191-72, 18 October 1972.

3. C. W. Nawrocki and J. F. Ferrie, "Zoom FFT — An Approximate Vernier Frequency Algorithm," NUSC Technical Memorandum SA2201-584-72, 22 November 1972.

4. G. D. Bergland, "A Guided Tour of the Fast Fourier Transform," IEEE Spectrum, vol. 6, July 1969, pp. 41-52.

5. C. L. Dolph, "A Current Distribution for Broadside Arrays Which Optimizes the Relationship Between Beam Width and Side-Lobe Level," Proceedings of the I. R. E. and Waves and Electrons, vol. 34, June 1946, pp. 335-348.

6. A. H. Nuttall, "Generation of Dolph-Chebyshev Weights for Large Numbers of Elements via a Fast Fourier Transform," NUSC Technical Memorandum TC-5-74, 15 April 1974.

7. J. F. Ferrie, G. C. Carter, and C. W. Nawrocki, "Availability of Markel's FFT Pruning Algorithm," NUSC Technical Memorandum TC-1-73, 15 January 1973.

REVERSE BLANK

NUSC Technical Report 5291
9 March 1976

Approximations for Statistics of Coherence Estimators

Albert H. Nuttall
G. Clifford Carter

ABSTRACT

Approximations for the bias, variance, and mean-square error of estimators of the magnitude-squared coherence and magnitude coherence are presented. The approximations are accurate for all values of true coherence and over the practically useful range of N, where N is the number of averages employed in the coherence estimators.

Approved for public release; distribution unlimited.

TABLE OF CONTENTS

	Page
LIST OF ILLUSTRATIONS	ii
LIST OF ABBREVIATIONS AND SYMBOLS	iii
INTRODUCTION	1
ESTIMATION OF MAGNITUDE-SQUARED COHERENCE	1
General Relations	2
Bias Approximation	3
Variance Approximation	4
Mean-Square Error Approximation	6
ESTIMATION OF MAGNITUDE COHERENCE	7
General Relations	7
Expansions About S = 0	8
Expansions About S = 1	9
Choice of Approximation	10
Variance Approximation	11
Bias Approximation	15
Mean-Square Error Approximation	17
SUMMARY	20
APPENDIX A — REDUCTION OF THE $_3F_2$ FUNCTION	A-1
APPENDIX B — EXPANSION ABOUT S = 1 FOR MAGNITUDE COHERENCE	B-1
APPENDIX C — VARIANCE APPROXIMATION FOR MAGNITUDE COHERENCE	C-1
REFERENCES	R-1

LIST OF ILLUSTRATIONS

Figure		Page
1	Bias of MSC Estimate	3-4
2	Variance of MSC Estimate	5
3	Mean-Square Error of MSC Estimate	6-7
4	Variance of MC Estimate	12-14
5	Bias of MC Estimate	16
6	Mean-Square Error of MC Estimate	17-19

LIST OF ABBREVIATIONS AND SYMBOLS

MSC	Magnitude-Squared Coherence
MC	Magnitude Coherence
N	number of independent averages
${}_3F_2$	generalized hypergeometric function
F	Gauss hypergeometric function
x(t), y(t)	jointly stationary processes
f	frequency
$\gamma_{xy}(f)$	complex coherence
C(f), C	magnitude-squared coherence
$\hat{C}(f)$, $\hat{C}$	estimate of magnitude-squared coherence
$E\{Q\}$	ensemble average of random variable Q
μ_m	m-th moment of $\hat{C}$
Γ	gamma function
S(f), S	magnitude coherence
$\hat{S}(f)$, $\hat{S}$	estimate of magnitude coherence
$\alpha, \nu, \beta, \lambda$	constants (see (31) and (32))
σ^2_{app}	approximate variance
A, B, D	constants (see (34))
b_{app}	approximate bias
G_N	constant (see (40))

APPROXIMATIONS FOR STATISTICS OF COHERENCE ESTIMATORS

INTRODUCTION

Expressions for the probability density function, the cumulative distribution function, and any moment of the estimates of magnitude-squared coherence (MSC) and magnitude coherence (MC) are available in references 1-5. The expressions for the moments usually involve a generalized hypergeometric function* ${}_3F_2$ and require a time-consuming computer effort for their evaluation. Also, the fundamental dependence of statistics like the bias, variance, and mean-square error on the number of averages N and the true coherence are not obvious, because of the lack of significant results for the ${}_3F_2$ function.

This report will seek to present accurate approximations for these statistics, of as simple a nature as possible, and capable of hand calculation. Also, the dependence on N and on the true coherence will be deduced, and thereby future experiments can be designed in which the required stability can be predicted and attained with ease and certainty. As a by-product, a technique for reducing a particular type of ${}_3F_2$ function to a Gauss hypergeometric function (reference 7, chapter 15) is presented.

ESTIMATION OF MAGNITUDE-SQUARED COHERENCE

The complex coherence between two jointly stationary random processes $x(t)$ and $y(t)$ is defined as

$$\gamma_{xy}(f) = \frac{G_{xy}(f)}{\left[G_{xx}(f)\, G_{yy}(f)\right]^{1/2}}, \tag{1}$$

where $G_{xy}(f)$ is the cross-spectral density at frequency f, and $G_{xx}(f)$ and $G_{yy}(f)$ are the auto-spectral densities. The MSC is

$$C(f) = \left|\gamma_{xy}(f)\right|^2 . \tag{2}$$

*See, for example, reference 6, section 9.14.

The MSC is frequently estimated according to

$$\hat{C}(f) \equiv \frac{\left|\hat{G}_{xy}(f)\right|^2}{\hat{G}_{xx}(f)\,\hat{G}_{yy}(f)} = \frac{\left|\sum_{n=1}^{N} X_n(f)\,Y_n^*(f)\right|^2}{\sum_{n=1}^{N}\left|X_n(f)\right|^2 \sum_{n=1}^{N}\left|Y_n(f)\right|^2}, \tag{3}$$

where N is the number of data segments employed, and $X_n(f)$, $Y_n(f)$ are the (discrete) Fourier transforms of the n-th weighted data segments of $x(t)$ and $y(t)$.

GENERAL RELATIONS

The m-th moment of the random variable* $\hat{C}$ for independent data segments is given in reference 1, (4) and reference 2, (3) as

$$E\{\hat{C}^m\} \equiv \mu_m = \frac{\Gamma(N)\,\Gamma(m+1)}{\Gamma(N+m)}(1-C)^N\,{}_3F_2\,(m+1, N, N; N+m, 1; C), \tag{4}$$

where C is the true MSC and ${}_3F_2$ is a generalized hypergeometric function. The power m need not be integer in (4).

For $m = 1$, the first moment of $\hat{C}$ can be reduced (reference 5, appendix B) to the simpler (and rapidly convergent) form

$$\mu_1 = \frac{1}{N} + \frac{N-1}{N+1} C\,F(1, 1; N+2; C)\ , \tag{5}$$

where F is the Gauss hypergeometric function. For $m = 2$, the second moment of $\hat{C}$ can be reduced to the simpler form (see appendix A)

$$\mu_2 = -\frac{N^3 - 2N^2 + 2N - 2}{N} + \frac{N-1}{N+1}\left[N^2 - (N-2)C\right] F(1, 1; N+2; C)\ , \tag{6}$$

which involves the F function with the same arguments as in (5). Equations (5) and (6) give exact results from which the bias, variance, and mean-square error of the MSC estimate $\hat{C}$ can be obtained.

---

*The f-dependence is suppressed for convenience.

BIAS APPROXIMATION

The bias of $\hat{C}$ is

$$\text{Bias}(\hat{C}) = E\{\hat{C}|C, N\} - C = \mu_1 - C \quad . \tag{7}$$

By expanding F in (5) in a power series in C and retaining terms to order N^{-2}, we obtain the approximation

$$\text{Bias}(\hat{C}) \cong \frac{1}{N}(1 - C)^2 \left(1 + \frac{2C}{N}\right) \quad . \tag{8}$$

Plots of (7) and (8) are given in figure 1 for $N = 8$ and 16. The discrepancy between the exact result (7) and the approximation (8) is barely discernible for $N = 8$ and is not discernible for $N = 16$. The discrepancy (between (7) and (8)) is even less for larger N. Equation (8) is a much simpler and more accurate approximation than reference 2, (5). The bias and approximation are observed to have a peak of value $1/N$ at the origin and to decrease monotonically with the value C of the true MSC.

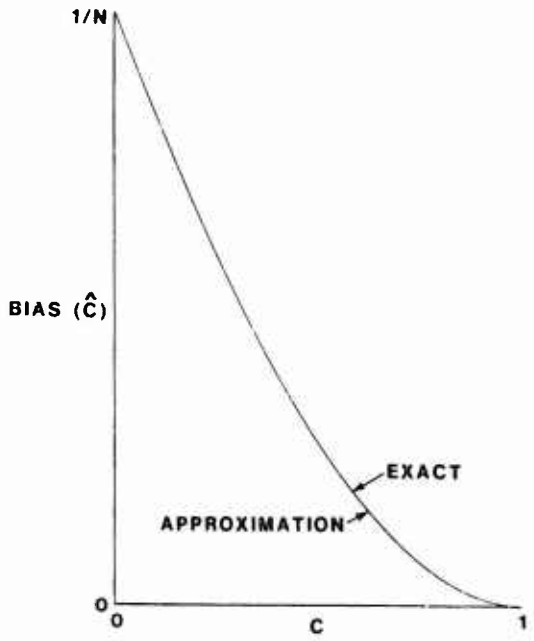


Figure 1A. $N = 8$

Figure 1. Bias of MSC Estimate

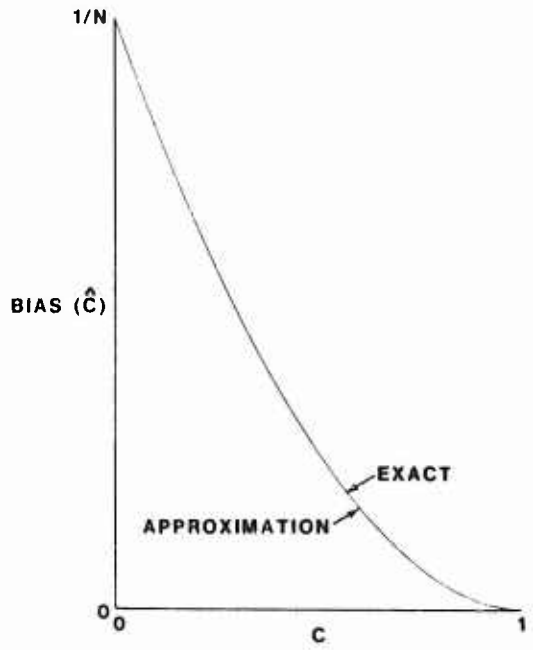


Figure 1B. N = 16

Figure 1 (Cont'd). Bias of MSC Estimate

VARIANCE APPROXIMATION

An expansion for the variance of $\hat{C}$ is given in reference 2, (6). If we expand the bracketed term to order N^{-1}, we obtain the approximation

$$\text{Variance}(\hat{C}) \cong \frac{N-1}{N(N+1)} (1-C)^2 \left[2C + \frac{1 - 6C + 13C^2}{N}\right] . \qquad (9)$$

This result can also be obtained from the exact expression

$$\text{Variance}(\hat{C}) = \mu_2 - \mu_1^2 \qquad (10)$$

combined with (5) and (6).

Plots of (9) and (10) are given in figure 2 for N = 8 and 16. The discrepancy between (9) and (10) is barely discernible for N = 16 and is not discernible for $N \geq 32$. Equation (9) is a much simpler and better approximation than reference 2, (6).

For large N, the peak of the variance occurs at $C \cong 1/3$ and is of value $8/27\ N^{-1}$. Thus, even when the true coherence is unknown, the maximum variance will be less than 0.3/N, for large N.

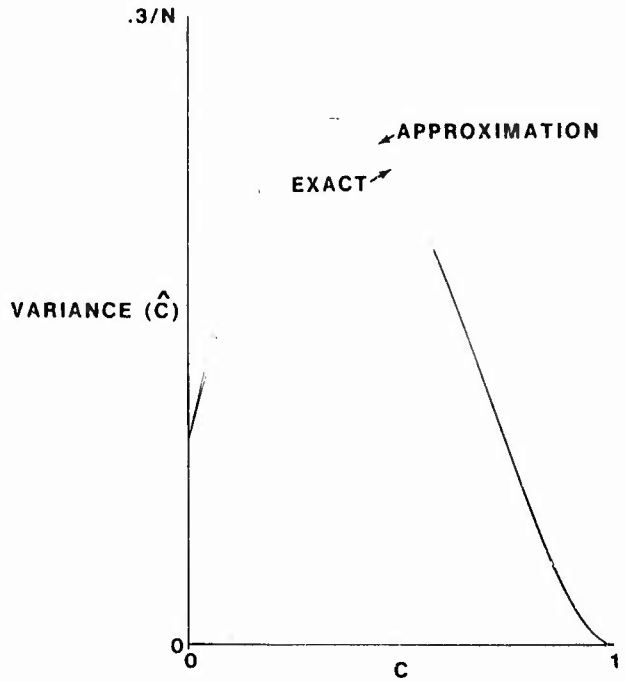


Figure 2A. N = 8

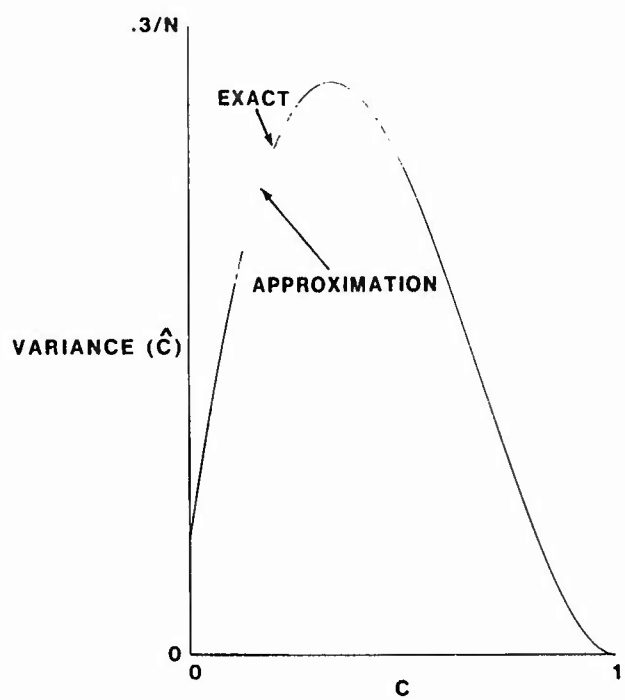


Figure 2B. N = 16

Figure 2. Variance of MSC Estimate

MEAN-SQUARE ERROR APPROXIMATION

The mean-square error of the MSC estimate $\hat{C}$ is

$$\text{Mean-Square Error}(\hat{C}) = E\left\{(\hat{C} - C)^2\right\}$$

$$= \left[\text{Bias}(\hat{C})\right]^2 + \text{Variance}(\hat{C})$$

$$= (\mu_1 - C)^2 + (\mu_2 - \mu_1^2) = \mu_2 - 2C\mu_1 + C^2 . \quad (11)$$

This exact result can be computed by means of (5) and (6). If we substitute approximations (8) and (9) in (11) and retain terms of the two highest orders in N, we obtain

$$\text{Mean-Square Error}(\hat{C}) \cong \frac{2}{N+1}(1 - C)^2\left[C + \frac{1 - 5C + 7C^2}{N}\right]. \quad (12)$$

Plots of (11) and (12) are presented in figure 3 for N = 8 and 16. The discrepancy between (11) and (12) is discernible for N = 16 but cannot be seen for $N \geq 32$.

For large N, the peak of the mean-square error occurs at $C \cong 1/3$ and is of value $8/27\ N^{-1}$.

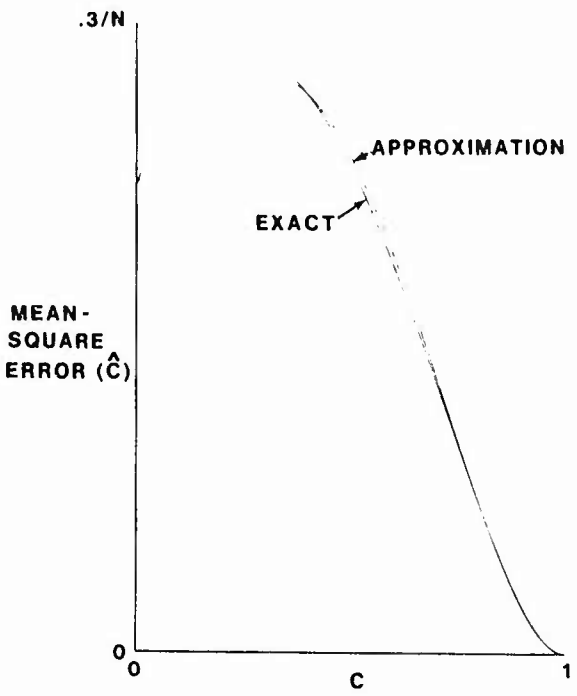


Figure 3A. N = 8

Figure 3. Mean-Square Error of MSC Estimate

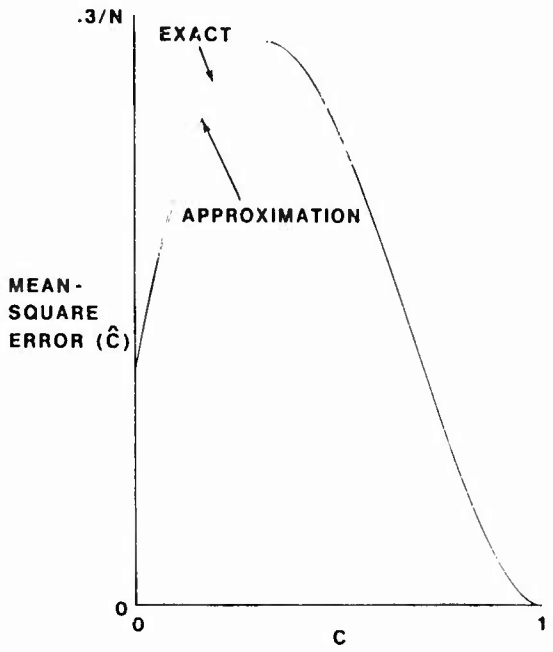


Figure 3B. N = 16

Figure 3 (Cont'd). Mean-Square Error of MSC Estimate

ESTIMATION OF MAGNITUDE COHERENCE

The magnitude coherence (MC) is defined as

$$S(f) = \left|\gamma_{xy}(f)\right| = \sqrt{C(f)} \tag{13}$$

upon use of (2). The estimate of MC is

$$\hat{S}(f) = \sqrt{\hat{C}(f)} \ , \tag{14}$$

where $\hat{C}(f)$ is defined in (3).

GENERAL RELATIONS

The first moment* of $\hat{S}$ is available from (4) by setting m = 1/2:

$$E\{\hat{S}\} = \frac{\Gamma(N)\Gamma(3/2)}{\Gamma(N + 1/2)}(1 - S^2)^N \, {}_3F_2\left(\frac{3}{2}, N, N; N + 1/2, 1; S^2\right) \ . \tag{15}$$

*The f-dependence is suppressed for convenience.

The second moment of $\hat{S}$ is directly available from (5):

$$E\{\hat{S}^2\} = \frac{1}{N} + \frac{N-1}{N+1} S^2 F(1, 1; N+2; S^2) \quad . \tag{16}$$

It will be noticed that (15) and (16) are even functions of S; this information will be useful in the approximate forms to be adopted later. Equations (15) and (16) give exact results from which the bias, variance, and mean-square error of the MC estimate $\hat{S}$ can be obtained.

A significant difference now exists between treatment of the MC estimate and the MSC estimate: whereas (4) could be reduced to an F function for m an integer, no such reduction has been discovered for (15). Further, (15) is not an appealing analytic result, as may be anticipated by noticing that, since (15) must equal unity at S = 1, and the leading factor contains an N-th order zero at S = 1, then ${}_3F_2(\ldots)$ must contain an N-th order pole at S = 1. No transformations or useful approximations of the ${}_3F_2$ function in (15) were discovered in references 6-11.

EXPANSIONS ABOUT S = 0

A direct series expansion of (4) yields

$$E\{\hat{S}^{2m}\} = \frac{\Gamma(N)\Gamma(m+1)}{\Gamma(N+m)} \left\{1 + \frac{mN(N-1)}{N+m} S^2 + \frac{mN(N-1)}{4(N+m)(N+1+m)} \left[(N^2-N)(m-1) + 2(m+1)\right] S^4 + \ldots \right\} \quad . \tag{17}$$

Now, if m = 1, the N^2 and N terms in the S^4 term drop out, and we get a useful development in which the terms decay with N:

$$E\{\hat{S}^2\} = \frac{1}{N} + \frac{N-1}{N+1} S^2 + \frac{N-1}{(N+1)(N+2)} S^4 + \ldots \quad . \tag{18}$$

But, if m = 1/2, we obtain

$$E\{\hat{S}\} = \frac{\Gamma(N)\Gamma(3/2)}{\Gamma(N+1/2)} \left\{1 + \frac{N(N-1)}{2N+1} S^2 - \frac{N(N-1)(N^2-N-6)}{4(2N+1)(2N+3)} S^4 + \ldots \right\} \tag{19}$$

and the coefficients of S^2, S^4, . . . increase with N, in direct contrast to results for MSC estimation. This increase is due to the two numerator terms and one denominator term in ${}_3F_2$ in (15) that depend on N.

EXPANSIONS ABOUT S = 1

If the results in (5) and (6) are expanded about $S = C = 1$ by means of reference 7, equation 15.3.11, we find the asymptotic expansions

$$E\{\hat{C}\} = C + \frac{1!}{N-2}(1-C)^2 - \frac{2!}{(N-2)(N-3)}(1-C)^3$$

$$+ \frac{3!}{(N-2)(N-3)(N-4)}(1-C)^4 + \ldots \qquad (20)$$

and

$$E\{\hat{C}^2\} = 1 - 2(1-C) + \frac{N+2}{N-2}(1-C)^2$$

$$- \frac{4(N+1)}{(N-2)(N-3)}(1-C)^3 + \frac{6(3N+2)}{(N-2)(N-3)(N-4)}(1-C)^4 + \ldots \qquad (21)$$

$$= C^2 + \frac{1}{N-2}(1-C^2)^2 - \frac{2}{(N-2)(N-3)}(1-C^2)^3$$

$$+ \frac{6 + \frac{N-N^2}{16}}{(N-2)(N-3)(N-4)}(1-C^2)^4 + \ldots \qquad (22)$$

upon regrouping terms. Expressions (20) and (22) are useful near $C = 1$ and indicate how rapidly $E\{\hat{C}^m\} - C^m$ approach zero as C approaches one, for $m = 1$ and 2. It will be observed from (20) and (22) that the coefficients of $(1 - C^m)^2$ and $(1 - C^m)^3$ are identical, and those of $(1 - C^m)^4$ are similar.

It was thought that $E\{\hat{S}\} = E\{\hat{C}^{1/2}\}$ might possess a similar expansion in powers of $(1-C^{1/2}) = (1-S)$ and provide a useful method of evaluating (15), at least near $S = 1$. In appendix B, it is indeed shown (after considerable labor) that

$$E\{\hat{S}\} = 1 - \frac{1}{2}(1-C) - \frac{1}{8}\frac{N-4}{N-2}(1-C)^2 - \frac{1}{16}\frac{N^2-7N+16}{(N-2)(N-3)}(1-C)^3 + \ldots \qquad (23)$$

$$= S + \frac{1}{N-2}(1-S)^2 - \frac{2}{(N-2)(N-3)}(1-S)^3 + \ldots \qquad (24)$$

(upon regrouping terms), which has the identical coefficients as (20) and (22), up through the order computed. Equation (24) shows that the bias of the MC estimate $\hat{S}$ approaches zero as S approaches one according to $(1-S)^2/(N-2)$. Also, (24) and (20) can be combined to show that

$$\text{Variance}(\hat{S}) \cong \frac{(1-S^2)^2}{2(N-2)} \text{ as } S \to 1 \ . \tag{25}$$

This corroborates reference 4, (8).

CHOICE OF APPROXIMATION

Expansions like (20)-(25) cannot be used to evaluate the desired statistics for small S; in fact, they are divergent asymptotic expansions. When this information is combined with the earlier results about S = 0, we find that direct analytic expansions of (15) are not fruitful, in contrast with the earlier approach for MSC results. Instead, we must adopt some convenient simple approximation and try to match it to the exact results in some fashion. (The techniques in reference 12, chapter 9, are relevant in this regard.)

Before we do that, however, it is necessary to digress. We know that

$$\text{Bias}(\hat{S}) = E\{\hat{S}\} - S \ , \tag{26}$$

$$\text{Variance}(\hat{S}) = E\{\hat{S}^2\} - E^2\{\hat{S}\} \ , \tag{27}$$

$$\text{Mean-Square Error}(\hat{S}) = \left[\text{Bias}(\hat{S})\right]^2 + \text{Variance}(\hat{S}) \ , \tag{28}$$

where the exact moments are given in (15) and (16). A very good approximation to $E\{\hat{S}^2\} = E\{\hat{C}\}$ is already available from (7) and (8), namely,

$$E\{\hat{C}\} \cong C + \frac{1}{N}(1-C)^2\left(1+\frac{2C}{N}\right) \ , \tag{29}$$

or

$$E\{\hat{S}^2\} \cong S^2 + \frac{1}{N}(1-S^2)^2\left(1+\frac{2S^2}{N}\right) . \tag{30}$$

Therefore, if we can approximate $E\{\hat{S}\}$ or $\text{Bias}(\hat{S})$ or $\text{Variance}(\hat{S})$ in (26) and (27), we will have approximations for all three statistics in (26)-(28).

Initial attempts concentrated on approximating the bias (26) by the form

$$\frac{(1-S)^2}{N-2} + \alpha(1-S)^{\nu}, \quad \nu \geq 3 \quad , \tag{31}$$

where α and ν were chosen so as to match the exact bias and its derivative at S = 0; these attempts were not successful for all N and S. A generalization to the form

$$\frac{(1-S)^2}{N-2} + (1-S)^{\nu}\left[\alpha + \beta S^2(S-\lambda)\right], \quad \lambda = \frac{1.15}{\sqrt{N}-2.85}, \quad \nu \geq 3 \quad , \tag{32}$$

was quite good for N up to 100, but deteriorated for larger N, despite also matching the exact second derivative of the bias at the origin. Numerous other forms were tried for approximating the bias but yielded poorer approximations.

VARIANCE APPROXIMATION

Succeeding attempts were aimed at approximating the variance (27). It will be recalled (from the discussion under (16)) that (27) is an even function of S. (This even property is not true of (26) or (28), because of the S term in (26).) The approximation to the variance was therefore also chosen to be even;* after much trial and error, an acceptable form was found to be

$$\text{Variance}\,(\hat{S}) \equiv \frac{(1-S^2)^2}{2(N-2)}\left[1 - \frac{3}{N}(1-S^2) + A\,\frac{(1-S^2)^2}{1 + BS^2 + DS^4}\right] \equiv \sigma^2_{app} \quad . \tag{33}$$

The leading term in (33) is dictated by (25); the second term in the bracket was deduced from observing the numerical values of the variance near S = 1; and the numerator of the third term is chosen to make it decay faster than the other two terms near S = 1. Equation (33) already matches the value and derivative of the exact variance at S = 1, and the three constants were chosen so as to match the value and first four derivatives of the exact variance at S = 0; see appendix C. The end result of the investigation is that the constants are given by

$$A = -0.571 + \frac{1.75}{N} + \frac{0.760}{N^2}$$

$$B = 0.752\,N - 3.26$$

$$D = 0.221\,N^2 - 1.66\,N \quad . \tag{34}$$

*See reference 12, pages 108 and 118.

Plots of the exact variance (27) and the approximate variance (33) are presented in figure 4 for N = 8, 16, 64, 256, and 1024. (Notice that the abscissa is S, not C.) The discrepancy does not go to zero as N increases, as it did for the MSC approximation; however, the discrepancy is small over the practical range of values of N (i.e., $N < 1000$), where N is the number of averages employed in the MC estimate.

The peak of Variance $(\hat{S})$ occurs at

$$S \cong \frac{4.6}{\sqrt{N}} \left(1 - \frac{9}{\sqrt{N}} + \frac{35}{N}\right) \text{ for } 64 \leq N \leq 1024 \tag{35}$$

and is of value

$$\text{Peak Variance } (\hat{S}) \cong \frac{0.49}{N} - \frac{10}{N^2} + \frac{290}{N^3} \text{ for } 64 \leq N \leq 1024 \ . \tag{36}$$

These results follow by fitting the exact numerical results in figure 4. For very large N, (36) suggests that the peak variance approaches $(2N)^{-1}$.

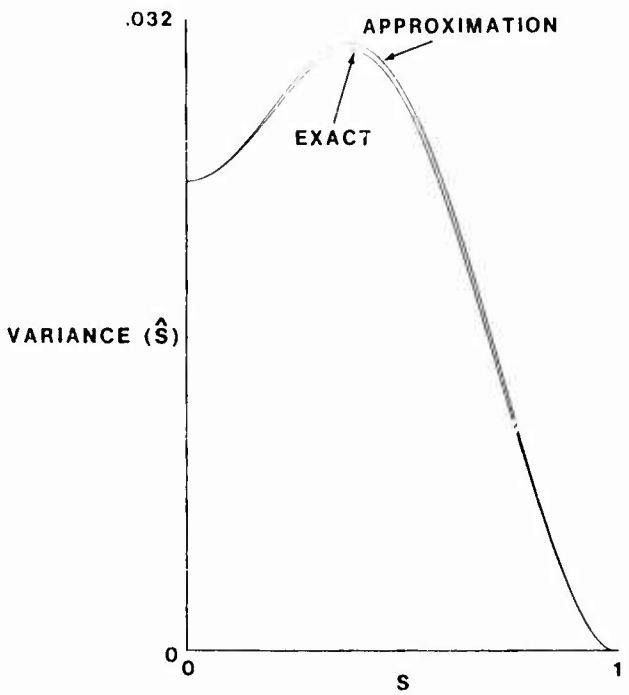


Figure 4A. N = 8

Figure 4. Variance of MC Estimate

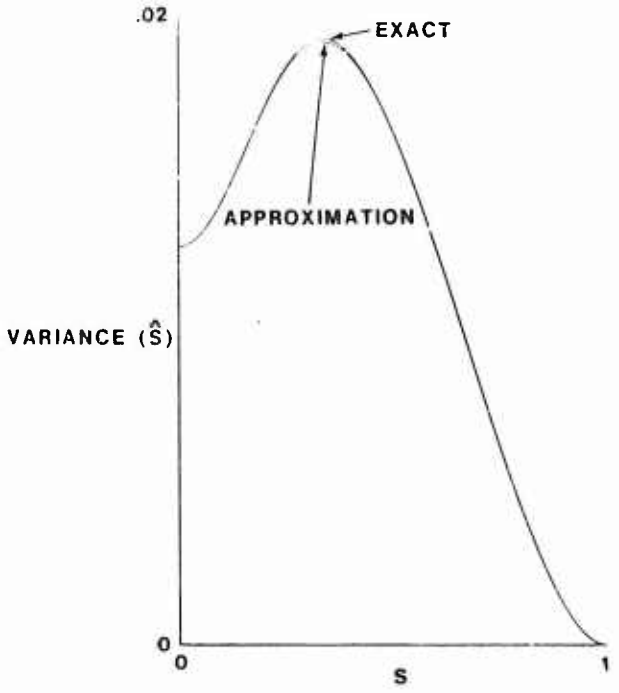


Figure 4B. N = 16

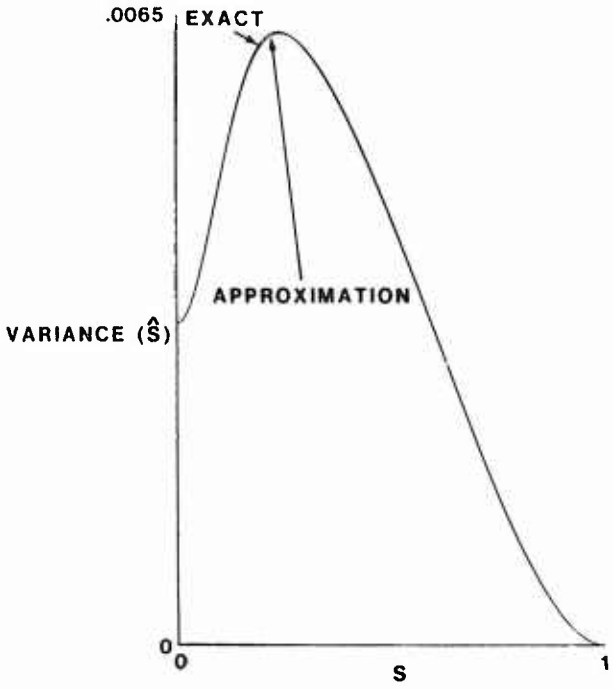


Figure 4C. N = 64

Figure 4 (Cont'd). Variance of MC Estimate

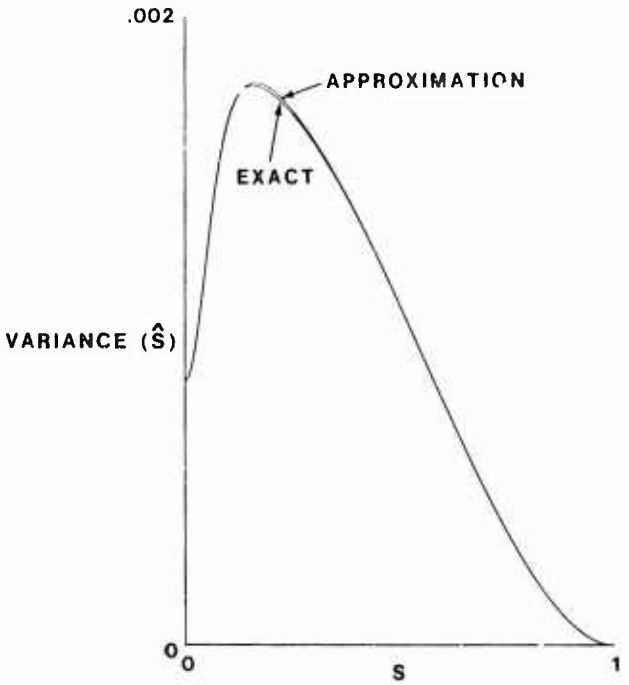


Figure 4D. N = 256

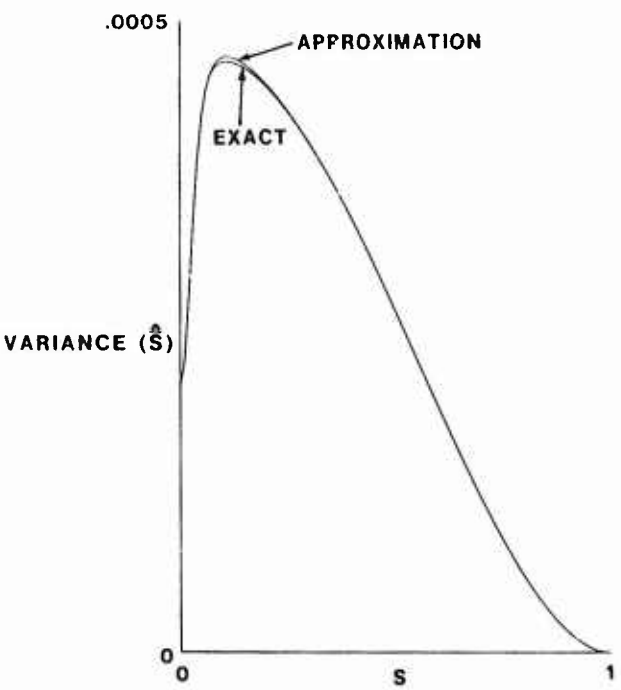


Figure 4E. N = 1024

Figure 4 (Cont'd). Variance of MC Estimate

At the origin, we have, from (15) and (16),

$$\text{Variance}\,(\hat{S}) = \frac{1}{N} - \left[\frac{\Gamma(N)\Gamma(3/2)}{\Gamma(N+1/2)}\right]^2$$

$$\cong \left(1 - \frac{\pi}{4}\right)\frac{1}{N} - \frac{\pi}{16}\frac{1}{N^2} = \frac{0.215}{N} - \frac{0.196}{N^2} \quad . \tag{37}$$

Here, we have employed the approximation (reference 7, equation 6.1.47)

$$\frac{\Gamma(N)\Gamma(3/2)}{\Gamma(N+1/2)} \cong \frac{\sqrt{\pi}/2}{\sqrt{N}}\left(1 + \frac{1}{8N}\right) \quad , \tag{38}$$

which is excellent even for N as small as 2.

BIAS APPROXIMATION

If we eliminate $E\{\hat{S}\}$ from (26) and (27), and then employ (30) and (33), we can express

$$\text{Bias}\,(\hat{S}) = \left[E\{\hat{S}^2\} - \text{Variance}\,(\hat{S})\right]^{1/2} - S$$

$$\cong \left[S^2 + \frac{1}{N}(1-S^2)^2\left(1 + \frac{2S^2}{N}\right) - \sigma_{app}^2\right]^{1/2} - S \equiv b_{app} \quad . \tag{39}$$

This approach is in line with the observation made under (30). The approximate variance σ_{app}^2 in (39) is given by (33) and (34).

Plots of the exact bias (26) and the approximate bias (39) are presented in figure 5 for N = 8 and 16. The exact bias decreases monotonically with S and has an origin value of

$$\text{Bias}\,(\hat{S}\,|\,S = 0) = \frac{\Gamma(N)\Gamma(3/2)}{\Gamma(N+1/2)} \equiv G_N \quad , \tag{40}$$

from (15); an excellent approximation to G_N is given in (38). The discrepancy between (26) and (39) is barely discernible for N = 8 and is not discernible for N = 16 up through N = 1024.

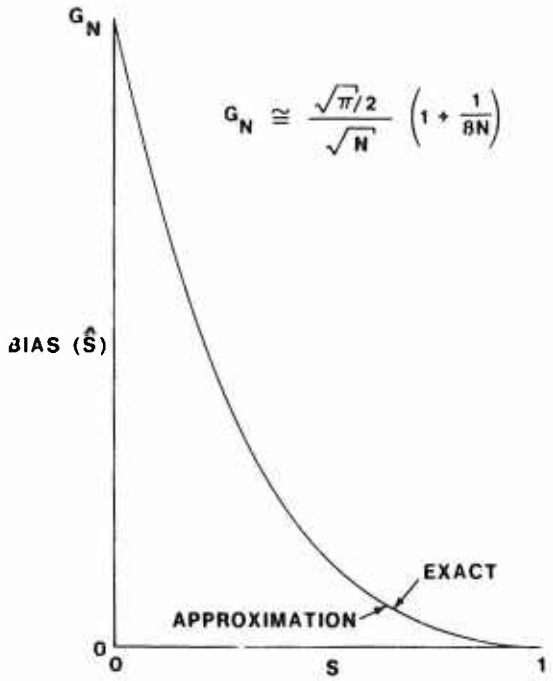


Figure 5A. N = 8

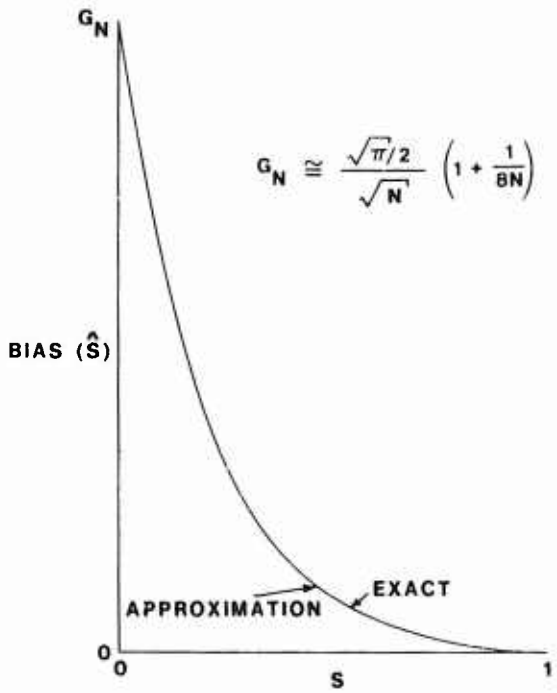


Figure 5B. N = 16

Figure 5. Bias of MC Estimate

MEAN-SQUARE ERROR APPROXIMATION

The approximation to the mean-square error is immediately available via (28):

$$\text{Mean-Square Error}\,(\hat{S}) \cong b_{app}^2 + \sigma_{app}^2 \ , \tag{41}$$

where the approximate bias and variance are given by (39) and (33), respectively. Plots of (28) and (41) are presented in figure 6 for N = 8, 16, 64, 256, and 1024. The discrepancy does not go to zero as N increases; however, it is small over the range of practically useful values of N.

The peak value of the mean-square error occurs at S = 0 and is of value 1/N, as is seen from (16). The mean-square error curve is composed of two distinct regions, one near the origin where the bias dominates, and one for larger S where the variance dominates; this explains the hump in the curves for larger N.

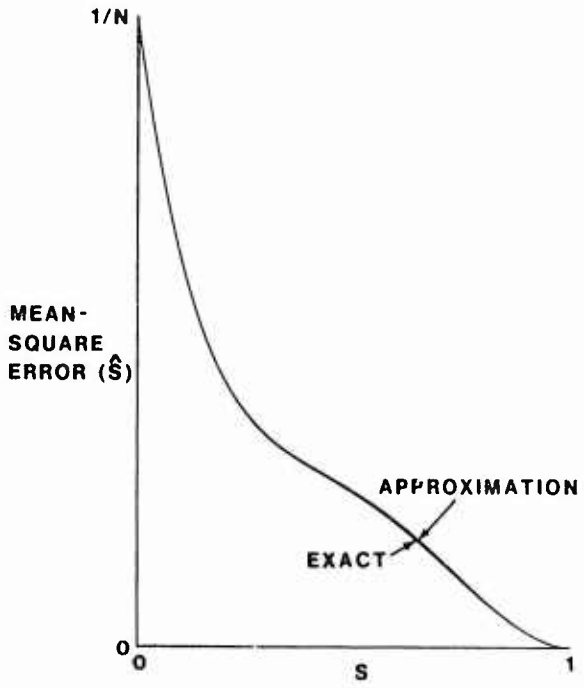


Figure 6A. N = 8

Figure 6. Mean-Square Error of MC Estimate

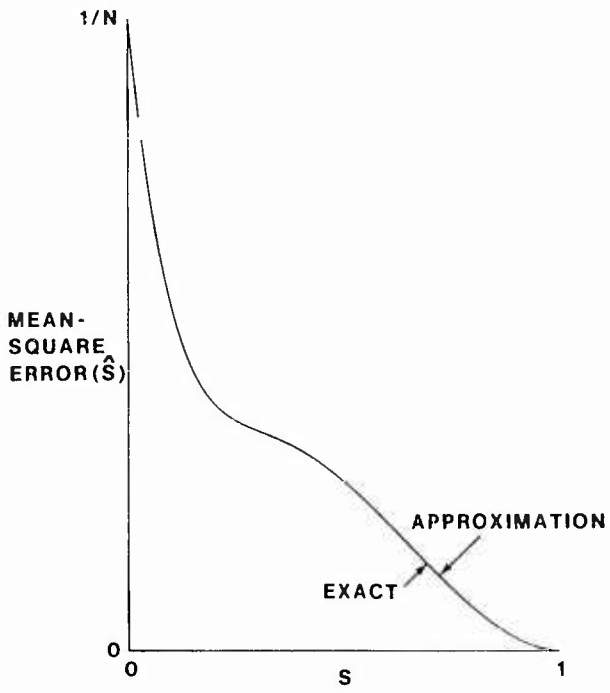


Figure 6B. N = 16

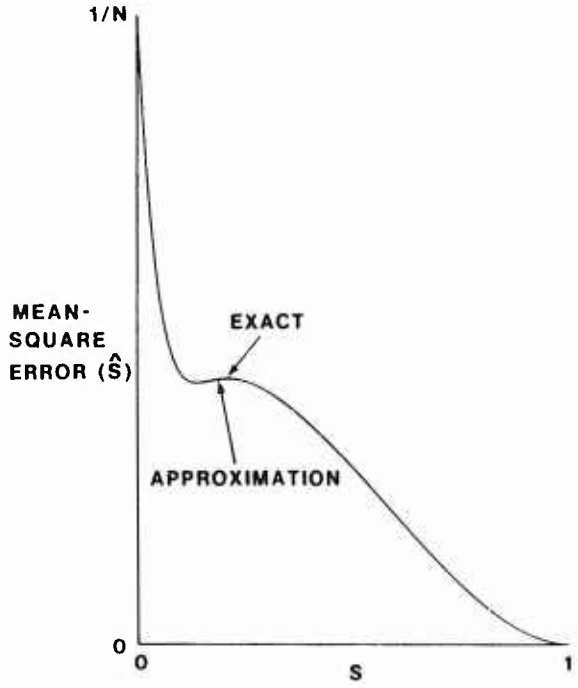


Figure 6C. N = 64

Figure 6 (Cont'd). Mean-Square Error of MC Estimate

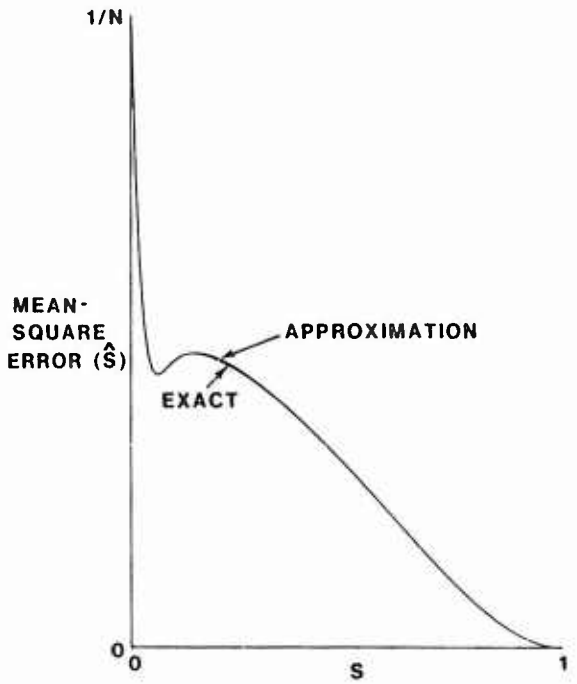


Figure 6D. N = 256

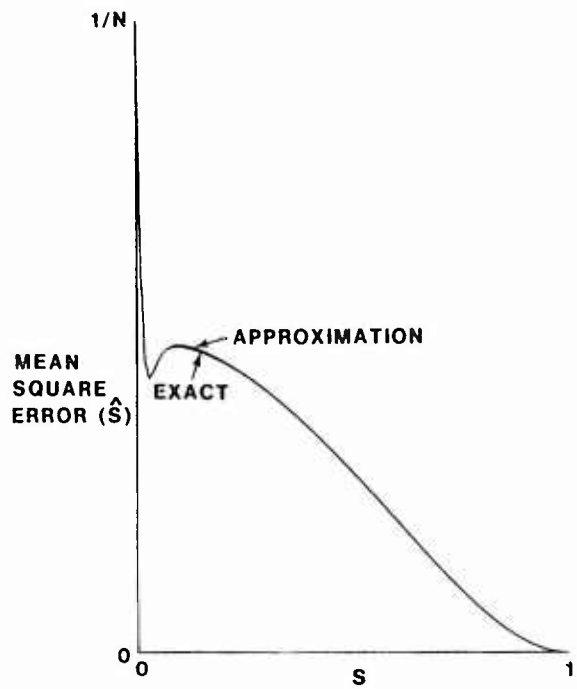


Figure 6E. N = 1024

Figure 6 (Cont'd). Mean-Square Error of MC Estimate

SUMMARY

Approximations for the MSC estimate are given by

$$\text{Bias}\,(\hat{\bar{C}}) \cong \frac{1}{N}\,(1-C)^2\left(1+\frac{2C}{N}\right) \tag{8}$$

$$\text{Variance}\,(\hat{\bar{C}}) \cong \frac{N-1}{N\,(N+1)}\,(1-C)^2\left[2C+\frac{1-6C+13C^2}{N}\right] \tag{9}$$

$$\text{Mean-Square Error}\,(\hat{\bar{C}}) \cong \frac{2}{N+1}\,(1-C)^2\left[C+\frac{1-5C+7C^2}{N}\right] . \tag{12}$$

Approximations for the MC estimate are given by

$$\text{Variance}\,(\hat{\bar{S}}) \cong \frac{(1-S^2)^2}{2\,(N-2)}\left[1-\frac{3}{N}\,(1-S^2)+A\,\frac{(1-S^2)^2}{1+BS^2+DS^4}\right] \equiv \sigma^2_{app} , \tag{33}$$

where

$$A = -0.571+\frac{1.75}{N}+\frac{0.760}{N^2}$$

$$B = 0.752\,N - 3.26$$

$$C = 0.221\,N^2 - 1.66\,N . \tag{34}$$

$$\text{Bias}\,(\hat{\bar{S}}) \cong \left[S^2+\frac{1}{N}\,(1-S^2)^2\left(1+\frac{2S^2}{N}\right)-\sigma^2_{app}\right]^{1/2} - S \equiv b_{app} \tag{39}$$

$$\text{Mean-Square Error}\,(\hat{\bar{S}}) \equiv b^2_{app}+\sigma^2_{app} . \tag{41}$$

All of these are capable of hand calculation over the entire range of true coherence. The approximations for the MSC estimate are particularly simple; those for the MC estimate are somewhat more complicated, but far more tractable than the exact answers involving a ${}_3F_2$ function. The fundamental dependencies of the statistics on N and true coherence have also been deduced. Although the discrepancies between approximations and exact values do not tend to zero for the MC statistics for large N, the approximations are useful at least over the range from $N = 8$ to $N = 1024$, which is believed to encompass the region of most practical interest. How good the approximations are for larger N has not been investigated quantitatively.

REVERSE BLANK

Appendix A

REDUCTION OF THE $_3F_2$ FUNCTION

From (4) in the main text, we have

$$\mu_2 = \frac{2}{N(N+1)}(1-C)^N \, {}_3F_2\,(3,\ N,\ N;\ N+2,\ 1;\ C)\ , \tag{A-1}$$

which is very slowly convergent for C near 1. Now, in (A-1), using reference 6, section 9.14, we have

$${}_3F_2\,(\cdots) = \sum_{k=0}^{\infty} \frac{(3)_k\,(N)_k}{(1)_k\,(N+2)_k}\ \frac{C^k}{k!}\,(N)_k\ . \tag{A-2}$$

But

$$\frac{(3)_k}{(1)_k} = \frac{(k+1)(k+2)}{2} \tag{A-3}$$

and

$$\frac{(N)_k}{(N+2)_k} = \frac{N(N+1)}{(N+k)(N+k+1)}\ . \tag{A-4}$$

Substituting (A-3) and (A-4) in (A-2) and (A-1) yields

$$\mu_2 = (1-C)^N \sum_{k=0}^{\infty} \frac{(k+1)(k+2)}{(k+N)(k+N+1)}\,\frac{C^k}{k!}(N)_k\ . \tag{A-5}$$

Now, a partial-fraction expansion yields

$$\frac{(k+1)(k+2)}{(k+N)(k+N+1)} = 1 + \frac{(N-1)(N-2)}{k+N} - \frac{N(N-1)}{k+N+1}\ ; \tag{A-6}$$

and, since we can express

$$\frac{1}{k+N} = \frac{1}{N}\ \frac{(N)_k}{(N+1)_k}\ ,$$

$$\frac{1}{k+N+1} = \frac{1}{N+1}\ \frac{(N+1)_k}{(N+2)_k}\ , \tag{A-7}$$

(A-5) takes the form

$$\mu_2 = (1-C)^N \left\{ \sum_{k=0}^{\infty} \frac{C^k}{k!} (N)_k + \frac{(N-1)(N-2)}{N} \sum_{k=0}^{\infty} \frac{(N)_k (N)_k}{(N+1)_k} \frac{C^k}{k!} \right.$$

$$\left. - \frac{N(N-1)}{N+1} \sum_{k=0}^{\infty} \frac{(N)_k (N+1)_k}{(N+2)_k} \frac{C^k}{k!} \right\} \qquad \text{(A-8)}$$

$$= (1-C)^N \left\{ F(n, b; b; C) + \frac{(N-1)(N-2)}{N} F(N, N; N+1; C) \right.$$

$$\left. - \frac{N(N-1)}{N+1} F(N, N+1; N+2; C) \right\} , \qquad \text{(A-9)}$$

upon employment of reference 7, equation 15.1.1. By use of reference 7, equation 15.3.3, this can be manipulated into the form

$$\mu_2 = 1 + \frac{(N-1)(N-2)}{N} (1-C)\ F(1, 1; N+1; C)$$

$$- \frac{N(N-1)}{N+1} (1-C)\ F(2, 1; N+2; C) , \qquad \text{(A-10)}$$

which is particularly good for developing in a series in $(1-C)$ by use of reference 7, equation 15.3.11.

At this point, a multitude of alternative forms for (A-10) are available by use of reference 7, page 558. Several rapidly convergent forms involving a single F function are now listed:

$$\mu_2 = - \frac{N^3 - 2N^2 + 2N - 2}{N} + \frac{N-1}{N+1} \left[N^2 - (N-2)\ C \right]\ F(1, 1; N+2; C) \qquad \text{(A-11)}$$

$$= \frac{2}{N(N+1)} - \frac{(N-1)(N-2)}{N+1} C$$

$$+ \frac{N-1}{(N+1)(N+2)} \left[N^2 - (N-2)\ C \right] C F(2, 1; N+3; C) \qquad \text{(A-12)}$$

$$= 1 + \frac{N-1}{N(N+1)} (1-C) \left\{ (N+1)(N-2) - \left[N^2 - (N-2)\ C \right] F(2, 1; N+2; C) \right\} . \qquad \text{(A-13)}$$

The form in (A-11) uses exactly the same F function as encountered in μ_1 in (5) and is more rapidly convergent than the latter two forms, for all values of C.

The reduction technique employed above for m = 2 in (4) can also be used for other integer values of m. However, it fails for m noninteger, because simplifications like (A-3) and (A-4) do not occur then.

Appendix B

EXPANSION ABOUT S = 1 FOR MAGNITUDE COHERENCE

The estimate of MSC is given in (3). We let

$$X_n(f) = (\tilde{a}_n + i\tilde{b}_n) \equiv \alpha_n$$

$$Y_n(f) = g(\tilde{a}_n + i\tilde{b}_n) + (\tilde{c}_n + i\tilde{d}_n) \equiv g\alpha_n + \beta_n \quad , \tag{B-1}$$

where $\tilde{a}_n$, $\tilde{b}_n$, $\tilde{c}_n$, $\tilde{d}_n$ are independent, zero-mean, unit-variance, real, Gaussian random variables. Then, for g real,

$$E\left\{X_n(f)\, Y_n^*(f)\right\} = E\left\{\alpha_n\, g(\alpha_n^* + \beta_n^*)\right\} = gE\left\{|\alpha_n|^2\right\} = 2g \quad ;$$

$$E\left\{|X_n(f)|^2\right\} = 2; \quad E\left\{|Y_n(f)|^2\right\} = 2(1+g^2) \quad . \tag{B-2}$$

Therefore, the MSC is

$$C = \frac{(2g)^2}{2 \times 2(1+g^2)} = \frac{g^2}{1+g^2}. \tag{B-3}$$

For a specified value C of the MSC, the required value of scale factor in (B-1) is

$$g = \left(\frac{C}{1 - C}\right)^{1/2} \quad . \tag{B-4}$$

Thus, as $S \to 1$, $C = S^2 \to 1$, $g \to \infty$, and $1/g \to 0$. Because we are interested in S near unity, we can concentrate on 1/g near zero.

If we define

$$A = \sum_{n=1}^{N} |\alpha_n|^2, \quad B = \sum_{n=1}^{N} |\beta_n|^2, \quad D = \sum_{n=1}^{N} \alpha_n \beta_n^* \quad , \tag{B-5}$$

then substitution of (B-1) in (3) yields

$$\hat{C} = \frac{\left|\sum_{n=1}^{N} \alpha_n (g\alpha_n^* + \beta_n^*)\right|^2}{\sum_{n=1}^{N} |\alpha_n|^2 \sum_{n=1}^{N} |g\alpha_n + \beta_n|^2} = \frac{|D + gA|^2}{A(B + 2gD_r + g^2A)}$$

$$= \frac{|D|^2 + 2gAD_r + g^2A^2}{AB + 2gAD_r + g^2A^2}, \qquad \text{(B-6)}$$

where D_r is the real part of D in (B-5). Rearranging (B-6), we obtain

$$\hat{C} = \frac{1 + \frac{1}{g}T + \frac{1}{g^2}U}{1 + \frac{1}{g}T + \frac{1}{g^2}V}, \qquad \text{(B-7)}$$

where

$$T = \frac{2D_r}{A}, \quad U = \frac{|D|^2}{A^2}, \quad V = \frac{B}{A}. \qquad \text{(B-8)}$$

Now a series expansion of (B-7) in powers of $1/g$ (as noted under (B-4)) yields

$$\hat{C} = 1 + \frac{a_2}{g^2} + \frac{a_3}{g^3} + \frac{a_4}{g^4} + \frac{a_5}{g^5} + \frac{a_6}{g^6} + \cdots, \qquad \text{(B-9)}$$

where

$$a_2 = U - V, \quad a_3 = -(U - V)T, \quad a_4 = (U - V)(T^2 - V),$$

$$a_5 = (U - V)(2V - T^2)T, \quad a_6 = (U - V)(T^4 + V^2 - 3T^2V). \qquad \text{(B-10)}$$

Since we are interested in the behavior of the MC estimate $\hat{S}$, we employ the expansion

$$(1 + \epsilon)^{1/2} = 1 + \frac{1}{2}\epsilon - \frac{1}{8}\epsilon^2 + \frac{1}{16}\epsilon^3 + \cdots \quad (|\epsilon| < 1) \qquad \text{(B-11)}$$

to obtain

$$\hat{S} = \sqrt{\hat{C}} = 1 + \left(\frac{a_2}{2}\right)\frac{1}{g^2} + \left(\frac{a_3}{2}\right)\frac{1}{g^3} + \left(\frac{a_4}{2} - \frac{a_2^2}{8}\right)\frac{1}{g^4}$$

$$+ \left(\frac{a_5}{2} - \frac{a_2 a_3}{4}\right)\frac{1}{g^5} + \left(\frac{a_6}{2} - \frac{a_3^2}{8} - \frac{a_2 a_4}{4} + \frac{a_2^3}{16}\right)\frac{1}{g^6} + \ldots . \qquad \text{(B-12)}$$

And, since we are interested in S near unity, we let

$$x = 1 - C \qquad \text{(B-13)}$$

and expand $\hat{S}$ in a power series in x. To do this, we utilize (B-4) and obtain

$$\frac{1}{g} = \sqrt{\frac{x}{1-x}} = x^{1/2}\left(1 + \frac{1}{2}x + \frac{3}{8}x^2 + \ldots\right)$$

$$\frac{1}{g^2} = x + x^2 + x^3 + \ldots$$

$$\frac{1}{g^3} = x^{3/2}\left(1 + \frac{3}{2}x + \frac{15}{8}x^2 + \ldots\right)$$

$$\frac{1}{g^4} = x^2\left(1 + 2x + 3x^2 + \ldots\right) = x^2 + 2x^3 + \ldots$$

$$\frac{1}{g^5} = x^{5/2}\left(1 + \frac{5}{2}x + \ldots\right)$$

$$\frac{1}{g^6} = x^3 + \ldots . \qquad \text{(B-14)}$$

Substitution of (B-14) in (B-12) yields

$$\hat{S} = 1 + x\left(\frac{1}{2}a_2\right) + x^{3/2}\left(\frac{1}{2}a_3\right) + x^2\left(\frac{1}{2}a_2 + \frac{1}{2}a_4 - \frac{1}{8}a_2^2\right)$$

$$+ x^{5/2}\left(\frac{3}{4}a_3 + \frac{1}{2}a_5 - \frac{1}{4}a_2 a_3\right)$$

$$+ x^3\left(\frac{1}{2}a_2 + a_4 - \frac{1}{4}a_2^2 + \frac{1}{2}a_6 - \frac{1}{8}a_3^2 - \frac{1}{4}a_2 a_4 + \frac{1}{16}a_2^3\right) + \ldots . \qquad \text{(B-15)}$$

Now we are ready to perform averages on the individual terms in (B-15) and obtain an expansion of $E\{\hat{S}\}$ in powers of $x = 1 - C$.

The method of obtaining $E\{a_2\}$ will be developed in full. The results for the other averages in (B-15) will merely be stated, and can easily be deduced from the method presented. From (B-10), (B-8), and (B-5),

$$a_2 = U - V = \frac{|D|^2 - BA}{A^2} = \frac{1}{A^2} \sum_{m,\, n=1}^{N} \beta_m^* \beta_n Q_{mn} \ , \qquad \text{(B-16)}$$

where we have defined

$$Q_{mn} = \alpha_m \alpha_n^* - A \delta_{mn} \ . \qquad \text{(B-17)}$$

Now, let

$$\underset{\sim}{\alpha} \equiv \left[\alpha_1 \ \alpha_2 \ \ldots \ \alpha_N\right] \ . \qquad \text{(B-18)}$$

Then, since Q_{mn} depends only on $\underset{\sim}{\alpha}$,

$$E\left\{U - V \middle| \underset{\sim}{\alpha}\right\} = \frac{1}{A^2} \sum_{m,\, n=1}^{N} Q_{mn} E\left\{\beta_m^* \beta_n\right\}$$

$$= \frac{2}{A^2} \sum_{n=1}^{N} Q_{nn} = \frac{2}{A^2} \left[A - AN\right] = -\frac{2(N-1)}{A} \ , \qquad \text{(B-19)}$$

where we have utilized the property

$$E\left\{\beta_m^* \beta_n\right\} = 2 \delta_{mn} \ , \qquad \text{(B-20)}$$

which follows directly from the definitions (B-1). Therefore, using (B-19), we have

$$E\{U - V\} = -2(N-1) E\left\{\frac{1}{A}\right\} \ . \qquad \text{(B-21)}$$

Now, A is given by (B-5) and (B-1) as

$$A = \sum_{n=1}^{N} (\tilde{a}_n^2 + \tilde{b}_n^2) \ . \qquad \text{(B-22)}$$

Therefore, the probability density function of A is

$$p(A) = \frac{A^{N-1} \exp(-A/2)}{2^N (N-1)!}, \quad A > 0 \ . \tag{B-23}$$

There follows immediately the m-th moment of 1/A as

$$E\{1/A^m\} = \frac{1}{2^m} \frac{1}{(N-1)(N-2) \ldots (N-m)}, \quad m < N \ . \tag{B-24}$$

Employing (B-24) in (B-21), we have

$$E\{a_2\} = E\{U - V\} = -1 \ . \tag{B-25}$$

By employing the generalizations of (B-20) to the fourth and sixth orders, namely,

$$E\left\{\beta_k \beta_\ell^* \beta_m \beta_n^*\right\} = 4\left(\delta_{k\ell}\, \delta_{mn} + \delta_{kn}\, \delta_{\ell m}\right) ,$$

$$E\left\{\beta_k \beta_\ell^* \beta_m \beta_n^* \beta_p \beta_q^*\right\} = 8\left(\delta_{k\ell}\, \delta_{mn}\, \delta_{pq} + \delta_{k\ell}\, \delta_{mq}\, \delta_{np}\right.$$

$$\left. + \delta_{kn} \delta_{\ell m}\, \delta_{pq} + \delta_{kn}\, \delta_{\ell p}\, \delta_{mq} + \delta_{kq}\, \delta_{\ell m}\, \delta_{np} + \delta_{kq}\, \delta_{\ell p} \delta_{mn}\right) , \tag{B-26}$$

we find the following quantities:

$$E\{a_3\} = 0, \quad E\{a_4\} = \frac{N-1}{N-2}, \quad E\{a_2^2\} = \frac{N}{N-2} ,$$

$$E\{a_5\} = 0, \quad E\{a_2 a_3\} = 0, \quad E\{a_6\} = -\frac{N-1}{N-3},$$

$$E\{a_3^2\} = \frac{2N}{(N-2)(N-3)}, \quad E\{a_2 a_4\} = -\frac{N^2}{(N-2)(N-3)},$$

$$E\{a_2^3\} = -\frac{N(N+1)}{(N-2)(N-3)} \ . \tag{B-27}$$

When we employ (B-27) in (B-15), there follows

$$E\{\hat{S}\} = 1 - \frac{1}{2}(1-C) - \frac{1}{8}\frac{N-4}{N-2}(1-C)^2$$

$$- \frac{1}{16}\frac{N^2-7N+16}{(N-2)(N-3)}(1-C)^3 + \ldots \quad . \tag{B-28}$$

This is the end result quoted in (23) in the main text.

Appendix C

VARIANCE APPROXIMATION FOR MAGNITUDE COHERENCE

From (19) and (40) in the main text, we have

$$E\{\hat{S}\} = Q_o + Q_1 S^2 + Q_2 S^4 + \ldots \quad , \tag{C-1}$$

where

$$Q_o = G_N$$

$$Q_1 = G_N \frac{N(N-1)}{2N+1}$$

$$Q_2 = G_N \frac{N(N-1)(6+N-N^2)}{4(2N+1)(2N+3)} \quad . \tag{C-2}$$

And, from (18), we have

$$E\{\hat{S}^2\} = R_o + R_1 S^2 + R_2 S^4 + \ldots \quad , \tag{C-3}$$

where

$$R_o = \frac{1}{N}$$

$$R_1 = \frac{N-1}{N+1}$$

$$R_2 = \frac{N-1}{(N+1)(N+2)} \quad . \tag{C-4}$$

Therefore,

$$\text{Variance}\,(\hat{S}) = \alpha + \beta S^2 + \gamma S^4 + \ldots \quad , \tag{C-5}$$

where

$$\alpha = R_o - Q_o^2$$

$$\beta = R_1 - 2Q_oQ_1$$

$$\gamma = R_2 - Q_1^2 - 2Q_oQ_2 \quad . \tag{C-6}$$

By use of (40) and reference 7, equation 6.1.47, we find

$$G_N = \frac{\sqrt{\pi}/2}{\sqrt{N}} \left[1 + \frac{1}{8N} + \frac{1}{128N^2} + \ldots \right] . \qquad \text{(C-7)}$$

Expanding the above expressions in powers of N^{-1}, we find

$$\alpha = \left(1 - \frac{\pi}{4}\right) \frac{1}{N} - \frac{\pi}{16} \frac{1}{N^2} - \frac{65\pi}{16384} \frac{1}{N^3} + \ldots$$

$$\beta = 1 - \frac{\pi}{4} - \left(2 - \frac{5\pi}{16}\right) \frac{1}{N} + \ldots$$

$$\gamma = - \frac{\pi}{32} N + \frac{7\pi}{128} + \ldots . \qquad \text{(C-8)}$$

Thus, (C-5) and (C-8) give a power series expansion of Variance $(\hat{S})$ that should be accurate for large N.

The variance approximation that we adopt is given in (33). We expand (33) in powers of S^2 and obtain

$$\sigma^2_{app} = \frac{1}{2(N-2)} \left[\left\{ 1 - \frac{3}{N} + A \right\} + S^2 \left\{ \frac{3}{N} - A(B+2) - 2\left(1 - \frac{3}{N} + A\right) \right\} \right.$$
$$\left. + S^4 \left\{ A\left((B+1)^2 - D\right) - 2\left(\frac{3}{N} - A(B+2)\right) + \left(1 - \frac{3}{N} + A\right) \right\} + \ldots \right] . \qquad \text{(C-9)}$$

We now select constants A, B, and D so that (C-5) and (C-9) match up through the power S^4. There follows

$$A = 2(N-2)\,\alpha - 1 + \frac{3}{N}$$

$$B = \frac{1}{A}\left[\frac{3}{N} - 2(N-2)(2\alpha + \beta)\right] - 2$$

$$D = (B+1)^2 - \frac{1}{A} 2(N-2)(3\alpha + 2\beta + \gamma) . \qquad \text{(C-10)}$$

We now employ the expansions for α, β, γ in (C-8) and obtain, finally,

$$A = -0.57080 + 1.7489/N + 0.76047/N^2 + \ldots$$

$$B = 0.75194N - 3.2639 + \ldots$$

$$D = 0.22142N^2 - 1.6648N + \ldots \qquad \text{(C-11)}$$

Equations (33) and (C-11) are the final results for the variance approximation. It has been found sufficient to retain only three decimals in the constants and to stop with the terms shown in (C-11).

REFERENCES

1. G. C. Carter and A. H. Nuttall, "Evaluation of the Statistics of the Estimate of Magnitude-Squared-Coherence," NUSC Technical Memorandum TC-193-71, 28 September 1971.

2. G. C. Carter and A. H. Nuttall, "Statistics of the Estimate of Coherence," Proceedings of the IEEE, vol. 60, no. 4, pp. 465-466, April 1972.

3. G. C. Carter, C. Knapp, and A. H. Nuttall, "Estimation of the Magnitude-Squared-Coherence Function Via Overlapped FFT Processing," IEEE Transactions on Audio and Electroacoustics, vol. AU-21, no. 4, pp. 377-344, August 1973.

4. G. C. Carter, C. Knapp, and A. H. Nuttall, "Statistics of the Estimate of the Magnitude-Coherence Function," IEEE Transactions on Audio and Electroacoustics, vol. AU-21, no. 4, pp. 388-389, August 1973.

5. G. C. Carter, "Estimation of the Magnitude-Squared-Coherence Function," M. S. Thesis, University of Connecticut, Storrs. Also in NUSC Technical Report 4343, 19 May 1972 (AD 743 945).

6. I. S. Gradshteyn and I. M. Ryzhik, Table of Integrals, Series and Products, Academic Press, New York, 1965.

7. Handbook of Mathematical Functions, U. S. Department of Commerce, National Bureau of Standards, Applied Mathematics Series No. 55, U. S. Government Printing Office, June 1964.

8. W. N. Bailey, Generalized Hypergeometric Series, Cambridge University Press, Great Britain, 1935.

9. Y. L. Luke, The Special Functions and Their Approximations, vols. I and II, Academic Press, New York, 1969.

10. H. Bateman, Higher Transcendental Functions, vols. I, II, and III, McGraw-Hill Book Co., Inc., New York, 1953.

11. E. D. Rainville, Special Functions, The Macmillan Company, New York, 1960.

12. C. Hastings, Jr., Approximations for Digital Computers, Princeton University Press, Princeton, New Jersey, 1955.

REVERSE BLANK

NUSC Technical Report 5303
26 March 1976

Spectral Analysis of a Univariate Process With Bad Data Points, Via Maximum Entropy and Linear Predictive Techniques

Albert H. Nuttall

ABSTRACT

A comparison of several methods for spectral estimation of a univariate process with equi-spaced samples, including maximum entropy, linear predictive, and autoregressive techniques, is made. The comparison is conducted via simulation for situations both with and without bad (or missing) data points. The case of bad data points required extensions of existing techniques in the literature and is documented fully here in the form of processing equations and FORTRAN programs. It is concluded that the maximum entropy (Burg) technique is as good as any of the methods considered, for the univariate case. The methods considered are particularly advantageous for short data segments.

This report also reviews several available techniques for spectral analysis under different states of knowledge and presents the interrelationships of the various approaches in a consistent notation. Hopefully, this non-rigorous presentation will clarify this method of spectral analysis for readers who are nonexpert in the field.

Approved for public release; distribution unlimited.

TABLE OF CONTENTS

	Page
LIST OF ILLUSTRATIONS	iii
LIST OF TABLES	iii
LIST OF ABBREVIATIONS AND SYMBOLS	iv
1. INTRODUCTION	1
2. CORRELATION KNOWN EXACTLY FOR ALL ARGUMENT VALUES	3
2.1 Linear Prediction Based on Infinite Past	3
2.2 Linear Prediction Based on Infinite Future	6
2.3 Linear Interpolation Based on Infinite Past and Future	7
3. CORRELATION KNOWN EXACTLY FOR A LIMITED RANGE OF ARGUMENT VALUES	11
3.1 Maximum Entropy Spectral Analysis (MESA)	11
3.2 Linear Predictive Filtering	17
3.3 All-Pole Digital Filter Model	21
4. CORRELATION UNKNOWN; FINITE DATA SET	27
4.1 Yule-Walker Equations	27
4.2 Unbiased Version of Yule-Walker Equations	33
4.3 Least-Squares Estimates of Box and Jenkins	34
4.4 Approximate Maximum Likelihood Estimates of Box and Jenkins	35
4.5 Prediction Using Valid Error Points	36
4.6 Forward and Backward Prediction Using Valid Error Points	38
4.7 Burg Technique	41
4.8 Summary of Properties of Techniques	47
5. CORRELATION UNKNOWN; FINITE DATA SET WITH BAD DATA POINTS	49
5.1 Forward and Backward Prediction Using Valid Error Points	49
5.2 Burg Technique	53

TABLE OF CONTENTS (Cont'd)

	Page
6. COMPARISONS	57
6.1 No Bad Data Points	57
6.2 Bad Data Points	61
7. DISCUSSION AND CONCLUSIONS	81
APPENDIX A. RECURSIVE SOLUTION	A-1
APPENDIX B. EVALUATION OF MAXIMUM ENTROPY	B-1
APPENDIX C. IMPLICATIONS OF ASSUMPTION OF WHITE SPECTRUM FOR MINIMUM ERROR; KNOWN CORRELATION	C-1
APPENDIX D. STABILITY OF RECURSION RELATION	D-1
APPENDIX E. IMPLICATIONS OF ASSUMPTION OF WHITE SPECTRUM; UNKNOWN CORRELATION	E-1
APPENDIX F. BOUND ON CROSS-GAIN	F-1
APPENDIX G. CLOSENESS OF ERROR MEASURES	G-1
APPENDIX H. SCALE FACTORS IN SPECTRAL ESTIMATES	H-1
APPENDIX I. BIASEDNESS OF BURG'S CORRELATION ESTIMATE	I-1
APPENDIX J. FORTRAN PROGRAMS	J-1
REFERENCES	R-1

LIST OF ILLUSTRATIONS

Figure		Page
1	Block Diagram of Predictive and Whitening Operations	4
2	Generation of All-Pole Process	22
3	Chain Interpretation of Burg Technique	43
4	Yule-Walker; N = 40, B = 0	63
5	Yule-Walker, Unbiased; N = 40, B = 0	64
6	Least Squares of Box and Jenkins; N = 40, B = 0	65
7	Approximate Maximum Likelihood of Box and Jenkins; N = 40, B = 0	66
8	Prediction, Valid Error Points; N = 40, B = 0	67
9	Forward and Backward Prediction; N = 40, B = 0	68
10	Burg; N = 40, B = 0	69
11	Burg, Uniform Noise; N = 40, B = 0	70
12	Forward and Backward Prediction; N = 40, B = 4	71
13	Burg; N = 40, B = 4	72
14	Forward and Backward Prediction; N = 100, B = 0	73
15	Burg; N = 100, B = 0	74
16	Forward and Backward Prediction; N = 100, B = 10	75
17	Burg; N = 100, B = 10	76
18	Forward and Backward Prediction; N = 100, B = 20	77
19	Burg; N = 100, B = 20	78
20	Forward and Backward Prediction; N = 100, B = 30	79
21	Burg; N = 100, B = 30	80

LIST OF TABLES

Table		Page
1	Properties of Estimated Correlation Matrices	48
2	Simulation Examples	58
3	Execution Times; No Bad Data Points	82

LIST OF ABBREVIATIONS AND SYMBOLS

MESA	Maximum Entropy Spectral Analysis
t	Time
$x(t)$	Random process
Δ	Sampling interval in time
x_n	Sample value $x(n\Delta)$
$\equiv$	Defined as
R_k	Correlation of $x(t)$ at delay $k\Delta$
$*$	Conjugate
N	Number of samples available
f	Frequency
$G_x(f)$	Spectrum of process $\{x_n\}$
i	$\sqrt{-1}$
$\hat{x}_k$	Predicted value of x_k
a_n	n-th coefficient of predictive filter
ϵ_k	Instantaneous error at time $k\Delta$
Overbar	Ensemble average
E	Ensemble average magnitude-squared error
$\tilde{a}_n$	n-th optimum predictive filter coefficient
$\tilde{\epsilon}_k$	Minimum-error sequence
E_j	Correlation of minimum-error sequence

LIST OF ABBREVIATIONS AND SYMBOLS (Cont'd)

$G_{\tilde{\epsilon}}(f)$	Spectrum of minimum-error sequence
$A(f)$	Transfer function of whitening filter
z	Complex variable
O	Unit circle in complex z-plane
C_j	Crosscorrelation between $\tilde{\epsilon}_k$ and x_k at delay $j\Delta$
$G_{\tilde{\epsilon}x}(f)$	Cross-spectrum between $\tilde{\epsilon}_k$ and x_k
p	Order to which R_k is known; assumed order of predictive filter
$\int_{1/\Delta}$	Integration over $\left(-\frac{1}{2\Delta}, \frac{1}{2\Delta}\right)$
$G_o(f)$	Approximation to $G_x(f)$
μ_K, λ	Lagrange multipliers
$\gamma(f)$	Auxiliary function; (37)
$B(z)$	Auxiliary polynomial; (38), (56)
α_k, b_ℓ	Constants
$\oint$	Counterclockwise integration around unit circle O in complex z-plane
$\delta_{k\ell}$	Kronecker delta; = 1 if $k=\ell$; = 0 otherwise
$\mathbf{R}$	Correlation matrix; (47)
$\boldsymbol{\delta}, \boldsymbol{\alpha}$	Column matrices; (48)
Superscript T	Transpose
$c_{k\ell}$	Element of inverse of matrix $\mathbf{R}$; (51)

LIST OF ABBREVIATIONS AND SYMBOLS (Cont'd)

θ	Arbitrary real constant
Superscript "	Conjugate transpose
a	Column matrix of $\{a_n\}$
Superscript caret	Estimate of quantity under caret
w_k	White noise
y_k	All-pole filter output process
$H(z)$	Digital filter transfer function
$G_w(f)$	Spectrum of $\{w_k\}$
β_n	Digital filter coefficient
$G_y(f)$	Spectrum of $\{y_k\}$
det	Determinant
F , F_o , $F^{(p)}$, $F_o^{(p)}$	Average magnitude-squared error for a member function
S_{n-m} , S_{nm}	Summations
D_ℓ	Sample crosscorrelation between $\tilde{\epsilon}_k$ and x_k
$\check{x}_k$	Backward-predicted value of x_k
$\check{\epsilon}_k$	Backward error
$\hat{R}_k$	Estimate of R_k
$P^{(p)}$	Auxiliary variable; (147)
$f_n^{(p)}$, $b_n^{(p)}$	Forward and backward residuals
g_p	Cross-gain

LIST OF ABBREVIATIONS AND SYMBOLS (Cont'd)

Num(p), Den(p)	Numerator and denominator, respectively, of (155) or (193)
$\mathfrak{Z}^{(p)}(z)$, $\mathfrak{B}^{(p)}(z)$	Transfer functions
$G_f^{(p)}(f)$, $G_b^{(p)}(f)$	Spectra of residuals
B	Number of bad or missing points
M_j	Location of j-th bad point in data sequence
$\sum'$	Summation over good data points; (170A)
I_p	Set of integers to be skipped; (173)
B_p	Number of distinct integers in I_p which are $\geq p+1$ and $\leq N$
$\notin$	Not contained in
$\hat{F}$, $\check{F}$	Average forward and backward errors, respectively
AIC	Akaike's Information Criterion

REVERSE BLANK

SPECTRAL ANALYSIS OF A UNIVARIATE PROCESS WITH BAD DATA POINTS, VIA MAXIMUM ENTROPY AND LINEAR PREDICTIVE TECHNIQUES

1. INTRODUCTION

The analysis of power density spectra of random processes via maximum entropy, linear predictive, and autoregressive techniques has attracted much attention recently, especially for short data segments. In particular, a good review article (reference 1) recently appeared in which 115 references are listed on the topic of linear prediction. Another good paper on this method of spectral analysis (including a comparison of techniques) is available in reference 2, where 66 references are cited. Additional related references, that this author is aware of, are given in references 3 through 15 of this report. The close links that exist between maximum entropy spectral analysis (MESA), autoregressive spectral analysis, predictive error filters, noise-whitening filters, and least-squares model building are pointed out very well in reference 14.

The purposes of this report are to review and interrelate several available techniques for spectral analysis under different states of knowledge, for equispaced samples, in a consistent notation; collect and compare the techniques via simulation in order to determine the best available technique(s); and extend the best technique(s) to handle the case of bad (or missing) data points and compare them via simulation. The only detailed comparison of techniques for no missing data points available thus far in the literature is that in reference 2, where the Burg technique and the Yule-Walker approach are compared. Here we will extend the comparison to include the Burg technique, the Yule-Walker approach, an unbiased version of the Yule-Walker approach, the approximate maximum likelihood and least-squares approaches of reference 16, the autocorrelation and covariance approaches of reference 1, and an extended version of the covariance approach. (A comparison with the maximum likelihood technique is reserved for a future report.) Also, we will compare the best of these approaches for the case of bad (or missing) data points and present FORTRAN programs for the recommended techniques.

Throughout this report, we assume we are dealing with equispaced samples of a stationary zero-mean random process x(t); that is, $x_n \equiv x(n\Delta)$, where Δ is the

sampling interval in time. In section 2, we will assume that the correlation function of the sampled process, $\{x_n\}$, namely,*

$$R_k = \overline{x_n \, x^*_{n-k}} = R^*_{-k}, \tag{1}$$

is known exactly for all k, and shall present two alternative equations to determine the spectrum of $\{x_n\}$; the latter of the two equations serves as a guide to the MESA, linear predictive, and autoregressive approaches. In section 3, it will be assumed that R_k is known only for a limited range of values of k, and three alternative approaches will be considered and shown to lead to identically the same spectral approximation. Next, in sections 4 and 5, the practical problem of an unknown correlation function and only a finite data set of $\{x_n\}$, $n = 1, 2, \ldots, N$, some of which may be bad, will be addressed, and several candidate techniques for spectral estimation will be presented. Finally, a comparison of the techniques, via simulation, will be conducted and conclusions drawn regarding the best available technique, both with and without bad data points. FORTRAN programs for the best technique for both situations will also be presented.

*The case of complex samples is treated, so that we can handle complex envelope or complex demodulated processes. Specialization to real processes is immediate, and (1) becomes $R_k = R_{-k}$. An overbar indicates an ensemble average.

2. CORRELATION KNOWN EXACTLY FOR ALL ARGUMENT VALUES

Suppose the correlation function in (1) of process $\{x_n\}$ is known for all k. The standard (double-sided) definition of the spectrum of $\{x_n\}$ is then (see, for example, reference 14, equation (10))

$$G_x(f) = \Delta \sum_{k=-\infty}^{\infty} R_k \exp(-i2\pi fk\Delta), \quad |f| < \frac{1}{2\Delta}. \tag{2}$$

$G_x(f)$ is real and nonnegative, but need not be even in frequency f for complex $\{R_k\}$.

2.1 LINEAR PREDICTION BASED ON INFINITE PAST

Suppose that sample values x_{k-1}, x_{k-2}, ... are available and are used to linearly predict the value of x_k. Then the one-step predicted value, based on the infinite past, is (for a zero-mean process)

$$\hat{x}_k \equiv \sum_{n=1}^{\infty} a_n x_{k-n}. \tag{3}$$

The values of the complex predictive filter coefficients $\{a_n\}_1^{\infty}$ are chosen such that the one-step prediction error

$$\epsilon_k \equiv \hat{x}_k - x_k = \sum_{n=0}^{\infty} a_n x_{k-n} \qquad (a_o = -1) \tag{4}$$

has minimum ensemble average magnitude-squared value. Figure 1 depicts the interrelationships.

The ensemble average magnitude-squared error is, employing (1), given by

$$E \equiv \overline{|\epsilon_k|^2} = \sum_{m,n=0}^{\infty} a_m a_n^* R_{n-m}. \tag{5}$$

For a minimum, we first compute (see reference 17, appendix A)

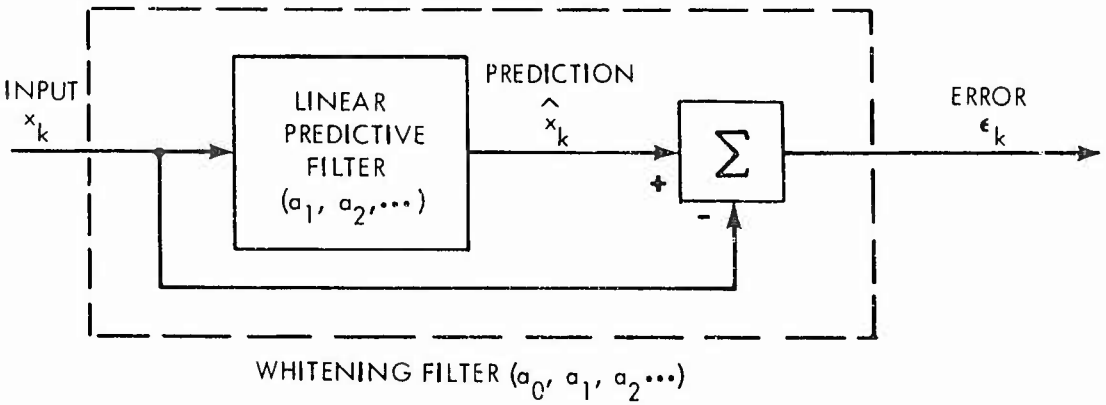


Figure 1. Block Diagram of Predictive and Whitening Operations

$$\frac{\partial E}{\partial a_\ell^*} = \sum_{m=0}^{\infty} R_{\ell-m}\, a_m, \quad \ell \geq 1 \tag{6}$$

and set it equal to zero, obtaining the optimum predictive filter coefficients $\{\tilde{a}_m\}_1^\infty$ as the solution of the set of equations*

$$\sum_{m=0}^{\infty} R_{\ell-m}\, \tilde{a}_m = 0, \quad \ell \geq 1 \qquad (\tilde{a}_o = a_o = -1). \tag{7}$$

The minimum-error sequence $\{\tilde{\epsilon}_k\}$ then possesses correlation

$$E_j \equiv \overline{\tilde{\epsilon}_k \tilde{\epsilon}^*_{k-j}} = \sum_{m,n=0}^{\infty} \tilde{a}_m \tilde{a}^*_n\, \overline{x_{k-m} x^*_{k-j-n}}$$

$$= \sum_{m,n=0}^{\infty} \tilde{a}_m \tilde{a}^*_n\, R_{j+n-m} = \sum_{n=0}^{\infty} \tilde{a}^*_n \sum_{m=0}^{\infty} R_{j+n-m}\, \tilde{a}_m, \tag{8}$$

*The same result, (7), can be obtained by setting the partial derivatives of E, with respect to the real and imaginary parts of a_ℓ, equal to zero.

where we have employed (4) and (1). Now the innermost sum on m in (8) is 0 for $j + n \geq 1$, by (7). And if $j \geq 1$ in (8), then $j + n \geq 1$ since $n \geq 0$ in the outermost sum in (8). Therefore, $E_j = 0$ for $j \geq 1$. Also since $E_{-j} = E_j^*$, we have

$$E_j = 0 \text{ for } j \neq 0; \tag{9}$$

that is, the minimum-error sequence $\{\tilde{\epsilon}_k\}$ is uncorrelated and therefore possesses a white spectrum. The linear filter characterized by coefficients $\{\tilde{a}_n\}_0^{(\infty)}$ is a whitening filter; see figure 1.

The correlation of $\{\tilde{\epsilon}_k\}$ for zero time delay is the power of the minimum error and is given by

$$E_o = \overline{|\tilde{\epsilon}_k|^2} = \sum_{n=0}^{(\infty)} \tilde{a}_n^* \sum_{m=0}^{(\infty)} R_{n-m} \tilde{a}_m$$

$$= \tilde{a}_o^* \sum_{m=0}^{(\infty)} R_{-m} \tilde{a}_m = R_o - \sum_{m=1}^{(\infty)} R_m^* \tilde{a}_m, \tag{10}$$

where we have used (8), (7), and (1). The spectrum of $\{\tilde{\epsilon}_k\}$ is therefore (using (9))

$$G_{\tilde{\epsilon}}(f) = \Delta \sum_{j=-(\infty)}^{(\infty)} E_j \exp(-i2\pi fj\Delta) = \Delta E_o, \ |f| < \frac{1}{2\Delta}, \tag{11}$$

which is white, as mentioned above.

But since the error sequence is given by a linear transformation of process $\{x_k\}$ according to (4) and figure 1, the spectrum of $\{\tilde{\epsilon}_k\}$ is given by the standard linear filter relation

$$G_{\tilde{\epsilon}}(f) = |A(f)|^2 G_x(f), \tag{12}$$

where

$$A(f) = \sum_{n=0}^{(\infty)} \tilde{a}_n \exp(-i2\pi fn\Delta) \tag{13}$$

is the transfer function of the whitening filter and is assumed to be stable.* Combining (11)-(13), we obtain an alternative expression to (2) for the spectrum of $\{x_k\}$ as

$$G_x(f) = \frac{G_{\tilde{\epsilon}}(f)}{\left|A(f)\right|^2} = \frac{\Delta E_o}{\left|\sum_{n=0}^{\infty} \tilde{a}_n \exp(-i2\pi f n \Delta)\right|^2}, \quad |f| < \frac{1}{2\Delta}. \tag{14}$$

Given the correlation values $\{R_k\}$, utilization of (14) requires solution of the set of equations in (7) for the filter coefficients $\{\tilde{a}_n\}$ and subsequent substitution in (10) and (14). Although this is not a practical alternative to (2) in this case, it does serve to indicate that there is possibly some potential in the idea of determining predictive filter coefficients to minimize the average magnitude-squared one-step prediction error and thereby obtain a white spectrum; this idea will prove to be quite fruitful later on.

As an aside, if we allow $a_{-1} \neq 0$ in (3) and minimize $\overline{|\epsilon_k|^2}$, we find $E_1 \neq 0$, although $E_j = 0$ for $j \geq 2$. Thus, the minimum-error sequence would not be white, and a convenient expression like (14) would not result.

It should also be noted that the crosscorrelations between the minimum-error sequence $\{\tilde{\epsilon}_k\}$ and all <u>past</u> values of the input, $\{x_k\}$, are zero; this follows by use of (4), (1), and (7).

2.2 LINEAR PREDICTION BASED ON INFINITE FUTURE

If sample values $x_{k+1}, x_{k+2}, \ldots$ are available and are used to linearly "predict" the value of x_k according to a backward regression (that is, combine future values),

$$\hat{x}_k \equiv \sum_{n=1}^{\infty} a_n^* x_{k+n}, \tag{15}$$

*That is, $\sum_{n=0}^{\infty} \tilde{a}_n z^{-n}$ has all its poles inside the unit circle, O, in the complex z-plane.

then the one-step error

$$\epsilon_k \equiv \hat{x}_k - x_k = \sum_{n=0}^{\infty} a_n^* x_{k+n} \qquad (a_o = -1) \tag{16}$$

has average magnitude-squared value

$$\overline{|\epsilon_k|^2} = \sum_{m,n=0}^{\infty} a_m a_n^* R_{n-m}, \tag{17}$$

which is identical to (5). Thus, the same optimum filter coefficients in (7) that minimized (5) would also minimize (17). The minimum-error sequence in (16) would also be white, and an expression for the spectrum of $\{x_k\}$ identical to (14) would result. The point of this result is that an equivalent expression for the spectrum of $\{x_k\}$ is obtained by the backward regression (15), rather than the forward regression (3) of the preceding subsection. This idea will prove useful later when we have to deal with finite data sets and unknown correlation functions.

The crosscorrelations between the minimum-error sequence and all <u>future</u> values of the input are zero; this follows by use of (16), (1), and (7).

2.3 LINEAR INTERPOLATION BASED ON INFINITE PAST AND FUTURE

If we attempt to combine the approaches of the previous two subsections, we are led into considering linear interpolation according to

$$\hat{x}_k \equiv \sum_{\substack{n=-\infty \\ n\neq 0}}^{\infty} a_n x_{k-n}. \tag{18}$$

The error

$$\epsilon_k \equiv \hat{x}_k - x_k = \sum_{n=-\infty}^{\infty} a_n x_{k-n} \qquad (a_o = -1) \tag{19}$$

has average magnitude-squared value

$$E \equiv \overline{|\epsilon_k|^2} = \sum_{m,n=-\omega}^{\omega} a_m a_n^* R_{n-m}, \tag{20}$$

using (1). Setting $\partial E/\partial a_\ell^* = 0$ for $\ell \neq 0$, we obtain for the optimum filter coefficients

$$\sum_{m=-\omega}^{\omega} R_{\ell-m} \tilde{a}_m = 0, \ \ell \neq 0 \qquad (\tilde{a}_o = a_o = -1). \tag{21}$$

There follows, by use of (1),

$$\tilde{a}_{-j} = \tilde{a}_j^*. \tag{22}$$

The correlation of the minimum-error sequence $\{\tilde{\epsilon}_k\}$ is now

$$E_j \equiv \overline{\tilde{\epsilon}_k \tilde{\epsilon}_{k-j}^*} = \sum_{m,n=-\omega}^{\omega} \tilde{a}_m \tilde{a}_n^* R_{j+n-m}$$

$$= \sum_{n=-\omega}^{\omega} \tilde{a}_n^* \sum_{m=-\omega}^{\omega} \tilde{a}_m R_{j+n-m} = \tilde{a}_{-j}^* \sum_{m=-\omega}^{\omega} \tilde{a}_m R_{-m} = -\tilde{a}_j E_o, \tag{23}$$

where we have employed (19), (1), (21), and (22). It is generally nonzero for $j \neq 0$. The spectrum of the minimum-error sequence is therefore

$$G_{\tilde{\epsilon}}(f) = -\Delta E_o \sum_{j=-\omega}^{\omega} \tilde{a}_j \exp(-i2\pi f j\Delta) = -\Delta E_o A(f), \ |f| < \frac{1}{2\Delta}, \tag{24}$$

where we have used (23) and assumed A(f) to be stable. This spectrum is not white; in fact, employing (12), (24) can be expressed as

$$G_{\tilde{\epsilon}}(f) = \frac{\Delta^2 E_o^2}{G_x(f)}, \ |f| < \frac{1}{2\Delta}, \tag{25}$$

which is the inverse of the input spectrum.

If we instead eliminate $G_{\tilde{\epsilon}}(f)$ from (12) and (24), we obtain an expression for the input spectrum in terms of filter A(f) in (24) as

$$G_x(f) = -\frac{\Delta E_o}{A^*(f)} = -\frac{\Delta E_o}{A(f)}, \quad |f| < \frac{1}{2\Delta}; \tag{26}$$

the realness of A(f) follows from (22).

There is an uncorrelated property between the minimum error and the input in the present case also. Namely, the crosscorrelation between the minimum-error sequence and the input is

$$C_j \equiv \overline{\tilde{\epsilon}_k x^*_{k-j}} = \sum_{n=-\infty}^{\infty} \tilde{a}_n \overline{x_{k-n} x^*_{k-j}} = \sum_{n=-\infty}^{\infty} \tilde{a}_n R_{j-n} = E_o \delta_{oj}, \tag{27}$$

using (19), (1), (21), and (23). Thus, the minimum-error sequence is uncorrelated with all past and future values of the input except at the same time instant. The cross-spectrum is

$$G_{\tilde{\epsilon}x}(f) \equiv \Delta \sum_{j=-\infty}^{\infty} C_j \exp(-i2\pi f j\Delta) = \Delta E_o, \quad |f| < \frac{1}{2\Delta}, \tag{28}$$

which is white.

Although (26) and (21) offer an alternative to (14) and (7) in the present case of known correlation function $\{R_k\}$, it suffers in the practical case of unknown correlation and a finite data set, by virtue of the estimate of the real denominator of (26) going through zero (or being complex if (22) is ignored) at some values of f. This is not a significant problem for (14) since both the real and imaginary parts of the estimate of (13) must simultaneously equal zero there, in order to constitute a problem.

Another important practical drawback of this interpolation approach is that ensemble average $\overline{|\epsilon_k|^2}$ would probably be approximated by $\sum_k |\epsilon_k|^2$, where the sum is conducted over those values of k at which a meaningful value of error ϵ_k can be formed for a segment of a single member function of an ensemble. But since the minimum-error sequence $\{\tilde{\epsilon}_k\}$ is not uncorrelated in this case (see (23)), minimization of $\sum_k |\epsilon_k|^2$ for a single member function segment is not synonymous with minimization of $\overline{|\epsilon_k|^2}$; rather, the minimiza-

tion of $\sum_k |\epsilon_k|^2$ will spuriously involve correlation between adjacent terms which are not included in $\overline{|\epsilon_k|^2}$ and which will bias the filter coefficients. Several simulation runs (on real data) confirmed this conclusion by yielding severely biased (and negative) estimates of spectrum $G_x(f)$, even when (22) was taken into account. Accordingly, the interpolation approach was dropped from further consideration.

3. CORRELATION KNOWN EXACTLY FOR A LIMITED RANGE OF ARGUMENT VALUES

In this section, R_k of (1) is assumed to be known exactly for $|k| \leq p$ and unknown for $|k| > p$. Since we are unable to compute the exact spectrum $G_X(f)$, given by (2), in this case, a different approach involving approximations to $G_X(f)$ is required. Three different techniques will be considered and shown to yield identically the same approximation to $G_X(f)$.

3.1 MAXIMUM ENTROPY SPECTRAL ANALYSIS (MESA)

The method in this subsection was originally given in reference 18 and elaborated upon in reference 19. We begin with (2) and note that

$$\int_{-\frac{1}{2\Delta}}^{\frac{1}{2\Delta}} df\, G_x(f)\, \exp(i2\pi fk\Delta) \equiv \int_{1/\Delta} df\, G_x(f)\, \exp(i2\pi fk\Delta) = R_k . \tag{29}$$

We wish to approximate $G_x(f)$ by a real nonnegative function $G(f)$ such that its entropy (reference 18, equation (1))

$$\Delta \int_{1/\Delta} df\, \ell n\, G(f) \tag{30}$$

is maximized, subject to the integral constraints

$$\int_{1/\Delta} df\, G(f)\, \exp(i2\pi fk\Delta) = R_k , \quad |k| \leq p . \tag{31}$$

To this aim, we form the quantity

$$Q \equiv \int_{1/\Delta} df\, \ell n\, G(f) - \sum_{k=-p}^{p} \mu_k \int_{1/\Delta} df\, G(f)\, \exp(i2\pi fk\Delta) , \tag{32}$$

where Lagrange multipliers $\mu_{-k} = \mu_k^*$. because of the restriction $R_{-k} = R_k^*$, as shown in (1). We perform a variation of (32) according to

$$Q+\delta Q = \int_{1/\Delta} df\, \ell n\left[G_o(f) + \epsilon\eta\ (f)\right] - \sum_{k=-p}^{p} \mu_k \int_{1/\Delta} df \left[G_o(f) + \epsilon\eta\,(f)\right] \exp(i2\pi fk\Delta)\,, \tag{33}$$

where $G_o(f)$ is the "optimum" approximation to $G_X(f)$ under criterion (30), and obtain, upon setting

$$\frac{\partial(Q+\delta Q)}{\partial\epsilon} = 0 \text{ at } \epsilon = 0\,, \tag{34}$$

the relation

$$G_o(f) = \frac{1}{\sum_{k=-p}^{p} \mu_k \exp(i2\pi fk\Delta)}\,, \quad |f| < \frac{1}{2\Delta}\,. \tag{35}$$

$G_o(f)$ is real since $\mu_{-k} = \mu_k^*$. Since it is also to be nonnegative, we can express

$$G_o(f) = \frac{1}{|\gamma(f)|^2}\,, \quad |f| < \frac{1}{2\Delta}\,, \tag{36}$$

where

$$\gamma(f) \equiv \sum_{k=0}^{p} \alpha_k \exp(i2\pi fk\Delta), \quad |f| < \frac{1}{2\Delta}, \tag{37}$$

and where $\gamma(f)$ has no zeros in the upper-half complex f-plane; that is, polynomial

$$B(z) \equiv \sum_{k=0}^{p} \alpha_k z^k \tag{38}$$

has no zeros inside the unit circle, O, in the complex z-plane. A proof that B(z) in (38) has no zeros inside O is given in reference 11, page 7, for example.* Specifically, it is shown that B(1/z) has all its poles and zeros inside O; that is, B(1/z) is minimum phase.

In order to determine the constants $\{\alpha_k\}_o^p$ in (37), we express (36) as

$$G_o(f)\gamma^*(f) = \frac{1}{\gamma(f)}, \quad |f| < \frac{1}{2\Delta} . \tag{39}$$

(We could equally well have multiplied by $\gamma(f)$ in the following.) Therefore, for all values of ℓ,

$$\int_{1/\Delta} df\, G_o(f)\gamma^*(f)\, \exp(i2\pi f\ell\Delta) = \int_{1/\Delta} df\, \frac{1}{\gamma(f)}\, \exp(i2\pi f\ell\Delta) . \tag{40}$$

But using (37), this can be expressed as

$$\sum_{k=0}^{p} \alpha_k^* \int_{1/\Delta} df\, G_o(f)\, \exp(i2\pi f(\ell-k)\Delta) = \int_{1/\Delta} df\, \frac{\exp(i2\pi f\ell\Delta)}{\sum_{k=0}^{p} \alpha_k \exp(i2\pi fk\Delta)}, \text{ all } \ell. \tag{41}$$

Now if ℓ is an integer in the range [0, p], the integral on the left side of (41) is equal to $R_{\ell-k}$ (via (29)) for any value of k in its range [0, p]; this is where the constraints are employed. Therefore, we have for integer ℓ,

$$\sum_{k=0}^{p} R_{\ell-k}\, \alpha_k^* = b_\ell , \quad 0 \le \ell \le p , \tag{42}$$

where

$$b_\ell \equiv \int_{1/\Delta} df\, \frac{\exp(i2\pi f\ell\Delta)}{\sum_{k=0}^{p} \alpha_k \exp(i2\pi fk\Delta)} , \quad 0 \le \ell \le p . \tag{43}$$

*The proof is couched in terms of the recursive solution of (46) presented in appendix A.

In (43), letting $z = \exp(i2\pi f\Delta)$ and using (38), we have

$$b_\ell = \frac{1}{i2\pi\Delta} \oint \frac{dz}{z} \frac{z^\ell}{B(z)}, \quad 0 \le \ell \le p, \tag{44}$$

where $\oint$ denotes counterclockwise integration around the unit circle O in the complex z-plane. Now B(z) has no zeros inside O by construction. Furthermore, B(z) can have no zeros on O, for then $\gamma(f)$ would be zero for some f, and $G_0(f)$ would possess infinite power, contradicting $R_0 < \infty$. Then (44) yields

$$b_\ell = \frac{1}{\Delta\alpha_0} \delta_{\ell 0}, \quad 0 \le \ell \le p, \tag{45}$$

and (42) becomes

$$\sum_{k=0}^{p} R_{\ell-k} \alpha_k^* = \frac{1}{\Delta\alpha_0} \delta_{\ell 0}, \quad 0 \le \ell \le p. \tag{46}$$

This is p+1 linear equations in p+1 unknowns.*

Now let correlation matrix **R** be defined as

$$\mathbf{R} = \begin{bmatrix} R_0 & R_{-1} & \cdots & R_{-p} \\ R_1 & R_0 & & \\ \cdot & & \cdot & \\ \cdot & & \cdot & \\ \cdot & & \cdot & \\ R_p & & & R_0 \end{bmatrix} \tag{47}$$

and define two column matrices

$$\boldsymbol{\delta} = [1 \quad 0 \quad 0 \quad \cdots \quad 0]^T, \quad \boldsymbol{\alpha} = [\alpha_0 \quad \alpha_1 \quad \cdots \quad \alpha_p]^T. \tag{48}$$

*The recursive solution of (46) is presented in appendix A.

R is Hermitian, Toeplitz, and nonnegative definite. Then (46) can be expressed as

$$R\alpha^* = \frac{1}{\Delta\alpha_o}\,\delta \tag{49}$$

with solution

$$\alpha^* = \frac{1}{\Delta\alpha_o}\,R^{-1}\,\delta\,. \tag{50}$$

Now let the inverse matrix

$$R^{-1} \equiv \begin{bmatrix} c_{oo} & c_{o1} & \cdots & c_{op} \\ c_{1o} & c_{11} & & \\ \cdot & & & \\ \cdot & & & \\ \cdot & & & \\ c_{po} & & & c_{pp} \end{bmatrix}. \tag{51}$$

Then (50) and (48) yield

$$\alpha_o^* = \frac{1}{\Delta\alpha_o}\,c_{oo},\quad |\alpha_o|^2 = \frac{1}{\Delta}\,c_{oo},\quad \alpha_o = \left(\frac{c_{oo}}{\Delta}\right)^{1/2}\exp(i\theta)\,, \tag{52}$$

where θ is an arbitrary real constant. (c_{oo} is always real.) Utilizing this result and (15) in (50), there follows

$$\alpha_k^* = \frac{c_{ko}}{\sqrt{\Delta c_{oo}}}\exp(-i\theta),\quad 0 \le k \le p\,, \tag{53}$$

and (37) becomes

$$\gamma(f) = \frac{\exp(i\theta)}{\sqrt{\Delta c_{oo}}} \sum_{k=0}^{p} c_{ko}^{*} \exp(i2\pi fk\Delta), \quad |f| < \frac{1}{2\Delta}. \tag{54}$$

Finally, using (36), the "optimum" spectrum (called the maximum entropy spectrum) is

$$G_o(f) = \frac{\Delta c_{oo}}{\left| \sum_{k=0}^{p} c_{ko} \exp(-i2\pi fk\Delta) \right|^2}, \quad |f| < \frac{1}{2\Delta}. \tag{55}$$

Equation (55) gives the maximum entropy spectrum in terms of the first column of the inverse of the correlation matrix R of available known correlation values; see (47). The forms of (55) and (46) are similar to those encountered earlier in (14) and (7), respectively; see also appendix A. The maximum value of the entropy defined in (30) is evaluated in appendix B and is given by $\ell n\ (\Delta / c_{oo})$.

Substitution of (53) in (38) yields

$$B(z) = \frac{\exp(-i\theta)}{\sqrt{\Delta c_{oo}}} \sum_{k=0}^{p} c_{ko} z^{k}. \tag{56}$$

Thus, investigation of the zeros of B(z) depends on the polynomial $\sum_{k=0}^{p} c_{ko} z^{k}$; it must have no zeros inside the unit circle O. But if we combine (46) and (53), we can write that

$$\sum_{k=0}^{p} R_{\ell-k} \frac{c_{ko}}{c_{oo}} = - R_{\ell}, \quad 1 \le \ell \le p. \tag{57}$$

Now reference 1, page 567, declares that all the zeros of $\sum_{k=0}^{p} c_{ko} z^{-k}$ must lie inside O since R is a correlation matrix. Therefore, polynomial B(z) has no zeros inside O.

3.2 LINEAR PREDICTIVE FILTERING

Here, as in the previous subsection, the available information is knowledge of R_k for $|k| \leq p$. A linear one-step prediction of x_k, based on the past p values, $x_{k-1}, \ldots, x_{k-p}$, is to be accomplished with minimum average magnitude-squared error; see figure 1. Now, however, instead of (3), we have for the predicted value the finite sum*

$$\hat{x}_k \equiv \sum_{n=1}^{p} a_n x_{k-n} . \tag{58}$$

The instantaneous error is

$$\epsilon_k \equiv \hat{x}_k - x_k = \sum_{n=0}^{p} a_n x_{k-n} \qquad (a_o = -1) . \tag{59}$$

(Equations (58) and (59) constitute stable digital filters regardless of the choice of coefficients.) The ensemble average magnitude-squared error is

$$E \equiv \overline{|\epsilon_k|^2} = \sum_{m,n=0}^{p} a_m a_n^* R_{n-m} = \mathbf{a}^H \mathbf{R}\, \mathbf{a} , \tag{60}$$

where we have used (1) and (47) and defined

$$\mathbf{a} = [a_o \; a_1 \; \ldots \; a_p]^T . \tag{61}$$

We now wish to minimize E by choice of filter coefficients $\{a_n\}$. However, we have the constraint on a_o in (59); this can be expressed mathematically as

$$\mathbf{a}^H \boldsymbol{\delta} = -1 , \tag{62}$$

where $\boldsymbol{\delta}$ is defined in (48). In order to minimize (60) subject to (62), we form the quantity

---

* The more general form including $\sum_{n=1}^{p} b_n x_{k-n}^*$ is not considered here.

$$a^H R a - \lambda a^H \delta - \lambda^* a^T \delta^*$$

$$= (a - \lambda R^{-1}\delta)^H R (a - \lambda R^{-1}\delta) - |\lambda|^2 \delta^H R^{-1} \delta, \tag{63}$$

where R^{-1} is defined in (51). Since R is nonnegative definite, being a correlation matrix, (63) is minimized by the choice of coefficients

$$\tilde{a} = \lambda R^{-1} \delta. \tag{64}$$

The Lagrange multiplier λ is obtained by substituting (64) in constraint (62), and using (51) and (48):

$$\lambda^* \delta^H R^{-1} \delta = -1, \quad \lambda = -\frac{1}{c_{oo}}. \tag{65}$$

Then (64) yields

$$\tilde{a}_k = -\frac{c_{ko}}{c_{oo}}, \quad 0 \le k \le p. \tag{66}$$

The minimum value of the error power is found by utilizing (64) and (65) in (60):

$$E_o \equiv \overline{|\tilde{\epsilon}_k|^2} = |\lambda|^2 \delta^H R^{-1} R R^{-1} \delta = |\lambda|^2 c_{oo} = \frac{1}{c_{oo}}, \tag{67}$$

where $\{\tilde{\epsilon}_k\}$ is the minimum-error sequence obtained by employing (66) in (59). (A recursion relation for $E_o^{(p)}$ is presented in (A-7); it can be started with $1/c_{oo}^{(o)} = R_o$.) Notice from (67) that c_{oo} must be positive, for non-negative definite R.

The transfer function of the optimum error filter from input x to output $\tilde{\epsilon}$ in figure 1 is, from (59) and (66),

$$A(f) \equiv \sum_{k=0}^{p} \tilde{a}_k \exp(-i2\pi fk\Delta)$$

$$= -\frac{1}{c_{oo}} \sum_{k=0}^{p} c_{ko} \exp(-i2\pi fk\Delta), \quad |f| < \frac{1}{2\Delta} . \tag{68}$$

Furthermore, the spectra in figure 1 are related by

$$G_{\tilde{\epsilon}}(f) = |A(f)|^2 \, G_x(f) . \tag{69}$$

Now let us assume that the spectrum of the minimum-error sequence is white over the band $(-\frac{1}{2\Delta}, \frac{1}{2\Delta})$; this is in line with the property (11) which held for the case when the infinite past was available. Then we say

$$\hat{G}_{\tilde{\epsilon}}(f) \equiv \frac{E_o}{1/\Delta} = \frac{\Delta}{c_{oo}}, \quad |f| < \frac{1}{2\Delta} , \tag{70}$$

where we have used (67). Substitution of (68) and (70) in (69) yields the linear predictive spectrum approximation to the input spectrum according to the definition

$$\hat{G}_x(f) \equiv \frac{\hat{G}_{\tilde{\epsilon}}(f)}{|A(f)|^2} = \frac{\Delta c_{oo}}{\left| \sum_{k=0}^{p} c_{ko} \exp(-i2\pi fk\Delta) \right|^2}, \quad |f| < \frac{1}{2\Delta}. \tag{71}$$

This is identical to the approximation (55) obtained by MESA. It is critically dependent on the assumption that the spectrum of the minimum-error $\tilde{\epsilon}$ in figure 1 is white.

Since (71) is identical with the maximum entropy spectrum, (55), it must follow that

$$\int_{1/\Delta} df \, \hat{G}_x(f) \exp(i2\pi fk\Delta) = R_k \text{ for } |k| \leq p ; \tag{72}$$

that is, although not specified in the current approach, the correlation function formed from the linear predictive spectrum $\hat{G}_x(f)$ in (71) has the same values at $k\Delta$ for $|k| \leq p$ as the known correlation values $\{R_k\}$.

The implications of the assumption (70) of a white spectrum for the minimum error are investigated in appendix C. It is shown that the crosscorrelation function between input x and output $\tilde{\epsilon}$ of figure 1,

$$C_\ell \equiv \overline{\tilde{\epsilon}_k \, x^*_{k-\ell}}, \tag{73}$$

must then satisfy

$$C_\ell = \left\{ \begin{array}{l} 1/c_{oo} \, , \ \ell = 0 \\ \\ 0 \quad , \ \ell \geq 1 \end{array} \right\} ; \tag{74}$$

that is, minimum-error sequence $\{\tilde{\epsilon}_k\}$ is assumed uncorrelated with all the past values of the input. It is also shown that the unknown correlation values R_k for $k > p$ can be approximated according to

$$R_k = - \sum_{n=1}^{p} \frac{c_{no}}{c_{oo}} R_{k-n} = \sum_{n=1}^{p} \tilde{a}_n R_{k-n} \, , \ k \geq p+1 \, . \tag{75}$$

This recursion relation, starting with known values $R_1, \ldots, R_p$, can be considered to be an extrapolation of the known correlation values into regions where they are unknown. Equation (75) is shown in appendix D to be a stable recursion when B(z) of (56) has no zeros inside O; this property has been discussed under (38), (56), and (A-9). It can also be shown that Fourier transformation of the extrapolated correlation approximants yields precisely (71). It is interesting to note that (75) has the same form as the predictive equation (58) for individual data values.

Since

$$\int_{1/\Delta} df \ \hat{G}_x(f) \ \exp(i2\pi fk\Delta) \tag{76}$$

is the autocorrelation at delay $k\Delta$, it is given by (72) for $|k| \leq p$, and by (75) for $k \geq p + 1$, where the latter correlations are extrapolated values. This follows

from setting $\hat{G}_{\epsilon}(f)$ white and choosing $\hat{G}_x(f)$ by (71), according to the analysis in appendixes C and D.

If sample values $x_{k+1}, \ldots, x_{k+p}$ were used to linearly "predict" x_k according to backward regression

$$\hat{x}_k = \sum_{n=1}^{p} a_n^* x_{k+n}, \tag{77A}$$

the one-step error $\epsilon_k = \hat{x}_k - x_k$ has average magnitude-squared value

$$E \equiv \overline{|\epsilon_k|^2} = \sum_{m,n=0}^{p} a_m a_n^* R_{n-m} \qquad (a_o = -1), \tag{77B}$$

which is identical to (60). Thus, the same optimum filter coefficients in (66) that minimized (60) would also minimize (77B), and an approach similar to that above would yield a spectral approximation identical to (71). The equivalence of the results of this backward regression to that of the forward regression in (58) will prove useful later when we deal with finite data sets and unknown correlation functions.

3.3 ALL-POLE DIGITAL FILTER MODEL

The available information about process $\{x_k\}$ is the same as in the previous two subsections, namely, knowledge of R_k for $|k| \leq p$. Consider a sampled autoregressive process $\{y_k\}$ in steady state generated by a stable all-pole digital filter, $H(z)$, excited by discrete white noise $\{w_k\}$; see figure 2. The noise is characterized by correlation

$$\overline{w_k w_{k-n}^*} = \delta_{no}, \text{ all } n, \tag{78A}$$

with no loss of generality, and has spectrum

$$G_w(f) = \Delta, \quad |f| < \frac{1}{2\Delta}. \tag{78B}$$

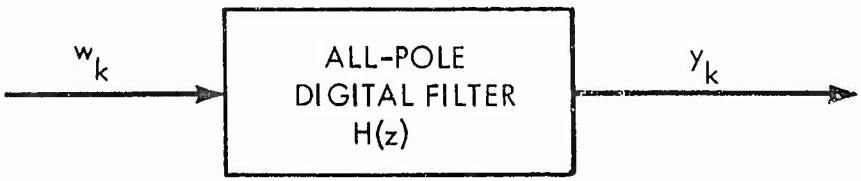


Figure 2. Generation of All-Pole Process

The digital filter is characterized by a p-th order autoregressive relationship,

$$\sum_{n=0}^{p} \beta_n y_{k-n} = w_k \ , \tag{79}$$

with transfer function

$$H(z) = \frac{1}{\sum_{n=0}^{p} \beta_n z^{-n}} \ . \tag{80}$$

We are going to choose digital filter coefficients $\{\beta_n\}_0^p$ so that autoregressive process $\{y_k\}$ has the same correlation values as process $\{x_k\}$, up through order p; that is, we will set

$$\overline{y_k y^*_{k-n}} = R_n \text{ for } |n| \leq p \ . \tag{81}$$

Then the spectrum of autoregressive process $\{y_k\}$, given by

$$G_y(f) = G_w(f) \left| H\left(\exp(i2\pi f\Delta)\right)\right|^2$$

$$= \frac{\Delta}{\left|\sum_{n=0}^{p} \beta_n \exp(-i2\pi fn\Delta)\right|^2}, \ |f| < \frac{1}{2\Delta} \ , \tag{82}$$

will be used as an approximation to the spectrum of $\{x_k\}$. The spectral relation in (82) holds only if H(z) is stable; that is, all the zeros of the denominator of (80) must lie inside O.

In order to evaluate the filter coefficients $\{\beta_n\}_o^p$, we notice that

$$\overline{w_k\, y^*_{k-n}} = 0 \text{ for } n > 0 \tag{83}$$

since noise samples $\{w_k\}$ are uncorrelated (see (78)) and filter H(z) is realizable (see (79)). The first step we take is to express (79) as

$$y_k = \frac{1}{\beta_o}\left[w_k - \sum_{n=1}^{p} \beta_n\, y_{k-n}\right]. \tag{84}$$

Then using (78) and (83),

$$\overline{w_k\, y^*_k} = \frac{1}{\beta^*_o}. \tag{85}$$

Now multiply both sides of (79) by $y^*_{k-\ell}$ and average; there follows

$$\sum_{n=0}^{p} \beta_n\, R_{\ell-n} = \frac{1}{\beta^*_o}\,\delta_{\ell o},\ 0 \le \ell \le p, \tag{86}$$

upon use of (81), (83), and (85). Now if we let $\beta_n = \sqrt{\Delta}\ \alpha^*_n$, (86) becomes identical to (46). Therefore, we can use solution (53) to obtain for the filter coefficients

$$\beta_n = \frac{c_{oo}}{\sqrt{c_{oo}}} \exp(-i\theta),\ 0 \le n \le p, \tag{87}$$

where θ is an arbitrary real constant.

Substitution of (87) in (82) yields the autoregressive spectrum approximation to the input spectrum as

$$\hat{G}_x(f) \equiv G_y(f) = \frac{\Delta c_{oo}}{\left| \sum_{n=0}^{p} c_{no} \exp(-i2\pi fn\Delta) \right|^2}, \quad |f| < \frac{1}{2\Delta} . \tag{88}$$

This is identical to the maximum entropy spectrum (55) and the linear predictive spectrum (71). The discussion surrounding (76) is relevant here also.

Substitution of (87) in digital filter (80) yields

$$H(z) = \frac{\sqrt{c_{oo}} \exp(i\theta)}{\sum_{n=0}^{p} c_{no} z^{-n}} . \tag{89}$$

This is stable if the denominator contains all its zeros within O; that is, H(z) is stable if and only if B(z) of (56) has no zeros inside O. This property has already been shown true in the discussions under (38), (56), and (A-9).

The relationship in (86) can be extended to $\ell = p + 1$ with the result that

$$\sum_{n=0}^{p} \beta_n R_{p+1-n} = 0 , \tag{90}$$

where R_{p+1} is now interpreted as the value of $\overline{y_k y_{k-p-1}^*}$, and was never specified. If we combine (90) with the last p equations of (86), we obtain

$$\sum_{n=0}^{p} \beta_n R_{\ell-n} = 0 , \quad 1 \le \ell \le p+1 . \tag{91}$$

In order for this set of p + 1 linear equations to possess a nonzero solution for $\{\beta_n\}_0^p$ (as it did above), we must have

$$\det \begin{bmatrix} R_1 & R_0 & R_{-1} & \cdots & R_{1-p} \\ R_2 & R_1 & R_0 & \cdots & R_{2-p} \\ \vdots & & & & \\ R_{p+1} & R_p & R_{p-1} & \cdots & R_1 \end{bmatrix} = 0 . \qquad (92)$$

This can be solved* for R_{p+1}. But since this is identical with reference 19, equation (1), we see that the all-pole digital filter model is identical to choosing R_{p+1} such that

$$\det \begin{bmatrix} R_0 & R_{-1} & \cdots & R_{-p} & R_{-p-1} \\ R_1 & R_0 & & & \\ \vdots & & \ddots & & \\ R_p & R_{p-1} & & & R_{-1} \\ R_{p+1} & R_p & \cdots & R_1 & R_0 \end{bmatrix} \qquad (93)$$

is maximized. Additional interpretations of (93) in terms of maximum uncertainty and entropy are presented in references 20 and 14.

*Of course, a far more practical method is given by (90) and (87), and more generally by (75).

REVERSE BLANK

4. CORRELATION UNKNOWN; FINITE DATA SET

In this section, the correlation values $\{R_k\}$ are unknown, and the only information available about the random process x(t) is a finite set of N samples $x_1, \ldots x_N$, from which we remove the sample mean. From these N samples, we desire an estimate of the spectrum $G_x(f)$. Yet we can not minimize or utilize any ensemble averages as was done in sections 2 and 3, since we have only a finite segment of one member function to work with.

The MESA and autoregressive methods of subsections 3.1 and 3.3 are not easily directly extended to the case of unknown correlation, because they make explicit use of this correlation information; see (31) and (81), respectively. A direct extension of these two methods would require us to decide on the form of the correlation estimates a priori, and could unnecessarily restrict the quality of the spectral estimate we finally obtain. The linear predictive method of sections 2 and 3.2, on the other hand, requires that the ensemble average magnitude-squared error be replaced by some estimating quantity that can be readily calculated from the available data $\{x_n\}_1^N$; as a by-product, we may get estimates of the correlation. Several candidate processing techniques based on subsection 3.2 will therefore be considered, and their processing equations derived. Also, some of the results of subsection 3.1 on MESA will be adapted and combined with the linear predictive approach to form a viable approach to spectral estimation; this technique was originally presented by Burg in reference 21. In section 6, all the techniques will be compared by means of simulation.

4.1 YULE-WALKER EQUATIONS

We begin by defining in this subsection

$$x_k = 0 \text{ for } k<1, \; k>N, \tag{94}$$

since these samples are unavailable. Taking (58) in subsection 3.2 as a guide, we attempt a linear prediction according to

$$\hat{x}_k = \sum_{n=1}^{p} a_n x_{k-n}, \text{ all } k, \tag{95}$$

where the choice of p is arbitrary for the moment. It should be noticed that although $\hat{x}_k$ is defined for all k, it is not expected to have a good chance of accurately predicting x_k for $k \leq p$ or $k \geq N+2$ since some zero values of x_k have

been utilized in those regions, according to (94). Nevertheless, we define an instantaneous error

$$\epsilon_k = \hat{x}_k - x_k = \sum_{n=0}^{p}{}' a_n x_{k-n}, \text{ all } k \qquad (a_o = -1); \tag{96}$$

it is expected to be valid or meaningful, however, only if $k \geq p + 1$ and $k \leq N$ (error ϵ_{N+1} must utilize a zero value for x_{N+1}). Digital filtering operations (95) and (96) are stable for any choice of coefficients $\{a_n\}$.

Since we cannot compute an ensemble average magnitude-squared error now, an average magnitude-squared error is defined for the available data of the single member function as

$$F \equiv \frac{1}{N} \sum_k \left|\epsilon_k\right|^2 = \sum_{m,n=0}^{p} a_m a_n^* \frac{1}{N} \sum_k x_{k-m} x_{k-n}^*, \tag{97}$$

where $\sum_k$ denotes summation over <u>all</u> nonzero values of the summand $\left|\epsilon_k\right|^2$, regardless of how meaningful they are. The normalizing factor 1/N is somewhat arbitrary; there are N+p nonzero terms in the first sum in (97), but only N-p meaningful terms.

We define, for all n, m

$$S_{n-m} \equiv \frac{1}{N} \sum_k x_{k-m} x_{k-n}^* = S_{m-n}^*, \tag{98}$$

in which case (97) yields

$$F = \sum_{m,n=0}^{p} a_m a_n^* S_{n-m}. \tag{99}$$

This relation uses S_ℓ only for $|\ell| \leq p$. In order to minimize F by choice of filter coefficients $\{a_n\}_1^p$, we compute

$$\frac{\partial F}{\partial a_\ell^*} = \sum_{m=0}^{p} S_{\ell-m} a_m, \quad 1 \leq \ell \leq p. \tag{100}$$

The optimum coefficients $\{\tilde{a}_n\}_1^p$ are therefore solutions of the p linear equations

$$\sum_{m=0}^{p} S_{\ell-m}\,\tilde{a}_m = 0,\quad 1 \le \ell \le p \qquad (\tilde{a}_o = a_o = -1) \tag{101}$$

or

$$\sum_{m=1}^{p} S_{\ell-m}\,\tilde{a}_m = S_\ell\,,\quad 1 \le \ell \le p\,. \tag{102}$$

These are the Yule-Walker equations for the optimum filter coefficients. The method here is called the autocorrelation method in reference 1. (As an aside, in analogy to subsections 2.2 and 3.2, identically the same equations (102) result when x_k is predicted on the basis of p future values, rather than p past values as was done here in (95); see (5) and (17) et seq. and (77) et seq.)

The minimum value of average error F is obtained by substituting (101) in (97) and (99):

$$F_o \equiv \frac{1}{N}\sum_k \left|\tilde{\epsilon}_k\right|^2 = \sum_{n=0}^{p} \tilde{a}_n^* \sum_{m=0}^{p} S_{n-m}\,\tilde{a}_m = \tilde{a}_o \sum_{m=0}^{p} S_{-m}\,\tilde{a}_m$$

$$= -\sum_{m=0}^{p} S_m^*\,\tilde{a}_m = S_o - \sum_{m=1}^{p} S_m^*\,\tilde{a}_m\,, \tag{103}$$

where we have employed (98) and (101).

The p x p matrix $[S_{\ell-m}]_1^p$ on the left side of (102) has the form of a legal correlation matrix in that it is Hermitian, Toeplitz, and nonnegative definite. The last property follows from

$$\sum_{\ell,m=1}^{p} S_{\ell-m}\alpha_m\alpha_\ell^* = \sum_{\ell,m=1}^{p} \alpha_m\alpha_\ell^*\,\frac{1}{N}\sum_k x_{k-m}x_{k-\ell}^*$$

$$= \frac{1}{N}\sum_k \left|\sum_{m=1}^{p} \alpha_m x_{k-m}\right|^2 \ge 0 \tag{104}$$

for any $\{\alpha_m\}_1^p$. Since (104) is greater than zero with probability one, (102) will possess a solution with probability one.

A convenient method of obtaining this solution is to combine (101) and (103) to get

$$-\sum_{m=0}^{p} S_{\ell-m}\,\tilde{a}_m = F_o\,\delta_{\ell o},\quad 0 \le \ell \le p. \tag{105}$$

Written out in detail, this is

$$\begin{bmatrix} S_o & S_{-1} & \cdots & S_{-p} \\ S_1 & S_o & & \\ \vdots & & \ddots & \\ S_p & & & S_o \end{bmatrix} \begin{bmatrix} 1 \\ -\tilde{a}_1 \\ \vdots \\ -\tilde{a}_p \end{bmatrix} = \begin{bmatrix} F_o \\ 0 \\ \vdots \\ 0 \end{bmatrix} \tag{106}$$

(The (p+1) x (p+1) matrix in (106) is nonnegative definite, as a simple extension of (104) shows.) But (106) is identical in form to (A-3), and the recursive solution presented in (A-4) through (A-7) applies directly.

The spectral estimate we adopt follows from results (68) through (71) in subsection 3.2 on linear predictive filtering for known correlation values: first, the optimum transfer function leading from $\{x_k\}$ to minimum-error sequence $\{\tilde{\epsilon}_k\}$ in (96) is

$$A(f) = \sum_{n=0}^{p} \tilde{a}_n \exp(-i2\pi fn\Delta). \tag{107}$$

However, we have a problem in trying to accurately estimate the average minimum-error power that would be used in the numerator of the assumed white spectrum for the error in (70). Although minimum average error F_o of (103) could be used, it is not recommended because not all the error terms in the sum in definition (97) are meaningful. Therefore, because of our inability to

accurately estimate the average minimum-error power in this case, we shall adopt as our spectral estimate

$$\hat{G}_x(f) \equiv \frac{\Delta \cdot 1}{\left|A(f)\right|^2} = \frac{\Delta}{\left|\sum_{n=0}^{p} \tilde{a}_n \exp(-i2\pi f n \Delta)\right|^2}, \quad |f| < \frac{1}{2\Delta} . \tag{108}$$

This is tantamount to assuming the average minimum-error power equal to unity (in addition to assuming the minimum-error spectrum white). This procedure also eliminates level perturbations in the spectral estimate (108) due to random fluctuations in the absolute level of the sample set $\{x_n\}_1^N$; that is, from (102) and (98), it is seen that the optimum values of the filter coefficients, $\{\tilde{a}_n\}_1^p$, would be the same if $\{Kx_n\}_1^N$ were the available samples, for any K. Therefore, estimate $\hat{G}_x(f)$ in (108) is also independent of the absolute level of the available samples. The choice (108) allows for convenient comparisons of the spectral estimates obtained by the various methods presented here.

As an alternative, (108) could be numerically integrated over $(-\frac{1}{2\Delta}, \frac{1}{2\Delta})$, and then (108) could be scaled so that the area under the estimated spectrum is equal to the sample power, $\frac{1}{N} \sum_{n=1}^{N} |x_n|^2$, if desired.

The implications of the assumption in (108) that the minimum-error sequence has a white spectrum are investigated in appendix E. It is shown that the sample crosscorrelation between input sequence $\{x_k\}$ and minimum-error sequence $\{\tilde{\epsilon}_k\}$, defined for the available data of the single member function as

$$D_\ell = \frac{1}{N} \sum_k \tilde{\epsilon}_k \, x^*_{k-\ell}, \text{ all } \ell , \tag{109}$$

is assumed to satisfy

$$D_\ell = 0, \; 1 \leq \ell ; \tag{110}$$

that is, the minimum-error sequence is uncorrelated (on a single member function basis) with all the past input. It is also shown that the quantities S_ℓ de-

fined in (98) (of which only S_ℓ for $|\ell| \leq p$ were used in (99) et seq.) can be estimated for $\ell \geq p + 1$ according to

$$S_\ell = \sum_{n=1}^{p} \tilde{a}_n S_{\ell-n}, \quad \ell \geq p + 1. \tag{111}$$

This relation, (111), which may not be true for the quantities S_ℓ actually obtained from data $\{x_n\}_1^N$ via (98), is due directly to the assumption that the sample spectrum of the minimum-error is white; see appendix E. The recursion relation (111) is stable, according to appendix D, if

$$1 - \sum_{n=1}^{p} \tilde{a}_n z^{-n} \tag{112}$$

possesses all its zeros within O. But since matrix $[S_{\ell-m}]$ in (102) has the form of a legal correlation matrix, we appeal directly to reference 1, page 567, to state that this property does indeed hold. Therefore, recursion (111) is stable.

It is worthwhile noting that no direct estimation of unknown correlation values $\{R_k\}$ was attempted in this approach; rather, we minimized the average error defined in (97) and solved directly for the filter coefficients in (102). However, if we rewrite (105) in the form

$$\sum_{m=0}^{p} S_{\ell-m} \tilde{a}_m = - F_o \delta_{\ell o}, \quad 0 \leq \ell \leq p, \tag{113}$$

and compare with (C-3), we see that the quantity S_ℓ could be adopted as an estimate of R_ℓ for $|\ell| \leq p$; that is, using (98), we could say

$$\hat{R}_\ell \equiv S_\ell = \frac{1}{N} \sum_k x_k x^*_{k-\ell}, \quad |\ell| \leq p, \tag{114}$$

(and then (111), with $\hat{R}$ replacing S, could be used to estimate R_ℓ for $|\ell| \geq p + 1$, rather than (98)). This is in fact the approach adopted by some authors; see, for example, reference 2, equation (19). However, (114) yields biased estimates because

$$\overline{\hat{R}_\ell} = \overline{S_\ell} = \left\{ \begin{array}{c} \frac{N-|\ell|}{N} R_\ell \,, \; |\ell| \le N \\ \\ 0, \text{ otherwise} \end{array} \right\} . \tag{115}$$

It is interesting to note that if (114) were adopted a priori as estimates of the unknown correlation values $\{R_k\}$, then the MESA and autoregressive approaches of subsections 3.1 and 3.3 could be utilized directly, if the right sides of (31) and (81) were replaced by $\{\hat{R}_k\}$. The spectral estimates would then be given by results identical to (108), except for a scale factor. The major drawback of this approach is the need to commit oneself to a specific form for the correlation estimates, such as (114), rather than letting the technique itself yield alternative estimates. The specific form used for the correlation estimates could limit the quality of the spectral estimate obtained; this contention is proven true by simulation in section 6.

4.2 UNBIASED VERSION OF YULE-WALKER EQUATIONS

One method of obtaining unbiased estimates of the correlation values $\{R_\ell\}$ is to define estimators

$$\hat{R}_\ell \equiv \frac{1}{N-\ell} \sum_k x_k x^*_{k-\ell} = \frac{1}{N-\ell} \sum_{k=\ell+1}^{N} x_k x^*_{k-\ell} \quad \text{for } 0 \le \ell \le p \,. \tag{116}$$

Of course $\hat{R}_{-\ell} \equiv \hat{R}^*_\ell$. These could then be used in (102) in the form

$$\sum_{m=1}^{p} \hat{R}_{\ell-m} \tilde{a}_m = \hat{R}_\ell \,, \; 1 \le \ell \le p \,, \tag{117}$$

to solve for the filter coefficients $\{\tilde{a}_m\}_1^p$. And (108) could again be adopted for the spectral estimate. The solution for the coefficients in (117) minimizes no error criterion; it merely utilizes unbiased correlation estimates. The discussion under (115) is relevant to this approach; how good the technique is will be ascertained in section 6.

The matrix $[\hat{R}_{\ell-m}]_1^p$ of estimated correlation values on the left side of (117) is Hermitian and Toeplitz; however, it is not necessarily nonnegative definite. (This last property is shown by considering the example p = 2, N = 3,

with $x_1 = 2$, $x_2 = x_3 = 3$, for then $\hat{R}_0 = 22/3$, and $\hat{R}_1 = 15/2$.) The recursive solution of appendix A could again be applied to a modified form of (117); see (105) and (106). If the recursive technique in (111) were utilized to extrapolate $\hat{R}_\ell$ according to .

$$\hat{R}_\ell \equiv \sum_{n=1}^{p} \tilde{a}_n \hat{R}_{\ell-n}, \quad \ell \geq p + 1 \tag{118}$$

and (116), it need not be stable unles $[\hat{R}_{\ell-m}]_1^p$ is nonnegative definite. Even if (118) were unstable, (108) could still be used as a spectral estimate of $G_x(f)$; there would, however, be a greater tendency of some pole-pairs of (108) to drift close to the unit circle, O, in the z-plane and give rise to spurious large peaks in the spectral estimate. This tendency is reduced for stable recursions (118), that is, if (112) possesses all its zeros within O.

4.3 LEAST-SQUARES ESTIMATES OF BOX AND JENKINS

In reference 16, appendix A7.5, a likelihood function approach to estimation of the coefficients in an all-pole (that is, autoregressive) filter model for generation of the process $\{x_n\}$ is considered. The end result (in our notation) is given in (A7.5.7) for real data by

$$S_{ij} \equiv \frac{1}{N} D_{i+1,j+1} = \frac{1}{N} \sum_{k=1}^{N-i-j} x_{i+k} x_{j+k}, \quad 0 \leq i, j \leq p \tag{119}$$

and in (A7.5.15) by

$$\sum_{j=1}^{p} S_{ij} \tilde{a}_j = S_{io}, \quad 1 \leq i \leq p. \tag{120}$$

This constitutes p linear equations in the p unknowns $\{\tilde{a}_j\}_1^p$. The matrix $[S_{ij}]_1^p$ occurring in (120) is symmetric, not necessarily Toeplitz, and not necessarily nonnegative definite. (The last property is shown by considering the example $N = 5$, $p = 2$, with $x_2 = x_3 = x_4 = 1$, for then $S_{11} = 3/5$, $S_{12} = S_{21} = 2/5$, $S_{22} = 1/5$, and the determinant is $-1/25$.) The quantities $\{S_{ij}\}$ also yield biased estimates of $\{R_{i-j}\}$, because

$$\overline{S_{ij}} = \frac{N - i - j}{N} R_{i-j} . \tag{121}$$

Nevertheless we will adopt (108) for our spectral estimate in this case. The fact that we encounter a non-Toeplitz matrix in (120) disallows the use of the recursive technique for solution in appendix A.

If the solution to (120) is substituted in (112), the zeros need not all lie inside O. Therefore, there would be a greater tendency for some pole-pairs of (108) to drift close to O than when all the zeros must lie inside O, as for subsection 4.1.

4.4 APPROXIMATE MAXIMUM LIKELIHOOD ESTIMATES OF BOX AND JENKINS

This technique is a slight modification of the previous one in subsection 4.3. Namely, in reference 16, under (A7.5.18), the coefficients are solutions of

$$\sum_{j=1}^{p} S_{ij} \tilde{a}_j = S_{io}, \quad 1 \le i \le p , \tag{122}$$

where (see (119))

$$S_{ij} \equiv \frac{1}{N-i-j} D_{i+1,j+1} = \frac{1}{N-i-j} \sum_{k=1}^{N-i-j} x_{i+k} x_{j+k}, \quad 0 \le i, j \le p . \tag{123}$$

The matrix $[S_{ij}]_1^p$ occurring in (122) is symmetric, not necessarily Toeplitz, and not necessarily nonnegative definite. (The last property is shown by considering the example $N = 5$, $p = 2$, with $x_2 = 2$, $x_3 = 1$, $x_4 = 2$, for then $S_{11} = 3$, $S_{12} = S_{21} = 2$, $S_{22} = 1$, and the determinant of these coefficients is -1). The quantities $\{S_{ij}\}$ yield unbiased estimates of $\{R_{i-j}\}$; however, every element in a particular diagonal can be different, even though they are estimating the same quantity. Also, the number of terms (in the sum in (123)) along a particular diagonal varies with the position of the element, thereby yielding differing degrees of stability. Equation (108) can be used with (122) to obtain the spectral estimate. Recursive solution of (122) is not allowed because of the non-Toeplitz character of the matrix $[S_{ij}]_1^p$. The comments at the end of subsection 4.3 are relevant here also.

4.5 PREDICTION USING VALID ERROR POINTS

The method of subsection 4.1 utilized an average error measure defined over all nonzero error terms; see (97). However, as noted under (96), instantaneous error ϵ_k is meaningful only if $k \geq p+1$ and $k \leq N$. Here we define an average magnitude-squared error by summing only over the set of valid error points:

$$F \equiv \frac{1}{N-p} \sum_{k=p+1}^{N} |\epsilon_k|^2 . \tag{124}$$

There are N - p terms in this sum. This procedure is tantamount to not running off the edges of the available data $\{x_n\}_1^N$. Employing (96), (124) can be written as

$$F = \sum_{m,n=0}^{p} a_m a_n^* S_{nm} , \tag{125}$$

where

$$S_{nm} \equiv \frac{1}{N-p} \sum_{k=p+1}^{N} x_{k-m} x_{k-n}^* = S_{mn}^* . \tag{126}$$

This quantity always contains N - p terms for $0 \leq n, m \leq p$. In order to minimize F, we compute

$$\frac{\partial F}{\partial a_\ell^*} = \sum_{m=0}^{p} S_{\ell m} a_m , \quad 1 \leq \ell \leq p . \tag{127}$$

The optimum predictive coefficients are therefore solutions of

$$\sum_{m=0}^{p} S_{\ell m} \tilde{a}_m = 0, \quad 1 \leq \ell \leq p \qquad (\tilde{a}_o = a_o = -1) , \tag{128}$$

or

$$\sum_{m=1}^{p} S_{\ell m} \tilde{a}_m = S_{\ell o}, \quad 1 \le \ell \le p. \tag{129}$$

The method here is called the covariance method in reference 1.

The minimum value of the average error F is obtained by substituting (128) in (124) and (125):

$$F_o \equiv \frac{1}{N-p} \sum_{k=p+1}^{N} \left|\tilde{\epsilon}_k\right|^2 = \sum_{n=0}^{p} \tilde{a}_n^* \sum_{m=0}^{p} S_{nm} \tilde{a}_m = \tilde{a}_o^* \sum_{m=0}^{p} S_{om} \tilde{a}_m$$

$$= - \sum_{m=0}^{p} S_{mo}^* \tilde{a}_m = S_{oo} - \sum_{m=1}^{p} S_{mo}^* \tilde{a}_m, \tag{130}$$

where we have used (126) and (128).

The p x p matrix $[S_{\ell m}]_1^p$ on the left side of (129) is a legal correlation matrix in that it is Hermitian and nonnegative definite. The last property follows from

$$\sum_{\ell,m=1}^{p} S_{\ell m} \alpha_m \alpha_\ell^* = \sum_{\ell,m=1}^{p} \alpha_m \alpha_\ell^* \frac{1}{N-p} \sum_{k=p+1}^{N} x_{k-m} x_{k-\ell}^*$$

$$= \frac{1}{N-p} \sum_{k=p+1}^{N} \left| \sum_{m=1}^{p} \alpha_m x_{k-m} \right|^2 \ge 0 \tag{131}$$

for any $\{\alpha_m\}_1^p$. Since $[S_{\ell m}]$ is not necessarily Toeplitz, however, the recursive solution in appendix A is not applicable. Numerical computation of $[S_{\ell m}]$ is eased by taking advantage of a recursive relation between $S_{\ell+1, m+1}$ and $S_{\ell m}$.

The spectral estimate we adopt is given by (108). However, note that we could, if desired, get an estimate here of the average minimum error power E_o, used in (70), according to

$$\hat{E}_0 = F_0 . \tag{132}$$

This quantity is meaningful because (130) involves only the valid error terms.

Equation (129) is similar to, but not identical with, the form of (117). The quantities $\{S_{nm}\}$, defined in (126), yield unbiased estimates of $\{R_{n-m}\}$; however, every element in a particular diagonal can be different, even though they are estimating the same quantity.

If the solution to (129) is substituted in (112), the zeros need not lie inside O, despite the nonnegative definite property demonstrated in (131). (The example

$$p = 1,\ N = 2,\ \text{yields}\ \tilde{a}_1 = x_2/x_1 \tag{133}$$

and gives a zero location of (112) which can lie anywhere in the z-plane.) Therefore, the comments at the end of subsection 4.3 are relevant here also.

4.6 FORWARD AND BACKWARD PREDICTION USING VALID ERROR POINTS

It was noted in subsections 2.2, 3.2, and 4.1 that "prediction" based on future values of the input $\{x_k\}$ yielded an equivalent spectral estimate to that obtained by prediction based on past values. Here we combine the two techniques. The forward-predicted value of x_k is

$$\hat{x}_k \equiv \sum_{n=1}^{p} a_n\, x_{k-n},\ p+1 \le k \le N, \tag{134}$$

where we limit k to the range $[p+1, N]$, in anticipation of the fact that we can only measure valid errors in that range; see (96) et seq. The backward-predicted value of x_k is

$$\check{x}_k \equiv \sum_{n=1}^{p} a_n^*\, x_{k+n},\ 1 \le k \le N-p, \tag{135}$$

where we again limit the range of k. (See, for example, (15), (22), and (77).) The forward and backward errors are, respectively,

$$\hat{\epsilon}_k \equiv \hat{x}_k - x_k = \sum_{n=0}^{p} a_n x_{k-n}, \quad p+1 \le k \le N,$$
$$\check{\epsilon}_k = \check{x}_k - x_k = \sum_{n=0}^{p}{}' a_n^* x_{k+n}, \quad 1 \le k \le N-p, \tag{136}$$

where $a_o = -1$.

An overall average magnitude-squared error is defined as

$$F = \frac{1}{2(N-p)}\left(\sum_{k=p+1}^{N} \left|\hat{\epsilon}_k\right|^2 + \sum_{k=1}^{N-p} \left|\check{\epsilon}_k\right|^2 \right) = \sum_{m,n=0}^{p} a_m a_n^* S_{nm}, \tag{137}$$

where, in this subsection,

$$S_{nm} \equiv \frac{1}{2(N-p)}\left(\sum_{k=p+1}^{N} x_{k-m} x_{k-n}^* + \sum_{k=1}^{N-p} x_{k+n} x_{k+m}^* \right). \tag{138}$$

This quantity always contains 2(N-p) terms for $0 \le n, m \le p$. Two useful properties of S_{nm} are immediately available:

$$S_{mn} = S_{nm}^*, \quad S_{p-n,\, p-m} = S_{nm}^*. \tag{139}$$

These properties, plus a recursive relation relating $S_{n+1,\, m+1}$ and S_{nm}, ease the numerical computation of matrix $[S_{nm}]$.

We minimize F by choice of $\{a_m\}_1^p$, getting (see (127) - (129))

$$\sum_{m=1}^{p} S_{nm} \tilde{a}_m = S_{no}, \quad 1 \le n \le p. \tag{140}$$

The minimum value of F is (see (130))

$$F_o = S_{oo} - \sum_{m=1}^{p} S^*_{mo}\, \tilde{a}_m . \tag{141}$$

The method here is an extended version of the covariance approach in reference 1.

The matrix $[S_{\ell m}]_1^n$ is Hermitian and nonnegative definite:

$$\sum_{\ell,m=1}^{p} S_{\ell m}\, \alpha_m \alpha^*_\ell = \frac{1}{2(N-p)}\left(\sum_{k=p+1}^{N} \left| \sum_{m=1}^{p} \alpha_m x_{k-m} \right|^2 + \sum_{k=1}^{N-p} \left| \sum_{m=1}^{p} \alpha^*_m x_{k+m} \right|^2 \right) \geq 0 \tag{142}$$

for any $\{\alpha_m\}_1^p$. However, this matrix is not necessarily Toeplitz; therefore, we cannot apply the recursive solution of appendix A.

The spectral estimate we adopt is obtained by substituting the solution of (140) in (108). An estimate of the average minimum error power E_o, used in (70), is available here according to

$$\hat{E}_o = F_o , \tag{143}$$

if desired, where F_o is given by (141). This is meaningful because (137) utilized only the valid error terms.

In analogy to (126), the quantities $\{S_{nm}\}$ in (138) yield unbiased estimates of $\{R_{n-m}\}$. Nevertheless, if the solution to (140) is substituted in (112), the zeros need not lie within O, despite the nonnegative definite property shown in (142). For $p = 1$ we find

$$\tilde{a}_1 = \frac{x_2 x^*_1 + x_3 x^*_2 + \ldots + x_N x^*_{N-1}}{\frac{1}{2}|x_1|^2 + |x_2|^2 + |x_3|^2 + \ldots + |x_{N-2}|^2 + |x_{N-1}|^2 + \frac{1}{2}|x_N|^2} . \tag{144}$$

And since

$$\frac{|x_k\, x^*_{k-1}|}{\frac{1}{2}|x_{k-1}|^2 + \frac{1}{2}|x_k|^2} \leq 1 , \tag{145}$$

it follows that

$$\left|\tilde{a}_1\right| \leq 1 . \tag{146}$$

So for p = 1, the zero of (112) must lie within O, (unless $x_k = A \exp(ikB)$ for all k, in which case it lies on O). However for p = 2, N = 3, and real data, the zeros of (112) lie at $r \pm \sqrt{r^2 - 1}$, where $r = \frac{x_1 + x_3}{2x_2}$. So if $|r| \leq 1$, both zeros lies on O, whereas if $|r| > 1$, one zero lies outside O. Therefore, the comments at the end of subsection 4.3 are relevant here also.

4.7 BURG TECHNIQUE

The key to this technique, first presented in reference 21, is the observation from equation (A-6) in appendix A that if the particular p-th order coefficient $a_p^{(p)}$ can be evaluated, the rest of the p-th order predictive filter coefficients, $a_k^{(p)}$, $1 \leq k \leq p - 1$, could be evaluated from (p - 1)-th order coefficients. This relation (A-6) holds true for the solution of normal equations (A-3) even if $\{R_k\}$ are replaced by estimated values. Explicitly, if estimates $\hat{R}_o, \hat{R}_1, \ldots, \hat{R}_{p-1}$, and $a_p^{(p)}$ are considered known in the matrix equation

$$\begin{bmatrix} \hat{R}_o & \hat{R}_{-1} & \cdots & \hat{R}_{-p} \\ \hat{R}_1 & \hat{R}_o & & \\ \vdots & & \ddots & \\ \hat{R}_p & & & \hat{R}_o \end{bmatrix} \begin{bmatrix} 1 \\ -a_1^{(p)} \\ \vdots \\ -a_p^{(p)} \end{bmatrix} = \begin{bmatrix} P^{(p)} \\ 0 \\ \vdots \\ 0 \end{bmatrix} , \tag{147}$$

then we have p + 1 linear equations in the p + 1 unknowns $a_1^{(p)}, \ldots, a_{p-1}^{(p)}, \hat{R}_p$, $P^{(p)}$. (Notice that whereas R_p was known and $a_p^{(p)}$ unknown in (A-3), the situation is reversed here for these two variables.) The solutions are given, for $p \geq 1$, by

$$a_k^{(p)} = a_k^{(p-1)} - a_p^{(p)} \, a_{p-k}^{(p-1)*} , \quad k = 1, 2, \ldots, p - 1 \text{ (no terms if } p = 1) \tag{148}$$

$$\hat{R}_p = \sum_{k=1}^{p} \hat{R}_{p-k}\, a_k^{(p)}, \quad \hat{\rho}_p = \sum_{k=1}^{p} \hat{\rho}_{p-k}\, a_k^{(p)}, \tag{149}$$

$$P^{(p)} = P^{(p-1)} \left(1 - \left|a_p^{(p)}\right|^2\right). \tag{150}$$

The quantities $\{\hat{\rho}_k\}$ in (149) are the estimated normalized correlation coefficients $\{\hat{R}_k/\hat{R}_o\}$. The recursion (150) is started with

$$P^{(0)} = \hat{R}_o \equiv \frac{1}{N} \sum_{n=1}^{N} \left|x_n\right|^2, \tag{151}$$

which is the sample power of the available samples. A method of evaluating $a_p^{(p)}$ for $p \geq 1$ is treated below.

The method presented here is a combination of references 21 and 7. It begins by defining zero-th order forward and backward sequences according to

$$f_n^{(o)} = x_n, \quad b_n^{(o)} = x_n, \quad 1 \leq n \leq N. \tag{152}$$

The p-th order forward and backward sequences (residuals) for $p \geq 1$ are defined according to

$$\left.\begin{aligned} f_n^{(p)} &\equiv f_n^{(p-1)} - g_p\, b_{n-1}^{(p-1)} \\ b_n^{(p)} &\equiv b_{n-1}^{(p-1)} - g_p^*\, f_n^{(p-1)} \end{aligned}\right\} \text{ for } p+1 \leq n \leq N. \tag{153}$$

(These can be interpreted as one-step forward and backward prediction errors.) A chain interpretation of (153) is presented in figure 3. (From the known correlation results in subsection 3.2, if we define

$$f_n^{(p)} = x_n - \sum_{k=1}^{p} a_k^{(p)}\, x_{n-k}, \quad b_n^{(p)} = x_{n-p} - \sum_{k=1}^{p} a_k^{(p)\,*}\, x_{n-p+k},$$

we find that figure 3 results, with g_p replaced by $a_p^{(p)}$.)

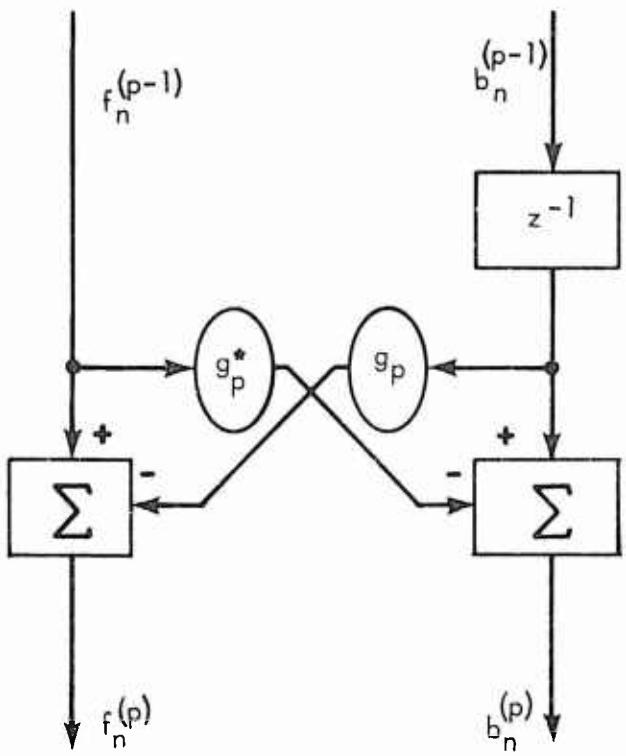


Figure 3. Chain Interpretation of Burg Technique

The average magnitude-squared value of the p-th order forward and backward sequences is

$$F^{(p)} \equiv \frac{1}{2(N-p)} \sum_{n=p+1}^{N} \left(\left| f_n^{(p)} \right|^2 + \left| b_n^{(p)} \right|^2 \right)$$

$$= \frac{1}{2(N-p)} \sum_{n=p+1}^{N} \left(\left| f_n^{(p-1)} - g_p \, b_{n-1}^{(p-1)} \right|^2 + \left| b_{n-1}^{(p-1)} - g_p^* \, f_n^{(p-1)} \right|^2 \right), \quad p \geq 1 . \tag{154}$$

We wish to minimize this average power at the p-th stage by choice of cross-gain g_p. We find the optimum choice to be

$$g_p = \frac{2 \sum_{n=p+1}^{N} f_n^{(p-1)} \, b_{n-1}^{(p-1)*}}{\sum_{n=p+1}^{N} \left(\left| f_n^{(p-1)} \right|^2 + \left| b_{n-1}^{(p-1)} \right|^2 \right)} \equiv \frac{\text{Num}(p)}{\text{Den}(p)} , \quad p \geq 1 . \tag{155}$$

When (155) is substituted in (153), the results are called the residuals. The minimum value of the residual power at the p-th stage is obtained by substituting (155) in (154) and is expressible as

$$F_o^{(p)} = \left(1 - \left|g_p\right|^2\right) \frac{\mathrm{Den}(p)}{2(N-p)}, \quad p \geq 1. \tag{156}$$

The quantities necessary for this evaluation are available when (155) is evaluated. The value of (156) will never be smaller than (141), since the procedure here is a step-by-step procedure, not a simultaneous procedure as used in subsection 4.6.

An immediate recursion for the transfer functions of the p-th stage in figure 3 is

$$\left.\begin{aligned} \mathcal{F}^{(p)}(z) &= \mathcal{F}^{(p-1)}(z) - g_p z^{-1} \mathcal{B}^{(p-1)}(z) \\ \mathcal{B}^{(p)}(z) &= z^{-1} \mathcal{B}^{(p-1)}(z) - g_p^* \mathcal{F}^{(p-1)}(z) \end{aligned}\right\}, \quad p \geq 1, \tag{157}$$

with starting values

$$\mathcal{F}^{(o)}(z) = \mathcal{B}^{(o)}(z) = 1. \tag{158}$$

If we let transfer functions

$$\mathcal{F}^{(p)}(z) = 1 - \sum_{k=1}^{p} a_k^{(p)} z^{-k},$$

$$\mathcal{B}^{(p)}(z) = -\sum_{k=0}^{p-1} a_{p-k}^{(p)*} z^{-k} + z^{-p} = z^{-p} \mathcal{F}^{(p)*}(z^{-1}), \tag{159}$$

the solution is

$$a_p^{(p)} = g_p, \quad p \geq 1, \tag{160}$$

with the lower order coefficients given by (148). Thus, the only remaining quantity, $a_p^{(p)}$, that was necessary for solution of (147) - (150) is given by (160)

and (155), along with (152) and (153). To the three lowest orders, the solutions are given by

$$p = 0, \quad P^{(0)} = \hat{R}_o = \frac{1}{N} \sum_{n=1}^{N} |x_n|^2 \tag{161}$$

$$p = 1, \quad a_1^{(1)} = g_1$$

$$\hat{R}_1 = \hat{R}_o \, a_1^{(1)}$$

$$P^{(1)} = P^{(0)} \left(1 - \left|a_1^{(1)}\right|^2\right) \tag{162}$$

$$p = 2, \quad a_2^{(2)} = g_2$$

$$a_1^{(2)} = a_1^{(1)} - a_2^{(2)} \, a_1^{(1)*}$$

$$\hat{R}_2 = \hat{R}_1 \, a_1^{(2)} + \hat{R}_o \, a_2^{(2)}$$

$$P^{(2)} = P^{(1)} \left(1 - \left|a_2^{(2)}\right|^2\right). \tag{163}$$

It will be observed that for $p = 1$, $a_1^{(1)}$ is identical to (144); in fact, the procedures are identical in this case. It should also be noted that at each stage, an estimate, $\hat{R}_p$, of the true correlation value R_p becomes available via (149), and is unchanged by the addition of any further stages (larger p).

It was demonstrated in (A-9) that the magnitude of $a_p^{(p)}$ was bounded by unity if the known correlation matrix R was nonnegative definite. The same property,

$$\left|a_p^{(p)}\right| \leq 1, \tag{164}$$

is true here in the case of unknown correlation when $a_p^{(p)}$ is determined by (160) and (155); see appendix F. This is sufficient to show that all zeros of (A-10)

lie inside O; see reference 11, for example. Therefore, the recursion (149) can be used in the form

$$\hat{R}_f = \sum_{k=1}^{p} \hat{R}_{f-k}\, a_k^{(p)}, \quad \ell \geq p+1 , \tag{165}$$

to extrapolate the estimated correlation values beyond p-th order, with the p-th order coefficients $\{a_k^{(p)}\}_1^p$, and is guaranteed to be stable. Division of (165) by $\hat{R}_0$ yields the normalized correlation coefficients. Recursion (165) is similar in form to those encountered in (75), (111), and (118).

The quantity $P^{(p)}$ that results as the solution (150) of matrix equation (147) is not the minimum average magnitude-squared error as it was for known correlation; see (A-3), (A-7), and (67). In fact, $P^{(p)}$ has no direct physical significance; it is merely the variable left over in that position in the normal equations (147) when modified from the case of known correlation values, (A-3). Rather, $F_o^{(p)}$ in (154) and (156) is the minimum average magnitude-squared error of the forward and backward residuals, (153), of the available data. Thus, as far as picking an "optimum" value of p at which to terminate the recursion in (147) - (150) is concerned, the latter quantity has more physical significance. However, the two quantities are very close to each other for no bad data points, especially for N-p large; see appendix G. Both quantities are readily calculated at any stage via (150) and (156), respectively.

The transfer functions from input x to the p-th order residuals are given in (159). Therefore, the spectra of the residuals are given by

$$G_f^{(p)}(f) = G_b^{(p)}(f) = \left| \mathcal{F}^{(p)}\left(\exp(i2\pi f\Delta)\right) \right|^2 G_x(f) . \tag{166}$$

Now if the chain in figure 3 has been carried to the stage where further values of cross-gain g_p would be substantially zero, then the residuals are approximately white. Therefore, an estimate of the input spectrum is available from (166) and (159) according to

$$\hat{G}_x(f) = \frac{\Delta}{\left| 1 - \sum_{k=1}^{p} a_k^{(p)} \exp(-i2\pi fk\Delta) \right|^2}, \quad |f| < \frac{1}{2\Delta} , \tag{167}$$

where the residual power has been set at unity; see the discussion under (108). Two alternatives to this scale factor are discussed in appendix H; namely, it is shown that $P^{(p)}$ and $F_0^{(p)}$ are both meaningful scale factors that could be applied to (167).

The estimated correlation values in (149) are generally biased. This may be anticipated from the complicated forms of (149), (148), and (155), since additional statistics than simply $\overline{x_{k+p}x_k^*}$ need to be known in order that $\hat{R}_p$ be capable of evaluation; that is, $\hat{R}_p$ depends on much more than just $\overline{x_{k+p}x_k^*}$, for the Burg method. This biasedness may be proven for a simple example with $p = 1$, $N = 3$. ($\hat{R}_0$ in (151) is unbiased; and for $p = 1$, $N = 2$, we find $\hat{R}_1 = x_2x_1^*$, which is unbiased.) For real data, with random variables $\{x_k\}_1^3$ being zero-mean unit-variance Gaussian, and $\overline{x_2x_1} = \overline{x_3x_2} = \pm\frac{1}{\sqrt{2}}$, $\overline{x_3x_1} = 0$, we find (in appendix I) that $\overline{\hat{R}_1} = \pm\frac{1}{\sqrt{2}}\ \frac{12 - 2\sqrt{3}}{9} = \pm\frac{1}{\sqrt{2}}\ (.9484)$. The bias is slight but non-zero.

In summary, the Burg algorithm for data processing consists of initialization (152); followed by the cross-gain calculation in (155); filter coefficients via (160) and (148); and normalized correlation coefficients (149) (if desired) at every stage. The update required at each stage is given by (153), and the extrapolated normalized correlation coefficients at any stage are available from (165), upon division by $\hat{R}_0$.

4.8 SUMMARY OF PROPERTIES OF TECHNIQUES

The solution for the filter coefficients in the techniques considered above can be put in the form

$$\hat{R}(-\tilde{a}) = F_0\ \delta\ . \tag{168}$$

The properties of the estimated correlation matrix $\hat{R}$ (if desired) are tabulated in table 1. (Actually, several of the "No" entries should be "Not Necessarily.")

It will be seen that none of the techniques possesses a "Yes" for all the properties. The Yule-Walker and Burg techniques possess everything but the unbiased property; however, the unbiased property, per se, of the correlation estimates is not necessarily a desirable feature for spectral estimation, as will

Table 1. Properties of Estimated Correlation Matrices

Technique	Correlation Estimates	Unbiased	Hermitian	Toeplitz	Nonnegative Definite	Stable Recursion
Yule-Walker	(114)	No	Yes	Yes	Yes	Yes
Unbiased Yule-Walker	(116)	Yes	Yes	Yes	No	No
Least Squares of Box and Jenkins	(119)	No	Yes	No	No	No
Approximate maximum likelihood of Box and Jenkins	(123)	Yes	Yes	No	No	No
Prediction	(126)	Yes	Yes	No	Yes	No
Forward and Backward Prediction	(138)	Yes	Yes	No	Yes	No
Burg	(149)	No	Yes	Yes	Yes	Yes

be seen by later simulation results. On the other hand, simultaneous satisfaction of the three properties of Hermitian, Toeplitz, and nonnegative definite guarantees that a stable recursion and nonspiky spectral estimates result; see reference 1, page 567.

5. CORRELATION UNKNOWN: FINITE DATA SET WITH BAD DATA POINTS

In some applications, some data values can be bad as a result of malfunctioning equipment or human errors in reading or recording, for example. Also, some data values can be missing as a result of equipment being inadvertently or intermittently turned off for calibration purposes, for example; or some sections of data can be contaminated by strong burst-like noise and be virtually useless in those sections. All of these problems can be characterized mathematically by saying that of the available data set $\{x_n\}_1^N$, the values x_n for the distinct integers

$$n = M_1, M_2, \ldots M_B \tag{169}$$

are known to be bad (or missing). The B bad locations $\{M_j\}_1^B$ are presumed to be known. The bad data points can be regularly spaced, or randomly spaced, or a combination, depending on the application, it will make no difference to the techniques to be developed here.

In this section, we wish to estimate the input spectrum despite the presence of known bad points. The last two methods in subsections 4.6 and 4.7 will be extended to cover this case. The reason we do not extend the other methods in section 4 will become clear when we compare the various techniques by simulation in section 6.

5.1 FORWARD AND BACKWARD PREDICTION USING VALID ERROR POINTS

The method to be presented here is very similar to that given earlier in subsection 4.6; accordingly the treatment will be briefer. For convenience and to enable a better estimation of the true spectrum with a limited number, p, of parameters, we subtract the sample mean of the N-B good data points so that

$$\frac{1}{N-B} \sum_{n=1}^{N}{}' x_n = 0 , \tag{170A}$$

where $\sum'$ denotes that we skip those values of n in the set (169); that is, we simply ignore the bad data points -- this is, in fact, the main theme of the methods to be presented. We attempt no interpolation on the bad points, nor do

we set them equal to zero or the sample mean. We also scale the good points so that the sample variance is unity:

$$\frac{1}{N-B-1} \sum_{n=1}^{N} \left| x_n \right|^2 = 1 . \tag{170B}$$

This helps avoid overflow and underflow problems in the numerical manipulation of large arrays encountered for large p.

A forward prediction of x_k is afforded by

$$\hat{x}_k \equiv \sum_{n=1}^{p} a_n x_{k-n} , \; p + 1 \leq k \leq N , \tag{171}$$

provided that $k-1, k-2, \ldots, k-p \neq M_1, M_2, \ldots, M_B$. Then a valid forward error can be defined as

$$\hat{\epsilon}_k \equiv \hat{x}_k - x_k = \sum_{n=0}^{p} a_n x_{k-n} \qquad (a_o = -1) , \; p + 1 \leq k \leq N , \tag{172}$$

provided that $k, k-1, \ldots, k-p \neq M_1, M_2, \ldots, M_B$; that is, $\hat{\epsilon}_k$ is defined for $p+1 \leq k \leq N$ except for k in the set of integers

$$I_p : \left\{ \begin{array}{llll} M_1, & M_1 + 1, & \ldots, & M_1 + p \\ M_2, & M_2 + 1, & \ldots, & M_2 + p \\ \vdots & & & \\ M_B, & M_B + 1, & \ldots, & M_B + p \end{array} \right\} . \tag{173}$$

If any numbers in set I_p are $< p+1$ or $> N$, they are not encountered in the error definition (172). Let B_p denote the number of <u>distinct</u> integers in I_p which are $\geq p+1$ and $\leq N$; this is the number of gaps (bad points) in the error sequence (172).

We now define an average forward error over the valid error points as

$$\hat{F} = \frac{1}{N-p-B_p} \sum_{\substack{k=p+1 \\ k \notin I_p}}^{N} \left|\hat{\epsilon}_k\right|^2 , \tag{174}$$

where $\notin$ denotes "not contained in," and $N-p-B_p$ is the number of terms in the sum. Substituting (172) in (174), we obtain

$$\hat{F} = \sum_{m,n=0}^{p} a_m a_n^* \frac{1}{N-p-B_p} \sum_{\substack{k=p+1 \\ k \notin I_p}}^{N} x_{k-m} x_{k-n}^* . \tag{175}$$

A backward prediction of x_k is available as

$$\check{x}_k \equiv \sum_{n=1}^{p} a_n^* x_{k+n} , \quad 1 \le k < N - p , \tag{176}$$

provided that $k+1, k+2, \ldots, k+p \neq M_1, M_2, \ldots, M_B$. And a backward error

$$\check{\epsilon}_k \equiv \check{x}_k - x_k = \sum_{n=0}^{p} a_n^* x_{k+n} \qquad (a_o = -1) , \quad 1 \le k \le N - p , \tag{177}$$

is available if $k, k+1, \ldots, k+p \neq M_1, M_2, \ldots, M_B$. Letting $\ell = k+p$ in (177), we can write

$$\check{\epsilon}_{\ell-p} = \sum_{n=0}^{p} a_n^* x_{\ell-p+n} , \quad p + 1 \le \ell \le N , \tag{178}$$

if ℓ is not contained in the set I_p defined in (173). The we can define an average backward error over the valid error points as

$$\check{F} = \frac{1}{N-p-B_p} \sum_{\substack{\ell=p+1 \\ \ell \notin I_p}}^{N} \left| \check{\epsilon}_{\ell-p} \right|^2 \tag{179}$$

$$= \sum_{m,n=0}^{p} a_m a_n^* \frac{1}{N-p-B_p} \sum_{\substack{\ell=p+1 \\ \ell \notin I_p}}^{N} x_{\ell-p+n} x_{\ell-p+m}^* , \tag{180}$$

where we have substituted (178).

We are now in a position to define an overall average error as

$$F = \frac{1}{2} (\hat{F} + \check{F}) = \sum_{m,n=0}^{p} a_m a_n^* S_{nm} \tag{181}$$

where, from (175) and (180),

$$S_{nm} = \frac{1}{2(N-p-B_p)} \sum_{\substack{k=p+1 \\ k \notin I_p}}^{N} \left(x_{k-m} x_{k-n}^* + x_{k-p+n} x_{k-p+m}^* \right). \tag{182}$$

It should be noticed that (182) does not tell us merely to sum over the "good" products, but rather to exclude set I_p. The number of terms in the sum (182) is the same for $0 \le n$, msp and is $N-p-B_p$. (For no bad points, (182) reduces to (138).) Two useful properties of S_{nm} are

$$S_{mn} = S_{nm}^* , \; S_{p-n,\, p-m} = S_{nm}^* . \tag{183}$$

The quantity S_{nm} is an unbiased estimate of R_{n-m}; however, the presence of bad points will increase the variance of S_{nm}; see reference 5. The matrix $[S_{nm}]_1^p$ is Hermitian and nonnegative definite.

The optimum predictive filter coefficients $\{\tilde{a}_m\}_1^p$ are obtained by minimizing (181):

$$\sum_{m=1}^{p} S_{\ell m}\, \tilde{a}_m = S_{\ell o}\,, \quad 1 \le \ell \le p\,. \tag{184}$$

The minimum average error is

$$F_o = S_{oo} - \sum_{m=1}^{p} S^*_{mo}\, \tilde{a}_m\,. \tag{185}$$

And since the sample variance of the good data points was set equal to unity in (170B), (185) is a relative error measure that can be used to decide what value of p should be used in (171) and (176); see reference 1, equations (41) and (89) et seq. The spectral estimate we adopt is obtained by substituting the solution of (184) into (108), as usual. The quantity F_o in (185) could be used as a scale factor, if desired, according to

$$\hat{E}_o = F_o\,. \tag{186}$$

5.2 BURG TECHNIQUE

The problem setting is the same as that for the previous subsection, including (169) - (170). The solution is identical to that for subsection 4.7, up to (150). Now we define zero-th order forward and backward sequences as

$$f_n^{(0)} = x_n\,,\ b_n^{(0)} = x_n\,,\ 1 \le n \le N\,,\ n \notin I_o\,, \tag{187}$$

where we again employ the definition (173). The first-order sequences are defined as

$$\left.\begin{aligned} f_n^{(1)} &= f_n^{(0)} - g_1\, b_{n-1}^{(0)} \\ b_n^{(1)} &= b_{n-1}^{(0)} - g_1^*\, f_n^{(0)} \end{aligned}\right\} \text{ for } 2 \le n \le N\,,\ n \notin I_1\,, \tag{188}$$

where the restriction of set I_1 is due to the fact that the first-order sequences cannot be formed (evaluated) in set I_1. We choose cross gain g_1 to minimize the average error

$$F^{(1)} \equiv \frac{1}{2(N-1-B_1)} \sum_{\substack{n=2 \\ n \notin I_1}}^{N} \left(\left| f_n^{(1)} \right|^2 + \left| b_n^{(1)} \right|^2 \right), \tag{189}$$

where $N-1-B_1$ is the number of terms in the sum. The solution is given by

$$g_1 = \frac{2 \sum_{\substack{n=2 \\ n \notin I_1}}^{N} f_n^{(0)} \, b_{n-1}^{(0)*}}{\sum_{\substack{n=2 \\ n \notin I_1}}^{N} \left(\left| f_n^{(0)} \right|^2 + \left| b_{n-1}^{(0)} \right|^2 \right)}. \tag{190}$$

With this value of g_1, we can now compute values for residuals $f_n^{(1)}$, $b_n^{(1)}$ in (188) and continue the procedure.

At stage p, we have

$$\left.\begin{aligned} f_n^{(p)} &= f_n^{(p-1)} - g_p \, b_{n-1}^{(p-1)} \\ b_n^{(p)} &= b_{n-1}^{(p-1)} - g_p^* \, f_n^{(p-1)} \end{aligned}\right\} \text{for } p+1 \le n \le N, \; n \notin I_p. \tag{191}$$

The choice of cross-gain g_p that minimizes average error

$$F^{(p)} \equiv \frac{1}{2(N-p-B_p)} \sum_{\substack{n=p+1 \\ n \notin I_p}}^{N} \left(\left| f_n^{(p)} \right|^2 + \left| b_n^{(p)} \right|^2 \right) \qquad \left(F^{(0)} = 1 \right), \tag{192}$$

is

$$g_p = \frac{2 \sum_{\substack{n=p+1 \\ n \notin I_p}}^{N} f_n^{(p-1)} \, b_{n-1}^{(p-1)*}}{\sum_{\substack{n=p+1 \\ n \notin I_p}}^{N} \left(\left| f_n^{(p-1)} \right|^2 + \left| b_{n-1}^{(p-1)} \right|^2 \right)} \equiv \frac{\mathrm{Num}(p)}{\mathrm{Den}(p)} , \qquad (193)$$

and the minimum value of (192) can be expressed as

$$F_o^{(p)} = \left(1 - \left|g_p\right|^2\right) \frac{\mathrm{Den}(p)}{2(N-p-B_p)} \qquad \left(F_o^{(0)} = 1\right) . \qquad (194)$$

This is also a relative error, due to the normalization (170B), and can be used as an indicator when to terminate the recursion procedure in (191).

It may be seen from (192) and (193) that the sums are merely taken over those values of n where the summands are defined. The number of terms in all the sums is $N-p-B_p$.

As in subsection 4.7, the filter coefficients are given by

$$a_p^{(p)} = g_p , \quad p \geq 1 , \qquad (195)$$

and for $p \geq 2$, by

$$a_k^{(p)} = a_k^{(p-1)} - a_p^{(p)} \, a_{p-k}^{(p-1)*} , \quad 1 \leq k \leq p-1 . \qquad (196)$$

Equations (147) through (150) still hold true. The starting value of $P^{(0)}$ is now 1, by virtue of normalization (170B). Recursion (165) for $\ell \geq p+1$ is still valid and is stable since

$$\left|a_p^{(p)}\right| = \left|g_p\right| \leq 1 , \qquad (197)$$

as may be seen from (193) and appendix F. The spectral estimate is again given by (167). The discussions in appendixes G and H are relevant here also.

REVERSE BLANK

6. COMPARISONS

All the techniques considered in section 4 will now be compared in terms of their resolution capability, bias, and statistical stability, by means of a simulation approach. In particular, the fourth-order autoregressive process which was intensively investigated in reference 2 (see figures 4a and 5a) will be the basic process of interest here also. It is characterized by

$$x_k = \sum_{n=1}^{4} \alpha_n x_{k-n} + w_k , \tag{198}$$

where

$$\alpha_1 = 2.7607 , \quad - 3.8106 , \quad \alpha_3 = 2.6535 , \quad \alpha_4 = - 0.9238 , \tag{199}$$

and where $\{w_k\}$ is Gaussian white noise. We restrict consideration to real processes here. We will not address the problem of how best to pick the value of p used in the techniques of sections 4 and 5, but shall instead set p equal to the known value, 4, and concentrate on the ability of the various techniques to estimate the parameters in (199), and thereby the spectrum of $\{x_k\}$, from a finite set of N data points.

The simulation method consists of the generation of 100 independent realizations of the process in (198) in steady state. The coefficients in (198) are estimated for each of the 100 realizations, and the corresponding 100 estimated spectra are computed by means of (108), for every technique in sections 4 and 5. The examples to be considered are summarized in table 2, where N is the number of data points in each realization (trial), and B is the number of bad points in each realization. The corresponding figures are collected together at the end of this section.

6.1 NO BAD DATA POINTS

In figure 4A, the 100 different estimated spectra, one for each of the 100 independent trials, are plotted for the Yule-Walker approach, and for N = 40 data points. In figure 4B, the (power) average spectrum of the 100 estimated spectra is plotted, along with the true spectrum of process (198) and (199). The true spectrum is scaled so that its area is equal to that of the average spectrum. It will be seen from figure 4A that there is a great deal of variability in the individual spectral estimates. From figure 4B, we observe that the

Table 2. Simulation Examples

Figure Number	Number of Data Points N	Number of Bad Points B	Technique
4	40	0	Yule-Walker
5	40	0	Yule-Walker, Unbiased
6	40	0	Least Squares of Box and Jenkins
7	40	0	Approximate Maximum Likelihood of Box and Jenkins
8	40	0	Prediction, Valid Error Points
9	40	0	Forward & Backward Prediction
10	40	0	Burg
11	40	0	Burg, Uniform Noise
12	40	4	Forward & Backward Prediction
13	40	4	Burg
14	100	0	Forward & Backward Prediction
15	100	0	Burg
16	100	10	Forward & Backward Prediction
17	100	10	Burg
18	100	20	Forward & Backward Prediction
19	100	20	Burg
20	100	30	Forward & Backward Prediction
21	100	30	Burg

average spectrum does not resolve the two narrowband peaks of the true spectrum*; in fact, this same conclusion is true for the individual spectra in figure 4A. A severe bias exists in the skirts of the average spectrum, which gives a gross overestimate of the power in bands away from the peaks. Thus, the Yule-Walker approach has poor resolution, severe bias, and substantial variability.

The corresponding results for the unbiased version of the Yule-Walker approacl are displayed in figure 5. Rather than improving the situation, it is found that the spectral estimates are worse in every regard. The spectral estimates with strong spikes near $f = \frac{1}{8\Delta}$ are manifestations of pole-pair locations of estimate (108) that are very close to the unit circle O. Recall from subsection 4.2 that the zeros of (112) need not lie inside O; see the discussion below (118).

The unbiased correlation estimates utilized above in the normal equations are of the same form as those suggested in reference 5 for missing data, when spectral estimation is attempted directly via (2). But since the performance of these unbiased correlation estimates is so poor here, they are not considered worthwhile in the presence of bad data points, when spectral estimation is accomplished via (108). Whether they are worthwhile for use in (2) is not known.

Results for the least-squares approach of Box and Jenkins are given in figure 6. The variability is less than that for the Yule-Walker estimates in figure 4A. And some resolution is achieved in figure 6B, in addition to good skirt selectivity. There is still, however, a large number of spiky spectral estimates, as anticipated in the discussion under (121).

Conditions are not much improved for the approximate maximum likelihood method of Box and Jenkins presented in figure 7. There happens to be one particular spectral estimate with a very large spike (a zero virtually on O) that severely influences the average power level. The variability in the estimated skirt level is quite small for this technique (as well as for the previous one).

In figure 8, the results for prediction using only the valid error points are presented. The resolution and bias in figure 8B are observed to be very good,

---

*This same conclusion is reached in reference 2, figure 5b, for the same number of data points. Increasing p (above 4) does recover some of the resolution of the two narrowband peaks, but it does not reduce the severe bias of the Yule-Walker approach.

and except for some spiky estimates in figure 8A, the variability of the individual estimates is fairly small.

The situation is still better when we consider forward and backward prediction, using only the valid error points, in figure 9. There are a couple of spiky estimates, but they are not excessively large, as they were previously. The bias and resolution are very good in figure 9B. Although the zeros of (112) need not remain inside O for this technique, it was found that in all 100 trials, no zeros were ever located outside of O. The presence of the two spiky estimates, however, indicates that on two occasions, a zero came close to the periphery of O.

One of the major drawbacks of this technique is the need to invert a non-Toeplitz matrix (or an equivalent operation) in order to evaluate the optimum filter coefficients; see (140). For large p, this is a significant numerical problem. We therefore attempted to convert the matrix $[S_{\ell m}]$ in (140) to a Toeplitz matrix, so that the recursive solution in appendix A could be utilized. We first averaged $[S_{\ell m}]_1^p$ down the diagonals and left the right-hand side of (140) as is; however, we lost resolution and got badly biased and more variable spectral estimates. Next we diagonally averaged $[S_{\ell m}]_0^p$ and left the right-hand side of (140) alone, but got the same bad effects. Finally, we diagonally averaged $[S_{\ell m}]_0^p$ and also replaced the terms on the right-hand side of (140) by the appropriate averages, but again to no avail. Thus, we are unable to significantly modify (140) without dire effects on the spectral estimate.

Finally, when the Burg technique is considered in figure 10, we observe the complete absence of spiky estimates; this is due mainly to the guaranteed location of the zeros of (A-10) inside O. In other respects, the results of figures 9 and 10 are very similar. There is a small bias in figure 10B, with the peaks being rounded off and the valley filled in; this is similar to figure 5 in reference 2.

All the results above have been conducted for Gaussian white noise $\{w_k\}$ in (198). To see the effect of the statistics of $\{w_k\}$ upon the spectral estimates, we changed to a uniform distribution. The results in figure 11 are virtually identical to those in figure 10. Accordingly, Gaussian statistics are kept for the remainder of the simulation.

6.2 BAD DATA POINTS

By virtue of the results of the preceding subsection, further consideration is limited to the forward and backward prediction technique and the Burg technique. The first example we consider is B = 4 bad data points out of a total of N = 40 data points; that is, in each of the 100 realizations of 40 data points, 4 points (no more, no less) were randomly selected as being bad, and the corresponding values of x_k were suppressed. In some of the realizations, the four data points may have been close together (for example, 10, 12, 14, 15), whereas in other realizations, they might have been far apart (for example, 1, 14, 27, 40).

The resulting spectral estimates are given in figures 12 and 13. The variability in the skirts is less for the forward and backward prediction technique than for the Burg technique. However, the spiky nature of the former technique is quite evident in comparison with the latter technique. Both techniques have suffered a significant loss of resolution near the narrowband peaks.

The reason for the significant degradation in performance of both techniques is that although only B/N = 4/40 (10%) of the points are bad, the number of valid error points, $N-p-B_p$ in (174) and (192), can decrease significantly. For example, for p = 4 and spaced bad points at $M_1 = 11$, $M_2 = 16$, $M_3 = 21$, $M_4 = 26$ (see (169)), we have

$$B_p = 20, \quad N - p - B_p = 16. \tag{200}$$

On the other hand, for contiguous bad points at $M_1 = 1$, $M_2 = 2$, $M_3 = 3$, $M_4 = 4$, we have

$$B_p = 4, \quad N - p - B_p = 32. \tag{201}$$

Thus, anywhere from 16 to 32 valid error points can be achieved. The stability of the spectral estimate for (200) will be less than that for (201). Generally, contiguous bad points are less damaging than spaced bad points, because more valid error points can be formed when the bad points are contiguous.

One of the points of the above example is that 4 bad data points out of 40 is rather detrimental. We consider now N = 100 data points. The first example of interest will serve as a comparison case and is B = 0. The results of spectral estimation for the forward and backward prediction technique and Burg

technique are given in figures 14 and 15, respectively. The results are virtually identical; there is excellent resolution and almost no bias for both techniques.

When B is increased to 10, the results in figures 16 and 17 are obtained. Despite 10% bad points, good performance in terms of stability, bias, and resolution is attained. The number, $N-p-B_D$, of valid data points can vary from 46 to 86; however, the likelihood of realizing as few as 46 on a random basis is very remote. The Burg technique has less-spiky estimates near the narrowband peaks, as expected; however, it is more variable in the skirts than the forward and backware prediction technique.

When B is increased to 20, the results in figures 18 and 19 indicate that the Burg technique has more variability, but is less spiky and has better resolution. The same conclusions hold true for B = 30 in figures 20 and 21; however, neither technique resolves the two narrowband peaks for this many bad data points.

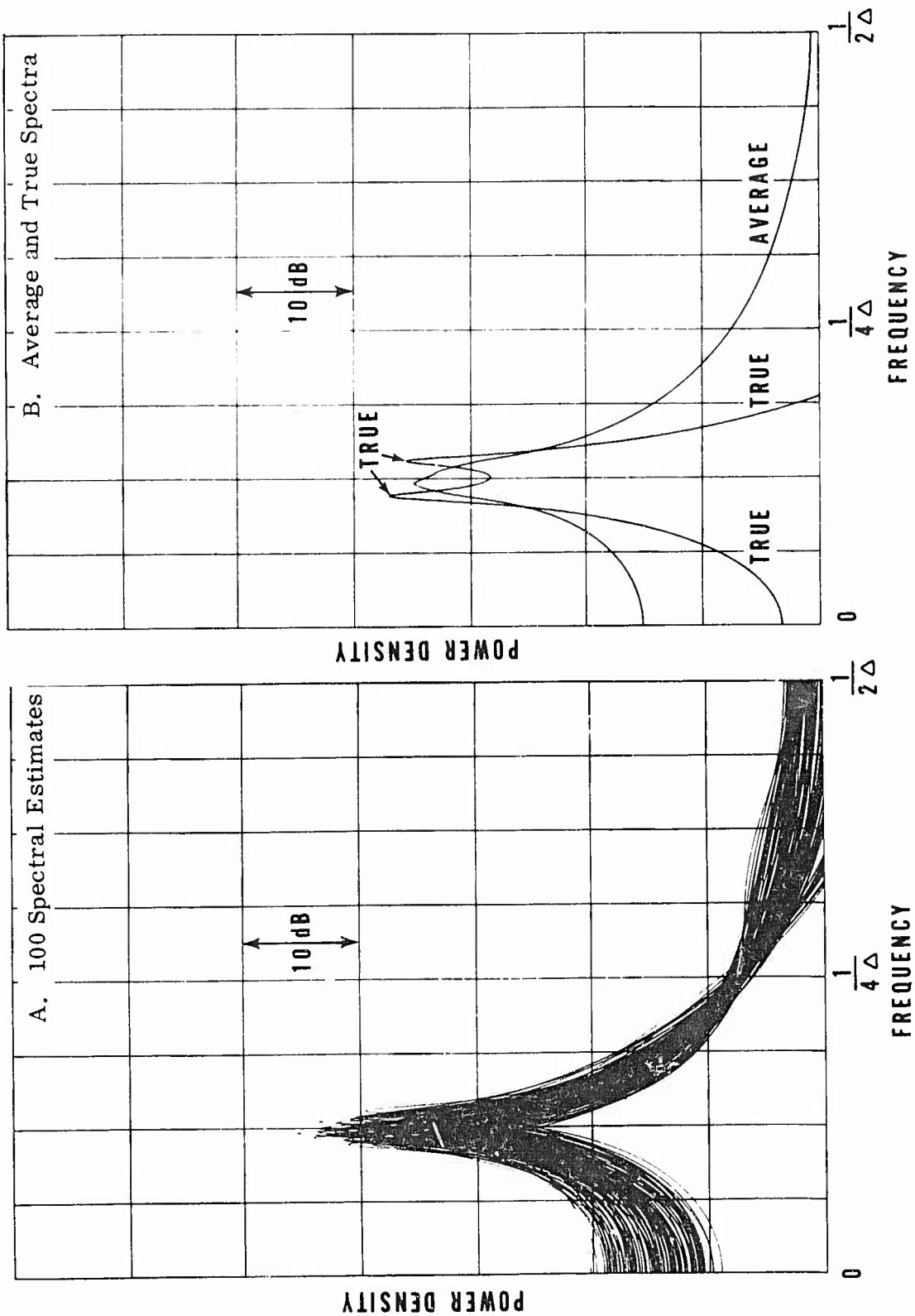


Figure 4. Yule-Walker; N = 40, B = 0

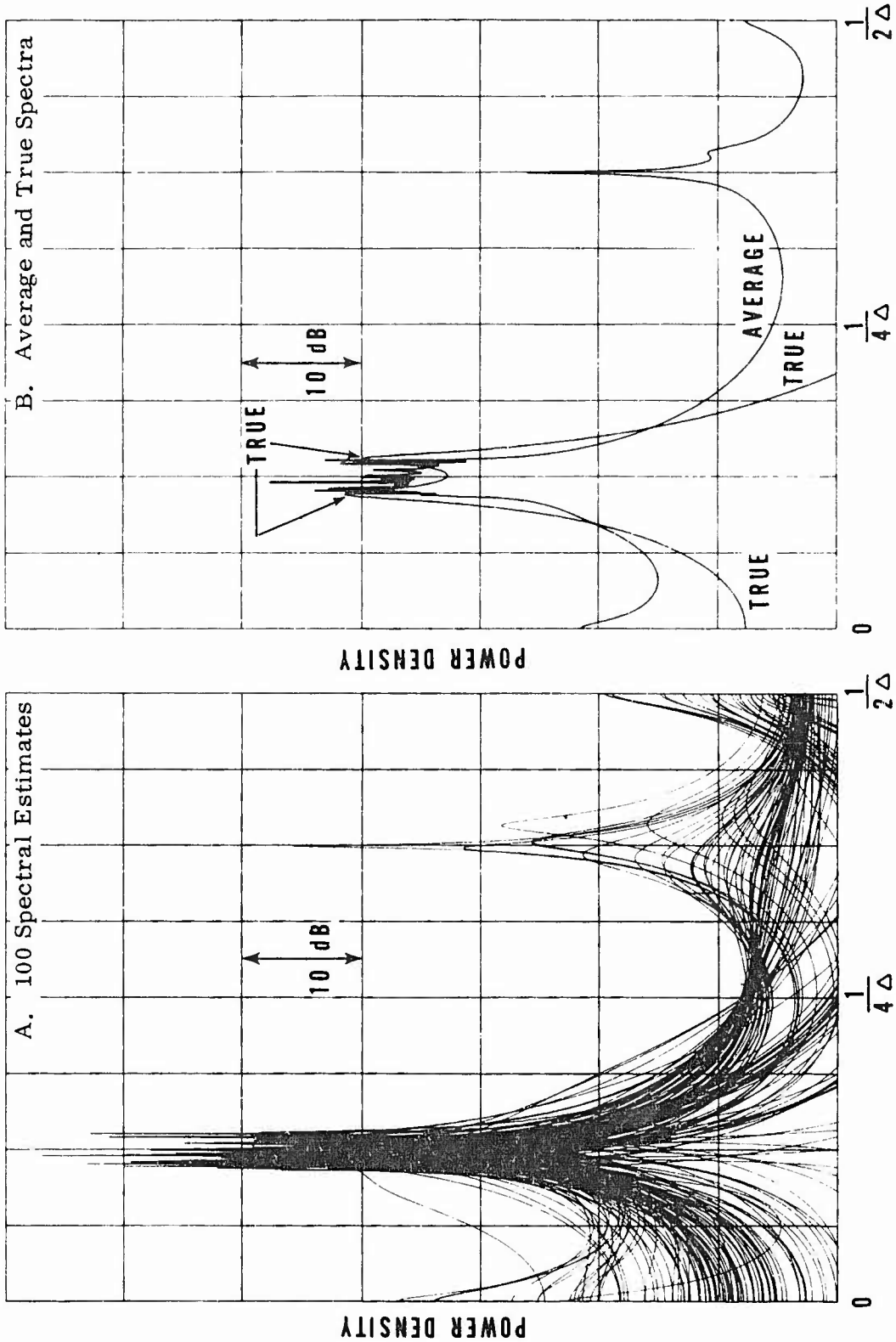


Figure 5. Yule-Walker, Unbiased; N = 40, B = 0

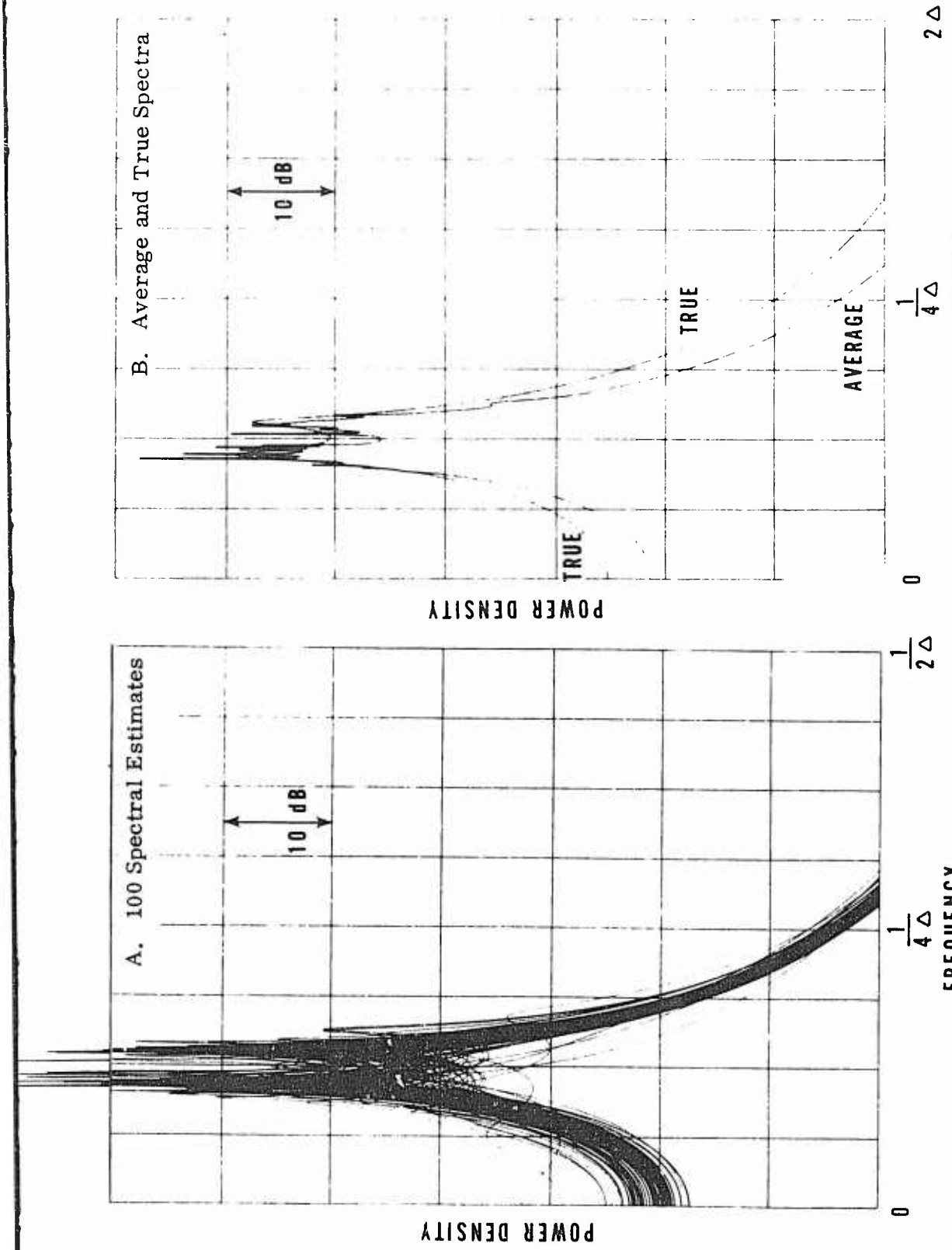


Figure 6. Least Squares of Box and Jenkins; N = 40, B = 0

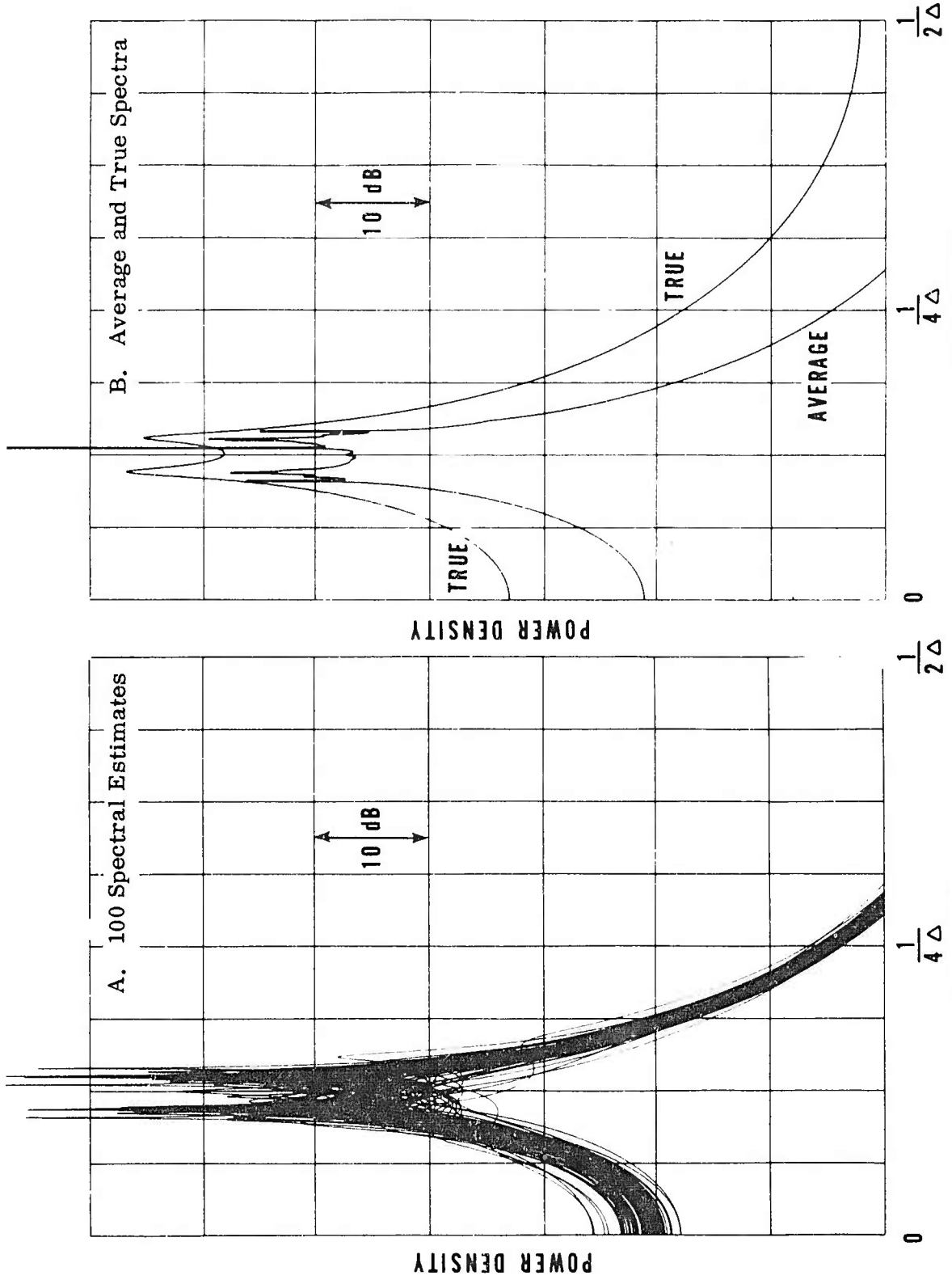


Figure 7. Approximate Maximum Likelihood of Box and Jenkins; N = 40, B = 0

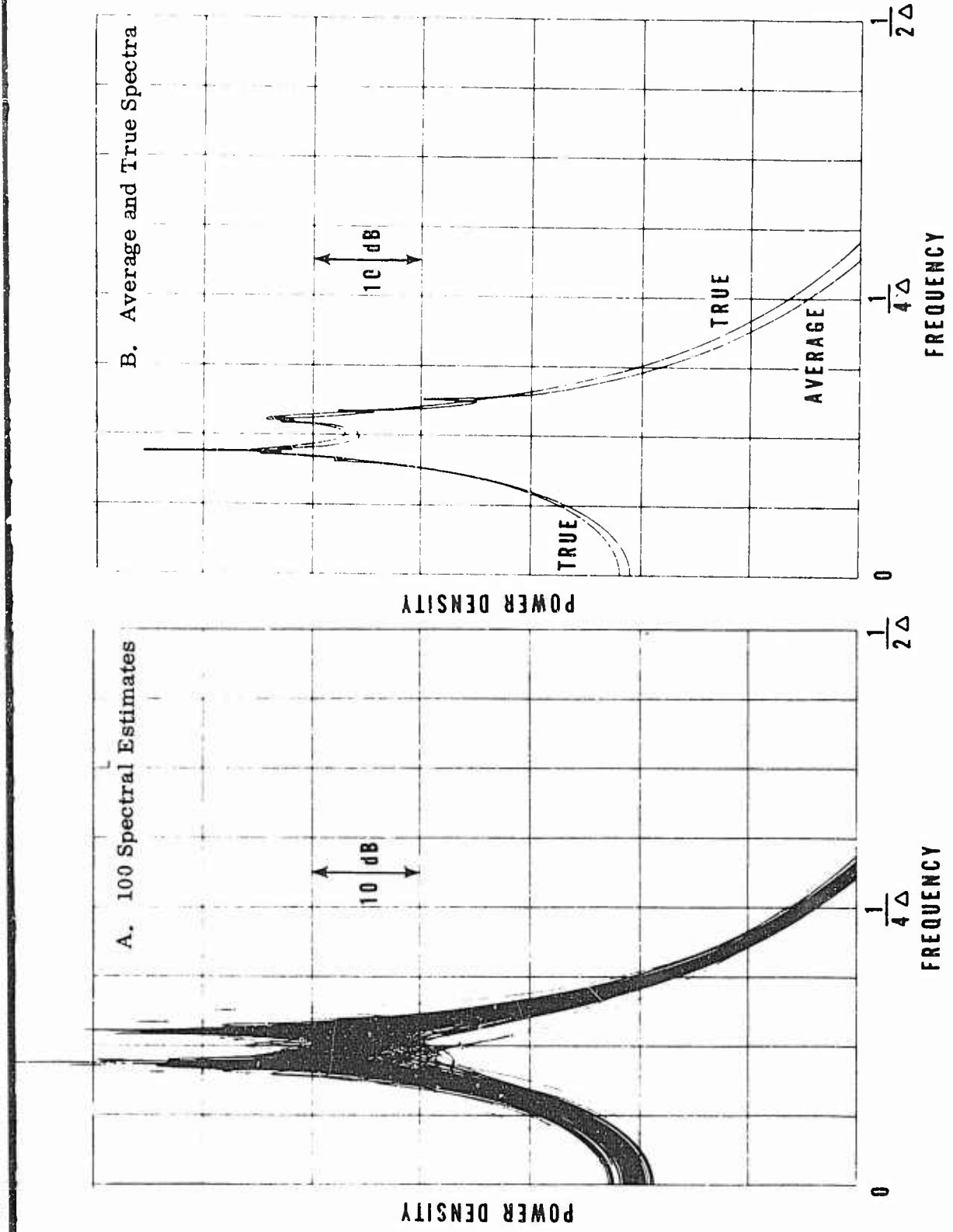


Figure 8. Prediction, Valid Error Points; N = 40, B = 0

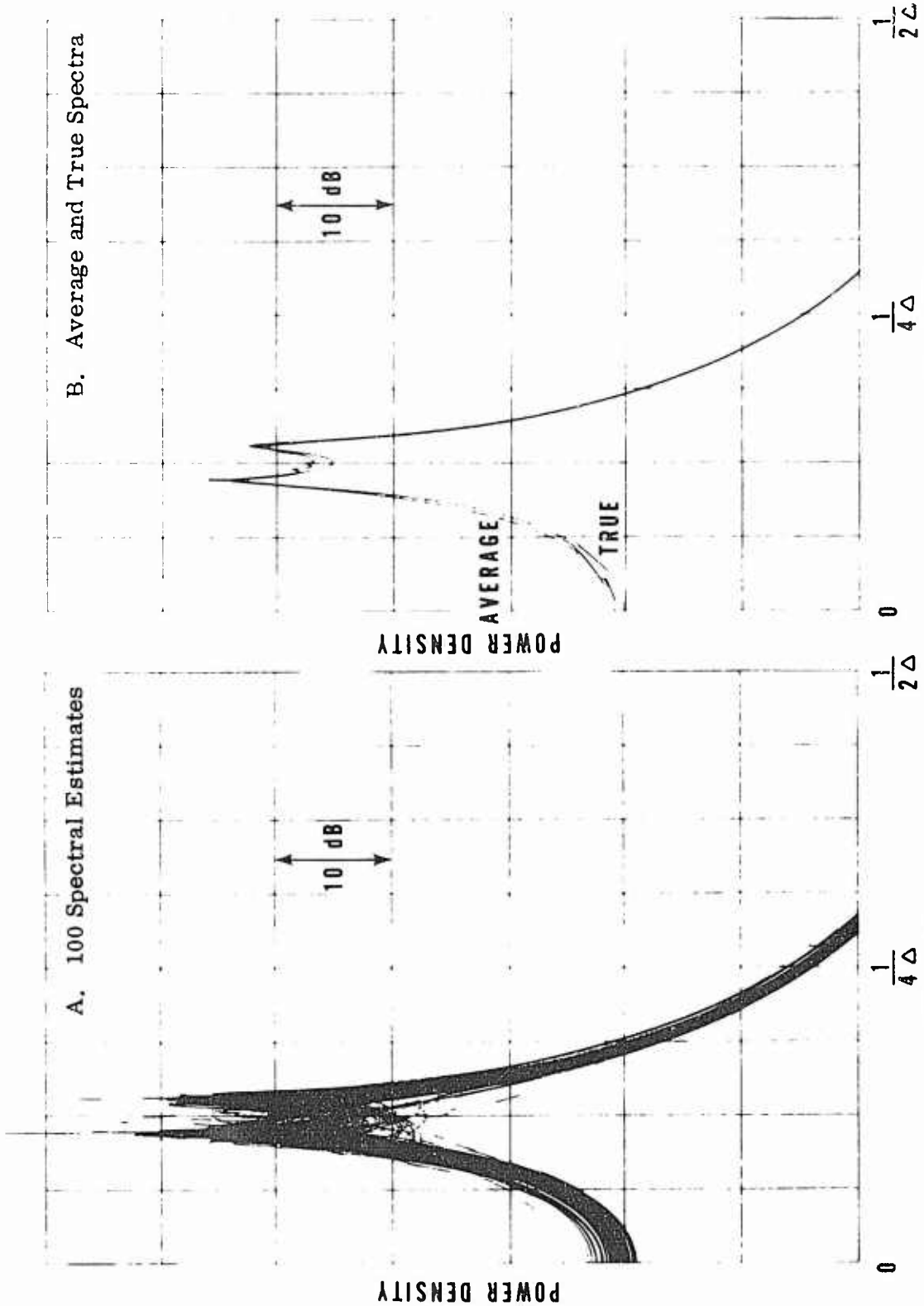


Figure 9. Forward and Backward Prediction; N = 40, B = 0

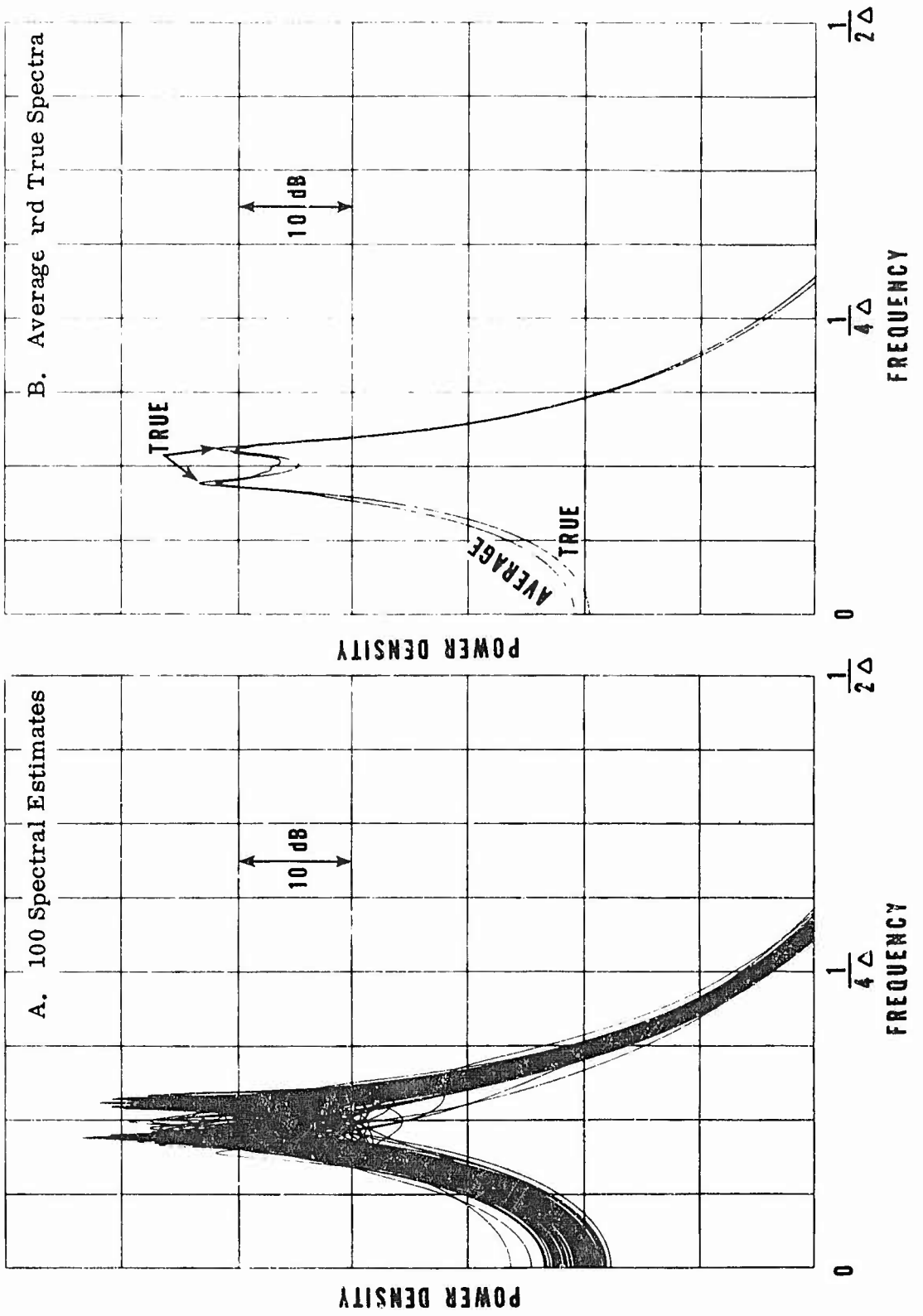


Figure 10. Burg; N = 40, B = 0

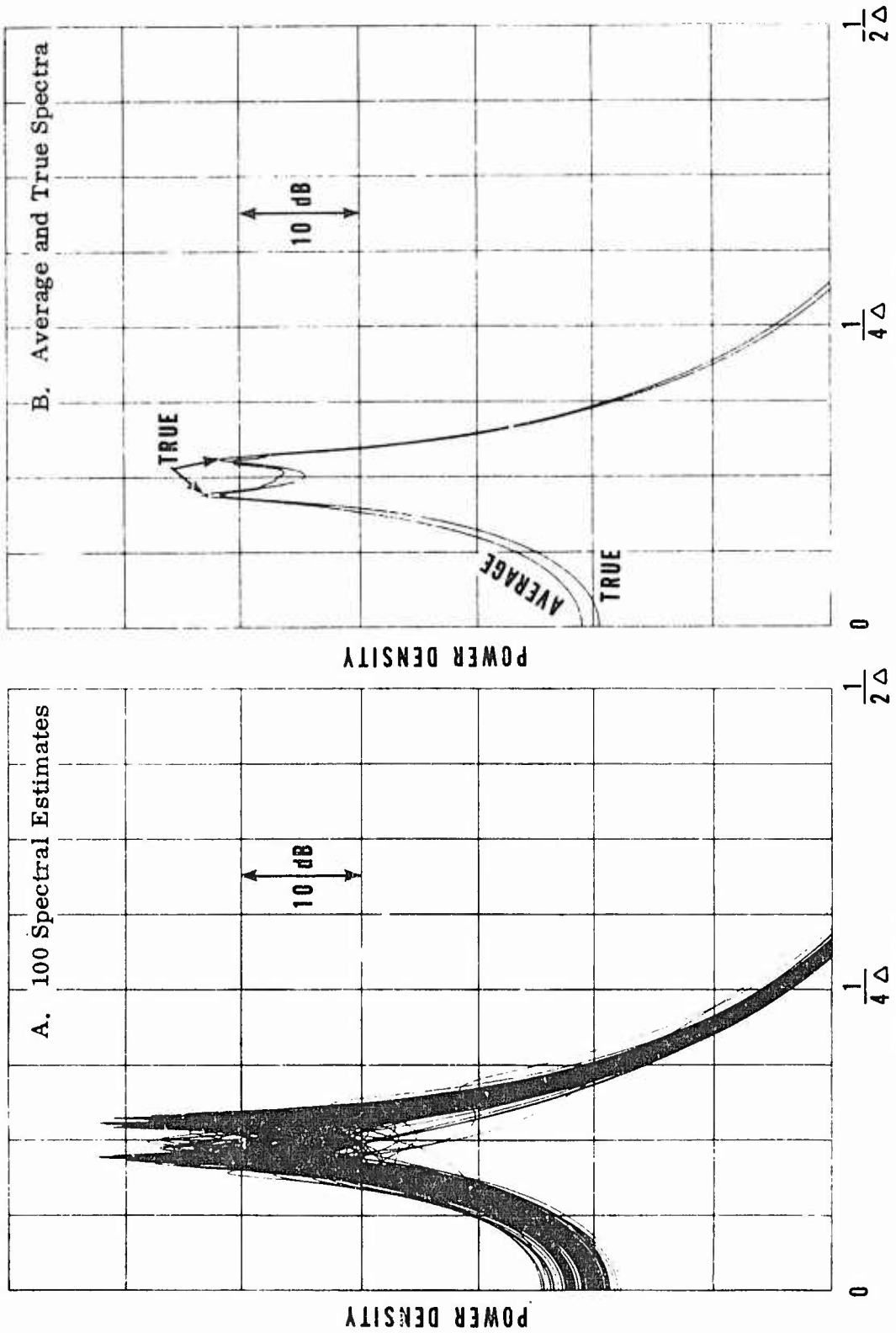


Figure 11. Burg, Uniform Noise; N = 40, B = 0

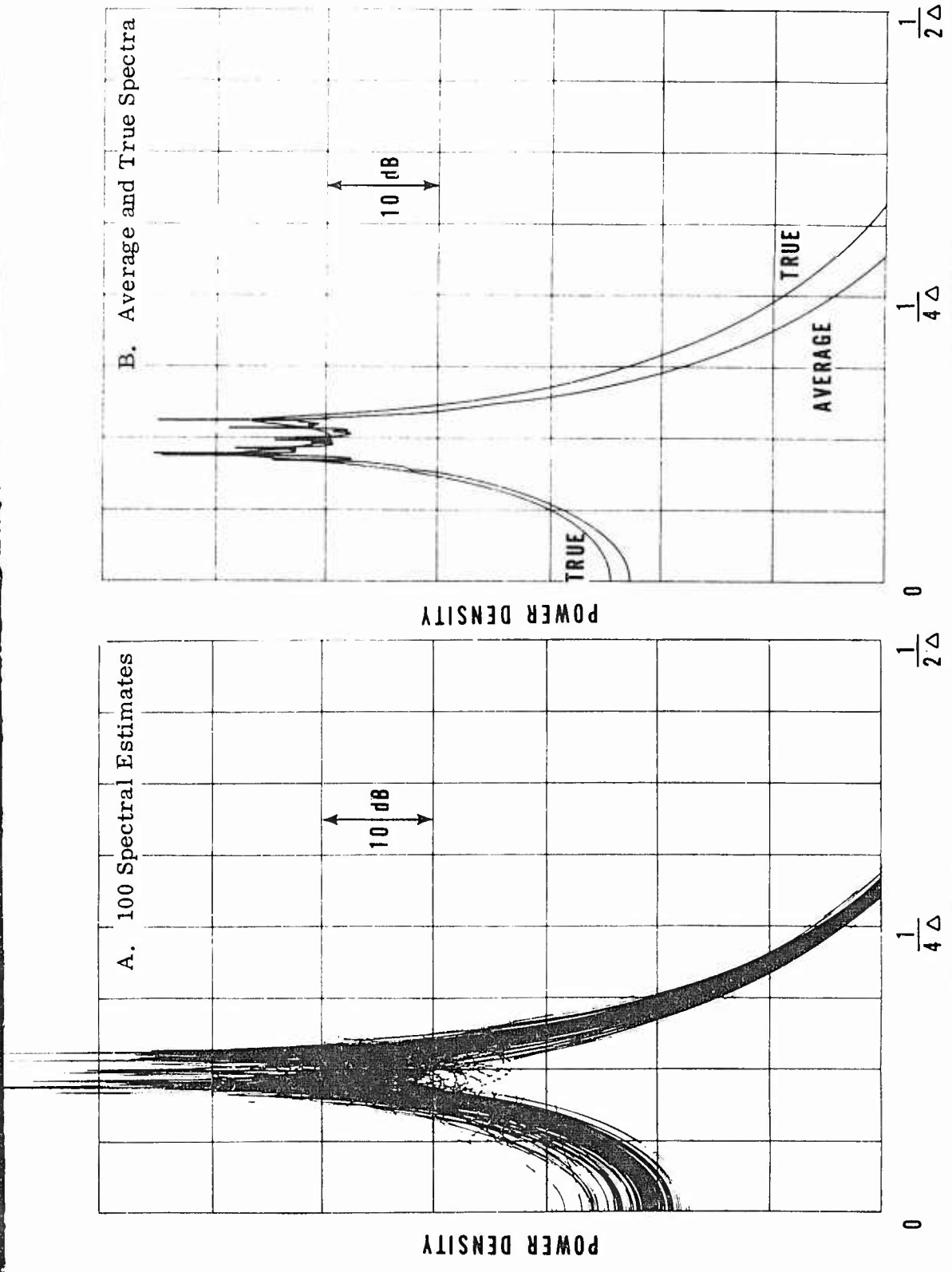


Figure 12. Forward and Backward Prediction; N = 40, B = 4

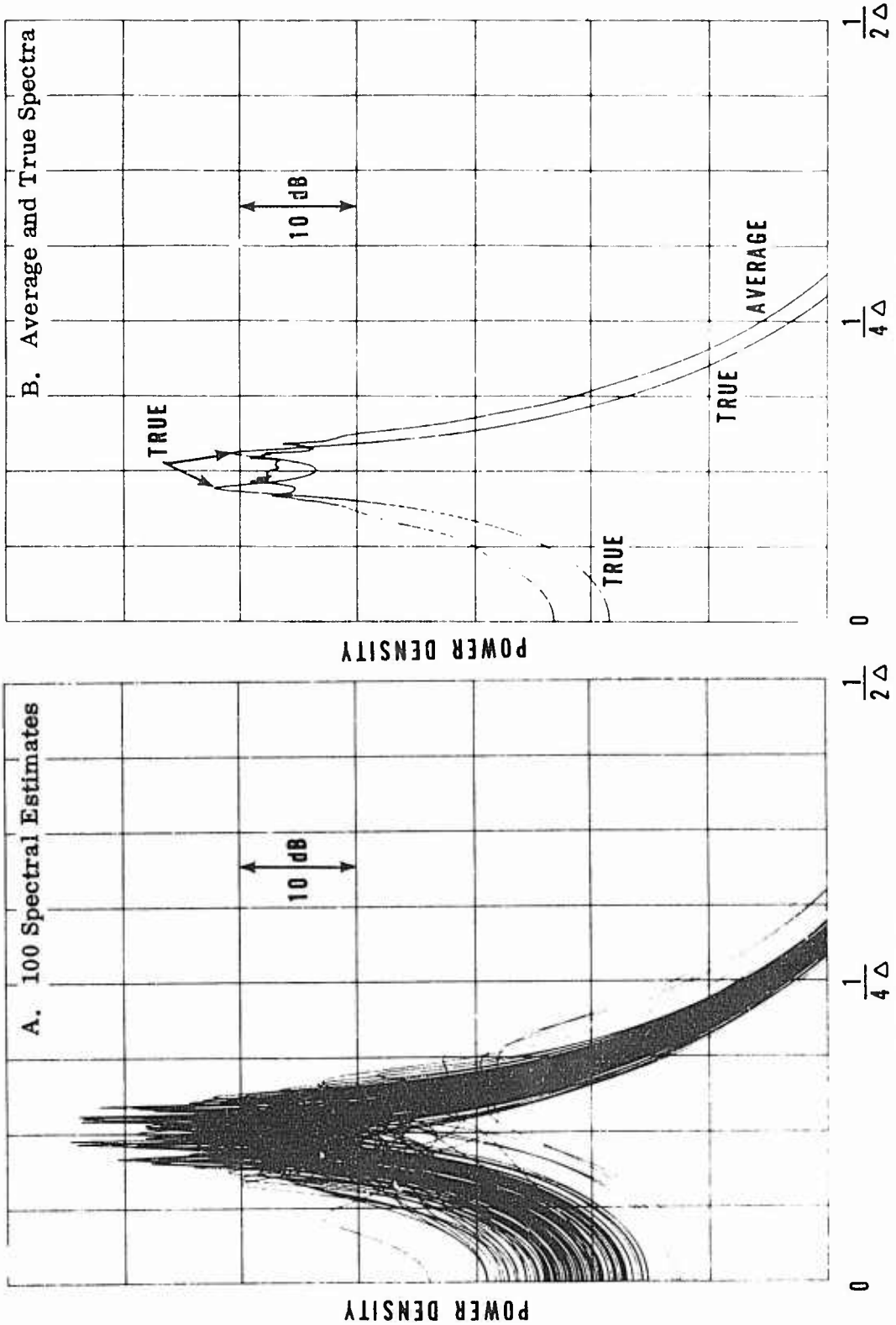


Figure 13. Burg; N = 40, B = 4

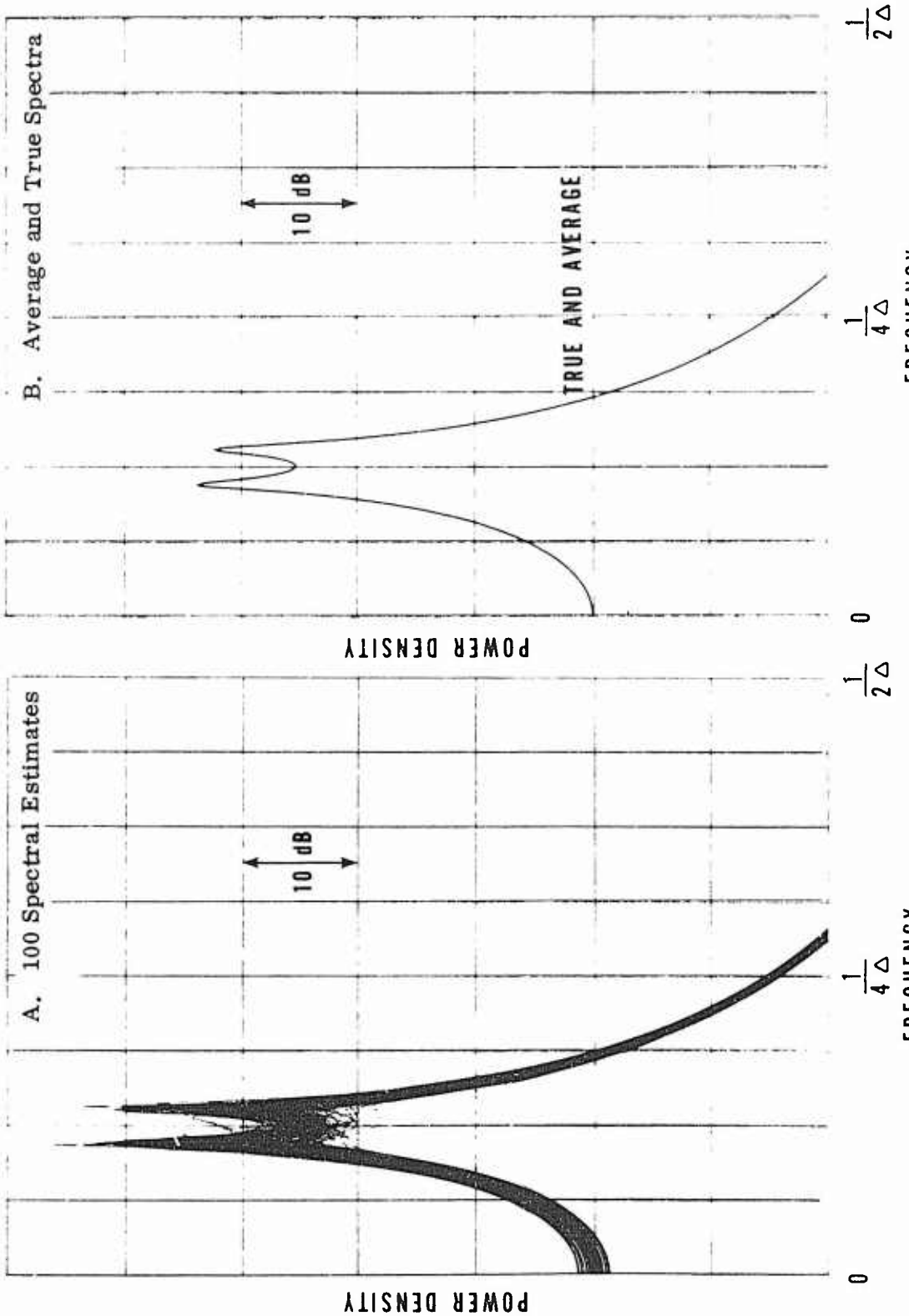


Figure 14. Forward and Backward Prediction; N = 100, B = 0

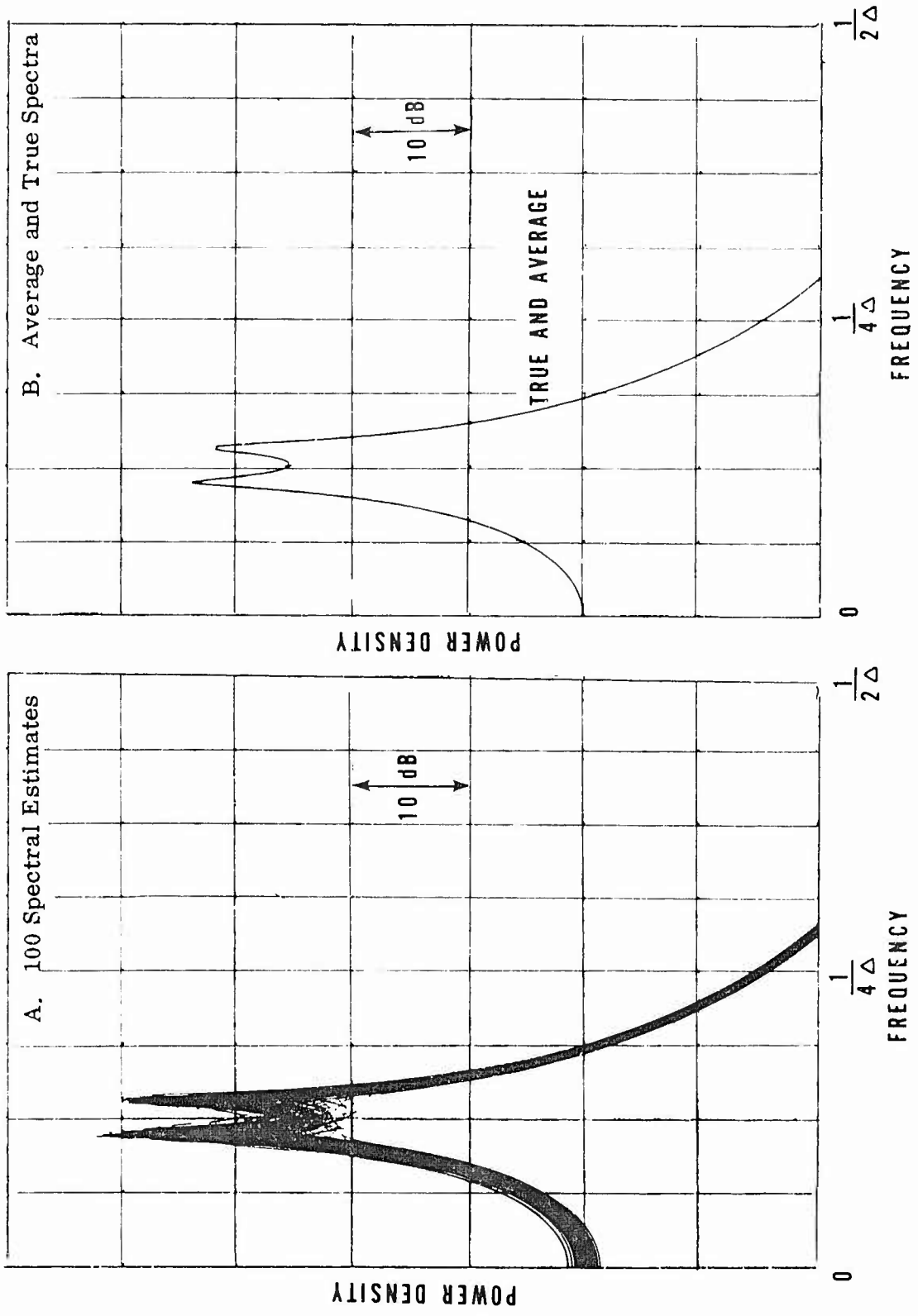


Figure 15. Burg; N = 100, B = 0

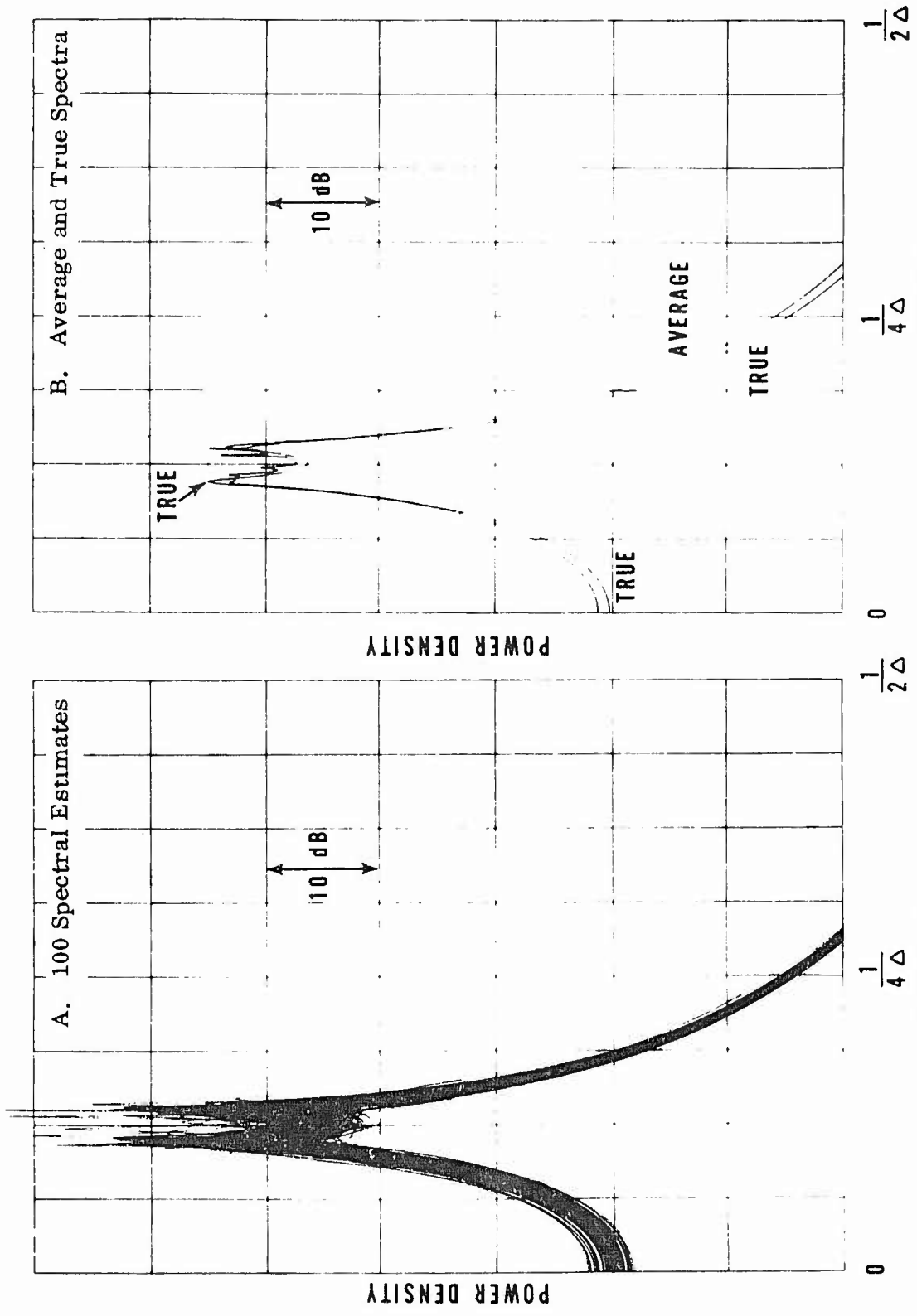


Figure 16. Forward and Backward Prediction; N = 100, B = 10

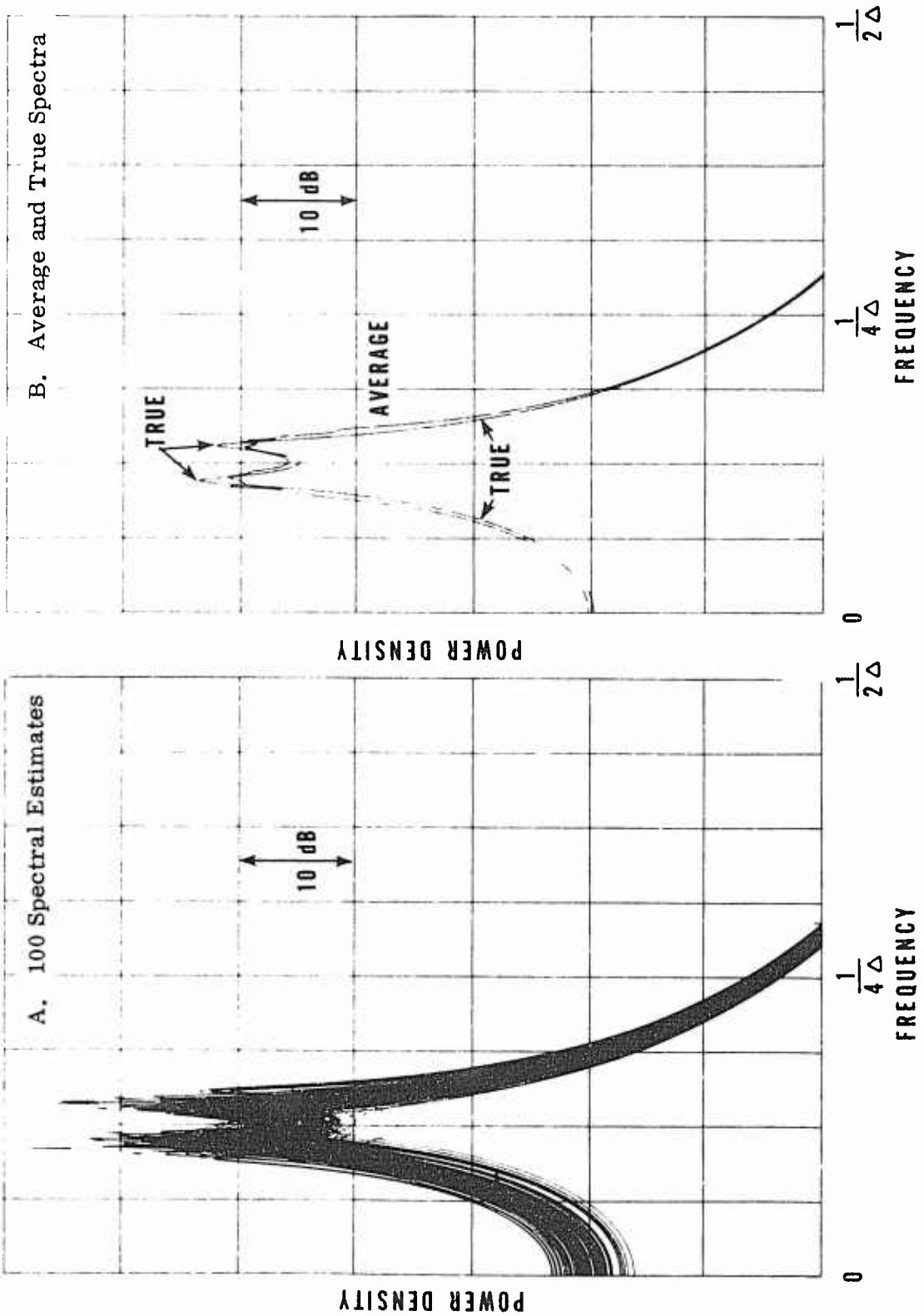


Figure 17. Burg; N = 100, B = 10

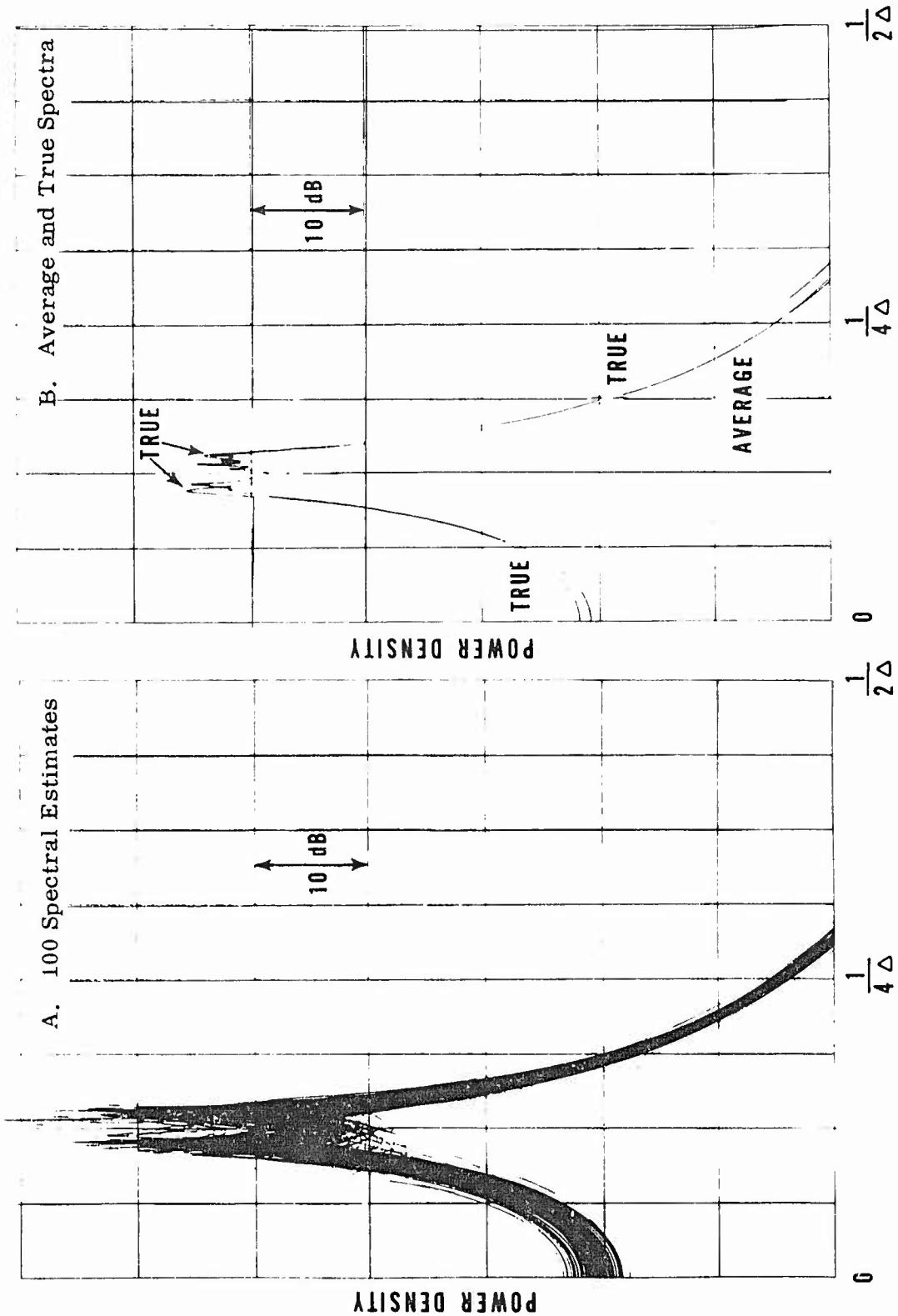


Figure 18. Forward and Backward Prediction; N = 100, B = 20

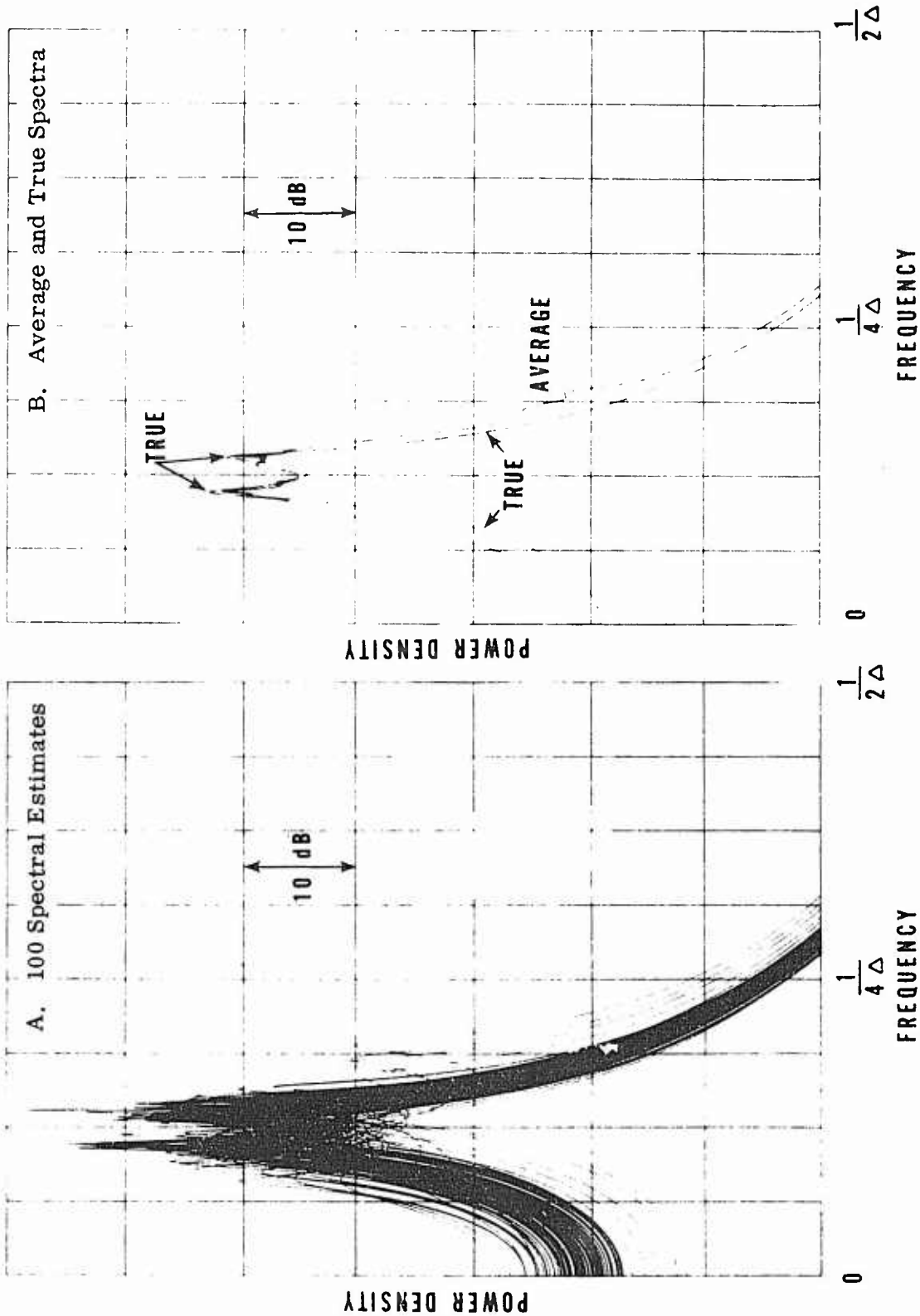


Figure 19. Burg; N = 100, B = 20

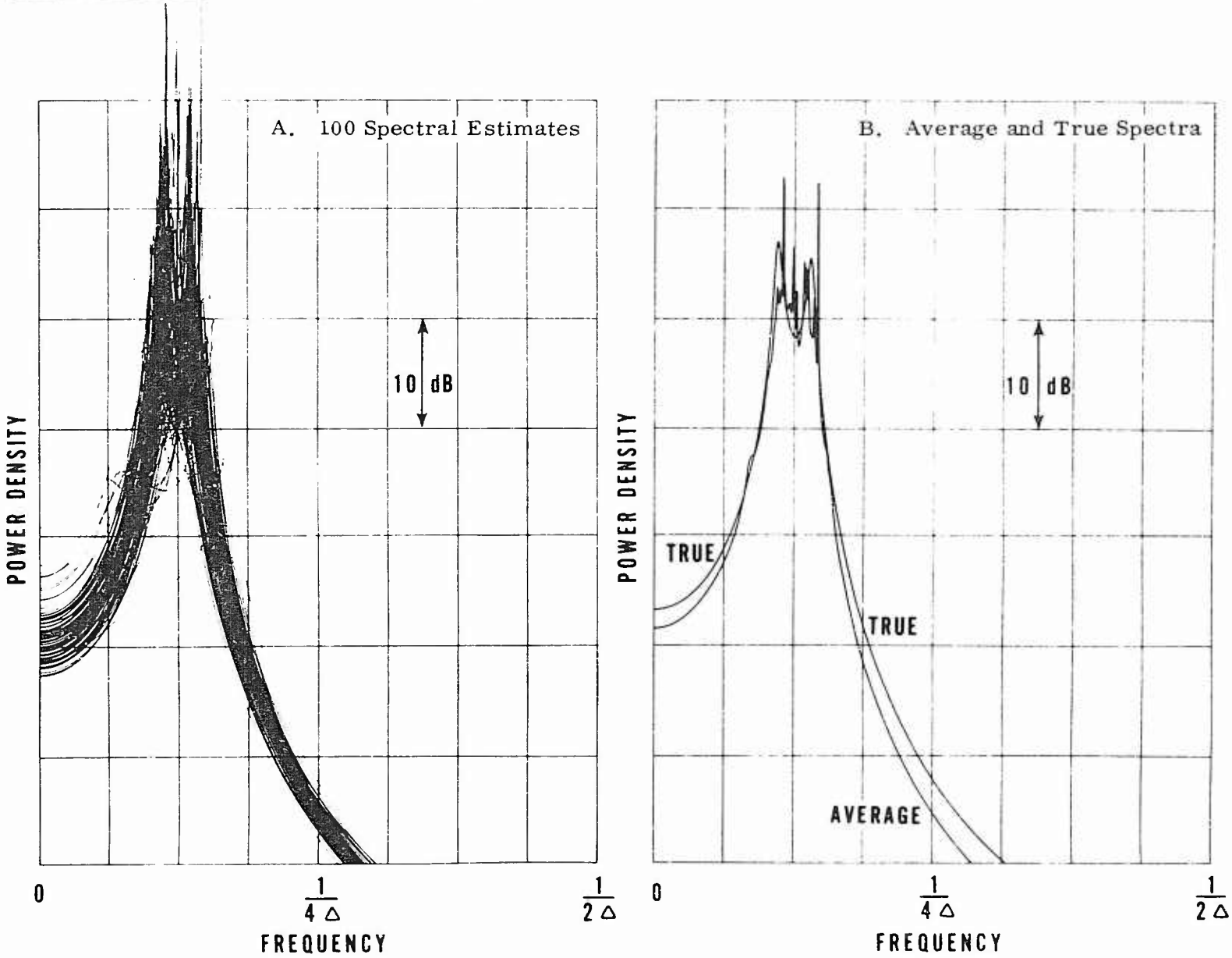


Figure 20. Forward and Backward Prediction; N = 100, B = 30

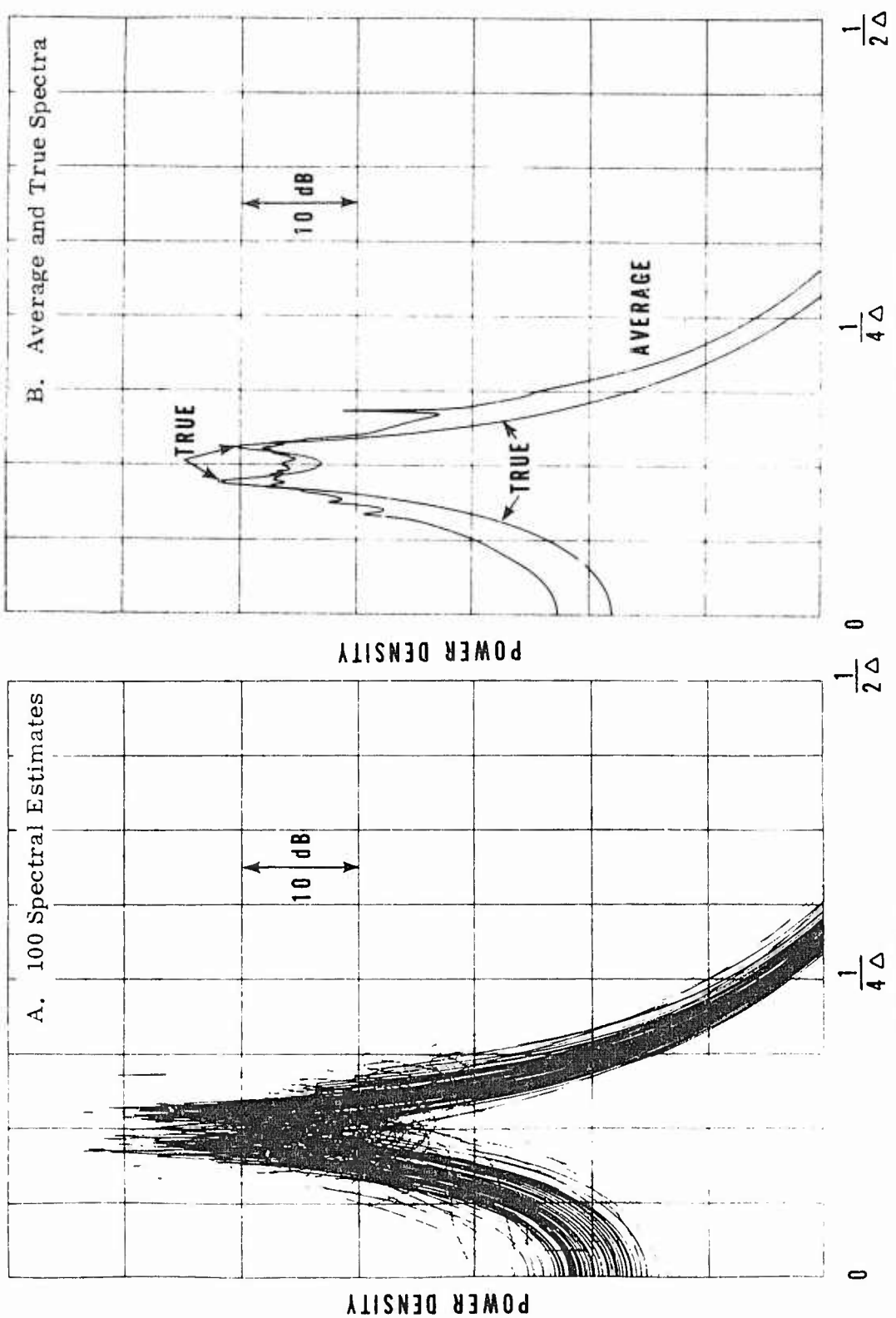


Figure 21. Burg: N = 100, B = 30

7. DISCUSSION AND CONCLUSIONS

Several methods of spectral estimation via linear predictive techniques have been considered for a univariate process, both with and without bad data points; the bad points can be regularly spaced, randomly spaced, or a combination. Two particular methods have been found to have better performance than the remainder, namely, the forward and backward prediction technique and the Burg technique. The former technique tends to have less variability on the skirts, but has more spiky estimates near the peaks of the spectrum; the latter technique has very few spiky estimates. Both techniques have comparable resolution and bias.

Since the best choice of filter order, p, is not known a priori, it is necessary in practice to make several guesses at this parameter and compute some error criterion that indicates when to terminate the recursion. In particular, Akaike's Information Criterion (reference 22) is often adopted as a termination procedure; it takes the form (reference 1, equations (91) and (41) or reference 22, page 719)

$$\text{AIC} = \ell n \ (\text{Relative Error}) + \frac{2p}{N_e} \qquad (\text{AIC}\,(p = 0) = 0) \ , \quad (202)$$

where N_e is the "effective" number of data points, and is taken as N-p (or N-p-B_p for bad points) here, at the p-th stage. The value of p at which (202) is a minimum is taken as the best estimate of this parameter; however, criterion (202) is not absolute, and the user can adjust it to fit his application (reference 1, page 575). A wide range of values of p may have to be investigated if little is known about the true spectrum a priori; an upper bound on p is given by Akaike as $3N^{1/2}$ (Ibid).

One of the ramifications of this successive guessing procedure is that for the forward and backward prediction technique, a different pxp matrix $[S_{nm}]_1^p$ must be inverted (or an equivalent operation conducted) at each stage (see (140) and (138)) in order to determine the filter coefficients and minimum error, (141). Although the matrix terms can be updated according to

$$S_{nm}^{(p+1)} = \frac{N-p}{N-p-1} S_{nm}^{(p)} - \frac{x_{p+1-m} x_{p+1-n}^* + x_{N-p+n} x_{N-p+m}^*}{2(N-p-1)} \ , \quad (203)$$

in addition to the relations in (139), the size of the matrix $[S_{nm}]_1^p$ grows with p, and the solution of (140) can be a time-consuming procedure, if many large values of p must be investigated. This fact, coupled with the fact that this spectral estimation technique can yield spiky estimates and an unstable recur-

sion relation (149), leads to the conclusion that, of the methods considered, the Burg technique is the recommended procedure for spectral analysis of univariate processes. A comparison with the maximum likelihood technique (reference 23) is underway and will be documented in a future report.

The solution for the filter coefficients in the Burg technique is accomplished recursively as shown in subsection 4.7 and automatically progresses through successively larger values of p at which error measures (150) and (156) are readily calculated. There is, of course, the need to update the forward and backward residuals via (153), and the calculation of cross-gain g_p in (155), both of which take time to effect. But the effort required actually decreases as p increases, since fewer terms are involved in (153) and (155); in exchange, the stability of the estimates also decreases.

FORTRAN programs for the Burg technique, both with and without bad data points, are given in appendix J. Some representative execution times on the Univac 1108 for the computation of the filter coefficients (SUBROUTINE BURG) are given in table 3, where N is the number of data points and PMAX is the maximum order of filter considered. The times are approximately linearly proportional to N and PMAX. The execution time for the evaluation of the power density estimate itself is governed by the FFT technique employed to evaluate (167) (SUBROUTINE POWERS).

Table 3. Execution Times; No Bad Data Points

N	PMAX	Time (sec)
100	10	0.038
100	20	0.073
1000	10	0.33
1000	50	1.78
10000	50	17.9
10000	150	48.4

The presence of bad data points is easily accommodated in the Burg technique, as shown in subsection 4.7. If the bad data points are contiguous, the loss in stability of the estimates is not as great as when the bad data points are spaced. The worst possible locations of bad data points occur when the closest spacing is $\geq p + 1$, since each bad data point causes the loss of $p + 1$ valid error points. Interpolation of spaced bad data points has proven poorer than the technique utilized here (of ignoring bad points) when the spectral content of the input process extends fairly close to the Nyquist frequency $(2\Delta)^{-1}$. Since the exact extent of the input spectrum is unknown a priori, interpolation can be a damaging procedure in some cases.

The spectral estimation technique investigated here is particularly advantageous for short data segments, where other methods are inapplicable. For example, if a piece of equipment fails frequently, short disjointed pieces of data may be all that are available. Or if a process is nonstationary, it may be necessary to cut the total data record into small segments in each of which it is believed that conditions are substantially stationary. For longer data records, where standard FFT techniques can be applied, it has been recommended that both spectral estimation procedures be applied and the results plotted together to glean maximum information about the true spectrum (see reference 12). This seems particularly useful when some pure tones are present in the input data; the standard FFT technique is ideally suited for the analysis of pure tones or very narrowband components.

REVERSE BLANK

Appendix A

RECURSIVE SOLUTION

If we employ (52) in (46), there results

$$\sum_{k=0}^{p} R_{\ell-k} \frac{\alpha_k^*}{\alpha_o^*} = \frac{1}{c_{oo}} \delta_{\ell o}, \quad 0 \le \ell \le p. \tag{A-1}$$

Now define

$$\frac{\alpha_k^*}{\alpha_o^*} = - a_k^{(p)}, \quad 0 \le k \le p, \tag{A-2}$$

where the dependence of the coefficients on the order p in (31) is indicated explicitly. Then (A-1) becomes

$$\begin{bmatrix} R_o & R_{-1} & \cdots & R_{-p} \\ R_1 & R_o & & \\ \vdots & & \ddots & \\ R_p & & & R_o \end{bmatrix} \begin{bmatrix} 1 \\ -a_1^{(p)} \\ \vdots \\ -a_p^{(p)} \end{bmatrix} = \begin{bmatrix} 1/c_{oo}^{(p)} \\ 0 \\ \vdots \\ 0 \end{bmatrix} \tag{A-3}$$

where the matrix R is Hermitian and where we have also indicated that the real quantity c_{oo} is dependent on p; see (47) and (51). Equation (A-3) constitutes p+1 linear equations in the p+1 unknowns $a_1^{(p)}, \ldots, a_p^{(p)}, 1/c_{oo}^{(p)}$.

The solution to (A-3) can be obtained recursively as follows (see, for example, reference 11 or reference 24, appendix B):

$$a_1^{(1)} = R_1/R_o, \quad \frac{1}{c_{oo}^{(1)}} = R_o - R_{-1} a_1^{(1)} = R_o \left(1 - \left|a_1^{(1)}\right|^2\right); \tag{A-4}$$

for $p \geq 2$:

$$a_p^{(p)} = \frac{R_p - \sum_{k=1}^{p-1} a_k^{(p-1)} R_{p-k}}{R_o - \sum_{k=1}^{p-1} a_k^{(p-1)} R_k^*} = \left[R_p - \sum_{k=1}^{p-1} a_k^{(p-1)} R_{p-k} \right] c_{oo}^{(p-1)}, \quad (A-5)$$

$$a_k^{(p)} = a_k^{(p-1)} - a_p^{(p)} a_{p-k}^{(p-1)*}, \quad k = 1, 2, \ldots, p-1, \quad (A-6)$$

$$\frac{1}{c_{oo}^{(p)}} = R_o - \sum_{k=1}^{p} a_k^{(p)} R_k^* = R_o - a_p^{(p)} R_p^* - \sum_{k=1}^{p-1} a_k^{(p)} R_k^* = \frac{1}{c_{oo}^{(p-1)}} \left(1 - \left| a_p^{(p)} \right|^2 \right). \quad (A-7)$$

The last step in (A-7) is obtained by substituting (A-6) and employing (A-5). It is very important to notice from (A-6) that once $a_p^{(p)}$ is specified, all the p-th order filter coefficients can be calculated from (p-1)th order coefficients. The same is true of (A-7).

If we use (A-2) and (53), the maximum entropy spectrum in (55) can be expressed as

$$G_o(f) = \frac{\Delta / c_{oo}^{(p)}}{\left| \sum_{k=0}^{p} a_k^{(p)} \exp(-i2\pi f k \Delta) \right|^2}, \quad |f| < \frac{1}{2\Delta}. \quad (A-8)$$

The similarity in form to (14) will be complete when it is shown (in (67)) that $1/c_{oo}^{(p)}$ is the minimum value of the average magnitude-squared error for a p-th order predictive filter; therefore $c_{oo}^{(p)}$ must be positive for all p, for non-negative definite R. Equation (A-7) offers a recursive calculation of the average error; it can be started with $\frac{1}{c_{oo}^{(p)}} = R_o$. (In fact, (A-5) through (A-7) can be used for $p \geq 1$ when that starting value is used.)

Since $c_{oo}^{(p)}$ must be positive for all p, (A-7) indicates that

$$\left| a_k^{(k)} \right| \leq 1 \text{ for } k = 1, 2, \ldots, p . \tag{A-9}$$

This is equivalent to having all the zeros of

$$\sum_{k=0}^{p} a_k^{(p)} z^{-k} , \tag{A-10}$$

(where the remaining coefficients are determined via (A-6)) inside the unit circle, O, in the complex z-plane; see reference 1, page 567. Therefore

$$B^{(p)}(z) \equiv \sum_{k=0}^{p} a_k^{(p)} z^k \tag{A-11}$$

has no zeros inside O.

Appendix B

EVALUATION OF MAXIMUM ENTROPY

The optimum spectrum is given by (36) and (37). The maximum entropy then follows from (30) as

$$\text{Ent} \equiv \Delta \int_{1/\Delta} df\, \ell n\, G_o(f) = -\Delta \int_{1/\Delta} df\, [\ell n \gamma(f) + \ell n \gamma^*(f)] \equiv \mathcal{E}_1 + \mathcal{E}_2 . \tag{B-1}$$

Consider

$$\mathcal{E}_1 = -\Delta \int_{1/\Delta} df\, \ell n \left\{ \sum_{k=0}^{p} \alpha_k \exp(i2\pi fk\Delta) \right\} . \tag{B-2}$$

Letting $z = \exp(i2\pi f\Delta)$ and using (38), (B-2) becomes

$$\mathcal{E}_1 = -\frac{1}{i2\pi} \oint \frac{dz}{z}\, \ell n\, B(z) , \tag{B-3}$$

where $\oint$ denotes counterclockwise integration around the unit circle, O, in the complex z-plane. Now

$$B(z) = \sum_{k=0}^{p} \alpha_k z^k = \alpha_p \prod_{k=1}^{p} (z - o_k) \tag{B-4}$$

where, from (A-14), zero locations $\{o_k\}$ satisfy

$$|o_k| > 1, \text{ all } k; \tag{B-5}$$

that is, all the zeros of B(z) lie outside O. (There can be multiple-order zeros in (B-4).) Also assume $p \geq 1$ for now. Then (B-3) can be expressed as

$$\mathcal{E}_1 = -\frac{1}{i2\pi}\oint \frac{dz}{z}\left[\ell n\ \alpha_p + \sum_{k=1}^{p} \ell n\ (z - o_k)\right]$$

$$= -\left[\ell n\ \alpha_p + \sum_{k=1}^{p} \frac{1}{i2\pi}\oint \frac{dz}{z}\,\ell n\ (z - o_k)\right]. \qquad \text{(B-6)}$$

But

$$\ell n\ (z - o_k) = \ell n\ (-o_k) + \ell n\ \left(1 - \frac{z}{o_k}\right)$$

$$= \ell n\ (-o_k) - \frac{z}{o_k} - \left(\frac{z}{o_k}\right)^2 - \ldots \text{ for } \left|\frac{z}{o_k}\right| < 1\,; \qquad \text{(B-7)}$$

that is, expansion (B-7) converges for $|z| < |o_k|$. But since $|o_k| > 1$, the region of integration in (B-6) remains in the convergence region of (B-7). Therefore, the integral in (B-6) is

$$\frac{1}{i2\pi}\oint \frac{dz}{z}\,\ell n\ (z - o_k) = \frac{1}{i2\pi}\oint \frac{dz}{z}\left\{\ell n\,(-o_k) - \frac{z}{o_k} - \left(\frac{z}{o_k}\right)^2 - \ldots\right\} = \ell n\ (-o_k)\,. \qquad \text{(B-8)}$$

Then from (B-6) and (B-4)

$$\mathcal{E}_1 = -\left[\ell n\ \alpha_p + \sum_{k=1}^{p} \ell n\ (-o_k)\right] = -\ell n\left[\alpha_p \prod_{k=1}^{p} (-o_k)\right]$$

$$= -\ell n\ B(0) = -\ell n\ \alpha_o\,. \qquad \text{(B-9)}$$

And from (B-1) and (B-4)

$$\mathcal{E}_2 = -\Delta \int_{1/\Delta} df\ \ell n\ \gamma^*(f) = -\Delta \int_{1/\Delta} df\ \ell n\left\{\sum_{k=0}^{p} \alpha_k^*\ \exp(i2\pi fk\Delta)\right\}$$

$$= -\frac{1}{i2\pi}\oint\frac{dz}{z}\,\ell n\left\{\sum_{k=0}^{p}\alpha_k^* z^{-k}\right\} = -\frac{1}{i2\pi}\oint\frac{dz}{z}\,\ell n\ B^*\left(\frac{1}{z^*}\right)$$

$$= -\frac{1}{i2\pi}\oint\frac{dz}{z}\,\ell n\left\{\alpha_p^*\prod_{k=1}^{p}\left(\frac{1}{z}-o_k^*\right)\right\}$$

$$= -\frac{1}{i2\pi}\oint\frac{dz}{z}\left[\ell n\ \alpha_p^* + \sum_{k=1}^{p}\ell n\left(\frac{1}{z}-o_k^*\right)\right]$$

$$= -\left[\ell n\ \alpha_p^* + \sum_{k=1}^{p}\frac{1}{i2\pi}\oint\frac{dz}{z}\,\ell n\left(\frac{1}{z}-o_k^*\right)\right]. \qquad \text{(B-10)}$$

Now

$$\ell n\left(\frac{1}{z}-o_k^*\right) = \ell n\left(-o_k^*\right) + \ell n\left(1-\frac{1}{o_k^* z}\right)$$

$$= \ell n\left(-o_k^*\right) - \frac{1}{o_k^* z} - \left(\frac{1}{o_k^* z}\right)^2 - \ldots \text{ for } \left|\frac{1}{o_k^* z}\right| < 1; \qquad \text{(B-11)}$$

that is, expansion (B-11) converges for $|z| > \frac{1}{|o_k^*|}$. But since $|o_k| > 1$, the region of integration in (B-10) remains in the convergence region of (B-11). Therefore, the integral in (B-10) is

$$\frac{1}{i2\pi}\oint\frac{dz}{z}\,\ell n\left(\frac{1}{z}-o_k^*\right) = \frac{1}{i2\pi}\oint\frac{dz}{z}\left\{\ell n\left(-o_k^*\right) - \frac{1}{o_k^* z} - \left(\frac{1}{o_k^* z}\right)^2 - \ldots\right\} = \ell n\left(-o_k^*\right). \qquad \text{(B-12)}$$

Then from (B-10) and (B-4)

$$\mathcal{E}_2^{\circ} = -\left[\ell n\ \alpha_p^* + \sum_{k=1}^{p}\ell n\ (-o_k^*)\right] = -\ell n\left[\alpha_p^*\prod_{k=1}^{p}(-o_k^*)\right]$$

$$= -\ell n\ B^*(0) = -\ell n\ \alpha_o^*. \qquad \text{(B-13)}$$

Combining (B-9) and (B-13) in (B-1), there follows for the maximum entropy

$$\text{Ent} = -\ell n \left|\alpha_o\right|^2 = \ell n \ (\Delta/c_{oo}) , \qquad \text{(B-14)}$$

where we have also employed (52). (For p = 0, a separate derivation yields (B-14) also.) Recall from (51) that c_{oo} is the upper-left corner element of R^{-1}, where R is defined by (47).

Appendix C

IMPLICATIONS OF ASSUMPTION OF WHITE SPECTRUM FOR MINIMUM ERROR; KNOWN CORRELATION

We define the crosscorrelation function between minimum error $\tilde{\epsilon}$ and input x in figure 1 as

$$C_\ell = \overline{\tilde{\epsilon}_k \, x^*_{k-\ell}}, \text{ all } \ell \, . \tag{C-1}$$

Substituting (59) and utilizing (1), this becomes

$$C_\ell = \sum_{n=0}^{p} \tilde{a}_n \, R_{\ell-n}, \text{ all } \ell \, . \tag{C-2}$$

Now from (64) and (65), we can express

$$R \, \tilde{a} = - \frac{1}{c_{oo}} \, \delta \, . \tag{C-3}$$

Thus, (C-2) immediately yields

$$C_\ell = \left\{ \begin{array}{c} -1/c_{oo}, \ \ell = 0 \\ \\ 0, \ 1 \leq \ell \leq p \end{array} \right\} ; \tag{C-4}$$

that is, minimum error value $\tilde{\epsilon}_k$ is uncorrelated with the past p inputs x_{k-1}, $\ldots$, x_{k-p}.

Now using (59) and (C-1), the autocorrelation function of the minimum error is

$$E_\ell \equiv \overline{\tilde{\epsilon}_k \, \tilde{\epsilon}^*_{k-\ell}} = \sum_{n=0}^{p} \tilde{a}^*_n \, \overline{\tilde{\epsilon}_k \, x^*_{k-\ell-n}} = \sum_{n=0}^{p} \tilde{a}^*_n \, C_{\ell+n}, \text{ all } \ell \, . \tag{C-5}$$

In particular, using (C-4),

$$E_1 = \tilde{a}_p^* \, C_{p+1} . \tag{C-6}$$

But from (C-2) and (66),

$$C_{p+1} = \sum_{n=0}^{p} \tilde{a}_n \, R_{p+1-n} = - R_{p+1} - \sum_{n=1}^{p} \frac{c_{no}}{c_{oo}} \, R_{p+1-n} . \tag{C-7}$$

Therefore, assuming $E_1 = 0$ is equivalent to assuming $C_{p+1} = 0$, (that is, minimum error $\tilde{\epsilon}_k$ uncorrelated with input x_{k-p-1}), which in turn is equivalent to requiring

$$R_{p+1} = - \sum_{n=1}^{p} \frac{c_{no}}{c_{oo}} \, R_{p+1-n} = \sum_{n=1}^{p} \tilde{a}_n \, R_{p+1-n} . \tag{C-8}$$

This relation, which may not be true for the actual process $\{x_k\}$, is a direct result of assumption (70); the quantity R_{p+1} in (C-8) is really an approximation to the true (unknown) correlation value.

Next from (C-5),

$$E_2 = \tilde{a}_{p-1}^* \, C_{p+1} + \tilde{a}_p^* \, C_{p+2} . \tag{C-9}$$

Assuming $E_2 = 0$ (in addition to $E_1 = 0$) is equivalent to also assuming $C_{p+2} = 0$, which in turn from (C-2) and (66) requires that we approximate according to

$$R_{p+2} = - \sum_{n=1}^{p} \frac{c_{no}}{c_{oo}} \, R_{p+2-n} = \sum_{n=1}^{p} \tilde{a}_n \, R_{p+2-n} . \tag{C-10}$$

Continuing in this way, it follows that assuming white noise for $\{\tilde{\epsilon}_k\}$, that is, assuming

$$E_\ell = 0 \text{ for } \ell \geq 1 , \tag{C-11}$$

is equivalent to assuming that $C_\ell = 0$ for $\ell \geq p + 1$; that is, the minimum error is uncorrelated with <u>all</u> past inputs. There follows the approximations

$$R_\ell = -\sum_{n=1}^{p} \frac{c_{no}}{c_{oo}} R_{\ell-n} = \sum_{n=1}^{p} \tilde{a}_n R_{\ell-n} \quad \text{for} \quad \ell \geq p+1 . \tag{C-12}$$

This recursion relation (starting with known values $R_1, R_2, \ldots, R_p$) can be considered to be an extrapolation of the known correlation values into regions where they are unknown.

If we augment (C-12) according to

$$R_{-\ell} = R_\ell^* \text{ for } \ell \geq p+1 , \tag{C-13}$$

then it can be shown that the spectrum defined by

$$\Delta \sum_{\ell=-\infty}^{\infty} R_\ell \exp(-i2\pi f \ell \Delta) = \frac{\Delta / c_{oo}}{\left| 1 - \sum_{n=1}^{p} \tilde{a}_n \exp(-i2\pi f n \Delta) \right|^2} , \tag{C-14}$$

which is identical to (71). The transform in (C-14) converges if $|R_\ell|$ decays with increasing $|\ell|$, that is, if B(z) of (56) has no zeros inside O.

Appendix D

STABILITY OF RECURSION RELATION

The recursion relation for approximated correlation values R_ℓ is given in (C-12) and (75) as

$$R_\ell = \sum_{k=1}^{p} \tilde{a}_k R_{\ell-k} \text{ for } \ell \geq p+1 . \tag{D-1}$$

Therefore,

$$U(z) \equiv \sum_{\ell=p+1}^{\infty} R_\ell \, z^{-\ell} = \sum_{k=1}^{p} \tilde{a}_k z^{-k} \sum_{\ell=p+1}^{\infty} R_{\ell-k} z^{-\ell+k} . \tag{D-2}$$

But

$$\sum_{\ell=p+1}^{\infty} R_{\ell-k} z^{-\ell+k} = \sum_{j=p+1-k}^{\infty} R_j z^{-j} = \sum_{j=p+1-k}^{p} R_j z^{-j}$$

$$+ \sum_{j=p+1}^{\infty} R_j z^{-j} \equiv V_k(z) + U(z) , \tag{D-3}$$

where

$$V_k(z) = R_{p+1-k} z^{-(p+1-k)} + V_{k-1}(z) , \; k \geq 2 ; \; V_1(z) = R_p z^{-p} . \tag{D-4}$$

$V_k(z)$ involves the starting values $R_{p+1-k}, \ldots, R_p$ for $1 \leq k \leq p$. Employment of (D-3) in (D-2) yields

$$U(z) = \sum_{k=1}^{p} \tilde{a}_k z^{-k} V_k(z) + U(z) \sum_{k=1}^{p} \tilde{a}_k z^{-k} , \tag{D-5}$$

or

$$U(z) = \frac{\sum_{k=1}^{p} \tilde{a}_k z^{-k} V_k(z)}{1 - \sum_{k=1}^{p} \tilde{a}_k z^{-k}} = - \frac{\sum_{k=1}^{p} c_{ko} z^{-k} V_k(z)}{\sum_{k=0}^{p} c_{ko} z^{-k}}, \qquad (D-6)$$

where we have utilized (66). In order that recursion (D-1) be stable, the denominator of (D-6) must possess all its zeros within the unit circle O in the complex z-plane. Therefore, B(z) of (56) must possess all its zeros outside O if recursion (D-1) is to be stable. This is guaranteed by the results in (A-9) et seq.

Appendix E

IMPLICATIONS OF ASSUMPTION OF WHITE SPECTRUM; UNKNOWN CORRELATION

The minimum error sequence is given by (96) and (101) as

$$\tilde{\epsilon}_k = \sum_{n=0}^{p} \tilde{a}_n x_{k-n}, \text{ all } k. \tag{E-1}$$

The sample autocorrelation of $\{\tilde{\epsilon}_k\}$ is defined here as

$$F_\ell \equiv \frac{1}{N} \sum_k \tilde{\epsilon}_k \tilde{\epsilon}^*_{k-\ell} = \sum_{m,n=0}^{p} \tilde{a}_m \tilde{a}^*_n S_{\ell+n-m} \tag{E-2}$$

using (E-1) and (98). The sample spectrum of $\{\tilde{\epsilon}_k\}$ is defined here as

$$H_{\tilde{\epsilon}}(f) \equiv \Delta \sum_{\ell \equiv -\infty}^{\infty} F_\ell \exp(-i2\pi f \ell \Delta) = H_x(f) \left|A(f)\right|^2, \ |f| < \frac{1}{2\Delta}, \tag{E-3}$$

where we have employed (E-2) and (107) and defined the sample spectrum of $\{x_k\}$ as

$$H_x(f) \equiv \Delta \sum_{\ell=-\infty}^{\infty} S_\ell \exp(-i2\pi f \ell \Delta), \ |f| < \frac{1}{2\Delta}. \tag{E-4}$$

Therefore, (E-3) yields

$$H_x(f) = \frac{H_{\tilde{\epsilon}}(f)}{\left|A(f)\right|^2}, \ |f| < \frac{1}{2\Delta}. \tag{E-5}$$

Now we will assume that the sample spectrum of $\{\tilde{\epsilon}_k\}$ is white; that is, we set

$$\hat{H}_{\tilde{\epsilon}}(f) \equiv K\Delta, \quad |f| < \frac{1}{2\Delta}, \tag{E-6}$$

where K is a constant. We then adopt an estimate of the sample spectrum of sequence $\{x_n\}_1^N$ according to

$$\hat{H}_x(f) \equiv \frac{\hat{H}_{\tilde{\epsilon}}(f)}{|A(f)|^2} = \frac{K\Delta}{\left|\sum_{n=0}^{p} \tilde{a}_n \exp(-i2\pi fn\Delta)\right|^2}, \quad |f| < \frac{1}{2\Delta}, \tag{E-7}$$

and adopt a scaled version of this quantity as a spectral estimate of process $\{x_n\}$:

$$\hat{G}_x(f) \equiv \frac{\Delta}{\left|\sum_{n=0}^{p} \tilde{a}_n \exp(-i2\pi fn\Delta)\right|^2}, \quad |f| < \frac{1}{2\Delta}. \tag{E-8}$$

The white assumption in (E-6) forces us to assume that

$$F_\ell = 0 \text{ for } \ell \neq 0, \tag{E-9}$$

as (E-3) shows. In order to see what this implies, we utilize the definition of the sample crosscorrelation in (109), along with (96) and (98), to obtain

$$D_\ell \equiv \frac{1}{N} \sum_k \tilde{\epsilon}_k x^*_{k-\ell} = \sum_{n=0}^{p} a_n S_{\ell-n}, \text{ all } \ell. \tag{E-10}$$

Use of (101) then shows that

$$D_\ell = 0 \text{ for } 1 \leq \ell \leq p. \tag{E-11}$$

Meanwhile, the sample autocorrelation in (E-2) can be written in the form

$$F_\ell = \sum_{n=0}^{p} \tilde{a}^*_n D_{\ell+n}, \text{ all } \ell, \tag{E-12}$$

upon employment of (E-10). There immediately follows from (E-9), (E-11), and (E-12)

$$F_1 = \tilde{a}_p^* D_{p+1} = 0 . \tag{E-13}$$

But then (E-9) and (E-10) indicate that

$$S_{p+1} = \sum_{n=1}^{p} \tilde{a}_n S_{p+1-n} , \tag{E-14}$$

where $\{\tilde{a}_n\}_1^p$ are the solutions of (102). But relation (E-14) may not be true for the quantity S_{p+1} actually obtained from data $\{x_n\}_1^N$ via (98). Thus, assumption $F_1 = 0$ is forcing us to assume that S_{p+1} can be obtained via (E-14) and (102), when $\{S_\ell\}_{-p}^p$ are obtained from (98).

Next from (E-12) and (E-11),

$$F_2 = \tilde{a}_{p-1}^* D_{p+1} + \tilde{a}_p^* D_{p+2} . \tag{E-15}$$

Assuming $F_2 = 0$ (in addition to $F_1 = 0$) is equivalent to also assuming $D_{p+2} = 0$, which in turn from (E-10) requires that

$$S_{p+2} = \sum_{n=1}^{p} \tilde{a}_n S_{p+2-n} . \tag{E-16}$$

Continuing in this way, it follows that assuming

$$F_\ell = 0 \text{ for } \ell \geq 1 \tag{E-17}$$

is equivalent to assuming $D_\ell = 0$ for $\ell \geq p + 1$; that is, the minimum-error sequence is uncorrelated (on a single member function basis) with all past inputs. There follows the estimates

$$S_\ell = \sum_{n=1}^{p} \tilde{a}_n S_{\ell-n} , \quad \ell \geq p + 1 . \tag{E-18}$$

Stability is discussed in (111) et seq.

Appendix F

BOUND ON CROSS-GAIN

The value of the cross-gain g_p in (155) can be written as

$$g_p = \frac{\sum_{n=p+1}^{N} f_n^{(p-1)}\, b_{n-1}^{(p-1)*}}{\left(\sum_{n=p+1}^{N} \left| f_n^{(p-1)} \right|^2 \sum_{n=p+1}^{N} \left| b_{n-1}^{(p-1)} \right|^2 \right)^{1/2}} \cdot \frac{2\left(\sum_{n=p+1}^{N} \left| f_n^{(p-1)} \right|^2 \sum_{n=p+1}^{N} \left| b_{n-1}^{(p-1)} \right|^2 \right)^{1/2}}{\sum_{n=p+1}^{N} \left(\left| f_n^{(p-1)} \right|^2 + \left| b_{n-1}^{(p-1)} \right|^2 \right)} \qquad \text{(F-1)}$$

The first factor in (F-1) is of the form of a correlation coefficient of the (p-1)-th order forward and backward sequences and can never exceed unity in magnitude (by Schwarz's inequality). The second factor in (F-1) is almost always very close to 1: let the pair of sums

$$\left\{ \sum_{n=p+1}^{N} \left| f_n^{(p-1)} \right|^2 \text{ and } \sum_{n=p+1}^{N} \left| b_{n-1}^{(p-1)} \right|^2 \right\} = \left\{ A \text{ and } A(1+r) \right\}, \qquad \text{(F-2)}$$

where $r \geq 0$ without loss of generality. The second factor in (F-1) then equals $\frac{(1+r)^{1/2}}{1+r/2}$, which is never larger than 1 and is tabulated below. Thus, g_p in (F-1) is virtually identical to the correlation coefficient of the forward and backward sequences, since r is near zero with high probability.

Table F.1 Second Factor in (F-1).

r	0	.1	.2	.3	.4	.5
$\frac{(1+r)^{1/2}}{1+r/2}$	1	.999	.996	.991	.986	.980

REVERSE BLANK

Appendix G

CLOSENESS OF ERROR MEASURES

Two possible error measures for the Burg technique were presented in (150) and (156). For p = 0, employing (154) and (152),

$$F^{(0)} = \frac{1}{N} \sum_{n=1}^{N} |x_n|^2 . \tag{G-1}$$

Comparing this result with (151), we find

$$F^{(0)} = P^{(0)} . \tag{G-2}$$

Thus, the two error measures are identical for p = 0.

Next from (150) and (151)

$$P^{(1)} = P^{(0)} \left(1 - \left|a_1^{(1)}\right|^2\right) = \left(1 - \left|a_1^{(1)}\right|^2\right) \frac{1}{N} \sum_{n=1}^{N} |x_n|^2 , \tag{G-3}$$

whereas from (156), (160), (155), and (152),

$$\begin{aligned} F_o^{(1)} &= \left(1 - \left|a_1^{(1)}\right|^2\right) \frac{\mathrm{Den}(1)}{2(N-1)} \\ &= \left(1 - \left|a_1^{(1)}\right|^2\right) \frac{1}{2(N-1)} \sum_{n=2}^{N} \left(\left|f_n^{(0)}\right|^2 + \left|b_{n-1}^{(0)}\right|^2\right) \\ &= \left(1 - \left|a_1^{(1)}\right|^2\right) \frac{\frac{1}{2}|x_1|^2 + |x_2|^2 + |x_3|^2 + \ldots + |x_{N-2}|^2 + |x_{N-1}|^2 + \frac{1}{2}|x_N|^2}{N-1} . \end{aligned} \tag{G-4}$$

But now reference to (151) and (G-3) reveals that, for N-1 large,

$$F_o^{(1)} \cong \left(1 - \left|a_1^{(1)}\right|^2\right) P^{(0)} = P^{(1)} . \tag{G-5}$$

Continuing with (150),

$$P^{(2)} = P^{(1)} \left(1 - \left|a_2^{(2)}\right|^2\right). \tag{G-6}$$

And (156), (160), and (155) combine to yield

$$F_o^{(2)} = \left(1 - \left|a_2^{(2)}\right|^2\right) \frac{Den(2)}{2(N-2)} = \left(1 - \left|a_2^{(2)}\right|^2\right) \frac{1}{2(N-2)} \sum_{n=3}^{N} \left(\left|f_n^{(1)}\right|^2 + \left|b_{n-1}^{(1)}\right|^2\right). \tag{G-7}$$

But from (154),

$$F_o^{(1)} = \frac{1}{2(N-1)} \sum_{n=2}^{N} \left(\left|f_n^{(1)}\right|^2 + \left|b_{n-1}^{(1)}\right|^2\right). \tag{G-8}$$

Comparing (G-7) and (G-8), we see that, for N-2 large,

$$F_o^{(2)} \cong \left(1 - \left|a_2^{(2)}\right|^2\right) F_o^{(1)} . \tag{G-9}$$

Then employing (G-5) and (G-6), we have

$$F_o^{(2)} \cong \left(1 - \left|a_2^{(2)}\right|^2\right) P^{(1)} = P^{(2)} , \tag{G-10}$$

which is the desired relationship. In general, for no bad data points, we have

$$F_o^{(p)} \cong P^{(p)} \text{ for } N-p \text{ large} . \tag{G-11}$$

Numerical computations have borne this result out, with the two quantities not having any ordered relationship; that is, either quantity can be larger (or smaller) at different stages, p. (G-9) generalizes to

$$F_o^{(p)} \cong \left(1 - \left|a_p^{(p)}\right|^2\right) F_o^{(p-1)} \text{ for } N-p \text{ large} . \tag{G-12}$$

Appendix H

SCALE FACTORS IN SPECTRAL ESTIMATES

Instead of using a unity value for the average minimum error or residual power in the numberator of (167), we could use the value given by (156). Then our spectral estimate would be

$$\hat{G}_x(f) = \frac{\Delta F_o^{(p)}}{\left|1 - \sum_{k=1}^{p} a_k^{(p)} \exp(-i2\pi fk\Delta)\right|^2}, \quad |f| < \frac{1}{2\Delta}. \tag{H-1}$$

An alternative approach is to use an arbitrary scale factor K and choose it so that the area under the spectral estimate is equal to the sample power (151), as suggested under (108); that is, set

$$\hat{G}_x(f) = \frac{\Delta K}{\left|1 - \sum_{k=1}^{p} a_k^{(p)} \exp(-i2\pi fk\Delta)\right|^2}, \quad |f| < \frac{1}{2\Delta}, \tag{H-2}$$

and force

$$\int_{-\frac{1}{2\Delta}}^{\frac{1}{2\Delta}} df\, \hat{G}_x(f) = P^{(0)} = \frac{1}{N} \sum_{n=1}^{N} |x_n|^2. \tag{H-3}$$

Substituting (H-2) in (H-3), and using (159), we have

$$P^{(0)} = \int_{-\frac{1}{2\Delta}}^{\frac{1}{2\Delta}} df\, \frac{\Delta K}{\left|1 - \sum_{k=1}^{p} a_k^{(p)} \exp(-i2\pi fk\Delta)\right|^2} = \frac{K}{\prod_{m=1}^{p} \left\{1 - \left|a_m^{(m)}\right|^2\right\}}. \tag{H-4}$$

The last step in (H-4) is proven as follows: from (A-8) and (29), we know that

$$\int_{-\frac{1}{2\Delta}}^{\frac{1}{2\Delta}} df \frac{\Delta}{\left|1 - \sum_{k=1}^{p} a_k^{(p)} \exp(-i2\pi fk\Delta)\right|^2} = R_o\, c_{oo}^{(p)} . \qquad \text{(H-5)}$$

But from (A-7),

$$R_o\, c_{oo}^{(p)} = \frac{R_o\, c_{oo}^{(p-1)}}{1 - \left|a_p^{(p)}\right|^2} = \frac{1}{\prod_{m=1}^{p} \left\{1 - \left|a_m^{(m)}\right|^2\right\}} , \qquad \text{(H-6)}$$

where we have employed $R_o\, c_{oo}^{(0)} = 1$. The relationship in (H-4) holds when the filter coefficients are determined via (148).

Therefore, (H-4) yields, with the aid of (150).

$$K = P^{(0)} \prod_{m=1}^{p} \left\{1 - \left|a_m^{(m)}\right|^2\right\} = P^{(p)} , \qquad \text{(H-7)}$$

and the estimate (H-2) becomes

$$\hat{G}_x(f) = \frac{\Delta P^{(p)}}{\left|1 - \sum_{k=1}^{p} a_k^{(p)} \exp(-i2\pi fk\Delta)\right|^2} , \quad |f| < \frac{1}{2\Delta} . \qquad \text{(H-8)}$$

The very close similarity of values between the alternatives (H-1) and (H-8) is made evident by the results of appendix G, in particular (G-11). Thus, there is virtually no difference between estimates (H-1) and (H-8), for no bad data points.

Appendix I

BIASEDNESS OF BURG'S CORRELATION ESTIMATE

For the Burg technique with p = 1, N = 3, we find from (162) and (144) that (for real data)

$$\hat{R}_1 = \frac{2}{3} \frac{x_2 \left(x_1 + x_3\right)\left(x_1^2 + x_2^2 + x_3^2\right)}{x_1^2 + 2x_2^2 + x_3^2} \,. \tag{I-1}$$

The mean of this random variable depends on more than just $\overline{x_2 x_1}$ $(= \overline{x_3 x_2})$; in fact, it depends on the third-order joint density of (x_1, x_2, x_3). As an example, let

$$x_1 = u, \; x_2 = \pm \frac{1}{\sqrt{2}} (u+v), \; x_3 = v, \tag{I-2}$$

where u and v are independent, zero-mean, unit-variance, Gaussian random variables. Then x_1, x_2, x_3 are zero-mean, unit-variance, Gaussian random variables with

$$\overline{x_2 x_1} = \overline{x_3 x_2} = \pm \frac{1}{\sqrt{2}}, \; \overline{x_3 x_1} = 0 \,. \tag{I-3}$$

Employing (I-2) in (I-1), we obtain

$$\hat{R}_1 = \pm \frac{1}{\sqrt{2}} \frac{1}{6} \frac{(u+v)^2 (3u^2 + 2uv + 3v^2)}{u^2 + uv + v^2} \,. \tag{I-4}$$

Therefore,

$$\overline{\hat{R}_1} = \pm \frac{1}{\sqrt{2}} \frac{1}{6} \frac{1}{2\pi} \iint_{-\infty}^{\infty} du \, dv \, \exp\left(-\frac{u^2 + v^2}{2}\right) \frac{(u+v)^2 (3u^2 + 2uv + 3v^2)}{u^2 + uv + v^2}$$

$$= \pm\frac{1}{\sqrt{2}}\ \frac{1}{6}\ \frac{1}{2\pi}\int_0^{\infty} dr\ r^3\ \exp(-r^2/2)\int_{-\pi}^{\pi} d\theta\ \frac{(C+S)^2\,(3C^2+2CS+3S^2)}{C^2+CS+S^2}, \qquad \text{(I-5)}$$

where we have changed to polar coordinates and let $C \equiv \cos\theta$, $S \equiv \sin\theta$. The integral on r in (I-5) is 2, and the integral on θ is $4\pi\left(2 - \frac{1}{\sqrt{3}}\right)$. Therefore,

$$\overline{\hat{R}_1} = \pm\frac{1}{\sqrt{2}}\ \frac{12 - 2\sqrt{3}}{9} = \pm\frac{1}{\sqrt{2}}\ (.9484), \qquad \text{(I-6)}$$

which is not equal to

$$\overline{x_2\,x_1} = \overline{x_3\,x_2} = \pm\frac{1}{\sqrt{2}}\ . \qquad \text{(I-7)}$$

Appendix J

FORTRAN PROGRAMS

The programs in this appendix are written for real data, but may be readily generalized to complex data by means of the general equations in the main text. From (H-8) and (H-7), for real data, the spectral estimate is given by

$$\hat{G}_x(f) = \frac{\Delta \prod_{k=1}^{p} \left\{1 - a_k^{(k)2}\right\} P^{(0)}}{\left|1 - \sum_{k=1}^{p} a_k^{(p)} \exp(-i2\pi fk\Delta)\right|^2}, \quad |f| < \frac{1}{2\Delta}. \tag{J-1}$$

Let frequency increment

$$\Delta_f \equiv \frac{1}{J\Delta} = \frac{1}{J/2}\,\frac{1}{2\Delta} = \frac{f_N}{J/2}, \tag{J-2}$$

where f_N is the Nyquist frequency, and J is an integer. Then, using (H-3) and the real behavior of the data,

$$P^{(0)} = 2\int_0^{\frac{1}{2\Delta}} df\, \hat{G}_x(f) \cong 2\Delta P^{(0)} \prod_{k=1}^{p} \left\{1 - a_k^{(k)2}\right\} \sum_{m=0}^{J/2} \Delta_f \cdot$$

$$\frac{\epsilon_m}{\left|1 - \sum_{k=1}^{p} a_k^{(p)} \exp(-i2\pi m\Delta_f k\Delta)\right|^2}$$

$$= \frac{2}{J} P^{(0)} \prod_{k=1}^{p} \left\{1 - a_k^{(k)2}\right\} \sum_{m=0}^{J/2} \frac{\epsilon_m}{\left|1 - \sum_{k=1}^{p} a_k^{(p)} \exp(-i2\pi mk/J)\right|^2} \equiv \sum_{m=0}^{J/2} \epsilon_m P_m, \tag{J-3}$$

where $\{\epsilon_m\}$ is a set of integration weights (for example, trapezoidal). So we can compute (independent of time increment Δ) the quantity

$$\frac{P_m}{P^{(0)}} = \frac{2}{J} \prod_{k=1}^{p} \left\{1 - a_k^{(k)2}\right\} \frac{1}{\left|1 - \sum_{k=1}^{p} a_k^{(p)} \exp(-i2\pi mk/J)\right|^2} \quad \text{for } 0 \le m \le \frac{J}{2}, \tag{J-4}$$

which represents the fractional power in the frequency band

$$\left(\frac{m - \frac{1}{2}}{J\Delta}, \frac{m + \frac{1}{2}}{J\Delta}\right); \tag{J-5}$$

that is,

$$\sum_{m=0}^{J/2} \epsilon_m \frac{P_m}{P^{(0)}} \cong 1 \tag{J-6}$$

if estimate $\hat{G}_X(f)$ in (J-1) has been sampled finely enough (that is, large J). The denominator of (J-4) is recognized as a J-point FFT of p+1 nonzero numbers; hence, J should be chosen as a power of 2 for speed purposes. The programs below yield the fraction of power in frequency bands of width $(J\Delta)^{-1}$, if J is an integer large enough that the spectral estimate (167) or (H-8) is adequately sampled to keep track of its peaks.

NO BAD DATA POINTS (SUBSECTION 4.7)

The data generation is accomplished via function IRAND, which generates integers uniformly distributed over $(0, 2^{35}-1)$; by RAND, which generates numbers uniformly distributed over (0,1); and by TINORM, which generates zero-mean unit-variance Gaussian variables. The FFT used below is that presented in reference 25.

```
C  SPECTRAL ESTIMATION      USER: CHANGE LINE 13 AND REPLACE LINES 17-31
C  N = NUMBER OF DATA POINTS
C  X(1),...,X(N) = INPUT DATA
C  PMAX = MAXIMUM ORDER OF FILTER
C  PBEST = BEST ORDER OF FILTER
C  A(1),...,A(PBEST) = PREDICTIVE FILTER COEFFICIENTS
C  PROD = PRODUCT(1-A(P)**2) FOR P=1 TO PBEST
C  RHO(1),...,RHO(PMAX) = NORMALIZED CORRELATION COEFFICIENTS
C  J = SIZE OF FFT  (MUST BE A POWER OF 2)
C  XX(1),...,XX(J/2+1) = FRACTIONAL POWERS, FROM DC TO NYQUIST FREQUENCY
C  CO(1),...,CO(J/4+1) = QUARTER COSINE TABLE
C  Y AND YY ARE REQUIRED AUXILIARY ARRAYS
      PARAMETER N=100, PMAX=10, J=2048, J41=J/4+1
      INTEGER PBEST
      DIMENSION X(N),Y(N),A(PMAX),RHO(PMAX),XX(J),YY(J),CO(J41)
C  INPUT DATA IN X(1),...,X(N)
      DEFINE IRAND=I*5**15+((1-SIGN(1,I*5**15))/2)*34359738367
      DEFINE RAND=FLOAT(I)/34359738367.
      I=5281
      NSTART=N+400     @ WILL DISCARD INITIAL 400 POINTS
      XX(1)=0.
      XX(2)=0.
      XX(3)=0.
      XX(4)=0.
      DO 11 L=5,NSTART
      I=IRAND
      XX(L)=2.7607*XX(L-1)-3.8106*XX(L-2)+2.6535*XX(L-3)-
     $0.9238*XX(L-4)+TINORM(RAND,$11)
11    CONTINUE
      DO 12 I=1,N
12    X(I)=XX(I+NSTART-N)
      PRINT 1,
1     FORMAT(/' INPUT DATA:')
      PRINT 4, (X(I),I=1,N)
C  EVALUATE PREDICTIVE FILTER COEFFICIENTS
      CALL BURG(N,PMAX,X,Y,PBEST,A,PROD,RHO)
      PRINT 9, X(N)
9     FORMAT(/' MEAN =',E14.8)
      PRINT 10, Y(N)
10    FORMAT(' STANDARD DEVIATION =',E13.8)
      PRINT 2, PBEST
2     FORMAT(/' PBEST =',I3)
      PRINT 3,
3     FORMAT(/' PREDICTIVE FILTER COEFFICIENTS:')
      PRINT 4, (A(I),I=1,PBEST)
4     FORMAT(5E20.8)
      PRINT 5, PROD
5     FORMAT(/' PRODUCT(1-A(P)**2) =',E13.8)
      PRINT 6,
6     FORMAT(/' NORMALIZED CORRELATION COEFFICIENTS:')
      PRINT 4, (RHO(I),I=1,PMAX)
      CALL QTRCOS(CO,J)
C  EVALUATE FRACTIONAL POWERS
      CALL POWERS(PBEST,A,PROD,J,XX,YY,CO)
      PRINT 7,
7     FORMAT(/' FRACTIONAL POWERS:')
      L=J/2+1
      PRINT 8, (XX(I),I=1,L)
8     FORMAT(2X,10E13.6)
      END
```

```
      SUBROUTINE BURG(N,PMAX,X,Y,PBEST,A,PROD,RHO)       C 2 FEB 1976
C  THIS SUBROUTINE COMPUTES THE PREDICTIVE FILTER COEFFICIENTS
C  N = NUMBER OF DATA POINTS; INTEGER INPUT
C  PMAX = MAXIMUM ORDER OF FILTER; INTEGER INPUT
C  X(1),X(2),...,X(N) = DATA ARRAY ON INPUT; ALTERED ON OUTPUT
C  ON OUTPUT, X(1),X(2),...,X(PMAX) = A(1;PMAX),A(2;PMAX),....A(PMAX;PMAX)
C  Y(1),Y(2),...,Y(N) = AUXILIARY ARRAY; SCRATCH INPUT
C  ON OUTPUT, Y(1),Y(2),...,Y(PMAX) = A(1;1),A(2;2),....A(PMAX;PMAX)
C  ON OUTPUT, X(N) = MEAN, AND Y(N) = STANDARD DEVIATION OF INPUT DATA
C  PBEST = BEST ORDER OF FILTER; INTEGER OUTPUT
C  A(1),A(2),...,A(PBEST) = PREDICTIVE FILTER COEFFICIENT ARRAY =
C  A(1;PBEST),A(2;PBEST),...,A(PBEST;PBEST); OUTPUT
C  PROD = PRODUCT(1-A(P;PBEST)**2) FOR P=1 TO PBEST; OUTPUT
C  RHO(1),...,RHO(PMAX) = NORMALIZED CORRELATION COEFFICIENTS; OUTPUT
C  DIMENSION X(N),Y(N),A(PMAX),RHO(PMAX)     IS REQUIRED IN MAIN PROGRAM
      INTEGER PMAX,PBEST,P
      DOUBLE PRECISION SA,SB
      DIMENSION X(1),Y(1),A(1),RHO(1)
      IF(PMAX.GT.3.*SQRT(N)) PRINT 2, PMAX,N
2     FORMAT(/' PMAX =',I4,' IS TOO LARGE FOR NUMBER OF DATA POINTS N ='
     $,I5)
C  COMPUTE MEAN
      S1=0.
      DO 1 I=1,N
1     S1=S1+X(I)
      S1=S1/N
C  SUBTRACT MEAN, AND SCALE TO UNIT VARIANCE
      S2=0.
      DO 3 I=1,N
      X(I)=X(I)-S1
3     S2=S2+X(I)**2
      S2=SQRT(S2/(N-1.))
      T=1./S2
      DO 5 I=1,N
      X(I)=X(I)*T
5     Y(I)=X(I)
C  BEGIN RECURSION
      P=0
      PRODUC=1.
      AICMIN=0.
      PBEST=0
      PROD=1.
6     P=P+1
C  CALCULATE CROSS-GAIN; EQ. 155
      SA=0.D0
      SB=0.D0
      L=P+1
      DO 7 I=L,N
      SA=SA+X(I)*Y(I-1)
7     SB=SB+X(I)**2+Y(I-1)**2
      G=2.*SA/SB
      PRODUC=PRODUC*(1.-G*G)
C  CALCULATE FILTER COEFFICIENTS; EQS. 160&148. STORE IN X(1),...,X(P)
      X(P)=G
      IF(P.EQ.1) GO TO 8
      L=P/2
      DO 9 I=1,L
      T=X(I)-G*X(P-I)
      X(P-I)=X(P-I)-G*X(I)
9     X(I)=T
C  CALCULATE NORMALIZED CORRELATION COEFFICIENT; EQ. 149
8     T=X(P)
      IF(P.EQ.1) GO TO 14
      L=P-1
      DO 15 I=1,L
15    T=T+X(I)*RHO(P-I)
14    RHO(P)=T
```

```
C  CALCULATE AKAIKE'S INFORMATION CRITERION; EQS. 156&202
      RELERR=(1.-G*G)*SNGL(SB)/(2.*(N-P))
      AIC=LOG(RELERR)+2.*FLOAT(P)/(N-P)
      IF(AIC.GE.AICMIN) GO TO 10
      AICMIN=AIC
      PBEST=P
      PROD=PRODUC
      DO 11 I=1,P
11    A(I)=X(I)
10    IF(P.EQ.PMAX) GO TO 16
C  UPDATE FORWARD AND BACKWARD SEQUENCES; EQ. 153
      L=P+1
      DO 12 I=N,L,-1
      T=X(I)-G*Y(I-1)
      Y(I)=Y(I-1)-G*X(I)
12    X(I)=T
      Y(P)=G
      GO TO 6
16    Y(PMAX)=G
      IF(PBEST.EQ.PMAX) GO TO 4
C  COMPUTE EXTRAPOLATED NORMALIZED CORRELATION
C  COEFFICIENTS FROM PBEST+1 TO PMAX; EQ. 165
      L=PBEST+1
      DO 17 P=L,PMAX
      A(P)=0.
      T=0.
      DO 18 I=1,PBEST
18    T=T+A(I)*RHO(P-I)
17    RHO(P)=T
4     X(N)=S1
      Y(N)=S2
      RETURN
      END


      SUBROUTINE POWERS(PBEST,A,PROD,J,XX,YY,CO)
C  THIS SUBROUTINE COMPUTES THE FRACTIONAL POWERS IN BANDS 1/(J*DELTA); EQ. J-4
C  PBEST = BEST ORDER OF FILTER; INTEGER INPUT
C  A(1),...,A(PBEST) = FILTER COEFFICIENT ARRAY; INPUT
C  PROD = PRODUCT(1-A(P)**2)  FOR P=1 TO PBEST; INPUT
C  J = SIZE OF FFT  (J/2+1=NUMBER OF FREQUENCY POINTS); INTEGER INPUT
C  XX = AUXILIARY ARRAY ON INPUT
C  XX(1),...,XX(J/2+1) = FRACTIONAL POWERS ON OUTPUT
C  YY = AUXILIARY ARRAY; SCRATCH INPUT
C  CO(1),...,CO(J/4+1) = QUARTER COSINE TABLE FOR FFT; INPUT
C  DIMENSION XX(J),YY(J),CO(J/4+1)  IS REQUIRED IN MAIN PROGRAM
C  DIMENSION A(PMAX)  IS REQUIRED IN MAIN PROGRAM, WHERE PMAX.GE.PBEST
      INTEGER PBEST
      DIMENSION A(1),XX(1),YY(1),CO(1)
      F=PROD*2./J
      XX(1)=1.
      YY(1)=0.
      DO 1 I=1,PBEST
      XX(I+1)=-A(I)
1     YY(I+1)=0.
      L=PBEST+2
      DO 2 I=L,J
      XX(I)=0.
2     YY(I)=0.
      L=1.4427*LOG(J)+.5       @ LOG2(J)
      CALL MKLFFT(XX,YY,CO,L,-1)
      L=J/2+1
      DO 3 I=1,L
3     XX(I)=F/(XX(I)**2+YY(I)**2)
      RETURN
      END
```

```
INPUT DATA:
      -.5595709E+01        .1134001E+02        .1590241E+02        .7492369E+01       -.2272714E+01
      -.2177161E+01        .8740469E+01        .2062052E+02        .1955965E+02        .1083377E+01
      -.2566002E+02       -.4116662E+02       -.3099371E+02        .2594106E+01        .3876933E+02
       .5440105E+02        .3007443E+02       -.7254209E+01       -.4834886E+02       -.6196347E+02
      -.3964567E+02        .5768167E+01        .4687120E+02        .8028019E+02        .3910616E+02
      -.2430066E+01       -.3939161E+02       -.5205120E+02       -.3743730E+02       -.5895646E+01
       .2565129E+02        .4365842E+02        .4210351E+02        .2374820E+02       -.3698461E+01
      -.2837123E+02       -.4038951E+02       -.3535496E+02       -.1517663E+02        .1364593E+02
       .3870157E+02        .4734531E+02        .3378484E+02        .1897963E+01       -.3461738E+02
      -.5657356E+02       -.5021730E+02       -.1806857E+02        .2234494E+02        .4667870E+02
       .4696502E+02        .2106791E+02       -.1173943E+02       -.3201909E+02       -.3215161E+02
      -.1795602E+02       -.4807980E+01        .1764450E+02        .2669157E+02        .2923187E+02
       .2265907E+02        .6785047E+01       -.1401527E+02       -.3243687E+02       -.3761855E+02
      -.2483226E+02       -.4575626E+00        .2316687E+02        .3591508E+02        .3164570E+02
       .1279135E+02       -.1108947E+02       -.2819874E+02       -.3117949E+02       -.1928172E+02
      -.1810665E+01        .1230663E+02        .1899450E+02        .1921426E+02        .1332588E+02
       .3538552E+00       -.1863298E+02       -.3507228E+02       -.3818424E+02       -.2116706E+02
       .1302307E+02        .4691040E+02        .4911280E+02        .4477004E+02        .3764144E+01
      -.5660955E+02       -.6045731E+02       -.5782363E+02       -.1161174E+00        .5824156E+02
       .8540372E+02        .6336034E+02        .6040977E+01       -.3297168E+02       -.7934845E+02

MEAN =  .1173513E+00
STANDARD DEVIATION = .3506007E+02

PBEST =  4

PREDICTIVE FILTER COEFFICIENTS:
       .2735131E+01       -.3782361E+01        .2640127E+01       -.9357775E+00

PRODUCT(1-A(P)**2) = .8895657E-03

NORMALIZED CORRELATION COEFFICIENTS:
       .7330239E+00        .8110486E-01       -.5961948E+00        .9366197E+00       -.7770162E+00
      -.2315720E+00        .5906175E+00        .7683069E+00        .7363477E+00        .3604352E+00
```

BAD DATA POINTS (SUBSECTION 5.2)

```
C  SPECTRAL ESTIMATION FOR BAD DATA POINTS       USER: CHANGE
C  LINE 17 AND REPLACE LINES 22-36 AND 41-46
C  N = NUMBER OF DATA POINTS
C  X(1),...,X(N) = INPUT DATA
C  BMAX = MAXIMUM NUMBER OF BAD DATA POINTS
C  B = ACTUAL NUMBER OF BAD DATA POINTS   (MUST HAVE B.LE.BMAX)
C  M(1),...,M(B) = LOCATIONS OF BAD DATA POINTS
C  PMAX = MAXIMUM ORDER OF FILTER
C  PBEST = BEST ORDER OF FILTER
C  A(1),...,A(PBEST) = PREDICTIVE FILTER COEFFICIENTS
C  PROD = PRODUCT(1-A(P)**2) FOR P=1 TO PBEST
C  RHO(1),...,RHO(PMAX) = NORMALIZED CORRELATION COEFFICIENTS
C  J = SIZE OF FFT  (MUST BE A POWER OF 2)
C  XX(1),...,XX(J/2+1) = FRACTIONAL POWERS, FROM DC TO NYQUIST FREQUENCY
C  CO(1),...,CO(J/4+1) = QUARTER COSINE TABLE
C  Y, YY, AND IP ARE REQUIRED AUXILIARY ARRAYS
      PARAMETER N= 100, BMAX= 25, PMAX=10, J=2048, J41=J/4+1
      INTEGER B,PBEST
      DIMENSION X(N),Y(N),A(PMAX),RHO(PMAX),XX(J),YY(J),CO(J41)
      DIMENSION M(BMAX),IP(N)
C  INPUT DATA IN X(1),...,X(N)
      DEFINE IRAND=I*5**15+((1-SIGN(1,I*5**15))/2)*34359738367
      DEFINE RAND=FLOAT(I)/34359738367.
      I=5281
      NSTART=N+400     @ WILL DISCARD INITIAL 400 POINTS
```

```
      XX(1)=0.
      XX(2)=0.
      XX(3)=0.
      XX(4)=0.
      DO 11 L=5,NSTART
      I=IRAND
      XX(L)=2.7607*XX(L-1)-3.8106*XX(L-2)+2.6535*XX(L-3)-
     $0.9238*XX(L-4)+TINORM(IRAND,$11)
11    CONTINUE
      DO 12 I=1,N
12    X(I)=XX(I+NSTART-N)
      PRINT 1,
1     FORMAT(/' INPUT DATA:')
      PRINT 4, (X(I),I=1,N)
C  ENTER B, AND ENTER BAD DATA LOCATIONS IN M(1),...,M(B)
      B=5
      M(1)=3
      M(2)=7
      M(3)=11
      M(4)=12
      M(5)=19
C  EVALUATE PREDICTIVE FILTER COEFFICIENTS
      CALL BURGBD(N,PMAX,X,B,M,IP,Y,PBEST,A,PROD,RHO)
      PRINT 9, X(N)
9     FORMAT(/' MEAN =',E14.6)
      PRINT 10, Y(N)
10    FORMAT(' STANDARD DEVIATION =',E13.8)
      PRINT 2, PBEST
2     FORMAT(/' PBEST =',I3)
      PRINT 3,
3     FORMAT(/' PREDICTIVE FILTER COEFFICIENTS:')
      PRINT 4, (A(I),I=1,PBEST)
4     FORMAT(5E20.8)
      PRINT 5, PROD
5     FORMAT(/' PRODUCT(1-A(P)**2) =',E13.8)
      PRINT 6,
6     FORMAT(/' NORMALIZED CORRELATION COEFFICIENTS:')
      PRINT 4, (RHO(I),I=1,PMAX)
      CALL QTRCOS(CO,J)
C  EVALUATE FRACTIONAL POWERS
      CALL POWERS(PBEST,A,PROD,J,XX,YY,CO)
      PRINT 7,
7     FORMAT(/' FRACTIONAL POWERS:')
      L=J/2+1
      PRINT 8, (XX(I),I=1,L)
8     FORMAT(2X,10E13.6)
      END

      SUBROUTINE BURGBD(N,PMAX,X,B,M,IP,Y,PBEST,A,PROD,RHO) 2 FEB 1976
C  THIS SUBROUTINE COMPUTES THE PREDICTIVE FILTER COEFFICIENTS FOR B BAD POINTS
C  N = NUMBER OF DATA POINTS; INTEGER INPUT
C  PMAX = MAXIMUM ORDER OF FILTER; INTEGER INPUT
C  X(1),X(2),...,X(N) = DATA ARRAY ON INPUT; ALTERED ON OUTPUT
C  ON OUTPUT, X(1),X(2),...,X(PMAX) = A(1,PMAX),A(2,PMAX),...,A(PMAX,PMAX)
C  B = NUMBER OF BAD DATA POINTS; INTEGER INPUT
C  M(1),M(2),...,M(B) = LOCATIONS OF BAD DATA POINTS; INTEGER INPUTS
C  THESE LOCATIONS MUST BE DISTINCT AND LIE IN THE RANGE [1,N]
C  IP(1),IP(2),...,IP(N) = AUXILIARY ARRAY; SCRATCH INPUT
C  Y(1),Y(2),...,Y(N) = AUXILIARY ARRAY; SCRATCH INPUT
C  ON OUTPUT, Y(1),Y(2),...,Y(PMAX) = A(1,1),A(2,2),...,A(PMAX,PMAX)
C  ON OUTPUT, X(N) = MEAN, AND Y(N) = STANDARD DEVIATION OF INPUT DATA
C  PBEST = BEST ORDER OF FILTER; INTEGER OUTPUT
C  A(1),A(2),...,A(PBEST) = PREDICTIVE FILTER COEFFICIENT ARRAY =
C  A(1,PBEST),A(2,PBEST),...,A(PBEST,PBEST); OUTPUT
```

```
C  PROD = PRODUCT(1-A(P)*PBEST)**2) FOR P=1 TO PBEST; OUTPUT
C  RHO(1),...,RHO(PMAX) = NORMALIZED CORRELATION COEFFICIENTS; OUTPUT
C  DIMENSION X(N),Y(N),A(PMAX),RHO(PMAX)     IS REQUIRED IN MAIN PROGRAM
C  DIMENSION M(BMAX),IP(N)    IS REQUIRED IN MAIN PROGRAM
       INTEGER PMAX,B,PBEST,P,BP
       DOUBLE PRECISION SA,SB
       DIMENSION X(1),M(1),IP(1),Y(1),A(1),RHO(1)
       IF(B.GT.0) GO TO 21
       CALL BURG(N,PMAX,X,Y,PBEST,A,PROD,RHO)
       RETURN
21     L=N-B
       IF(PMAX.GT.3.*SQRT(L)) PRINT 2, PMAX,L
2      FORMAT(/' PMAX =',I4,' IS TOO LARGE FOR NUMBER OF GOOD DATA POINTS
     $ N-B =',I5)
C  SET UP IP ARRAY FOR P=0; EQ. 173
       DO 22 I=1,N
22     IP(I)=1
       DO 23 L=1,B
       I=M(L)
23     IP(I)=0
C  COMPUTE MEAN OF GOOD DATA POINTS
       S1=0.
       DO 1 I=1,N
       IF(IP(I).EQ.0) GO TO 1
       S1=S1+X(I)
1      CONTINUE
       S1=S1/(N-B)
C  SUBTRACT MEAN, AND SCALE TO UNIT VARIANCE, FOR GOOD DATA POINTS
       S2=0.
       DO 3 I=1,N
       IF(IP(I).EQ.0) GO TO 3
       X(I)=X(I)-S1
       S2=S2+X(I)**2
3      CONTINUE
       S2=SQRT(S2/(N-B-1.))
       T=1./S2
       DO 5 I=1,N
       IF(IP(I).EQ.0) GO TO 5
       X(I)=X(I)*T
       Y(I)=X(I)
5      CONTINUE
C  BEGIN RECURSION
       P=0
       PRODUC=1.
       AICMIN=0.
       PBEST=0
       PROD=1.
6      P=P+1
C  UPDATE IP ARRAY; EQ. 173
       DO 24 L=1,B
       I=M(L)+P
       IF(I.GT.N) GO TO 24
       IP(I)=0
24     CONTINUE
       BP=0
       L=P+1
       DO 25 I=L,N
25     BP=BP+1-IP(I)
       K=N-P-BP
       IF(K.LT.25) PRINT 26, K,P
26     FORMAT(/' NUMBER OF VALID ERROR POINTS IS ONLY',I3,' FOR P=',I3)
C  CALCULATE CROSS-GAIN; EQ. 193
       SA=0.D0
```

```
      SB=0.D0
      L=P+1
      DO 7 I=L,N
      IF(IP(I).EQ.0) GO TO 7
      SA=SA+X(I)*Y(I-1)
      SB=SB+X(I)**2+Y(I-1)**2
7     CONTINUE
      G=2.*SA/SB
      PRODUC=PRODUC*(1.-G*G)
C  CALCULATE FILTER COEFFICIENTS; EQS. 1958196. STORE IN X(1),...,X(P)
      X(P)=G
      IF(P.EQ.1) GO TO 8
      L=P/2
      DO 9 I=1,L
      T=X(I)-G*X(P-I)
      X(P-I)=X(P-I)-G*X(I)
9     X(I)=T
C  CALCULATE NORMALIZED CORRELATION COEFFICIENT; EQ. 149
8     T=X(P)
      IF(P.EQ.1) GO TO 14
      L=P-1
      DO 15 I=1,L
15    T=T+X(I)*RHO(P-I)
14    RHO(P)=T
C  CALCULATE AKAIKE'S INFORMATION CRITERION; EQS. 1958202
      RELERR=(1.-G*G)*SNGL(SB)/(2.*K)
      AIC=LOG(RELERR)+2.*FLOAT(P)/K
      IF(AIC.GE.AICMIN) GO TO 10
      AICMIN=AIC
      PBEST=P
      PROD=PRODUC
      DO 11 I=1,P
11    A(I)=X(I)
10    IF(P.EQ.PMAX) GO TO 16
C  UPDATE FORWARD AND BACKWARD SEQUENCES; EQ.191
      L=P+1
      DO 12 I=N,L,-1
      IF(IP(I).EQ.0) GO TO 12
      T=X(I)-G*Y(I-1)
      Y(I)=Y(I-1)-G*X(I)
      X(I)=T
12    CONTINUE
      Y(P)=G
      GO TO 6
16    Y(PMAX)=G
      IF(PBEST.EQ.PMAX) GO TO 4
C  COMPUTE EXTRAPOLATED NORMALIZED CORRELATION
C  COEFFICIENTS FROM PBEST+1 TO PMAX; EQ. 165
      L=PBEST+1
      DO 17 P=L,PMAX
      A(P)=0.
      T=0.
      DO 18 I=1,PBEST
18    T=T+A(I)*RHO(P-I)
17    RHO(P)=T
4     X(N)=S1
      Y(N)=S2

      RETURN
      END
```

```
      SUBROUTINE POWERS(PBEST,A,PROD,J,XX,YY,CO)
C  THIS SUBROUTINE COMPUTES THE FRACTIONAL POWERS IN BANDS 1/(J*DELTA); EQ. J-4
C  PBEST = BEST ORDER OF FILTER; INTEGER INPUT
C  A(1),...,A(PBEST) = FILTER COEFFICIENT ARRAY; INPUT
C  PROD = PRODUCT(1-A(P)**2)  FOR P=1 TO PBEST; INPUT
C  J = SIZE OF FFT  (J/2+1=NUMBER OF FREQUENCY POINTS); INTEGER INPUT
C  XX = AUXILIARY ARRAY ON INPUT
C  XX(1),...,XX(J/2+1) = FRACTIONAL POWERS ON OUTPUT
C  YY = AUXILIARY ARRAY; SCRATCH INPUT
C  CO(1),...,CO(J/4+1) = QUARTER COSINE TABLE FOR FFT; INPUT
C  DIMENSION XX(J),YY(J),CO(J/4+1)  IS REQUIRED IN MAIN PROGRAM
C  DIMENSION A(PMAX)  IS REQUIRED IN MAIN PROGRAM, WHERE PMAX.GE.PBEST
      INTEGER PBEST
      DIMENSION A(1),XX(1),YY(1),CO(1)
      F=PROD*2./J
      XX(1)=1.
      YY(1)=0.
      DO 1 I=1,PBEST
      XX(I+1)=-A(I)
1     YY(I+1)=0.
      L=PBEST+2
      DO 2 I=L,J
      XX(I)=0.
2     YY(I)=0.
      L=1.4427*LOG(J)+.5        LOG2(J)
      CALL MKLFFT(XX,YY,CO,L,-1)
      L=J/2+1
      DO 3 I=1,L
3     XX(I)=F/(XX(I)**2+YY(I)**2)
      RETURN
      END
```

REFERENCES

1. J. Makhoul, "Linear Prediction : A Tutorial Review," Proceedings of the IEEE, vol. 63, no. 4, April 1975, pp. 561-580.

2. T. J. Ulrych and T. N. Bishop, "Maximum Entropy Spectral Analysis and Autoregressive Decomposition," Reviews of Geophysics and Space Physics, vol. 13, no. 1, February 1975, pp. 183-200.

3. H. Akaike, "On the Use of a Linear Model for the Identification of Feedback Systems," Annals of the Institute of Statistical Mathematics, vol. 20, no. 3, 1968, pp. 425-439.

4. J. P. Burg, "New Concepts in Power Spectra Estimation," 40th Meeting of Society of Exploration Geophysicists, New Orleans, Louisiana, November 1970.

5. R. H. Jones, "Spectrum Estimation with Missing Observations," Annals of the Institute of Statistical Mathematics, vol. 23, no. 3, 1971, pp. 387-398.

6. E. Parzen, "Some Recent Advances in Time Series Analysis," Statistical Models and Turbulence, edited by M. Rosenblatt, Springer-Verlag, New York, 1971, pp. 470-492.

7. D. C. Riley and J. P. Burg, "Time and Space Adaptive Deconvolution Filters," 42 Meeting of Society of Exploration Geophysicists, Anaheim, Calif., 1972.

8. B. Veltman, et al., "Some Remarks on the Use of Auto-correlation Functions with the Analysis and Design of Signals," Signal Processing, edited by J. W. R. Griffiths, P. L. Stocklin, and C. Van Schooneveld, Academic Press, London and New York, 1973.

9. R. H. Jones, "Autoregressive Spectrum Estimation," Third Conference on Probability and Statistics in Atmospheric Science, Boulder, Colo., 19-22 June 1973.

10. W. R. King, W. H. Swindell, and L. J. O'Brien, Final Report on Development of a Curvilinear Ray Theory Model and Maximum Entropy Spectral

Analysis, Texas Instruments Inc., Report ALEX(03)-FR-74-01, 28 February 1974.

11. E. M. Hofstetter, "An Introduction to the Mathematics of Linear Predictive Filtering as Applied to Speech Analysis and Synthesis," Lincoln Lab, Mass. Inst. of Tech., Technical Note 1973-36, Rev. 1, 12 April 1974.

12. R. H. Jones, "Identification and Autoregressive Spectrum Estimation," Proceedings of Conference on Decision and Control, Phoenix, Arizona, 20-22 November 1974.

13. E. Parzen, "Some Recent Advances in Time Series Modeling," IEEE Transaction on Automatic Control, vol. AC-19, no. 6, December 1974, pp. 723-730.

14. R. N. McDonough, "Maximum-Entropy Spatial Processing of Array Data," Geophysics, vol. 39, no. 6, December 1974, pp. 843-851.

15. F. J. Harris, A Maximum Entropy Filter, Naval Undersea Center Report NUC TP 442, January 1975.

16. G. E. Box and G. M. Jenkins, Time Series Analysis; Forecasting and Control, Holden-Day, San Francisco, Calif., 1970.

17. A. H. Nuttall, "Trigonometric Smoothing and Interpolation of Sampled Complex Functions, via the FFT," NUSC Technical Memorandum TC-94-71, 19 April 1971.

18. J. P. Burg, "Maximum Entropy Spectral Analysis," 37th Meeting of Society of Exploration Geophysicists, Oklahoma City, Oklahoma, 31 October 1967.

19. J. A. Edward and M. M. Fitelson, "Notes on Maximum-Entropy Processing," IEEE Transactions on Information Theory, vol IT-19, March 1973, pp. 232-234.

20. A van den Bos, "Alternative Interpretation of Maximum Entropy Spectral Analysis," IEEE Transactions on Information Theory, vol. IT-17, no. 4, July 1971, pp. 493-494.

21. J. P. Burg, "A New Analysis Technique for Time Series Data," NATO Advanced Study Institute on Signal Processing, Enschede, Netherlands, volume 1, August 1968.

22. H. Akaike, "A New Look at Statistical Model Identification," IEEE Transactions on Automatic Control, vol. AC-19, December 1974, pp. 716-723. (This entire volume is devoted to Systems Identification and Time Series Analysis.)

23. R. T. Lacoss, "Data Adaptive Spectral Analysis Methods," Geophysics, vol. 36, no. 4, August 1971, pp. 661-675.

24. N. Wiener, Extrapolation, Interpolation, and Smoothing of Stationary Time Series, John Wiley and Sons, Inc., New York, May 1950.

25. J. F. Ferrie, G. C. Carter, and C. W. Nawrocki, "Availability of Markel's FFT Algorithm," NUSC Technical Memorandum TC-1-73, 15 January 1973.

NUSC Technical Document 5419
19 May 1976

FORTRAN Program for Multivariate Linear Predictive Spectral Analysis, Employing Forward and Backward Averaging

Albert H. Nuttall

ABSTRACT

A FORTRAN program for multivariate linear predictive spectral analysis, employing forward and backward averaging, is presented. The program is written for general M, where M is the number of processes, with the exception of an internal function and three internal subroutines which are written for M = 2 in this version of the program, but can easily be generalized to general M. This program generalizes Burg's algorithm to the multivariate case. The theory behind this program will be published in a forthcoming NUSC Technical Report.

Approved for public release; distribution unlimited.

FORTRAN PROGRAM FOR MULTIVARIATE LINEAR PREDICTIVE SPECTRAL ANALYSIS, EMPLOYING FORWARD AND BACKWARD AVERAGING

INTRODUCTION

The Burg algorithm for spectral analysis has proven to be a very attractive method for a univariate process. * Extension to a multivariate process has been desired for some time and has now been accomplished, and is documented here in the form of a FORTRAN program. Publication of this program will make immediately available to those interested users a powerful method of spectral analysis; the theory behind this program will be published soon in a NUSC Technical Report. The basic analytical problem was to minimize the sum of the traces of the forward and backward error matrices by choice of the partial correlation coefficients, subject to a linear matrix constraint which guaranteed that the forward-extrapolated and backward-extrapolated correlation estimates were Hermitians of each other. Solution of a bilinear matrix equation is required in the process.

It has just come to the author's attention that a similar procedure has been presented by R. H. Jones.† Comparison of the details of the two procedures and programs has not been undertaken yet.

---

*A. H. Nuttall, "Spectral Analysis of a Univariate Process with Bad Data Points, via Maximum Entropy and Linear Predictive Techniques," NUSC Technical Report 5303, 26 March 1976.

†R. H. Jones, "Multivariate Maximum Entropy Spectral Analysis," Applied Time Series Analysis Symposium, Tulsa, Oklahoma, 14-15 May 1976.

REVERSE BLANK

```
C   MULTIVARIATE LINEAR PREDICTIVE SPECTRAL ANALYSIS,
C   EMPLOYING FORWARD AND BACKWARD AVERAGING; REAL PROCESSES
C   THIS PROGRAM IS WRITTEN FOR GENERAL M, WITH THE EXCEPTION
C   OF FUNCTION DETERM AND SUBROUTINES SDM, INVERT, AND SOLVE.
C   USER: CHANGE LINES 14 AND 22, AND REPLACE SUBROUTINE DATA
C   M = ORDER OF MULTIVARIATE PROCESS; INTEGER INPUT
C   N = NUMBER OF DATA POINTS IN EACH PROCESS; INTEGER INPUT
C   X(1,1)...X(N,1),...,X(1,M)...X(N,M) = INPUT DATA; ALTERED ON OUTPUT
C   PMAX = MAXIMUM ORDER OF FILTER; INTEGER INPUT
C   NF = SIZE OF FFT (MUST BE A POWER OF 2 TO USE MKLFFT); INTEGER INPUT
C   PBEST = BEST ORDER OF FILTER; INTEGER OUTPUT
C   UBEST = MATRIX OF COEFFICIENTS IN SPECTRAL ESTIMATE; OUTPUT
      PARAMETER M=2     ⊙ BIVARIATE PROCESS
      PARAMETER N=100, PMAX = 20, NF=1024, NF41=NF/4+1
      INTEGER PBEST,P
      DIMENSION X(N,M),Y(N,M),Z(N,M),UBEST(M,M),AP(M,M,PMAX),
     $BP(M,M,PMAX),AVE(M),XX(NF,M,M),YY(NF,M,M),COSI(NF41),
     $U(M,M),V(M,M),UI(M,M),VI(M,M),A(M,M),B(M,M),
     $WA(M,M),WB(M,M),WC(M,M),WD(M,M),WE(M,M)
      EQUIVALENCE(X,Y)
C   INPUT DATA IN X(1,1)...X(N,1),...,X(1,M)...X(N,M)
      CALL DATA
      PRINT 1,
1     FORMAT(/' INPUT DATA:')
      DO 2 I=1,M
      PRINT 3, I
3     FORMAT('   PROCESS NUMBER',I2)
2     PRINT 4, (X(K,I),K=1,N)
4     FORMAT(5E20.9)
C   EVALUATE PARTIAL CORRELATION COEFFICIENTS
      CALL PCC
      PRINT 5,
5     FORMAT(/' SAMPLE MEANS:')
```

```
      PRINT 6, (AVE(I),I=1,M)
6     FORMAT(4E20.8)
      PRINT 7, PBEST
7     FORMAT(/' PBEST =',I3)
      PRINT 8,
8     FORMAT(/' UBEST:')
      PRINT 6, ((UBEST(I,J),I=1,M),J=1,M)
      PRINT 9,
9     FORMAT(/' FORWARD PARTIAL CORRELATION COEFFICIENTS:')
      DO 10 L=1,PMAX
10    PRINT 6, ((AP(I,J,L),I=1,M),J=1,M)
      PRINT 11,
11    FORMAT(/' BACKWARD PARTIAL CORRELATION COEFFICIENTS:')
      DO 12 L=1,PMAX
12    PRINT 6, ((BP(I,J,L),I=1,M),J=1,M)
C  EVALUATE PREDICTIVE FILTER COEFFICIENTS
      CALL PFC
      PRINT 13,
13    FORMAT(/' FORWARD PREDICTIVE FILTER COEFFICIENTS:')
      DO 14 L=1,PBEST
14    PRINT 6, ((AP(I,J,L),I=1,M),J=1,M)
C  EVALUATE PREDICTIVE-ERROR FILTER TRANSFER FUNCTION
      CALL PEFTF
C  EVALUATE SPECTRAL DENSITY MATRIX AND COHERENCE
      K=NF/2+1
      CALL SDM
      PRINT 15,
15    FORMAT(/' SPECTRAL DENSITY MATRIX AND COHERENCE FOR M=2:')
      PRINT 16,
16    FORMAT(11X,'AUTO11',14X,'AUTO22',10X,'REAL(CROSS12)',7X,'IMAG(CROS
     $S12)',9X,'MAG SQ COH',11X,'ARGUMENT')
      PRINT 17, (XX(L,1,1),XX(L,2,2),XX(L,1,2),YY(L,1,2),YY(L,1,1),YY(L,
     $2,2),L=1,K)
17    FORMAT(6E20.8)
```

```
      SUBROUTINE DATA
C   THIS SUBROUTINE GENERATES DATA FOR M=2, BIVARIATE PROCESS
      DEFINE IRAND=I*5**15+((1-SIGN(1,I*5**15))/2)*34359738367
      DEFINE RAND=FLOAT(I)/34359738367.
      I=5281
      L=N+100     N WILL DISCARD INITIAL 100 POINTS
      XX(1,1,1)=0.
      XX(1,2,1)=0.
      DO 1 K=2,L
      I=IRAND
      XX(K,1,1)=0.65*XX(K-1,1,1)-0.75*XX(K-1,2,1)+RAND-0.5
      I=IRAND
1     XX(K,2,1)=0.65*XX(K-1,1,1)+0.55*XX(K-1,2,1)+RAND-0.5
      DO 2 K=1,N
      X(K,1)=XX(K+L-N,1,1)
2     X(K,2)=XX(K+L-N,2,1)
      RETURN
```

```
      SUBROUTINE PCC
C     THIS SUBROUTINE COMPUTES PBEST, UBEST, AND THE PARTIAL
C     CORRELATION COEFFICIENTS FOR P = 1 TO PMAX; ANY M
      I=N
      J=PMAX
      IF(J.GT..5*SQRT(I)) PRINT 1, J,I
1     FORMAT(/' PMAX =',I4,' IS TOO LARGE FOR NUMBER OF DATA POINTS N ='
     *,I5)
      FAC=MAX(2.,LOG10(N))*M*M/N
C     SUBTRACT MEANS; FILL IN DATA ARRAYS
      ONP=1./N
      ONP1=1./(N-1)
      DO 2 I=1,M
      TA=0.
      DO 3 K=1,N
3     TA=TA+Y(K,I)
      TA=TA*ONP
      AVE(I)=TA
      DO 2 K=1,N
      Y(K,I)=Y(K,I)-TA
2     Z(K,I)=Y(K,I)
C     INITIALIZE CORRELATION ARRAYS
      CALL AUTO(2,N-1,Y,WC)
      DO 4 I=1,M
      DO 4 J=I,M
      TA=Y(1,I)*Y(1,J)
      TB=Y(N,I)*Y(N,J)
      U(I,J)=(WC(I,J)+TA+TB)*ONP
      WA(I,J)=(WC(I,J)+TB)*ONP1
4     WB(I,J)=(WC(I,J)+TA)*ONP1
      CALL EQUAL(U,V)
      CALL CROSS(2,N,Y,Y,WC)
      CALL SCALE(ONP1,WC,WC)
```

```
C   BEGIN RECURSION
      AICMIN=LOG(DETERM(U))
      PBEST=0
      CALL EQUAL(U,UBEST)
      DO 5 P=1,PMAX
      ONP=1./(N-P)
      ONP1=1./(N-P-1)
C   EVALUATE MATRICES REQUIRED IN MATRIX EQUATION
      CALL INVERT(V,VI)
      CALL MULT(VI,WB,WD)
      CALL MULT(WD,VI,WB)
      CALL INVERT(U,UI)
      CALL MULT(UI,WA,WD)
      CALL MULT(WD,UI,WA)
      CALL MULT(WC,VI,WD)
      CALL MULT(UI,WC,WE)
      CALL ADD(WD,WE,WC)
C   SOLVE MATRIX EQUATION
      CALL SOLVE
C   EVALUATE PARTIAL CORRELATION COEFFICIENTS
      CALL MULT(WC,VI,A)
      CALL TRANS(WC,WD)
      CALL MULT(WD,UI,B)
      CALL EQUAL(A,AP(1,1,P))
      CALL EQUAL(B,BP(1,1,P))
C   UPDATE MATRICES U AND V
      CALL MULT(A,WB,WE)
      CALL SUB(U,WE,U)
      CALL MULT(B,WC,WE)
      CALL SUB(V,WE,V)
C   UPDATE DATA SEQUENCES Y AND Z
      L=P+1
      DO 6 K=N,L,-1
      DO 7 I=1,M
      TA=Z(K-1,I)
```

```
      DO 8 J=1,M
8     TA=TA-B(I,J)*Y(K,J)
7     Z(K,I)=TA
      DO 9 I=1,M
      TA=Y(K,I)
      DO 10 J=1,M
10    TA=TA-A(I,J)*Z(K-1,J)
9     Y(K,I)=TA
6     CONTINUE
C  EVALUATE OPTIMUM ERROR MATRICES
      CALL AUTO(P+2,N,Y,WD)
      CALL AUTO(P+1,N-1,Z,WE)
      DO 11 I=1,M
      DO 11 J=1,M
      IF(I.LE.J) GO TO 12
      WA(I,J)=WA(J,I)
      WB(I,J)=WB(J,I)
      GO TO 11
12    WA(I,J)=(WD(I,J)+Y(P+1,I)*Y(P+1,J))*ONP
      WB(I,J)=(WE(I,J)+Z(N,I)*Z(N,J))*ONP
11    CONTINUE
C  CALCULATE AKAIKE'S INFORMATION CRITERION
      AIC=LOG(DETERM(U))+FAC*P
      IF(AIC.GE.AICMIN) GO TO 13
      AICMIN=AIC
      PBEST=P
      CALL EQUAL(U,UBEST)
13    IF(P.EQ.PMAX) GO TO 5
C  CALCULATE NEW CORRELATION MATRICES
      CALL SCALE(ONP1,WD,WA)
      CALL SCALE(ONP1,WE,WB)
      CALL CROSS(P+2,N,Y,Z,WC)
      CALL SCALE(ONP1,WC,WC)
5     CONTINUE
      RETURN
```

```
      SUBROUTINE PFC
C   THIS SUBROUTINE COMPUTES THE PREDICTIVE FILTER COEFFICIENTS; ANY M
      IF(PBEST.LE.1) RETURN
      DO 1 P=2,PBEST
      IA=P-1
      DO 2 L=1,IA
      IB=P-L
      CALL MULT(AP(1,1,P),BP(1,1,IB),WA)
      CALL SUB(AP(1,1,L),WA,WA)
      CALL MULT(BP(1,1,P),AP(1,1,L),WB)
      CALL SUB(BP(1,1,IB),WB,BP(1,1,IB))
2     CALL EQUAL(WA,AP(1,1,L))
1     CONTINUE
      RETURN

      SUBROUTINE PEFTF
C   THIS SUBROUTINE COMPUTES THE PREDICTIVE-ERROR
C   FILTER TRANSFER FUNCTION; ANY M
      K=1.4427*LOG(NF)+.5
      CALL QTRCOS(COSI,NF)
      DO 1 I=1,M
      DO 1 J=1,M
      XX(1,I,J)=0.
      IF(I.EQ.J) XX(1,1,J)=1.
      YY(1,I,J)=0.
      IA=PBEST+1
      DO 2 L=2,IA
      XX(L,I,J)=-AP(I,J,L-1)
2     YY(L,I,J)=0.
      IA=PBEST+2
      DO 3 L=IA,NF
      XX(L,I,J)=0.
3     YY(L,I,J)=0.
1     CALL MKLFFT(XX(1,I,J),YY(1,I,J),COSI,K,-1)
      RETURN
```

```
      SUBROUTINE SUM
C  THIS SUBROUTINE COMPUTES THE SPECTRAL DENSITY MATRIX AND COHERENCE FOR M=2
      DO 1 L=1,K
      WA(1,1)=XX(L,2,2)
      WA(1,2)=-XX(L,1,2)
      WA(2,1)=-XX(L,2,1)
      WA(2,2)=XX(L,1,1)
      WB(1,1)=YY(L,2,2)
      WB(1,2)=-YY(L,1,2)
      WB(2,1)=-YY(L,2,1)
      WB(2,2)=YY(L,1,1)
      TA=DETERM(WA)-DETERM(WB)
      TB=WA(1,1)*WB(2,2)+WA(2,2)*WB(1,1)-WA(1,2)*WB(2,1)-WA(2,1)*WB(1,2)
      TA=1./(TA**2+TB**2)
      CALL TRANS(WA,WC)
      CALL MULT(UBEST,WC,WD)
      CALL MULT(WB,WD,WC)
      TB=WC(1,2)-WC(2,1)
      CALL MULT(WA,WD,WC)
      CALL TRANS(WB,WD)
      CALL MULT(UBEST,WD,WE)
      CALL MULT(WB,WE,WD)
      CALL ADD(WC,WD,WC)
      YY(L,1,1)=(WC(1,2)**2+TB**2)/(WC(1,1)*WC(2,2))    ! MSC
      YY(L,2,2)=ATAN2(TB,WC(1,2))    ! ARGUMENT
      XX(L,1,1)=TA*WC(1,1)    ! AUTO11
      XX(L,2,2)=TA*WC(2,2)    ! AUTO22
      XX(L,1,2)=TA*WC(1,2)    ! REAL(CROSS12)
      YY(L,1,2)=TA*TB         ! IMAG(CROSS12)
      XX(L,2,1)=0.
      YY(L,2,1)=0.
1     CONTINUE
      RETURN
```

```
      SUBROUTINE CROSS(N1,N2,A,B,C)     @ A,B,A NG
C  THIS SUBROUTINE COMPUTES A CROSS CORRELATION MATRIX; ANY M
      DIMENSION A(N,M),B(N,M),C(M,M)
      DOUBLE PRECISION T
      DO 1 I=1,M
      DO 1 J=1,M
      T=0.D0
      DO 2 K=N1,N2
2     T=T+A(K,I)*B(K-1,J)
1     C(I,J)=T
      RETURN

      SUBROUTINE AUTO(N1,N2,A,B)    @  A,A NG
C  THIS SUBROUTINE COMPUTES AN AUTO CORRELATION MATRIX; ANY M
      DIMENSION A(N,M),B(M,M)
      DOUBLE PRECISION T
      DO 1 I=1,M
      DO 1 J=1,M
      IF(I.LE.J) GO TO 2
      B(I,J)=B(J,I)
      GO TO 1
2     T=0.D0
      DO 3 K=N1,N2
3     T=T+A(K,I)*A(K,J)
      B(I,J)=T
1     CONTINUE
      RETURN

      SUBROUTINE EQUAL(A,B)
C  THIS SUBROUTINE SETS TWO MXM MATRICES EQUAL
      DIMENSION A(M,M),B(M,M)
      DO 1 I=1,M
      DO 1 J=1,M
1     B(I,J)=A(I,J)
      RETURN
```

```
      SUBROUTINE SCALE(T,A,B)    @  A,A OK
C  THIS SUBROUTINE SCALES AN MXM MATRIX
      DIMENSION A(M,M),B(M,M)
      DO 1 I=1,M
      DO 1 J=1,M
1     B(I,J)=T*A(I,J)
      RETURN

      SUBROUTINE TRANS(A,B)    @  A,A NG
C  THIS SUBROUTINE TRANSPOSES AN MXM MATRIX
      DIMENSION A(M,M),B(M,M)
      DO 1 I=1,M
      DO 1 J=1,M
1     B(I,J)=A(J,I)
      RETURN

      SUBROUTINE ADD(A,B,C)      @  A,B,A OK
C  THIS SUBROUTINE ADDS TWO MXM MATRICES
      DIMENSION A(M,M),B(M,M),C(M,M)
      DO 1 I=1,M
      DO 1 J=1,M
1     C(I,J)=A(I,J)+B(I,J)
      RETURN

      SUBROUTINE SUB(A,B,C)      @  A,B,A OK
C  THIS SUBROUTINE SUBTRACTS TWO MXM MATRICES
      DIMENSION A(M,M),B(M,M),C(M,M)
      DO 1 I=1,M
      DO 1 J=1,M
1     C(I,J)=A(I,J)-B(I,J)
      RETURN
```

```
      SUBROUTINE MULT(A,B,C)     @  A,B,A NG
C  THIS SUBROUTINE MULTIRLIES TWO MXM MATRICES
      DIMENSION A(M,M),B(M,M),C(M,M)
      REAL T
      DO 1 I=1,M
      DO 1 J=1,M
      T=0.
      DO 2 K=1,M
2     T=T+A(I,K)*B(K,J)
1     C(I,J)=T
      RETURN

      SUBROUTINE INVERT(A,B)    @  A,A NG
C  THIS SUBROUTINE INVERTS A 2X2 MATRIX
      DIMENSION A(2,2),B(2,2)
      TA=1./DETERM(A)
      B(1,1)=A(2,2)*TA
      B(2,2)=A(1,1)*TA
      B(1,2)=-A(1,2)*TA
      B(2,1)=-A(2,1)*TA
      RETURN
```

```
      SUBROUTINE SOLVE
C  THIS SUBROUTINE SOLVES MATRIX EQUATION FOR M=2, BIVARIATE PROCESS
      TA=WA(1,1)+WA(2,2)+WB(1,1)+WB(2,2)
      TB=DETERM(WA)-DETERM(WB)
      CALL MULT(WC,WB,WD)
      WE(1,1)=WA(2,2)
      WE(1,2)=-WA(1,2)
      WE(2,1)=-WA(2,1)
      WE(2,2)=WA(1,1)
      CALL MULT(WE,WC,WA)
      CALL ADD(WD,WA,WD)
      CALL SCALE(TA,WB,WB)
      WB(1,1)=WB(1,1)+TB
      WB(2,2)=WB(2,2)+TB
      CALL INVERT(WB,WE)
      CALL MULT(WD,WE,WC)
      RETURN

      FUNCTION DETERM(A)
C  THIS FUNCTION COMPUTES THE DETERMINANT OF A 2X2 MATRIX
      DIMENSION A(2,2)
      DETERM=A(1,1)*A(2,2)-A(1,2)*A(2,1)
      RETURN
      END
```

```
      SUBROUTINE MRLFFT(X,Y,CC,M,ISN)
      DIMENSION X(1),Y(1),CC(1),L(12)
      EQUIVALENCE (L12,L(1)),(L11,L(2)),(L10,L(3)),(L9,L(4)),(L8,L(5)),
     1(L7,L(6)),(L6,L(7)),(L5,L(8)),(L4,L(9)),(L3,L(10)),(L2,L(11)),
     2(L1,L(12))
      N=2**M
      ND4=N/4
      ND4P1=ND4+1
      ND4P2=ND4P1+1
      ND2P2=ND4+ND4P2
      DO 8 LO=1,M
      LMX=2**(M-LO)
      LIX=2*LMX
      ISCL=N/LIX
      DO 8 LM=1,LMX
      IARG=(LM-1)*ISCL+1
      IF(IARG.LE.ND4P1) GO TO 4
      C=-CC(ND2P2-IARG)
      S=ISN*CC(IARG-ND4)
      GO TO 6
    4 C=CC(IARG)
      S=ISN*CC(ND4P2-IARG)
    6 DO 8 LI=LIX,N,LIX
      J1=LI-LIX+LM
      J2=J1+LMX
      T1=X(J1)-X(J2)
      T2=Y(J1)-Y(J2)
      X(J1)=X(J1)+X(J2)
      Y(J1)=Y(J1)+Y(J2)
      X(J2)=C*T1-S*T2
      Y(J2)=C*T2+S*T1
    8 CONTINUE
      DO 40 J=1,12
      L(J)=1
      IF(J-M) 31,31,40
```

```
   31 L(J)=2**(M+1-J)
   40 CONTINUE
      JN=1
      DO 60 J1=1,L1
      DO 60 J2=J1,L2,L1
      DO 60 J3=J2,L3,L2
      DO 60 J4=J3,L4,L3
      DO 60 J5=J4,L5,L4
      DO 60 J6=J5,L6,L5
      DO 60 J7=J6,L7,L6
      DO 60 J8=J7,L8,L7
      DO 60 J9=J8,L9,L8
      DO 60 J10=J9,L10,L9
      DO 60 J11=J10,L11,L10
      DO 60 JR=J11,L12,L11
      IF(JN-JR) 51,51,52
   51 R=X(JN)
      X(JN)=X(JR)
      X(JR)=R
      FI=Y(JN)
      Y(JN)=Y(JR)
      Y(JR)=FI
   52 JN=JN+1
   60 CONTINUE
      RETURN
      END


      SUBROUTINE QTRCOS(C,N)
      DIMENSION C(1)
      N41=N/4+1
      SCL=6.283185307/N
      DO 1 I=1,N41
      C(I)=COS((I-1)*SCL)
      RETURN
      END
```

INPUT DATA:
PROCESS NUMBER 1

.539017290+00	.245720774+00	-.482462563+00	-.992351741+00	-.624363147+0
.311439447+00	.745712250+00	.943723917+00	.151725411+00	-.768593825+0
-.137811743+00	.258360229+00	.797701389+00	.712606726+00	.801285848+00
.436427981+00	-.447039306-01	-.712001279+00	-.113687564+01	-.928196430+00
-.334296368+00	.578125685+00	.136806943+01	.101646697+01	.507132798+00
-.105504647+01	-.205701426+01	-.194855675+01	-.141357696+01	-.190089338+00
.186863446+01	.314386600+01	.213840547+01	-.460096721+00	-.231132931+01
-.360816958+01	-.284176603+01	-.235473484+00	.166777730+01	.334291941+01
.268775697+01	.568884477+00	-.226317665+01	-.359439639+01	-.267972845+01
-.435471714+00	.217180708+01	.354075885+01	.232882616+01	-.226566900+00
-.253764409+01	-.329867983+01	-.273452786+01	-.406073399+00	.250713751+01
.446607794+01	.321279564+01	.910315067+00	-.134065935+01	-.278673139+01
-.255580643+01	-.111350261+01	.952319160+00	.318501863+01	.370616418+01
.173904091+01	-.891706161+00	-.248540881+01	-.278242433+01	-.134156680+01
.821645573+00	.300343323+01	.354829520+01	.262362026+01	-.899125412-01
-.343308693+01	-.477496344+01	-.349630961+01	-.690292142+00	.243947476+01
.406036778+01	.364338505+01	.546732336+00	-.188848424+01	-.325925767+01
-.261742641+01	-.130845191+01	.124780042+01	.265499102+01	.276964760+01
.154117967+01	-.164883353+01	-.359906724+01	-.334951061+01	-.186946419+01
.179766156+00	.239384729+01	.251525083+01	.163953295+01	-.348173000+00

PROCESS NUMBER 2

.84303e592+00	.e69348198+00	.160710171+00	.143860e16+00	-.811205745+00
-.9e9363019+00	-.e81254640-01	.719463959+00	.559866265+00	-.304195061-01
-.e595550e1+00	-.324309267+0C	.1031781e6+00	.347221136+00	.806906846+00
.573e04117+00	.392593741+00	.141012892+00	.846649855-01	-.19283e110+00
-.118136658+01	-.e622690e9+0C	-.200975716+00	.6e4971411+00	.140607059+01
.117015797+01	.e14815375-01	-.819632486+00	-.173084117+01	-.219331250+01
-.173391955+01	.581636146+00	.242631036+01	.290413064+01	.171095636+01
-.102425857+00	-.251422542+01	-.280791241+01	-.195120275+01	.509945005+00
.254005781+01	.300857615+01	.182085487+01	-.845298506+00	-.268139764+01
-.315916e00+01	-.173311681+01	.924678788+00	.250485858+01	.302334699+01
.194512719+01	-.499722436+0J	-.291389978+01	-.355933656+01	-.253520629+01
.436254069+00	.279261303+01	.313536388+01	.251057035+01	.872932166+00
-.126357e09+01	-.250785863+01	-.257481125+01	-.997304127+00	.135073581+01
.268305531+01	.233738655+01	.826688573+00	-.111395001+01	-.216378626+01
-.252566388+01	-.107619643+01	.986667454+00	.300149566+01	.382641739+01
.235223493+01	-.816001907+0J	-.327553758+01	-.450584e14+01	-.257751539+01
-.218958363+00	.294191515+01	.364813358+01	.282662770+01	-.603196919-01
-.199258408+01	-.276155442+01	-.265696651+01	-.647379011+00	.173391402+01
.316297090+01	.262459749+01	.383558452+00	-.196807757+01	-.27e345471+01
-.241e50638+01	-.101002751+01	.115360206+01	.196722519+01	.166847882+01

SAMPLE MEANS:

.12088474-01 .29368686-01

PBEST = 1

UBEST:

.85827529-01	-.16895235-02	-.16895533-02	.94233543-01

FORWARD PARTIAL CORRELATION COEFFICIENTS:

.87178199+00	.63438967+00	-.77056313+00	.56007387+00
-.23906691-01	.16050778+00	-.44208146-01	-.14140500+00
.12861929+00	.10583678+00	-.69130776-01	-.13053089+00
-.11691187+00	.23187558+00	.17878873+00	.41780444-02
.40615016-01	.27998135-01	-.10429599+00	.16929921-01
.24605042+00	-.12032283-01	-.16857674-01	-.43390963-02
.17854212+00	.10247301+00	.91585344-01	-.11016705+00
.18917018+00	.93947226-01	-.27802812-01	.86785080-02
.83620687-01	.13179397+00	-.10202888+00	-.22455782+00
-.52716018-01	.16927882+00	-.40031603-01	-.26368762-01
-.34835575-01	.69706881-01	.57877776-01	-.15375618-01
.17867703+00	.15723763+00	.12828297-01	-.60952150-01
.34596313-02	.39651371-02	-.48080474-02	.25300868-01
.27076123-01	-.60010745-01	-.26705663+00	-.25429490-01
-.32320119-01	.20140195-01	.16263054+00	-.18064264+00
-.68684286-02	.12352235+00	-.13155429+00	-.23900040+00
-.31237028-01	.77121304-02	.46082551-01	-.13080224+00
-.67714986-01	.12319486+00	-.60138148-02	.23447769+00
.30910177+00	.99847924-01	-.17542228+00	.78581150-01
.10105012+00	-.43833962-01	-.79558321-01	.11067312-01

BACKWARD PARTIAL CORRELATION COEFFICIENTS:

.56634543+00	-.63158400+00	.77095323+00	.86551043+00
-.38619705-01	-.68005920-01	.91898256-01	-.10944276+00
.98088672-01	-.39144080-01	.49347097-01	-.11626068+00
-.31436418-01	.18277526+00	.21200653+00	.10165400+00
-.32122347-02	-.11529624+00	.32075942-01	.26184274-01
.23053678+00	.80639576-01	-.63253236-02	-.77234688-02
.21251928+00	.19567088+00	.52191904-01	-.68660371-01
.17527212+00	.40069454-01	.85478141-01	.43810577-01
.40505521-01	-.12052401+00	.31185572-01	-.22440251+00
-.58472257-01	-.74855364-01	.12981139+00	.26606044-01
-.54029082-02	.64966278-01	.52912593-01	.11350412-01
.18511250+00	.92376648-01	.12131841+00	-.91881800-02
.24479130-02	-.21931030-02	.13060269-01	.33258257-01
-.92941155-01	-.37001477+00	-.65932078-01	-.82644233-01
.30723351-01	.19210216+00	-.41189335-01	-.17412099+00
-.60926581-01	-.20000201+00	.19977054-01	-.22807021+00
-.19100688-01	.29983650-01	-.40489737-01	-.13174640+00
-.54098301-01	-.26089670-02	.18686700+00	.28881325+00
.27324250+00	-.85220627-01	.14391930+00	.10810987+00
.71641948-01	-.61657626-01	-.27087901-01	-.96299216-02

FORWARD PREDICTIVE FILTER COEFFICIENTS:

.87178199+00	.63436967+00	-.77056313+00	.56007387+00

SPECTRAL DENSITY MATRIX AND COHERENCE FOR M=2:

AUTO11	AUTO22	REAL(CROSS12)	IMAG(CROSS12)
.24793549+00	.12047345+00	.51711873-01	.00000000
.24797525+00	.12050044+00	.51719926-01	.26336852-02
.24809457+00	.12058142+00	.51744096-01	.52694282-02
.24829362+00	.12071651+00	.51784420-01	.79092910-02
.24857263+00	.12090589+00	.51840938-01	.10556343-01
.24893196+00	.12114982+00	.51913725-01	.13209068-01
.24937204+00	.12144863+00	.52002873-01	.15874360-01
.24989347+00	.12180273+00	.52108493-01	.18551543-01
.25049686+00	.12221259+00	.52230716-01	.21243350-01
.25118301+00	.12267879+00	.52369693-01	.23951967-01
.25195276+00	.12320195+00	.52525603-01	.26679592-01
.25280716+00	.12378281+00	.52698649-01	.29428473-01
.25374722+00	.12442217+00	.52889045-01	.32200889-01
.25477422+00	.12512091+00	.53097029-01	.34999179-01
.25588945+00	.12588002+00	.53322877-01	.37825725-01
.25709441+00	.12670057+00	.53566889-01	.40682976-01
.25839065+00	.12758373+00	.53829365-01	.43573427-01

MAG SQ COH	ARGUMENT
.89526267-01	.00000000
.89751875-01	.50978114-01
.90428364-01	.10148646+00
.91554744-01	.15156364+00
.93129297-01	.20086448+00
.95149682-01	.24916648+00
.97612908-01	.29627483+00
.10051529+00	.34202566+00
.10385252+00	.38628722+00
.10761967+00	.42896022+00
.11181120+00	.46997543+00
.11642097+00	.50929184+00
.12144226+00	.54689309+00
.12686775+00	.58278427+00
.13268963+00	.61698785+00
.13889957+00	.64954069+00
.14548868+00	.68049063+00

NUSC Technical Report 5501
13 October 1976

Multivariate Linear Predictive Spectral Analysis Employing Weighted Forward and Backward Averaging: A Generalization of Burg's Algorithm

Albert H. Nuttall

ABSTRACT

A method for multivariate linear predictive spectral analysis, employing weighted forward and backward averaging, is presented and programmed in FORTRAN. The method constitutes a generalization of Burg's univariate algorithm to the multivariate case. The essential analytical procedure is to minimize the trace of the sum of the weighted forward and backward error matrices by choice of the partial correlation coefficients, subject to a linear matrix constraint which guarantees that the forward-extrapolated and backward-extrapolated correlation matrix estimates are Hermitians of each other. The choice of error weighting is important and is discussed. Solution of a bilinear matrix equation is required in the algorithm.

Approved for public release; distribution unlimited.

TABLE OF CONTENTS

	Page
LIST OF ILLUSTRATIONS	ii
LIST OF TABLES	ii
LIST OF SYMBOLS	ii
1. INTRODUCTION	1
2. KNOWN CORRELATION	3
2.1 Derivation of Equations	3
2.2 Properties and Interpretations	8
2.3 Extrapolation of Correlation Values	12
2.4 Spectral Approximation	16
2.5 Example	18
3. UNKNOWN CORRELATION, FINITE DATA SET	19
3.1 Philosophy of Approach	19
3.2 Comparative Features	24
3.3 Properties and Interpretations	26
3.4 Evaluation of Partial Correlation Coefficients	27
3.5 Weighting of Error Matrices	32
3.6 Solution of Bilinear Matrix Equation	37
3.7 Spectral Estimation	39
3.8 Termination Procedure	42
3.9 Examples	44
4. SUMMARY	48
APPENDIX A - PROPERTIES OF A SPECTRAL DENSITY MATRIX	A-1
APPENDIX B - MINIMIZATION OF TRACE OF ERROR MATRIX	B-1
APPENDIX C - INTERRELATIONSHIPS OF U_p AND V_p	C-1
APPENDIX D - HERMITIAN PROPERTY OF EXTRAPOLATED CORRELATIONS	D-1
APPENDIX E - RELATIONSHIP OF DETERMINANTS	E-1
APPENDIX F - SPECTRUM FROM EXTRAPOLATED CORRELATIONS	F-1
APPENDIX G - HERMITIAN PROPERTY OF ONE-STEP EXTRAPOLATED CORRELATION MATRIX ESTIMATES	G-1
APPENDIX H - INTERRELATIONSHIPS OF U_p AND V_p FOR UNKNOWN CORRELATION CASE	H-1
APPENDIX I - MINIMIZATION OF TRACE OF WEIGHTED ERROR MATRICES	I-1
APPENDIX J - COMPUTATION OF FILTER TRANSFER FUNCTION	J-1
APPENDIX K - PROGRAM FOR SPECTRAL ANALYSIS	K-1
REFERENCES	R-1

LIST OF ILLUSTRATIONS

Figure		Page
1	Chain Representation of Residuals	7

LIST OF TABLES

Table		
1	Timing of SUBROUTINE PCC	48

LIST OF SYMBOLS

t	Time
X, $X(t)$, X_n	Multivariate stationary, zero-mean, random process eq. (1)
M	Dimensionality of X, $X(t)$, X_n
Δ	Common sampling interval in time
R_k	Correlation matrix of input process $\{X_n\}$ at delay $k\Delta$, eq. (2)
Overbar	Ensemble average
Superscript T	Transpose
Superscript *	Conjugate
Superscript H	Conjugate Transpose
N	Number of M-dimensional data samples available
f	Frequency (Hz)
i	$\sqrt{-1}$
$G(f)$	Spectrum of $\{X_n\}$, eq. (3)
p	Range of values of k for which R_k is known; order of prediction filter
$\hat{X}_k$	Forward predicted value of X_k, eq. (4)

LIST OF SYMBOLS

$A_n, A_n^{(p)}$	n-th coefficient of forward predictive filter, eq. (4)
Y_k, Z_k	Instantaneous error, eqs. (5) and (9)
tr	Trace of a square matrix
$\check{X}_{k-p}$	Backward predicted value of X_{k-p}, eq. (8)
$B_n, B_n^{(p)}$	n-th coefficient of backward predictive filter, eq. (8)
U_p, V_p	Correlation matrices of residuals, eqs. (12) and (30)
C_{p-1}, D_{p-1}	Auxiliary matrices, eqs. (13), (35), and (36)
$Y_k^{(p)}, Z_k^{(p)}$	p-th order forward and backward residuals, eq. (17)
I	Identity matrix
$A_p^{(p)}, B_p^{(p)}$	Partial correlation coefficients
z	Variable of z-transforms
$\mathcal{H}_A^{(p)}(z), \mathcal{H}_B^{(p)}(z)$	Transfer functions (z-transforms) of p-th stage, eq. (23)
D	Arbitrary MxM matrix
$\tilde{X}_n$	Scaled process, eq. (24)
$\tilde{R}_k$	Correlation of scaled process, eq. (25)
$\tilde{A}_n^{(p)}$	n-th coefficient for scaled process, eq. (28)
det	Determinant of a square matrix
q, q_n	Arbitrary Mx1 complex matrix
$F_m^{(p)}$	Crosscorrelation of residual and input, eq. (38)
$\hat{R}_m^{(p)}$	Forward extrapolated correlation matrix, eq. (52)
$\check{R}_{-m}^{(p)}$	Backward extrapolated correlation matrix, eq. (55)
$G^{(p)}(f)$	p-th order spectral approximation, eqs. (67) and (69)
$H_A^{(p)}(f), H_B^{(p)}(f)$	Transfer functions of p-th stage, eqs. (68) and (70)
W_k	White noise, eq. (73)

LIST OF SYMBOLS

δ_{m0}	Kronecker delta: 1 if m = 0; 0 otherwise
$R_m^{(p-1)}$	Forward extrapolated correlation estimate, eq. (86)
$R_{-m}^{(p-1)}$	Backward extrapolated correlation estimate, eq. (92)
V_{p-1}	Estimate of the correlation of backward residual at zero time delay, eq. (89)
U_{p-1}	Estimate of the correlation of forward residual at zero time delay, eq. (95)
S_{mn}	Correlation matrix, eq. (103)
$Y_k^{(p)}, Z_k^{(p)}$	Errors (residuals), eq. (111)
E_p, F_p	Error matrices, eqs. (112) and (115)
$S_{p-1}^{(\ )}$	Auxiliary correlation matrices, eq. (114)
Λ_a	Weighting matrix, eq. (117)
Λ	Hermitian non-negative matrix = $\Lambda_a^H \Lambda_a$
$\Lambda_{p-1}, \Gamma_{p-1}$	Weighting matrices, eq. (121)
G_p	Auxiliary matrix, eq. (122)
α, β, μ, ν	Auxiliary matrices, eqs. (126) and (127)
Ψ_{p-1}, Ψ_{p-1}	Square root matrices, eq. (142)
$\tilde{Y}_k^{(p-1)}, \tilde{Z}_k^{(p-1)}$	Scaled processes, eq. (143)
$q_k^{(p)}, \chi_k^{(p)}$	Error processes, eqs. (144) and (148)
$\tilde{A}_p^{(p)}, \tilde{B}_p^{(p)}$	Scaled partial correlation coefficients, eqs. (145) and (149)
$\mathcal{E}_p, \mathcal{F}_p$	Estimated correlations of errors, eqs. (146) and (150)
a_k, A_k	Auxiliary quantities, eqs. (160) and (161)
$G^{(p)}(f)$	Spectral estimate, eqs. (165) and (167)
Adj	Adjoint of a square matrix
FFT	Fast Fourier transform

LIST OF SYMBOLS

N_F	Number of frequency cells in range $\left(-\frac{1}{2\Delta}, \frac{1}{2\Delta}\right)$
$R_A(f), I_A(f)$	Real and imaginary parts of Adjoint, eq. (172)
$M(f)$	Auxiliary matrix, eqs. (174) and (179)
$XX(f), YY(f)$	Real and imaginary parts of $H_A^{(p)}(f)$, eq. (175)
$XX_A(f), YY_A(f)$	Adjoints, eqs. (176) and (177)
AIC_p	Akaike Information Criterion, eq. (180)
$\ln$	Natural logarithm
p_{max}	Maximum value of p considered
p_{best}	Best order of p for spectral estimate

INTRODUCTION

Spectral analysis of stationary random processes via linear predictive, maximum entropy, and autoregressive techniques has attracted much attention lately, especially for short data segments; see, for example, the bibliographies listed in references 1, 2, and 3. For a univariate process, it appears that the Burg algorithm (Ref. 4), which guarantees a stable correlation recursion, is as good as any of the currently available techniques of similar nature that employ an all-pole model of the available process (Ref. 3).

Accordingly, it is desirable to develop a spectral analysis technique for the multivariate case in such a way that: we employ a physically meaningful error minimization for the determination of the filter coefficients; the technique yields a stable correlation recursion; and it reduces to Burg's algorithm for the univariate case. It will be shown in the following that we have accomplished these goals, with the exception that we have not proved (or disproved) the stability requirement. A FORTRAN program for this spectral analysis technique was published in Ref. 5, along with an example of its application. Virtually simultaneously, the same technique was investigated independently and published in Ref. 6. In this report, we will document the derivations and equations that lead to the program presented in Ref. 5, and indicate an extension of that result.

Our approach in this report will be to investigate, in some detail, first the case where the correlation of the multivariate process under consideration is known for a limited range of argument values, and to extract all the relevant important properties of the solution so that they may be forced to be satisfied later when we treat the unknown correlation case. This property-

extraction procedure will be found to: furnish guides to the analysis of the unknown correlation case; allow us to cut down on computer execution time and storage by employing the properties; and make us aware of some of the shortcomings of the unknown (versus known) correlation cases. This procedure should also be helpful to those who are not thoroughly familiar with spectral analysis of multivariate processes and their properties.

Throughout this report, we assume we are dealing with equispaced samples of a stationary zero-mean complex random process X(t) of dimensionality M; that is, sample

$$X(n\Delta) \equiv X_n \equiv \left[x_n^{(1)} \cdots x_n^{(M)}\right]^T \tag{1}$$

is an M x 1 column matrix, where Δ is the common sampling interval for all the component processes of X(t). It is not assumed that X(t) is Gaussian.

In section 2, we will assume that the correlation matrix of process $\{X_n\}$, namely the M x M matrix*

$$R_k \equiv \overline{X_n X_{n-k}^H} = R_{-k}^H \tag{2}$$

is known exactly for a limited range of values of k, and will show how an approximation for the spectrum of process $\{X_n\}$ can be obtained. In section 3, the input correlation matrix R_k will be unknown, and all that is available is a finite set of N data samples, $X_1, X_2, \ldots, X_N$, from which an estimate of the spectrum of process $\{X_n\}$ is desired. The end result will be a FORTRAN program for multivariate spectral analysis.

*The case of complex samples is treated so that we can handle complex envelope or complex demodulated processes. Specialization to real processes is immediate, and (2) becomes $R_k = R_{-k}^T$. An overbar indicates an ensemble average, superscript T denotes a transpose, and superscript H denotes a conjugate transpose. Matrices are indicated by capital letters.

2. KNOWN CORRELATION

If the correlation in (2) is known for all k, the standard (double-sided) definition of the spectrum of process $\{X_n\}$ is

$$G(f) = \Delta \sum_{k=-\infty}^{\infty} \exp(-i2\pi f k\Delta)\, R_k \ , \quad |f| < \frac{1}{2\Delta} \ . \tag{3}$$

The complex M x M matrix G(f) is Hermitian and non-negative definite for any value of frequency f (see appendix A), but need not be even in frequency f. When R_k is not known for all k, but only for a range $|k| \le p$, an approximation to (3) must be accepted; this problem will be pursued below.

2.1 DERIVATION OF EQUATIONS

Suppose M-dimensional samples X_{k-p} .. , X_{k-1} are available, and we attempt a one-step linear prediction of X_k according to the p-th order operation

$$\hat{X}_k \equiv \sum_{n=1}^{p} A_n X_{k-n} \ , \tag{4}$$

where complex coefficient matrix A_n is M x M, n = 1, 2, ..., p. The instantaneous error at time kΔ is defined as

$$Y_k = X_k - \hat{X}_k = -\sum_{n=0}^{p} A_n X_{k-n} \ , \quad A_0 \equiv -I. \tag{5}$$

The linear operators in (4) and (5) constitute stable linear filters regardless of the choice of coefficients; the filter of (4) is called the predictive filter, that of (5) is called the predictive error filter. Notice that we are not assuming that process $\{X_n\}$ actually satisfies an autoregressive relation; rather we are simply attempting to linearly predict $\{X_n\}$ on the basis of the most recent p past values.

The minimum value of the scalar error

$$\overline{Y_k^H Y_k} = \mathrm{tr}\, \overline{Y_k Y_k^H} \quad , \tag{6}$$

by choice of coefficients $\{A_n\}_1^p$, is given (in appendix B) by the solution of the linear matrix equations

$$\sum_{n=1}^{p} A_n^{(p)} R_{m-n} = R_m \quad , \quad 1 \le m \le p, \tag{7}$$

where the explicit dependence on the order p is indicated. Knowledge of R_k for $|k| \le p$ is required in (7).

Before we discuss the solution of (7) for $\{A_n^{(p)}\}_1^p$, we consider one-step linear "backward prediction" of process $\{X_n\}$. Suppose samples X_k, X_{k-1}, ..., X_{k-p+1} are available, and we attempt a one-step linear prediction of X_{k-p} according to

$$\check{X}_{k-p} = \sum_{n=1}^{p} B_n X_{k-p+n} \quad . \tag{8}$$

The instantaneous error is defined as

$$Z_k = X_{k-p} - \check{X}_{k-p} = -\sum_{n=0}^{p} B_n X_{k-p+n} \quad , \quad B_0 = -I. \tag{9}$$

The minimum value of the scalar error

$$\overline{Z_k^H Z_k} = \mathrm{tr}\, \overline{Z_k Z_k^H} \quad , \tag{10}$$

by choice of coefficients $\{B_n\}_1^p$, may be shown (in a manner similar to that of appendix B) to be given by the solution of the linear matrix equations

$$\sum_{n=1}^{p} B_n^{(p)} R_{n-m} = R_{-m} \quad , \quad 1 \le m \le p. \tag{11}$$

For the optimum coefficients in (7) and (11), we find (see appendix B) that the optimum error matrices take the form

$$\text{opt}\ \overline{Y_k Y_k^H} = R_0 - \sum_{n=1}^{p} A_n^{(p)} R_{-n} \equiv U_p\ , \quad U_0 \equiv R_0\ ,$$
$$\text{opt}\ \overline{Z_k Z_k^H} = R_0 - \sum_{n=1}^{p} B_n^{(p)} R_n \equiv V_p\ , \quad V_0 \equiv R_0\ . \tag{12}$$

In general, these two matrices, their diagonal elements, and their traces are unequal (as the simple example of p=1 will show). However, their determinants are equal, as will be shown in subsection 2.2.

The solutions of (7) and (11) can be accomplished simultaneously in a recursive fashion (Ref. 7). Define

$$C_{p-1} \equiv -\sum_{n=0}^{p-1} A_n^{(p-1)} R_{p-n}\ , \qquad A_0^{(p)} \equiv -I,$$
$$D_{p-1} \equiv -\sum_{n=0}^{p-1} B_n^{(p-1)} R_{n-p}\ , \qquad B_0^{(p)} \equiv -I. \tag{13}$$

Then

$$A_p^{(p)} = C_{p-1} V_{p-1}^{-1}\ , \quad B_p^{(p)} = D_{p-1} U_{p-1}^{-1} \tag{14}$$

and

$$\left.\begin{aligned} A_n^{(p)} &= A_n^{(p-1)} - A_p^{(p)} B_{p-n}^{(p-1)} \\ B_n^{(p)} &= B_n^{(p-1)} - B_p^{(p)} A_{p-n}^{(p-1)} \end{aligned}\right\} \quad 1 \le n \le p-1 \qquad (p \ge 2). \tag{15}$$

These relations will be simplified somewhat in subsection 2.2. For M=1, a univariate process, (7) and (11) immediately yield

$$A_n^{(p)} = B_n^{(p)*} \quad \text{for} \quad M = 1, \tag{16}$$

where we have used (2) in the form $R_k = R_{-k}^*$ for a univariate process. No such simple relation as (16) holds for $M \geq 2$.

We will now derive a chain interpretation of the above results that will prove very useful later when we have to deal with the unknown correlation case. For the optimum filter coefficients $\left\{A_n^{(p)}\right\}_1^p$ and $\left\{B_n^{(p)}\right\}_1^p$, define the p-th order forward and backward residuals (see (5) and (9)) as the outputs of the forward and backward predictive error filters:

$$Y_k^{(p)} = -\sum_{n=0}^{p} A_n^{(p)} X_{k-n} = X_k - A_1^{(p)} X_{k-1} - \cdots - A_p^{(p)} X_{k-p} ,$$

$$Z_k^{(p)} = -\sum_{n=0}^{p} B_n^{(p)} X_{k-p+n} = X_{k-p} - B_1^{(p)} X_{k-p+1} - \cdots - B_p^{(p)} X_k . \qquad (17)$$

Then using (15), we can express

$$\begin{aligned} Y_k^{(p)} &= X_k - \sum_{n=1}^{p-1} A_n^{(p)} X_{k-n} - A_p^{(p)} X_{k-p} \\ &= X_k - \sum_{n=1}^{p-1} \left(A_n^{(p-1)} - A_p^{(p)} B_{p-n}^{(p-1)} \right) X_{k-n} - A_p^{(p)} X_{k-p} \\ &= -\sum_{n=0}^{p-1} A_n^{(p-1)} X_{k-n} + A_p^{(p)} \sum_{n=1}^{p} B_{p-n}^{(p-1)} X_{k-n} \\ &= Y_k^{(p-1)} + A_p^{(p)} \sum_{j=0}^{p-1} B_j^{(p-1)} X_{k-p+j} = Y_k^{(p-1)} - A_p^{(p)} Z_{k-1}^{(p-1)} . \end{aligned} \qquad (18)$$

And similarly

$$\begin{aligned} Z_k^{(p)} &= X_{k-p} - \sum_{n=1}^{p-1} B_n^{(p)} X_{k-p+n} - B_p^{(p)} X_k \\ &= X_{k-p} - \sum_{n=1}^{p-1} \left(B_n^{(p-1)} - B_p^{(p)} A_{p-n}^{(p-1)} \right) X_{k-p+n} - B_p^{(p)} X_k \\ &= -\sum_{n=0}^{p-1} B_n^{(p-1)} X_{k-p+n} + B_p^{(p)} \sum_{n=1}^{p} A_{p-n}^{(p-1)} X_{k-p+n} \\ &= Z_{k-1}^{(p-1)} + B_p^{(p)} \sum_{j=0}^{p-1} A_j^{(p-1)} X_{k-j} = Z_{k-1}^{(p-1)} - B_p^{(p)} Y_k^{(p-1)} . \end{aligned} \qquad (19)$$

Thus p-th order residuals $Y_K^{(p)}$ and $Z_K^{(p)}$ are related to the (p-1)th order residuals simply through the coefficients $A_p^{(p)}$ and $B_p^{(p)}$. A block diagram of the relationships in (18) and (19) is given in figure 1, where $z^{-1}I$ denotes an M x M matrix filter of unit delay.

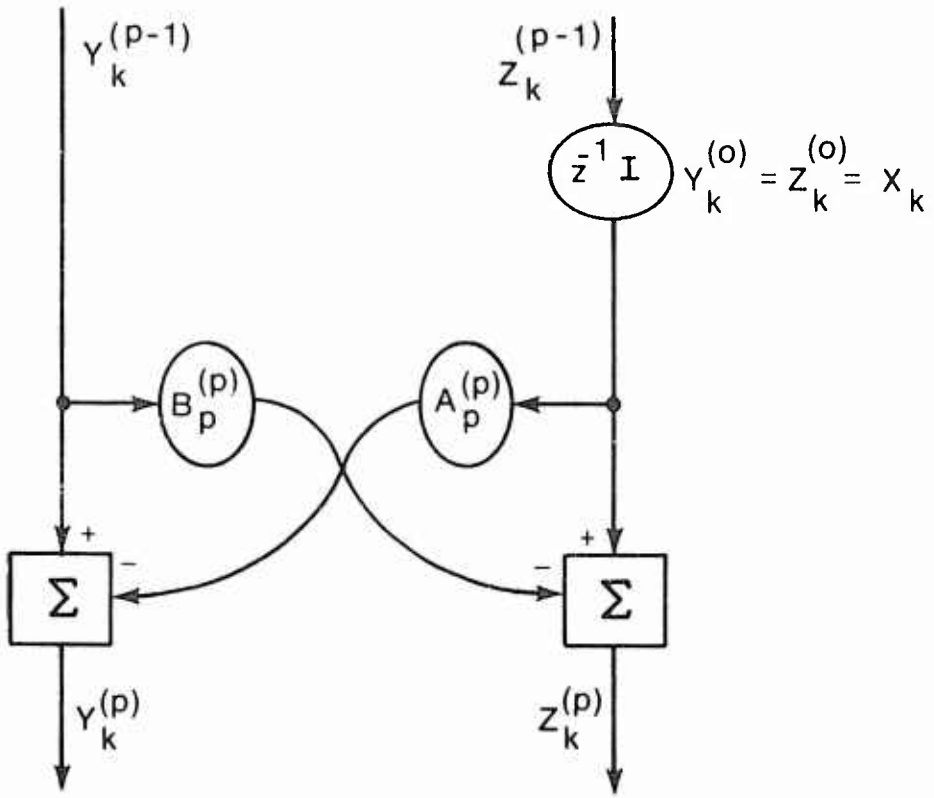


Figure 1. Chain Representation of Residuals

Thus matrix operators $A_p^{(p)}$ and $B_p^{(p)}$ can be interpreted as those coefficients which minimize

$$\overline{Y_k^{(p)H} Y_k^{(p)}} \quad \text{and} \quad \overline{Z_k^{(p)H} Z_k^{(p)}} \tag{20}$$

respectively, at the output of the p-th stage in figure 1, where $\{A_n^{(p)}\}_1^{p-1}$ and $\{B_n^{(p)}\}_1^{p-1}$ are determined by minimizations at lower order stages. $A_p^{(p)}$ and $B_p^{(p)}$ are called the partial correlation coefficients. Stated alternatively, stage by stage minimizations of (20), via choices of partial correlation coefficients $A_p^{(p)}$ and $B_p^{(p)}$, respectively, results in the same overall filter as if the powers in

$$-\sum_{n=0}^{p} A_n X_{k-n} \quad \text{and} \quad -\sum_{n=0}^{p} B_n X_{k-p+n} \tag{21}$$

were minimized by the choices of $\{A_n\}_1^p$ and $\{B_n\}_1^p$, respectively, each in one simultaneous optimization. This will furnish an important reference point

for the unknown correlation case in section 3.

If we let the transfer functions (z-transforms) to the outputs of the p-th stage in figure 1 be denoted by $\mathcal{H}_A^{(p)}(z)$ and $\mathcal{H}_B^{(p)}(z)$, it immediately follows, from figure 1 or equations (18) and (19), that

$$\begin{aligned}
\mathcal{H}_A^{(p)}(z) &= \mathcal{H}_A^{(p-1)}(z) - z^{-1} A_p^{(p)} \mathcal{H}_B^{(p-1)}(z), \\
\mathcal{H}_B^{(p)}(z) &= z^{-1} \mathcal{H}_B^{(p-1)}(z) - B_p^{(p)} \mathcal{H}_A^{(p-1)}(z), \\
\mathcal{H}_A^{(0)}(z) &= \mathcal{H}_B^{(0)}(z) = I.
\end{aligned} \tag{22}$$

In closed form, these predictive error filter transfer functions are expressible as (see (17))

$$\begin{aligned}
\mathcal{H}_A^{(p)}(z) &= -\sum_{n=0}^{p} z^{-n} A_n^{(p)} = I - \sum_{n=1}^{p} z^{-n} A_n^{(p)}, \\
\mathcal{H}_B^{(p)}(z) &= -\sum_{n=0}^{p} z^{n-p} B_n^{(p)} = -\sum_{j=0}^{p} z^{-j} B_{p-j}^{(p)} \\
&= z^{-p}\left[I - \sum_{n=1}^{p} z^{n} B_n^{(p)}\right].
\end{aligned} \tag{23}$$

2.2 PROPERTIES AND INTERPRETATIONS

Suppose that process $\{X_n\}$ were scaled according to

$$\tilde{X}_n = D X_n \tag{24}$$

where M x M matrix D is arbitrary, but invertible. Then the correlation of the scaled process is

$$\tilde{R}_k \equiv \overline{\tilde{X}_n \tilde{X}_{n-k}^H} = D \overline{X_n X_{n-k}^H} D^H = D R_k D^H. \tag{25}$$

Now from (7), since the solutions $\{A_n^{(p)}\}$ and $\{\bar{A}_n^{(p)}\}$ must satisfy

$$\sum_{n=1}^{p} A_n^{(p)} R_{m-n} = R_m, \quad 1 \le m \le p, \tag{26}$$

$$\sum_{n=1}^{p} \tilde{A}_n^{(p)} \tilde{R}_{m-n} = \tilde{R}_m \,, \quad 1 \le m \le p, \tag{27}$$

respectively, the solutions are related by a similarity transformation:

$$\tilde{A}_n^{(p)} = D A_n^{(p)} D^{-1} \,, \quad 1 \le n \le p. \tag{28}$$

This is called the scaling property. A similar property holds for the backward coefficients $\{B_n^{(p)}\}$.

An immediate by-product of the scaling property is that $A_n^{(p)}$ and $\tilde{A}_n^{(p)}$ have the same eigenvalues:

$$\det\left(\tilde{A}_n^{(p)} - \lambda I\right) = \det\left(D A_n^{(p)} D^{-1} - \lambda I\right) = \det\left(A_n^{(p)} - \lambda I\right). \tag{29}$$

Similarly, $B_n^{(p)}$ and $\tilde{B}_n^{(p)}$ have the same eigenvalues, regardless of scaling matrix D.

The remainder of this subsection will deal with the quantities U_p and V_p defined in (12), and C_p and D_p defined in (13). The quantity U_p can be interpreted physically as the correlation matrix of the p-th order forward residual; see (12), (5), and (17). Similarly, V_p is the correlation matrix of the p-th order backward residual; see (12), (9), and (17). That is,

$$U_p = \overline{Y_k^{(p)} Y_k^{(p)H}} \,, \quad V_p = \overline{Z_k^{(p)} Z_k^{(p)H}} \,. \tag{30}$$

Thus U_p and V_p are Hermitian:

$$U_p^H = U_p \,, \quad V_p^H = V_p \,; \tag{31}$$

and U_p and V_p are non-negative definite:

$$\mathcal{V}^H U_p \mathcal{V} = \mathcal{V}^H \overline{Y_k^{(p)} Y_k^{(p)H}} \mathcal{V} = \overline{\left|\mathcal{V}^H Y_k^{(p)}\right|^2} \ge 0 \tag{32}$$

for any M x 1 matrix $\mathcal{V}$. In appendix C, it is shown that simple recursions hold for U_p and V_p:

$$U_p = (I - A_p^{(p)} B_p^{(p)}) U_{p-1} \ , \ U_0 = R_0 \ ,$$
$$V_p = (I - B_p^{(p)} A_p^{(p)}) V_{p-1} \ , \ V_0 = R_0 \ . \tag{33}$$

It immediately follows from (33) that (see appendix C)

$$\det U_p = \det V_p \ , \ p \geq 0 . \tag{34}$$

This property was proved in Ref. 8, page 240.

The quantity C_p defined in (13) can be interpreted as the cross-correlation matrix between the p-th order forward and backward residuals at one unit of delay: $\overline{Y_k^{(p)} Z_{k-1}^{(p)H}} = \sum_{n=0}^{p} \sum_{m=0}^{p} A_n^{(p)} \overline{X_{k-n} X_{k-1-p+m}^H} B_m^{(p)H}$

$$= \sum_{m=0}^{p} \left(\sum_{n=0}^{p} A_n^{(p)} R_{p+1-m-n} \right) B_m^{(p)H} = - \sum_{n=0}^{p} A_n^{(p)} R_{p+1-n} = C_p , \tag{35}$$

where we have used (17), (2), (7), and (13). Similarly

$$\overline{Z_{k-1}^{(p)} Y_k^{(p)H}} = \sum_{m=0}^{p} \sum_{n=0}^{p} B_m^{(p)} \overline{X_{k-1-p+m} X_{k-n}^H} A_n^{(p)H}$$

$$= \sum_{n=0}^{p} \left(\sum_{m=0}^{p} B_m^{(p)} R_{p-1+n+m} \right) A_n^{(p)H} = - \sum_{m=0}^{p} B_m^{(p)} R_{-p-1+m} = D_p , \tag{36}$$

where we have used (17), (2), (11), and (13). It immediately follows from (35) and (36) that

$$D_p^H = C_p \ . \tag{37}$$

Thus it is not necessary to do the additional calculation of D_p in the solution given in (13).

Another interpretation of C_p is available as follows:

$$F_m^{(p)} \triangleq \overline{Y_k^{(p)} X_{k-m}^H} = - \sum_{n=0}^{p} A_n^{(p)} \overline{X_{k-n} X_{k-m}^H} = - \sum_{n=0}^{p} A_n^{(p)} R_{m-n} = \begin{cases} U_p , & m = 0 \\ 0 , & 1 \leq m \leq p \\ C_p , & m = p+1 \end{cases} \tag{38}$$

where we have employed (17), (2), (12), (7), and (13) in order. Thus the p-th order forward residual is uncorrelated with the p most recent past

values of the input, and the crosscorrelation at p + 1 units of delay is just C_p. Similarly, the backward residual satisfies

$$\overline{Z_k^{(p)} X_{k-p+m}^H} = -\sum_{n=0}^{p} B_n^{(p)} \overline{X_{k-p+n} X_{k-p+m}^H} = -\sum_{n=0}^{p} B_n^{(p)} R_{n-m} = \begin{cases} V_p, & m = 0 \\ 0, & 1 \le m \le p \\ D_p, & m = p+1 \end{cases} . \quad (39)$$

Yet another interpretation of C_p and D_p will be given in subsection 2.3.

As the order p in the linear prediction (4) increases, (38) yields

$$F_m^{(p)} = \overline{Y_k^{(p)} X_{k-m}^H} \to \begin{cases} U_\infty, & m = 0 \\ 0, & 1 \le m \end{cases} \quad \text{as} \quad p \to \infty . \quad (40)$$

Therefore the autocorrelation matrix of the forward residual becomes

$$\overline{Y_k^{(p)} Y_{k-m}^{(p)H}} = -\sum_{n=0}^{p} \overline{Y_k^{(p)} X_{k-m-n}^H} A_n^{(p)H} \to \begin{cases} U_\infty, & m = 0 \\ 0, & 1 \le m \end{cases} \quad \text{as} \quad p \to \infty . \quad (41)$$

That is, p-th order residual $Y_k^{(p)}$ tends to white noise with a correlation matrix at zero time delay of value U_∞, which is not necessarily diagonal.

The Hermitian property in (37) allows us to combine (14) into the equation

$$A_p^{(p)} V_{p-1} = U_{p-1} B_p^{(p)H} , \quad (42)$$

where we utilized (31). This constraint on the partial correlation coefficients will be of paramount importance in the unknown correlation case. It immediately follows from (42) and (34) that

$$\det A_p^{(p)} = \det B_p^{(p)H} = \left(\det B_p^{(p)}\right)^* \tag{43}$$

No such simple relation holds between $\det A_n^{(p)}$ and $\det B_n^{(p)}$ for $n<p$, except for $M = 1$, a univariate process.

2.3 EXTRAPOLATION OF CORRELATION VALUES

In subsection 2.1, we minimized the error in prediction (4) and found that for a p-th order prediction, knowledge of R_k for $|k| \le p$ was required; see (7). Now suppose that this is all the knowledge available about $\{R_k\}$; that is, suppose R_k is unknown for $|k|>p$. What can be done about approximating these unknown values?

One approach is as follows: we assume that the p-th order residual process $\{Y_k^{(p)}\}$ in (17) is white (i.e., uncorrelated for all non-zero delays), and that $A_p^{(p)} \neq 0$ (otherwise we could reduce the value of p). That is, we assume we can do nothing more in prediction by choosing more terms in the sum (4), which is tantamount to assuming maximum uncertainty (entropy) about the residual process $\{Y_k^{(p)}\}$. This is a very extensive assumption; we now investigate its ramifications.

We know from (38) that

$$F_m^{(p)} = \overline{Y_k^{(p)} X_{k-m}^H} = -\sum_{n=0}^{p} A_n^{(p)} R_{m-n}, \quad \text{all } m, \tag{44}$$

must satisfy

$$F_m^{(p)} = 0 \quad \text{for} \quad 1 \le m \le p. \tag{45}$$

Additionally, employing (17), the autocorrelation matrix of the p-th order residual is

$$\overline{Y_k^{(p)} Y_{k-j}^{(p)H}} = -\sum_{n=0}^{p} \overline{Y_k^{(p)} X_{k-j-n}^H} A_n^{(p)H} = -\sum_{n=0}^{p} F_{n+j}^{(p)} A_n^{(p)H}, \quad \text{all } j. \tag{46}$$

Now for j = 1, the white noise assumption on process $\{Y_k^{(p)}\}$ yields, via (46) and (45),

$$0 = -\sum_{n=0}^{p} F_{n+1}^{(p)} A_n^{(p)H} = -F_{p+1}^{(p)} A_p^{(p)H}; \quad \text{i.e.} \quad F_{p+1}^{(p)} = 0. \tag{47}$$

And for j = 2, the white assumption (in conjunction with (47)) yields

$$0 = -\sum_{n=0}^{p} F_{n+2}^{(p)} A_n^{(p)H} = -F_{p+2}^{(p)} A_p^{(p)H}; \quad \text{i.e.} \quad F_{p+2}^{(p)} = 0. \tag{48}$$

Continuing in this way, the white assumption is tantamount to assuming that

$$F_m^{(p)} = 0 \quad \text{for} \quad p+1 \le m. \tag{49}$$

Returning to expression (44), this means that we are assuming that

$$-\sum_{n=0}^{p} A_n^{(p)} R_{m-n} = 0 \quad \text{for} \quad p+1 \le m; \tag{50}$$

that is,

$$R_m = \sum_{n=1}^{p} A_n^{(p)} R_{m-n} \quad \text{for} \quad p+1 \le m. \tag{51}$$

Using more explicit notation, and denoting these assumed values of correlation as forward extrapolations $\{\hat{R}_m^{(p)}\}$, we have

$$\hat{R}_m^{(p)} \equiv \sum_{n=1}^{p} A_n^{(p)} \hat{R}_{m-n}^{(p)} \quad , \quad p+1 \le m, \tag{52}$$

where "starting values"

$$\hat{R}_m^{(p)} \equiv R_m \quad , \quad 0 \le m \le p. \tag{53}$$

Equation (52) is called the correlation recursion equation. It is interesting to note that the form of the correlation recursion (52) is identical to the form (4) for the individually predicted waveform values.

The correlation values in (52) are called the maximum entropy correlation extrapolations. The recursion is stable if and only if (see (23))

$$\det\left(I - \sum_{n=1}^{p} z^{-n} A_n^{(p)}\right) = \det \mathcal{A}_A^{(p)}(z) \tag{54}$$

possesses all its zeros within the unit circle in the complex z-plane; this property will be treated in subsection 2.4.

A similar procedure for backward correlation extrapolation, assuming that residual process $\{Z_k^{(p)}\}$ is white, yields

$$\check{R}_{-m}^{(p)} \equiv \sum_{n=1}^{p} B_n^{(p)} \check{R}_{n-m}^{(p)} \quad , \quad p+1 \le m, \tag{55}$$

where

$$\check{R}_{-m}^{(p)} \equiv R_{-m} \quad , \quad 0 \le m \le p. \tag{56}$$

Backward recursion (55) is identical in form to the backward prediction (8). The recursion (55) is stable if and only if (see (23)).

$$\det\left(I - \sum_{n=1}^{p} z^{-n} B_n^{(p)}\right) = \det\left(z^{-p} a_B^{(p)}(z^{-1})\right) \tag{57}$$

possesses all its zeros within the unit circle.

As a special case of (52) and (53), the one-step forward extrapolated correlation based on a p-th order prediction is

$$\hat{R}_{p+1}^{(p)} = \sum_{n=1}^{p} A_n^{(p)} \hat{R}_{p+1-n}^{(p)} = \sum_{n=1}^{p} A_n^{(p)} R_{p+1-n} \ . \tag{58}$$

But from (13), we now can see that

$$C_p = -\sum_{n=0}^{p} A_n^{(p)} R_{p+1-n} = R_{p+1} - \hat{R}_{p+1}^{(p)} \ . \tag{59}$$

That is, C_p is the difference between the true correlation value R_{p+1} and the one-step forward extrapolated correlation $\hat{R}_{p+1}^{(p)}$ based upon knowledge of $\{R_k\}_{-p}^{p}$.

A similar procedure shows that

$$D_p = R_{-p-1} - \check{R}_{-p-1}^{(p)} \ . \tag{60}$$

That is, D_p is the difference between the true correlation value R_{-p-1} and the one-step backward extrapolated correlation $\check{R}_{-p-1}^{(p)}$ based upon knowledge of $\{R_k\}_{-p}^{p}$.

When (59) and (60) are combined with the Hermitian property in (37), we see that

$$\check{R}_{-p-1}^{(p)\,H} = \hat{R}_{p+1}^{(p)} \ . \tag{61}$$

This is a special case of the more general property (demonstrated in appendix D) that

$$\hat{R}_{-m}^{(p)H} = \hat{R}_{m}^{(p)} \quad , \quad p+1 \le m \; ; \tag{62}$$

that is, the backward and forward extrapolated correlation matrices are Hermitians of each other. This is a desirable property of the extrapolations and is consistent with the same property, (2), which holds for the known correlation values, $\{R_k\}_{-p}^{p}$.

It was noted in (54) and (57) that the zeros of $\det \mathcal{A}_A^{(p)}(z)$ and $\det \mathcal{A}_B^{(p)}(z^{-1})$ must be within the unit circle in order that recursions (52) and (55), respectively, be stable. It is shown in appendix E that

$$\det\left(I - \sum_{n=1}^{p} z^{-n} A_n^{(p)}\right) = \det\left(I - \sum_{n=1}^{p} z^{-n} B_n^{(p)H}\right). \tag{63}$$

That we need consider only the zeros of one of these quantities; the location of these zeros is considered below.

It is also shown in appendix E that

$$\operatorname{tr} A_1^{(p)} = \left(\operatorname{tr} B_1^{(p)}\right)^* \tag{64}$$

and

$$\det A_p^{(p)} = \left(\det B_p^{(p)}\right)^* . \tag{65}$$

2.4 SPECTRAL APPROXIMATION

Equations (52) and (53) define the forward extrapolated correlations for all $m \ge 0$. We extend these to negative m via

$$\hat{R}_{m}^{(p)} \equiv \hat{R}_{-m}^{(p)H} \quad , \quad m \le 0, \tag{66}$$

which is consistent with (2)'. We will now use the Fourier transform of this infinite sequence, as in (3), as an approximation to the spectrum of process $\{X_n\}$. In appendix F, it is shown that the approximate spectrum is given by

$$G^{(p)}(f) = \Delta\, H_A^{(p)}(f)^{-1}\, U_p\, H_A^{(p)}(f)^{-1^H}, \quad |f| < \frac{1}{2\Delta}, \tag{67}$$

where

$$H_A^{(p)}(f) = -\sum_{n=0}^{p} \exp(-i2\pi f n\Delta) A_n^{(p)} \tag{68}$$

is the forward predictive error filter transfer function. Since U_p is nonnegative definite by (32), spectral approximation $G^{(p)}(f)$ is nonnegative definite for any f; it is also obviously Hermitian by (31). Thus the desirable properties of appendix A are achieved by approximation (67). In order to evaluate (67), one M x M matrix inverse (of $H_A^{(p)}(f)$) is needed at each value of f of interest.

A similar procedure applied to the backward correlation recursion of (55) and (56) yields the spectral approximation

$$G^{(p)}(f) = \Delta\, H_B^{(p)}(f)^{-1}\, V_p\, H_B^{(p)}(f)^{-1^H}, \quad |f| < \frac{1}{2\Delta}, \tag{69}$$

where

$$H_B^{(p)}(f) = -\sum_{n=0}^{p} \exp(-i2\pi f n\Delta) B_{p-n}^{(p)} \tag{70}$$

is the backward predictive error filter transfer function. Since the extrapolated correlations via (52) or (55) are equal, as shown in subsection 2.3, the same notation, $G^{(p)}(f)$, is used for both (67) and (69); however, we have two different factorizations for the unique spectral approximation $G^{(p)}(f)$.

In appendix F, it is also shown that the zeros of $\det \mathcal{A}_A^{(p)}(z)$ (see (22) and (23)) all lie inside the unit circle in the complex z-plane. Additionally, the poles of $\mathcal{A}_A^{(p)}(z)^{-1}$ all lie inside the unit circle, and the zeros of $\mathcal{A}_A^{(p)}(z)^{-1}$

all lie at z = 0. Thus the recursion (52) is stable. This point is discussed in Ref. 7, p. 132.

2.5 EXAMPLE

A simple example for M = 2 will be considered. Let the process be generated according to

$$X_k = G X_{k-1} + W_k , \tag{71}$$

where

$$G = \begin{bmatrix} .85 & -.75 \\ .65 & .55 \end{bmatrix} \tag{72}$$

and white noise W_k satisfies

$$\overline{W_k W_{k-m}^H} = \delta_{m0} I. \tag{73}$$

Then it may be shown that

$$R_m = G R_{m-1} + \delta_{m0} I, \quad m \geq 0, \tag{74}$$

with solution

$$R_0 = \begin{bmatrix} 25.135 & 4.862 \\ 4.862 & 21.643 \end{bmatrix} , \quad R_1 = \begin{bmatrix} 17.718 & -12.099 \\ 19.012 & 15.064 \end{bmatrix} . \tag{75}$$

By means of (7) and (11), we find

$$A_1^{(n)} = \begin{bmatrix} .85 & -.75 \\ .65 & .55 \end{bmatrix} , \quad B_1^{(1)} = \begin{bmatrix} .55930 & .75279 \\ -.64400 & .84070 \end{bmatrix} , \tag{76}$$

and $A_1^{(p)} = A_1^{(n)}$, $A_n^{(p)} = 0$, $2 \leq n \leq p$. We observe $A_1^{(1)} \neq B_1^{(1)}$, $A_1^{(1)} B_1^{(1)} \neq B_1^{(1)} A_1^{(1)}$, and $A_1^{(n)-1} \neq B_1^{(1)}$. The determinants of (76) are both .955.

Evaluation of (12) gives

$$U_1 = I , \quad V_1 = \begin{bmatrix} .91330 & .28934 \\ .28934 & 1.18659 \end{bmatrix} \tag{77}$$

These matrices and their traces and eigenvalues are unequal, but their determinants are both 1.

3. UNKNOWN CORRELATION

In this section, the correlation values $\{R_k\}$ are unknown, and the only information available about the random process is a finite set of N data points $X_1, X_2, \ldots, X_N$, from which we have removed the sample mean. From these N data points, we desire an estimate of the spectrum G(f). But we cannot minimize or utilize any ensemble averages as was done in section 2, since we have only a finite segment of one member function to work with.

3.1 PHILOSOPHY OF APPROACH

For the known correlation case above, we had the set of normal equations

$$\left.\begin{aligned} \sum_{n=1}^{p} A_n^{(p)} R_{m-n} &= R_m \\ \sum_{n=1}^{p} B_n^{(p)} R_{n-m} &= R_{-m} \end{aligned}\right\}, \quad 1 \le m \le p, \tag{78A, 78B}$$

where $\{A_n^{(p)}\}_1^p$ and $\{B_n^{(p)}\}_1^p$ were the unknowns. Now in the unknown correlation case, we make a change by assuming that $A_p^{(p)}$ and $B_p^{(p)}$ are known* (along with R_m for $|m| \le p-1$, from lower order solutions), and by letting R_p and R_{-p} be unknown. The equations in the unknowns are still linear, and the solution is given by

$$\left.\begin{aligned} A_n^{(p)} &= A_n^{(p-1)} - A_p^{(p)} B_{p-n}^{(p-1)} \\ B_n^{(p)} &= B_n^{(p-1)} - B_p^{(p)} A_{p-n}^{(p-1)} \end{aligned}\right\}, \quad 1 \le n \le p-1 \qquad (p \ge 2), \tag{79A, 79B}$$

*The manner of specifying $A_p^{(p)}$ and $B_p^{(p)}$ will be considered in subsection 3.4.

$$R_p = \sum_{n=1}^{p} A_n^{(p)} R_{p-n} \quad , \tag{80A}$$

$$R_{-p} = \sum_{n=1}^{p} B_n^{(p)} R_{n-p} \quad . \tag{80B}$$

(It must be noted that R_k in this section denotes an estimate of the true (unknown) correlation value; for notational convenience, no distinguishing symbol has been added to R_k to emphasize this distinction.) However, we shall insist that the correlation estimates (80) that we obtain at the p-th stage satisfy

$$R_p = R_{-p}^H \quad , \tag{81}$$

in keeping with property (2). Since equations (78) and (81) are identical to those encountered in the known correlation case, the mathematical definitions and interrelationships employed there can be applied here also. However, some of the properties and physical interpretations may be different, since we are now dealing with estimates, rather than true values.

To solve (78), we begin by defining

$$R_0 = \frac{1}{N} \sum_{k=1}^{N} X_k X_k^H = R_0^H \quad . \tag{82}$$

Now consider p=1 in (78); we have

$$A_1^{(1)} R_0 = R_1 \quad , \qquad B_1^{(1)} R_0 = R_{-1} \quad . \tag{83}$$

Now if $A_1^{(1)}$ and $B_1^{(1)}$ are known, we can compute unknowns R_1 and R_{-1}. But by constraint (81), $A_1^{(1)}$ and $B_1^{(1)}$ must be chosen such that

$$A_1^{(1)} R_0 = R_0 B_1^{(1)H} \quad . \tag{84}$$

Thus when we select $A_1^{(1)}$ and $B_1^{(1)}$, constraint (84) must be kept in mind; that is,

$A_1^{(1)}$ and $B_1^{(1)}$ cannot be specified independently of each other.

At stage $p(\geq 2)$, if $A_p^{(p)}$ is known (and $\{R_k\}_{1-p}^{p-1}$ are known from earlier stages with property $R_k = R_{-k}^H$, $0 \leq k \leq p-1$), we could solve the linear equations (78A) for $\{A_n^{(p)}\}_1^p$ and R_p, according to (79A) and (80A), where the lower order quantities in (79) and (80) are available from earlier stages. Similarly if $B_p^{(p)}$ is known, we use (79B) and (80B) to solve (78B). However, by (81), we must constrain the selection of $A_p^{(p)}$ and $B_p^{(p)}$.

To see exactly what constraint (81) implies about the selection of $A_p^{(p)}$ and $B_p^{(p)}$, notice that, for $p \geq 2$, (and defining $B_0^{(p-1)} = -I$)

$$R_p = \sum_{n=1}^{p} A_n^{(p)} R_{p-n} = \sum_{n=1}^{p-1} \left(A_n^{(p-1)} - A_p^{(p)} B_{p-n}^{(p-1)}\right) R_{p-n} + A_p^{(p)} R_0$$

$$= \sum_{n=1}^{p-1} A_n^{(p-1)} R_{p-n} - A_p^{(p)} \sum_{n=1}^{p} B_{p-n}^{(p-1)} R_{p-n}$$

$$= \sum_{n=1}^{p-1} A_n^{(p-1)} R_{p-n} - A_p^{(p)} \sum_{j=0}^{p-1} B_j^{(p-1)} R_j , \tag{85}$$

where we have employed (80A) and (79A). Now define forward extrapolated correlation estimates based on order p-1 according to (see (52) and (53))

$$R_m^{(p-1)} \equiv \sum_{n=1}^{p-1} A_n^{(p-1)} R_{m-n}^{(p-1)} \quad \text{for} \quad m \geq p, \tag{86}$$

where

$$R_m^{(p-1)} \equiv R_m , \quad 0 \leq m \leq p-1. \tag{87}$$

Then, in particular, the one-step forward extrapolated correlation estimate based on order p-1 is

$$R_p^{(p-1)} = \sum_{n=1}^{p-1} A_n^{(p-1)} R_{p-n}^{(p-1)} = \sum_{n=1}^{p-1} A_n^{(p-1)} R_{p-n} . \tag{88}$$

Also define (see (12))

$$V_{p-1} = -\sum_{n=0}^{p-1} B_n^{(p-1)} R_n \ . \tag{89}$$

This quantity has the physical interpretation as the estimate of the correlation matrix of the (p-1)th order backward residual at zero time delay (see (30)); its properties are considered in subsection 3.3. Then by means of (88) and (89), (85) can be expressed as

$$R_p = R_p^{(p-1)} + A_p^{(p)} V_{p-1} \ . \tag{90}$$

(This equation is similar to a combination of (14) and (59) for the known correlation case.)

At the same time, by (80B) and (79B) (and defining $A_0^{(p-1)} = -I$),

$$\begin{aligned} R_{-p} &= \sum_{n=1}^{p} B_n^{(p)} R_{n-p} = \sum_{n=1}^{p-1} \left(B_n^{(p-1)} - B_p^{(p)} A_{p-n}^{(p-1)} \right) R_{n-p} + B_p^{(p)} R_0 \\ &= \sum_{n=1}^{p-1} B_n^{(p-1)} R_{n-p} - B_p^{(p)} \sum_{n=1}^{p} A_{p-n}^{(p-1)} R_{n-p} \\ &= \sum_{n=1}^{p} B_n^{(p-1)} R_{n-p} - B_p^{(p)} \sum_{j=0}^{p-1} A_j^{(p-1)} R_{-j} \ . \end{aligned} \tag{91}$$

Now define backward extrapolated correlation estimates based on order p-1 as (see (55) and (56))

$$R_{-m}^{(p-1)} = \sum_{n=1}^{p-1} B_n^{(p-1)} R_{n-m}^{(p-1)} \quad \text{for} \quad m \geq p, \tag{92}$$

where

$$R_{-m}^{(p-1)} = R_{-m} \ , \ 0 \leq m \leq p-1. \tag{93}$$

Then, in particular,

$$R_{-p}^{(p-1)} = \sum_{n=1}^{p-1} B_n^{(p-1)} R_{n-p}^{(p-1)} = \sum_{n=1}^{p-1} B_n^{(p-1)} R_{n-p} \,. \tag{94}$$

Also define (see (12))

$$U_{p-1} = - \sum_{n=0}^{p-1} A_n^{(p-1)} R_{-n} \,. \tag{95}$$

This quantity is an estimate of the correlation matrix of the (p-1)th order forward residual at zero time delay (see (30)). Then by means of (94) and (95), (91) can be expressed as

$$R_{-p} = R_{-p}^{(p-1)} + B_p^{(p)} U_{p-1} \,. \tag{96}$$

(This equation is similar to a combination of (14) and (60) for the known correlation case.) But now it can be shown (see appendix G) that the extrapolated correlation estimates in (88) and (94) satisfy

$$R_{-p}^{(p-1)H} = R_p^{(p-1)} \,. \tag{97}$$

Therefore, if (81) is to be satisfied, (90) and (96) in conjunction with (97) force

$$A_p^{(p)} V_{p-1} = U_{p-1}^H B_p^{(p)H} \,. \tag{98}$$

(This reduces to (84) for p=1.) Thus the selection procedure of $A_p^{(p)}$ and $B_p^{(p)}$ at the p-th stage must be done according to (98), where V_{p-1} and U_{p-1} are quantities already available from the (p-1)th stage, according to (89) and (95). The precise selection procedure will be undertaken in subsection 3.4.

3.2 COMPARATIVE FEATURES

There are alternative techniques to the estimation of the correlation matrices and the spectral density matrix that could be considered. For example, the standard Yule-Walker technique (e.g., Ref 2, page 186) uses correlation estimates

$$R_p \equiv \frac{1}{N} \sum_K X_k X_{k-p}^H \quad , \tag{99}$$

where the sum is over all nonzero summands, and then solves recursively for $\{A_n^{(p)}\}_1^p$ and $\{B_n^{(p)}\}_1^p$ via the method in subsection 2.1. This <u>apriori</u> decision on the form (99) of the correlation estimate gives poorer spectral estimates for M=1 (Refs. 2 and 3), and probably does so for M>1. The estimated correlation matrix $[R_{m-n}]_0^p$ is Hermitian, block Toeplitz, and nonnegative definite:

$$\left[v_0^H \cdots v_p^H\right]\left[R_{m-n}\right]\begin{bmatrix} v_0 \\ \vdots \\ v_p \end{bmatrix} = \sum_{n,m=0}^{p} v_n^H R_{m-n} v_m = \sum_{n,m=0}^{p} v_n^H \left(\frac{1}{N}\sum_K X_{k-n} X_{k-m}^H\right) v_m$$

$$= \frac{1}{N}\sum_K \left| \sum_{n=0}^{p} v_n^H X_{k-n} \right|^2 \geq 0 \quad \text{for any } \{v_n\}_0^p \quad , \tag{100}$$

where v_n is Mx1. However the stability of the correlation recursion (52) is unknown to this author. The estimate (99) is unchanged by the addition of more stages, that is, larger values of p.

Another technique would be to minimize the prediction error

$$Y_k \equiv \sum_{n=0}^{p} A_n X_{k-n} \ , \quad p+1 \le k \le N \qquad (A_0 = -I) \tag{101}$$

over the available data points directly, by choice of $\{A_n\}_1^p$. We have the error matrix

$$\frac{1}{N-p} \sum_{k=p+1}^{N} Y_k Y_k^H = \sum_{n,m=0}^{p} A_n S_{mn} A_m^H \ , \tag{102}$$

where

$$S_{mn} \equiv \frac{1}{N-p} \sum_{k=p+1}^{N} X_{k-n} X_{k-m}^H \ , \quad 0 \le m, n \le p. \tag{103}$$

The optimum coefficients for minimum trace of the error matrix, (102), are solutions of

$$\sum_{n=1}^{p} A_n^{(p)} S_{mn} = S_{m0} \ , \quad 1 \le m \le p. \tag{104}$$

Matrix $[S_{mn}]_1^p$ is not block Toeplitz, and a significant computer problem exists for M>1 when it is noted that solution of linear equations (104) must be done anew for each different value of p. This was a good technique for spectral estimation when M=1 (see Ref. 3); however, computer time was greater than for the Burg technique. Moreover, stability of the correlation recursion (52) is unlikely in view of the (occasionally unstable) results for M=1 in Ref. 3.

This technique could be extended to include backward prediction in addition to (101). However, the lack of the block Toeplitz property and lack of stability make it a very undesirable technique.

The technique suggested here (in subsection 3.1) lets the correlation estimate be yielded according to solution (80), once partial correlation coefficients $A_p^{(p)}$ and $B_p^{(p)}$ have been specified. And we shall see in subsection 3.4 that these latter quantities are determined according to a physically meaningful minimization problem. Stability of the correlation recursion (52) has not been proved; however, numerous examples have all yielded stable solutions. The estimate (80) is unchanged by the addition of more stages, that is, larger values of p. And it will be seen that the current technique reduces to Burg's algorithm (Ref. 4) for M=1. Thus the current technique appears to be very attractive among those techniques that employ an all-pole representation of the input process.

3.3 PROPERTIES AND INTERPRETATIONS

The quantities U_{p-1} and V_{p-1} were defined in (95) and (89) and were interpreted as estimates of the correlation matrices of the (p-1)th order forward and backward residuals, respectively, at zero time delay. It is shown in appendix H that they satisfy the recurrence relations

$$\begin{aligned} U_p &= \left(I - A_p^{(p)} B_p^{(p)}\right) U_{p-1} , \qquad U_0 = R_0 , \\ V_p &= \left(I - B_p^{(p)} A_p^{(p)}\right) V_{p-1} , \qquad V_0 = R_0 , \end{aligned} \tag{105}$$

just as for the known correlation case. It is also shown that

$$U_p^H = U_p , \quad V_p^H = V_p , \tag{106}$$

and

$$\det U_p = \det V_p . \tag{107}$$

However, we are not able to prove U_p or V_p nonnegative definite without specifying the method by which A_p and $B_p^{(p)}$ are selected; no relations like (30) and (32) exist here.

By means of (106), the constraint (98) on selection of $A_p^{(p)}$ and $B_p^{(p)}$ takes the form (see 42))

$$A_p^{(p)} V_{p-1} = U_{p-1} B_p^{(p)H} . \tag{108}$$

This will be used in the next subsection.

3.4 EVALUATION OF PARTIAL CORRELATION COEFFICIENTS

We recall from subsection 2.1 that, in the known correlation case, the partial correlation coefficients $A_p^{(p)}$ and $B_p^{(p)}$ minimized

$$\operatorname{tr} \overline{Y_k^{(p)} Y_k^{(p)H}} \quad \text{and} \quad \operatorname{tr} \overline{Z_k^{(p)} Z_k^{(p)H}} , \tag{109}$$

respectively, when lower order stages had already been optimized. We extend this idea to the unknown correlation case as follows: let (as in (18) and (19))

$$Y_k^{(0)} \equiv X_k , \; Z_k^{(0)} \equiv X_k , \quad 1 \le k \le N, \tag{110}$$

and for $p \ge 1$, define errors (residuals)

$$\left.\begin{aligned} Y_k^{(p)} &\equiv Y_k^{(p-1)} - A_p^{(p)} Z_{k-1}^{(p-1)} \\ Z_k^{(p)} &\equiv Z_{k-1}^{(p-1)} - B_p^{(p)} Y_k^{(p-1)} \end{aligned}\right\} , \; p+1 \le k \le N . \tag{111}$$

The block diagram for (111) is identical to that in figure 1 on page 7.

Define for $p \geq 1$, the error (residual) matrix over the available data points as

$$E_p \equiv \frac{1}{N-p} \sum_{k=p+1}^{N} Y_k^{(p)} Y_k^{(p)H} = E_p^H ; \tag{112}$$

this nonnegative definite matrix is an unbiased estimator of $\overline{Y_k^{(p)} Y_k^{(p)H}}$.

Substitution of (111) in (112) yields

$$E_p = S_{p-1}^{(yy)} - A_p^{(p)} S_{p-1}^{(yz)H} - S_{p-1}^{(yz)} A_p^{(p)H} + A_p^{(p)} S_{p-1}^{(zz)} A_p^{(p)H} , \tag{113}$$

where

$$S_{p-1}^{(yy)} \equiv \frac{1}{N-p} \sum_{k=p+1}^{N} Y_k^{(p-1)} Y_k^{(p-1)H} = S_{p-1}^{(yy)H} , \tag{114A}$$

$$S_{p-1}^{(yz)} \equiv \frac{1}{N-p} \sum_{k=p+1}^{N} Y_k^{(p-1)} Z_{k-1}^{(p-1)H} , \tag{114B}$$

$$S_{p-1}^{(zz)} \equiv \frac{1}{N-p} \sum_{k=p+1}^{N} Z_{k-1}^{(p-1)} Z_{k-1}^{(p-1)H} = S_{p-1}^{(zz)H} . \tag{114C}$$

Also define for $p \geq 1$, error matrix

$$F_p \equiv \frac{1}{N-p} \sum_{k=p+1}^{N} Z_k^{(p)} Z_k^{(p)H} = F_p^H . \tag{115}$$

Substitution of (111) in (115) yields

$$F_p = S_{p-1}^{(zz)} - B_p^{(p)} S_{p-1}^{(yz)} - S_{p-1}^{(yz)H} B_p^{(p)H} + B_p^{(p)} S_{p-1}^{(yy)} B_p^{(p)H} . \tag{116}$$

Now error matrices E_p and F_p are Hermitian and nonnegative definite. Therefore matrix $\Lambda_a E_p \Lambda_a^H$ is Hermitian and nonnegative definite for any MxM weighting matrix Λ_a:

$$V^H (\Lambda_a E_p \Lambda_a^H) V = (\Lambda_a^H V)^H E_p (\Lambda_a^H V) \geq 0 \tag{117}$$

for any Mx1 matrix $\mathcal{V}$. Also since

$$tr(\Lambda_a E_p \Lambda_a^H) = tr(\Lambda_a^H \Lambda_a E_p) \equiv tr(\Lambda E_p), \tag{118}$$

only the product $\Lambda = \Lambda_a^H \Lambda_a$ matters in so far as the trace of $\Lambda_a E_p \Lambda_a^H$ is concerned; notice that Λ is Hermitian and nonnegative definite. We shall be interested in minimizing the traces of weighted error matrices $\Lambda_a E_p \Lambda_a^H$ and $\Gamma_a F_p \Gamma_a^H$; the exact choice of, and the reason for, weightings Λ_a and Γ_a will be undertaken in the next subsection.

Now if we were to minimize $tr(\Lambda_{p-1} E_p)$ by choice of $A_p^{(p)}$, we would find (see appendix B for method) that we must solve

$$\Lambda_{p-1} A_p^{(p)} S_{p-1}^{(yz)} = \Lambda_{p-1} S_{p-1}^{(yz)}, \tag{119}$$

and the choice of Λ_{p-1} would be irrelevant. Also, if we were to minimize $tr(\Gamma_{p-1} F_p)$ by choice of $B_p^{(p)}$, we would find that we must solve

$$\Gamma_{p-1} S_{p-1}^{(yy)} B_p^{(p)H} = \Gamma_{p-1} S_{p-1}^{(yz)}, \tag{120}$$

and the choice of Γ_{p-1} would be irrelevant. Furthermore, we would not satisfy constraint (108) generally. But since the behavior of error matrix F_p is just as important as that of E_p, we should take both matrices into account in any error minimization; in fact, for known correlation, recall that the determinants of residual matrices U_p and V_p were equal.

We therefore choose to minimize the sum of the traces of the weighted error matrices

$$\mathrm{tr}\left(\Lambda_{p-1} E_p\right) + \mathrm{tr}\left(\Gamma_{p-1} F_p\right) = \mathrm{tr}\left(\Lambda_{p-1} E_p + \Gamma_{p-1} F_p\right), \tag{121}$$

where Λ_{p-1} and Γ_{p-1} are Hermitian and nonnegative definite, by choice of $A_p^{(p)}$ and $B_p^{(p)}$ subject to constraint (108). If we let

$$A_p^{(p)} V_{p-1} = U_{p-1} B_p^{(p)H} \equiv G_p , \tag{122}$$

then we can express

$$\begin{aligned} &\Lambda_{p-1} E_p + \Gamma_{p-1} F_p = \\ &\Lambda_{p-1}\left[S_{p-1}^{(yy)} - G_p V_{p-1}^{-1} S_{p-1}^{(yx)H} - S_{p-1}^{(yx)} V_{p-1}^{-1} G_p^H + G_p V_{p-1}^{-1} S_{p-1}^{(xx)} V_{p-1}^{-1} G_p^H\right] \\ &+\Gamma_{p-1}\left[S_{p-1}^{(xx)} - G_p^H U_{p-1}^{-1} S_{p-1}^{(yx)} - S_{p-1}^{(yx)H} U_{p-1}^{-1} G_p + G_p^H U_{p-1}^{-1} S_{p-1}^{(yy)} U_{p-1}^{-1} G_p\right] \end{aligned} \tag{123}$$

in terms of the single unknown matrix G_p. Our problem therefore is to minimize the trace of (123) by choice of the single quantity G_p, subject to no constraints; we can then solve for the best coefficients according to

$$A_p^{(p)} = G_p V_{p-1}^{-1} , \quad B_p^{(p)} = G_p^H U_{p-1}^{-1} . \tag{124}$$

Also we can compute the correlation estimate from (90) and (88) according to

$$R_p = R_p^{(p-1)} + G_p . \tag{125}$$

In appendix I, it is shown that the minimum of the trace of (123) is realized when G_p is the solution of the bilinear matrix equation (Ref. 9)

$$G_p \alpha + \beta G_p = \mu + \nu , \tag{126}$$

where

$$\alpha = V_{p-1}^{-1} S_{p-1}^{(zz)} V_{p-1}^{-1} \Gamma_{p-1}^{-1}$$
$$\beta = \Lambda_{p-1}^{-1} U_{p-1}^{-1} S_{p-1}^{(yy)} U_{p-1}^{-1} \qquad (127)$$
$$\mu = S_{p-1}^{(yz)} V_{p-1}^{-1} \Gamma_{p-1}^{-1}$$
$$\nu = \Lambda_{p-1}^{-1} U_{p-1}^{-1} S_{p-1}^{(yz)}$$

Uniqueness of the solution of (126) is considered in subsection 3.6. (It is interesting to note that the separate minimizations in (119) and (120) yield

$$G_p \alpha - \mu = \nu - \beta G_p = 0. \qquad (128)$$

Thus whereas both these quantities had to be equal separately to the zero matrix, we now require only that they be equal to each other.)

For the special case of M=1 (a univariate process), (105) and (108) yield

$$U_p = V_p, \quad B_p^{(p)} = A_p^{(p)*} \qquad (M = 1). \qquad (129)$$

Then (126) and (127) can be solved for the scalar

$$G_p = \frac{\left(\Gamma_{p-1}^{-1} + \Lambda_{p-1}^{-1}\right) S_{p-1}^{(yz)}}{\Gamma_{p-1}^{-1} S_{p-1}^{(zz)} + \Lambda_{p-1}^{-1} S_{p-1}^{(yy)}} U_{p-1} \qquad (M = 1). \qquad (130)$$

Now, if and only if

$$\Gamma_{p-1} = \Lambda_{p-1} \qquad (M = 1), \tag{131}$$

(130) reduces to Burg's algorithm (Ref. 4); in fact, it can be shown that (131) is the only choice of weights in (130) which guarantees a stable correlation recursion for M=1. Thus we shall insist that the weights satisfy (131) when we deal with their selection below.

3.5 WEIGHTING OF ERROR MATRICES

It is necessary to apply weighting to error matrices E_p and F_p in (112) and (115), prior to minimization of the trace in (121), for several reasons. First, without weighting, the larger amplitude components of errors (111) would receive most of the emphasis in the minimization; thus, some weighting inversely proportional to the component strengths is desired. Second, it is desired that stable correlation recursions result and that matrices U_p and V_p be nonnegative definite. Without weighting, it has been discovered (by an example to be presented in subsection 3.9) that both of these requirements can be violated. Third, we will insist that the scaling property introduced in subsection 2.2 hold for the unknown correlation case as well; that is, if

$$\tilde{X}_k = D X_k \ , \quad D \ \text{arbitrary} \ , \tag{132}$$

we shall insist that the coefficients satisfy

$$\left.\begin{aligned} \tilde{A}_n^{(p)} &= D A_n^{(p)} D^{-1} \\ \tilde{B}_n^{(p)} &= D B_n^{(p)} D^{-1} \end{aligned}\right\} \ , \ 1 \le n \le p, \quad \text{all } p. \tag{133}$$

The matrix equation (126) can be combined with (122) to yield the simultaneous set of equations

$$\begin{aligned} A_p^{(p)} S_{p-1}^{(zz)} V_{p-1}^{-1} \Gamma_{p-1}^{-1} + \Lambda_{p-1}^{-1} U_{p-1}^{-1} S_{p-1}^{(yy)} B_p^{(p)H} &= S_{p-1}^{(yz)} V_{p-1}^{-1} \Gamma_{p-1}^{-1} + \Lambda_{p-1}^{-1} U_{p-1}^{-1} S_{p-1}^{(yz)}, \\ A_p^{(p)} V_{p-1} - U_{p-1} B_p^{(p)H} &= 0. \end{aligned} \tag{134}$$

We now consider several possible choices of weightings Λ_{p-1} and Γ_{p-1} that tend to simplify the form of (134). The first choice is no weighting:

$$\Lambda_{p-1} = I, \quad \Gamma_{p-1} = I. \qquad \text{Choice 1} \tag{135}$$

The problem with this choice is that the weighting is not related to the error component strengths, and it may be readily verified that the solutions to (134) and (135) do not satisfy the scaling property (133). Also an unstable correlation recursion can occur. However, the solutions do reduce to Burg's algorithm for M=1; see (131).

Our next candidate weighting is

$$\Lambda_{p-1} = U_{p-1}^{-1}, \quad \Gamma_{p-1} = V_{p-1}^{-1}, \qquad \text{Choice 2} \tag{136}$$

which are Hermitian and are nonnegative definite if U_{p-1} and V_{p-1} are nonnegative definite. This weighting is inversely proportional to the component strengths, as desired; more will be said on this below. The equations (134) become

$$\begin{aligned} A_p^{(p)} S_{p-1}^{(zz)} + S_{p-1}^{(yy)} B_p^{(p)H} &= 2 S_{p-1}^{(yz)}, \\ A_p^{(p)} V_{p-1} - U_{p-1} B_p^{(p)H} &= 0. \end{aligned} \tag{137}$$

The solutions of (137) satisfy the scaling property (133), and they reduce to Burg's algorithm for M=1; (129) shows that (131) is satisfied for the choice (136). Although stability of the correlation recursions (52)

and (55), and nonnegative definiteness of U_p and V_p, have not been proven for general M≥2, no counter examples have been discovered.

We next consider

$$\Lambda_{p-1}^{-1} = S_{p-1}^{(yy)^{-1}} U_{p-1} \;, \quad \Gamma_{p-1}^{-1} = V_{p-1} S_{p-1}^{(zz)^{-1}} \;, \qquad \text{Choice 3} \tag{138}$$

in which case (134) becomes

$$\begin{aligned} A_p^{(p)} + B_p^{(p)H} &= S_{p-1}^{(yz)} S_{p-1}^{(zz)^{-1}} + S_{p-1}^{(yy)^{-1}} S_{p-1}^{(yz)} \;, \\ A_p^{(p)} V_{p-1} - U_{p-1} B_p^{(p)H} &= 0. \end{aligned} \tag{139}$$

However, the weighting (138) is not necessarily Hermitian, is not necessarily nonnegative definite, and is not directly related to the error component strengths. Also the solutions of (139) do not satisfy the scaling property. Furthermore, the solutions do not reduce to Burg's algorithm for M=1, and can yield unstable correlation recursions for M=1.

The last choice is

$$\Lambda_{p-1}^{-1} = U_{p-1} S_{p-1}^{(yy)^{-1}} U_{p-1} \;, \quad \Gamma_{p-1}^{-1} = V_{p-1} S_{p-1}^{(zz)^{-1}} V_{p-1} \;, \qquad \text{Choice 4} \tag{140}$$

which are Hermitian and nonnegative definite, and for which (134) becomes

$$\begin{aligned} A_p^{(p)} V_{p-1} + U_{p-1} B_p^{(p)H} &= S_{p-1}^{(yz)} S_{p-1}^{(zz)^{-1}} V_{p-1} + U_{p-1} S_{p-1}^{(yy)^{-1}} S_{p-1}^{(yz)} \;, \\ A_p^{(p)} V_{p-1} - U_{p-1} B_p^{(p)H} &= 0. \end{aligned} \tag{141}$$

This choice is a very interesting one in that the solutions of (141) are immediate and do not require that a bilinear matrix equation be solved. The weighting (140) is inversely proportional to the error component strengths, and the solutions of (141) do satisfy the scaling property. In fact, this choice is very close to Choice 2, since U_{p-1} and $S_{p-1}^{(yy)}$ are both estimates of the correlation matrix of process $\{Y_k^{(p-1)}\}$ at zero time delay, and should be

fairly close to each other. However, the solutions of (141) do not reduce to Burg's algorithm for M=1, and the correlation recursion (52) can be unstable, even for M=1. In fact, the solutions to (141) are identical to those for Choice 3 for M=1.

Therefore, of the four choices considered, only Choice 2 in (136) yields solutions that satisfy the scaling property (133) and reduces to Burg's algorithm for M=1. The stability of the correlation recursions has not been proved or disproved for choice (136) of weighting.

There is another strong reason for choosing weighting (136), which has to do with a whitening interpretation. We recall that U_{p-1} and V_{p-1}, defined in (95) and (89), are estimates of the correlation matrices of processes $\{Y_k^{(p-1)}\}$ and $\{Z_k^{(p-1)}\}$, respectively, at zero time delay. Now let (for non-negative definite U_{p-1} and V_{p-1})

$$U_{p-1} = \mathcal{U}_{p-1}\mathcal{U}_{p-1}^H \quad , \quad V_{p-1} = \mathcal{V}_{p-1}\mathcal{V}_{p-1}^H \quad , \tag{142}$$

where $\mathcal{U}_{p-1}$ and $\mathcal{V}_{p-1}$ are (lower triangular) square root matrices. Then scaled processes

$$\tilde{Y}_k^{(p-1)} \equiv \mathcal{U}_{p-1}^{-1} Y_k^{(p-1)} \quad , \quad \tilde{Z}_k^{(p-1)} \equiv \mathcal{V}_{p-1}^{-1} Z_k^{(p-1)} \quad , \quad p \le k \le N \, , \tag{143}$$

each have estimated correlation matrices at zero time delay equal to I; that is, all the components of $\{\tilde{Y}_k^{(p-1)}\}$ (or $\{\tilde{Z}_k^{(p-1)}\}$) have unit power and are uncorrelated with each other at zero time delay.

Now define, for $p+1 \le k \le N$,

$$q_k^{(p)} \equiv \mathcal{U}_{p-1}^{-1} Y_k^{(p)} = \mathcal{U}_{p-1}^{-1}\left(Y_k^{(p-1)} - A_p^{(p)} Z_{k-1}^{(p-1)}\right) = \tilde{Y}_k^{(p-1)} - \tilde{A}_p^{(p)} \tilde{Z}_{k-1}^{(p-1)} \quad , \tag{144}$$

where

$$\tilde{A}_p^{(p)} \equiv U_{p-1}^{-1} A_p^{(p)} V_{p-1} . \tag{145}$$

Also define the estimated correlation matrix at zero time delay of process $\{q_k^{(p)}\}$ as

$$\mathcal{E}_p \equiv \frac{1}{N-p} \sum_{k=p+1}^{N} q_k^{(p)} q_k^{(p)H} = \frac{1}{N-p} \sum_{k=p+1}^{N} U_{p-1}^{-1} Y_k^{(p)} Y_k^{(p)H} U_{p-1}^{-1H} = U_{p-1}^{-1} E_p U_{p-1}^{-1H}, \tag{146}$$

where we have used (144) and (112). Therefore

$$\operatorname{tr} \mathcal{E}_p = \operatorname{tr}\left(U_{p-1}^{-1} E_p U_{p-1}^{-1H}\right) = \operatorname{tr}\left(U_{p-1}^{-1H} U_{p-1}^{-1} E_p\right) = \operatorname{tr}\left(U_{p-1}^{-1} E_p\right), \tag{147}$$

where we have used (I-1) and (142). Thus, minimizing the trace of $U_{p-1}^{-1} E_p$, by choice of $A_p^{(p)}$, is equivalent to minimizing the trace of $\mathcal{E}_p$ by choice of $\tilde{A}_p^{(p)}$ (see (144)), where process $\{q_k^{(p)}\}$ is the error in prediction of (p-1)th order processes with estimated correlation matrices at zero time delay equal to I.

In a similar fashion, for $p+1 \le k \le N$,

$$Z_k^{(p)} \equiv V_{p-1}^{-1} Z_k^{(p)} = V_{p-1}^{-1}\left(Z_{k-1}^{(p-1)} - B_p^{(p)} Y_k^{(p-1)}\right) = \tilde{Z}_{k-1}^{(p-1)} - \tilde{B}_p^{(p)} \tilde{Y}_k^{(p-1)} \tag{148}$$

where

$$\tilde{B}_p^{(p)} \equiv V_{p-1}^{-1} B_p^{(p)} U_{p-1} . \tag{149}$$

And

$$\mathcal{J}_p \equiv \frac{1}{N-p} \sum_{k=p+1}^{N} Z_k^{(p)} Z_k^{(p)H} = \frac{1}{N-p} \sum_{k=p+1}^{N} V_{p-1}^{-1} Z_k^{(p)} Z_k^{(p)H} V_{p-1}^{-1H} = V_{p-1}^{-1} F_p V_{p-1}^{-1} \tag{150}$$

with

$$\operatorname{tr} \mathcal{J}_p = \operatorname{tr}\left(V_{p-1}^{-1} F_p\right). \tag{151}$$

If we solve (145) and (149) for $A_p^{(p)}$ and $B_p^{(p)}$, and then utilize constraint (108) along with (142), we find that the constraint takes the form

$$\tilde{A}_p^{(p)} = \tilde{B}_p^{(p)H} . \tag{152}$$

This could be used as the starting point in a minimization of error matrices $\mathcal{E}_p$ and $\mathcal{J}_p$. In fact, if we minimize the unweighted trace of $\mathcal{E}_p+\mathcal{J}_p$ by choice of $\tilde{A}_p^{(p)}$, we find the optimum choice to be given by

$$\tilde{A}_p^{(p)} \tilde{S}_{p-1}^{(zz)} + \tilde{S}_{p-1}^{(yy)} \tilde{A}_p^{(p)} = 2\tilde{S}_{p-1}^{(yz)} , \tag{153}$$

where the notation is an obvious modification of (114). By employing (145), (143), and (142), we can show that (153) is equivalent to (137), as it must be. (This alternative approach may be useful for proving the stability of the correlation recursion.)

3.6 SOLUTION OF BILINEAR MATRIX EQUATION

If we substitute definitions (127) into bilinear matrix equation (126), and premultiply by $\Lambda_{p-1}^{1/2}$ and postmultiply by $\Gamma_{p-1}^{1/2}$, we obtain the equation

$$\tilde{G}_p \tilde{\alpha} + \tilde{\beta} \tilde{G}_p = \tilde{\mu} + \tilde{\nu}, \tag{154}$$

where

$$\begin{aligned}
\tilde{G}_p &\equiv \Lambda_{p-1}^{1/2} G_p \Gamma_{p-1}^{1/2} \\
\tilde{\alpha} &= \Gamma_{p-1}^{-1/2} V_{p-1}^{-1} S_{p-1}^{(xx)} V_{p-1}^{-1} \Gamma_{p-1}^{-1/2} \\
\tilde{\beta} &= \Lambda_{p-1}^{-1/2} U_{p-1}^{-1} S_{p-1}^{(ww)} U_{p-1}^{-1} \Lambda_{p-1}^{-1/2} \\
\tilde{\mu} &= \Lambda_{p-1}^{1/2} S_{p-1}^{(wx)} V_{p-1}^{-1} \Gamma_{p-1}^{-1/2} \\
\tilde{\nu} &= \Lambda_{p-1}^{-1/2} U_{p-1}^{-1} S_{p-1}^{(yw)} \Gamma_{p-1}^{1/2} .
\end{aligned} \tag{155}$$

Now the Hermitian matrices $\tilde{\alpha}$ and $\tilde{\beta}$ are non-negative definite; e.g.,

$$q^H \tilde{\alpha} q = \left(V_{p-1}^{-1} \Gamma_{p-1}^{-1/2} q\right)^H S_{p-1}^{(22)} \left(V_{p-1}^{-1} \Gamma_{p-1}^{-1/2} q\right) \geq 0 \tag{156}$$

for any MX1 matrix q, since $S_{p-1}^{(22)}$ is non-negative definite. We have employed the Hermitian property of V_{p-1} and Γ_{p-1} above; see (118) et seq. This means that the eigenvalues of $\tilde{\alpha}$ and $\tilde{\beta}$ must be non-negative. Therefore the solution of (154) exists and is unique (Ref. 10, eq. 3).

Solution of the bilinear matrix equation (126) or (154) has been addressed by many authors (Refs. 9 - 17). In particular, for the equation involving MxM matrices,

$$XB + AX = C, \tag{157}$$

one form for the solution is given by

$$X = PQ^{-1}, \tag{158}$$

where

$$P = \sum_{k=0}^{M-1} (-1)^k A_k C B^{M-1-k},$$
$$Q = \sum_{k=0}^{M} (-1)^k a_k B^{M-k}, \tag{159}$$

are MxM matrices. The constants $\{a_k\}$ are given by (Ref. 18, pp. 87-88)

$$a_k = -\frac{1}{k} tr\left(A A_{k-1}\right), \quad 1 \leq k \leq M \qquad (a_0 = 1), \tag{160}$$

and the matrices $\{A_k\}$ are given by

$$A_k = A A_{k-1} + a_k I, \quad 1 \leq k \leq M \qquad (A_0 = I). \tag{161}$$

Here, M-2 full matrix multiplications are necessary when we note that $A_M = 0$

by the Cayley-Hamilton theorem.

For M = 2, (159) takes the form

$$\left.\begin{aligned} P &= C B - (A - \mathrm{tr}(A)\, I)\, C \\ Q &= (\mathrm{tr}\, A + \mathrm{tr}\, B) B + (\det A - \det B) I \end{aligned}\right\} \quad \text{for } M = 2, \tag{162}$$

where we have used the Cayley-Hamilton theorem to express

$$B^2 = \mathrm{tr}(B)\, B - \det(B)\, I \quad \text{for } M = 2. \tag{163}$$

Equations (162) and (158) are the forms used in the FORTRAN program for M = 2.

3.7 SPECTRAL ESTIMATION

Having obtained correlation estimates $\{R_m\}_0^P$ by means of (82) and (80A), we now extrapolate these, as in subsection 2.3 (equations (52) and (66)), to yield

$$\begin{aligned} R_m &= \sum_{n=1}^{P} A_n^{(p)} R_{m-n}, \quad p+1 \le m, \\ R_m &= R_{-m}^H, \quad m < 0. \end{aligned} \tag{164}$$

This defines an infinite sequence $\{R_m\}_{-\infty}^{\infty}$ which is assumed stable; its Fourier transform will be taken as the spectral estimate of the process under consideration. In a manner identical to that given in appendix F, it is found that

$$G^{(p)}(f) = \Delta \sum_{m=-\infty}^{\infty} \exp(-i 2\pi f m \Delta) R_m = \Delta\, H_A^{(p)}(f)^{-1}\, U_p\, H_A^{(p)}(f)^{-1^H}, \quad |f| < \frac{1}{2\Delta}, \tag{165}$$

where U_p and $H_A^{(p)}(f)$ are given by (95) and (68), respectively. It follows that

$$\int_{-\frac{1}{2\Delta}}^{\frac{1}{2\Delta}} df\, G^{(p)}(f) = R_0 = \text{sample power (80)}. \tag{166}$$

Also, as in subsection 2.4, an alternative factorization is available as

$$G^{(p)}(f) = \Delta\, H_B^{(p)}(f)^{-1}\, V_p\, H_B^{(p)}(f)^{-1^H}, \quad |f| < \frac{1}{2\Delta}, \tag{167}$$

where V_p and $H_B^{(p)}(f)$ are given in (89) and (70). If U_p or V_p is non-negative definite, then $G^{(p)}(f)$ is non-negative definite, as desired for a spectral estimate. Since (165) and (167) are equal, we concentrate henceforth on form (165).

Since

$$H_A^{(p)}(f)^{-1} = \frac{\text{Adj } H_A^{(p)}(f)}{\det H_A^{(p)}(f)} , \tag{168}$$

(165) can be expressed as

$$G^{(p)}(f) = \Delta \left| \det H_A^{(p)}(f) \right|^{-2} \left[\text{Adj } H_A^{(p)}(f) \right] U_p \left[\text{Adj } H_A^{(p)}(f) \right]^H . \tag{169}$$

Since $G^{(p)}(f)$ is Hermitian, matrix $G^{(p)}(f)$ need be computed only on and above its main diagonal, at each frequency of interest. Efficient computation of $H_A^{(p)}(f)$ by means of an FFT is undertaken in appendix J. It is shown that we need to perform M^2 N_F-point FFTs of p+1 non-zero numbers, in order to evaluate $H_A^{(p)}(f)$ at N_F frequency cells in the frequency range $\left(-\frac{1}{2\Delta}, \frac{1}{2\Delta}\right)$.

Real Multivariate Process

The results above have been derived for a complex multivariate process $\{X_k\}$. For a real multivariate process, U_p is real and $\{A_m^{(p)}\}_0^p$ are real. Then

$$H_A^{(p)}(-f) = H_A^{(p)}(f)^* \quad \text{for a real process,} \tag{170}$$

and

$$G^{(p)}(-f) = \Delta H_A^{(p)}(f)^{*^{-1}} U_p H_A^{(p)}(f)^{*^{-1}H}$$

$$= \Delta H_A^{(p)}(f)^{-1^*} U_p H_A^{(p)}(f)^{-1H^*} = G^{(p)}(f)^* \quad \text{for a real process.} \tag{171}$$

Thus we need compute matrix $G^{(p)}(f)$ only for $f \geq 0$, for a real multivariate process.

In order to avoid complex matrix multiplications, we develop (169) more explicitly; let

$$Adj\ H_A^{(p)}(f) = R_A(f) + i\, I_A(f), \tag{172}$$

where $R_A(f)$ and $I_A(f)$ are real MxM matrices at each f. Then since U_p is real, $U_p^T = U_p$, and upon substituting (172) in (169), we find

$$G^{(p)}(f) = \Delta \left| \det H_A^{(p)}(f) \right|^{-2} \left[R_A(f) U_p R_A(f)^T + I_A(f) U_p I_A(f)^T + i\, M(f) - i\, M(f)^T \right] \tag{173}$$

for a real process,

where

$$M(f) \equiv I_A(f)\, U_p\, R_A(f)^T. \tag{174}$$

Since M(f) is real, the quantity $i\,M(f) - i\,M(f)^T$ is zero on the main diagonal; therefore we need not compute the main diagonal of M(f). All the matrix multiplications in (173) are real.

Real Bivariate Process

We now further specialize to M = 2, a bivariate process. Let the real and imaginary parts of the filter transfer function $H_A^{(p)}$ be denoted by XX and YY, respectively (where these symbols are unrelated to X and Y introduced earlier); that is

$$H_A^{(p)}(f) \equiv XX(f) + i\, YY(f). \tag{175}$$

Then from (172), for 2 X 2 matrices,

$$R_A(f) = Re\left\{Adj\, H_A^{(p)}(f)\right\} = Adj\, Re\left\{H_A^{(p)}(f)\right\} = Adj\, XX(f) \equiv XX_A(f), \tag{176}$$

and

$$I_A(f) = \mathrm{Im}\left\{\mathrm{Adj}\, H_A^{(p)}(f)\right\} = \mathrm{Adj}\ \mathrm{Im}\left\{H_A^{(p)}(f)\right\} = \mathrm{Adj}\ YY(f) \equiv YY_A(f). \tag{177}$$

Substitution of (176) and (177) in (173) yields spectral estimate

$$G^{(p)}(f) = 4\left|\det H_A^{(p)}(f)\right|^{-2}\left[XX_A(f)U_p\, XX_A(f)^T + YY_A(f)U_p\, YY_A(f)^T + i\,M(f) - i\,M(f)^T\right]$$
$$\text{for a real bivariate process,} \tag{178}$$

where

$$M(f) = YY_A(f)\ U_p\ XX_A(f)^T. \tag{179}$$

The 2X2 matrices involved in (178) are all real, and $XX_A(f)$ and $YY_A(f)$ are the adjoints of the real and imaginary parts of $H_A^{(p)}(f)$, respectively. The form (178) is used in the program for the spectral estimate of a real bivariate process.

3.8 TERMINATION PROCEDURE

For unknown correlation, the correct value of p to use in (79) and (80) is unknown. We adopt the Akaike information criterion (AIC) derived in Ref. 19, page 719:

$$AIC_p = N \ln \det U_p + 2M^2p$$
$$= N \ln \det V_p + 2M^2p, \tag{180}$$

where we have utilized (107); namely, we compute AIC_p for $p = 0, 1, .., p_{max}$, and we use that value of p, p_{best}, for which AIC_p is a minimum. Selection of p_{max} is discussed below.

For purposes of updating U_p and V_p, we can combine (105), (106), and (122) to yield

$$U_p = U_{p-1} - A_p^{(p)} \epsilon_p^{\dagger}, \quad V_p = V_{p-1} - B_p^{(p)H} G_p, \tag{181}$$

in terms of the solution, G_p, of bilinear matrix equation (126).

At this point, it is worthwhile to review the procedure adopted here. From the actual data, we could have estimated the input correlation matrix via (99) (or some scaled version of it). Also we could have used (112) and (115) as error matrix estimates; in fact, these matrices are guaranteed Hermitian and non-negative definite. However, since $\det E_p \neq \det F_p$, we would have had to settle on some average like

$$\ln\left(\det E_p \cdot \det F_p\right)^{1/2} = \frac{1}{2}\left(\ln \det E_p + \ln \det F_p\right) \tag{182}$$

for purposes of the information criterion. As for the spectral estimate, we could have adopted, instead of (165), the quantity $\Delta H_A^{(p)}(f)^{-1} E_p H_A^{(p)}(f)^{-1H}$, or $\Delta H_B^{(p)}(f)^{-1} F_p H_B^{(p)}(f)^{-1H}$, for example.

Instead, we have chosen consistently to stick with the results of the normal equations (78). Thus the estimate of the input correlation matrix is obtained from (80)(and (82)); the estimates of the correlation matrices of the residuals are given by (89) and (95) (or more computationally convenient via (181)); and the spectral estimate is given in terms of U_p or V_p by (165) or (167), respectively, for $p=p_{best}$. The major gap in this procedure is that we have not proved that U_p or V_p is non-negative definite for Choice 2 of weighting in (136); however, no counter examples have been discovered.

Our selection of P_{max} is accomplished as follows: in ref. 1, page 575, Akaike is quoted as suggesting $P_{max} \approx 3N^{1/2}$ for M = 1, a univariate process. Since the number of coefficients evaluated is p, and the number of available data

points is N, this ratio was upper bounded by $3N^{-1/2}$. We extend this idea directly to the multivariate case: the number of scalar coefficients evaluated is $M^2 p$, and the number of available scalar data points is MN. Upper bounding this ratio by $3N^{-1/2}$, we find we should choose the filter order

$$p_{max} \leq \frac{3N^{1/2}}{M} \tag{183}$$

in terms of the number of data points, N, and the dimensionality of the time series, M.

3.9 EXAMPLES

It is worthwhile to summarize here the sequence of calculations required. For data $X_1, X_2, \ldots, X_N$ available (with the sample mean removed), we have

$$\begin{aligned}
&Y_k^{(0)} = Z_k^{(0)} = X_k, \quad 1 \leq k \leq N \\
&S_0^{(yy)} = \frac{1}{N-1}\sum_{k=2}^{N} X_k X_k^H = S_0^{(yy)H} \\
&S_0^{(zz)} = \frac{1}{N-1}\sum_{k=2}^{N} X_{k-1} X_{k-1}^H = \frac{1}{N-1}\sum_{k=1}^{N-1} X_k X_k^H = S_0^{(zz)H} \\
&S_0^{(yz)} = \frac{1}{N-1}\sum_{k=2}^{N} X_k X_{k-1}^H . \\
&U_0 = V_0 = R_0 = \frac{1}{N}\sum_{k=1}^{N} X_k X_k^H = U_0^H = V_0^H .
\end{aligned} \tag{184}$$

Then for $p \geq 1$ and choice (136) of weighting,

$$\begin{aligned}
&\alpha = V_{p-1}^{-1} S_{p-1}^{(zz)} \\
&\beta = S_{p-1}^{(yy)} U_{p-1}^{-1} \\
&\mu = \nu = S_{p-1}^{(yz)} \\
&G_p \text{ via (126)} \\
&A_p^{(p)} = G_p V_{p-1}^{-1}, \quad B_p^{(p)} = G_p^H U_{p-1}^{-1} \\
&U_p = U_{p-1} - A_p^{(p)} G_p^H \\
&V_p = V_{p-1} - B_p^{(p)} G_p \\
&AIC_p = N \ln \det U_p + 2M^2 p
\end{aligned} \tag{185}$$

$$\left.\begin{aligned} Y_k^{(p)} &= Y_k^{(p-1)} - A_p^{(p)} Z_{k-1}^{(p-1)} \\ Z_k^{(p)} &= Z_{k-1}^{(p-1)} - B_p^{(p)} Y_k^{(p-1)} \end{aligned}\right\} \quad , p+1 \le k \le N \tag{186}$$

$$\begin{aligned} S_p^{(yy)} &= \frac{1}{N-p-1} \sum_{k=p+2}^{N} Y_k^{(p)} Y_k^{(p)H} = S_p^{(yy)H} \\ S_p^{(zz)} &= \frac{1}{N-p-1} \sum_{k=p+2}^{N} Z_{k-1}^{(p)} Z_{k-1}^{(p)H} = \frac{1}{N-p-1} \sum_{k=p+1}^{N-1} Z_k^{(p)} Z_k^{(p)H} = S_p^{(zz)H} \\ S_p^{(yz)} &= \frac{1}{N-p-1} \sum_{k=p+2}^{N} Y_k^{(p)} Z_{k-1}^{(p)H} \quad . \end{aligned} \tag{187}$$

For $p = p_{max}$, it is not necessary to compute (186) through (187). When the best value of p, p_{best}, is found from AIC_p, we can then compute the spectral estimate (165).

We now consider an example for M = 2, N = 4:

$$X_1 = \begin{bmatrix} -1 \\ -1 \end{bmatrix} , \; X_2 = \begin{bmatrix} 1 \\ 2 \end{bmatrix} , \; X_3 = \begin{bmatrix} -1 \\ -2 \end{bmatrix} , \; X_4 = \begin{bmatrix} 1 \\ 1 \end{bmatrix} , \tag{188}$$

$$U_0 = V_0 = R_0 = \begin{bmatrix} 1.0 & 1.5 \\ 1.5 & 2.5 \end{bmatrix}$$

Then for weighting (136), we find

$$G_1 = -\frac{1}{12} \begin{bmatrix} 11 & 18 \\ 18 & 28 \end{bmatrix} , \; A_1^{(1)} = B_1^{(1)} = -\frac{1}{6} \begin{bmatrix} 1 & 3 \\ 6 & 2 \end{bmatrix} \tag{189}$$

The eigenvalues of $A_1^{(1)}$ are $(-3 \pm \sqrt{73})/12$, which are both bounded by 1 in magnitude, as they must be for the correlation recursion (164) for p = 1 to be stable. Also,

$$U_1 = V_1 = \frac{1}{72} \begin{bmatrix} 7 & 6 \\ 6 & 16 \end{bmatrix} , \tag{190}$$

which is non-negative definite. Thus, for weighting (136), all the desirable properties are realized.

However, for no weighting, (135), we find, for the same example (188),

$$G_1 = -\frac{1}{18}\begin{bmatrix} 20 & 30 \\ 30 & 43 \end{bmatrix}, \quad A_1^{(1)} = B_1^{(1)} = \frac{1}{9}\begin{bmatrix} -10 & 0 \\ -21 & 4 \end{bmatrix}. \tag{191}$$

The eigenvalues of $A_1^{(1)}$ are 4/9 and -10/9; since the latter is larger than 1 in magnitude, the recursion $R_m = A_1^{(1)} R_{m-1}$, $m \geq 1$, is unstable. Also

$$U_1 = V_1 = -\frac{1}{162}\begin{bmatrix} 38 & 57 \\ 57 & 53 \end{bmatrix}, \tag{192}$$

which is not a non-negative definite matrix. It is found that the spectral estimate obtained from (165) has frequency ranges where the two autospectra (diagonal terms of (165)) are negative, and where the magnitude-squared coherence can be negative or greater than 1. These are all unacceptable.

For the alternative example for M = 2, N = 4, of

$$X_1 = \begin{bmatrix} -.25 \\ -1.19 \end{bmatrix}, \quad X_2 = \begin{bmatrix} -1.25 \\ .81 \end{bmatrix}, \quad X_3 = \begin{bmatrix} .75 \\ .81 \end{bmatrix}, \quad X_4 = \begin{bmatrix} .75 \\ -.43 \end{bmatrix}, \tag{193}$$

and no weighting, we find a stable correlation recursion, but U_1 and V_1 are not non-negative definite, and values of the magnitude-squared coherence greater than 1 are realized in some frequency ranges. Because of these unacceptable behaviors, the choice of no weighting, (135), is discarded from future consideration.

An example for M = 2, N = 100, and weighting (136), generated via (71) - (73) of subsection 2.5 yielded the results below; the program and its output are given in appendix K. We find $p_{best}=1$ and

$$A_1^{(1)} = \begin{bmatrix} .87151 & -.77024 \\ .63432 & .56035 \end{bmatrix}, \quad B_1^{(1)} = \begin{bmatrix} .56613 & .77098 \\ -.63142 & .86573 \end{bmatrix}, \qquad (194)$$

$$U_1 = .09110 \begin{bmatrix} .97698 & -.00867 \\ -.00867 & 1.02364 \end{bmatrix}, \quad V_1 = .09110 \begin{bmatrix} .93178 & .34488 \\ .34488 & 1.20087 \end{bmatrix}. \qquad (195)$$

It is worthwhile to compare these estimates for N = 100 with the exact values in (76) and (77). The scale factor .09110 in (195) is unimportant and is due to the fact that the white noise used here had variance 1/12 rather than 1 as in (73); except for the scale factor, the matrices in (195) have determinants equal to 1. The estimated magnitude-squared coherence reaches a maximum of .999745, versus the true peak of .999013.

Observations from other examples of real bivariate processes have pointed out that: the eigenvalues of $A_1^{(1)}$ and $B_1^{(1)}$ are identical and are bounded by 1 in magnitude; the eigenvalues of $A_p^{(p)}$ and $B_p^{(p)}$ are not identical for $p \geq 2$, and can be larger than 1 in magnitude; and the eigenvalues of $A_n^{(p)}$ and $B_n^{(p)}$ for $n<p$ can be larger than 1 in magnitude.

Timing Results

Some sample execution times on a UNIVAC 1108 for SUBROUTINE PCC, which evaluates the partial correlation coefficients, are presented below for M = 2, a bivariate real process.

Table 1. Timing of Subroutine PCC

N	p_{max}	Time of Execution (sec)
100	10	0.25
100	15	0.35
1000	10	2.63
1000	40	9.23
10000	50	120
10000	150	326

The execution time is almost linearly proportional to N and p_{max}. The execution time for PEFTF was 1.25 seconds, and that for SDM was 0.55 seconds, both for N_F = 1024 frequency cells; see appendix K for program.

4. SUMMARY

A method for multivariate linear predictive spectral analysis, employing weighted forward and backward averaging, has been presented and programmed in FORTRAN. The method constitutes a generalization of Burg's univariate algorithm (Ref. 4) to the multivariate case.

The choice of weighting in the error minimization is very important, and several candidates have been considered. The weighting retained, (136), is the only one of those considered that satisfies both the scaling property (133) for all M, and reduces to Burg's algorithm for M = 1. Also, the weighting retained is equivalent to minimizing the unweighted traces of

error processes that are the differences of approximately white processes; in fact, (136) could be used as the starting point of the error minimization.

The major gaps in the analysis are that we have not proved that U_p and V_p are non-negative definite, and we have not proved that correlation recursion (164) is stable; however, no counterexamples have been encountered. The major analytical block in this endeavor is the bilinear matrix equation, (126), which requires special treatment for its solution.

Appendix A

PROPERTIES OF A SPECTRAL DENSITY MATRIX

Suppose an arbitrary linear filter with impulse response $\{H_n\}$ is excited by input $\{X_k\}$. The output at time $k\Delta$ is

$$Y_k = \sum_n H_n X_{k-n} , \tag{A-1}$$

where the sum is over all non-zero summands. X_k and Y_k are M x 1 matrices, whereas H_n is M x M. In steady state, the spectra of the processes in (A-1) are related by

$$G_Y(f) = H(f)\, G_X(f)\, H(f)^H , \tag{A-2}$$

where transfer function

$$H(f) \equiv \sum_n \exp(-i2\pi f n\Delta)\, H_n , \tag{A-3}$$

and f frequency in Hz and is real.

Now

$$G_x(f)^H = \Delta \sum_{k=-\infty}^{\infty} \exp(i2\pi f k\Delta) R_k^H = \Delta \sum_{n=-\infty}^{\infty} \exp(-i2\pi f n\Delta) R_n = G_x(f), \tag{A-4}$$

where we have employed (2). Thus $G_X(f)$ is Hermitian at any value of f. Similarly $G_Y(f)$ is Hermitian at any f.

Also

$$R_o^{(Y)} \equiv \overline{Y_K Y_K^H} \tag{A-5}$$

is non-negative definite for any H(f), because

$$q^H R_o^{(Y)} q = q^H \overline{Y_k Y_K^H}\, q = \overline{\left| q^H Y_K \right|^2} \geq 0 \tag{A-6}$$

for any M x 1 column matrix q . Therefore

$$R_0^{(Y)} = \int_{-\frac{1}{2\Delta}}^{\frac{1}{2\Delta}} df\, G_Y(f) = \int_{-\frac{1}{2\Delta}}^{\frac{1}{2\Delta}} df\, H(f) G_X(f) H(f)^H \qquad \text{(A-7)}$$

is non-negative definite for any H(f). It then follows that

$$G_X(f) \text{ is non-negative definite for all } f. \qquad \text{(A-8)}$$

To prove this, assume that $G_X(f_1)$ is not non-negative definite; than if we choose $H(f) \sim 1\ \delta(f-f_1)$, that is, an impulsive transfer function near frequency f_1, we get $R_0^{(Y)} \sim G_X(f_1)$ from (A-7), which contradicts the conclusion that $R_0^{(Y)}$ must be non-negative definite.

Thus a spectral density matrix must always be Hermitian and non-negative definite for all f. In particular, this implies that all the auto spectra (diagonal terms of the matrix) must be real and non-negative. It also implies that all coherences are bounded by unity in magnitude.

Appendix B

MINIMIZATION OF TRACE OF ERROR MATRIX

From (4) and (5), we have

$$Y_k = X_k - \sum_{n=1}^{P} A_n X_{k-n} = X_k - a\chi_k \tag{B-1}$$

where

$$a \equiv [A_1 \cdots A_p], \quad \chi_k \equiv \begin{bmatrix} X_{k-1} \\ \vdots \\ X_{k-p} \end{bmatrix}. \tag{B-2}$$

Let

$$\overline{X_k \chi_k^H} = c, \quad \overline{\chi_k \chi_k^H} = Q. \tag{B-3}$$

Here, a is M x Mp, χ_k is Mpx1, c is MxMp, and Q is MpxMp. We notice that $Q^H = Q$, and $v^H Q v = \overline{|v^H \chi_k|^2} > 0$ for any Mpx1 matrix $v \neq 0$, if no exact linear relation exists between the elements of $X_{k-1}, \ldots, X_{k-p}$; that is, Q is Hermitian and positive definite.

Now

$$\overline{Y_k Y_k^H} = \overline{(X_k - a\chi_k)(X_k^H - \chi_k^H a^H)}$$

$$= R_0 - ac^H - ca^H + aQa^H \tag{B-4}$$

$$= R_0 - cQ^{-1}c^H + (a - cQ^{-1})Q(a - cQ^{-1})^H. \tag{B-5}$$

Let

$$a - cQ^{-1} = \begin{bmatrix} v_1^H \\ \vdots \\ v_M^H \end{bmatrix} \tag{B-6}$$

where v_j is an Mpx1 matrix. Then for the M x M matrix in (B-5),

$$L \equiv (a - \mathcal{C}Q^{-1})Q(a - \mathcal{C}Q^{-1})^H = [\ell_{jm}]_{j,m=1}^{M}, \tag{B-7}$$

where complex scalar

$$\ell_{jm} = v_j^H Q v_m . \tag{B-8}$$

The real quantity $\ell_{jj} = v_j^H Q v_j > 0$ for any $v_j \neq 0$, since Q is Hermitian and positive definite; the minimum value of ℓ_{jj} is zero and is attained if and only if $v_j = 0$. Therefore, tr L is minimized, attaining value zero, by the choice $v_j = 0$, $1 \le j \le M$. Thus $\text{tr}\,\overline{Y_K Y_K^H} = \overline{Y_K^H Y_K}$ is minimized by the choice of a as

$$a_{opt} \equiv [A_1^{(p)} \cdots A_p^{(p)}] = \mathcal{C}Q^{-1}, \tag{B-9}$$

since the leading two terms in (B-5) are independent of a.

Then we have opt L = 0 and

$$\text{opt}\ \overline{Y_K Y_K^H} = R_0 - \mathcal{C}Q^{-1}\mathcal{C}^H = R_0 - a_{opt}\mathcal{C}^H = R_0 - a_{opt} Q a_{opt}^H . \tag{B-10}$$

Also

$$\min \overline{Y_K^H Y_K} = \text{tr}\ \text{opt}\ \overline{Y_K Y_K^H} = \text{tr}(R_0 - \mathcal{C}Q^{-1}\mathcal{C}^H) = \overline{X_K^H X_K} - \text{tr}(\mathcal{C}Q^{-1}\mathcal{C}^H). \tag{B-11}$$

It should be noted that the solution (B-9) is attainable directly from (B-4) if the coefficient of a^H (or a) is set equal to zero; this observation will be useful later.

Equations (B-9) and (B-10) can be developed as follows:

$a_{opt} Q = \mathcal{C}$ yields, with the use of (B-2) and (B-3),

$$[A_1^{(p)} \cdots A_p^{(p)}] \begin{bmatrix} R_0 & R_1 & \cdots & R_{p-1} \\ R_{-1} & \ddots & & \\ \vdots & & & \\ R_{1-p} & & & R_0 \end{bmatrix} = [R_1 \cdots R_p]; \tag{B-12}$$

that is,

$$\sum_{n=1}^{p} A_n^{(p)} R_{m-n} = R_m , \quad 1 \le m \le p. \tag{B-13}$$

And (B-10) can be expressed as

$$\text{opt } \overline{Y_k Y_k^H} = R_0 - \left[A_1^{(p)} \cdots A_p^{(p)}\right] \begin{bmatrix} R_1^H \\ \vdots \\ R_p^H \end{bmatrix} = R_0 - \sum_{n=1}^{p} A_n^{(p)} R_n . \tag{B-14}$$

Equations (B-13) and (B-14) are the main results of this appendix.

If an exact linear relation exists between the elements of $X_{k-1}, \cdots, X_{k-p}$, then

$$X_{k-1} = \sum_{j=2}^{p} G_j X_{k-j} \quad \text{for some } \{G_j\}_2^p \neq 0. \tag{B-15}$$

In this case, (B-1) yields

$$Y_{k-1} = X_{k-1} - \sum_{n=1}^{p} A_n X_{k-1-n} = X_{k-1} - \sum_{j=2}^{p} A_{j-1} X_{k-j} - A_p X_{k-1-p} . \tag{B-16}$$

Therefore we can get zero error by choosing

$$A_n^{(p)} = \left\{ \begin{array}{c} G_{n+1} , \ 1 \le n \le p-1 \\ 0, \ n = p \end{array} \right\} . \tag{B-17}$$

Thus $A_p^{(p)} = 0$ if an exact linear relation exists between the elements of $X_{k-1}, \cdots, X_{k-p}$.

Also we have the following general theorem:

No exact linear relation between elements of $X_k, \cdots, X_{k-p}$ $\iff$ $\begin{bmatrix} R_0 & \cdots & R_p \\ \vdots & \searrow & \\ R_p & & R_0 \end{bmatrix}$ is positive definite. (B-18)

To prove this, let

$$X_k = \begin{bmatrix} X_k \\ \vdots \\ X_{k-p} \end{bmatrix} , \quad D = \begin{bmatrix} d_1 \\ \vdots \\ d_{M(p+1)} \end{bmatrix} . \tag{B-19}$$

Then $F_K \equiv D^H X_K$ is a scalar. Now if and only if an exact linear relation exists, $F_K = 0$ for some $D \neq 0$, no matter which member function of the ensemble we select (with probability one). We also notice that

$$\overline{|F_K|^2} = D^H \overline{X_K X_K^H} D \tag{B-20}$$

and that the ensemble average in (B-20) is equal to the matrix in (B-18).

Assume that $F_K \neq 0$ for any $D \neq 0$. Then $\overline{|F_K|^2} > 0$ for any $D \neq 0$, and the right-hand side of (B-20) is positive for any $D \neq 0$. Therefore $\overline{X_K X_K^H}$ is positive definite.

Conversely if $\overline{X_K X_K^H}$ is positive definite, the right-hand side of (B-20) is positive for any $D \neq 0$. Then $\overline{|F_K|^2} > 0$ for any $D \neq 0$, yielding $F_K \neq 0$ for any $D \neq 0$.

Appendix C

INTERRELATIONSHIPS OF U_p AND V_p

We start with the definition (12) and develop U_p as

$$\begin{aligned} U_p &= R_0 - \sum_{m=1}^{p} A_m^{(p)} R_{-m} \\ &= R_0 - \sum_{m=1}^{p-1} \left(A_m^{(p-1)} - A_p^{(p)} B_{p-m}^{(p-1)}\right) R_{-m} - A_p^{(p)} R_{-p} \qquad \text{(by (15))} \\ &= R_0 - \sum_{m=1}^{p-1} A_m^{(p-1)} R_{-m} + A_p^{(p)} \sum_{m=1}^{p} B_{p-m}^{(p-1)} R_{-m} \\ &= U_{p-1} + A_p^{(p)} \sum_{j=0}^{p-1} B_j^{(p-1)} R_{j-p} \qquad \text{(by (12))} \\ &= U_{p-1} - A_p^{(p)} D_{p-1} \qquad \text{(by (13))} \\ &= U_{p-1} - A_p^{(p)} B_p^{(p)} U_{p-1} \qquad \text{(by (14))} \\ &= \left(I - A_p^{(p)} B_p^{(p)}\right) U_{p-1} . \end{aligned} \tag{C-1}$$

This relation holds for $p \geq 1$, with $U_0 = R_0$. A similar derivation for V_p yields

$$V_p = \left(I - B_p^{(p)} A_p^{(p)}\right) V_{p-1} \quad , \; p \geq 1 \; ; \quad V_0 = R_0 . \tag{C-2}$$

The determinant of U_p is given by

$$\begin{aligned} \det U_p &= \det\left(I - A_p^{(p)} B_p^{(p)}\right) \cdot \det U_{p-1} \\ &= \det A_p^{(p)} \cdot \det\left(A_p^{(p)^{-1}} - B_p^{(p)}\right) \cdot \det U_{p-1} \; , \end{aligned} \tag{C-3}$$

whereas the determinant of V_p is

$$\begin{aligned} \det V_p &= \det\left(I - B_p^{(p)} A_p^{(p)}\right) \cdot \det V_{p-1} \\ &= \det\left(A_p^{(p)^{-1}} - B_p^{(p)}\right) \cdot \det A_p^{(p)} \cdot \det V_{p-1} . \end{aligned} \tag{C-4}$$

Now if det U_{p-1} = det V_{p-1}, then (C-3) and (C-4) indicate that

$$\det U_p = \det V_p \,. \tag{C-5}$$

But since $U_o = V_o = R_o$, det U_o = det V_o. Therefore (C-5) holds for $p \geq 0$, by induction.

Appendix D

HERMITIAN PROPERTY OF EXTRAPOLATED CORRELATIONS

We know that

$$R_{-k}^{H} = R_k \quad \text{for} \quad |k| \le p. \tag{D-1}$$

We then solve

$$\sum_{n=1}^{p} A_n^{(p)} R_{k-n} = R_k \,, \quad 1 \le k \le p \tag{D-2}$$

for $\{A_n^{(p)}\}_1^p$, and set

$$\hat{R}_k^{(p)} = \sum_{n=1}^{p} A_n^{(p)} \hat{R}_{k-n}^{(p)} \quad \text{for all } k \ge 1; \; \hat{R}_k^{(p)} = R_k \text{ for } |k| \le p. \tag{D-3}$$

We then define

$$\hat{R}_{-k}^{(p)} = \hat{R}_k^{(p)\,H} \quad \text{for} \quad p+1 \le k. \tag{D-4}$$

In a similar fashion for the backward case, we solve

$$\sum_{n=1}^{p} B_n^{(p)} R_{n-k} = R_{-k} \,, \quad 1 \le k \le p \tag{D-5}$$

for $\{B_n^{(p)}\}_1^p$, and set

$$\check{R}_{-k}^{(p)} = \sum_{n=1}^{p} B_n^{(p)} \check{R}_{n-k}^{(p)} \quad \text{for all } k \ge 1; \; \check{R}_{-k}^{(p)} = R_{-k} \text{ for } |k| \le p. \tag{D-6}$$

We then define

$$\check{R}_k^{(p)} = \check{R}_{-k}^{(p)\,H} \quad \text{for} \quad p+1 \le k. \tag{D-7}$$

We know from the definitions above that

$$\check{R}^{(p)H}_{-k} = \hat{R}^{(p)}_{k} \quad \text{for} \quad |k| \le p. \tag{D-8}$$

Now we assume that

$$\check{R}^{(p)H}_{-k} = \hat{R}^{(p)}_{k} \quad \text{for} \quad |k| \le m, \text{ where } m \ge p; \tag{D-9}$$

that is, from (D-6) and (D-3),

$$\check{R}^{(p)H}_{-k} = \sum_{n=1}^{p} \check{R}^{(p)H}_{n-k} B^{(p)H}_{n} = \sum_{n=1}^{p} A^{(p)}_{n} \hat{R}^{(p)}_{k-n} = \hat{R}^{(p)}_{k} \quad \text{for} \quad 1 \le k \le m. \tag{D-10}$$

Now from recursion definition (D-6),

$$\begin{aligned}
\check{R}^{(p)H}_{-m-1} &= \sum_{n=1}^{p} \check{R}^{(p)H}_{n-m-1} B^{(p)H}_{n} \\
&= \sum_{n=1}^{p} \hat{R}^{(p)}_{m+1-n} B^{(p)H}_{n} && \text{(by (D-9))} \\
&= \sum_{n=1}^{p} \sum_{j=1}^{p} A^{(p)}_{j} \hat{R}^{(p)}_{m+1-n-j} B^{(p)H}_{n} && \text{(by (D-3))} \\
&= \sum_{j=1}^{p} A^{(p)}_{j} \sum_{n=1}^{p} \check{R}^{(p)}_{n-(m+1-j)} B^{(p)H}_{n} && \text{(by (D-9))} \\
&= \sum_{j=1}^{p} A^{(p)}_{j} \hat{R}^{(p)}_{m+1-j} && \text{(by (D-10))} \\
&= \hat{R}^{(p)}_{m+1} && \text{(by (D-3))}.
\end{aligned} \tag{D-11}$$

Therefore we have extended (D-9) by one step, and the proof follows for all $k \ge p+1$ by induction.

Appendix E

RELATIONSHIP OF DETERMINANTS

The forward correlation recursion is given in (52) as

$$\hat{R}_m^{(p)} = \sum_{n=1}^{p} A_n^{(p)} \hat{R}_{m-n}^{(p)} \quad , \; p+1 \le m. \tag{E-1}$$

The z-transform of this sequence is

$$\hat{\mathcal{R}}(z) \equiv \sum_{m=p+1}^{\infty} z^{-m} \hat{R}_m^{(p)} = \sum_{n=1}^{p} z^{-n} A_n^{(p)} \sum_{m=p+1}^{\infty} z^{-(m-n)} \hat{R}_{m-n}^{(p)} \; . \tag{E-2}$$

The inner sum on m can be expressed as (see (53))

$$\sum_{m=p+1}^{p+n} z^{-(m-n)} R_{m-n} + \sum_{m=p+1+n}^{\infty} z^{-(m-n)} \hat{R}_{m-n}^{(p)} \equiv \mathcal{R}_n(z) + \hat{\mathcal{R}}(z). \tag{E-3}$$

Therefore,

$$\hat{\mathcal{R}}(z) = \sum_{n=1}^{p} z^{-n} A_n^{(p)} \mathcal{R}_n(z) + \sum_{n=1}^{p} z^{-n} A_n^{(p)} \hat{\mathcal{R}}(z) \tag{E-4}$$

or

$$\hat{\mathcal{R}}(z) = \left(I - \sum_{n=1}^{p} z^{-n} A_n^{(p)} \right)^{-1} \sum_{n=1}^{p} z^{-n} A_n^{(p)} \mathcal{R}_n(z) \, . \tag{E-5}$$

At the same time, we define the z-transform of the backward correlation recursion as

$$\check{\mathcal{R}}(z) \equiv \sum_{m=p+1}^{\infty} z^{-m} \check{R}_{-m}^{(p)} \tag{E-6}$$

and note that, via (62),

$$\check{\mathcal{R}}^{H}(z) = \sum_{m=p+1}^{\infty} z^{-m} \check{R}_{-m}^{(p)^H} = \sum_{m=p+1}^{\infty} z^{-m} \hat{R}_m^{(p)} = \hat{\mathcal{R}}(z) \, . \tag{E-7}$$

A comment on notation is timely here. If matrix

$$G(z) \equiv \sum_n z^{-n} D_n \quad , \tag{E-8}$$

where z is a complex scalar variable, then

$$G^H(z) \equiv \sum_n z^{-n} D_n^H \quad . \tag{E-9}$$

But

$$G(z)^H = \sum_n (z^*)^{-n} D_n^H \quad , \tag{E-10}$$

which is not always equal to (E-9), unless z is real.

But let us also develop definition (E-7) by means of backward recursion (55), in a manner similar to that above in (E-1) through (E-5). We find

$$\overset{\vee}{R}^H(z) = \sum_{m=p+1}^{\infty} z^{-m} \overset{\vee}{R}^{(p)H}_{-m} = \sum_{m=p+1}^{\infty} z^{-m} \sum_{n=1}^{p} \overset{\vee}{R}^{(p)H}_{n-m} B_n^{(p)H} \quad \text{(by (55))}$$

$$= \sum_{n=1}^{p} z^{-n} \left(\sum_{m=p+1}^{\infty} z^{-(m-n)} \overset{\vee}{R}^{(p)H}_{n-m} \right) B_n^{(p)H} \quad . \tag{E-11}$$

The inner sum on m is

$$\sum_{m=p+1}^{p+n} z^{-(m-n)} R^H_{n-m} + \sum_{m=p+1+n}^{\infty} z^{-(m-n)} \overset{\vee}{R}^{(p)H}_{n-m} = R_n(z) + \overset{\vee}{R}^H(z), \tag{E-12}$$

where we used (56), (2), (E-3), and (E-11). Therefore

$$\overset{\vee}{R}^H(z) = \sum_{n=1}^{p} z^{-n} R_n(z) B_n^{(p)H} + \overset{\vee}{R}^H(z) \sum_{n=1}^{p} z^{-n} B_n^{(p)H} \tag{E-13}$$

or

$$\overset{\vee}{R}^H(z) = \sum_{n=1}^{p} z^{-n} R_n(z) B_n^{(p)H} \left(I - \sum_{n=1}^{p} z^{-n} B_n^{(p)H} \right)^{-1} \quad . \tag{E-14}$$

Combining (E-5) and (E-14) according to (E-7), we see that

$$\det\left(I-\sum_{n=1}^{p} z^{-n} A_n^{(p)}\right) \quad \text{and} \quad \det\left(I-\sum_{n=1}^{p} z^{-n} B_n^{(p)H}\right) \tag{E-15}$$

must have the same zeros, since these two quantities determine the singularity locations of (E-5) and (E-14). The quantity $R_n(z)$ defined in (E-3) is singular only at $z = 0$.

Furthermore

$$\det\left(I-\sum_{n=1}^{p} z^{-n} A_n^{(p)}\right) = z^{-Mp}\det\left(z^{p} I - z^{p-1} A_1^{(p)} - \cdots - A_p^{(p)}\right) = \frac{\prod_{j=1}^{Mp}(z-z_j)}{z^{Mp}} \tag{E-16}$$

and

$$\det\left(I-\sum_{n=1}^{p} z^{-n} B_n^{(p)H}\right) = z^{-Mp}\det\left(z^{p} I - z^{p-1} B_1^{(p)H} - \cdots - B_p^{(p)H}\right) = \frac{\prod_{j=1}^{Mp}(z-z_j)}{z^{Mp}}, \tag{E-17}$$

where we have utilized tne observations that the quantities in (E-15) have the same zeros, the same pole at z=0, and the same scale factor. Therefore the two determinants in (E-15) are equal.

Also since

$$\det\left(I-\sum_{n=1}^{p} z^{-n} G_n\right) = 1 - z^{-1}\operatorname{tr} G_1 - \cdots + (-1)^{M} z^{-Mp}\det G_p, \tag{E-18}$$

it follows that

$$\operatorname{tr} A_1^{(p)} = \operatorname{tr} B_1^{(p)H} = \left(\operatorname{tr} B_1^{(p)}\right)^{*} \tag{E-19}$$

and

$$\det A_p^{(p)} = \det B_p^{(p)H} = \left(\det B_p^{(p)}\right)^{*}. \tag{E-20}$$

Numerical examples show that generally

$$\left|\operatorname{tr} A_k^{(p)}\right| \neq \left|\operatorname{tr} B_k^{(p)}\right| \quad \text{for} \quad 1 < k \leq p \tag{E-21}$$

and

$$\left|\det A_k^{(p)}\right| \neq \left|\det B_k^{(p)}\right| \quad \text{for} \quad k < p. \tag{E-22}$$

Appendix F

SPECTRUM FROM EXTRAPOLATED CORRELATIONS

The forward correlation recursion is given by

$$\hat{R}_m^{(p)} = \sum_{n=1}^{p} A_n^{(p)} \hat{R}_{m-n}^{(p)} \quad , \quad m \geq p+1 \; , \tag{F-1}$$

where

$$\hat{R}_m^{(p)} = R_m \quad , \quad |m| \leq p \tag{F-2}$$

and

$$\hat{R}_{-m}^{(p)} = \hat{R}_m^{(p)^H} \quad , \; m \geq p+1 . \tag{F-3}$$

We wish to evaluate the z-transform of $\{\Delta \hat{R}_m^{(p)}\}$:

$$\mathcal{G}^{(p)}(z) \equiv \Delta \sum_{m=-\infty}^{\infty} z^{-m} \hat{R}_m^{(p)} \; . \tag{F-4}$$

In order to do so, consider a fictitious process $\{\hat{X}_n\}$ with the correlation given by (F-1) through (F-3). Consider the output of the optimum predictive error filter, given by

$$\hat{Y}_k \equiv - \sum_{n=0}^{p} A_n^{(p)} \hat{X}_{k-n} \; , \; \text{all} \; k. \tag{F-5}$$

The crosscorrelation

$$\hat{C}_m = \overline{\hat{Y}_k \hat{X}_{k-m}^H} = - \sum_{n=0}^{p} A_n^{(p)} \overline{\hat{X}_{k-n} \hat{X}_{k-m}^H} = - \sum_{n=0}^{p} A_n^{(p)} \hat{R}_{m-n}^{(p)} \; , \; \text{all} \; m. \tag{F-6}$$

Using (7) and (F-1), we see that

$$\hat{C}_m = 0 \quad \text{for} \quad m \geq 1 \qquad \left(\hat{C}_m \neq 0 \quad \text{for} \quad m \leq 0\right) ; \tag{F-7}$$

that is, predictive error filter output $\hat{Y}_k$ is uncorrelated with all past values of input $\hat{X}_k$.

Also, output autocorrelation

$$\hat{D}_m \equiv \overline{\hat{Y}_k \hat{Y}_{k-m}^H} = -\sum_{n=0}^{P} \overline{\hat{Y}_k \hat{X}_{k-m-n}^H} A_n^{(p)H} = -\sum_{n=0}^{P} \hat{C}_{m+n} A_n^{(p)H}, \qquad \text{(F-8)}$$

using (F-5) and (F-6). But now employment of (F-7) in (F-8) shows that

$$\hat{D}_m = 0 \quad \text{for} \quad m \geq 1. \qquad \text{(F-9)}$$

Also (F-7), (F-6), (F-2), and (12) yield

$$\hat{D}_0 = \hat{C}_0 = -\sum_{n=0}^{P} A_n^{(p)} \hat{R}_{-n}^{(p)} = -\sum_{n=0}^{P} A_n^{(p)} R_{-n} = U_p. \qquad \text{(F-10)}$$

And since, from definition (F-8),

$$\hat{D}_{-m} = \hat{D}_m^H, \qquad \text{(F-11)}$$

we have

$$\hat{D}_m = \begin{cases} U_p, & m = 0 \\ 0, & \text{otherwise} \end{cases}; \qquad \text{(F-12)}$$

that is, predictive error filter output $\hat{Y}_k$ is white for input $\hat{X}_k$. (Of course, U_p is not diagonal).

At the same time, autocorrelation $\hat{D}_m$ can be expressed (by means of (F-5)) as

$$\hat{D}_m = \sum_{n=0}^{P} \sum_{j=0}^{P} A_n^{(p)} \overline{\hat{X}_{k-n} \hat{X}_{k-m-j}^H} A_j^{(p)H} = \sum_{n=0}^{P} \sum_{j=0}^{P} A_n^{(p)} \hat{R}_{m+j-n}^{(p)} A_j^{(p)H}, \text{ all } m. \qquad \text{(F-13)}$$

Therefore the z-transform of $\{\Delta \hat{D}_m\}$ is

$$\Delta \sum_{m=-\infty}^{\infty} z^{-m} \hat{D}_m = \sum_{n=0}^{P} z^{-n} A_n^{(p)} \Delta \sum_{m=-\infty}^{\infty} z^{-(m+j-n)} \hat{R}_{m+j-n}^{(p)} \sum_{j=0}^{P} z^{j} A_j^{(p)H}$$

$$= \mathcal{A}_A^{(p)}(z)\, \mathcal{G}^{(p)}(z)\, \mathcal{A}_A^{(p)H}(z^{-1}), \tag{F-14}$$

where we have used (F-13), (23), (F-4), and (E-9). When we couple (F-14) with (F-12), we obtain

$$\Delta U_p = \mathcal{A}_A^{(p)}(z)\, \mathcal{G}^{(p)}(z)\, \mathcal{A}_A^{(p)H}(z^{-1}) \tag{F-15}$$

or

$$\mathcal{G}^{(p)}(z) = \Delta \left[\mathcal{A}_A^{(p)}(z)\right]^{-1} U_p \left[\mathcal{A}_A^{(p)H}(z^{-1})\right]^{-1}, \tag{F-16}$$

where matrix U_p is independent of z. This is one of the main results of this appendix.

If we let (for f real)

$$z = \exp(i2\pi f\Delta), \quad |f| < \frac{1}{2\Delta}, \tag{F-17}$$

and denote the forward predictive error filter transfer function and spectral estimate as

$$\mathcal{A}_A^{(p)}\left(\exp(i2\pi f\Delta)\right) = -\sum_{n=0}^{P} \exp(-i2\pi f n\Delta) A_n^{(p)} = H_A^{(p)}(f),$$
$$\mathcal{G}^{(p)}\left(\exp(i2\pi f\Delta)\right) = \Delta \sum_{m=-\infty}^{\infty} \exp(-i2\pi f m\Delta) \hat{R}_m^{(p)} = G^{(p)}(f), \tag{F-18}$$

respectively, then the spectrum of process $\{\hat{X}_n\}$ can be expressed as

$$G^{(p)}(f) = \Delta\, H_A^{(p)}(f)^{-1}\, U_p\, H_A^{(p)}(f)^{-1^H}, \tag{F-19}$$

where we have utilized the result that (see (E-8)) through (E-10))

$$\left[\mathcal{A}_A^{(p)H}\left(\exp(-i2\pi f\Delta)\right)\right]^{-1} = \left[\mathcal{A}_A^{(p)}\left(\exp(i2\pi f\Delta)\right)^H\right]^{-1} = H_A^{(p)}(f)^{H^{-1}} = H_A^{(p)}(f)^{-1^H}. \tag{F-20}$$

The procedure for the backward correlation recursion parallels that above to yield (using (23))

$$\mathcal{G}^{(p)}(z) = \Delta \left[\mathcal{A}_B^{(p)}(z)\right]^{-1} V_p \left[\mathcal{A}_B^{(p)H}(z^{-1})\right]^{-1} \tag{F-21}$$

and

$$G^{(p)}(f) = \Delta\ H_B^{(p)}(f)^{-1} V_p\ H_B^{(p)}(f)^{-1H} . \tag{F-22}$$

ZERO LOCATIONS OF $\mathcal{A}_A^{(p)}(z)^{-1}$

Assume that $\mathcal{A}_A^{(p)}(z)^{-1} \equiv Q(z)$ has a zero at $z=z_1 \neq 0$; that is,

$$\text{assume}\quad Q(z_1) = 0,\ \text{the zero matrix}, \tag{F-23}$$

where $0 < |z_1|$. But

$$\mathcal{A}_A^{(p)}(z) = -\sum_{n=0}^{p} z^{-n} A_n^{(p)} = -z^{-p}\left[A_p^{(p)} + z A_{p-1}^{(p)} + \cdots + z^{p-1} A_1^{(p)} - z^p I\right]. \tag{F-24}$$

Therefore $\mathcal{A}_A^{(p)}(z_1)$ is finite for $0<|z_1|$, yielding

$$Q(z_1)\,\mathcal{A}_A^{(p)}(z_1) = 0 \neq I. \tag{F-25}$$

Therefore assumption (F-23) is invalid, indicating that

$$Q(z) \neq 0 \quad \text{for} \quad 0 < |z| . \tag{F-26}$$

Now from (F-24)

$$\mathcal{A}_A^{(p)}(z) \sim -z^{-p} A_p^{(p)} \quad \text{as} \quad |z| \to 0; \tag{F-27}$$

therefore,

$$Q(z) \sim -z^p A_p^{(p)^{-1}} \quad \text{as} \quad |z| \to 0. \tag{F-28}$$

Thus Q(z) has a p-th order zero at z=0, but is not equal to the zero matrix for $0 < |z|$. Of course, the individual elements of matrix Q(z) can have zeros anywhere.

POLE LOCATIONS OF $\mathcal{H}_A^{(p)}(z)^{-1}$

Since from (F-24)

$$\mathcal{H}_A^{(p)}(z) = -z^{-p} Q_p(z), \tag{F-29}$$

where $Q_p(z)$ is a matrix of polynomials in z of order p, it follows that

$$Q(z) = -z^p Q_p(z)^{-1} = -\frac{z^p}{\det Q_p(z)} \hat{Q}_{(M-1)p}(z), \tag{F-30}$$

where $\hat{Q}_{(M-1)p}(z)$ is a matrix of polynomials in z of order (M-1)p. Therefore the poles of Q(z) are caused by the zeros of det $Q_p(z)$; that is, the poles of $\mathcal{H}_A^{(p)}(z)^{-1}$ are caused by the zeros of det $\mathcal{H}_A^{(p)}(z)$. As $|z| \to \infty$, $\mathcal{H}_A^{(p)}(z) \sim I$ from (F-24); therefore, $Q(z) \sim I$ as $|z| \to \infty$, so that Q(z) has no poles at $|z| = \infty$. Thus the poles of Q(z) are located where det $\mathcal{H}_A^{(p)}(z) = 0$.

We now consider the problem of determining when det $\mathcal{H}_A^{(p)}(z) = 0$; the following derivation is based upon Ref. 7. Let

$$\mathcal{Y}_K = \begin{bmatrix} X_K \\ \vdots \\ X_{K-p+1} \end{bmatrix} \tag{F-31}$$

be an Mpx1 matrix. Define prediction

$$\hat{\mathcal{Y}}_K = C \mathcal{Y}_{K-1}, \tag{F-32}$$

where C is MpxMp. And define error

$$\delta_k = \varphi_k - \hat{\varphi}_k = \varphi_k - C\varphi_{k-1} . \tag{F-33}$$

Then

$$\begin{aligned}\overline{\delta_k \delta_k^H} &= \overline{(\varphi_k - C\varphi_{k-1})(\varphi_k^H - \varphi_{k-1}^H C^H)} \\ &= \mathcal{U}_0 - C\mathcal{U}_{-1} - \mathcal{U}_1 C^H + C\mathcal{U}_0 C^H \\ &= \mathcal{U}_0 - \mathcal{U}_1\mathcal{U}_0^{-1}\mathcal{U}_1^H + (C - \mathcal{U}_1\mathcal{U}_0^{-1})\mathcal{U}_0(C - \mathcal{U}_1\mathcal{U}_0^{-1})^H\end{aligned} \tag{F-34}$$

where

$$\mathcal{U}_m \equiv \overline{\varphi_k \varphi_{k-m}^H} . \tag{F-35}$$

The minimum value of $\mathrm{tr}\ \overline{\delta_k \delta_k^H}$ is realized when (see appendix B) we select

$$C = \mathcal{U}_1\mathcal{U}_0^{-1} . \tag{F-36}$$

The corresponding value of

$$\overline{\delta_k \delta_k^H} = \mathcal{U}_0 - \mathcal{U}_1\mathcal{U}_0^{-1}\mathcal{U}_1^H = \mathcal{U}_0 - C\mathcal{U}_0 C^H , \tag{F-37}$$

since $\mathcal{U}_0^H = \mathcal{U}_0$. Now let the left eigenvectors and eigenvalues of the optimum C be denoted as

$$\xi_m^H C = \lambda_m \xi_m^H , \quad 1 \le m \le Mp . \tag{F-38}$$

(The eigenvectors $\{\xi_m\}$ may not all be linearly independent). Then

$$\begin{aligned}0 \le \overline{|\xi_m^H \delta_k|^2} &= \xi_m^H \overline{\delta_k \delta_k^H} \xi_m = \xi_m^H (\mathcal{U}_0 - C\mathcal{U}_0 C^H)\xi_m \\ &= \xi_m^H \mathcal{U}_0 \xi_m (1 - |\lambda_m|^2) .\end{aligned} \tag{F-39}$$

Now $\mathcal{U}_0$ is Hermitian, block Toeplitz, non-negative definite, and has the form

$$\mathcal{U}_0 = \overline{\mathcal{S}_K \mathcal{S}_K^H} = \begin{bmatrix} R_0 & R_1 & \cdots & R_{p-1} \\ R_{-1} & \ddots & & \\ \vdots & & & \\ R_{1-p} & & & R_0 \end{bmatrix}. \tag{F-40}$$

Therefore $|\lambda_m| \le 1$ for $1 \le m \le Mp$; that is, all the eigenvalues of C are bounded by unity in magnitude. Furthermore, Ref. 7, p. 134, shows that if there is no exact linear relation between the elements of $X_k, X_{k-1}, \ldots, X_{k-p}$, then $|\lambda_m| < 1$ for $1 \le m \le Mp$ (see also appendix B).

Now we develop the error in (F-33) in more detail:

$$\mathcal{S}_k = \mathcal{S}_k - C\mathcal{S}_{k-1} = \begin{bmatrix} X_k \\ \vdots \\ X_{k-p+1} \end{bmatrix} - \begin{bmatrix} C_{11} & \cdots & C_{1p} \\ \vdots & & \\ C_{p1} & \cdots & C_{pp} \end{bmatrix} \begin{bmatrix} X_{k-1} \\ \vdots \\ X_{k-p} \end{bmatrix}$$

$$= \begin{bmatrix} X_k - \sum_{m=1}^{p} C_{1m} X_{k-m} \\ \vdots \\ X_{k-p+1} - \sum_{m=1}^{p} C_{pm} X_{k-m} \end{bmatrix}. \tag{F-41}$$

Minimizing $\operatorname{tr} \overline{\mathcal{S}_k \mathcal{S}_k^H}$ can be seen to make C of the form

$$C = \begin{bmatrix} A_1^{(p)} & A_2^{(p)} & \cdots & A_p^{(p)} \\ I & 0 & & 0 \\ 0 & I & 0 & \\ \vdots & & \ddots & \ddots \\ 0 & & I & 0 \end{bmatrix}. \tag{F-42}$$

Therefore (Ref. 7, eqs. (35) and (36)),

$$\det(C - \lambda I) = (-\lambda)^{Mp} \det \mathcal{A}_A^{(p)}(\lambda). \tag{F-43}$$

If we were to assume that $\det \mathcal{N}_A^{(p)}(z_i)=0$, where $|z_i| \geq 1$, we would have $\det(C-z_iI)=0$. But this contradicts $|\lambda_m|<1$ for $1 \leq m \leq M_p$. Therefore, the zeros of $\det \mathcal{N}_A^{(p)}(z)$ all lie inside the unit circle; that is, the poles of Q(z) all lie inside the unit circle.

Appendix G

HERMITIAN PROPERTY OF ONE-STEP EXTRAPOLATED CORRELATION MATRIX ESTIMATES

From (78), at the (p-1)th stage, we know that

$$R_{-m}^{H} = \sum_{n=1}^{p-1} R_{n-m}^{H} B_n^{(p-1)H} = \sum_{n=1}^{p-1} R_{m-n} B_n^{(p-1)H} = \sum_{n=1}^{p-1} A_n^{(p-1)} R_{m-n} = R_m \,, \quad 1 \le m \le p-1. \tag{G-1}$$

Now we start with (94) and express

$$\begin{aligned} R_{-p}^{(p-1)H} &= \sum_{n=1}^{p-1} R_{n-p}^{H} B_n^{(p-1)H} = \sum_{n=1}^{p-1} R_{p-n} B_n^{(p-1)H} \\ &= \sum_{n=1}^{p-1} \sum_{j=1}^{p-1} A_j^{(p-1)} R_{p-n-j} B_n^{(p-1)H} && \text{(by (G-1))} \\ &= \sum_{j=1}^{p-1} A_j^{(p-1)} \sum_{n=1}^{p-1} R_{p-n-j} B_n^{(p-1)H} \\ &= \sum_{j=1}^{p-1} A_j^{(p-1)} R_{p-j} && \text{(by (G-1))} \\ &= R_p^{(p-1)} && \text{(by (98))}. \end{aligned} \tag{G-2}$$

Thus, the one-step extrapolated correlation matrix estimates, based on order p-1, are Hermitians of each other.

Appendix H

INTERRELATIONSHIPS OF U_p AND V_p FOR UNKNOWN CORRELATION CASE

We develop the definition (95) as follows:

$$
\begin{aligned}
U_p &= -\sum_{n=0}^{p} A_n^{(p)} R_{n} = R_0 - \sum_{n=1}^{p-1} A_n^{(p)} R_{-n} - A_p^{(p)} R_{-p} \\
&= R_0 - \sum_{n=1}^{p-1} \left(A_n^{(p-1)} - A_p^{(p)} B_{p-n}^{(p-1)} \right) R_{-n} - A_p^{(p)} \sum_{n=1}^{p} B_n^{(p)} R_{n-p} \quad \text{(by (79A) and (80B))} \\
&= -\sum_{n=0}^{p-1} A_n^{(p-1)} R_{-n} + A_p^{(p)} \sum_{n=1}^{p-1} B_{p-n}^{(p-1)} R_{-n} \\
&\quad - A_p^{(p)} \left[\sum_{n=1}^{p-1} \left(B_n^{(p-1)} - B_p^{(p)} A_{p-n}^{(p-1)} \right) R_{n-p} + B_p^{(p)} R_0 \right] \quad \text{(by (79B))}.
\end{aligned}
\tag{H-1}
$$

Now

$$
\sum_{n=1}^{p-1} B_n^{(p-1)} R_{n-p} = \sum_{j=1}^{p-1} B_{p-j}^{(p-1)} R_{-j} \, . \tag{H-2}
$$

Therefore

$$
\begin{aligned}
U_p &= U_{p-1} + A_p^{(p)} B_p^{(p)} \left[\sum_{n=1}^{p-1} A_{p-n}^{(p-1)} R_{n-p} - R_0 \right] \quad \text{(by (95))} \\
&= U_{p-1} + A_p^{(p)} B_p^{(p)} \sum_{n=1}^{p} A_{p-n}^{(p-1)} R_{n-p} \\
&= U_{p-1} - A_p^{(p)} B_p^{(p)} U_{p-1} \quad \text{(by (95))} \\
&= \left(I - A_p^{(p)} B_p^{(p)} \right) U_{p-1} \, .
\end{aligned}
\tag{H-3}
$$

In a similar manner, we can show that

$$
V_p = \left(I - B_p^{(p)} A_p^{(p)} \right) V_{p-1} \, . \tag{H-4}
$$

In order to show that U_p is Hermitian, we recall the constraint (98) and express

$$U_p = U_{p-1} - A_p^{(p)} B_p^{(p)} U_{p-1} = U_{p-1} - A_p^{(p)} V_{p-1}^H A_p^{(p)H} . \qquad \text{(H-5)}$$

Therefore if $U_{p-1}^H = U_{p-1}$ and $V_{p-1}^H = V_p$, it immediately follows that

$$U_p^H = U_p . \qquad \text{(H-6)}$$

Similarly since

$$V_p = V_{p-1} - B_p^{(p)} A_p^{(p)} V_{p-1} = V_{p-1} - B_p^{(p)} U_{p-1}^H B_p^{(p)H} ,$$

it also immediately follows that

$$V_p^H = V_p . \qquad \text{(H-7)}$$

But properties (H-6) and (H-7) are obviously true for p = 0, because

$$U_0 = V_0 = R_0 = R_0^H . \qquad \text{(H-8)}$$

Therefore (H-6) and (H-7) are true for all p, by induction.

In order to relate the determinants of U_p and V_p, we express (H-3) and (H-4) as

$$U_p = A_p^{(p)} (A_p^{(p)-1} - B_p^{(p)}) U_{p-1} , \quad V_p = (A_p^{(p)-1} - B_p^{(p)}) A_p^{(p)} V_{p-1} . \qquad \text{(H-9)}$$

Therefore if $\det U_{p-1} = \det V_{p-1}$, then

$$\det U_p = \det V_p . \qquad \text{(H-10)}$$

But (H-10) is obviously true for p=0 by (H-8). Therefore (H-10) is true for all p, by induction.

Properites (H-6), (H-7), and (H-10) applied to (98) immediately show that

$$\det B_p^{(p)} = (\det A_p^{(p)})^* . \qquad \text{(H-11)}$$

Appendix I

MINIMIZATION OF TRACE OF WEIGHTED ERROR MATRICES

We wish to minimize the trace of (123) by choice of matrix G_p. We use the fact that, for square matrices P and Q,

$$tr(PQ) = \sum_{m,n} P_{mn} Q_{nm} = \sum_{m,n} Q_{nm} P_{mn} = tr(QP), \qquad (I\text{-}1)$$

to express

$$tr\left(\Lambda_{p-1} E_p + \Gamma_{p-1} F_p\right) = tr\Big[\Lambda_{p-1} S_{p-1}^{(yy)} + \Gamma_{p-1} S_{p-1}^{(aa)} - G_p V_{p-1}^{-1} S_{p-1}^{(ya)H} \Lambda_{p-1} - \Gamma_{p-1} S_{p-1}^{(ya)H} U_{p-1}^{-1} G_p$$
$$+ \left(\Lambda_{p-1} G_p V_{p-1}^{-1} S_{p-1}^{(aa)} V_{p-1}^{-1} + U_{p-1}^{-1} S_{p-1}^{(yy)} U_{p-1}^{-1} G_p \Gamma_{p-1} - \Lambda_{p-1} S_{p-1}^{(ya)} V_{p-1}^{-1} - U_{p-1}^{-1} S_{p-1}^{(ya)} \Gamma_{p-1}\right) G_p^H\Big]. \qquad (I\text{-}2)$$

Now (I-2) is an analytic function of the variables $Re(G_{mn})$ and $Im(G_{mn})$. Therefore the minimum of (I-2) is realized simply by setting the coefficient of G_p^H equal to zero (Ref. 20). We obtain, after premultiplying by Λ_{p-1}^{-1} and post-multiplying by Γ_{p-1}^{-1}, the equation for G_p:

$$G_p V_{p-1}^{-1} S_{p-1}^{(aa)} V_{p-1}^{-1} \Gamma_{p-1}^{-1} + \Lambda_{p-1}^{-1} U_{p-1}^{-1} S_{p-1}^{(yy)} U_{p-1}^{-1} G_p = S_{p-1}^{(ya)} V_{p-1}^{-1} \Gamma_{p-1}^{-1} + \Lambda_{p-1}^{-1} U_{p-1}^{-1} S_{p-1}^{(ya)}. \qquad (I\text{-}3)$$

(G_p is not Hermitian or Toeplitz, as numerical examples will show.) In terms of $A_p^{(p)}$ and $B_p^{(p)}$, we have the simultaneous equations

$$A_p^{(p)} S_{p-1}^{(aa)} V_{p-1}^{-1} \Gamma_{p-1}^{-1} + \Lambda_{p-1}^{-1} U_{p-1}^{-1} S_{p-1}^{(ya)} B_p^{(p)H} = S_{p-1}^{(ya)} V_{p-1}^{-1} \Gamma_{p-1}^{-1} + \Lambda_{p-1}^{-1} U_{p-1}^{-1} S_{p-1}^{(ya)} \qquad (I\text{-}4)$$

$$A_p^{(p)} V_{p-1} - U_{p-1} B_p^{(p)H} = 0$$

where we utilized (122).

Appendix J

COMPUTATION OF FILTER TRANSFER FUNCTION

The forward predictive error filter transfer function is given in (68) as

$$H_A^{(p)}(f) = -\sum_{n=0}^{p} \exp(-i\,2\pi f n\Delta)\, A_n^{(p)} \quad , \quad |f| < \frac{1}{2\Delta} \,. \tag{J-1}$$

Now divide the frequency range $(-\frac{1}{2\Delta}, \frac{1}{2\Delta})$ into N_F cells of width

$$\Delta_f = \frac{1}{N_F}\,\frac{1}{\Delta} \,. \tag{J-2}$$

Then for $|m| \le N_F/2$,

$$\begin{aligned} H_A^{(p)}(m\,\Delta_f) = H_A^{(p)}\left(\frac{m}{N_F\Delta}\right) &= -\sum_{n=0}^{p} \exp(-i\,2\pi mn/N_F)\, A_n^{(p)} \\ &= \sum_{n=0}^{N_F-1} \exp(-i\,2\pi mn/N_F)\, Z_n \,, \end{aligned} \tag{J-3}$$

where

$$Z_n = \left\{ \begin{array}{l} -A_n^{(p)} \,, \; 0 \le n \le p \\ 0, \; p+1 \le n \le N_F-1 \end{array} \right\} \,. \tag{J-4}$$

Now if we let the sum in (J-3) be denoted as an N_F-pcint FFT,

$$\sum_{n=0}^{N_F-1} \exp(-i\,2\pi mn/N_F) Z_n = \tilde{Z}_m \,, \quad 0 \le m \le N_F-1, \tag{J-5}$$

then (J-3) becomes

$$H_A^{(p)}\left(\frac{m}{N_F\Delta}\right) = \left\{ \begin{array}{l} \tilde{Z}_m \,, \; 0 \le m \le N_F/2 \\ \tilde{Z}_{N_F+m} \,, \; -N_F/2 \le m \le -1 \end{array} \right\} \,. \tag{J-6}$$

Then quantity $\tilde{Z}_m$ in (J-5) is an MxM matrix for each value of m.

Appendix K

PROGRAM FOR SPECTRAL ANALYSIS

In this appendix we present the program for the procedure summarized in (184) - (187) and (165). The spectral estimate, (165), is computed at frequencies $\{m/(N_F\Delta)\}$:

$$G^{(p)}\left(\frac{m}{N_F\Delta}\right) = \Delta\, H_A^{(p)}\left(\frac{m}{N_F\Delta}\right)^{-1} U_p \left[H_A^{(p)}\left(\frac{m}{N_F\Delta}\right)^{-1}\right]^H , \quad |m| \le N_F/2, \tag{K-1}$$

where the forward predictive error transfer function $H_A^{(p)}\left(\frac{m}{N_F\Delta}\right)$ is given by (J-6). The specific scaling adopted is based upon (166), which takes the sampled form

$$\sum_{m=-N_F/2}^{N_F/2} w_m \Delta_f G^{(p)}(m\Delta_f) \cong R_0 , \tag{K-2}$$

where $\{w_m\}$ is a set of integration weights (e.g., trapezoidal). The approximation is a good one if $G^{(p)}(f)$ is sampled finely enough; that is, if N_F is large enough to resolve the peaks and valleys of $G^{(p)}(f)$. If we employ (J-2), (K-2) becomes

$$\sum_{m=-N_F/2}^{N_F/2} w_m \frac{1}{N_F\Delta} G^{(p)}\left(\frac{m}{N_F\Delta}\right) \cong R_0 ; \tag{K-3A}$$

or, for trapezoidal weighting,

$$\sum_{m=-\frac{N_F}{2}+1}^{N_F/2} \frac{1}{N_F\Delta} G^{(p)}\left(\frac{m}{N_F\Delta}\right) \cong R_0 , \tag{K-3B}$$

where we have employed the periodic nature of $G^{(p)}(f)$ (See (165) and (68)).

Thus the sum of samples $\frac{1}{N_F\Delta} G^{(p)}\left(\frac{m}{N_F\Delta}\right)$ equals the sample power, (80).

For a real multivariate process, we can employ (171); a modified form emerges:

$$\mathrm{Re} \sum_{m=0}^{N_F/2} \tilde{w}_m \frac{2}{N_F\Delta} G^{(p)}\left(\frac{m}{N_F\Delta}\right) \cong R_0 \quad \text{for real process,} \tag{K-4}$$

where $\{\tilde{w}_m\}$ is another set of integration weights. This is the form programmed in the following; the quantities computed are

$$\frac{2}{N_F\Delta} G^{(p)}\left(\frac{m}{N_F\Delta}\right) = \frac{2}{N_F} H_A^{(p)}\left(\frac{m}{N_F\Delta}\right)^{-1} U_p \left[H_A^{(p)}\left(\frac{m}{N_F\Delta}\right)^{-1}\right]^H \quad \text{for } 0 \le m \le \frac{N_F}{2} . \tag{K-5}$$

The real part of their weighted sum equals the sample power, R_0. The FFT used here to evaluate (J-5) is given in Ref. 21; it is limited to powers of 2, but could be replaced if desired. Input parameters are N, PMAX, and NF in line 22, and the input data call is in line 37 and SUBROUTINE DATA; all these quantities have to be changed by the user to fit his particular application. The program is written for a real multivariate process (general M), with the exception of FUNCTION DETERM, SUBROUTINEs SDM, INVERT, and SOLVE, and the printout of the spectral density matrix, (K-5). Arrays used in the program are explained by comment statements. A sample printout follows the program.

```
C  MULTIVARIATE LINEAR PREDICTIVE SPECTRAL ANALYSIS-
C  EMPLOYING WEIGHTED FORWARD AND BACKWARD AVERAGING.
C  THIS PROGRAM IS WRITTEN FOR REAL PROCESSES AND GENERAL M, WITH THE
C  EXCEPTION OF FUNCTION DETERM AND SUBROUTINES SDM, INVERT, AND SOLVE,
C  AND THE PRINT OUT OF THE SPECTRAL DENSITY MATRIX.
C  USER: CHANGE LINES 22 AND 37, AND REPLACE SUBROUTINE DATA.
C  M = DIMENSIONALITY OF MULTIVARIATE PROCESS; INTEGER INPUT
C  N = NUMBER OF DATA POINTS IN EACH PROCESS; INTEGER INPUT
C  X(1,1)...X(N,1),...,X(1,M)...X(N,M) = INPUT DATA; ALTERED ON OUTPUT
C  PMAX = MAXIMUM ORDER OF FILTER; INTEGER INPUT
C  NF = SIZE OF FFT (MUST BE A POWER OF 2 TO USE MKLFFT); INTEGER INPUT
C  AVE = MEANS OF INPUT DATA; OUTPUT
C  R = COVARIANCE MATRIX OF INPUT DATA; OUTPUT
C  AIC = AKAIKE'S INFORMATION CRITERION; OUTPUT
C  PBEST = BEST ORDER OF FILTER; INTEGER OUTPUT
C  UBEST = MATRIX OF COEFFICIENTS IN SPECTRAL ESTIMATE; OUTPUT
C  AP = MATRIX OF FORWARD PARTIAL CORRELATION COEFFICIENTS; THEN =
C  MATRIX OF FORWARD PREDICTIVE FILTER COEFFICIENTS FOR PBEST; OUTPUT
C  BP = MATRIX OF BACKWARD PARTIAL CORRELATION COEFFICIENTS; OUTPUT
C  XX,YY = SPECTRAL MATRICES; OUTPUT
      PARAMETER M=2     @ BIVARIATE PROCESS
      PARAMETER N= 100 , PMAX= 10, NF=1024, NF41=NF/4+1
      INTEGER PBEST,P
      DIMENSION X(N,M),Y(N,M),Z(N,M),UBEST(M,M),AP(M,M,PMAX),
     $BP(M,M,PMAX),AVE(M),XX(NF,M,M),YY(NF,M,M),COSI(NF41),
     $U(M,M),V(M,M),UI(M,M),VI(M,M),A(M,M),B(M,M),R(M,M),
     $WA(M,M),WB(M,M),WC(M,M),WD(M,M),WE(M,M),AIC(PMAX),AICO(2)
      EQUIVALENCE (X,Y),(AIC(1),AICO(2))
C  PRINT OUT VALUES OF PARAMETERS
      I=N
      J=PMAX
      K=M
      L=NF
      PRINT 1, I,J,K,L
1     FORMAT(1H1,' N =',I6,10X,'PMAX =',I4,10X,'M =',I2,10X,'NF =',I5)
C  INPUT DATA IN X(1,1)...X(N,1),...,X(1,M)...X(N,M)
      CALL DATA
      PRINT 2
2     FORMAT(/' INPUT DATA:')
      J=N-99
      L=N-200
      DO 3 I=1,M
      PRINT 4, I
      IF(N.LE.200) GO TO 5
      PRINT 6, (X(K,I),K=1,100)
      PRINT 7, L
7     FORMAT (I6,' INPUT DATA POINTS NOT PRINTED HERE')
      PRINT 6, (X(K,I),K=J,N)
      GO TO 3
5     PRINT 6, (X(K,I),K=1,N)
3     CONTINUE
4     FORMAT('   PROCESS NUMBER',I2)
6     FORMAT(5E20.8)
C  EVALUATE PARTIAL CORRELATION COEFFICIENTS
      CALL PCC
      PRINT 8
```

```
8       FORMAT(/' MEANS OF INPUT DATA:')
        PRINT 6, (AVE(I),I=1,M)
        PRINT 9
9       FORMAT(/' COVARIANCE MATRIX OF INPUT DATA:')
        PRINT 6, ((R(I,J),I=1,M),J=1,M)
        PRINT 10
10      FORMAT(/' AKAIKE INFORMATION CRITERION:')
        PRINT 11, (P,AIC(P),P=0,PMAX)
11      FORMAT(I10,E20.8)
        PRINT 12, PBEST
12      FORMAT(/' PBEST =',I3)
        PRINT 13
13      FORMAT(/' UBEST:')
        PRINT 6, ((UBEST(I,J),I=1,M),J=1,M)
        PRINT 14
14      FORMAT(/' FORWARD PARTIAL CORRELATION COEFFICIENTS:')
        DO 15 P=1,PMAX
15      PRINT 16, P,((AP(I,J,P),I=1,M),J=1,M)
16      FORMAT(I10,6E20.8)
        PRINT 17
17      FORMAT(/' BACKWARD PARTIAL CORRELATION COEFFICIENTS:')
        DO 18 P=1,PMAX
18      PRINT 16, P,((BP(I,J,P),I=1,M),J=1,M)
        IF(PBEST.EQ.0) GO TO 19
C   EVALUATE PREDICTIVE FILTER COEFFICIENTS
        CALL PFC
        PRINT 20
20      FORMAT(/' FORWARD PREDICTIVE FILTER COEFFICIENTS FOR PBEST:')
        DO 21 P=1,PBEST
21      PRINT 16, P,((AP(I,J,P),I=1,M),J=1,M)
C   EVALUATE PREDICTIVE-ERROR FILTER TRANSFER FUNCTION
19      CALL PEFTF
C   EVALUATE SPECTRAL DENSITY MATRIX AND COHERENCE
        K=NF/2+1
        CALL SDM
        PRINT 22
22      FORMAT(/' SPECTRAL DENSITY MATRIX AND COHERENCE FOR M=2:')
        PRINT 23
23      FORMAT(8X,'BIN',10X,'AUTO11',14X,'AUTO22',10X,'REAL(CROSS12)',7X,'
       $IMAG(CROSS12)',9X,'MAG SQ COH',11X,'ARGUMENT')
        PRINT 16, (L,XX(L,1,1),XX(L,2,2),XX(L,1,2),YY(L,1,2),YY(L,1,1),YY(
       $L,2,2), L=1,K)
        SUBROUTINE DATA
C   THIS SUBROUTINE GENERATES DATA FOR M=2, BIVARIATE PROCESS
        DEFINE IRAND=I*5**15+((1-SIGN(1,I*5**15))/2)*34359738367
        DEFINE RAND=FLOAT(I)/34359738367.
        I=5281
        TA=0.
        TB=0.
        DO 1 K=1,100    @ WILL DISCARD THESE INITIAL POINTS
        I=IRAND
        T=.85*TA+.75*TB+RAND*.5
        I=IRAND
```

```
      TB=.65*TA+.55*TB+RAND-.5
1     TA=T
      X(1,1)=TA
      X(1,2)=TB
      DO 2 K=2,N
      I=IRAND
      T=.85*TA-.75*TB+RAND-.5
      I=IRAND
      TB=.65*TA+.55*TB+RAND-.5
      TA=T
      X(K,1)=TA
2     X(K,2)=TB
      RETURN
      SUBROUTINE PCC
C     THIS SUBROUTINE COMPUTES PBEST, UBEST, AND THE PARTIAL
C     CORRELATION COEFFICIENTS FOR P = 1 TO PMAX; ANY M
      I=N
      J=PMAX
      IA=3.*SQRT(N)/M
      IF(PMAX.GT.IA) PRINT 1, J,I,IA
1     FORMAT(/' PMAX =',I4,' IS TOO LARGE FOR NUMBER OF DATA POINTS N ='
     $,I5,';  SEARCH LIMITED TO P =',I4)
      IA=MIN(IA,PMAX)      @ UPPER BOUND ON PMAX; EQ 183
      FAC=2.*M*M/N         @ FAC=0.  WOULD FORCE PBEST EQUAL TO PMAX
C     SUBTRACT MEANS; FILL IN DATA ARRAYS; EQ 110
      DO 2 I=1,M
      TA=0.
      DO 3 K=1,N
3     TA=TA+Y(K,I)
      TA=TA/N
      AVE(I)=TA
      DO 2 K=1,N
      Y(K,I)=Y(K,I)-TA
2     Z(K,I)=Y(K,I)
C     INITIALIZE CORRELATION MATRICES; EQS 82, 114, AND 105
      CALL AUTO(2,N-1,Y,WC)
      DO 4 I=1,M
      DO 4 J=I,M
      TA=Y(1,I)*Y(1,J)
      TB=Y(N,I)*Y(N,J)
      R(I,J)=(WC(I,J)+TA+TB)/N
      WA(I,J)=WC(I,J)+TB
      WB(I,J)=WC(I,J)+TA
      R(J,I)=R(I,J)
      WA(J,I)=WA(I,J)
4     WB(J,I)=WB(I,J)
      CALL EQUAL(R,U)
      CALL EQUAL(R,V)
      CALL CROSS(2,N,Y,Y,WC)
C     BEGIN RECURSION
      AIC(0)=LOG(DETERM(U))
      AICMIN=AIC(0)
      PBEST=0
```

```
      CALL EQUAL(U,UBEST)
      DO 5 P=1,IA
C  EVALUATE MATRICES REQUIRED IN BILINEAR MATRIX EQUATION; EQ 126
      CALL INVERT(V,VI)
      CALL MULT(VI,WB,WD)
      CALL EQUAL(WD,WB)
      CALL INVERT(U,UI)
      CALL EQUAL(WA,WD)
      CALL MULT(WD,UI,WA)
      CALL ADD(WC,WC,WC)
C  SOLVE BILINEAR MATRIX EQUATION; EQS 157-161
      CALL SOLVE
C  EVALUATE PARTIAL CORRELATION COEFFICIENTS; EQ 124
      CALL MULT(WC,VI,A)
      CALL TRANS(WC,WD)
      CALL MULT(WD,UI,B)
      CALL EQUAL(A,AP(1,1,P))
      CALL EQUAL(B,BP(1,1,P))
C  UPDATE MATRICES U AND V; EQ 18₁
      CALL MULT(A,WD,WE)
      CALL SUB(U,WE,U)
      CALL MULT(B,WC,WE)
      CALL SUB(V,WE,V)
C  CALCULATE AKAIKE'S INFORMATION CRITERION; EQ 180
      AIC(P)=LOG(DETERM(U))+FAC*P
      IF(AIC(P).GE.AICMIN) GO TO 6
      AICMIN=AIC(P)
      PBEST=P
      CALL EQUAL(U,UBEST)
6     IF(P.EQ.IA) GO TO 5
C  UPDATE DATA SEQUENCES Y AND Z; EQ 111
      L=P+1
      DO 7 K=N,L,-1
      DO 8 I=1,M
      TA=Z(K-1,I)
      DO 9 J=1,M
9     TA=TA-B(I,J)*Y(K,J)
8     Z(K,I)=TA
      DO 10 I=1,M
      TA=Y(K,I)
      DO 11 J=1,M
11    TA=TA-A(I,J)*Z(K-1,J)
10    Y(K,I)=TA
7     CONTINUE
C  CALCULATE NEW CORRELATION MATRICES; EQ 114
      CALL AUTO(P+2,N,Y,WA)
      CALL AUTO(P+1,N-1,Z,WB)
      CALL CROSS(P+2,N,Y,Z,WC)
5     CONTINUE
      IF(M.EQ.1) RETURN
      K=M-1
      DO 12 I=1,K
      L=I+1
      DO 12 J=L,M
```

```
      UBEST(I,J)=.5*(UBEST(I,J)+UBEST(J,I))
12    UBEST(J,I)=UBEST(I,J)
      RETURN
C
      SUBROUTINE PFC
C  THIS SUBROUTINE COMPUTES THE PREDICTIVE
C  FILTER COEFFICIENTS; ANY M; EQ 79
      IF(PBEST.LE.1) RETURN
      DO 1 P=2,PBEST
      IA=P-1
      DO 2 L=1,IA
      IB=P-L
      CALL MULT(AP(1,1,P),BP(1,1,IB),WA)
      CALL SUB(AP(1,1,L),WA,WA)
      CALL MULT(BP(1,1,P),AP(1,1,L),WB)
      CALL SUB(BP(1,1,IB),WB,BP(1,1,IB))
2     CALL EQUAL(WA,AP(1,1,L))
1     CONTINUE
      RETURN
C
      SUBROUTINE PEFTF
C  THIS SUBROUTINE COMPUTES THE PREDICTIVE-ERROR
C  FILTER TRANSFER FUNCTION; ANY M; EQS 68 AND (J-3)-(J-6)
      K=1.4427*LOG(NF)+.5
      CALL QTRCOS(COSI,NF)
      DO 1 I=1,M
      DO 1 J=1,M
      XX(1,I,J)=0.
      IF(I.EQ.J) XX(1,I,J)=1.
      YY(1,I,J)=0.
      IF(PBEST.EQ.0) GO TO 2
      IA=PBEST+1
      DO 3 L=2,IA
      XX(L,I,J)=-AP(I,J,L-1)
3     YY(L,I,J)=0.
2     IA=PBEST+2
      DO 4 L=IA,NF
      XX(L,I,J)=0.
4     YY(L,I,J)=0.
1     CALL MKLFFT(XX(1,I,J),YY(1,I,J),COSI,K,-1)
      RETURN
C
      SUBROUTINE SDM
C  THIS SUBROUTINE COMPUTES THE SPECTRAL DENSITY
C  MATRIX AND COHERENCE FOR M=2; EQS 178 AND K-5
      T=2./NF
      DO 1 L=1,K
      WA(1,1)=XX(L,2,2)
      WA(1,2)=-XX(L,1,2)
      WA(2,1)=-XX(L,2,1)
      WA(2,2)=XX(L,1,1)
      WB(1,1)=YY(L,2,2)
      WB(1,2)=-YY(L,1,2)
      WB(2,1)=-YY(L,2,1)
      WB(2,2)=YY(L,1,1)
```

```
      TA=DETERM(WA)-DETERM(WB)
      TB=WA(1,1)*WB(2,2)+WA(2,2)*WB(1,1)-WA(1,2)*WB(2,1)-WA(2,1)*WB(1,2)
      TA=T/(TA**2+TB**2)
      CALL TRANS(WA,WC)
      CALL MULT(UBEST,WC,WD)
      CALL MULT(WB,WD,WC)
      TB=WC(1,2)-WC(2,1)
      CALL MULT(WA,WD,WC)
      CALL TRANS(WB,WD)
      CALL MULT(UBEST,WD,WE)
      CALL MULT(WB,WE,WD)
      CALL ADD(WC,WD,WC)
      YY(L,1,1)=(WC(1,2)**2+TB**2)/(WC(1,1)*WC(2,2))     @ MAG SQ COH
      YY(L,2,2)=ATAN2(TB,WC(1,2))                        @ ARGUMENT
      XX(L,1,1)=TA*WC(1,1)                               @ AUTO11
      XX(L,2,2)=TA*WC(2,2)                               @ AUTO22
      XX(L,1,2)=TA*WC(1,2)                               @ REAL(CROSS12)
      YY(L,1,2)=TA*TB                                    @ IMAG(CROSS12)
      XX(L,2,1)=0.
      YY(L,2,1)=0.
1     CONTINUE
      RETURN
C
      SUBROUTINE CROSS(N1,N2,A,B,C)     @ A,B,A NG
C  THIS SUBROUTINE COMPUTES A CROSS CORRELATION MATRIX; ANY M; EQ 114B
      DIMENSION A(N,M),B(N,M),C(M,M)
      DOUBLE PRECISION T
      DO 1 I=1,M
      DO 1 J=1,M
      T=0.D0
      DO 2 K=N1,N2
2     T=T+A(K,I)*B(K-1,J)
1     C(I,J)=T
      RETURN
C
      SUBROUTINE AUTO(N1,N2,A,B)    @  A,A NG
C  THIS SUBROUTINE COMPUTES AN AUTO CORRELATION MATRIX; ANY M; EQ 114A
      DIMENSION A(N,M),B(M,M)
      DOUBLE PRECISION T
      DO 1 I=1,M
      DO 1 J=I,M
      T=0.D0
      DO 2 K=N1,N2
2     T=T+A(K,I)*A(K,J)
      B(I,J)=T
1     B(J,I)=B(I,J)
      RETURN
C
      SUBROUTINE EQUAL(A,B)
C  THIS SUBROUTINE SETS TWO MXM MATRICES EQUAL
      DIMENSION A(M,M),B(M,M)
      DO 1 I=1,M
      DO 1 J=1,M
1     B(I,J)=A(I,J)
      RETURN
```

```
      SUBROUTINE TRANS(A,B)      @  A,A NG
C  THIS SUBROUTINE TRANSPOSES AN MXM MATRIX
      DIMENSION A(M,M),B(M,M)
      DO 1 I=1,M
      DO 1 J=1,M
1     B(I,J)=A(J,I)
      RETURN
C
      SUBROUTINE ADD(A,B,C)      @  A,B,A OK
C  THIS SUBROUTINE ADDS TWO MXM MATRICES
      DIMENSION A(M,M),B(M,M),C(M,M)
      DO 1 I=1,M
      DO 1 J=1,M
1     C(I,J)=A(I,J)+B(I,J)
      RETURN
C
      SUBROUTINE SUB(A,B,C)      @  A,B,A OK
C  THIS SUBROUTINE SUBTRACTS TWO MXM MATRICES
      DIMENSION A(M,M),B(M,M),C(M,M)
      DO 1 I=1,M
      DO 1 J=1,M
1     C(I,J)=A(I,J)-B(I,J)
      RETURN
C
      SUBROUTINE MULT(A,B,C)     @  A,B,A NG
C  THIS SUBROUTINE MULTIPLIES TWO MXM MATRICES
      DIMENSION A(M,M),B(M,M),C(M,M)
      DO 1 I=1,M
      DO 1 J=1,M
      T=0.
      DO 2 K=1,M
2     T=T+A(I,K)*B(K,J)
1     C(I,J)=T
      RETURN
C
      SUBROUTINE INVERT(A,B)     @  A,A NG
C  THIS SUBROUTINE INVERTS A 2X2 MATRIX
      DIMENSION A(2,2),B(2,2)
      TA=1./DETERM(A)
      B(1,1)=A(2,2)*TA
      B(2,2)=A(1,1)*TA
      B(1,2)=-A(1,2)*TA
      B(2,1)=-A(2,1)*TA
      RETURN
C
      SUBROUTINE SOLVE
C  THIS SUBROUTINE SOLVES BILINEAR MATRIX EQUATION
C  FOR M=2, BIVARIATE PROCESS; EQS 157, 158, AND 162
      TA=WA(1,1)+WA(2,2)+WB(1,1)+WB(2,2)
      TB=DETERM(WA)-DETERM(WB)
      CALL MULT(WC,WB,WD)
      WE(1,1)=WA(2,2)
      WE(1,2)=-WA(1,2)
      WE(2,1)=-WA(2,1)
      WE(2,2)=WA(1,1)
```

```
      CALL MULT(WE,WC,WA)
      CALL ADD(WD,WA,WD)
      WB(1,1)=TA*WB(1,1)+TB
      WB(2,2)=TA*WB(2,2)+TB
      WB(1,2)=TA*WB(1,2)
      WB(2,1)=TA*WB(2,1)
      CALL INVERT(WB,WE)
      CALL MULT(WD,WE,WC)
      RETURN
C
      FUNCTION DETERM(A)
C  THIS FUNCTION COMPUTES THE DETERMINANT OF A 2X2 MATRIX
      DIMENSION A(2,2)
      DETERM=A(1,1)*A(2,2)-A(1,2)*A(2,1)
      RETURN
      END
  SUBROUTINE MKLFFT(X,Y,CC,M,ISN)
  DIMENSION X(1),Y(1),CC(1),L(12)
  EQUIVALENCE (L12,L(1)),(L11,L(2)),(L10,L(3)),(L9,L(4)),(L8,L(5)),
 1(L7,L(6)),(L6,L(7)),(L5,L(8)),(L4,L(9)),(L3,L(10)),(L2,L(11)),
 2(L1,L(12))
  N=2**M
  ND4=N/4
  ND4P1=ND4+1
  ND4P2=ND4P1+1
  ND2P2=ND4+ND4P2
  DO 8 LO=1,M
  LMX=2**(M-LO)
  LIX=2*LMX
  ISCL=N/LIX
  DO 8 LM=1,LMX
  IARG=(LM-1)*ISCL+1
  IF(IARG.LE.ND4P1) GO TO 4
  C=-CC(ND2P2-IARG)
  S=ISN*CC(IARG-ND4)
  GO TO 6
4 C=CC(IARG)
  S=ISN*CC(ND4P2-IARG)
6 DO 8 LI=LIX,N,LIX
  J1=LI-LIX+LM
  J2=J1+LMX
  T1=X(J1)-X(J2)
  T2=Y(J1)-Y(J2)
  X(J1)=X(J1)+X(J2)
  Y(J1)=Y(J1)+Y(J2)
  X(J2)=C*T1-S*T2
  Y(J2)=C*T2+S*T1
8 CONTINUE
  DO 40 J=1,12
  L(J)=1
  IF(J-M) 31,31,40
31 L(J)=2**(M+1-J)
```

```
40 CONTINUE
   JN=1
   DO 60 J1=1,L1
   DO 60 J2=J1,L2,L1
   DO 60 J3=J2,L3,L2
   DO 60 J4=J3,L4,L3
   DO 60 J5=J4,L5,L4
   DO 60 J6=J5,L6,L5
   DO 60 J7=J6,L7,L6
   DO 60 J8=J7,L8,L7
   DO 60 J9=J8,L9,L8
   DO 60 J10=J9,L10,L9
   DO 60 J11=J10,L11,L10
   DO 60 JR=J11,L12,L11
   IF(JN-JR) 51,51,52
51 R=X(JN)
   X(JN)=X(JR)
   X(JR)=R
   FI=Y(JN)
   Y(JN)=Y(JR)
   Y(JR)=FI
52 JN=JN+1
60 CONTINUE
   RETURN
   END

      SUBROUTINE QTRCOS(C,N)
      DIMENSION C(1)
      N41=N/4+1
      SCL=6.283185307/N
      DO 1 I=1,N41
1     C(I)=COS((I-1)*SCL)
      RETURN
      END
```

N = 100 PMAX = 10 M = 2 NF = 1024

INPUT DATA:

PROCESS NUMBER 1

.53901729+00	.24572077+00	-.48246256+00	-.99235174+00	-.62436315+00
.31143945+00	.74571225+00	.94372392+00	.15172541+00	-.76859383+00
-.13781174+00	.25836023+00	.79770139+00	.71260673+00	.80128585+00
.43642798+00	-.44703931-01	-.71200128+00	-.11368756+01	-.92819643+00
-.33429637+00	.57812569+00	.13680694+01	.10164690+01	.50713280+00
-.10550485+01	-.20570143+01	-.19485568+01	-.14135770+01	-.19008934+00
.18386345+01	.31438660+01	.21384055+01	-.46009872+00	-.23113293+01
-.36081896+01	-.28417680+01	-.23547348+00	.16677773+01	.33429194+01
.28877570+01	.56888448+00	-.22631766+01	-.33943964+01	-.26797284+01
-.43547171+00	.21718071+01	.35407588+01	.23288262+01	-.22656890+00
-.25376441+01	-.32986798+01	-.27345279+01	-.40607340+00	.25071375+01
.44460779+01	.32127956+01	.91031507+00	-.13406594+01	-.27867314+01
-.25558064+01	-.11135026+01	.95231916+00	.31850186+01	.37061642+01
.17390409+01	-.89170610+00	-.24854088+01	-.27824243+01	-.13415888+01
.82164557+00	.30034332+01	.35482952+01	.26236263+01	-.89912541-01
-.34330869+01	-.47749634+01	-.34963096+01	-.69029214+00	.24394748+01
.40683678+01	.36433851+01	.54673234+00	.18884842+01	-.32592577+01
-.28174284+01	-.13084519+01	.12478004+01	.28549910+01	.27696476+01
.13411797+01	-.16488338+01	-.35990672+01	-.33495106+01	-.18694348+01
.17976616+00	.23938473+01	.25152508+01	.16395330+01	-.34817306+00

PROCESS NUMBER 2

.84303659+00	.86934820+00	.16071917+00	.14386062+00	-.81120574+00
-.96936302+00	-.68125464-01	.71946396+00	.53986827+00	-.30419506-01
-.85955505+00	-.32430927+00	.10317814+00	.34722114+00	.80690885+00
.57330412+00	.39259374+00	.14101289+00	.84664986-01	-.19283811+00
-.11813866+01	-.86226903+00	-.20097572+00	.66497141+00	.14060706+01
.11701580+01	.81481338-01	-.81963249+00	-.17308412+01	-.21933125+01
-.17339195+01	.58163619+00	.24263104+01	.29041306+01	.17109564+01
-.18242586+00	-.25142254+01	-.28079124+01	-.19512028+01	.50994501+00
.25400578+01	.30085762+01	.18208549+01	-.84529851+00	-.28813978+01
-.31391280+01	-.17331168+01	.92467879+00	.25048586+01	.30233470+01
.19451272+01	-.49972244+00	-.29138998+01	-.33593366+01	-.25352063+01
.43625407+00	.27926130+01	.31353639+01	.25105703+01	.87293217+00
-.12635761+01	-.25078586+01	-.25748112+01	-.99730413+00	.13507358+01
.26830553+01	.23373865+01	.82668857+00	-.11139500+01	-.21637863+01
-.25236639+01	-.10761964+01	.98666745+00	.30014957+01	.38264174+01
.23522349+01	-.81600191+00	-.32755376+01	-.45058461+01	-.25775154+01
-.21895836+00	.29419152+01	.36481336+01	.28266277+01	-.60319692-01
-.19925841+01	-.27615544+01	-.26589665+01	-.64737901+00	.17339140+01
.31629709+01	.26245979+01	.38355845+00	-.19680776+01	-.27634547+01
-.24165064+01	-.10100275+01	.11536021+01	.19672252+01	.16684788+01

MEANS OF INPUT DATA:

.12088474-01	.29368686-01

COVARIANCE MATRIX OF INPUT DATA:

.46218387+01	.91577268+00	.91577268+00	.37956951+01

AKAIKE INFORMATION CRITERION:

0	.28156752+01
1	-.47116107+01
2	-.46664973+01
3	-.46229553+01

4	-.46316842+01
5	-.45650773+01
6	-.45422159+01
7	-.45357835+01
8	-.44974548+01
9	-.44907100+01
10	-.44389324+01

PBEST = 1

UBEST:

.89002132-01	-.79014897-03	-.79014897-03	.93252867-01

FORWARD PARTIAL CORRELATION COEFFICIENTS:

1	.87150693+00	.63431677+00	-.77024333+00	.56034775+00
2	-.24060294-01	.15673790+00	-.46089508-01	-.13923085+00
3	.12915299+00	.10394043+00	-.69120812-01	-.12937856+00
4	-.11394597+00	.22871864+00	.18147939+00	.72523244-02
5	.39759100-01	.27629165-01	-.10585008+00	.16504833-01
6	.24732786+00	-.11105661-01	-.13494856-01	-.36488586-02
7	.18216120+00	.10071856+00	.96155114-01	-.10703941+00
8	.19121648+00	.93589546-01	-.25144000-01	.10180847-01
9	.82219786-01	.12730163+00	-.10475686+00	-.22288333+00
10	-.53422038-01	.16764631+00	-.42075946-01	-.26114821-01

BACKWARD PARTIAL CORRELATION COEFFICIENTS:

1	.56612993+00	-.63141833+00	.77098253+00	.86572675+00
2	-.38369942-01	-.66131392-01	.95437832-01	-.11108892+00
3	.97749089-01	-.38619501-01	.51535051-01	-.11780613+00
4	-.33532630-01	.18090538+00	.21567873+00	.98908506-01
5	-.22097769-02	-.11387029+00	.31994226-01	.28316177-01
6	.22834081+00	.77628009-01	-.75839960-02	-.71869090-02
7	.20997133+00	.19255909+00	.53676562-01	-.89760510-01
8	.17425043+00	.38450344-01	.85870568-01	.43625234-01
9	.39914736-01	-.11974496+00	.33887566-01	-.22667238+00
10	-.58663283-01	-.74213017-01	.13284003+00	.24026474-01

FORWARD PREDICTIVE FILTER COEFFICIENTS FOR PBEST:

1	.87150893+00	.63431677+00	-.77024333+00	.56034775+00

SPECTRAL DENSITY MATRIX AND COHERENCE FOR M=2:

BIN	AUTO11	AUTO22	REAL(CROSS12)	IMAG(CROSS12)	MAG SQ COH	ARGUMENT
1	.48031416-03	.24469207-03	.10474293-03	.00000000	.93347806-01	.00000000
2	.48039190-03	.24474571-03	.10475898-03	.51851717-05	.93569521-01	.49455843-01
3	.48062528-03	.24490670-03	.10480719-03	.10374396-04	.94234384-01	.98664136-01
4	.48101453-03	.24517527-03	.10488758-03	.15571732-04	.95341385-01	.14738464+00
5	.48156022-03	.24555178-03	.10500028-03	.20781259-04	.96888931-01	.19539113+00
6	.48226298-03	.24603673-03	.10514542-03	.26007074-04	.98874767-01	.24247721+00
7	.48312366-03	.24663077-03	.10532316-03	.31253307-04	.10129598+00	.28846080+00
8	.48414344-03	.24733472-03	.10553375-03	.36524137-04	.10414911+00	.33318695+00
9	.48532356-03	.24814953-03	.10577746-03	.41823766-04	.10743000+00	.37652935+00
10	.48666550-03	.24907630-03	.10605455-03	.47156497-04	.11113392+00	.41839078+00
11	.48817101-03	.25011633-03	.10636541-03	.52526663-04	.11525556+00	.45870120+00
12	.48984205-03	.25127100-03	.10671042-03	.57938682-04	.11978902+00	.49741631+00
13	.49168070-03	.25254195-03	.10709001-03	.63397053-04	.12472785+00	.53451476+00
14	.49368939-03	.25393093-03	.10750468-03	.68906375-04	.13006503+00	.56999511+00
15	.49567071-03	.25543986-03	.10795494-03	.74471342-04	.13579307+00	.60387272+00

LIST OF REFERENCES

1. J. Makhoul, "Linear Prediction: A Tutorial Review, "Proceedings of the IEEE, vol. 63, no. 4, April 1975, pp. 561-580.

2. T. J. Ulrych and T. N. Bishop, "Maximum Entropy Spectral Analysis and Autoregressive Decomposition," Reviews of Geophysics and Space Physics, vol. 13, no. 1, February 1975, pp. 183-200.

3. A. H. Nuttall, Spectral Analysis of a Univariate Process with Bad Data Points, via Maximum Entropy and Linear Predictive Techniques, NUSC Technical Report 5303, 26 March 1976.

4. J. P. Burg, "A New Analysis Technique for Time Series Data," NATO Advanced Study Institute on Signal Processing, Enschede, Netherlands, vol. 1, August 1968.

5. A. H. Nuttall, FORTRAN Program for Multivariate Linear Predictive Spectral Analysis, Employing Forward and Backward Averaging, NUSC Technical Document 5419, 19 May 1976.

6. R. H. Jones, "Multivariate Maximum Entropy Spectral Analysis," Applied Time Series Analysis Symposium, Tulsa Oklahoma, 14-15 May 1976. A revised version will appear in Applied Time Series Analysis, editor D. Findley, Academic Press, 1977.

7. P. Whittle,"On the Fitting of Multivariate Autoregressions, and the Approximate Canonical Factorization of a Spectral Density Matrix," Biometrika, vol. 50, 1963, pp. 129-134.

8. H. Akaike, "Block Toeplitz Matrix Inversion," SIAM J. Appl. Math., vol. 24, no. 2, March 1973, pp. 234-241.

9. G. Kreisselmeier, "A Solution of the Bilinear Matrix Equation AY+YB = -Q," SIAM J. Appl. Math., vol. 23, no. 3, Nov. 1972, pp. 334-338.

10. A. Jameson, "Solution of the Equation AX+XB = C by Inversion of an MxM or NxN Matrix," SIAM J. Appl. Math., vol. 16, no. 5, Sept. 1968, pp. 1020-1023.

11. C. S. Lu, "Solution of the Matrix Equation AX+XB = C," Electronics Letters, vol. 7, no. 8, April 22, 1971, pp. 185-186.

12. S. Barnett, "Remarks on Solution of AX+XB = C," Electronics Letters, vol. 7, no. 14, July 15, 1971, p. 385.

13. I. S. Pace and S. Barnett, "Comparison of Numerical Methods for Solving Liapunov Matrix Equations," Int. J. Control, vol. 15, no. 5, 1972, pp. 907-915.

14. R. E. Hartwig, "Resultants and the Solution of AX-XB = -C," SIAM J. Appl. Math., vol. 23, no. 1, July 1972, pp. 104-117.

15. V. Kučera, "The Matrix Equation AX+XB = C," SIAM J. Appl. Math., vol. 26, no. 1, Jan. 1974, pp. 15-25.

16. R. E. Hartwig, "AX-XB = C, Resultants and Generalized Inverses," SIAM J. Appl. Math., vol. 28, no. 1, Jan. 1975, pp. 154-183.

17. S. Barnett, "Simplification of Certain Linear Matrix Equations," IEEE Trans on Automatic Control, February 1976, pp. 115-116.

18. F. R. Gantmacher, "The Theory of Matrices," vol. I, Chelsea Publishing Co., N.Y., 1959.

19. H. Akaike, "A New Look at the Statistical Model Identification," IEEE Trans. on Automatic Control, vol. AC-19, no. 6, Dec. 1974, pp. 716-723.

20. A. H. Nuttall, "Trigonometric Smoothing and Interpolation of Sampled Complex Functions, via the FFT," NUSC Technical Memorandum TC-94-71, 19 April 1971.

21. J. F. Ferrie, G. C. Carter, and C. W. Nawrocki, "Availability of Markel's FFT Algorithm," NUSC Technical Memorandum TC-1-73, 15 January 1973.

NUSC Report No. 5505
3 December 1976

FORTRAN Program for Linear Predictive Spectral Analysis of a Complex Univariate Process

Albert H. Nuttall

ABSTRACT

A FORTRAN program for evaluating (1) the linear predictive complex filter coefficients and (2) the power density spectrum of a complex univariate process is presented, and its use is demonstrated. A pitfall of using this approach for estimating the cross-spectrum of two real processes is pointed out, and a limitation of the complex predictive filter for waveform estimation is considered.

Approved for public release; distribution unlimited.

TABLE OF CONTENTS

Page

LIST OF ILLUSTRATIONS ii

LIST OF SYMBOLS iii

1. INTRODUCTION 1

2. USE OF PROGRAM FOR SPECTRAL ANALYSIS 2

3. ESTIMATION OF CROSS-SPECTRUM OF TWO REAL PROCESSES 7

4. A LIMITATION OF COMPLEX PREDICTIVE FILTER 11

5. DISCUSSION 17

APPENDIX A--FORTRAN PROGRAM FOR SPECTRAL ANALYSIS A-1

APPENDIX B--PROPERTY OF AUTOREGRESSIVE MODEL B-1

APPENDIX C--NONANALYTIC WHITE NOISE EXCITATION C-1

APPENDIX D--A METHOD OF GENERATING ANALYTIC PROCESSES D-1

APPENDIX E--CAPABILITY OF A MORE GENERAL PREDICTION MODEL E-1

LIST OF REFERENCES R-1

LIST OF ILLUSTRATIONS

Figure		Page
1	Spectrum of Surface-Bottom Forward Scatter	5
2	Spectrum of Direct Path	6

LIST OF SYMBOLS

N	Number of complex data points
PMAX	Maximum order of filter considered
J	Size of FFT for spectral estimate
PBEST	Best order of filter
Δ	Sampling interval in time
t	Time
u(t), v(t)	Real processes
Asterisk	Conjugate
α, β	Complex constants
x(t)	Complex process
$R_{xx}(\tau)$	Correlation of x(t) at delay τ
$R_{uv}(\tau)$	Crosscorrelation of u(t) and v(t)
f	Frequency
$G_{xx}(f)$	Auto-Spectrum of x(t)
R(f), I(f)	Real and imaginary parts of $G_{uv}(f)$
Re z	Real part of z
Im z	Imaginary part of z
$\hat{x}_k$	Estimate of x_k
a_n	n-th predictive coefficient
p	Order of predictive filter
$\tilde{x}_k$	More general estimate of x_k; (19)
g_n, h_n	Complex filter coefficients

LIST OF SYMBOLS (Cont'd)

w_k	Excitation process in autoregression
δ_{on}	Kronecker delta: = 1 if n = 0, = 0 otherwise
Overbar	Ensemble average
R_n, $\mathcal{R}_n$	Correlations of $\{x_k\}$; (28) and (29)
$G(f)$, $\mathcal{G}(f)$	Spectra of $\{x_k\}$; (31) and (32)
$\hat{\varepsilon}_k$, $\tilde{\varepsilon}_k$	Errors in prediction

FORTRAN PROGRAM FOR LINEAR PREDICTIVE SPECTRAL ANALYSIS OF A COMPLEX UNIVARIATE PROCESS

1. INTRODUCTION

Spectral analysis of a complex univariate process via linear predictive and maximum entropy techniques is considered in reference 1, and Fortran programs for real data are presented there in appendix J. In this report, we present a program for handling the case of complex data, yielding as an output the auto-spectrum of the process.* Complex data can be encountered, for example, when a narrowband real process is complex-demodulated to a low frequency and sampled at a rate comparable to the bandwidth of the process. When the new center frequency is zero, the process is called the complex envelope.

In section 2, an example of the use of the program is presented, and the changes that the user must make for his application are pointed out. In section 3, the possibility of using this program to estimate the cross-spectrum of two real processes is investigated and found to be undesirable. In section 4, a limitation of the complex predictive filter for complex waveform estimation is considered, and a possible generalization is indicated to alleviate the problem.

---

*The theory and notation for this case were developed fully in reference 1 and will not be repeated here, for sake of brevity; the reader is referred to that earlier material for all details.

2. USE OF PROGRAM FOR SPECTRAL ANALYSIS

The program for spectral analysis of a complex process consists of five parts: a main program and four subroutines, as listed in appendix A. Input parameters to the main program (listed in statement 15) are

N, number of complex data points,
PMAX, maximum order of filter considered, and
J, size of FFT for spectral estimate.

The sample program generates a data example in lines 20-33 and must be replaced by the user to fit his particular applications.

A sample output for N = 100, PMAX = 10, is presented below. It indicates that PBEST = 1, which agrees with the actual value of p (see statement 21 of the main program). The fractional powers sum up to 0.99999829 instead of 1; the difference is a measure of whether the spectral estimate has been adequately sampled in frequency. (If the error is too large, J may be increased.)

Since the autospectrum of a complex process is real, but not necessarily even, it is necessary to compute the spectrum over both negative and positive frequencies. Thus bin 1 corresponds to zero frequency; bin J/2 + 1 corresponds to $\pm$ Nyquist frequency, $\pm 1/(2\Delta)$: and bin J corresponds to frequency $-1/(J\Delta)$, where Δ is the sampling interval in time.

An example of a spectral estimate of 1000 samples of a complex envelope of surface-bottom forward scatter at a 20° grazing angle at frequency 750 Hz over a 20 nautical-mile path is presented in figure 1, where the sampling rate is 1 Hz. There is observed to be a pair of spectral peaks at $\pm 1/4$ Nyquist frequency, a strong very low frequency component, and a rather symmetric spectrum about zero frequency. In figure 2, the direct path is employed instead, the sampling rate is 0.1 Hz, but 1000 samples are still used. The center portion of the spectral estimate reveals a double peak near zero frequency and a rapid drop-off away from this frequency. With these few data points, resolution capability of this quality is very hard to achieve by any other spectral analysis techniques.

INPUT DATA:

-.2539492E+00	-.8951166E+00	.4536105E+00	-.2610464E+00	.3755559E+00	.4360030E+00	-.3372201E+00	.6557265E+00
-.8555661E+00	.2525350E-01	-.1659231E+00	-.3633280E+00	.9682664E-02	-.8352922E+00	.7605867E+00	-.3225437E+00
.8477816E+00	.9471585E-01	.5988406E+00	.2705816E+00	.3339350E+00	.6823717E+00	-.6059322E+00	.1078538E+01
-.9486116E+00	.1216878E+00	-.6661106E+00	-.2039573E+00	.1486239E+00	-.8437252E+00	.7876657E+00	-.4316485E+00
.1024675E+01	.9076193E-02	.4482694E+00	.5610925E+00	-.4205226E+00	.7278903E+00	-.7750475E+00	.4104407E+00
-.6277671E+00	.1809231E+00	-.2804774E+00	-.4708469E-01	.3635850E-01	-.4308911E+00	.7079704E+00	-.7052009E+00
.1229269E+01	.4143486E-01	.1200071E+01	.5982084E+00	-.8167860E-01	.7186627E+00	-.6499661E+00	.6328607E+00
-.4396759E+00	.3667754E+00	-.5762945E+00	-.2285531E+00	-.1172210E+00	-.6718681E+00	.2253534E+00	-.4832207E+00
.4299714E+00	.3068308E+00	-.2165946E+00	.9622887E+00	-.7432526E+00	.7319095E+00	-.1168311E+01	.2378776E+00
-.5340162E+00	-.1019848E+01	.3940973E+00	-.1315885E+01	.1404353E+01	-.4380959E+00	.9017414E+00	.7869984E+00
-.1865911E+00	.1215061E+01	-.1397781E+01	.2303766E+00	-.1221668E+01	-.5466162E+00	-.4688498E+00	-.6850595E+00
.2355604E+00	-.1148132E+01	.1382508E+01	-.5833971E+00	.1359893E+01	.5955449E+00	.3161057E+00	.1075656E+01
-.1138091E+01	.9863622E+00	-.1492634E+01	-.4063459E+00	-.4693016E+00	-.1358166E+01	.3942589E+00	-.1484605E+01
.9331566E+00	-.5134167E+00	.7873784E+00	.4623887E+00	.4284305E+00	.9165726E+00	-.8906238E-01	.1150111E+01
-.4366261E+00	.3296487E+00	-.9267212E+00	.7406392E+00	-.8625970E+00	-.3579939E-01	-.2225074E+00	-.8605970E+00
.6460511E+00	-.5375357E+00	.5618232E+00	-.3986387E+00	.6124994E+00	.4739014E-01	.8565150E+00	.3538466E-01
.4299756E+00	.7346645E+00	-.6406501E+00	.1016616E+01	-.1409099E+01	.3697511E+00	-.7234079E+00	-.1174324E+01
.4345019E+00	-.8560326E+00	.6433180E+00	-.3110645E+00	.1031275E+01	.6982308E+00	.2972769E+00	.9603551E+00
-.2504676E+00	.5294065E+00	-.7971136E+00	.2945691E-02	-.1002636E+01	-.7346041E+00	-.6471465E+00	-.1619057E+01
.7054031E+00	-.1163662E+01	.1320268E+01	-.4406653E+00	.1505335E+01	.4404662E+00	.5226194E+00	.1560663E+01
-.3791662E+00	.9526753E+00	-.8698356E+00	.6215147E+00	-.2809470E+01	.1538174E+00	-.1060939E+01	-.6096780E+00
.1652277E+00	-.1546543E+01	.6668556E+00	-.1095972E+01	.9042032E+00	-.7296715E+00	.1389129E+01	.5827792E+00
.7169074E+00	.1227424E+01	-.6440133E+00	.9336474E+00	-.8002643E+00	.2636432E+00	.1060563E+00	-.4073306E+00
.5159649E+00	-.3696665E+00	.2401589E+00	.4595078E+00	-.4900862E+00	.8407669E+00	-.4478550E+00	.4151837E+00
-.2036469E+00	-.2594119E+00	-.3276602E+00	-.2554016E+00	-.4947675E+00	-.5116457E+00	-.3849582E+00	-.6441827E+00

MEAN = (.4676050E-02, .4938406E-02)
STANDARD DEVIATION = .1159733E+01

POEST = 1

PREDICTIVE FILTER COEFFICIENTS FOR POEST:

.6297609E+00	.6775263E+00

PRODUCT(1-ABS(A(P))**2) = .1443376E+00

NORMALIZED CORRELATION COEFFICIENTS:

.6297609E+00	.6775263E+00	-.6242147E-01	.8533624E+00	-.8175007E+00	.8951494E+00	-.7243652E+00	-.1065387E+00
-.3840052E+00	-.5576722E+00	.1361342E+00	-.6115226E+00	.5000486E+00	-.2928812E+00	.5133544E+00	.1543459E+00
.2167293E+00	.4450148E+00	-.1657604E+00	.4284531E+00				

FRACTIONAL POWERS:

.4729E-03	.4864E-03	.5005E-03	.5152E-03	.5307E-03	.5469E-03	.5640E-03	.5818E-03	.6006E-03	.6203E-03
.6411E-03	.6630E-03	.6860E-03	.7103E-03	.7360E-03	.7632E-03	.7919E-03	.8224E-03	.8547E-03	.8890E-03
.9254E-03	.9643E-03	.1006E-02	.1049E-02	.1096E-02	.1144E-02	.1201E-02	.1256E-02	.1322E-02	.1389E-02
.1460E-02	.1540E-02	.1625E-02	.1717E-02	.1818E-02	.1927E-02	.2047E-02	.2178E-02	.2323E-02	.2482E-02
.2657E-02	.2852E-02	.3069E-02	.3311E-02	.3583E-02	.3889E-02	.4234E-02	.4626E-02	.5074E-02	.5587E-02
.6179E-02	.6865E-02	.7666E-02	.8604E-02	.9712E-02	.1102E-01	.1259E-01	.1448E-01	.1671E-01	.1947E-01
.2278E-01	.2661E-01	.3108E-01	.3606E-01	.4112E-01	.4572E-01	.4899E-01	.5018E-01	.4887E-01	.4551E-01
.4087E-01	.3578E-01	.3068E-01	.2640E-01	.2256E-01	.1932E-01	.1662E-01	.1437E-01	.1251E-01	.1095E-01
.9652E-02	.8554E-02	.7622E-02	.6829E-02	.6148E-02	.5560E-02	.5050E-02	.4606E-02	.4216E-02	.3872E-02
.3569E-02	.3299E-02	.3058E-02	.2842E-02	.2648E-02	.2473E-02	.2315E-02	.2171E-02	.2041E-02	.1922E-02
.1813E-02	.1713E-02	.1621E-02	.1536E-02	.1458E-02	.1386E-02	.1319E-02	.1256E-02	.1199E-02	.1144E-02
.1094E-02	.1047E-02	.1003E-02	.9623E-03	.9236E-03	.8872E-03	.8530E-03	.8208E-03	.7905E-03	.7618E-03
.7347E-03	.7091E-03	.6848E-03	.6618E-03	.6400E-03	.6192E-03	.5996E-03	.5810E-03	.5631E-03	.5461E-03
.5299E-03	.5145E-03	.4997E-03	.4857E-03	.4722E-03	.4593E-03	.4470E-03	.4350E-03	.4236E-03	.4130E-03

.402e75-03	.392e82-03	.383094-03	.373866-03	.364991-03	.356460-03	.348249-03	.340344-03	.33272A-03	.325399-03
.318e13-03	.311e69-03	.304903-03	.298546-03	.292406-03	.286476-03	.280734-03	.275202-03	.269843-03	.264658-03
.259e41-03	.254783-03	.250078-03	.245521-03	.241105-03	.236824-03	.232674-03	.228648-03	.224743-03	.220953-03
.217274-03	.213702-03	.210233-03	.206863-03	.203589-03	.200406-03	.197312-03	.194304-03	.191377-03	.188531-03
.185761-03	.183064-03	.180432-03	.177887-03	.175399-03	.172976-03	.170615-03	.168315-03	.166073-03	.163888-03
.161758-03	.159681-03	.157655-03	.155680-03	.153752-03	.151872-03	.150037-03	.148246-03	.146498-03	.144791-03
.143125-03	.141498-03	.139908-03	.138356-03	.136840-03	.135358-03	.133911-03	.132496-03	.131113-03	.129762-03
.128441-03	.127150-03	.125887-03	.124652-03	.123445-03	.122264-03	.121109-03	.119980-03	.118875-03	.117794-03
.116736-03	.115701-03	.114689-03	.113698-03	.112728-03	.111780-03	.110851-03	.109942-03	.109052-03	.108181-03
.107329-03	.106495-03	.105678-03	.104878-03	.104095-03	.103329-03	.102579-03	.101844-03	.101125-03	.100422-03
.997324-04	.990378-04	.983573-04	.977507-04	.971178-04	.964962-04	.959917-04	.952981-04	.947170-04	.941483-04
.935917-04	.930464-04	.925139-04	.919923-04	.914820-04	.909827-04	.904943-04	.900165-04	.895493-04	.890923-04
.886455-04	.882090-04	.877815-04	.873641-04	.869562-04	.865576-04	.861682-04	.857878-04	.854164-04	.850538-04
.846998-04	.843542-04	.840173-04	.836885-04	.833680-04	.830555-04	.827509-04	.824543-04	.821653-04	.818841-04
.816104-04	.813442-04	.810853-04	.808338-04	.805895-04	.803523-04	.801222-04	.798990-04	.796828-04	.794734-04
.792706-04	.790744-04	.788856-04	.787030-04	.785268-04	.783572-04	.781940-04	.780371-04	.778865-04	.777423-04
.776044-04	.774726-04	.773467-04	.772271-04	.771135-04	.770060-04	.769045-04	.768090-04	.767194-04	.766358-04
.765580-04	.764861-04	.764200-04	.763598-04	.763053-04	.762567-04	.762138-04	.761767-04	.761453-04	.761197-04
.760999-04	.760857-04	.760772-04	.760745-04	.760775-04	.760862-04	.761007-04	.761208-04	.761466-04	.761784-04
.762159-04	.762591-04	.763079-04	.763626-04	.764232-04	.764895-04	.765617-04	.766393-04	.767238-04	.768137-04
.769094-04	.770113-04	.771191-04	.772329-04	.773528-04	.774788-04	.776110-04	.777494-04	.778939-04	.780448-04
.782020-04	.783655-04	.785355-04	.787120-04	.788950-04	.790846-04	.792808-04	.794837-04	.796935-04	.799100-04
.801335-04	.803641-04	.806015-04	.808462-04	.810981-04	.813573-04	.816239-04	.818980-04	.821796-04	.824689-04
.827660-04	.830711-04	.833839-04	.837048-04	.840340-04	.843715-04	.847173-04	.850717-04	.854348-04	.858067-04
.861875-04	.865773-04	.869764-04	.873848-04	.878027-04	.882303-04	.886676-04	.891150-04	.895724-04	.900402-04
.905185-04	.910075-04	.915073-04	.920182-04	.925403-04	.930740-04	.936193-04	.941765-04	.947458-04	.953275-04
.959218-04	.965291-04	.971492-04	.977828-04	.984301-04	.990912-04	.997696-04	.100456-03	.101161-03	.101891-03
.102646-03	.103397-03	.104134-03	.104918-03	.105718-03	.106536-03	.107371-03	.108225-03	.109096-03	.109987-03
.110897-03	.111827-03	.112777-03	.113747-03	.114739-03	.115753-03	.116789-03	.117847-03	.118930-03	.120036-03
.121167-03	.122323-03	.123505-03	.124714-03	.125950-03	.127214-03	.128507-03	.129829-03	.131182-03	.132566-03
.133982-03	.135431-03	.136915-03	.138433-03	.139987-03	.141578-03	.143207-03	.144876-03	.146584-03	.148335-03
.150128-03	.151965-03	.153848-03	.155778-03	.157756-03	.159784-03	.161864-03	.163996-03	.166184-03	.168429-03
.170734-03	.173098-03	.175522-03	.178013-03	.180572-03	.183199-03	.185898-03	.188672-03	.191522-03	.194452-03
.197463-03	.200558-03	.203751-03	.207030-03	.210405-03	.213879-03	.217456-03	.221140-03	.224936-03	.228847-03
.232880-03	.237036-03	.241323-03	.245746-03	.250311-03	.255023-03	.259888-03	.264914-03	.270108-03	.275476-03
.281026-03	.286765-03	.292709-03	.298859-03	.305228-03	.311825-03	.318662-03	.325751-03	.333103-03	.340733-03
.348653-03	.356880-03	.365427-03	.374313-03	.383556-03	.393173-03	.403187-03	.413613-03	.424490-03	.435839-03
.447680-03	.460013-03								

SUM OF FRACTIONAL POWERS = .9999982E+00

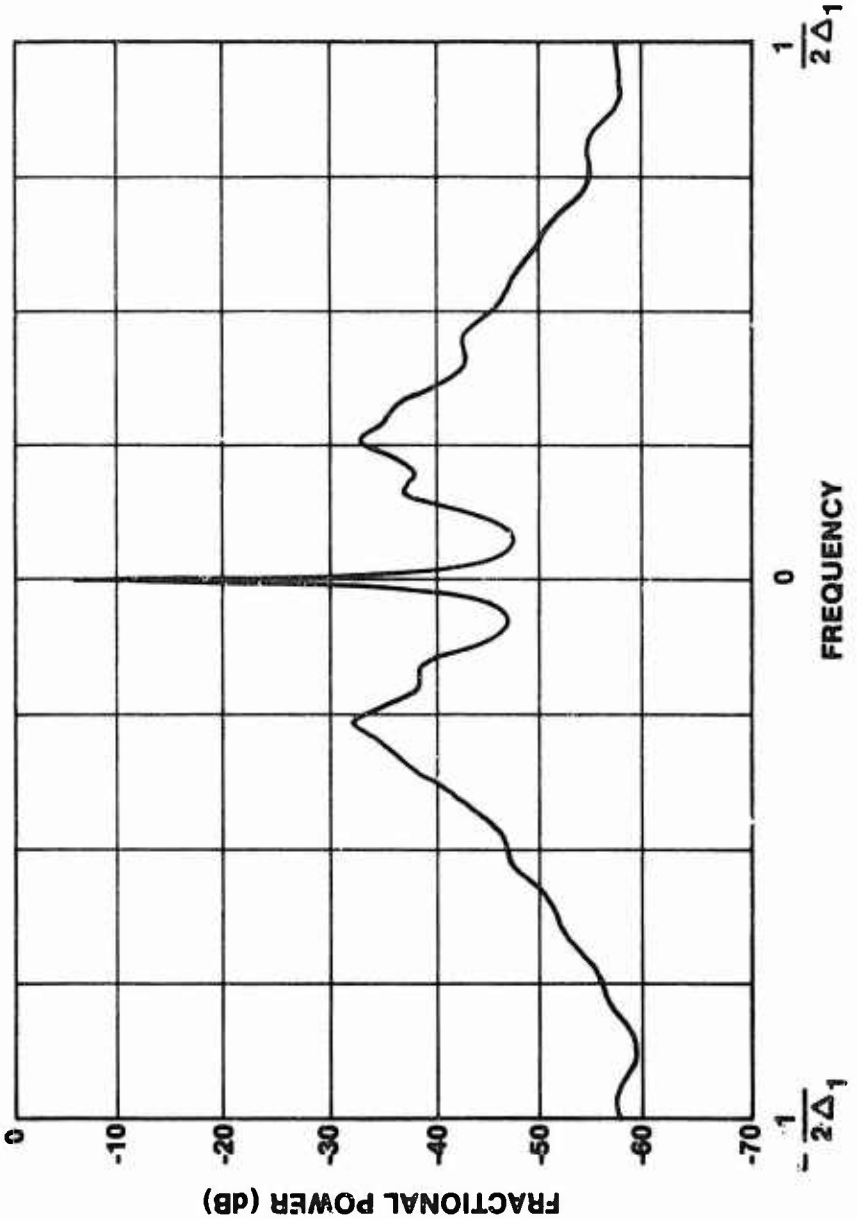


Figure 1. Spectrum of Surface-Bottom Forward Scatter

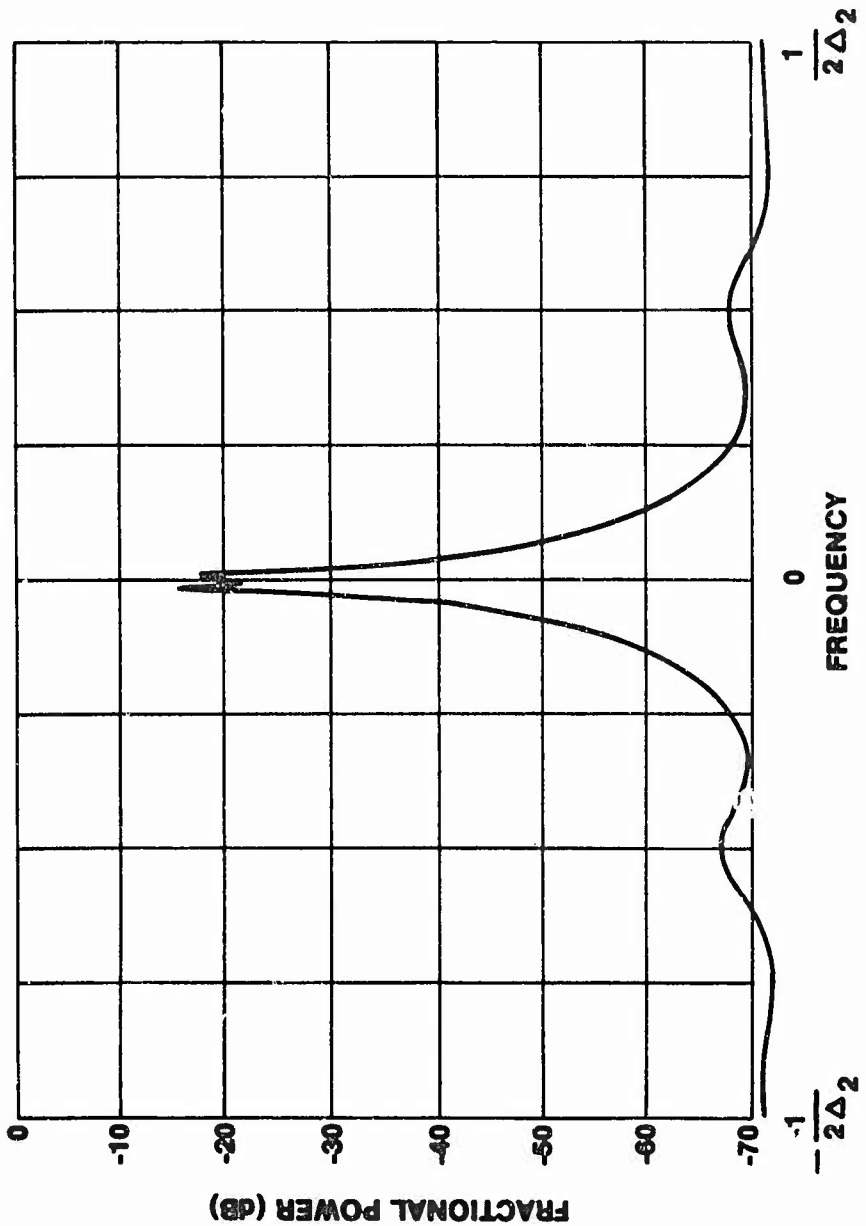


Figure 2. Spectrum of Direct Path

3. ESTIMATION OF CROSS-SPECTRUM OF TWO REAL PROCESSES

Suppose that processes u(t) and v(t) are real, zero-mean, and stationary. If we form the complex process

$$x(t) = \alpha u(t) + \beta v(t), \tag{1}$$

where α and β are complex, then the autocorrelation of x(t) is

$$R_{xx}(\tau) \equiv \overline{x(t)x^*(t-\tau)} = R^*_{xx}(-\tau)$$

$$= |\alpha|^2 R_{uu}(\tau) + |\beta|^2 R_{vv}(\tau) + \alpha\beta^* R_{uv}(\tau) + \alpha^*\beta R_{uv}(-\tau), \tag{2}$$

where the crosscorrelation of u(t) and v(t) is

$$R_{uv}(\tau) \equiv \overline{u(t)v(t-\tau)}\ . \tag{3}$$

The auto-spectrum of x(t) is the nonnegative real (noneven) function

$$G_{xx}(f) \equiv \int_{-\infty}^{\infty} d\tau \exp(-i2\pi f\tau) R_{xx}(\tau)$$

$$= |\alpha|^2 G_{uu}(f) + |\beta|^2 G_{vv}(f) + \alpha\beta^* G_{uv}(f) + \alpha^*\beta G^*_{uv}(f), \tag{4}$$

where the cross-spectrum of u(t) and v(t) is

$$G_{uv}(f) \equiv \int_{-\infty}^{\infty} d\tau \exp(-i2\pi f\tau) R_{uv}(\tau) = G^*_{uv}(-f). \tag{5}$$

Now let us decompose the cross-spectrum as

$$G_{uv}(f) = R(f) + iI(f), \tag{6}$$

for which (5) yields

$$R(-f) = R(f),\ I(-f) = -I(f). \tag{7}$$

Utilizing (6) and (7) in (4), we obtain

$$G_{xx}(f) = |\alpha|^2 G_{uu}(f) + |\beta|^2 G_{vv}(f)$$

$$+ 2\mathrm{Re}(\alpha\beta^*)R(f) - 2\mathrm{Im}(\alpha\beta^*)I(f),$$

$$G_{xx}(-f) = |\alpha|^2 G_{uu}(f) + |\beta|^2 G_{vv}(f)$$

$$+ 2\mathrm{Re}(\alpha\beta^*)R(f) + 2\mathrm{Im}(\alpha\beta^*)I(f). \qquad (8)$$

Solving (8) for R(f) and I(f), the real and imaginary parts, respectively, of cross-spectrum $G_{uv}(f)$, we obtain

$$R(f) = \frac{1}{4}\frac{1}{\mathrm{Re}(\alpha\beta^*)}\left[G_{xx}(f) + G_{xx}(-f) - 2|\alpha|^2 G_{uu}(f) - 2|\beta|^2 G_{vv}(f)\right],$$

$$I(f) = -\frac{1}{4}\frac{1}{\mathrm{Im}(\alpha\beta^*)}\left[G_{xx}(f) - G_{xx}(-f)\right], \qquad (9)$$

if $\mathrm{Re}(\alpha\beta^*) \neq 0$ and $\mathrm{Im}(\alpha\beta^*) \neq 0$. Since α and β are arbitrary, we choose $\alpha\beta^* = (1 - i)/2$, for which $|\alpha|^2|\beta|^2 = |\alpha\beta^*|^2 = 1/2$. For simplicity, we choose $|\alpha|^2 = |\beta|^2 = 1/\sqrt{2}$; then (9) becomes

$$R(f) = \frac{G_{xx}(f) + G_{xx}(-f)}{2} - \frac{G_{uu}(f) + G_{vv}(f)}{\sqrt{2}}$$

$$= \mathrm{EVEN}\{G_{xx}(f)\} - \frac{G_{uu}(f) + G_{vv}(f)}{\sqrt{2}},$$

$$I(f) = \frac{G_{xx}(f) - G_{xx}(-f)}{2} = \mathrm{ODD}\{G_{xx}(f)\}. \qquad (10)$$

Now we need only compute R(f) and I(f) for $f \geq 0$, as (7) indicates.

An alternative method to (10) was presented in reference 2, equation (4). However, that method required calculating four auto-spectra, whereas the current method requires calculating only three auto-spectra: $G_{uu}(f)$ and $G_{vv}(f)$ are real and even, whereas $G_{xx}(f)$ is real, but not necessarily even.

The choices of α and β in (1) are still not unique. If we let

$$\alpha = 2^{-1/4} e^{i\theta}, \quad \beta = 2^{-1/4} e^{i\phi}, \tag{11}$$

then

$$\alpha\beta^* = 2^{-1/2} e^{i(\theta-\phi)} = \frac{1 - i}{2} = 2^{-1/2} e^{-i\pi/4}. \tag{12}$$

Therefore, we must have $\theta - \phi = -\pi/4$. There are two obvious choices:

Choice 1

$$\theta = 0, \ \phi = \pi/4$$

$$\alpha = 2^{-1/4}, \ \beta = 2^{-1/4}\left(\frac{1 + i}{\sqrt{2}}\right)$$

$$x(t) = 2^{-1/4}\left[u(t) + \frac{1 + i}{\sqrt{2}} v(t)\right], \tag{13}$$

which is not very symmetric.

Choice 2

$$\theta = -\pi/8, \ \phi = \pi/8$$

$$\alpha = 2^{-1/4} e^{-i\pi/8} \equiv a - ib$$

$$\beta = 2^{-1/4} e^{i\pi/8} = a + ib$$

$$a = 2^{-1/4} \cos(\pi/8), \ b = 2^{-1/4} \sin(\pi/8)$$

$$x(t) = a[v(t) + u(t)] + ib[v(t) - u(t)], \tag{14}$$

which is the preferred form.

For known autocorrelations or auto-spectra, (10) furnishes a valid way of calculating the real and imaginary parts of the cross-spectrum of real processes $u(t)$ and $v(t)$. However, when the auto-spectra are

unknown, spectral estimates must be substituted in (10). Although R(f) and I(f) can both take on positive or negative values in any frequency range, there is a constraint on their magnitudes. Namely, the magnitude-coherence is upper-bounded by unity. However, several numerical examples using the programs in appendix A, for cases where the true magnitude-coherence was near unity, yielded estimated magnitude-coherences greater than unity in some frequency ranges. This was traced to the fact that the estimate of $G_{xx}(f)$ can be too small and/or the estimates of $G_{uu}(f)$ and $G_{vv}(f)$ can be too large. This type of coherence estimate is intolerable; hence, estimation of cross-spectra of real processes by means of the auto-spectrum of a complex process is discouraged. The same conclusion is offered for the method in reference 2.

4. A LIMITATION OF COMPLEX PREDICTIVE FILTER

The theory behind the program presented in appendix A has been given in reference 1 and is based on a linear predictive technique. Specifically, given p past values of complex process $\{x_k\}$, a linear one-step prediction of x_k is attempted according to reference 1, equation 58:

$$\hat{x}_k \equiv \sum_{n=1}^{p} a_n x_{k-n}. \tag{15}$$

If we express all the quantities in (15) in terms of their real and imaginary parts according to definitions

$$\hat{x}_k = \hat{u}_k + i\hat{v}_k, \quad x_k = u_k + iv_k, \quad a_n = \alpha_n + i\beta_n, \tag{16}$$

then (15) can be expressed as

$$\hat{u}_k = \sum_{n=1}^{p} (\alpha_n u_{k-n} - \beta_n v_{k-n}),$$

$$\hat{v}_k = \sum_{n=1}^{p} (\beta_n u_{k-n} + \alpha_n v_{k-n}). \tag{17}$$

But (17) is not as general as the form for prediction given by (μ_n, ν_n, β_n, α_n real):

$$\tilde{u}_k = \sum_{n=1}^{p} (\mu_n u_{k-n} + \nu_n v_{k-n}),$$

$$\tilde{v}_k = \sum_{n=1}^{p} (\beta_n u_{k-n} + \alpha_n v_{k-n}). \tag{18}$$

It is apparent that the mean-square errors of predictions in (18) could be made smaller than those in (17), in general.

The complex estimate of x_k that can be formed from (18) is

$$\tilde{x}_k \equiv \tilde{u}_k + i\tilde{v}_k = \sum_{n=1}^{p} (g_n x_{k-n} + h_n x^*_{k-n}), \tag{19}$$

where

$$g_n = \frac{1}{2}[\mu_n + \alpha_n + i(\beta_n - \nu_n)],$$

$$h_n = \frac{1}{2}[\mu_n - \alpha_n + i(\beta_n + \nu_n)]. \tag{20}$$

(The form (19) is the one alluded to in reference 1, footnote to equation (58).) The coefficients $\{g_n\}_1^p$ and $\{h_n\}_1^p$ in (19) are two completely independent sets of complex constants that can be chosen. Since the complex predictive filter in (15) is obviously a special case of (19), it is expected to have a more limited ability in waveform prediction than (19); however, (15) may suffice for spectral approximation purposes. (For a real process, (19) reduces to (15).)

Now suppose that a pair of real processes were actually generated according to p-th order autoregressions,

$$u_k = \sum_{n=1}^{p} (\mu_n u_{k-n} + \nu_n v_{k-n}) + d_k,$$

$$v_k = \sum_{n=1}^{p} (\beta_n u_{k-n} + \alpha_n v_{k-n}) + b_k, \tag{21}$$

where all the quantities are real. Then complex process

$$x_k \equiv u_k + iv_k = \sum_{n=1}^{p} (g_n x_{k-n} + h_n x^*_{k-n}) + w_k, \tag{22}$$

where g_n and h_n are given by (20), and

$$w_k \equiv d_k + ib_k. \tag{23}$$

Now if $\alpha_n = -\mu_n$, $\beta_n = \nu_n$, for $1 \leq n \leq p$ in (21), we get $g_n = 0$, $h_n = \mu_n + i\nu_n$, and (22) yields autoregression

$$x_k = \sum_{n=1}^{p} h_n x^*_{k-n} + w_k. \tag{24}$$

So a linear prediction according to (15) is not expected to do too well on the actual waveform values given by (24), no matter what the statistics of $\{w_k\}$ are. However, the spectral approximation available via (15) of $G_x(f)$ for process (24) can be very good if p is chosen large enough in (15).

As an example, let p = 1 in (24):

$$x_k = hx^*_{k-1} + w_k, \tag{25}$$

where h and w_k are complex with

$$|h| < 1, \tag{26a}$$

$$\overline{w_k w^*_{k-n}} = \delta_{on}, \ \overline{w_k w_{k-n}} = 0. \tag{26b}$$

The excitation process described in (26b) is an analytic process, as witnessed by the zero value for the second ensemble average. We find averages

$$\overline{w_k x_{k-n}} = 0, \ \overline{w_k x^*_{k-n}} = \delta_{on}, \ n \geq 0, \tag{27}$$

and correlations

$$R_n \equiv \overline{x_k x^*_{k-n}} = \frac{1}{1 - |h|^2} \begin{Bmatrix} |h|^n, \ n = 0, 2, 4, \ldots \\ 0, \ n = 1, 3, 5, \ldots \end{Bmatrix}, \tag{28}$$

$$\mathcal{R}_n \equiv \overline{x_k x_{k-n}} = \frac{h}{1 - |h|^2} \begin{Bmatrix} 0, \ n = 0, 2, 4, \ldots \\ |h|^{n-1}, \ n = 1, 3, 5, \ldots \end{Bmatrix}. \tag{29}$$

Since (29) is not zero for all n, process $\{x_k\}$ of (25) is not an analytic process.

If we use the facts (derivable from the definitions above) that

$$R_{-n} = R^*_n, \ \mathcal{R}_{-n} = \mathcal{R}_n, \tag{30}$$

we find that the spectra

$$G(f) \equiv \Delta \sum_{n=-\infty}^{\infty} R_n \exp(-i2\pi fn\Delta)$$

$$= \Delta \frac{1 + |h|^2}{|1-|h|^2 \exp(-i2\pi f2\Delta)|^2}, \tag{31}$$

and

$$\mathcal{G}(f) \equiv \Delta \sum_{n=-\infty}^{\infty} \mathcal{R}_n \exp(-i2\pi fn\Delta)$$

$$= \Delta \frac{2h \cos(2\pi f\Delta)}{|1 - |h|^2 \exp(-i2\pi f2\Delta)|^2}. \tag{32}$$

Generally, spectrum G(f) is real and positive and $\mathcal{G}(f)$ is complex and even about f = 0. For this particular example, (25), G(f) is also even about f = 0.

If we attempt prediction on the process (25) according to (15) and we minimize

$$\overline{|\hat{\varepsilon}_k|^2} \equiv \overline{|\hat{x}_k - x_k|^2}, \tag{33}$$

we find

$$\hat{a}_n = \begin{cases} 0, & n \neq 2 \\ |h|^2, & n = 2 \end{cases} \tag{34}$$

and

$$\min \overline{|\hat{\varepsilon}_k|^2} = \begin{cases} (1 - |h|^2)^{-1}, & p = 1 \\ 1 + |h|^2, & p \geq 2 \end{cases}. \tag{35}$$

Now (34) is hardly the same result as the actual autoregression (25). Nevertheless we find spectral approximation

$$\hat{G}(f) = \left\{ \begin{array}{c} \Delta(1 - |h|^2)^{-1}, \; p = 1 \\ G(f), \; p \geq 2 \end{array} \right\}, \tag{36}$$

from (34); that is, the spectral approximation is exact for $p \geq 2$, despite the obvious error of (34) in terms of waveform prediction.

If instead we attempt prediction on process (25) according to (19) and we minimize

$$\overline{|\tilde{\varepsilon}_k|^2} \equiv \overline{|\tilde{x}_k - x_k|^2}, \tag{37}$$

we find, of course,

$$g_n = 0, \; h_n = \left\{ \begin{array}{c} 0, \; n \neq 1 \\ h, \; n = 1 \end{array} \right\} \tag{38}$$

and

$$\min \overline{|\tilde{\varepsilon}_k|^2} = 1 = \overline{|w_k|^2}. \tag{39}$$

For $|h|^2$ near 1, the error (35) for $p \geq 2$ is approximately twice as great as (39).

For the general autoregression in (22), it is shown in appendix B that for analytic white noise $\{w_k\}$, $\{h_n\}_1^p = 0$ if and only if $\{\mathcal{R}_m\}_o^p = 0$. Thus, given a complex data sequence $\{x_n\}_1^N$ of unknown origin, we can define

$$\hat{\mathcal{R}}_m \equiv \frac{1}{N - m} \sum_{n=m+1}^{N} x_n x_{n-m}, \; 0 \leq m,$$

$$\hat{R}_o \equiv \frac{1}{N} \sum_{n=1}^{N} |x_n|^2. \tag{40}$$

Then, if $|\hat{\mathcal{R}}_m|/\hat{R}_o << 1$ for $0 \leq m \leq q$, the autoregressive model (19) with $\{h_n\}_1^p = 0$ can be used with some confidence for $p \leq q$ to predict the actual waveform. But, even if some $\hat{\mathcal{R}}_m \neq 0$, the autoregressive model (19) with $\{h_n\}_1^p = 0$ can still be used to estimate the spectrum of the process

$\{x_k\}$; however, in order to attain equivalent spectral estimates, it has been observed that more data points, N, are needed when some $h_n \neq 0$ than when $\{h_n\}_1^p = 0$.

If a process is generated according to autoregression

$$x_k = \sum_{n=1}^{p} g_n x_{k-n} + w_k, \tag{41}$$

where process $\{w_k\}$ is not analytic, then $\{\mathcal{R}_m\}$ are not necessarily zero. Thereby prediction (15) will not necessarily give accurate predictions, although the spectral estimate can still be adequate; this situation is discussed further in appendix C. Generation of analytic processes is considered in appendix D, and a more thorough look at the prediction capability of (19) is considered in appendix E.

5. DISCUSSION

A program for estimating the autospectrum of a complex univariate process via linear predictive techniques has been presented. Although it can be used to estimate the cross-spectrum of two real processes, it is not recommended because estimated values of magnitude-coherence greater than unity can result. Instead, the methods of multivariate techniques presented in reference 3 should be employed; in fact, the theory for complex multivariate processes is developed there and a working program given.

Although the program presented here presumes that none of the data points are bad, it may be readily generalized to include bad data points. The method and program presented in reference 1 furnish the necessary background for this extension.

Application of the linear predictive technique in (15) is most successful when the complex process under investiagtion is analytic. Otherwise, the more general prediction technique in (19) is worthy of consideration.

Appendix A

FORTRAN PROGRAM FOR SPECTRAL ANALYSIS

The following program for spectral analysis of a complex process consists of five parts: a main program and four external subroutines. The subroutine BURGCX computes the complex predictive filter coefficients, POWERC computes the fractional power in bands $(J\Delta)^{-1}$ Hz wide, MKLFFT effects a fast Fourier transform (reference 4), and QTRCOS generates a table of cosine values (reference 4).

```
C  SPECTRAL ESTIMATION FOR COMPLEX DATA
C  USER: CHANGE LINE 15 AND REPLACE LINES 20-33
C  N = NUMBER OF COMPLEX DATA POINTS; INTEGER INPUT
C  X(1),...,X(N) = COMPLEX INPUT DATA; ALTERED ON OUTPUT
C  PMAX = MAXIMUM ORDER OF FILTER; INTEGER INPUT
C  J = SIZE OF FFT  (MUST BE A POWER OF 2 TO USE MKLFFT); INTEGER INPUT
C  PBEST = BEST ORDER OF FILTER; INTEGER OUTPUT
C  A(1),...,A(PBEST) = COMPLEX PREDICTIVE FILTER COEFFICIENTS; OUTPUT
C  PROD = PRODUCT(1-ABS(A(P))**2) FOR P=1 TO PBEST; OUTPUT
C  RHO(1),...,RHO(PMAX) = COMPLEX NORMALIZED CORRELATIONS; OUTPUT
C  XX(1),...,XX(J) = FRACTIONAL POWERS; OUTPUT
C  CO(1),...,CO(J/4+1) = QUARTER COSINE TABLE FOR FFT PURPOSES
C  Y IS A REQUIRED COMPLEX AUXILIARY ARRAY
C  YY IS A REQUIRED AUXILIARY ARRAY
      PARAMETER N= 100, PMAX=10, J= 512, J41=J/4+1
      INTEGER PBEST
      COMPLEX X(N),Y(N),A(PMAX),RHO(PMAX)
      DIMENSION XX(J),YY(J),CO(J41)
C  COMPLEX INPUT DATA IN X(1),...,X(N)
      COMPLEX A1,Z(1400)
      DEFINE IRAND=I*5**15-((1-SIGN(1,I*5**15))/2)*34359738367
      DEFINE RAND=FLOAT(I)/34359738367.
      I=5281
      A1=(.65,.65)
      Z(1)=(0.,0.)
      DO 21 L=2,1400
      I=IRAND
      R1=RAND-.5
      I=IRAND
      R2=RAND-.5
21    Z(L)=A1*Z(L-1)+CMPLX(R1,R2)
      DO 22 I=1,N
22    X(I)=Z(I+1400-N)
      PRINT 1
1     FORMAT(1H1,' INPUT DATA:')
      PRINT 4, (X(I),I=1,N)
C  EVALUATE PREDICTIVE FILTER COEFFICIENTS
      CALL BURGCX(N,PMAX,X,Y,PBEST,A,PROD,RHO)
      PRINT 9, X(N)
9     FORMAT(/' MEAN = (',E13.8,',',E13.8,')')
      R1=REAL(Y(N))
      PRINT 10, R1
10    FORMAT(' STANDARD DEVIATION =',E13.8)
      PRINT 2, PBEST
2     FORMAT(/' PBEST =',I3)
      IF(PBEST.EQ.0) GO TO 12
      PRINT 3
3     FORMAT(/' PREDICTIVE FILTER COEFFICIENTS FOR PBEST:')
      PRINT 4, (A(I),I=1,PBEST)
4     FORMAT(4(E18.8,E15.8))
12    PRINT 5, PROD
```

```
5       FORMAT(/' PRODUCT(1-ABS(A(P))**2) =',E13.6)
        PRINT 6
6       FORMAT(/' NORMALIZED CORRELATION COEFFICIENTS:')
        PRINT 4, (RHO(I),I=1,PMAX)
        CALL QTRCOS(CO,J)
C  EVALUATE FRACTIONAL POWERS
        CALL POWERC(PBEST,A,PROD,J,XX,YY,CO,SUM)
        PRINT 7
7       FORMAT(/' FRACTIONAL POWERS:')
        PRINT 8, (XX(I),I=1,J)
8       FORMAT(2X,10E13.6)
        PRINT 11, SUM
11      FORMAT(/' SUM OF FRACTIONAL POWERS =',E13.6)
        END



      SUBROUTINE BURGCX(N,PMAX,X,Y,PBEST,A,PROD,RHO)
C  THIS SUBROUTINE COMPUTES THE COMPLEX PREDICTIVE FILTER COEFFICIENTS
C  N = NUMBER OF COMPLEX DATA POINTS; INTEGER INPUT
C  PMAX = MAXIMUM ORDER OF FILTER; INTEGER INPUT
C  X(1),X(2),...,X(N) = COMPLEX DATA ARRAY ON INPUT; ALTERED ON OUTPUT
C  ON OUTPUT, X(1),X(2),...,X(PMAX) = A(1;PMAX),A(2;PMAX),...,A(PMAX;PMAX)
C  Y(1),Y(2),...,Y(N) = COMPLEX AUXILIARY ARRAY; SCRATCH INPUT
C  ON OUTPUT, Y(1),Y(2),...,Y(PMAX) = A(1;1),A(2;2),...,A(PMAX;PMAX)
C  ON OUTPUT, X(N) = MEAN, AND Y(N) = STANDARD DEVIATION OF INPUT DATA
C  PBEST = BEST ORDER OF FILTER; INTEGER OUTPUT
C  A(1),A(2),...,A(PBEST) = COMPLEX PREDICTIVE FILTER COEFFICIENT ARRAY =
C  A(1;PBEST),A(2;PBEST),...,A(PBEST;PBEST); OUTPUT
C  PROD = PRODUCT(1-ABS(A(P;PBEST))**2) FOR P=1 TO PBEST; OUTPUT
C  RHO(1),...,RHO(PMAX) = COMPLEX NORMALIZED CORRELATIONS; OUTPUT
C  COMPLEX X(N),Y(N),A(PMAX),RHO(PMAX)  IS REQUIRED IN MAIN PROGRAM
      INTEGER PMAX,PBEST,P
      DOUBLE PRECISION SAR,SAI,SB
      COMPLEX S1,G,T
      COMPLEX X(1),Y(1),A(1),RHO(1)
      IF(PMAX.GT.3.*SQRT(N)) PRINT 2, PMAX,N
2     FORMAT(/' PMAX =',I4,' IS TOO LARGE FOR NUMBER OF DATA POINTS N ='
     $,I5)
C  COMPUTE MEAN
      S1=(0.,0.)
      DO 1 I=1,N
1     S1=S1+X(I)
      S1=CMPLX(REAL(S1)/N,AIMAG(S1)/N)
C  SUBTRACT MEAN, AND SCALE TO UNIT VARIANCE
      S2=0.
      DO 3 I=1,N
      X(I)=X(I)-S1
3     S2=S2+REAL(X(I))**2+AIMAG(X(I))**2
      S2=SQRT(S2/(N-1.))
      B=1./S2
      DO 5 I=1,N
      A(I)=CMPLX(REAL(X(I))*B,AIMAG(X(I))*B)
5     Y(I)=X(I)
```

```
C  BEGIN RECURSION
       P=0
       PRODUC=1.
       AICMIN=0.
       PBEST=0
       PROD=1.
6      P=P+1
C  CALCULATE CROSS-GAIN; EQ. 155
       SAR=0.D0
       SAI=0.D0
       SB=0.D0
       L=P+1
       DO 7 I=L,N
       T1=REAL(X(I))
       T2=AIMAG(X(I))
       T3=REAL(Y(I-1))
       T4=AIMAG(Y(I-1))
       SAR=SAR+T1*T3+T2*T4
       SAI=SAI+T2*T3-T1*T4
7      SB=SB+T1**2+T2**2+T3**2+T4**2
       B=2.*SAR/SB
       C=2.*SAI/SB
       G=CMPLX(B,C)
       B=1.-B*B-C*C
       PRODUC=PRODUC*B
C  CALCULATE FILTER COEFFICIENTS; EQS. 160&148. STORE IN X(1),...,X(P)
       X(P)=G
       IF(P.EQ.1) GO TO 8
       L=P/2
       DO 9 I=1,L
       T=X(I)-G*CONJG(X(P-I))
       X(P-I)=X(P-I)-G*CONJG(X(I))
9      X(I)=T
C  CALCULATE NORMALIZED CORRELATION COEFFICIENT; EQ. 149
8      T=X(P)
       IF(P.EQ.1) GO TO 14
       L=P-1
       DO 15 I=1,L
15     T=T+X(I)*RHO(P-I)
14     RHO(P)=T
C  CALCULATE AKAIKE'S INFORMATION CRITERION; EQS. 156&202
       RELERR=B*SNGL(SB)/(2.*(N-P))
       AIC=LOG(RELERR)+4.*FLOAT(P)/(N-P)
       IF(AIC.GE.AICMIN) GO TO 10
       AICMIN=AIC
       PBEST=P
       PROD=PRODUC
       DO 11 I=1,P
11     A(I)=X(I)
10     IF(P.EQ.PMAX) GO TO 16
C  UPDATE FORWARD AND BACKWARD SEQUENCES; EQ. 153
       L=P+1
       DO 12 I=N,L,-1
       T=X(I)-G*Y(I-1)
       Y(I)=Y(I-1)-CONJG(G)*X(I)
```

```
12      X(I)=T
        Y(P)=G
        GO TO 6
16      Y(PMAX)=G
        IF(PBEST.EQ.PMAX) GO TO 4
C   COMPUTE EXTRAPOLATED NORMALIZED CORRELATION
C   COEFFICIENTS FROM PBEST+1 TO PMAX; EQ. 165
        L=PBEST+1
        DO 17 P=L,PMAX
        A(P)=(0.,0.)
        T=(0.,0.)
        DO 18 I=1,PBEST
18      T=T+A(I)*RHO(P-I)
17      RHO(P)=T
4       X(N)=S1
        Y(N)=CMPLX(S2,0.)
        RETURN
        END



        SUBROUTINE POWERC(PBEST,A,PROD,J,XX,YY,CO,SUM)
C   THIS SUBROUTINE COMPUTES THE FRACTIONAL POWERS IN BANDS 1/(J*DELTA)
C   PBEST = BEST ORDER OF FILTER; INTEGER INPUT
C   A(1),...,A(PBEST) = COMPLEX FILTER COEFFICIENT ARRAY; INPUT
C   PROD = PRODUCT(1-ABS(A(P))**2;,FOR P=1 TO PBEST; INPUT
C   J = SIZE OF FFT; INTEGER INPUT
C   XX = AUXILIARY ARRAY ON INPUT
C   XX(1),...,XX(J) = FRACTIONAL POWERS ON OUTPUT
C   YY = AUXILIARY ARRAY; SCRATCH INPUT
C   CO(1),...,CO(J/4+1) = QUARTER COSINE TABLE FOR FFT; INPUT
C   DIMENSION XX(J),YY(J),CO(J/4+1)  IS REQUIRED IN MAIN PROGRAM
C   COMPLEX A(PMAX)  IS REQUIRED IN MAIN PROGRAM, WHERE PMAX.GE.PBEST
        INTEGER PBEST
        DIMENSION XX(1),YY(1),CO(1)
        COMPLEX A(1)
        F=PROD/J
        XX(1)=1.
        YY(1)=0.
        IF(PBEST.EQ.0) GO TO 4
        DO 1 I=1,PBEST
        XX(I+1)=+REAL(A(I))
1       YY(I+1)=+AIMAG(A(I))
4       L=PBEST+2
        DO 2 I=L,J
        XX(I)=0.
2       YY(I)=0.
        L=1.4427*LOG(J)+.5      @ LOG2(J)
        CALL MKLFFT(XX,YY,CO,L,-1)
        SUM=0.
        DO 3 I=1,J
        XX(I)=F/(XX(I)**2+YY(I)**2)
3       SUM=SUM+XX(I)
        RETURN
        END
```

```
      SUBROUTINE MRLFFT(X,Y,CC,M,ISN)
      DIMENSION X(1),Y(1),CC(1),L(12)
      EQUIVALENCE (L12,L(1)),(L11,L(2)),(L10,L(3)),(L9,L(4)),(L8,L(5)),
     1(L7,L(6)),(L6,L(7)),(L5,L(8)),(L4,L(9)),(L3,L(10)),(L2,L(11)),
     2(L1,L(12))
      N=2**M
      ND4=N/4
      ND4P1=ND4+1
      ND4P2=ND4P1+1
      ND2P2=ND4+ND4P2
      DO 8 LO=1,M
      LMX=2**(M-LO)
      LIX=2*LMX
      ISCL=N/LIX
      DO 8 LM=1,LMX
      IARG=(LM-1)*ISCL+1
      IF(IARG.LE.ND4P1) GO TO 4
      C=-CC(ND2P2-IARG)
      S=ISN*CC(IARG-ND4)
      GO TO 6
    4 C=CC(IARG)
      S=ISN*CC(ND4R2-IARG)
    6 DO 8 LI=LIX,N,LIX
      J1=LI-LIX+LM
      J2=J1+LMX
      T1=X(J1)-X(J2)
      T2=Y(J1)-Y(J2)
      X(J1)=X(J1)+X(J2)
      Y(J1)=Y(J1)+Y(J2)
      X(J2)=C*T1-S*T2
      Y(J2)=C*T2+S*T1
    8 CONTINUE
      DO 40 J=1,12
      L(J)=1
      IF(J-M) 31,31,40
   31 L(J)=2**(M+1-J)
   40 CONTINUE
      JN=1
      DO 60 J1=1,L1
      DO 60 J2=J1,L2,L1
      DO 60 J3=J2,L3,L2
      DO 60 J4=J3,L4,L3
      DO 60 J5=J4,L5,L4
      DO 60 J6=J5,L6,L5
      DO 60 J7=J6,L7,L6
      DO 60 J8=J7,L8,L7
      DO 60 J9=J8,L9,L8
      DO 60 J10=J9,L10,L9
      DO 60 J11=J10,L11,L10
      DO 60 JR=J11,L12,L11
      IF(JN-JR) 51,51,52
   51 R=X(JN)
      X(JN)=X(JR)
      X(JR)=R
      FI=Y(JN)
```

```
      Y(JN)=Y(JR)
      Y(JR)=FI
   52 JN=JN+1
   60 CONTINUE
      RETURN
      END



      SUBROUTINE QTRCOS(C,N)
      DIMENSION C(1)
      N41=N/4+1
      SCL=6.283185307/N
      DO 1 I=1,N41
    1 C(I)=COS((I-1)*SCL)
      RETURN
      END
```

Appendix B

PROPERTY OF AUTOREGRESSIVE MODEL

The process of interest here is given by the autoregressive model (22):

$$x_k = \sum_{n=1}^{p} (g_n x_{k-n} + h_n x^*_{k-n}) + w_k, \tag{B-1}$$

where excitation $\{w_k\}$ is analytic white noise. That is,

$$\overline{w_k w^*_{k-m}} = \delta_{om}, \qquad \overline{w_k w_{k-m}} = 0. \tag{B-2}$$

It then follows easily that

$$\overline{w_k x^*_{k-m}} = \delta_{om}, \qquad \overline{w_k x_{k-m}} = 0, \qquad m \geq 0. \tag{B-3}$$

Use of (B-2) and (B-3) then yields correlations

$$R_m \equiv \overline{x_k x_{k-m}} = \sum_{n=1}^{p} (g_n R_{m-n} + h_n R^*_{m-n}), \qquad m \geq 0, \tag{B-4}$$

$$R_m \equiv \overline{x_k x^*_{k-m}} = \sum_{n=1}^{p} (g_n R_{m-n} + h_n R^*_{m-n}) + \delta_{om}, \qquad m \geq 0. \tag{B-5}$$

For given coefficients $\{g_n\}_1^p$ and $\{h_n\}_1^p$, (B-4) and (B-5) constitute simultaneous equations in the unknown correlations.

Now let us suppose that

$$h_n = 0, \qquad 1 \leq n \leq p . \tag{B-6}$$

Then, from (B-4), the first p + 1 equations yield

$$\begin{aligned} \mathcal{R}_o - g_1\mathcal{R}_1 - \ldots - g_p\mathcal{R}_p &= 0 \\ &\vdots \\ \mathcal{R}_p - g_1\mathcal{R}_{p-1} - \ldots - g_p\mathcal{R}_o &= 0. \end{aligned} \tag{B-7}$$

Therefore

$$\mathcal{R}_m = 0, \; 0 \leq m \leq p, \tag{B-8}$$

and from (B-4) and (B-6) it follows that $\mathcal{R}_m$ is zero for all m.

Conversely, assume that

$$\mathcal{R}_m = 0, \; 0 \leq m \leq p. \tag{B-9}$$

Then, from (B-4), the first p equations yield

$$\begin{aligned} h_1R_1 + h_2R_2 + \ldots + h_pR_p &= 0 \\ &\vdots \\ h_1R_{2-p} + h_2R_{3-p} + \ldots + h_pR_1 &= 0. \end{aligned} \tag{B-10}$$

Therefore

$$h_n = 0, \; 1 \leq n \leq p, \tag{B-11}$$

and from (B-4) and (B-11) it follows that $\mathcal{R}_m$ is zero for all m.

Thus we have shown that $\{h_n\}_1^p = 0$ if and only if $\{\mathcal{R}_m\}_o^p = 0$ in the autoregression (B-1) with analytic white noise excitation.

Appendix C

NONANALYTIC WHITE NOISE EXCITATION

Suppose a process is generated according to autoregression

$$x_k = \sum_{n=1}^{p} g_n x_{k-n} + w_k, \tag{C-1}$$

where excitation $\{w_k\}$ satisfies

$$\overline{w_k w_{k-m}^*} = B\delta_{om}, \qquad \overline{w_k w_{k-m}} = \mathcal{B}\delta_{om}. \tag{C-2}$$

$\mathcal{B}$ is complex and nonzero; therefore $\{w_k\}$ is not an analytic process, although it is white.

Then $\{\mathcal{R}_m\}$ need not equal zero, even for autoregression (C-1). For example, for

$$p = 1,\ g_1 = g,\ |g| < 1,\ g \text{ complex}, \tag{C-3}$$

we find correlations

$$R_o = \frac{B}{1 - |g|^2}, \quad R_m = g^m R_o,\ m \geq 1, \quad R_{-m} = R_m^*, \tag{C-4}$$

$$\mathcal{R}_o = \frac{\mathcal{B}}{1 - g^2}, \quad \mathcal{R}_m = g^m \mathcal{R}_o,\ m \geq 1, \quad \mathcal{R}_{-m} = \mathcal{R}_m. \tag{C-5}$$

The corresponding spectra are

$$G(f) = \frac{\Delta B}{\left|1 - ge^{-i2\pi f\Delta}\right|^2}, \tag{C-6}$$

$$\mathcal{G}(f) = \frac{\Delta \mathcal{B}}{1 - 2g\cos(2\pi f\Delta) + g^2}. \tag{C-7}$$

Since the $\{R_m\}$ are not zero, appendix B shows that the coefficients $\{h_n\}$ would not be zero in model (B-1) with an analytic excitation.

Optimum prediction on process (C-1) using (15) gives

$$\hat{a}_n = \begin{cases} g, & n = 1 \\ 0, & n \neq 1 \end{cases}, \qquad \text{(C-8)}$$

with a minimum mean square error equal to B, and the spectral estimate is identically (C-6). Thus, for this example, the nonanalyticity of the excitation is no problem.

For the more general model of (C-1) with $p > 1$, it can be shown that all $\{R_m\}$ are independent of the value of $\mathcal{B}$. Then, although (15) may not be too accurate for waveform prediction, it can still be used for spectral estimation purposes.

Optimum prediction on process (C-1) using (19) gives

$$\hat{g}_1 = g, \qquad \text{other coefficients} = 0, \qquad \text{(C-9)}$$

with a minimum mean square error equal to B. This yields the same result as above.

Appendix D

A METHOD OF GENERATING ANALYTIC PROCESSES

Suppose linear filter H(f) is excited by complex input x(t), yielding output y(t). Then correlation

$$R_y(\tau) \equiv \overline{y(t)y^*(t-\tau)} = \int df \exp(i2\pi f\tau) G_x(f) |H(f)|^2 , \quad \text{(D-1)}$$

and spectrum

$$G_y(f) \equiv \int d\tau \exp(-i2\pi f\tau) R_y(\tau) = G_x(f) |H(f)|^2 . \quad \text{(D-2)}$$

Also correlation

$$\mathcal{R}_y(\tau) \equiv \overline{y(t)y(t-\tau)}$$

$$= \int df \exp(i2\pi f\tau) \mathcal{G}_x(f) H(f) H(-f), \quad \text{(D-3)}$$

and spectrum

$$\mathcal{G}_y(f) \equiv \int d\tau \exp(-i2\pi f\tau) \mathcal{R}_y(\tau) = \mathcal{G}_x(f) H(f) H(-f) . \quad \text{(D-4)}$$

Complex process y(t) is defined as being analytic if (D-3) is zero for all τ. Suppose that filter

$$H(f) = 0 \text{ for } f < 0. \quad \text{(D-5)}$$

Denote the output of filter (D-5) by $y_+(t)$. Then (D-4) shows that $\mathcal{G}_y(f)$ and $\mathcal{R}_y(\tau)$ are both identically zero for all argument values. Therefore single-sided waveform $y_+(t)$ is an analytic process.

Let complex envelope

$$\underline{y}(t) \equiv y_+(t) \exp(-i2\pi f_o t). \quad \text{(D-6)}$$

Then

$$\mathcal{R}_{\underline{y}}(\tau) \equiv \overline{\underline{y}(t)\underline{y}^*(t - \tau)} = \mathcal{R}_{y+}(\tau) \exp(-i2\pi f_o \tau) = 0 \qquad \text{(D-7)}$$

for any f_o. Thus the complex envelope of any stationary process is an analytic process.

On the other hand, for the two real processes u(t) and v(t), no linear combination, $\alpha u(t) + \beta v(t)$, where α and β are complex, ever yields an analytic process unless $R_{uu}(\tau)$, $R_{vv}(\tau)$, and $R_{uv}(\tau)$ satisfy very special restrictions. Thus the process constructed in (1) was not analytic and could not have been expected to yield good prediction capability via (15).

Appendix E

CAPABILITY OF A MORE GENERAL PREDICTION MODEL

If p is infinite in (19), we have prediction

$$\tilde{x}_k = \sum_{n=1}^{\infty} (g_n x_{k-n} + h_n x^*_{k-n}). \tag{E-1}$$

Minimization of $\overline{|\tilde{\varepsilon}_k|^2} \equiv \overline{|\tilde{x}_k - x_k|^2}$ yields the simultaneous equations

$$\sum_{n=1}^{\infty} (g_n R_{m-n} + h_n \mathcal{R}^*_{m-n}) = R_m, \quad 1 \leq m,$$

$$\sum_{n=1}^{\infty} (g_n \mathcal{R}_{m-n} + h_n R^*_{m-n}) = \mathcal{R}_m, \quad 1 \leq m. \tag{E-2}$$

It can then be shown that $\tilde{\varepsilon}_k$ is a white process with

$$\min \overline{|\tilde{\varepsilon}_k|^2} = R_o - \sum_{n=1}^{\infty} (g_n R^*_n + h_n \mathcal{R}^*_n). \tag{E-3}$$

Also it can be shown that

$$\overline{\tilde{\varepsilon}_k \tilde{\varepsilon}_{k-m}} = 0 \text{ for } m \neq 0, \tag{E-4}$$

with

$$\overline{\tilde{\varepsilon}_k^{\,2}} = \mathcal{R}_o - \sum_{n=1}^{\infty} (g_n \mathcal{R}_n + h_n R_n). \tag{E-5}$$

However, $\tilde{\varepsilon}_k$ is not an analytic process since (E-5) is not zero. The simplest example to demonstrate this is

$$R_n = R_o \delta_{on}, \; \mathcal{R}_n = \mathcal{R}_o \delta_{on}, \tag{E-6}$$

for which (E-3) and (E-5) yield R_o and $\mathcal{R}_o$, respectively.

The spectral relations for (E-1) take the forms

$$G_{\tilde{X}}(f) = G_X(f)|A(f)|^2 + G_X(-f)|B(f)|^2$$

$$+ \mathcal{G}_X(f)\, A(f)B^*(f) + [\mathcal{G}_X(f)A(f)B^*(f)]^* \qquad \text{(E-7)}$$

and

$$\mathcal{G}_{\tilde{X}}(f) = \mathcal{G}_X(f)A(f)A(-f) + \mathcal{G}_X^*(f)B(f)B(-f)$$

$$+ G_X(f)A(f)B(-f) + G_X(-f)A(-f)B(f), \qquad \text{(E-8)}$$

where

$$A(f) \equiv \sum_{n=1}^{\infty} g_n \exp(-i2\pi f n\Delta)$$

and

$$B(f) \equiv \sum_{n=1}^{\infty} h_n \exp(-i2\pi f n\Delta) \qquad \text{(E-9)}$$

are considered known after solution of (E-2) for coefficients $\{g_n\}$ and $\{h_n\}$. Equations (E-7) and (E-8) can be solved for $G_X(f)$ and $\mathcal{G}_X(f)$:

$$\begin{bmatrix} A_-A^* & B_-B^* & A_-B^* & A^*B_- \\ B\,B^* & A\,A^* & A\,B^* & A^*B \\ A_-B & A\,B_- & A\,A_- & B\,B_- \\ A^*B^* & A^*B_-^* & B^*B_-^* & A^*A_-^* \end{bmatrix} \begin{bmatrix} G_{X_-} \\ G_X \\ G_X \\ G_X^* \end{bmatrix} = \begin{bmatrix} G_{\tilde{X}_-} \\ G_{\tilde{X}} \\ \mathcal{G}_{\tilde{X}} \\ \mathcal{G}_{\tilde{X}}^* \end{bmatrix}, \qquad \text{(E-10)}$$

where

$$A \equiv A(f),\ A_- \equiv A(-f),$$

$$G_X \equiv G_X(f),\ G_{X_-} \equiv G_X(-f),$$

$$\mathcal{G}_X \equiv \mathcal{G}_X(f),\ \mathcal{G}_X^* \equiv \mathcal{G}_X^*(f). \qquad \text{(E-11)}$$

This requires the inverse of a 4 x 4 complex matrix at each value of frequency f.

Thus an alternative spectral estimation technique is available from the more general prediction model in (E-1). Whether it is worthwhile in terms of stability and resolution is unknown, as it has not been pursued.

LIST OF REFERENCES

1. A. H. Nuttall, Spectral Analysis of a Univariate Process with Bad Data Points, via Maximum Entropy and Linear Predictive Techniques, NUSC Technical Report 5303, 26 March 1976.

2. T. Ulrych and O. Jensen, "Cross-Spectral Analysis Using Maximum Entropy," Geophysics, vol. 39, no. 3, June 1974, pp. 353-354.

3. A. H. Nuttall, Multivariate Linear Predictive Spectral Analysis, Employing Weighted Forward and Backward Averaging: A Generalization of Burg's Algorithm, NUSC Technical Report 5501, 13 October 1976. Program also available in NUSC Technical Document 5419, 19 May 1976.

4. J. F. Ferrie, G. C. Carter, and C. W. Nawrocki, "Availability of Markel's FFT Algorithm," NUSC Technical Memorandum TC-1-73, 15 January 1973.

NUSC Report 5529
3 December 1976

Probability Distribution of Spectral Estimates Obtained Via Overlapped FFT Processing of Windowed Data

Albert H. Nuttall

ABSTRACT

The characteristic function of spectral estimates obtained via overlapped FFT processing of windowed data is presented for a random process containing a signal tone and Gaussian noise. For the special case of noise-alone, the probability distribution of the estimate is plotted and compared with an approximation utilizing only the first two moments and found to be in excellent agreement in probability over the range (.0001, .9999) for several data windows, overlaps, and time-bandwidth products. This result means that knowledge of the equivalent degrees of freedom of the spectral estimate is adequate for a complete probabilistic description, even when the overlap results in significant statistical dependence of the component FFT outputs.

Approved for public release; distribution unlimited.

TABLE OF CONTENTS

	Page
LIST OF ILLUSTRATIONS	ii
LIST OF SYMBOLS	iii
INTRODUCTION	1
CHARACTERISTIC FUNCTION FOR SIGNAL PLUS NOISE	2
MEAN AND VARIANCE FOR SIGNAL PLUS NOISE	5
PROBABILITY DISTRIBUTION FOR NOISE-ALONE	9
FLUCTUATIONS OF CROSS SPECTRAL ESTIMATE	22
DISCUSSION	25
APPENDIX A — DERIVATION OF CHARACTERISTIC FUNCTION	A-1
APPENDIX B — DERIVATION OF COVARIANCE MATRIX	B-1
APPENDIX C — NUMERICAL COMPUTATION OF CUMULATIVE PROBABILITY DISTRIBUTION	C-1
REFERENCES	R-1

LIST OF ILLUSTRATIONS

Figure		Page
1	Spectral Estimates for Signal Plus Noise.	8
2	Exact Distribution for Hanning Window	14
3	Approximation for Hanning Window.	16
4	Exact Distribution for Cubic Window	18
5	Appi ·mation for Cubic Window.	20

LIST OF SYMBOLS

FFT	Fast Fourier Transform
f	Analysis frequency
$\hat{G}(f)$	Power spectral estimate
P	Number of pieces in average
$Y_p(f)$	Fourier transform of p-th weighted data segment
t	Time
$x(t)$	Available complex data process
$w(t)$	Data window
L	Length of data window
S	Shift of adjacent data windows
$s(t)$	Signal waveform
$n(t)$	Noise waveform
A	Signal tone amplitude
f_o	Signal tone frequency
θ	Signal tone phase
Y_{ps}, Y_{pn}	Signal and noise components of p-th transform
$W(f)$	Spectral window (Fourier transform of $w(t)$)
B	Bandwidth of spectral window
$C(\xi)$	Characteristic function of $\hat{G}(f)$
$\mathbf{K}$	Covariance matrix of $\{Y_{pn}\}$
λ_p	p-th eigenvalue of $\mathbf{K}$

LIST OF SYMBOLS (cont'd)

$\mathbf{m}$	Column matrix of $\{Y_{ps}\}$
$\mathbf{Q}$	Normalized modal matrix of $\mathbf{K}$
μ	Transformed means (eq. 11)
Superscript T	Transpose of matrix
$G_n(f)$	Noise spectral density at frequency f
$\phi_w(\tau)$	Autocorrelation of w(t) (eq. 14)
r_m	Normalized autocorrelation (eq. 16)
$\mathbf{R}$	Matrix of $\{r_m\}$ (eq. 15)
Var	Variance
Superscript H	Conjugate transpose of matrix
$Q_s(f)$	Output signal power of window filter centered at f
$Q_n(f)$	Output noise power of window filter centered at f
EDF	Equivalent degrees of freedom (eq. 25)
$\hat{dB}$	Decibel equivalent of $\hat{G}(f)$ (eq. 29)
$\hat{g}$	Normalized spectral estimate (eq. 34)
$C_g(\xi)$	Characteristic function of $\hat{g}$
$\lambda_p^{(R)}$	p-th eigenvalue of $\mathbf{R}$
v	Threshold value
B_k	Coefficients (eq. 37)
t	Random variable with same mean and variance as $\hat{g}$.
$C_t(\xi)$	Characteristic function of t
b	Constant in $C_t(\xi)$

LIST OF SYMBOLS (cont'd)

K	Equivalent degrees of freedom for noise-alone
Γ	Gamma function
${}_1F_1$	Confluent hypergeometric function
BT	Product of analysis bandwidth and available record length
$G_{xy}(f)$, $\hat{G}_{xy}(f)$	Cross spectrum and its estimate
A	Amplitude of cross spectral estimate

PROBABILITY DISTRIBUTION OF SPECTRAL ESTIMATES OBTAINED VIA OVERLAPPED FFT PROCESSING OF WINDOWED DATA

INTRODUCTION

Estimation of the autospectrum of a stationary random process by means of overlapped FFT processing of windowed data (the so-called direct method) is a popular and efficient method, especially for data with pure tones present. Stable spectral estimates, as measured by the equivalent degrees of freedom of the spectral estimate, result when the product of the available record length and the desired frequency resolution (the time-bandwidth product) is large in comparison with unity. (See, for example, references 1 and 2 and the references listed therein.)

The equivalent degrees of freedom of the spectral estimate is an incomplete probabilistic descriptor, because it depends only on the mean and variance of the random variable. In this report, we address the problem of obtaining the characteristic function of the spectral estimate with overlap processing, of a signal tone present in Gaussian noise, and thence the cumulative probability distribution (perhaps by numerical means as given in references 3 and 4). For the case of signal-absent also, we will compare the exact probability distribution with an approximate distribution that uses only the first two moments of the spectral estimate, to see when the approximate distribution can

be used as a valid probabilistic description. Some related work is available in reference 5 and the papers cited therein.

A discussion of the relative stability of the spectral estimates with signal tones present, and of a cross-spectral estimate, completes the presentation.

CHARACTERISTIC FUNCTION FOR SIGNAL PLUS NOISE

The method and conditions of processing are described fully in reference 1 and, for sake of brevity, will not be repeated here. The power spectral estimate at analysis frequency, f, is given by (reference 1, pp. 2-4)

$$\hat{G}(f) = \frac{1}{P} \sum_{p=1}^{P} |Y_p(f)|^2, \tag{1}$$

where P is the total number of weighted data segments. Here*

$$Y_p(f) = \int dt \, \exp(-i2\pi ft) \, x(t) \, w\left[t - \frac{1}{2} L - (p-1)S\right], \tag{2}$$

where x(t) is the available (complex) data process, w(t) is the data window of length L, and S is the amount of shift each adjacent data window undergoes. The fractional overlap is therefore 1 - S/L.

*Integrals without limits are over the range of non-zero integrand.

If we let x(t) be composed of a pure signal tone*

$$s(t) = A \exp(i2\pi f_o t + i\theta) \tag{3}$$

and zero-mean Gaussian noise n(t), (2) can be expressed as

$$Y_p = Y_{ps} + Y_{pn} , \tag{4}$$

where the variable f is suppressed for notational convenience and complex (non-random) constant

$$Y_{ps} = A\, W(f-f_o) \exp\left[i\theta - i2\pi(f-f_o)\left(\frac{1}{2} L + (p-1)S\right)\right] , \tag{5}$$

where

$$W(f) \equiv \int dt \exp(-i2\pi ft)\, w(t). \tag{6}$$

$|W(f)|^2$ is called the spectral window (see equation (5), reference 1), and has analysis bandwidth B. Now if analysis frequency, f, is not within a bandwidth, B, of tone frequency, f_o, (5) will be zero; therefore, we limit consideration to $|f-f_o|<B$. The remaining term in (4),

$$Y_{pn} = \int dt \exp(-i2\pi ft)\, n(t)\, w\left[t - \frac{1}{2} L - (p-1)S\right] , \tag{7}$$

is complex Gaussian since n(t) is Gaussian.

Substituting (4) in (1), the spectral estimate is given by

$$\hat{G}(f) = \frac{1}{P}\sum_{p=1}^{P} |Y_{ps} + Y_{pn}|^2 , \tag{8}$$

*The generalization to several separated tones will be obvious.

where $\{Y_{ps}\}$ are complex constants and $\{Y_{pn}\}$ are complex correlated Gaussian zero-mean random variables, and the correlation is due to the overlapped processing.

In appendix A, the characteristic function of forms like (8) is evaluated; it specializes here to the form

$$C(\xi) = \prod_{p=1}^{P} \left\{ (1-i\lambda_p \xi/P)^{-1} \exp\left(\frac{i|\mu_p|^2 \lambda_p \xi/P}{1-i\lambda_p \xi/P} \right) \right\}, \tag{9}$$

where $\{\lambda_p\}$ are the eigenvalues of P x P matrix

$$\mathbf{K} \equiv \left[E\left\{ Y_{pn} Y^*_{qn} \right\} \right]_1^P , \tag{10}$$

and

$$\mu = \mathbf{Q}^H \mathbf{K}^{-\frac{1}{2}} \mathbf{m} , \tag{11}$$

where $\mathbf{Q}$ is the normalized modal matrix of $\mathbf{K}$, and

$$\mathbf{m} = \left[Y_{1s} \ldots Y_{Ps} \right]^T . \tag{12}$$

The evaluation of $\mathbf{K}$ in (10) is considered in appendix B. It is given by

$$\mathbf{K} = \left[K_{q-p} \right] = G_n(f) \phi_w(0) \mathbf{R} , \tag{13}$$

where $G_n(f)$ is the noise spectral density at analysis frequency, f;

$$\phi_w(\tau) = \int dt\ w(t) w^*(t-\tau); \tag{14}$$

and

$$\mathbf{R} = \left[r_{q-p}\right] = \begin{bmatrix} 1 & r_1 & r_2 & \cdots & r_{P-1} \\ r_{-1} & \ddots & & & \\ \vdots & & & & \\ \vdots & & & & \\ r_{1-P} & & & & 1 \end{bmatrix} , \tag{15}$$

where

$$r_m = \frac{\phi_w(mS)}{\phi_w(0)} \quad . \tag{16}$$

A Fourier transformation of (9) would yield the probability density function of the spectral estimate (8), for a tone present. This would have to be done numerically, but has not been pursued here.

MEAN AND VARIANCE FOR SIGNAL PLUS NOISE

By means of (A-16), the mean and variance* of spectral estimate, $\hat{G}(f)$, in (8) can be expressed as

$$\text{Mean}\left\{\hat{G}(f)\right\} = K_o + \frac{1}{P}\sum_{k=1}^{P} |m_k|^2 \ , \tag{17}$$

$$\text{Var}\left\{\hat{G}(f)\right\} = \frac{1}{P}\sum_{k=1-P}^{P-1}\left(1-\frac{|k|}{P}\right)|K_k|^2 + \frac{2}{P^2}\,\mathbf{m}^H\mathbf{K}\,\mathbf{m} \ , \tag{18}$$

in terms of the quantities in (12) and (13). Employing the explicit relationships in (12) and (13), there follows

$$\text{Mean}\left\{\hat{G}(f)\right\} = G_n(f)\phi_w(0) + A^2|W(f-f_o)|^2 \ , \tag{19}$$

*More generally, the cumulants are given by (A-7).

and

$$\text{Var}\left\{\hat{G}(f)\right\} = \left[G_n(f)\phi_w(0)\right]^2 \frac{1}{P}\sum_{k=1-P}^{P-1}\left(1-\frac{|k|}{P}\right)|r_k|^2$$

$$+2A^2|W(f-f_o)|^2 G_n(f)\phi_w(0)\frac{1}{P}\sum_{k=1-P}^{P-1}\left(1-\frac{|k|}{P}\right)r_k \exp\left(ik2\pi(f-f_o)S\right) \quad , \quad (20)$$

where we have employed (15) and (5).

At this point, it is convenient to define the output signal power of a window filter with transfer function, W, centered at f as

$$Q_s(f) = A^2|W(f-f_o)|^2 \quad , \quad (21)$$

and the output noise power of the same filter as

$$Q_n(f) = \int d\mu\, G_n(\mu)|W(\mu-f)|^2 \cong G_n(f)\int d\mu|W(\mu-f)|^2 = G_n(f)\phi_w(0). \quad (22)$$

Then (19) and (20) take the forms

$$\text{Mean}\left\{\hat{G}(f)\right\} = Q_n(f) + Q_s(f) \quad (23)$$

and

$$\text{Var}\left\{\hat{G}(f)\right\} = Q_n^2(f)\frac{1}{P}\sum_{k=1-P}^{P-1}\left(1-\frac{|k|}{P}\right)|r_k|^2$$

$$+2Q_s(f)Q_n(f)\frac{1}{P}\sum_{k=1-P}^{P-1}\left(1-\frac{|k|}{P}\right)r_k \exp(ik2\pi(f-f_o)S). \quad (24)$$

From (24), we see that the presence of signal ($A \neq 0$) always increases the <u>absolute</u> level of the variance of the spectral estimate over that for noise-alone. If the noise is absent, the variance of the estimate is zero. If the signal is absent, the equivalent degrees of freedom, defined as

$$EDF_n \equiv \frac{2(\text{Mean})^2}{\text{Variance}} = \frac{2}{\frac{1}{P}\sum_{k=1-P}^{P-1}\left(1-\frac{|k|}{P}\right)|r_k|^2}, \qquad (25)$$

is identical to equation (8), reference 1, as it should be.

On the other hand, for $Q_s(f) >> Q_n(f)$,

$$EDF_s \equiv \frac{2(\text{Mean})^2}{\text{Variance}} \cong \frac{Q_s(f)}{Q_n(f)\,\frac{1}{P}\sum_{k=1-P}^{P-1}\left(1-\frac{|k|}{P}\right) r_k \exp(ik2\pi(f-f_o)S)}, \qquad (26)$$

When a strong signal is present, EDF_s is larger than EDF_n by approximately the ratio $\frac{1}{2}\,Q_s(f)/Q_n(f) >> 1$, since the ratio of sums in (25) and (26) is approximately unity for $f \cong f_o$ and reasonable overlaps (see (27) below). That is, the relative fluctuation in the spectral estimate is reduced by the addition of signal, even though the absolute variance increases.

For Hanning weighting and 50% overlap (S = L/2), we find $r_o = 1$, $r_{\pm 1} = 1/6$, $r_k = 0$ for $k \geq 2$. Then the two sums in (25) and (26) take on the values

$$1 + (1-\tfrac{1}{P})\tfrac{1}{18}\ ,\ 1 + (1-\tfrac{1}{P})\tfrac{1}{3}\cos\left[2\pi(f-f_o)S\right], \qquad (27)$$

respectively. The former value is slightly larger than unity, whereas the latter value varies between approximately 2/3 and 4/3, depending on the exact location of the signal tone frequency, f_o, with respect to the analysis frequency, f. For an FFT approach, at least one bin has

its frequency location, f, such that $|f-f_o| \leq (2L)^{-1}$; thus, at least one frequency bin is located such that the latter value in (27) is larger than unity.

Figure 1A represents the power spectral estimate, (1), plotted on a linear scale proportional to watts. The "ribbon width" in the region of noise-alone is denoted by a. The amount of fluctuation of the estimate at f_o is denoted by b and is larger than a. (The quantity b is observable only by rerunning the spectral estimation procedure for independent noise segments.)

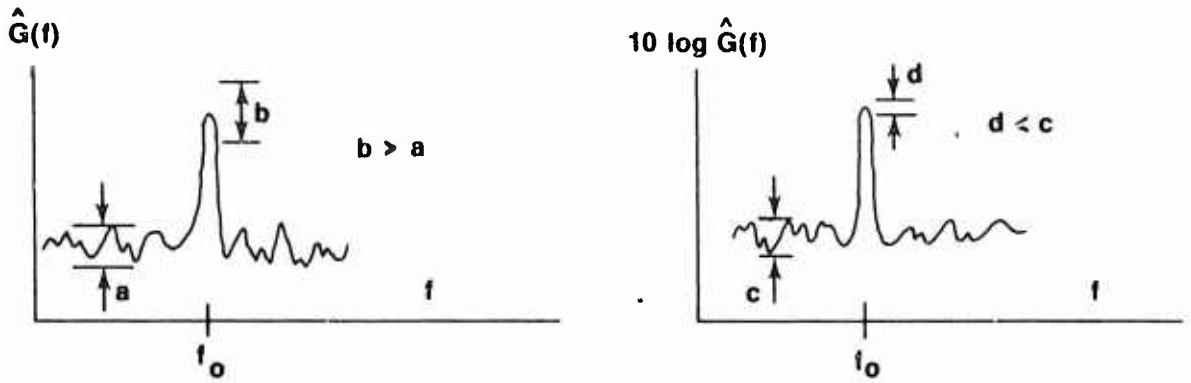


Figure 1. Spectral Estimates for Signal Plus Noise

If, instead, the power spectral estimate is plotted on a dB scale (see figure 1B), the noise-alone ribbon width, c, is larger than the fluctuation, d, of the estimate at f_o. The mathematics behind this

conclusion follows. Let the spectral estimate at frequency f be expressed as

$$\hat{G}(f) = m+x, \tag{28}$$

where m is non-random and x has zero-mean and variance σ^2. Then

$$\hat{dB} \equiv 10 \log \hat{G}(f) = 10 \log m + 10 \log(1+\frac{x}{m}). \tag{29}$$

Now suppose that $\sigma/m<<1$, which could be realized by means of a large number of pieces, P, or a high signal to noise ratio; then

$$\hat{dB} \cong 10 \log m + \frac{10}{\ln 10} \frac{x}{m} . \tag{30}$$

The last term in (30) is proportional to the relative stability of the spectral estimate (28); in fact

$$\text{Var}\left\{\hat{dB}\right\} \cong \left(\frac{10}{\ln 10}\right)^2 \frac{\sigma^2}{m^2} , \tag{31}$$

which can be made arbitrarily small. Thus a plot like figure 1 is easily achievable and should be anticipated for a pure tone in Gaussian noise.

PROBABILITY DISTRIBUTION FOR NOISE-ALONE

For noise-alone, the mean and variance of spectral estimate, $\hat{G}(f)$, are available from (19), (20), and (16) as

$$\begin{aligned} \text{Mean}\left\{\hat{G}(f)\right\} &= G_n(f)\phi_w(0), \\ \text{Var}\left\{\hat{G}(f)\right\} &= G_n^2(f) \frac{1}{P} \sum_{k=1-P}^{P-1} \left(1- \frac{|k|}{P}\right) |\phi_w(kS)|^2 , \end{aligned} \tag{32}$$

which agree with equations (5) and (6), reference 1, respectively. More generally, the characteristic function follows from (9) as

$$C(\xi) = \left[\prod_{p=1}^{P} \{1 - i\lambda_p \xi/P\} \right]^{-1} . \tag{33}$$

Now let us define a normalized random variable

$$\hat{g} \equiv \frac{\hat{G}(f)}{G_n(f)\phi_w(0)} ; \tag{34}$$

notice that the scale factor is independent of P and the amount of overlap. Thus the mean $E\{\hat{g}\} = 1$, and the characteristic function of $\hat{g}$ is

$$C_g(\xi) = \left[\prod_{p=1}^{P} \{1 - i\lambda_p^{(R)} \xi/P\} \right]^{-1} , \tag{35}$$

where $\{\lambda_p^{(R)}\}$ are the eigenvalues of matrix $\mathbf{R}$ in (15). Then by a partial fraction expansion, the probability that random variable $\hat{g}$ remains below a threshold value, v, is found to be

$$\text{Prob}\,(\hat{g}<v) = 1 - \sum_{k=1}^{P} B_k \exp\left(- \frac{v}{\lambda_k^{(R)}/P} \right), \quad v>0, \tag{36}$$

where

$$B_k = \frac{\left[\lambda_k^{(R)}\right]^{P-1}}{\prod_{\substack{p=1 \\ p\neq k}}^{P} \left\{\lambda_k^{(R)} - \lambda_p^{(R)}\right\}} , \qquad 1 \le k \le P. \tag{37}$$

We have assumed all the eigenvalues of $\mathbf{R}$ to be unequal; this is the case if the overlap is greater than 0, which is the case of most practical interest. The eigenvalues are all non-negative since $\mathbf{R}$ is a non-negative definite matrix (see appendix B).

Equation (36) is an exact expression for the cumulative probability distribution in terms of the eigenvalues of matrix $\mathbf{R}$. If we consider another random variable, t, with the same mean and variance as $\hat{g}$, a candidate approximate characteristic function is (guided by form (35))

$$C_t(\xi) = (1-i\xi/b)^{-b} , \tag{38}$$

where, in order to maintain the same variance, we choose

$$\frac{1}{b} = \frac{1}{P^2}\sum_{p=1}^{P} \lambda_p^{(R)^2} = \frac{1}{P^2}\sum_{p,q=1}^{P} |r_{p-q}|^2 = \frac{1}{P}\sum_{k=1-P}^{P-1} \left(1-\frac{|k|}{P}\right)|r_k|^2 . \tag{39}$$

Equation (8), reference 1, shows that b = K/2, i.e., half of the equivalent degrees of freedom. Then the approximate probability density function is

$$p(t) = \frac{1}{\Gamma(b)}\, b^b t^{b-1} e^{-bt} , \quad t>0, \tag{40}$$

and the approximate cumulative probability distribution is (equations 6.5.2 and 6.5.12, reference 6):

$$\int_0^v dt\, p(t) = \frac{1}{\Gamma(b+1)}\, (bv)^b e^{-bv}\, {}_1F_1(1;1+b;bv), \quad v>0. \tag{41}$$

(A further simpler approximation, not pursued here, would be to set b_1 = integer part of b, $b_2 = b_1 + 1$, and bracket the results above by two simpler sums.)

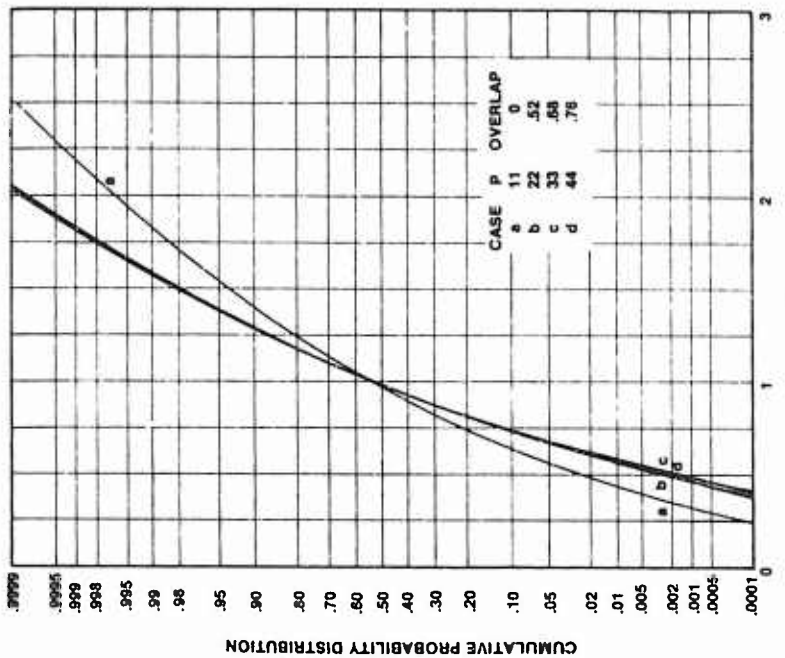
We shall now make quantitative comparisons between exact result (36) and approximation (41) which has the same mean and variance. The question is: is b in (39) and (41) a sufficient statistic to accurately quantitatively describe the exact cumulative probability distribution (36), for representative data windows, overlap, number of pieces, and time-bandwidth products, over the range of probabilities of interest to most users? If so, then attention can be confined to the equivalent degrees of freedom and its maximization alone, as was done in reference 1; this simplification would be most worthwhile and of obvious importance.

The actual numerical computation of the cumulative probability distribution Prob($\hat{g}$<v), is considered in appendix C. In figure 2, the exact cumulative probability distribution for Hanning windowing is presented for time-bandwidth product BT = 8, 16, 32, 64, where T is the available record length and B is the desired resolution bandwidth. In each plot, the overlap is varied from 0 to approximately 75%, and the distribution plotted on a normal probability ordinate covering the range (.0001, .9999). The fact that the curves are not straight lines over this range means that a Gaussian approximation to the power spectral estimate would not suffice. However, the Gaussian approximation would be a fairly good one for larger BT and P (see figure 2D, for example).

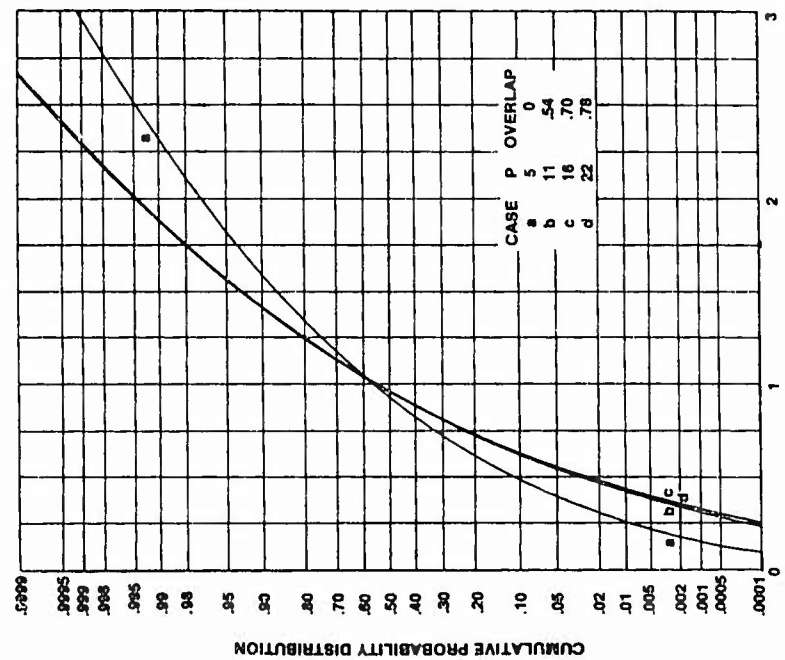
The fact that the curves in figure 2 are virtually identical for overlaps greater than 50% means that there is little point in choosing overlaps greater than this amount. This confirms the choices of overlap made in reference 1, where attention was confined to the equivalent degrees of freedom. The ideal distribution would be a vertical line at $v = 1$; the closeness of these curves to the ideal is a measure of the spread of the spectral estimate.

The corresponding results for the approximation (41) are presented in figure 3. The curves are virtually identical to those of figure 2 over the complete range of probabilities considered, for various values of BT and overlap.

For a cubic window, the exact results and the approximation are given in figures 4 and 5, respectively. The conclusions are identical to those made for the Hanning window.

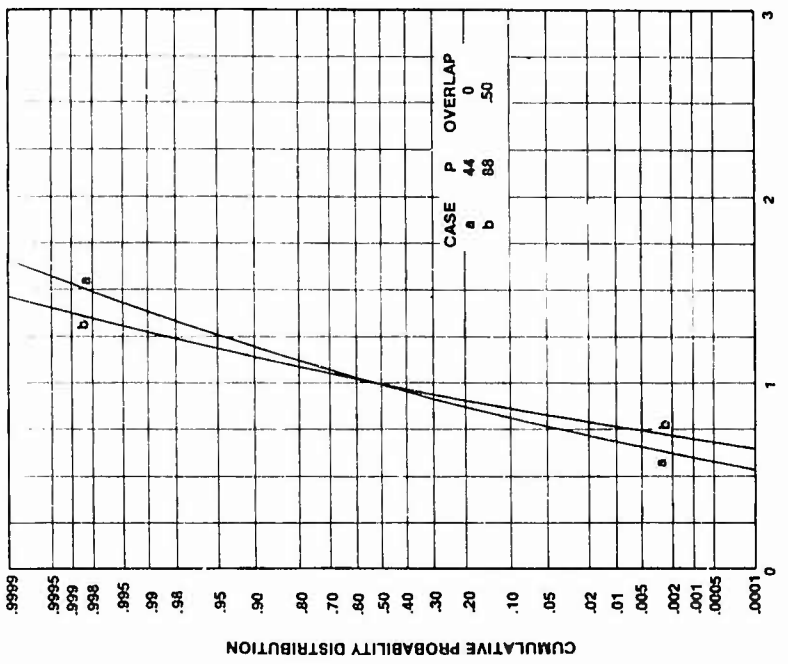


2B. BT=16

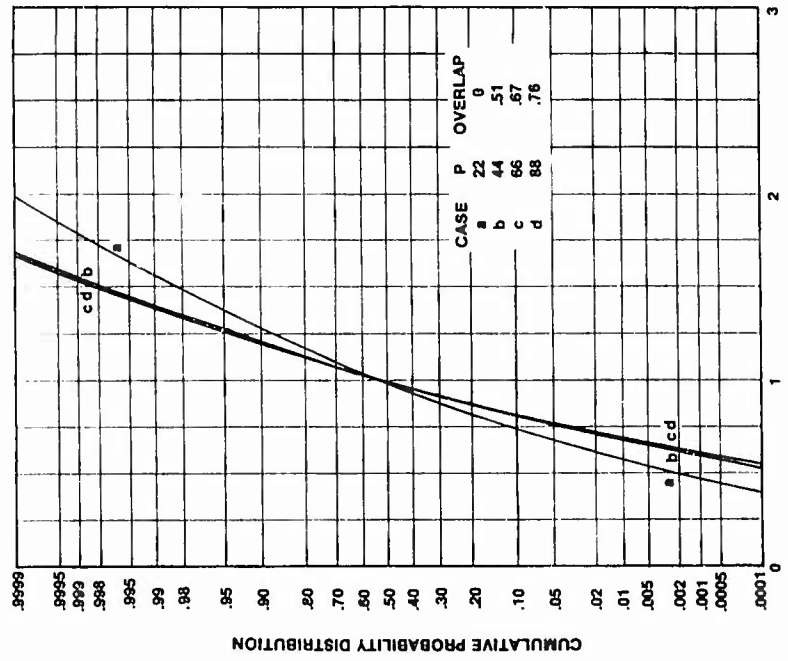


2A. BT=8

Figure 2. Exact Distribution for Hanning Window

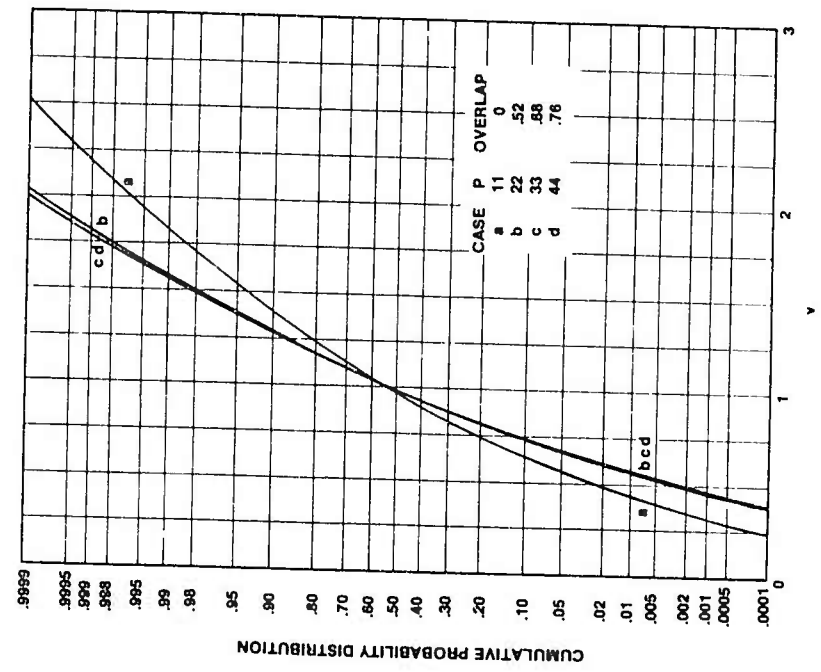


2D. BT=64

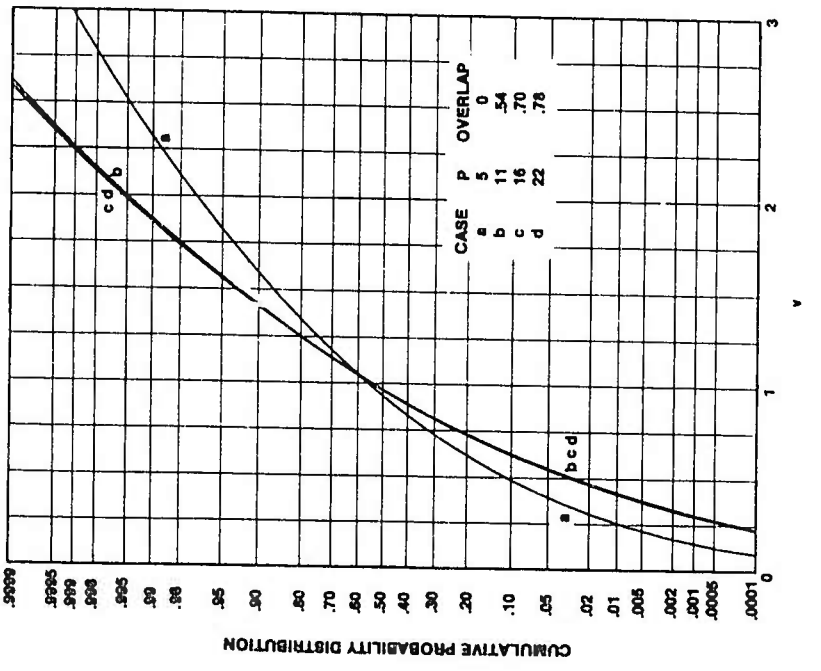


2C. BT=32

Figure 2. (Cont'd) Exact Distribution for Hanning Window

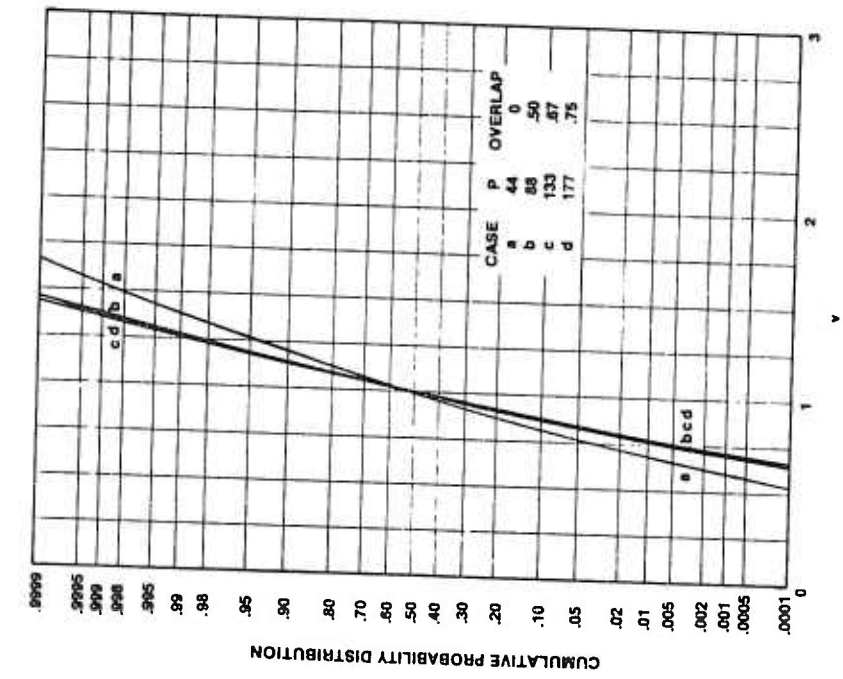


3B. BT=16

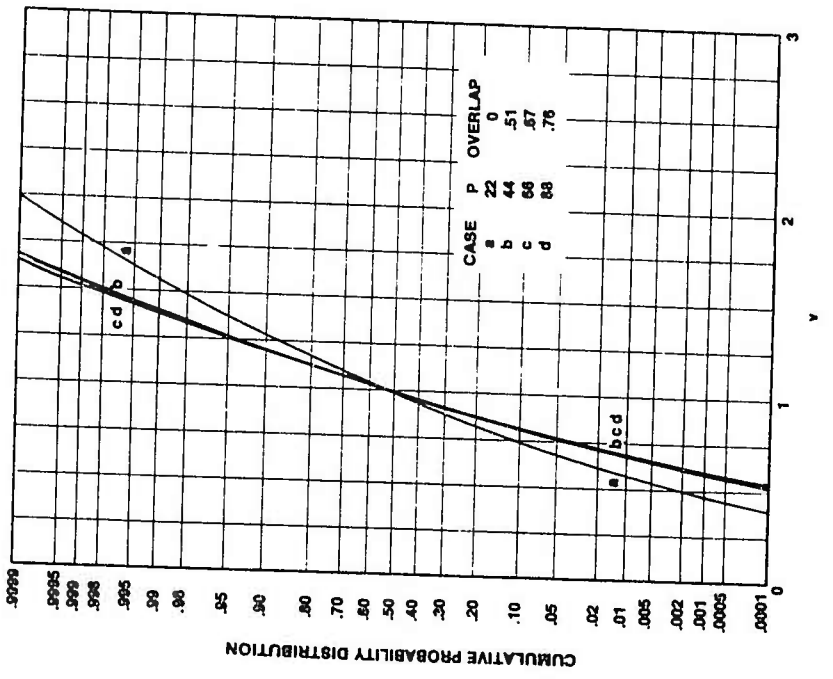


3A. BT=8

Figure 3. Approximation for Hanning Window

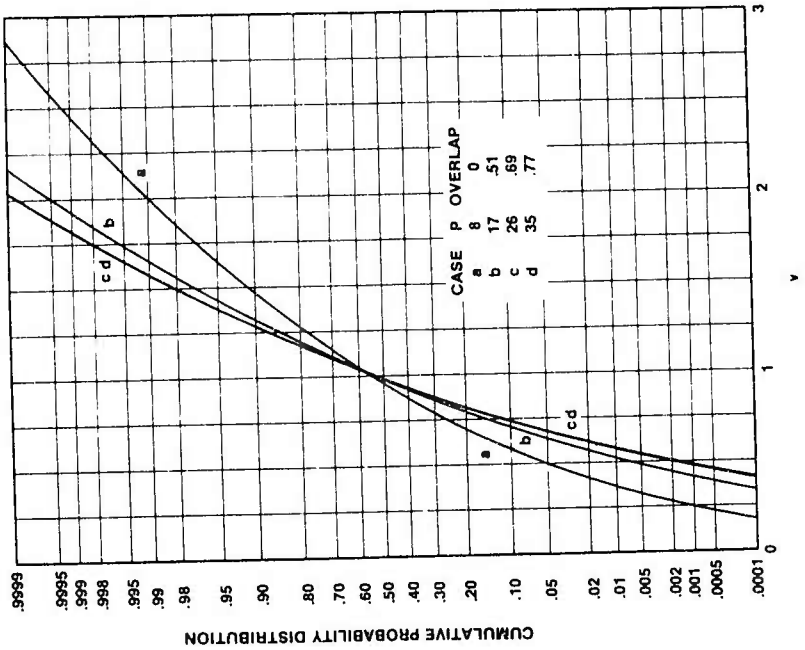


3D. BT=64

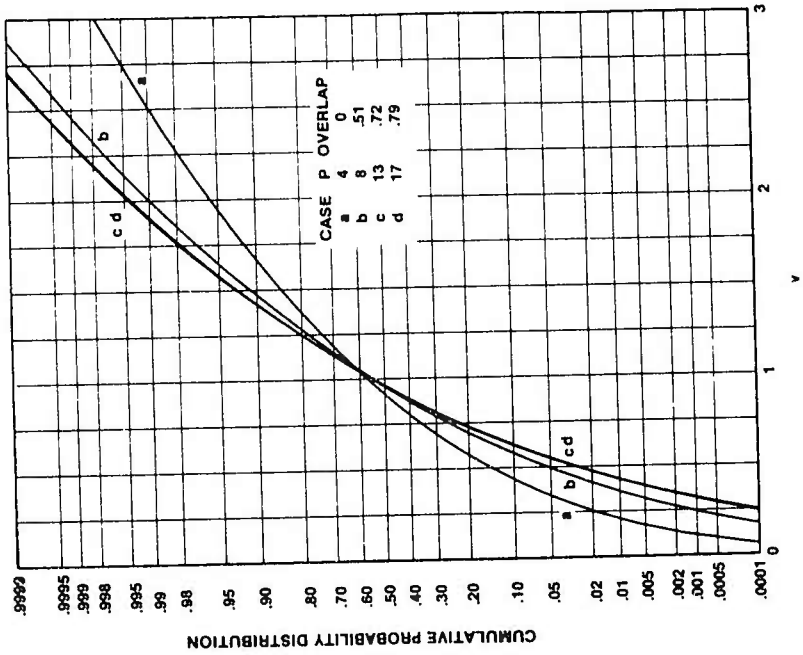


3C. BT=32

Figure 3. (Cont'd) Approximation for Hanning Window

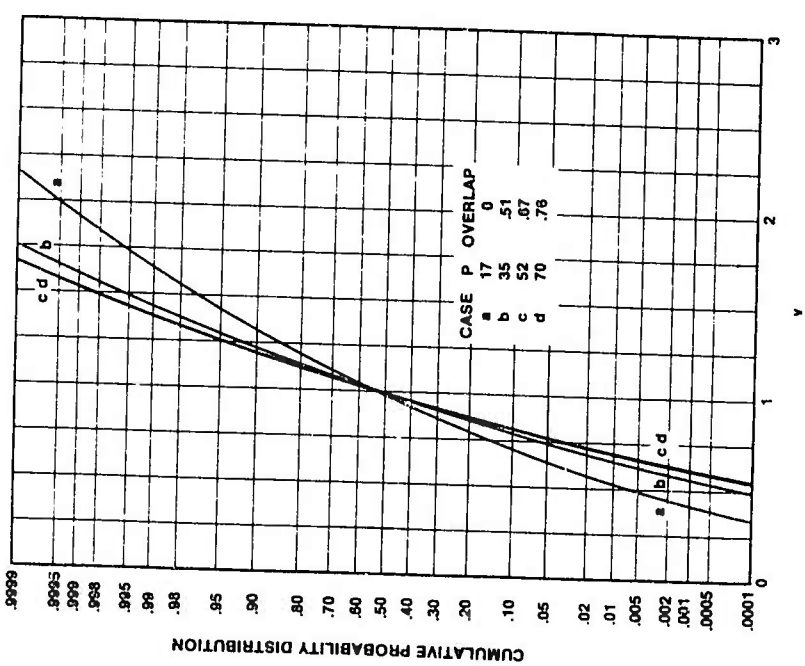


4B. BT=16

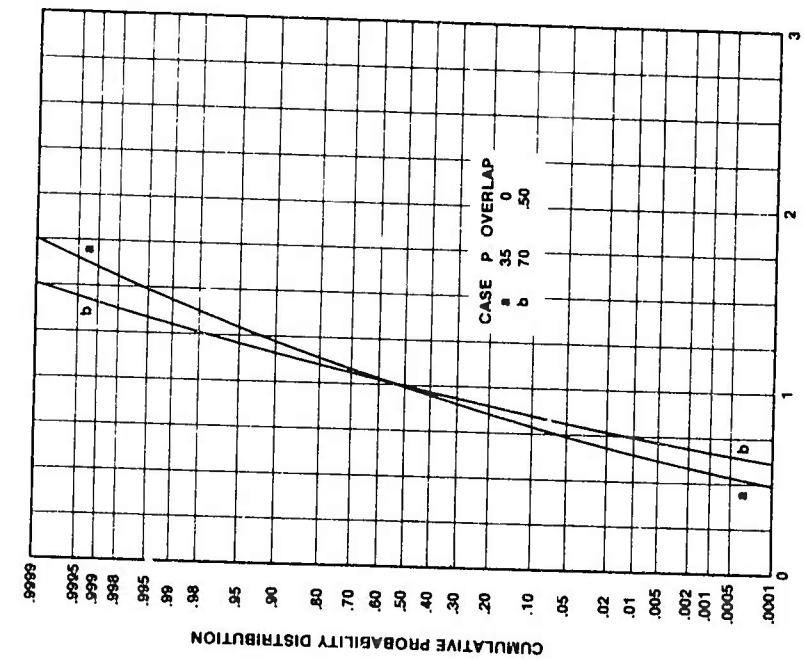


4A. BT=8

Figure 4. Exact Distribution for Cubic Window

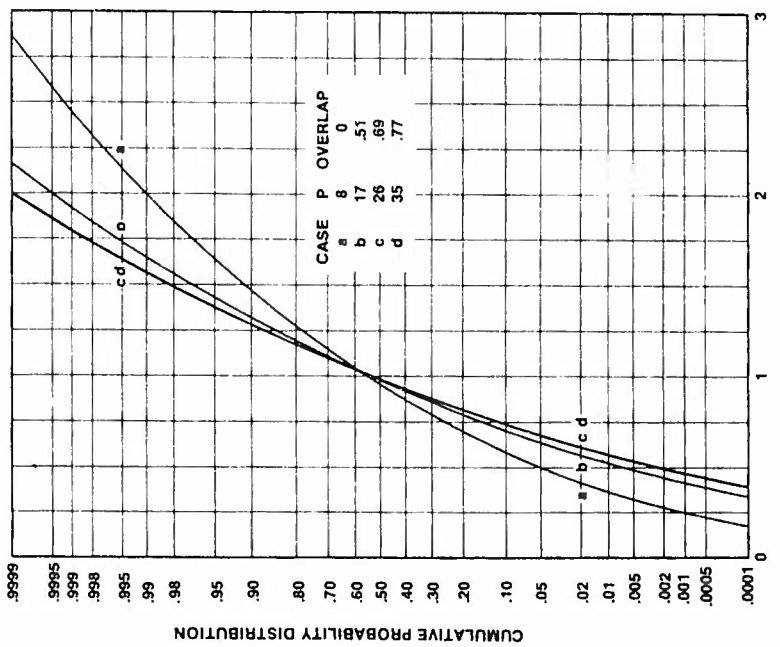


4C. BT=32

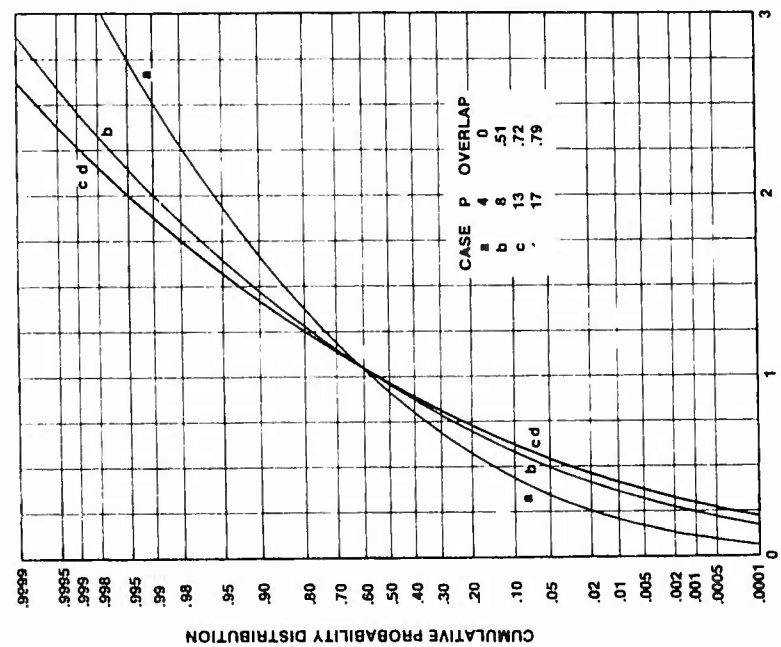


4D. BT=64

Figure 4. (Cont'd) Exact Distribution for Cubic Window

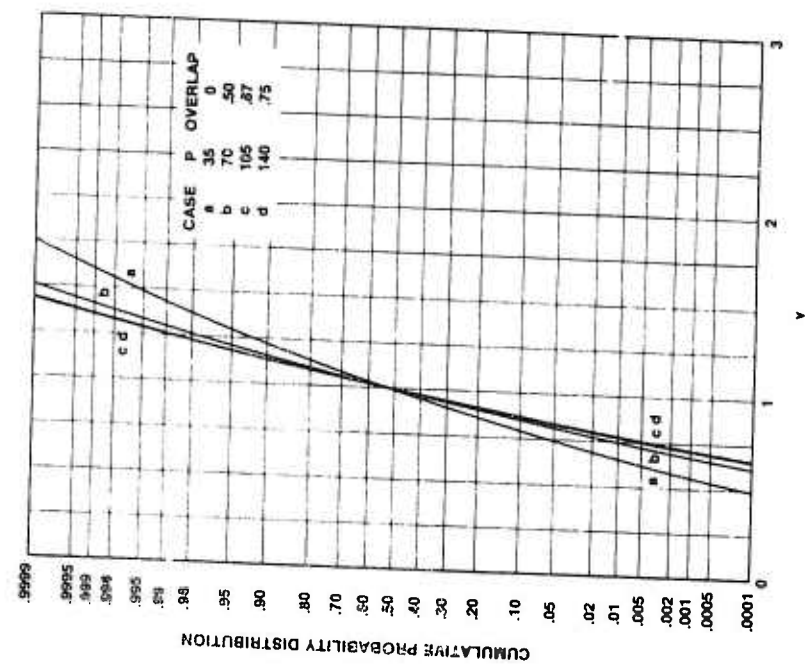


5B. BT=16

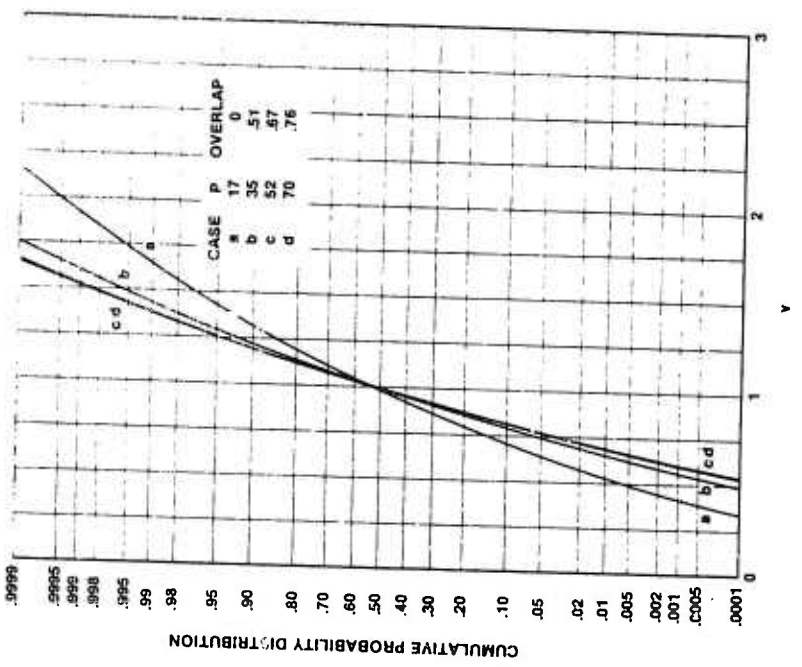


5A. BT=8

Figure 5. Approximation for Cubic Window



5D. BT=64



5C. BT=32

Figure 5. (Cont'd) Approximation for Cubic Window

FLUCTUATIONS OF CROSS SPECTRAL ESTIMATE

This topic is not directly related to the earlier material on autospectral estimation; however, it is an important observation and merits a comment. For two uncorrelated processes, x and y, the cross spectrum $G_{xy}(f) = 0$. However, the cross spectral estimate, $\hat{G}_{xy}(f)$, satisfies the equations (reference 2):

$$E\left\{\hat{G}_{xy}(f)\right\} = 0,$$

$$E\left\{\hat{G}_{xy}^{2}(f)\right\} = 0,$$

and

$$E\left\{\left|\hat{G}_{xy}(f)\right|^{2}\right\} = \frac{2}{K} G_{xx}(f)G_{yy}(f) \equiv 2\sigma^{2}, \tag{42}$$

where K is the equivalent degrees of freedom. Now, if K>>1, $\hat{G}_{xy}(f)$ is approximately complex Gaussian. Therefore, if we define the amplitude estimate

$$A \equiv \left|\hat{G}_{xy}(f)\right|, \tag{43}$$

it has probability density function

$$p(x) = \frac{x}{\sigma^{2}} \exp\left(-\frac{x^{2}}{2\sigma^{2}}\right), \quad x>0. \tag{44}$$

Then the mean of A is

$$E\left\{A\right\} = \left(\frac{\pi}{2}\right)^{\frac{1}{2}} \sigma = \left(\frac{\pi}{2} \frac{G_{xx}(f)G_{yy}(f)}{K}\right)^{\frac{1}{2}}, \tag{45}$$

which is a rather slow decay with K. Then the ratio of the mean amplitude, (45), to the square root of the product of the auto-spectra is

$$\frac{E\{A\}}{\left[G_{xx}(f)G_{yy}(f)\right]^{\frac{1}{2}}} = \left(\frac{\pi}{2K}\right)^{\frac{1}{2}} = \frac{1.253}{K^{\frac{1}{2}}} . \tag{46}$$

If, for example, K = 32, this ratio is .222 which is -6.55 dB; this is not very far down relative to unity coherence, though the two processes are uncorrelated.

Also,

$$\text{Var}\{A\} = \left(2-\frac{\pi}{2}\right)\sigma^2 = \left(2-\frac{\pi}{2}\right)\frac{G_{xx}(f)G_{yy}(f)}{K} , \tag{47}$$

and, therefore,

$$\frac{\text{Standard deviation}\{A\}}{\text{Mean}\{A\}} = \left(\frac{4-\pi}{\pi}\right)^{\frac{1}{2}} = 0.52, \tag{48}$$

independent of K (or P). So for a zero cross-spectrum value, $A = |\hat{G}_{xy}(f)|$ will always have the same amount of relative variation, regardless of the number of pieces P (for large P); thus, on a dB scale, the "ribbon width" of the cross-spectral estimate is independent of P, when the two processes are uncorrelated.

DISCUSSION

An exact expression for the characteristic function of the power spectral estimate of a pure tone in Gaussian noise has been attained, and then specialized to noise-alone. In the noise-alone case, a numerical computation of the cumulative distribution function has been conducted. Comparison of the latter with an approximation utilizing only the mean and variance shows excellent agreement over a wide range of probabilities, regardless of the exact window, overlap, or the time-bandwidth product. This means that concentration on the equivalent degrees of freedom, particularly on its maximization, is sufficient for a probabilistic description of the auto-spectral estimate. Maximizing the equivalent degrees of freedom results in a narrower probability density function, as witnessed by the increased steepness of the cumulative probability distributions presented.

An entirely different method of auto- and cross-spectral estimation has been presented in references 7 and 8, and is mentioned here as a viable, attractive alternative, particularly for short data segments. Since only a few parameters are estimated, the estimates are potentially more stable, whereas the technique considered here (and in reference 1) assigns independent degrees of freedom to each and every frequency cell of interest and, therefore, requires the estimation of many more parameters.

Appendix A

DERIVATION OF CHARACTERISTIC FUNCTION

The first half of appendix C of reference 9 considers the Hermitian form

$$F = \mathbf{X}^H \mathbf{B} \mathbf{X}, \tag{A-1}$$

with mean and covariance of the complex random variable matrix $\mathbf{X}$,

$$E\{\mathbf{X}\} = \mathbf{m}, \quad \mathrm{Cov}\{\mathbf{X}\} = E\left\{(\mathbf{X}-\mathbf{m})(\mathbf{X}-\mathbf{m})^H\right\} = \mathbf{K}, \tag{A-2}$$

where matrix $\mathbf{X}$ is P x 1, and matrix $\mathbf{B}$ is Hermitian and P x P. Defining P x P matrix

$$\mathbf{A} = \mathbf{K}^{\frac{1}{2}} \mathbf{B} \mathbf{K}^{\frac{1}{2}}, \tag{A-3}$$

with corresponding normalized modal matrix $\mathbf{Q}$ and (diagonal) eigenvalue matrix $\boldsymbol{\lambda}$, we can express (A-1) as

$$F = \mathbf{V}^H \boldsymbol{\lambda} \mathbf{V} = \sum_{k=1}^{P} \lambda_k |v_k|^2, \tag{A-4}$$

where matrix $\mathbf{V}$ is P x 1 with mean and covariance

$$E\{\mathbf{V}\} = \mathbf{Q}^H \mathbf{K}^{-\frac{1}{2}} \mathbf{m} \equiv \boldsymbol{\mu}, \quad \mathrm{Cov}\{\mathbf{V}\} = \mathbf{I}. \tag{A-5}$$

Then a slight generalization* of the second half of appendix C of reference 9 (see also reference 10) yields the characteristic function of random variable F in (A-4) as

*We must also have $E\left\{(\mathbf{X}-\mathbf{m})(\mathbf{X}-\mathbf{m})^T\right\} = \mathbf{O}$, in addition to (A-2).

$$C(\xi) = \prod_{k=1}^{P} \left\{ (1-i\lambda_k\xi)^{-1} \exp\left(\frac{i|\mu_k|^2\lambda_k\xi}{1-i\lambda_k\xi} \right) \right\} , \qquad \text{(A-6)}$$

where $\{\lambda_k\}$ and $\{\mu_k\}$ are the elements of matrices $\boldsymbol{\lambda}$ and $\boldsymbol{\mu}$. The cumulants of F follow easily from (A-6) as

$$c_n = (n-1)! \sum_{k=1}^{P} \lambda_k^n \left(1+n|\mu_k|^2 \right) . \qquad \text{(A-7)}$$

In particular, the first two cumulants are

$$\text{Mean } \{F\} = c_1 = \sum_{k=1}^{P} \lambda_k \, (1+|\mu_k|^2)$$

$$\text{Var } \{F\} = c_2 = \sum_{k=1}^{P} \lambda_k^2 \, (1+2|\mu_k|^2) . \qquad \text{(A-8)}$$

For the case of zero-mean variables, i.e., $\mathbf{m} = \mathbf{0}$, (A-5) yields $\boldsymbol{\mu} = \mathbf{0}$, and the characteristic function becomes

$$C(\xi) = \prod_{k=1}^{P} \left\{ (1-i\lambda_k\xi)^{-1} \right\} \quad \text{for zero-mean variables.} \qquad \text{(A-9)}$$

The cumulants are then

$$c_n = (n-1)! \sum_{k=1}^{P} \lambda_k^n \quad \text{for zero-mean variables.} \qquad \text{(A-10)}$$

(It is not necessary to evaluate $\mathbf{K}^{\frac{1}{2}}$ for eigenvalue purposes alone, because the eigenvalues $\{\lambda_k\}$ of matrix $\mathbf{A}$ defined in (A-3) are the same as the eigenvalues of $\mathbf{KB}$ or $\mathbf{BK}$.)

As a specific application of the general results above, we consider

$$\mathbf{B} = \mathbf{I}\ ,\ \mathbf{m} = [m_1 \cdots m_p]^T,\ \mathbf{K} = \left[K_{p-q}\right]\ . \tag{A-11}$$

Then from (A-3), we see that $\mathbf{A} = \mathbf{K}$. In order to evaluate (A-8), we notice that

$$\sum_{k=1}^{P} \lambda_k = \sum_{p=1}^{P} A_{pp} = PK_o\ , \tag{A-12}$$

$$\sum_{k=1}^{P} \lambda_k |\mu_k|^2 = \mu^H \lambda \mu = \mathbf{m}^H \mathbf{K}^{-\frac{1}{2}} \mathbf{Q} \lambda \mathbf{Q}^H \mathbf{K}^{-\frac{1}{2}} \mathbf{m}$$

$$= \mathbf{m}^H \mathbf{K}^{-\frac{1}{2}} \mathbf{A} \mathbf{K}^{-\frac{1}{2}} \mathbf{m} = \mathbf{m}^H \mathbf{m} = \sum_{k=1}^{P} |m_k|^2\ , \tag{A-13}$$

$$\sum_{k=1}^{P} \lambda_k^2 = \sum_{p,q=1}^{P} A_{pq} A_{qp} = \sum_{p,q=1}^{P} |K_{p-q}|^2 = \sum_{k=1-P}^{P-1} (P-|k|)|K_k|^2\ , \tag{A-14}$$

$$\sum_{k=1}^{P} \lambda_k^2 |\mu_k|^2 = \mu^H \lambda \lambda \mu = \mathbf{m}^H \mathbf{K}^{-\frac{1}{2}} \mathbf{Q} \lambda \lambda \mathbf{Q}^H \mathbf{K}^{-\frac{1}{2}} \mathbf{m}$$

$$= \mathbf{m}^H \mathbf{K}^{-\frac{1}{2}} \mathbf{A} \mathbf{Q} \lambda \mathbf{Q}^H \mathbf{K}^{-\frac{1}{2}} \mathbf{m} = \mathbf{m}^H \mathbf{K}^{-\frac{1}{2}} \mathbf{K} \mathbf{K} \mathbf{K}^{-\frac{1}{2}} \mathbf{m} = \mathbf{m}^H \mathbf{K} \mathbf{m}\ , \tag{A-15}$$

Then (A-8) yields

$$\text{Mean}\ \{F\} = c_1 = PK_o + \sum_{k=1}^{P} |m_k|^2\ ,$$

$$\text{Var}\ \{F\} = c_2 = \sum_{k=1-P}^{P-1} (P-|k|)|K_k|^2 + 2\,\mathbf{m}^H \mathbf{K} \mathbf{m}\ . \tag{A-16}$$

The specialization to zero-mean variables is obtained by dropping the last terms in (A-16).

Appendix B

DERIVATION OF COVARIANCE MATRIX

We are interested in deriving the two averages

$$E\left\{Y_{pn}\, Y^{*}_{qn}\right\} \quad \text{and} \quad E\left\{Y_{pn}\, Y_{qn}\right\} \tag{B-1}$$

because they are needed for appendix A and to see if the conditions required there are satisfied. We have, from (7),

$$E\left\{Y_{pn}\, Y^{*}_{qn}\right\} = \iint dt\, du\, \exp(-i2\pi f(t-u))\, E\left\{n(t)n^{*}(u)\right\}\, w\left[t-\frac{1}{2}L-(p-1)S\right] \cdot$$

$$w^{*}\left[u-\frac{1}{2}L-(q-1)S\right] . \tag{B-2}$$

Letting the noise correlation in (B-2) be denoted by $R_n(t-u)$, and its spectrum by G_n, (B-2) becomes

$$E\left\{Y_{pn}\, Y^{*}_{qn}\right\} = \int d\mu\, G_n(\mu) \int dt\, \exp(i2\pi(\mu-f)t)\, w\left[t-\frac{1}{2}L-(p-1)S\right] \cdot$$

$$\left\{\int du\, \exp(i2\pi(\mu-f)u)\, w\left[u-\frac{1}{2}L-(q-1)S\right]\right\}^{*}$$

$$= \int d\mu\, G_n(\mu)\, |W(f-\mu)|^2\, \exp\left[i2\pi(f-\mu)(q-p)S\right] . \tag{B-3}$$

This quantity is a function only of the difference of indices q and p.

If spectral window $|W|^2$ is narrower than the detail in noise spectrum G_n in the neighborhood of analysis frequency f, (B-3) simplifies to

$$E\left\{Y_{pn}Y^{*}_{qn}\right\} \cong G_n(f)\int d\mu |W(f-\mu)|^2 \exp\left[i2\pi(f-\mu)(q-p)S\right]$$

$$= G_n(f)\phi_w((q-p)S), \tag{B-4}$$

where

$$\phi_w(\tau) \equiv \int dt\ w(t)w^*(t-\tau) \tag{B-5}$$

is the autocorrelation function of data window w.

Now let

$$\frac{\phi_w(mS)}{\phi_w(0)} \equiv r_m\ . \tag{B-6}$$

Then

$$E\left\{Y_{pn}Y^{*}_{qn}\right\} = G_n(f)\phi_w(0)r_{q-p}\ , \tag{B-7}$$

and from (10),

$$\mathbf{K} = G_n(f)\phi_w(0)\,\mathbf{R}\ , \tag{B-8}$$

where P x P matrix

$$\mathbf{R} \equiv \begin{bmatrix} 1 & r_1 & r_2 \cdots r_{P-1} \\ r_{-1} & \ddots & \\ \vdots & & \\ \vdots & & \\ r_{1-P} & & 1 \end{bmatrix} \tag{B-9}$$

is Hermitian, Toeplitz, and non-negative definite.* For real weighting w, $\mathbf{R}$ is a real symmetric Toeplitz matrix. The matrix in (B-8) is the one required in (A-11) and (10).

*This property is easily proven by use of definitions (B-5) and (B-6).

The second quantity we desire is, by use of (7),

$$E\left\{Y_{pn}Y_{qn}\right\} = \iint dt\, du\, \exp(-i2\pi f(t+u))\, E\left\{n(t)n(u)\right\}\, w\left[t-\tfrac{1}{2}L-(p-1)S\right] \cdot$$

$$w\left[u-\tfrac{1}{2}L-(q-1)S\right] . \qquad \text{(B-10)}$$

Letting the noise correlation in (B-10) be denoted by $\mathcal{R}_n(t-u)$, and its spectrum (Fourier transform) by $\mathcal{C}_n$, (B-10) becomes

$$E\left\{Y_{pn}Y_{qn}\right\} = \int d\mu\, \mathcal{C}_n(\mu) \int dt\, \exp(i2\pi(\mu-f)t)\, w\left[t-\tfrac{1}{2}L-(p-1)S\right] \cdot$$

$$\int du\, \exp(-i2\pi(\mu+f)t)\, w\left[u-\tfrac{1}{2}L-(q-1)S\right]$$

$$= \int d\mu\, \mathcal{C}_n(\mu) W(f-\mu) W(f+\mu)\, \exp\left[-i2\pi f(L-2S+pS+qS)-i2\pi\mu(q-p)S\right] . \qquad \text{(B-11)}$$

If analysis frequency f is greater than the bandwidth B of spectral window W, then W(f-μ) and W(f+μ) do not overlap on the μ-axis, and (B-11) yields

$$E\left\{Y_{pn}Y_{qn}\right\} \cong 0 \text{ if } f>B. \qquad \text{(B-12)}$$

Thus, the property desired in appendix A (footnote to equation (A-6)) holds true if f>B.

Appendix C

NUMERICAL COMPUTATION OF CUMULATIVE PROBABILITY DISTRIBUTION

The numerical computation of the cumulative probability distribution $\text{Prob}(\hat{g}<v)$ is not accomplished here directly via the sum in (36). The reason is that, for large P, (36) is an alternating sum of terms of large magnitude, and accuracy is lost in the final result. Instead, the methods in references 3 and 4 are utilized on characteristic function (35): for a random variable limited to positive values, the cumulative probability distribution can be expressed as (reference 4)

$$P(v) = 1 - \frac{2}{\pi} \text{Re}\left\{ \int_0^\infty d\xi \ \frac{f_i(\xi)}{\xi} \exp(-i\xi v) \right\} , \ v>0, \qquad \text{(C-1)}$$

where $f_i(\xi)$ is the imaginary part of the characteristic function $f(\xi)$. We have $f_i(\xi)/\xi \sim E\{\hat{g}\} = 1$ as $\xi \to 0$. We approximate (C-1) according to

$$P(v) \cong 1 - \frac{2}{\pi} \text{Re}\left\{ \int_0^{\xi_2} d\xi \ \frac{f_i(\xi)}{\xi} \exp(-i\xi v) \right\}, \qquad \text{(C-2)}$$

and then sample and approximate this expression according to

$$P(n\ \Delta v) \cong 1 - \frac{2}{\pi} \text{Re}\left\{ \Delta\xi \sum_{k=0}^{L} w_k \ \frac{f_i(k\ \Delta\xi)}{k\ \Delta\xi} \exp\left[-ik\Delta\xi\ n\ \Delta v\right] \right\}, \qquad \text{(C-3)}$$

where $L\ \Delta\xi = \xi_2$, and $\{w_k\}$ are Trapezoidal weights of integration. We choose sampling increment

$$\Delta\xi = \frac{2\pi}{N\ \Delta v} , \qquad \text{(C-4)}$$

where N is chosen large enough that $f_i(\xi)/\xi$ does not change much in

$\Delta\xi$. Then

$$P(n\,\Delta v) = 1 - \frac{2}{\pi}\,\mathrm{Re}\left\{\Delta\xi \sum_{k=0}^{L} w_k \frac{f_i(k\,\Delta\xi)}{k\,\Delta\xi} \exp\left[-i2\pi kn/N\right]\right\}$$

$$= 1 - \frac{2}{\pi}\,\Delta\xi\,\mathrm{Re}\left\{\sum_{k=0}^{N-1} g_k \exp\left[-i2\pi kn/N\right]\right\} \qquad \text{(C-5)}$$

where

$$g_k = \sum_{j=0}^{J} w_{k+jN} \frac{f_i((k+jN)\,\Delta\xi)}{(k+jN)\,\Delta\xi},$$

$$0 \le k \le N-1,\ \frac{L+1}{N} - 1 \le J \le \frac{L+1}{N} \quad . \qquad \text{(C-6)}$$

Equation (C-5) is an N-point FFT; therefore, we choose N as a power of 2 for speed purposes.

The only remaining question is the choice of limit ξ_2 in (C-2). From (35), we know that

$$|f_i(\xi)| \le |f(\xi)| \le \frac{1}{\prod_{p=1}^{P} \max\left\{1,\ r_p\xi\right\}}, \qquad \text{(C-7)}$$

where $r_p \equiv \lambda_p^{(R)}/P$. Therefore

$$|f_i(\xi)| \le \frac{1}{\prod_{p=IP}^{P} \max\left\{r_p\xi\right\}} \quad , \qquad \text{(C-8)}$$

where IP can be 1 or 2 or ... or P. Therefore the error, E, in using (C-2) rather than (C-1) is bounded according to

$$E \le \frac{2}{\pi}\int_{\xi_2}^{\infty} \frac{d\xi}{\prod_{p=IP}^{P}\left\{r_p\right\}}\,\xi^{-P+IP-2} = \frac{2}{\pi}\left[\prod_{p=IP}^{P}\left\{r_p\right\}\right]^{-1}\frac{\xi_2^{-P+IP-1}}{P+1-IP} \quad . \qquad (C\text{-}9)$$

This equation can be solved for

$$\xi_2 = P\left[\frac{2}{\pi E\prod_{p=IP}^{P}\left\{\lambda_p^{(R)}\right\}(P+1-IP)}\right]^{\frac{1}{P+1-IP}} \quad , \qquad (C\text{-}10)$$

with the guarantee that the error will be less than E if we choose ξ_2 according to (C-10). Since IP is not unique, we choose ξ_2 to be the minimum value over the range of IP=1, 2,..., P, for then the integration range in (C-2) can be kept to a minimum.

In summary, we:

specify Δv, E, P, BT

compute $\left\{\lambda_p^{(R)}\right\}$ and ξ_2

choose N = 1024 (say)

compute $\Delta\xi = \frac{2\pi}{N\,\Delta v}$

compute $L = \xi_2/\Delta\xi$

let $J = (L+1)/N$

compute (C-6)

compute FFT $\left\{g_k\right\}$ and printout (C-5)

choose N = 2048, go back to step 4, and observe change in printout.

A program for this procedure for the Hanning window follows. The subroutines TRIMXD and EIGVLD are presented in reference 11, and subroutines DPMCOS and DPMFFT are given in reference 12.

In order to execute the approximation (41), the line under statement number 2 is changed to CALL PROBA(BT, P, Y). This subroutine for the Cubic window is also presented below.

```
      INTEGER P
      DIMENSION X(51),Y(51),Z(200),YNORM(25)
      DATA YNORM/-3.71902,-3.29053,-3.09023,-2.87816,-2.57583,-2.32635,
     $-2.05375,-1.64485,-1.28155,-.84162,-.52440,-.25335,0.,.25335,.5244
     $,.84162,1.28155,1.64485,2.05375,2.32635,2.57583,2.87816,3.09023,
     $3.29053,3.71902/
      C=1.44058253   C HANNING
      CALL MODESG(Z,0)
      CALL SUBJEG(Z,0.,YNORM(1),3.,YNORM(25))
      CALL OBJCTG(Z,1150.,335.,285.,2735.)
      DO 11 IBT=3,6
      BT=2.**IBT
      CALL SETSMG(Z,30,2.)
      CALL LINESG(Z,0,0.,YNORM(1))
      CALL LINESG(Z,1,0.,YNORM(25))
      CALL LINESG(Z,1,3.,YNORM(25))
      CALL LINESG(Z,1,3.,YNORM(1))
      CALL LINESG(Z,1,0.,YNORM(1))
      CALL SETSMG(Z,30,1.)
      DO 21 J=1,11
      CALL LINESG(Z,0,J*.25,YNORM(1))
21    CALL LINESG(Z,1,J*.25,YNORM(25))
      DO 22 J=2,24
      CALL LINESG(Z,0,0.,YNORM(J))
22    CALL LINESG(Z,1,3.,YNORM(J))
      CALL SETSMG(Z,30,2.)
      DO 23 I=1,51
23    X(I)=.06*(I-1)
      DO 1 IP=1,4
      P=(BT/C)*IP
      SL=(BT/C-1.)/(P-1)
      PRINT 2, BT,P,SL
2     FORMAT(////' BT ='E13.8,'      P ='I4,'      S/L ='E13.8)
      CALL PROBUP(BT,P,Y)
      PRINT 3, Y
3     FORMAT(/5E20.8)
      DO 4 I=1,51
      Q=MIN(Y(I),.999999)
      Q=MAX(Q,.000001)
4     Y(I)=TINORM(Q,$1)
      CALL LINESG(Z,51,X,Y)
1     CONTINUE
      CALL PAGEG(Z,0,1,1)
```

```
11    CONTINUE
      CALL EXITG(Z)
      END
      SUBROUTINE PROBDP(BT,P,ANS)
      PARAMETER M=100  @ MAXIMUM NUMBER OF PIECES
      PARAMETER N=2048,N41=N/4+1
      DOUBLE PRECISION R(M,M),D(M),B(M),E(M),W(M),F(M),GR(N),GI(N),CO(N4
     $1),C,ERROR,DELV,PI,SL,TPE,XI2,PR,AT,DELXI,S,U,WFIDXI
      INTEGER P,P1
      DIMENSION ANS(1)
      C=1.44058258D0  @ HANNING
      IF(P.LE.M) GO TO 1
      J=M
      PRINT 2, P,J
2     FORMAT(/' P ='I4,' IS GREATER THAN M ='I3/)
      DO 3 J=1,51
3     ANS(J)=-1.
      RETURN
1     ERROR=1.D-12
      DELV=.06D0
      PI=3.14159265358979324D0
      P1=P-1
      SL=(BT/C-1.D0)/P1
      DO 4 K=0,P1
4     D(K+1)=U(K*SL)
      DO 5 J=1,P
      DO 5 K=1,P
      L=ABS(J-K)+1
5     R(J,K)=D(L)
      CALL TRIMXD(P,M,R,D,B)
      CALL EIGVCD(P,E,D,B,W,F)
      TPE=2.D0/(PI*ERROR)
      XI2=1.0100
      PR=0.D0
      DO 6 J=P,1,-1
      PR=PR+LOG(E(J))
      AT=1.D0/(P-J+1.D0)
      S=P*EXP(AT*(LOG(TPE*AT)-PR))
6     XI2=MIN(XI2,S)
      NF=N/2
7     DELXI=2.D0*PI/(NF*DELV)
      S=XI2/DELXI
      JC=(S+1.D0)/NF
      N1=NF-1
      DO 8 K=0,N1
      S=0.D0
      DO 9 J=0,JC
9     S=S+WFIDXI((K+J*NF)*DELXI)
      GR(K+1)=S
8     GI(K+1)=0.D0
      CALL DPMCOS(CO,NF)
      J=1.4427*LOG(NF)+.5
      CALL DPMFFT(GR,GI,CO,J,-1)
      S=2.D0*DELXI/PI
      DO 10 J=1,51
```

```
10      ANS(J)=1.D0-S*GR(J)
        IF(NF.EQ.N) RETURN
        DO 11 J=1,46,5
11      PRINT 12, ANS(J),ANS(J+1),ANS(J+2),ANS(J+3),ANS(J+4)
        PRINT 12, ANS(51)
12      FORMAT(/5E20.8)
        NF=N
        GO TO 7
        FUNCTION U(T)  @ HANNING
        DOUBLE PRECISION T,SI
        IF(T.GE.1.D0) GO TO 1
        SI=2.D0*PI*T
        U=2.D0/3.D0*(1.D0-T)*(1.D0+.5D0*COS(SI))+(.5D0/PI)*SIN(SI)
        RETURN
1       U=0.D0
        RETURN
        FUNCTION WFIDXI(X)
        DOUBLE PRECISION X,XTOP,AL,BE,BI,TEMP,SQ
        IF(X.GT.0.D0) GO TO 1
        XTOP=1.0100
        WFIDXI=.5D0
        RETURN
1       IF(X.GT.XTOP) GO TO 3
        AL=1.D0
        BE=-E(P)*X/P
        DO 2 JI=1,P1
        BI=E(JI)*X/P
        TEMP=AL+BE*BI
        BE=BE-AL*BI
2       AL=TEMP
        SQ=AL*AL+BE*BE
        IF(SQ*(X*ERROR)**2.GT.10.D0) XTOP=MIN(XTOP,X)
        WFIDXI=-BE/(SQ*X)
        RETURN
3       WFIDXI=0.D0
        RETURN
        END
        SUBROUTINE PROBA(BT,P,ANS)
        DOUBLE PRECISION GD,D,BV,F11L
        INTEGER P,P1
        DIMENSION ANS(1)
        C=1.82009566   @ CUBIC
        P1=P-1
        SL=(BT/C-1.)/P1
        B=1.
        DO 1 K=1,P1
1       B=B+2.*(1.-FLOAT(K)/P)*U(K*SL)**2
        CAPK=2.*P/B
        PRINT 101, CAPK
101     FORMAT(/' CAPK IS 'E15.8)
        B=P/B
        IB=B
        FB=B-IB
        CALL GAMMA(1.+FB,G,$2,$2)
        GD=LOG(DBLE(G))
        DO 5 K=1,IB
        D=FB+K
```

```
5       GD=GD+LOG(D)
        DO 3 K=1,51
        V=.06*(K-1)
        IF(V.GT.0.) GO TO 6
        ANS(K)=0.
        GO TO 3
6       BV=B*V
        ANS(K)=EXP(B*LOG(BV)-BV+F11L(DBLE(B+1.),BV)-GD)
3       CONTINUE
        RETURN
2       PRINT 4, B
4       FORMAT(/' PROBLEM AT B  = 'E15.8)
        RETURN
        FUNCTION F11L(A,XD)
        DOUBLE PRECISION SD,TD,AD,XD,A
        SD=1.D0
        TD=1.D0
        AD=A-1.D0
        DO 1 K=1,1000
        TD=TD*XD/(AD+K)
        SD=SD+TD
1       IF(ABS(TD).LE.1.D-8*ABS(SD)) GO TO 2
        PRINT 3,
3       FORMAT(/' 1000 TERMS'/)
2       F11L=LOG(SD)
        RETURN
        FUNCTION U(T)  G CUBIC
        IF(T.GE.1.) GO TO 1
        U=1024./151.*(1.-T)**7
        IF(T.GE.0.75) RETURN
        U=U-8192./151.*(.75-T)**7
        IF(T.GE.0.5) RETURN
        U=U+28672./151.*(.5-T)**7
        IF(T.GE.0.25) RETURN
        U=U-57344./151.*(.25-T)**7
        RETURN
1       U=0.
        RETURN
        END
```

REFERENCES

1. A. H. Nuttall, Spectral Estimation by Means of Overlapped Fast Fourier Transform Processing of Windowed Data, NUSC Technical Report 4169, 13 October 1971.

2. A. H. Nuttall, Estimation of Cross-Spectra via Overlapped Fast Fourier Transform Processing, NUSC Technical Report 4169-S, 11 July 1975. (Also NUSC Technical Memorandum TC-83-72, 18 April 1972.)

3. A. H. Nuttall, Numerical Evaluation of Cumulative Probability Distribution Functions Directly from Characteristic Functions, USL Report 1032, 11 August 1969. (Also Proc. IEEE, vol. 57, no. 11, Nov. 1969, pp. 2071-2072.)

4. A. H. Nuttall, Alternate Forms and Computational Considerations for Numerical Evaluation of Cumulative Probability Distributions Directly from Characteristic Functions, NUSC Report NL-3012, 12 August 1970. (Also Proc. IEEE, vol. 58, no. 11, Nov. 1970, pp. 1872-1873.)

5. M. M. Siddiqui, Approximations to the Distribution of Quadratic Forms," The Annals of Mathematical Statistics, vol. 36, 1965, pp. 677-682.

6. Handbook of Mathematical Functions, U. S. Dept. of Comm., National Bureau of Standards, Applied Mathematics Series, no. 55, U. S. Government Printing Office, Washington, D.C., June 1964.

7. A. H. Nuttall, Spectral Estimation of a Univariate Process with Bad Data Points, via Maximum Entropy and Linear Predictive Techniques, NUSC Technical Report 5303, 26 March 1976.

8. A. H. Nuttall, Multivariate Linear Predictive Spectral Analysis, Employing Weighted Forward and Backward Averaging: A Generalization of Burg's Algorithm, NUSC Technical Report 5501, 13 October 1976. (Also, program is in NUSC Technical Document 5419, 19 May 1976.)

9. A. H. Nuttall and P. G. Cable, Operating Characteristics for Maximum Likelihood Detection of Signals in Gaussian Noise of Unknown Level; Part I, Coherent Signals of Unknown Level, NUSC Technical Report 4243, 27 March 1972.

REFERENCES (Cont'd)

10. G. L. Turin, "The Characteristic Function of Hermitian Quadratic Forms in Complex Normal Variables," Biometrika, vol. 47, nos. 1 and 2, 1960, pp. 199-201.

11. M. J. Goldstein and N. Brockman, "On Several Double Precision Subroutines for Computing the Eigenvalues and/or Eigenvectors of Hermitian Matrices," NUSC Technical Memorandum 2070-253-70, 10 July 1970.

12. J. F. Ferrie, "Double Precision Version of Markel's FFT Algorithm," NUSC Technical Memorandum TD 113-15-73, 11 June 1973.

Subject Matter Index

Acoustic signal processing, 4513

All-pole filter model, 5303

Approximate distribution, 5529

Approximate spectral analysis, 4767

Approximations for statistics, 5291

Autoregression, 5303, 5505

Average magnitude error, 4113

Bad data points, 5303

Bias, 5303

Bias of coherence estimators, 5291

Burg technique, 5303, 5505

Characteristic function, 1032

Coherence estimation, 5291

Complex univariate process, 5505

Cross-spectral estimation, 4169-S

Cumulative probability distribution function, 1032, 3012

Delay weighting, 4767

Dolph-Chebyshev weighting, 4767

Equivalent degrees of freedom, 5529

Equivalent-noise bandwidth, 4513

Fast Four Transform (FFT), 3012, 4113, 4169, 4169-S, 4513, 4767

Forward and backward averaging, 5303, 5419, 5501

Generalization of Burg's algorithm, 5419, 5501

Half-power bandwidth, 4169, 4169-S, 4513

Linear prediction, 5303, 5419, 5501 5505

Magnitude coherence, 5291

Magnitude-squared coherence, 5291

Maximum entropy, 5303, 5501, 5505

Mean-square error of coherence estimators, 5291

Minimum-bias windows, 4513

Multivariate process, 5419, 5501

Overlapped FFT processing, 4513, 5529

Overlapped time weighting, 4767

Probability distribution, 5529, 1032

Resolution, 5303

RMS bandwidth, 4513

Short modified periodograms, 4169, 4169-S

Spectral analysis, 5303, 5419, 5501, 5505

Spectral estimation, 4169, 4169-S, 4513, 5291, 5529

Statistics of coherence estimators, 5291

Statistical bandwidth, 4169, 4169-S

Time delay measurements, 5291

Variance of coherence estimators, 5291

Vernier spectral analysis, 4767

Weighted error matrices, 5501

Windowed data, 4169, 4169-S, 5529

Yule-Walker equations, 5303